DOCTOR OF PHILOSOPHY

Conjugated Polymers Based on 4-Substituted Fluorenes and Fluorenones

Kommanaboyina, Srikanth

Award date:
2016

Awarding institution:
Bangor University

Conjugated Polymers Based on 4-Substituted Fluorenes and Fluorenones

Srikanth Kommanaboyina

School of Chemistry

Prifysgol Bangor University

A thesis submitted to Bangor University

for the degree of Doctor of Philosophy

October 2016

Dedicated to my Parents,

Wife, Daughter and Brothers

Contents

Declaration and Consent

Details of the Work

I hereby agree to deposit the following item in the digital repository maintained by Bangor University and/or in any other repository authorized for use by Bangor University.

Author Name: Srikanth Kommanaboyina

Title: Conjugated Polymers Based on 4-Sunstituted Fluorenes and Fluorenines

Supervisor/Department: Professor Igor F. Perepichka, School of Chemistry

Funding body (if any): Bangor University, 125th Anniversary Scholarship

Qualification/Degree obtained: PhD

This item is a product of my own research endeavours and is covered by the agreement below in which the item is referred to as "the Work". It is identical in content to that deposited in the Library, subject to point 4 below.

Non-exclusive Rights

Rights granted to the digital repository through this agreement are entirely non-exclusive. I am free to publish the Work in its present version or future versions elsewhere.

I agree that Bangor University may electronically store, copy or translate the Work to any approved medium or format for the purpose of future preservation and accessibility. Bangor University is not under any obligation to reproduce or display the Work in the same formats or resolutions in which it was originally deposited.

Bangor University Digital Repository

I understand that work deposited in the digital repository will be accessible to a wide variety of people and institutions, including automated agents and search engines via the World Wide Web.

I understand that once the Work is deposited, the item and its metadata may be incorporated into public access catalogues or services, national databases of electronic theses and dissertations such as the British Library's EThOS or any service provided by the National Library of Wales.

I understand that the Work may be made available via the National Library of Wales Online Electronic Theses Service under the declared terms and conditions of use (http://www.llgc.org.uk/index.php?id=4676). I agree that as part of this service the National Library of Wales may electronically store, copy or convert the Work to any approved medium or format for the purpose of future preservation and accessibility. The National Library of Wales is not under any obligation to reproduce or display the Work in the same formats or resolutions in which it was originally deposited.

Statement 1:

This work has not previously been accepted in substance for any degree and is not being concurrently submitted in candidature for any degree unless as agreed by the University for approved dual awards.

Signed …….. (candidate)

Date ……..

Statement 2:

This thesis is the result of my own investigations, except where otherwise stated. Where correction services have been used, the extent and nature of the correction is clearly marked in a footnote(s).

Other sources are acknowledged by footnotes giving explicit references. A bibliography is appended.

Signed ……. (candidate)

Date …….

Statement 3:

I hereby give consent for my thesis, if accepted, to be available for photocopying, for inter-library loan and for electronic repositories, and for the title and summary to be made available to outside organisations.

Signed ……. (candidate)

Date …….

NB: Candidates on whose behalf a bar on access has been approved by the Academic Registry should use the following version of **Statement 3:**

Statement 3 (bar):

I hereby give consent for my thesis, if accepted, to be available for photocopying, for inter-library loans and for electronic repositories after expiry of a bar on access.

Signed …… (candidate)

Date ……

<u>Statement 4</u>:

Choose **<u>one</u>** of the following options

a) I agree to deposit an electronic copy of my thesis (the Work) in the Bangor University (BU) Institutional Digital Repository, the British Library ETHOS system, and/or in any other repository authorized for use by Bangor University and where necessary have gained the required permissions for the use of third party material.	
*b) I agree to deposit an electronic copy of my thesis (the Work) in the Bangor University (BU) Institutional Digital Repository, the British Library ETHOS system, and/or in any other repository authorized for use by Bangor University when the approved **bar on access** has been lifted.*	
*c) I agree to submit my thesis (the Work) electronically via Bangor University's e-submission system, however I **opt-out** of the electronic deposit to the Bangor University (BU) Institutional Digital Repository, the British Library ETHOS system, and/or in any other repository authorized for use by Bangor University, due to lack of permissions for use of third party material.*	

Options B should only be used if a bar on access has been approved by the University.

In addition to the above I also agree to the following:

1. That I am the author or have the authority of the author(s) to make this agreement and do hereby give Bangor University the right to make available the Work in the way described above.
2. That the electronic copy of the Work deposited in the digital repository and covered by this agreement, is identical in content to the paper copy of the Work deposited in the Bangor University Library, subject to point 4 below.
3. That I have exercised reasonable care to ensure that the Work is original and, to the best of my knowledge, does not breach any laws – including those relating to defamation, libel and copyright.
4. That I have, in instances where the intellectual property of other authors or copyright holders is included in the Work, and where appropriate, gained explicit permission for the inclusion of that material in the Work, and in the electronic form of the Work as accessed through the open access digital repository, *or* that I have identified and removed that material for which adequate and appropriate permission has not been obtained and which will be inaccessible via the digital repository.
5. That Bangor University does not hold any obligation to take legal action on behalf of the Depositor, or other rights holders, in the event of a breach of intellectual property rights, or any other right, in the material deposited.
6. That I will indemnify and keep indemnified Bangor University and the National Library of Wales from and against any loss, liability, claim or damage, including without limitation any related legal fees and court costs (on a full indemnity bases), related to any breach by myself of any term of this agreement.

Signature: ……

Date : …….

Acknowledgments

I would like to thank Bangor University for providing me 125th Anniversary Scholarship for the academic years 2011–2014, which fully covered my tuition fees and my living expenses in UK and without which this work would be impossible.

I have been fortunate to have such a well admirable supervisor, Professor Igor. F. Perepichka. His enthusiasm and advices have encouraged me enormously throughout my research work. I am always thankful to him for being a part of his research group, for his constant guidance and supervision. Big thanks to my supervisor for always finding time to discuss about my research work and shown a new research direction. This four years research journey with my supervisor is memorable. My further acknowledgements are to Prof. Mark Baird and Dr. Hongyun Tai for their co-supervision as Research Committee members and encouragement towards my research work.

My acknowledgements to the past and present research group members Dr. Michal Krompiec, Dr. Sanjay Ghosh, Elena Klimareva, Daniel Congrave and Mohammed Al-Mashhadani for their valuable research discussion and fruitful ideas. I also acknowledge the contribution of Bangor undergraduate project students Samuel Adamson, Martin Reid Thomas, Charlotte Booth, Simon Anderson and Issac Reids with their short projects that have made the progress of my research on polyfluorenes faster. I am thankful to visiting students in the group Mea Versleijen, Sara Abdul-Sattar Ahmed, Daphne de Graaff, Gethin Griffith and Remco Struik for their help in some experimental work on polyfluorene studies and worthful contribution to my research. My thanks to Dr. Hongyun Tai for allowing me to characterise the polymers using the GPC instrument in her group. Special thanks to Dr. Viacheslav Tverezovskiy and Simon Curling for using DSC and SEM instruments.

My acknowledgements to colleagues Mohammed Hassan, Anna Tochwin, Klarah Sherzad Baols, Charlotte Jones, Mohammed Altahan and Sohad Alshareef. My acknowledgement to all the technical staff members of the School of Chemistry Denis Williams, David Hughes, Gwynfor Davies, Glynne Evans, and Nicholas Welsby, as well as to administrative staff members Caroline Randall, Siobhan Jones, Tracey Roberts and Bryony Jones for all their supports, helps and advices during my research stay in Bangor.

I am thankful to my Bangor and U.K. friends Santosh Choudhary, Shweta Choudhary, Swaroop. C, Sanjay Priyadarshi, Nishant Reddy, Jayesh, Pooja, Prashant Kumar, Rakesh, Sruthi Sunny, Komal, Chintan Deasi, Jeenal, Karl Sadil and Cecil Condron for their kind affection and concern.

I am thankful to my close friends: Amzad Ali. M, Suresh. Y, Sandeep. G, Solomon. R, Sukeerthi. S, Hari Prasad. M, Srinivas. Ch, Ratan. Ch, Jagadesh. Ch, Madhu. M, Ranjit. V, Omar. M, Madan Mohan. Y and all other friends came across in my journey.

Last but not least my very special thanks to my parents: Vana Purna Chandra Kala Rao. K and Venkata Lakshmi Koteswaramma. K, wife and daughter: Sriteja. K (Raveena) and Trishna. A, brothers, sister-in-laws and their kids: Raghu Babu. K, Lakshmi Srinadh. K, Bhargavi. K, Maha Lakshmi. K, Siva Nitya Aashika. K, Neha Aashvika. K, Joshitha Sreya. K, and Karthik. K. I am thankful to Ram Chandra Murthy. D, Venkata Yathirajulu. D, Venkata Lakshmi. D, Srinivas. D, and kommanaboyina, dintakurthy family members.

List of abbreviations

acac	Acetylacetone
ACN	Acetonitrile
Alk	Alkyl
Alq_3	Tris(8-hydroxyquinoline)aluminium
Ar	Aryl
ASE	Amplified spontaneous emission
BHJ	Bulky heterojunction
$B_2(pin)_2$	Bis(pinacolato)diboron
B3LYP	Becke's exchange and Lee-Yang-Parr's correlation functional
bipy	2,2'-Bipyridyl
CD	Circular dichroism spectrum
CDT	Cambridge Display Technology company
CIE	Commission Internationale de l'Eclairage (colour diagram)
COD	1,5-Cyclooctadiene
COSY	Correlation spectroscopy
Da	Dalton
DC	Drop cast
DDO	Dodecyloxy
DDS	Dodecylthio
$DDSO_2$	Dodecylsulfonyl
DCE	Dichloroethane
DCM	Dichloromethane
DFB	Distributed feedback (laser)
DFT	Density functional theory
DMF	*N,N*-Dimethylformamide
DMSO	Dimethyl sulfoxide
dppf	1,1'-Bis(diphenylphosphino)ferrocene
DPV	Differential pulse voltammetry
DSC	Differential scanning calorimetry
EA	Ethyl acetate
E_A	Electron affinity
E_g	Band gap energy (of polymer)

E_{HL}	HOMO–LUMO gap energy
EDG	Electron-donating group
EI	Electron impact
EL	Electroluminescence
ETL	Electron transporting layer
ETM	Electron transporting material
EWG	Electron-withdrawing group
FRET	Fluorescence resonance energy transfer (Förster resonance energy transfer)
FT-IR	Fourier transform infrared spectroscopy
GC-MS	Gas chromatography – mass spectrometry
GIXD	Grazing-incidence-X-ray scattering
GPC	Gel permeating chromatography
GRIM	Grignard metathesis method
$HPCy_3BF_4$	Tricyclohexylphosphonium tetrafluoroborate
HOMO	Highest occupied molecular orbital
$HPCy_3BF_4$	Tricyclohexylphosphonium tetrafluoroborate
HTL	Hole transporting layer
HTM	Hole transporting material
Hz	Hertz
IBM	International business machines company
ICT	Intramolecular charge transfer
IR	Infra-red
I_P	Ionisation potential
ITO	Indium-tin oxide
KCTP	Kumada catalyst transfer polycondensation
LUMO	Lowest unoccupied molecular orbital
LCD	Liquid crystal display
LED	Light-emitting diode
LE	Locally excited state
LEP	Light-emitting polymer
LPPP	Ladder poly(*para*-phenylene)
MALDI	Matrix-assisted laser desorption/ionisation (mass spectrum / spectrometry)
MEH-PPV	Poly(2-methyloxy-5-(2-ethylhexyloxy)-1,4-phenylenevinylene)
MCH	Methylcyclohexane
Me	Methyl

M_n	Number average molecular weight
MS	Mass spectrometry, mass spectrum
M_w	Weight average molecular weight
MW	Microwave
NIS	*N*-Iodosuccinimide
NCS	*N*-Chlorosuccinimide
NMR	Nuclear magnetic resonance
OCz	N-Octylcarbazole
OFET	Organic field-effect transistor
OLED	Organic light-emitting diode
OLAN	Organolithium-activated nickel
OPV	Organic photovoltaics
PA	Polyacetylene
PCE	Power conversion efficiency
PDAF	Poly(dialkylfluorene)
$Pd_2(dba)_3$	Tris(benzylideneacetone)dipalladium(0)
PDI	Polydispersity index
PE	Petroleum ether (bp = 40–60 ^oC)
PEDOT	Poly(3,4-ethylenedioxythiophene)
PEDOT:PSS	Poly(3,4-ethylenedioxythiophene) polystyrenesulfonate
Ph	Phenyl
PFs	Polyfluorenes
PF6	Poly(9,9-dihexylfluorene)
PF7	Poly(9,9-diheptylfluorene)
PF8	Poly(9,9-dioctylfluorene)
PF9	Poly(9,9-dinonylfluorene)
PF6/8	Poly(9,9-di(4-octyloxyphenyl)fluorene)
PIF	Poly(indenofluorene)
PL	Photoluminescence
PLQY	Photoluminescence quantum yield
PLED	Polymer light emitting diode
PPP	Poly(*para*-phenylene)
R_f	Retention factor (in TLC)
RT	Room temperature
SC	Spin cast

SCE	Standard calomel electrode
SC-H	Spin cast (at high concentration)
SC-L	Spin cast (at low concentration)
SM-OLED	Small molecule organic light-emitting diode
TADF	Thermally activated delayed fluorescence
TBAB	Tetrabutylammonium bromide
T_d	Thermal decomposition
T_g	Glass transition temperature
TGA	Thermogravimetric analysis
THF	Tetrahydrofuran
TLC	Thin layer chromatography
TPA	Triphenylamine
TOF	Time-of-flight
Tol	Toluene
UV	Ultraviolet
UV-Vis	Ultraviolet-visible spectra, ultraviolet-visible spectroscopy
wt %	Weight percent
WPLED	White polymer light-emitting diode
XPS	X-ray photoelectron spectroscopy
λ_{abs}	Maximum of the band in the electron absorption spectrum
λ_{PL}	Maximum of the band in the photoluminescence spectrum
Φ_{PL}	Photoluminescence quantum yield

Abstract

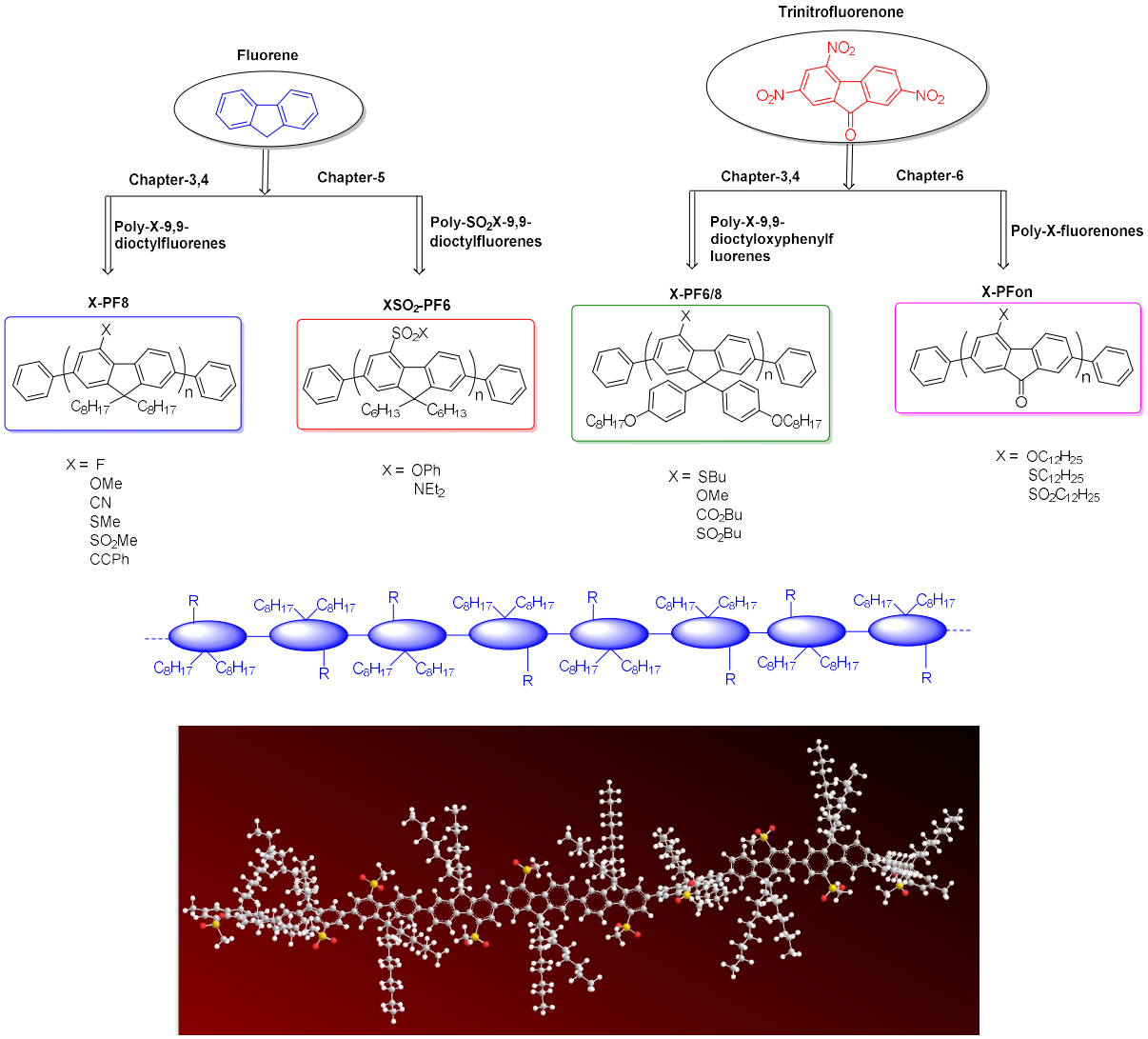

Organic electronics is fastly growing field of science and technology and semiconducting conjugated polymers are playing a significant role for the advancement of optoelectronic device applications. Photoluminescent and electroluminescent conjugated polymers made scientific and technological profound growth a wide range of light-emitting applications. Polyfluorenes is one of the most important class of luminescent materials with bright blue emission, thermal and environment stability and high quantum efficiency and tunable properties though modifications and copolymerisation with a great potential for various applications in electronics and photonics.

The Thesis deals with the design, synthesis and study of novel class of functionalised polyfluorenes, namely with 4-substituted polyfluorenes and polyfluorenones. While most of

previous researches on polyfluorenes were focused on their functionalisation at the C-9 carbon atom to change solubility, morphology and other properties or on copolymerisation of fluorenes with other building block to tune electronic properties of materials, in this work we systematically study novel polyfluorenes (and polyfluorenones) functionalised at position 4 of the benzene ring of the fluorene moiety. Such functionalisation allowed directly effect on electronic energy levels of polymers tuning their characteristics. Two families of polyfluorenes and polyfluorenones have been synthesised and the effects of such substitution with electron-donating and electron-withdrawing groups have been studied by electrochemical and photophysical methods demonstrating a potential of novel materials in further development in this field

The thesis consists of six chapters.

Chapters 1 and 2 give general introduction into the area of conjugated polymers and overview of the field of polyfluorenes, including their synthesis and the most important properties (related to this work), ending with the formulation of the aims and objectives of the Thesis.

Chapter 3 describes our studies toward functionalisation of fluorene in position 4 with various groups to access the monomers for 4-functionalised polymers. Two main approaches for such functionalisation have been developed that allowed to synthesise 4-functionalised fluorene monomers, i.e 2,7-dibromo-4-X-9,9-R,R-fluorenes with a number number of electron-donating and electron-withdrawing groups: X = OCH_3, SCH_3, SC_4H_9, $C{\equiv}C\text{-}C_6H_5$, F, CN, $CO_2C_4H_9$, SO_2CH_3, $SO_2C_4H_9$ (with solubilising groups R = n-octyl or 4-octyloxyphenyl).

Chapter 4 describes synthesis and characterisation of polyfluorenes **X-PF8** and **X-PF6/8** obtained from these monomers by Ni(0)-mediated Yamamoto polymerisation. The obtained polymers showed high molecular weights (M_w = 24,700–185,000 Da, Mn = 9,700–78,700 Da) and excellent thermal stability (T_d ~ 400 ^oC). They absorb at λ_{abs} = 379–411 nm and demonstrate bright emission in a blue region with finely resolved vibronic structure of their photoluminescence spectra (λ_{PL} = 415–435 nm for the first vibronic peaks). The polymers show very high photoluminescence quantum yields in both the solution (Φ_{PL} = 63–93%) and the solid state ((Φ_{PL} = 12–41%). Both series of polymers (**X-PF8** and **X-PF6/8**) showed quasi-reversibe or irreversible p- and n-doping in cyclic voltammetry experiments, from which the energies of their HOMO and LUMO levels and the band gaps have been estimated. It has been shown that EDG and EWG substituents in position 4 of the fluorene moiety can efficiently tune the HOMO and LUMO energy levels of the **X-PF8** and **X-PF6/8** polymers by over 0.5 eV, whereas their band gaps remain almost the same as in the unsubstituted polyfluorene. The experimental data have been supported by DFT calculations.

The formation of β-phase in the **X-PF8** polymers have been studied and it has been demonstrated pronounces effect of groups X on its stability.

Chapter 5 describes an alternative approach to 4-functionalised polyfluorenes by direct chlorosulfonation reaction of the fluorene moiety and further modifications at the sulfone site to access a wider range of possible substituted polyfluorenes. Two novel polymers **XSO_2-PF6** (X = PhO- or Et_2N-) have been synthesised and characterised by electrochemical and optical methods, expanding the range of accessible 4-substituted polyfluorenes.

Chapter 6 deals with 4-substituted polyfluorenones as electron-deficient polymers for electron transporting materials. Basing on the chemistry developed in Chapter 3, here we have elaborated advanced methods for the synthesis of several novel soluble 4-substituted polyfluorenones (**X-PFon**) and have demonstrated that they possess high electron affinity with reversible electrochemical n-doping and an emission in an orange-red region.

Overall, this research has developed a new class of polyfluorenes and polyfluorenones functionalised at position 4 of the fluorene moiety for efficient tuning of the electronic properties of materials. Considering the huge number of fluorene-based homopolymers and copolymers synthesised and studied to date and their wide range of applications (organic light emitting diodes, solar cell field-effect transistors, lasing materials, sensors etc), described approach is expected to have large impact on further progress in the field, developing and application of novel materials based on 4-functionalised fluorenes in organic electronics.

CHAPTER 1

Introduction to Conjugated Polymers

1.1 History and background of conjugated polymers

From the past century, electronics development became one of the foremost technological revolutions, which brought many new innovative solutions and expanded the boundaries in many technological fields such as information processing, telecommunication etc. This has resulted in drastic changes to many aspects of our everyday life including computers, television, domestic appliance, transport, telephones etc. Many others are still developing making the life and communication between people completely different from what we had only a few decades before. Many of these changes are the results of academic research and the commercialisation of new technologies by hi-tech industry and are based on novel technological solutions and novel types of electronic devices, in which electron flow through the active layer of a device is a key point of their operation. Such devices were traditionally made from metals and inorganic semiconductors (e.g. silicon). Due to characteristic properties of such materials, some problems existed including limited variations in their structure (and consequently variations in the properties), processing of materials and fabrication required devices from them. For example, processing of silicon and fabrication of Si-based devices involves enormous complexity.

With this respect, organic semiconductors represent an exciting alternative to inorganic materials for the future of electronics.[1] Hitherto organic π-conjugated polymers with semiconductive properties offer wide opportunities for structural variations to tune their characteristics, for making cheaper and efficient devices, with the advantage of having environmentally friendly technologies for materials production and device fabrications. Moreover, they allow access to new fields of technologies and devices, which cannot be realised on inorganic materials. For the past three decades or so, organic semiconductors and particularly organic conjugated polymers have been utilised as functional materials in a number of device applications such as organic light emitting diodes (OLEDs), organic photovoltaics (OPV) (plastic solar cells), organic field effect transistors (OFETs), memory devices, logic circuits, sensors/biosensors (Figure 1.1).[2,3,4,5] Currently many academic laboratories and hi-tech companies are involved in research, development, technology transfer and commercialisation of products and devices based on semiconductor polymers.

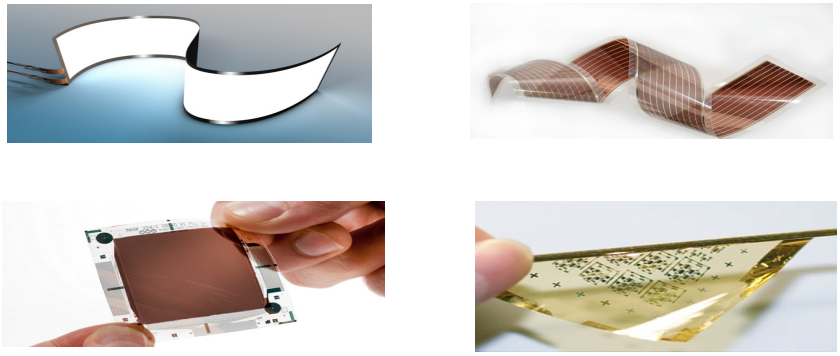

Figure 1.1 Conjugated polymers applications: white light OLED (top left), OPV (top right), organic sensor (bottom left) and organic transistors (bottom right).[2]

For most of the last century, polymers were considered to be insulators and were utilised as elastic, plastic sacks, paints, channels electrical parts and so on. In the year 1960, Pohl and their colleagues blended polysulfurnitride $(SN)_x$ as a semiconducting polymer and laid a starting stride for the exploration in conjugated polymers. Later in 1976, Prof. Alan MacDiarmid was welcomed by Prof. Hideki Shirakawa to his research laboratory and performed integrated polyacetylene (PA) greatly under the high vacuum line to stay away from dampness or oxygen, under the vicinity of argon. Accidently, bromine was doped into integrated polyacetylene, which was tested in Prof. Alan Heeger's research laboratory and an enormous growth of its electrical conductivity (several orders of magnitude) was observed after this doping with bromine vapours. This has resulted in first pioneering publication on high electrical conductivity of organic polymer, polyacetylene (PA) when doped with halogens (bromine, iodine) (Figure 1.2).[6] In 2000, these three eminent scientists, H. Shirakawa, A. J. Heeger and A. MacDiarmid were awarded with the Nobel Prize in Chemistry for their extraordinary discovery and further development of the new field of electrically conductive organic polymers that revolutionised our current life in every aspect.[7,8,9]

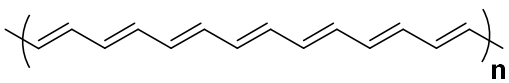

Polyacetylene (PA)

Figure 1.2 Polyacetylene chemical structure.

During the “infant age” of organic electronics (1970s–1980s), the main interest of researchers was focused on metallic type of electrical conductivity in small molecules and polymers (so-called organic metals). It was soon recognised that organic materials with semiconductive properties offer much more opportunities for developments and technological

applications, because all "traditional electronics" is based on semiconductive materials. Since then, many new organic conjugated polymers have been introduced and broadly studied, and some of them have been commercialised in various electronic devices.[10] In general, organic semiconductors are based on π-conjugated organic molecules or macromolecules and mainly composed of carbon and hydrogen atoms, but other elements such as nitrogen, sulfur, selenium, oxygen, phosphor etc can also present in many semiconductive structures. Important benefits of organic materials are their cheap production by general organic synthesis methods, solubility in common solvents and processability. Weak intermolecular interactions allow them to be solubilised, thus the materials can be purified using simple and mild techniques such as recrystallisation, precipitation, Soxhlet extraction or column chromatography. Furthermore, processing from solutions is easier and less energy consuming than the high vacuum, high temperature purification and deposition of inorganic materials (even for vacuum deposited organic materials which are used in small molecule OLED devices, the deposition temperature is substantially lower (~150–200 ^{o}C) compared to inorganic materials). Organic materials can also be easily deposited via printing processes from a solution and after drying from the solvent the active semiconductor layer can be obtained. Another exciting point is the light weight and flexibility of organic semiconductors that makes possible to create flexible devices. These novel properties offer new applications of organic semiconductive materials, which can hardly be realised using inorganic materials flexible displays, textile-integrated light-harvesting devices, biocompatible electronic devices, cheap disposable electronics etc.

1.2 Band theory of a semiconductor

The band theory is the outcome of improvement of the Schrödinger equation and defines the energy of the electrons in the material. In inorganic materials, the electrons are positioned in confined energy levels that form the bands, which can be endorsed towards other vacant energy levels by the applied of external stimuli.[11,12] The highest occupied molecular orbital (HOMO) and the other occupied energy levels which are of lower energy in the region form the valence band (VB) where the electrons sit. The lowest unoccupied molecular orbital (LUMO) and the higher energy levels form an unoccupied band, which is termed a conduction band (CB) because of promoting an electron from VB to this band leads to the electrical conductivity of the material.[13,14] According to the energy structure diagram, three dissimilar kinds of materials can be distinguished such as metals, semiconductors, and insulators (Figure 1.3). For metals, the valence band and the conduction band overlap (or coincide, or, at least, are very close, – less then Bolzman kT), which permits the electrons to

move from VB to CB without an additional source of energy.[15] On the other hand, insulators possess a substantial energy gap between the VB and CB, and the amount of energy required to overcome this forbidden gap is too high and normally would lead to the degradation of the material before such an event occurs. Lastly, in semiconductors, the energetically forbidden gap is small enough to permit the excitation of electrons via thermal or light activation.

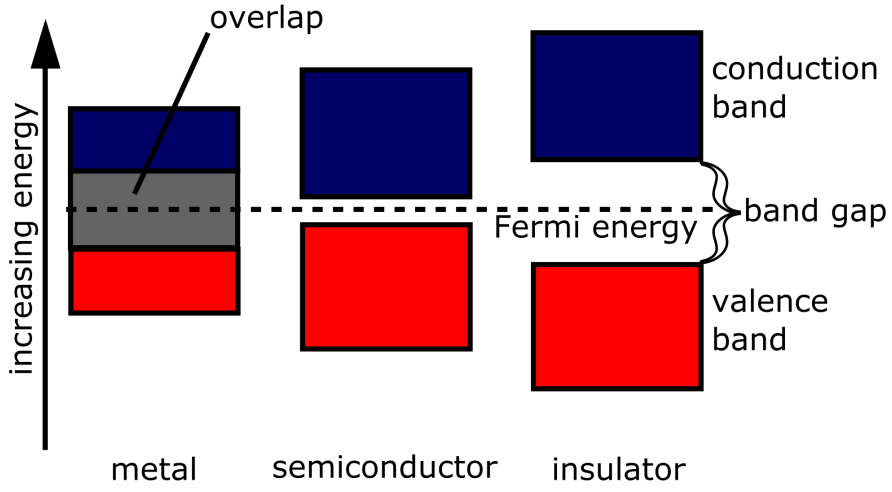

Figure 1.3 Energy band gap of metal, semiconductor and insulator.[11]

1.3 Photoexcitation

The process of exciting atoms or molecules by absorption of the light and evolution of energy in the excited state through radiative or non-radiative processes without any involvement of the chemical changes called as photophysics. When a molecule is photochemically excited to higher energy states S_1, S_2, S_3…S_n (characteristic times 10^{-13} to 10^{-11} s), the excited higher energy state electrons last for a short time and retain to the lower excited singlet energy states by dissipation of energy. Here, the energy states denoted as S_1,S_2,S_3……S_n consist of different energy levels which undergo vibrational relaxation within the state. The photon emission occurs by the transition from lowest singlet S_1 or triplet T_1 states to the ground energy state S_0, according to the Kasha's rule.[16] The deactivation routes of an excited molecule are classified into two main categories, radiative and non-radiative transition processes. Radiative process are fluorescence, phosphorescence and radiative energy transfer. The non-radiative process are internal conversion (IC), intersystem crossing (ISC), Förster resonance energy transfer (FRET). All these physical processes are shown in the Jablonski diagram (Figure 1.4).[17]

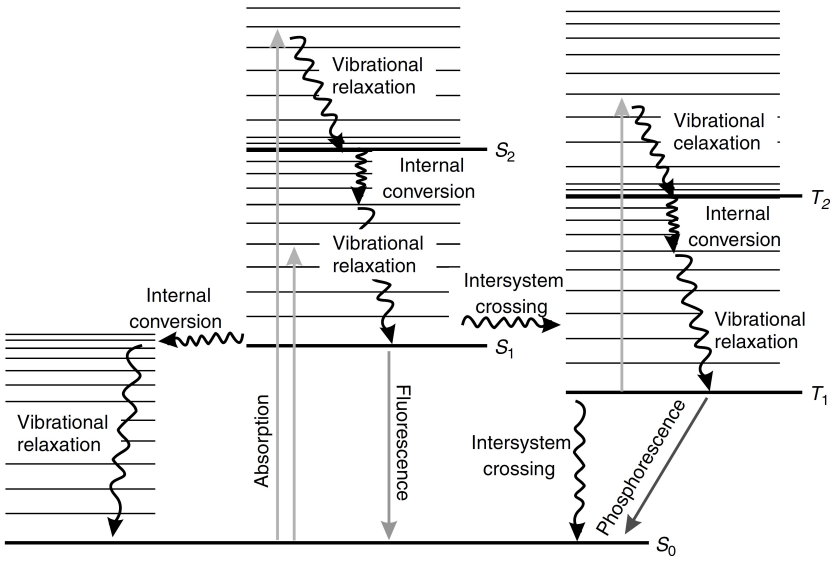

Figure 1.4 Jablonski diagram.[17]

1.3.1 Non-radiative process

Radiationless transition between two electronic states may be represented as the presence of the point of intersection at their potential energy surfaces. The major non-radiative deactivation routes from the excited states of the molecule are vibrational relaxation, internal conversion (IC), intersystem crossing (ISC), and fluorescence resonance energy transfer (Förster resonance energy transfer, FRET).

Vibrational relaxation (VR): In an electronically excited process, the electrons in a molecule are promoted to several higher energy vibrational levels. Afterthat, the molecule quickly dissipates energy to surroundings in the form of non-radiative process (through collisions) to relax to the lowest excited state S_1 (Figure 1.4). This vibrational relaxation process is extremely fast, with a lifetime of $< 10^{-12}$ s, which is substantially shorter than the lifetime of the lowest electronically excited singlet state.

***Internal conversion (IC)*:** It is an intermolecular radiationless passage from the electronic energy states of same spin multiplicity or else in between the different vibrational levels of the same electronic state (Figure 1.4).[18,19] The internal conversion rate constant of $S_1 \rightarrow S_0$ is lower (10^{-9} – 10^{-7} s) compared to the rate constant of the higher energy states like $S_2 \rightarrow S_1$ etc. (10^{-14} – 10^{-11} s). Moreover, it has been observed that internal conversion efficiency decreases with an increase of energy gap between the S_1 and S_0 states.[20,21] Some molecules can also show an internal conversion between the $T_2 \rightarrow T_1$ states.[22]

***Intersystem crossing (ISC)*:** It is the radiationless transition process, where the transition occurs between different spin multiplicity states, e.g. S_1–T_1 (Figure 1.4).[18] Due to the presence of large energy gaps between the excited state S_1 and to ground state S_0, the direct non-radiative transition from S_1 to S_0 is impossible. Considering these circumstance molecules has two alternative ways to reach the ground state energy level S_0 i.e through fluorescence emission or else by crossover to the lowest triplet energy state T_1 (i.e by the non-radiative process). The energy difference of the $T_1 - S_0$ and $S_1 - T_1$ states are generally in the order of 20,000 cm^{-1} and of 3,000–9,000 cm^{-1}, respectively. Thus, the probability of the intersystem crossing ($S_1 \rightarrow T_1$) is considerably greater than the probability of the $T_1 \rightarrow S_1$ transition. The IC rates are in the order of $10^{-8} - 10^{-3}$ s.[23]

***FRET*:** Fluorescence resonance energy transfer (or Förster resonance energy transfer) is defined as the distance interactions between two light sensitive chromophoric molecules in the excited electronic states where the excitation energy is transferred from a donor molecule to an acceptor molecule without emission of a photon. Thus occurs when own emission of the donor molecule overlap with an absorption of the acceptor molecule. In this case, an excitation of a donor chromophore may lead to the energy transfer to an acceptor chromophore through non-radiative dipole–dipole coupling (which can then relax to the ground state by radiative or non-radiative way). FRET process can occur intermolecularly between a donot and an acceptor molecules, as well as intramolecularly when the molecule contains both donor and acceptor parts

1.3.2. Singlet and triplet states

Two different types of electronic orbital configuration are produced by an absorption of the photon. In one of the state, the electron spins are paired, i.e anti-parallel, so the state has no spin magnetic moment. In the other state, the electron spins are unpaired, i.e parallel, and the state has a net spin magnetic moment. The paired spin which remains as a single state in the presence of magnetic field termed as a singlet state. Unpaired spin which interacts with the magnetic field and splits into the three quantised states is termed as a triplet state (Figure 1.5). According to the Hund's rule, the triplet state has lower energy than corresponding singlet state due to the repulsive spin-spin interaction between the electrons of the same spin. The difference in energy varies according to the degree of spatial interaction of involved orbitals. Excited states produced by direct absorption of a photon by S_0 ground state are singlet states, which are designated as S_1, S_2,...., S_n, the higher energies are denoted with a higher subscript

number (1,2,3……n). Spin state is preserved on an excitation. However, because a triplet state T_1 is of lower energy than S_1, ISC $S_1 - T_1$ can occur to produce triplet species. For some compounds, singlet→triplet absorption bands can be identified with sensitive spectrophotometers, these bands can be enhanced by the presence of paramagnetic species heavy atoms, magnetic fields and molecular oxygen.

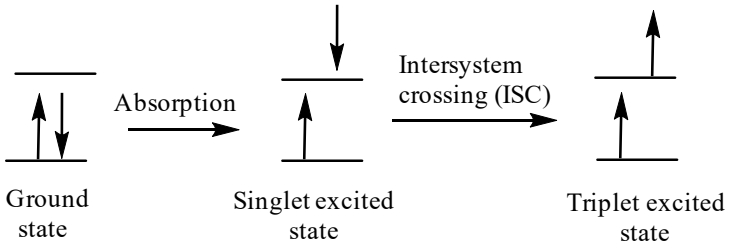

Figure 1.5 Singlet and triplet excited energy states.

1.3.3 Radiative process

The emission of light from a substance is defined as luminescence and occur when more energetic excited state relaxes into the ground state with an emission of a photon. When a molecule absorbs the photon of certain wavelength, the electron transfer takes place from the ground state S_0 to the higher energy states (S_1,S_2….S_n), followed by the loss of the energy and radiative relaxation of the excited state with an expulsion of as a photon. There are various types of luminescence categorised basing on their mode of excitation, e.g. photoluminescence (emission after an absorption of a photon by light irradiation: fluorescence, phosphorescence), electroluminescence (an emission from the excited state produced by an applied voltage to the material), chemiluminescence (an emission due to a chemical reaction), bioluminescence (in living organisms), sonoluminescence (an emission stimulated by ultrasound), etc.

***Fluorescence*:** On photoexcitation, the ground state vibrational level molecules undergo an excitation to one of the higher vibrational levels in the excited electronic state. This excited state is usually the first excited singlet state. Molecules in higher vibrational levels of the excited state quickly relax to the lowest vibrational level by the energy exchange with other molecules through collision or else by vibrational and rotational relaxation. Fluorescence occurs when the molecule returns to the electronic ground state from the excited singlet state with an emission of a photon (Figure 1.6). The transition $S_0 \rightarrow S_1$ is quantum mechanically "allowed" (spin state allowed) and the fluorescence lifetimes are typically of $10^{-8} - 10^{-10}$ s.

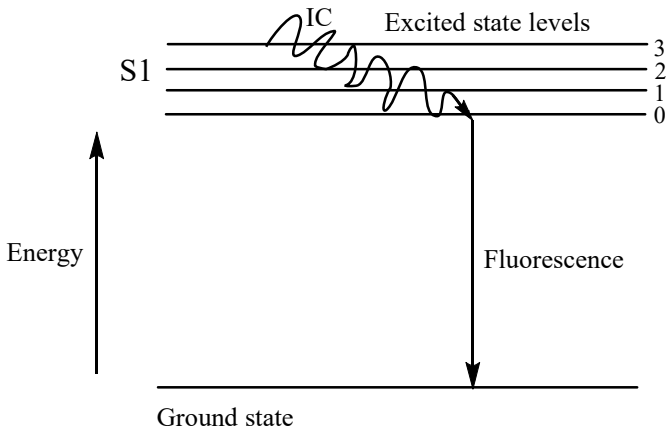

Figure 1.6 Fluorescence emission.

***Phosphorescence*:** Phosphorescence is a slow transition process, which occurs from the excited triplet state T_1 produced by ISC from S_1 state to ground state S_0 (the direct transition from the S_0 ground state to the T_1 excited state is highly implausible). Because it is spin-forbiden process, the lifetime of the T_1 state is longer than of S_1 state (typically, from 10^{-4} to 10 s) and the relaxation $T_1 \rightarrow S_0$ is slower. Also, because the energy level of T_1 state is lower than that of S_1 state, the phosphorescence occurs at longer wavelength. Practically, the phosphorescence shows the characteristic feature as slow emission where the emission continues after the source of excitation is removed (Figure 1.7).

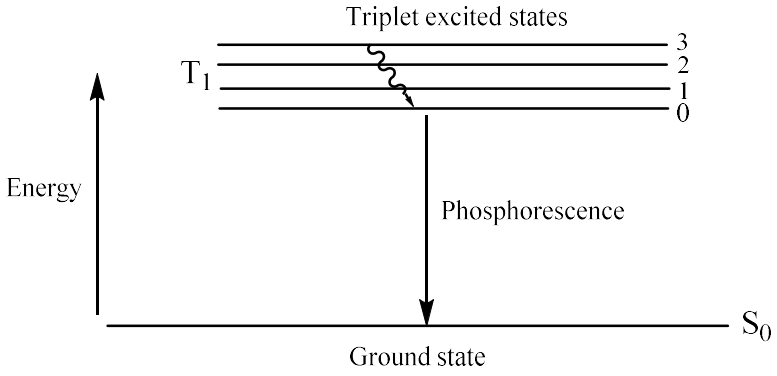

Figure 1.7 Phosphorescence emission.

1.4 Intramolecular charge transfer

Intramolecular charge transfer (ICT) is well studied process in photochemistry and biochemistry.[24,25,26] The ICT is well-documented for organic π-conjugated molecules, which consists of a donor (D) and an acceptor (A) groups or moieties. On photoexcitation of such molecules, charge transfer takes place from the donor to the acceptor group (or parts of the molecule). The process is especially efficient when D and A parts are connected through π-

conjugated bridge. The ICT leads to the substantial difference in the geometry and the electronic structure of the ground and the excited states. In some cases the excited ICT state can be emissive. One of a good example of twisted ICT is the *N,N*-dimethylaminobenzonitrile (DMABN). In the 1960s, Lippert et al.[27] reported the dual photoluminescence from DMABN (i.e. an emission from the locally excited state (LE) of the molecule and from the ICT state). Later, Grabowski et al.[28] explained the mechanism of dual fluorescence by internal twisting in the molecule after an absorption of a photon: an excitation leads to rotation of $N(CH_3)_2$ group which become perpendicular to the acceptor part of the molecule (-Ph-CN). This results to a change of amino nitrogen hybridisation from pyramidal to planar geometry facilitating the ICT process. The excited ICT state in DMABN is emissive and the photoluminescence can simultaneously from the LE and ICT states. Many other emissive donor-acceptor molecules were studied to understand the mechanism of ICT emission (e.g., another widely studied compound: 4-(dicyanomethylene)- 2-methyl-6-(p-dimethylaminostyryl)-4H-pyran (DCM) (Figure 1.8).[29,30]

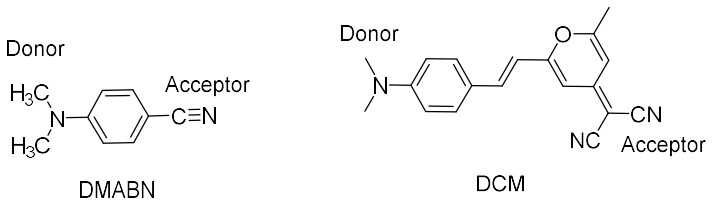

Figure 1.8 Examples of intramolecular charge transfer (ICT) compounds.[29,30]

1.5 Semiconducting properties of organic π-conjugated polymers

In order to attain a semiconducting behaviour in conjugated polymers, the π-conjugated electrons should be able to move easily without destroying its chemical structure. The organic π-electrons are the best candidates since they require less energy to remove them from their bonding state. Because the σ-bond holds two atoms in a molecule and keeps its atoms connected together, only molecules with π-bonds afford semiconducting properties.[31,32] The ethylene molecule has 7.6 eV of the energy gap between its HOMO and LUMO levels, which is too large to obtain a semiconducting behaviour. To decrease this energy gap, a molecule has to contain more delocalised π-bonds, so called conjugation effect. The conjugation effect occurs in a molecule when two or more π-bonds are adjacent and appropriately arranged in space. In that case, the π-electrons are not located around the source atoms but are partially delocalised into the whole π-system.

1.6 Classes of conjugated polymers

Historically, conjugated polymers are mainly classified into three types: the first generation of conjugated polymers (e.g. polyacetylene), the second generation conjugated polymers (e.g. poly(alkylthiophenes) and poly(*p*-phenylenevinylenes) (PPV), and the third generation polymers (semiconducting polymers with more complex molecular structures).[33] Some of the main classes of conjugated polymers are shown in Figure 1.9: polyacetylene, polythiophene, polypyrrole, poly(*p*-phenylenevinylene), poly(*p*-phenylene), and polyfluorene.[34] Polyacetylene was the first reported polymer to demonstrate high electrical conductivity with an addition of p- or n-dopants, but it was never commercialised due to its instability in the air, insolubility and poor processability.

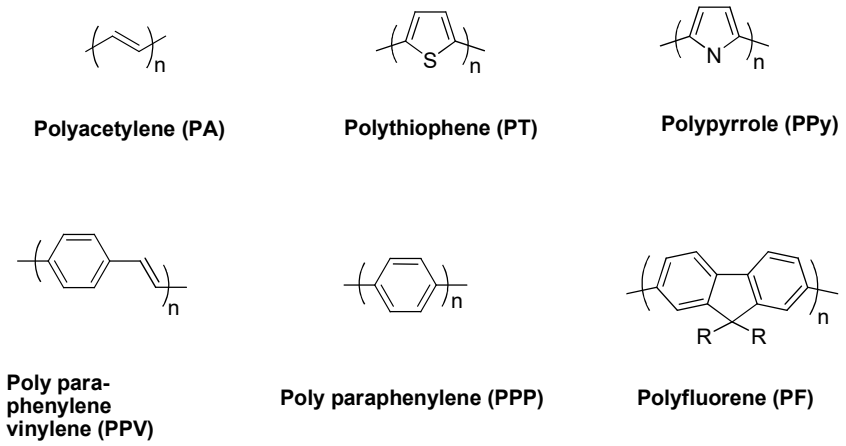

Figure 1.9 Various conjugated polymers.

1.6.1 Conjugated polyphenylenes

Polyphenylenes are one of the most extensively studied class of conjugated polymers from past two decades onwards toward various electronic device applications.[35] The simplest and most important polymer was poly(*p*-phenylene) (PPP) with light emission in the blue region, and some its derivatives have been developed in late 60's and used significantly for other applications.[36,37] However, unsubstituted PPP is insoluble material and its characterisation is limited. Upon introduction of solubilising substituents, PPPs become soluble, however this leads to an increase in the torsional angles between the repeating units, and consequently decreases the conjugation and the electronic properties of materials.[34,38,39] Several approaches have been applied to overcome this problem, such as planarisation of phenylene units via carbon or heteroatoms bridges (Si or N) for increasing the conjugation length. This particularly resulted in the enormous developments of linear polyphenylene derivatives such as ladder-type PPPs (LPPPs) and bridged heteroatoms of stepladder polyphenylenes (Figure 1.10).

Several different methods can be used for synthesis of polyphenylene-type materials, e.g. aromatisation of poly(cyclohexa-1,3-diene) as the precursor polymer, oxidative coupling of monomers and polycondensation or coupling polymerisation methods (Yamamoto polymerisation of aryl dihalides using Ni(0) reagents or Suzuki coupling of dihaloarenes with aryl diboronic acids).[40] The oxidation of benzene by the Kovacic method or nickel coupling of 1,4-dihalobenzenes gives an insoluble powder (Scheme 1.1). The material also shows some defects in its structure due to 1,2-coupling or formation of condensed polyaromatic units.[41]

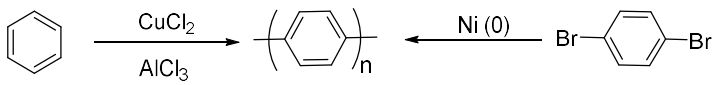

1.1 1.2 1.3

Scheme 1.1 Examples of oxidation and coupling routes to PPP.

PPP films can also be prepared by electropolymerisation under either reductive or oxidative conditions, but the electroluminescent (EL) properties have been found to be highly dependent on the polymerisation conditions.[42] The study of the photoluminescence (PL) efficiency of PPP thin films of various chain length concluded that for highly ordered PPP films, the chain length of 25–30 units was optimal. Oriented films of PPP have been prepared by the fraction deposition method and found to show highly polarised fluorescence.

Linear and ladder-type polyphenylenes.

Poly(*p*-phenylene) (PPP) has a large bandgap of ca. 3.5 eV, good thermal stability and was be used as blue-emitting polymer OLED (PLED)[43] soon after the discovery of electroluminescence in conjugated polymers by Sir Richard Friend and co-workers.[44] Whereas PPP itself is insoluble and unprocessable material and solubilising groups increase the torsional angles and decrease the conjugation length, an introduction of side chains which connect two neighbouring benzene rings together result in so-called laddered poly(*p*-phenylenes) (LPPP), which are soluble and fully planar polymers (Figure 1.10). These structural changes lead to the shift of their absorption and emission toward lower energies.[45,46] Fully planarised backbone alignment leads to strong enhancement of the conjugation length resulting in bathochromic shifts of both optical absorption and emission of LPPP compared to PPP. The PL emission spectra of LPPP polymers are red shifted to 600 nm (compared to blue-emitting PPP) and (apart of an increased conjugation length) this was explained partially by the excimer formation due to higher possibilities for the interaction of neighbouring polymer chains (and partly by keto defects formed on LPPP oxidation).[47,48]

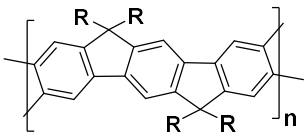

LPPP

Figure 1.10 Ladder-type polyphenylenes.

Poly(p-phenylenevinylenes).

These are the linear conjugated polymers derived from polyphenylenes, in which 1,4-phenylene rings are separated by ethylene bridges (Figure 1.4). They are renowned semiconducting polymers and are widely used in the OLED and other electronic applications. In 1990s years, unsubstituted PPV was prepared through solution-processable precursor route and used as the electroluminescent polymer in OLEDs. Many other chemical methods of PPV synthesis have been developed to the date.[49]

1.6.2 Polythiophenes

Polythiophenes are one of the most studied class of conjugated polymers with a wide range of applications in organic electronics (OLED, OFET, OPV, photoresists, batteries, non-linear optics, sensors, conductive electrodes, supercapacitors etc.)[50,51] This electron-rich class of conjugated polymers can be easily p-doped by chemical or electrochemical methods. In a doped state, polythiophenes undergo bathochromic shifts (from the visible region to NIR-region), Undoped polythiophenes show luminescence in the visible region, while the efficiency of their emission is relatively low, although some substituted polythiophenes are highly emissive and can be used (homo- and copolymers) in OLED applications.[52] Partially doped PT was also used for the light-emitting electrochemical cells (LECs). The band gap of unsubstituted polythiophene is around 2 eV, so it emits in the orange-red region, but the substitution in the positions 3,4 sterically disturbs the polymer backbone increasing torsional angles between the monomer units that results in substantial hypsochromic shifts in their absorption and emission up to the blue region. The photoluminescence quantum yield (PLQY) of poly(3-alkylthiophenes), one of the most prominent and popular thiophenes polymer for organic electronics (particularly, for OPV), is 30-40% in solutions, but in the solid state its PLQY drops down drastically to 1–4%. These drastic changes are due to the presence of heavy sulfur atoms facilitating non-radiative decays of interchain interactions and intersystem crossing in the solid state.

Polythiophenes also possess an interesting feature of thermochromism, which can be observed, for example, in poly(3-alkyl)thiophene films.[53] This thermochromism occurs due to the thermal movements of side chains: the more planar structures of the chains existing at low temperature shift to random coil conformations on the increase of the temperature.[54,55] This process is reversible and the materials can retain initial colour upon cooling.

Several different methods have been used for the preparation of polythiophenes: electropolymerisation, chemical oxidative polymerisation, and metal-catalysed coupling reactions. The films of unsubstituted polythiophene are insoluble and they were synthesised through electropolymerisation. This method, while being unsuitable for bulk synthesis of materials and now well controlled with respect to polymer structure uniformity, is very popular in chemistry research community as it is very easy and simple, and allows to synthesise quickly the polymer to study its basic physical and electronic properties.[56] In second, chemical oxidative polymerisation, $FeCl_3$ method was widely used to produce high molecular weight polymers, but the control of regioregularity (in the case of 3-substituted thiophenes) remains a serious issue for this method.[57,58] Grignard reagent polycondensation-type of polymerisation was reported by Yamamoto to give high yields of polythiophenes.[59]. This third method is based on the nickel catalysed Yamamoto polymerisation reaction.[60] The reaction proceeds with 2,5-dibromothiophene on treatment with the magnesium in THF solvent followed by treatment with $Ni(bipy)Cl_2$ to afford polythiophene. Nearly at the same time, Lin and Dudek, followed the same route for the preparation of intermediate 2-magnesiobromo-5-bromothiophene have developed similar methods by using acetylacetonates of Ni, Pd, Co and Fe as catalysts instead of nickel catalyst (Scheme 1.2).[61]

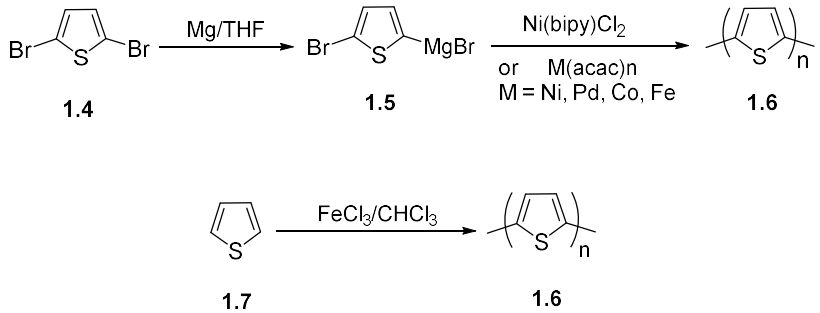

Scheme 1.2 Synthesis of polythiophene via metal coupling (**1.4**–**1.6**) and chemical oxidation.[61]

For 3-substituted thiophene monomers, the molecules have different possibility of couplings between the thiophene units, i.e. head-to-tail (HT), head-to-head (HH), or tail-to-tail (TT) fashion as shown in Figure 1.11. Such variations in coupling types lead to the

random regularity of the structure of the polymer chain, different torsional angles between the thiophene units and strongly affect the solid state morphology of the polymer films and their electronic properties. The best electronic properties are observed when the polymer chain have HT sequence of thiophenes units, but the methods of synthesis of such regioregular structures remained elusive until the pioneering work of Richard McCullough. In his method, McCullough has made the most important step forward toward a regioregular structure, elaborating Ni-catalysed polymerisation of 3-alkyl-2-magnesiobromo-5-bromothiophenes that gave polymers with a high degree (over 95–98%) of HT coupling (Scheme 1.3).[62,63] It should also be mentioned similar work of Rieke, performed independently and in parallel to McCullough work on regioregular polythiophenes through organo-zinc intermediates.[64]

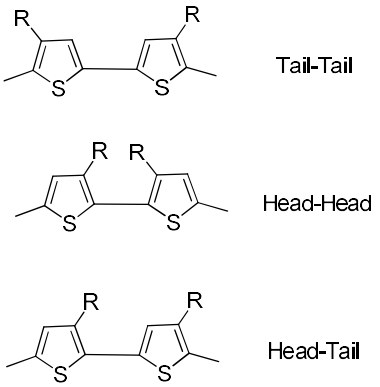

Figure 1.11 Linkage patterns for alkylthiophene rings in the polymer.

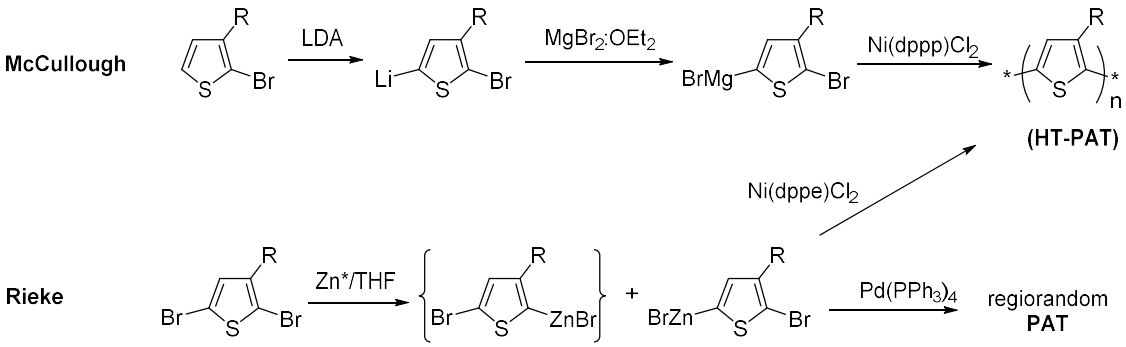

Scheme 1.3. McCullough and Rieke methods of synthesis of regioregular HT-poly(3-alkylthiophenes) (**HT-PAT**), along with formation of regiorandom polythiophene (**PAT**) in the case of Pd-catalysed coupling by Rieke method.[52,63,64]

1.6.3 Polyfluorenes (PFs).

Among many reported classes of conjugated polymers, polyfluorenes (PFs, Figure 1.12) have many advantages such as facile synthesis, chemical and thermal stability, bright blue-light emission in solution and in the solid state, reasonably high hole and electron mobilities in

bulk material etc. Polyfluorenes belong to the class of rigid rod phenylene-type polymers with rigid backbone structure and flexible side chains, which can be varied by functionalisation at the C-9 position. Due to the high CH acidity of C-9 carbon, fluorene can be easily functionalised after deprotonation in basic media by a wide range of electrophiles. As the chemistry of polyfluorenes is the main topic of research in this thesis, more detailed review on this class of conjugated polymers will be given in a separate Chapter 2.

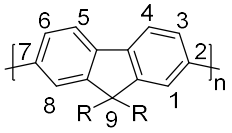

Figure 1.12 Polyfluorene (PF) chemical structure (for the most known polymer of this series poly(9,9-dioctylfluorene (**PF8**), R = C_8H_{17}).

1.6.4 Polycarbazoles (PCz)

Different types of polycarbazoles (and their derivatives) are known as materials useful for organic electronic applications: (i) poly(*N*-vinylcarbazole) with carbazole units in the side chains, which is used for photoconductive materials, (ii) non-conjugated poly(3,6-carbazoles) with a linkage at 3,6-positions, and (ii) conjugated poly(2,7-carbazole) (Figure 1.13). Polycarbazole (PCz) is the simplest nitrogen-bridged polyphenylene, well studied as an organic semiconductor. In addition to this, it forms charge transfer complexes with electron acceptors due to electron rich character of the carbazole moiety.[65] The discovery of poly(*N*-vinylcarbazole) was an important step forward in developing materials for photoreceptors for electrophotography (photocopiers) in the 1970s years.[66] It was also used as a host material in OLEDs and photovoltaic cells due to high singlet energy state and an absence of low triplet energy state.[67]

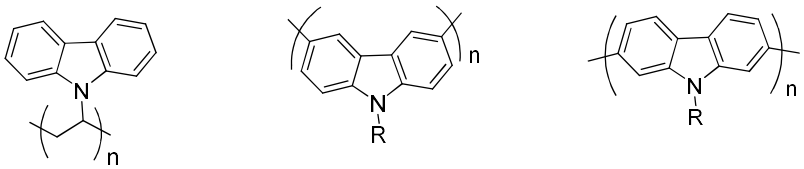

Figure 1.13 Different types of polycarbazoles.

The presence of nitrogen bridge atom between two phenylene moieties in carbazole changes the electronic properties of the system, which becomes different from that in polyfluorenes. While in polyfluorenes, chain growth take place at positions 2 and 7, electrophilic substitution in carbazole occurs at 3 and 6 positions (and then at 1 and 8).

Consequently, conjugated poly(2,7-carbazoles) can not be prepared directly by oxidative or other methods directly from carbazole. Also, its 2,7-dihalogenated derivatives (as monomers for further coupling polymerisation) can not be obtained by halogenation of carbazoles. Therefore, poly(3,6-carbazoles) is the most accessible polymer from carbazole, which can be readily prepared by oxidative polymerisation or by organometallic cross-coupling reactions from 3,6-disubstituted carbazoles.[68] However, this type of polymers, representing certain interest due to the electron-rich character of carbazole moiety is non-conjugated polymer and areas of their applications are limited.

Morin and Leclerc et al. first reported the efficient route for the preparation of poly(2,7-N-alkylcarbazole)s by multi-step synthesis of 2,7-dibromocarbazole monomer **1.11** and its Suzuki polymerisation reaction as depicted in Scheme 1.4.[69]

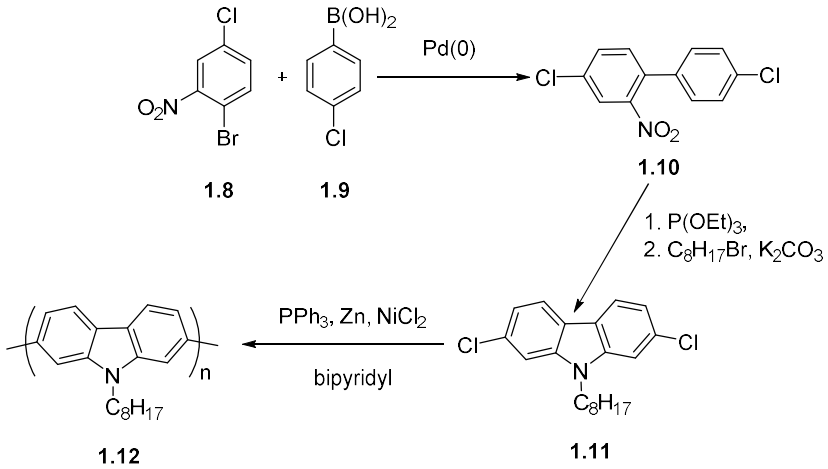

Scheme 1.4 Synthetic route to poly(*N*-octylcarbazole).[69]

Various 2,7-dihalocarbazoles (similar to **1.11**) have then been developed and used in the synthesis of poly(2,7-carbazole) derivatives using Suzuki cross-coupling polymerisation with 2,7-diboronic esters leading to a wide variety of copolymers.[70] These polymers produced a stable blue emission with no appearance of longer wavelength side emission (green emission), as observed in polyfluorene homopolymers, even after thermal annealing and also in OLED operation.[71,72] In recent years, these types of polymers have been used as hole transporting materials and in solar cells.[73]

1.6.5 Polydibenzosiloles (silafluorenes)

After the discovery of the high electricalconductivity of polyacetylene in 1977,[74,75] the field of conjugated polymers grew drastically and properties of conjugated polymers have gained much more attention in recent years particularly toward their electroluminescence and

applications in OLED. From past decade onwards significant efforts were done to develop multicolour OLEDS displays. The development of novel polyfluorene derivatives is growing rapidly for the commercial applications due to their high quantum efficiency of their emission, good solubility and charge carrier mobility. One of the drawbacks of polyfluorene-based OLEDs is their poor spectral stability, which was identified as low energy green emission due to excimers and keto-defects. Excimers can be suppressed by increasing interchain distance with the placement of bulky substituents to the polymers. The keto-defect can be rectified by careful synthesis of monomers and polymers or by replacement of bridgehead C-9 by heteroatoms. Many hetero-analogues of polyfluorenes, having sulfur, silicon, germanium or phosphorus atoms as a bridge between the benzene rings (instead of carbon), have been developed (**1.12-1.16**, Figure 1.14).[76,77,78] Particularly, special attention was paid in recent years to dibenzosiloles (silafluorenes), fluorene analogues in which the C-9 carbon atom in the bridge is replaced by four-valent and electronically similar silicon atom.

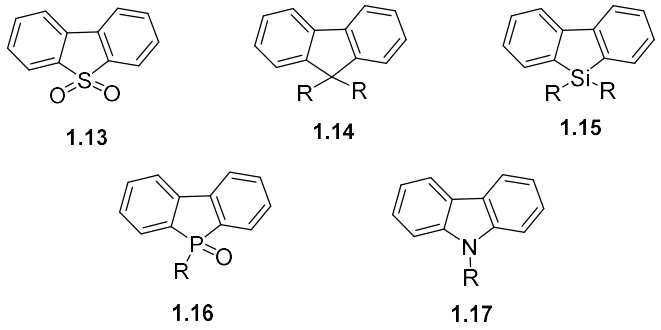

Figure 1.14 Fluorenes and different types of its heteroanalogs (at C-9) (**1.13**–**1.17**) used in synthesis of conjugated polymers.[76–78]

Gilman and Gorsich first reported the example of dibenzosilole in the 1955.[79] After that, dibenzosiloles were studied as incorporating units in the polymer in 1983.[80] Later on, they were used in dye-sensitized solar cells and in photoresists. An important step forward was made by Holmes and coworkers in 2005, who designed multistep synthetic procedure to access poly(2,7-dibenzosiloles) as depicted in Scheme 1.5.[81] A year later, Huang and coworkers prepared several copolymers of dibenzosiloles and studied them as materials for OFETs and OPV solar cells.[82]

The properties of poly(9,9-dihexyldibenzosilole) are quite similar to poly(9,9-dioctylfluorene), **PF8.**[81] This polymer absorbs at λ_{max} = 390 nm and emits at 425, 449, and 482 nm (vibronic peaks). So, its band gap, HOMO, and LUMO energy levels are quite similar to that of polyfluorenes. It has higher glass transition temperature (T_g = 149 ^oC) and higher decomposition temperature (T_d = 442^o C) compared to polyfluorenes. Moreover, it is more

stable toward oxidation/degradation. Thus, an annealing at 250º C for 16 h in an air did not show any signature of degradation (no changes in PL emission spectra) (Figure 1.15).[81,83]

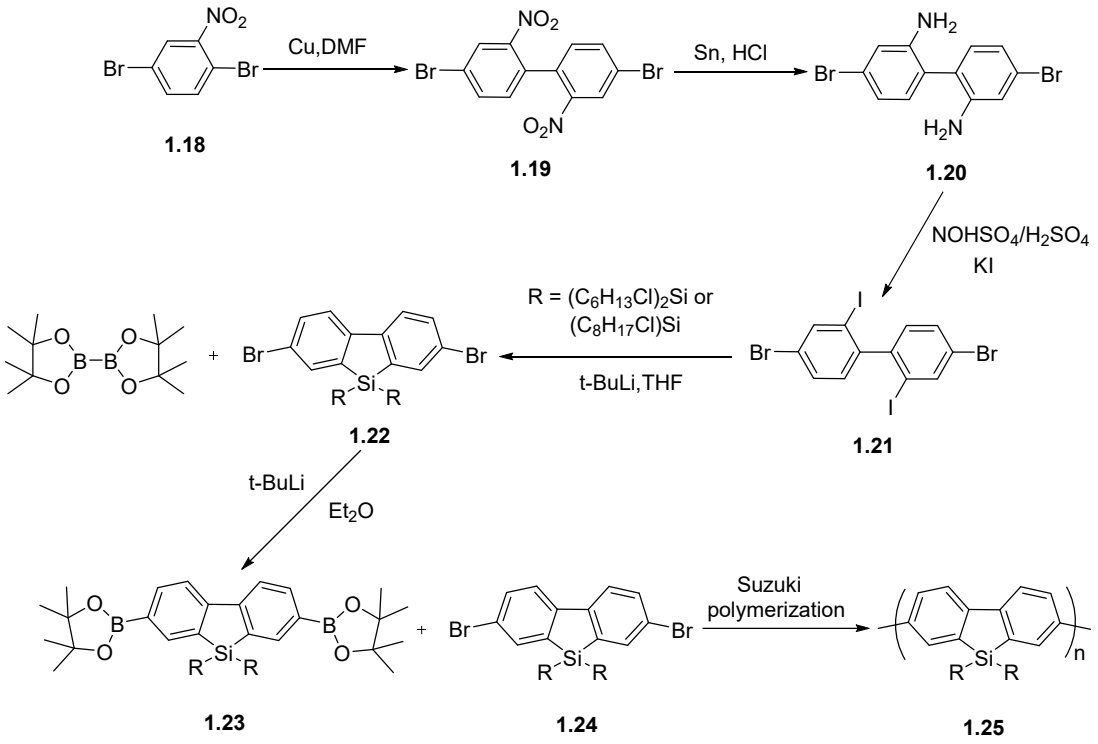

Scheme 1.5 Synthetic route to poly(2,7-dibenzosiloles) **1.25**.[81]

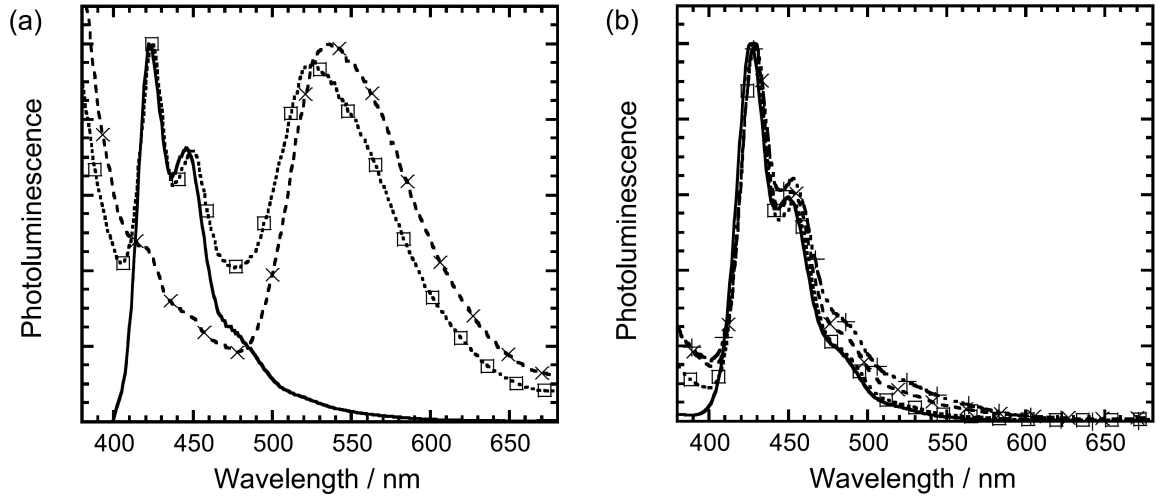

Figure 1.15 Normalised photoluminescence spectra of thin films of polymers before annealing (solid lines) and after annealing for 2 h at 150 °C (squares, dotted lines), 4 h at 200 °C (×, dashed lines), 24 h at 250 °C (+, dot-dashed line):
(a) poly(9,9-dioctylfluorene), **PF8**; (b) poly(dihexyldibenzosilole), **1.25** (R = C_6H_{13}).[83]

1.7 Applications of conjugated polymers

Conjugated polymers have tremendous importance for the modern electronics industry. Their academic research and hi-tech applications are enormous: electroluminescent materials for OLEDs,[84,85,86,87] including white-light emitting polymer OLEDs for solid state lighting,[88,89] OPV (plastic solar cells),[90,91,92,93,94,95] OFET,[96,97,98,99] electrochromic materials,[100,101,102,] photochromic materials,[103] electrically conductive transparent electrodes,[104,105,106] batteries and supercapacitors, sensors/biosensor and many others. From the beginning of this century, explosively expanded commercialisation of novel products based on conjugated polymers and devices with their use had started. Looking back on this enormous growth of research and newer applications in the past two decades, it is even difficult to predict now where this field will be in the next twenty years and which new materials, technologies and applications it is going to offer to us in future.

Organic conjugated polymers have many advantages that make them unique materials: low cost and environmentally friendly production, excellent solubility in common organic solvents and possibility to realise solution-based processes of device fabrications, good processability, light weight, flexibility and possibility of use of flexible substrates for ultra-thin devices etc.

Development and studies of conjugated polymers for OLEDs in academic laboratories have breakthroughs in commercial devices.[107,108].Considerable interests have been shown in the development of organic light-emitting diodes (OLEDs) based on conjugated polymers due to their wide-range applications (Figure 1.16). For full-colour displays, there are needs in materials, which would emit three primary colours (i.e. blue, green and red, RGB), combination of which can produce any colour on the pallet. Many studies are focused on exploring efficient, stable and pure blue light-emitting polymers, which still remain a challenge, whereas green- and red-emitting PLEDs have substantially higher stabilities and lifetimes (due to their lower HOMO-LUMO energy gap and consequently lower degradation on device operation when electrical energy is converted into the energy of the light).

Figure 1.16. Applications of OLEDs.

There is a great potential of applications of light-emitting polymers (LEPs) in optoelectronic devices as such polymer OLEDs have numerous advantages over inorganic LEDs, e.g. cost-efficient fabrication of large area display, low driving voltage, light weight and flexibility of materials for producing curved or flexible displays, transparent OLEDs displays embedded in windows etc. Organic OLED can emit over the entire visible spectrum region with impressive efficiency and brightness and possibilities of development of new materials is huge by current chemistry methods.

1.8 Working principle of OLED

Fluorescence of a material is one possible mechanism of the relaxation of an excited state into the ground state. By the excitation of an electron from the HOMO level to the LUMO level, two new energy states are generated upon relaxation within the original HOMO-LUMO energy gap. Each energetic state is filled with one electron of the opposite spin. This excited state may then relax to the ground state with the emission of a photon (at longer wavelength than an absorbed light). This process is called photoluminescence.

Another process, which is called electroluminescence is similar to photoluminescence, but here the excited state is produced differently, i.e. not by absorption of photon energy, but from electrical energy pumped from electrodes. For this, the material should possess semiconductive properties to be able to transport this energy (actually charges) to the place where an excited state is produced. Let's consider the simplified structure and operational principle of OLED (Figure 1.17). Organic light emitting diode (OLED) is a flat thin device, made by placing organic semiconducting thin film between two conductive electrodes (one of them should be transparent in the visible region,).[109] In practice, more complex configurations of OLED devices are used, which, apart from the emissive layer (EL) also include hole transport layer (HTL) and electron transport layer (ETL) to increase the device performance; normally, transparent indium-tin oxide (ITO) is used as the anode and calcium, magnesium,

barium or aluminium are used as cathodes.[110,111] When an electrical potential is applied to the electrodes, positive and negative charges are injected into a semiconductive material and travel in opposite directions (in the electromagnetic field). When they meet each other, an excited state of the molecule (or fragment of the macromolecule in the case of polymers) is produced, which relaxes with an expulsion of a photon, the energy of which (and accordingly the wavelength of emission) is related to band gap of the material (the difference between the HOMO and LUMO energies).

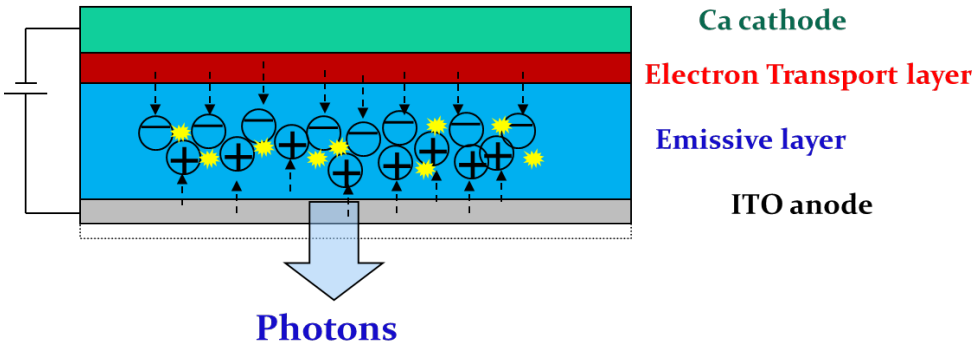

Figure 1.17. OLED structure and working principle.[112]

In the next chapter a more detailed description of one of the most interesting and important classes of conjugated polymers are presented, namely – polyfluorenes, including their syntheses, chemistry, photophysical and morphological behaviour.

References

1 A. Bousquet, H. Awadaa, R. C. Hiorns, C. Dagron-Lartigaua, and L. Billon, *Progr. Polym. Sci*., **2014**, *39*, 1847–1877. (DOI: org/10.1016/j.progpolymsci.2014.03.003).

2 A. Facchetti, *Chem. Mater.*, **2011**, *23*, 733–758. (DOI:10.1021/cm102419z).

3 R. H. Friend, R. W. Gymer, A. B. Holmes, J. H. Burroughes, R. N. Marks, C. Taliani, D. D. C. Bradley, D. A. Dos Santos, J. L. Brédas, M. Logdlund, and W. R. Salaneck, *Nature,* **1999**, *397*, 121–128. (DOI:10.1038/16393).

4 P.-L. T. Boudreault, A. Najari, and M. Leclerc, *Chem. Mater*., **2011**, *23*, 456–469. (DOI:10.1021/cm1021855).

5 N. T. Kalyania and S. J. Dhobleb, *Renewable and Sustainable Energy Reviews*., **2012**, *16*, 2696–2723. (DOI:10.1016/j.rser.2012.02.021).

6 H. Shirakawa, E. J. Louis, A. G. Mac Diarmid, C. K. Chiang, and A. J. Heeger, *J. Chem. Soc. Chem. Commun.*, **1977**, 578–580. (DOI: 10.1039/C39770000578).

7 H. Shirakawa, *Angew. Chem. Int. Ed.,* **2001**, *40*, 2574–2580. (DOI: 10.1002/1521-3773(20010716)40).

8 A. G. M. Diarmid, *Angew. Chem. Int. Ed.,* **2001**, *40*, 2581–2590. (DOI:10.1002/1521-3773(20010716)40). .

9 A. J. Heeger, *Angew. Chem. Int. Ed.,* **2001**, *40*, 2591–2611. (DOI:10.1002/1521-3773(20010716)40:14<2591).

10 A. J. Heeger, N. S. Sariciftci, and E. B. Namdas, *Semiconducting and Metallic Polymers,* (*OUP), Oxford*, **2010**.

11 K. M. Molapo, P. M. Ndangili, R. F. Ajayi, G. Mbambisa, S. M. Mailu, N. Njomo, M. Masikini, P. Baker, and E. I. Iwuoha, *Int. J. Electrochem. Sci.*, **2012**, *7*, 11859–11875. (DOI.org/10.1155/2014/520910).

12 J. Zaumseil and H. Sirringhaus, *Chem. Rev*., **2007**, *107*, 1296–1323. (DOI: 10.1021/cr0501543).

13 K. Walzer, B. Maennig, M. Pfeiffer, and K. Leo, *Chem. Rev*., **2007**, *107*, 1233–1271. (DOI: 10.1021/cr050156n).

14 J. G. C. Veinot and T. J. Marks, *Acc. Chem. Res*., **2005**, *38*, 632–643. (DOI: 10.1021/ar030210r).

15 S. Günes, H. Neugebauer, and N. S. Sariciftci, *Chem. Rev*., **2007**, *107*, 1324–1338. (DOI: 10.1021/cr050149z).

16 M. Kasha, Discuss. Faraday Soc., **1950**, *9*, 14–19. (DOI: 10.1039/DF9500900014).

17 A. Jablonski, *Nature*, **1933**, *131*, 839–840. (DOI:10.1038/131839b0).

18 K. L. Litvinenko, N. M. Webber, and S. R. Meech *J. Phys. Chem. A*, **2003**, *107*, 2616–2623. (DOI: 10.1021/jp027376e).

19 G. W. Robinson and R. P. Frosch, *J. Chem. Phys*., **1963**, *38*, 1187–1203. (DOI:.org/10.1063/1.1733823).

20 H. Yamaguchi, M. Higashi, and K. Fujimori, *Spec. Chim. Act. A*., **1990**, *46*, 1719–1720. (DOI: 10.1021/jm00165a028).

21 L. S. Föster and Dadby, *J. Phys. Chem*., **1962**, *66*, 838–840. (DOI: 10.1021/j100811a017).

22 K. Hamanoue, T. Nakayama, and M. Ito, *Chem. Soc. Faraday Trans*., **1991**, *87*, 3487–3493. (DOI: 10.1039/FT9918703487).

23 J. F. Rabek, *Experimental Methods in Photochemistry and Photophysics*, John Wiley and Sons, New York, **1982**.

24 Z. R. Grabowski and K. Rotkiewicz, *Chem. Rev*., **2003**, *103*, 3899–4032. (DOI: 10.1021/cr940745l).

25 A. Onkelinx, F. C. De Schryver, L. Viance, M. Van der Auweraer, K. Iwai, M. Yamamoto, M. Ichikawa, H. Masuhara, M. Maus, and W. Retting, *J. Am. Chem. Soc*., **1996**, *118* 2892–2902. (DOI: 10.1021/ja953697a).

26 M. El-Kemary, M. Elkhouly, M. Fujitsuka, and O. Ito, *J. Phys. Chem. A*, **2000**, *104*, 1196–2000. (DOI: 10.1021/jp9928457).

27 E. Lippert, W. Lìder, F. Moll, W. Nogele, H. Boos, H. Prigge, and I. Seibold-Blankenstein, *Angew. Chem*. **1961**, *73*, 695–706. (DOI: 10.1002/ange.19610732103).

28 Z. R. Grabowski and J. Dobkowski, *Pure Appl. Chem*. **1983**, *55*, 245–252. (DOI.org/10.1351/pac198855020245)

29 C. Zhong, *Phys. Chem. Chem. Phys*., **2015**, *17*, 9248–925. (DOI: 10.1039/c4cp02381a).

30 J. Donovalová, M. Cigáň, H. Stankovičová, J. Gašpar, M. Danko, A. Gáplovský, and P. Hrdlovič, *Molecules*, **2012**, *17*, 3259–3276. (DOI:10.3390/molecules17033259).

31 R. H. Friend, D. C. Bott, D. D. C. Bradley, C. K. Chai, W. J. Feast, P. J. S. Foot, J. R. M. Giles, M. E. Horton, C. M. Pereira, and P. D. Townsend, *Phil. Trans. Royal Soc. London*, **1985**, *A314*, 37–49. (DOI:10.1029/2002GL015463).

32 R. H. Friend, G. J. Denton, J. J. M. Halls, N. T. Harrison, A. B. Holmes, A. Köhler, A. Luxb, S. C. Moratti, K. Pichler, N. Tessler, and K. Towns, *Synth. Metals*, **1997**, *84*, 463–470. (DOI:10.1016/S0379-6779(97)80830-2).

33 A. J. Heeger, *Chem. Soc. Rev.,* **2010**, *39*, 2354–2371. (DOI: 10.1039/B914956M).

34 X. Guo, M. Baumgarten, and K. Müllen, *Progr. Polym. Sci.*, **2013**, *38*, 1832–1908. (DOI:10.1016/j.progpolymsci.2013.09.005).

35 A. C. Grimsdale and K. Müllen, *Macromol Rapid Commun.,* **2007**, *28*, 1676–1702. (DOI: 10.1002/marc.200700247).

36 S. B. Mainthia, P. L. Kronick, and M. M. Labes, *J. Chem. Phys*., **1964**, *41*, 2206. (DOI.org/10.1063/1.1726237).

37 M. Akiyama, Y. Iwakura, S. Shiraishi, and Y. J. Imai, *J. Polym. Sci. B: Polym. Lett.*, **1966**, *4*, 305–308. (DOI: 10.1002/pol.1966.110040501).

38 T. Vahlenkamp and G. Wegner, *Macromol Chem Phys*., **1994**, *195*, 1933–1952. (DOI: 10.1002/macp.1994.021950605).

39 Y. Yang, Q. Pei, and A. J. Heeger, *J Appl Phys.*, **1996**, *79*, 934–936. (DOI: org/10.1063/1.360875).

40 A. D. Schlüter, *J. Polym. Sci. A: Polym. Chem*., **2001**, *39,* 1533–1556. (DOI: 10.1002/pola.1130).

41 P. Kovacic and M. B. Jones, *Chem. Rev*., **1987**, *87*, 357–379. (DOI: 10.1021/cr00078a005).

42 P. Argyrakis, M.V. Kobryanskii, M.I. Sluch, and A.G. Vitukhnovsky, *Synth. Metals,***1997**, *91*, 159–160. (DOI:10.1016/S0379-6779(98)80079-9).

43 G. Grem, G. Leditzky, B. Ullrich, and G. Leising, *Adv. Mater*., **1992**, *4*, 36–37. (DOI: 10.1002/adma.19920040107).

44 J. H. Burroughes, D. D. C. Bradley, A. R. Brown, R. N. Marks, K. Mackay, R. H. Friend, P. L. Burn, and A. B. Holmes, *Nature*, **1990**, *347*, 539–541. (DOI:10.1038/347539a0).

45 U. Scherf and K. Müllen, *Makromol. Chem. Rapid Commun*., **1991**, *12*, 489–497. (DOI: 10.1002/marc.1991.030120806).

46 U. Scherf and K. Müllen, *Macromolecules*, **1992**, *25*, 3546–3548. (DOI: 10.1021/ma00039a037).

47 G. Grem, C. Paar, J. Stampfl, G. Leising, J. Huber, and U. Scherf, *Chem. Mater*., **1995**, *7*, 2–4. (DOI: 10.1021/cm00049a001).

48 L. Romaner, G. Heimel, H. Wiesenhofer, P.S. D. Freitas, U. Scherf, J. L. Brédas, E. Zojer, and E. J. W. List, *Chem. Mater.*, **2004**, *16*, 4667–4674. (DOI: 10.1021/cm0496164).

49 A. J. Blayney, I. F. Perepichka, F. Wudl, and D. F. Perepichka, *Isr. J. Chem*., **2014**, *54*, 674–688. (DOI: 10.1002/ijch.201400067).

50 J. Roncali, *Chem. Rev*., **1992**, *92*, 711–738. (DOI: 10.1021/cr00012a009).

51 I. F. Perepichka and D. F. Perepichka (Eds), *Handbook of Thiophene-Based Materials: Applications in Organic Electronics and Photonics* (*Vol. 1: Synthesis and Theory, Vol. 2: Properties and Applications)*, Wiley, **2009**, 910 pp.

52 I. F. Perepichka, D. F. Perepichka, H. Meng, and F. Wudl, *Adv. Mater.*, **2005**, *17*, 2281–2305. (DOI: 10.1002/adma.200500461).

53 C. Roux, J. Y. Bergeron, and M. Leclerc, *Makromol. Chem*., **1993**, *194*, 869–877. (DOI: 10.1002/macp.1993.021940311).

54 G. Zerbi, B. Chierichetti, and O. Inganas, *J. Chem. Phys.,***1991**, *94*, 4637–4645. (DOI: dx.doi.org/10.1063/1.460592).

55 G. Zerbi, B. Chierichetti, and O. Inganas, *J. Chem. Phys.,* **1991**, *94*, 4646–4658. (DOI: dx.doi.org/10.1063/1.460593).

56 J. Roncali, *J. Mater. Chem*., **1999**, *9*, 1875–1893. (DOI: 10.1039/A902747E).

57 M. Leclerc, F. M. Diaz, and G. Wegner, *Makromol. Chem*., **1989**, *190*, 3105–3116. (DOI: 10.1002/macp.1989.021901208).

58 M. Pomerantz, J. J. Tseng, H. Zhu, S. J. Sproull, J. R. Reynolds, R. Uitz, H. G. Amott, and M. I. Haider, *Synth. Metals*, **1991**, *41*, 825–830. (DOI:10.1016/0379-6779(91)91505-5).

59 T. Yamamoto, A. Morita, Y. Miyazaki, T. Maruyama, H. Wakayama, Z. H. Zhou, Y. Nakamura, T. Kanbara, S. Sasaki, and K. Kubota, *Macromolecules*, **1992**, *25*, 1214–1223. (DOI: 10.1021/ma00030a003).

60 Y. Yamamoto, K. Sanechika, and A. Yamamoto, *J. Polym. Sci., Polym. Lett. Ed.*, **1980**, *18*, 9–12. (DOI: 10.1002/pol.1980.130180103).

61 J. W. -P. Lin and L. P. Dudek, *J. Polym. Sci.A: Polym. Chem.*, **1980**, *18*, 2869–2873. (DOI: 10.1002/pol.1980.170180910).

62 R. D. McCullough, *Adv. Mater*., **1998**, *10*, 93–116. (DOI: 10.1002/(SICI)1521-4095(199801)10).

63 R. D. McCullough, *Adv. Mater*. **1998**, *10*, 93–116. (DOI: 10.1002/(SICI)1521-4095(199801)10:2<93).

64 R. D. Rieke, S-H. Kim, and X. Wu, *J. Org. Chem*., **1997**, *62*, 6921–6927. (DOI: 10.1021/jo970778b).

65 C. Li, M. Y. Liu, N. G. Pschirer, M. Baumgarten, and K. Müllen, *Chem.Rev*., **2010**, *110*, 6817–6855. (DOI: 10.1021/cr100052z).

66 W. E. Moerner and S. M. Silence, *Chem. Rev*., **2002**, *94*, 127–155. (DOI: 10.1021/cr00025a005).

67 I. Tanaka, M. Suzuki, and S. Tokoto, *Jpn. J. Appl. Phys. Part 1*, **2003**, *42*, 2737–2740. (DOI:10.1143/JJAP.42.2737).

68 J. V. Grazulevicius, P. Strohriegl, J. Pielichowski, and K. Pielichowski, *Progr. Polym. Sci*., **2003**, *28*, 1297–1353. (DOI:10.1016/S0079-6700(03)00036-4).

69 G. Zotti, G. Schiavon, S. Zecchin, J. F. Morin, and M. Leclerc, *Macromolecules*, **2002**, *35*, 2122–2128. (DOI: 10.1021/ma011311c).

70 J. Bouchard, S. Wakim, and M. Leclerc, *J Org Chem*., **2004**, *69*, 5705–5711. (DOI: 10.1021/jo049419o).

71 J. F. Morin and M. Leclerc, *Macromolecules*, **2001**, *34*, 4680–4682. (DOI: 10.1021/ma010152u).

72 J. F. Morin and M. Leclerc, *Macromolecules*., **2002**, *35*, 8413–8417. (DOI: 10.1021/ma020880x).

73 P. L. T. Boudreault, S. Beaupré, and M. Leclerc, *Polym. Chem.,* **2010**, *1*, 127–136. (DOI: 10.1039/B9PY00236G).

74 H. Shirakawa, E. J. Louis, A. G. Mac Diarmid, C. K. Chiang, and A. J. Heeger, *J. Chem. Soc. Chem. Commun.*, **1977**, 578–580. (DOI: 10.1039/C39770000578).

75 C. K. Chiang, C. R. Jr. Fincher, Y. W. Park, A. J. Heeger, H. Shirakawa, E. J. Louis, S. C. Gau, and A. G. MacDiarmid, *Phys. Rev. Lett*., **1977**, *39*, 1098–1101. (DOI: .org/10.1103/PhysRevLett.39.1098).

76 Y-G. Kim, B. C. Thompson, N. Ananthakrishnan, G. Padmanaban, S. Ramakrishnan, and J. R. Reynolds, *J. Mater. Res*., **2005**, *20*, 3188–3198. (DOI: 10.1117/2.1200704.0745).

77 J-F. Morin and M. Leclerc, *Macromolecules*, **2001**, *34*, 4680–4682. (DOI: 10.1021/ma010152u).

78 I. I. Perepichka, I. F. Perepichka, M. R. Bryce, and L.-O. Pålsson, *Chem. Commun.*, **2005**, 3397–3399. (DOI: 10.1039/B417717G).

79 H. Gilman and R. D. Gorsich, *J. Am. Chem. Soc.,* **1955**, *77*, 6380–6381. (DOI: 10.1021/ja01628a098).

80 I. Gverdtsiteli, D. E. Diberidze, and E. Chernyshev, *Chem. Abs*., **1983**, *101*, 73165. (DOI: 10.1071/CH08497).

81 K. L. Chan, M. J. McKiernan, C. R. Towns, and A. B. Holmes, *J. Am. Chem. Soc*., **2005**, *127*, 7662–7663 (DOI: 10.1021/ja0508065).

82 R.-F. Chen, Q.-L. Fan, S.-J. Liu, R. Zhu, K.-Y. Pu, and W. Huang, *Synth. Metals,* **2006**, *156*, 1161–1167. (DOI:10.1016/j.synthmet.2006.06.014).

83 W. W. H. Wong and A. B. Holmes, in: *Polyfluorenes*, U. Scherf and D. Neher (Eds), Springer, 2008 – *Advances in Polymer Science,* **2008**, *212*, 85–98. (DOI 10.1007/12_2008_148).

84 A. Kraft, A. C. Grimsdale, and A. B. Holmes, *Angew. Chem. Int. Ed.*, **1998**, *37*, 402–408. (DOI: 10.1002/(SICI)1521-3773(19980302)37).

85 U. Mitschke and P. Baüerle, *J. Mater. Chem.,* **2000**, *10,* 1471–1507. (DOI: 10.1039/A908713C).

86 D. F. Perepichka, I. F. Perepichka, H. Meng, and F. Wudl, Chapter 2 in Book: *Organic Light-Emitting Materials and Devices*, Z. R. Li and H. Meng (Eds), CRC Press, Boca Raton, FL, **2006**, pp. 45–293.

87 A .C. Grimsdale, K. L. Chan, R. E. Martin, P. G. Jokisz, and A. B. Holmes, *Chem. Rev.*, **2009**, *109*, 897–1091. (DOI: 10.1021/cr000013v).

88 L.Ying, C.-L Ho, H. Wu, Y. Cao, and W.-Y.Wong, *Adv. Mater*., **2014**, *26*, 2459–2473. (DOI: 10.1002/adma.201304784).

89 K. T. Kamtekar, A. P. Monkman, and M. R. Bryce, *Adv. Mater*. **2010,** *22*, 572–582. (DOI: 10.1002/adma.200902148).

90 J. Yan and B. R. Saunders, *RSC Adv*., **2014**, *4*, 43286–43314. (DOI: 10.1039/c4ra07064j).

91 C. L. Chochos, N. Tagmatarchisc and V. G. Gregoriou, *RSC Adv.,* **2013**, *3*, 7160–7181. (DOI: 10.1039/c3ra22926b)..

92 J. L. Delgado, P-A Bouit, S. Filippone, M. A. Herranza, and N. Martín, *Chem. Commun*., **2010**, *46*, 4853–4865. (DOI: 10.1039/c003088k).

93 O. Inganäa, F. Zhang, and M. R. Andersson, *Acc. Chem. Res.*, **2009**, *42*, 1731–1739. (DOI: 10.1021/ar900073s).

94 C. L. Chocho and S. A. Choulis, *Progr. Polym. Sci.,* **2011**, *36*, 1326–1414. (DOI:10.1016/j.progpolymsci.2011.04.003).

95 E. Bundgaard and F. C. Krebs, *Sol. Energy Mater. Sol. Cells*, **2007**, *91*, 954–985. (DOI:10.1016/j.solmat.2007.01.015).

96 C. Wang, H. Dong, W. Hu, Y. Liu, and Daoben Zhu, *Chem. Rev*., **2012**, *112*, 2208–2267. (DOI: dx.doi.org/10.1021/cr100380z).

97 K-J. Baeg, M. Caironi, and Y.-Y. Noh, *Adv. Mater.,* **2013**, *25*, 4210–4244. (DOI: 10.1002/adma.201205361).

98 C. B. Nielsen and I. McCulloch, *Progr. Polym. Sci.*, **2013**, *38*, 2053– 2069.

(DOI: org/10.1016/j.progpolymsci.2013.05.003).

99 F. Würthner and M. Stolte, *Chem. Commun*., **2011**, *47*, 5109–5115. (DOI: 10.1039/c1cc10321k).

100 P. M. Beaujuge and J. R. Reynolds, *Chem. Rev*., **2010,** *110*, 268–320. (DOI: 10.1021/cr900129a).

101 G. Sonmez, *Chem. Commun.,* 2005, 5251–5259. (DOI: 10.1039/b510230h).

102 G. Sonmez and F. Wudl, *J. Mater. Chem*., **2005**, *15,* 20–22. (DOI: 10.1039/b412513d).

103 T. J. Wigglesworth, A. J. Myles, and N. R. Branda, *Eur. J. Org. Chem*., **2005**, 1233–1238. (DOI: 10.1002/ejoc.200400623).

104 Y. H. Kim, C. Sachse, M. L. Machala, C. May, L. Müller-Meskamp, and K. Leo, *Adv. Funct. Mater*., **2011**, *21*, 1076–1081. (DOI: 10.1002/adfm.201002290).

105 S. Kirchmeyer and K. Reuter, *J. Mater. Chem*., **2005**, *15*, 2077–2088. (DOI: 10.1039/b417803n).

106 L. B. Groenendaal, F. Jonas, D. Freitag, H. Pielartzik, and J. R. Reynolds, *Adv. Mater*., **2000**, *12*, 481–494. (DOI: 10.1002/(SICI)1521-4095(200004)12:7<481).

107 M. Zhu and C. Yang, *Chem. Soc. Rev*., **2013**, *42*, 4963–4976. (DOI: 10.1039/C3CS35440G).

108 A. C. Arias, J. D. MacKenzie, I. McCulloch, J. Rivnay, and A. Salleo, *Chem. Rev.,* **2010**, *110*, 3–24. (DOI: 10.1021/cr900150b).

109 W. Brutting, J. Frischeisen, T. D. Schmidt, B. J. Scholz, and C. Mayr, *Phys. Stat. Solidi A*, **2013**, *210*, 44–65. (DOI 10.1002/pssa.201228320).

110 Q. Wang and D. Ma, *Chem. Soc. Rev*., **2010**, *39*, 2387–2398. (DOI: 10.1039/B909057F).

111 C. Adachi, M. A. Baldo, and S. R. Forrest, *Appl. Phys. Lett*., **2000**, *77*, 904–906. (DOI: org/10.1063/1.1306639).

112 A. C. Grimsdale, K. L. Chan, R. E. Martin, P. G. Jokisz, and A. B. Holmes, *Chem. Rev.,* **2009,** *109*, 897–1091. (DOI: 10.1021/cr000013v).

CHAPTER 2

Polyfluorenes

2.1 Introduction

Phenylene-related polymers have significant importance for OLEDs (PLEDs), particularly because they have a high band gap and can be used as potential materials for blue light emitting devices.[1] Among light-emitting organic materials, the stability of blue emitters is substantially lower, compared to the long wavelength emitting materials. Poly(para-phenylene)s (PPPs) are among known blue emitters.[2] On substitution with long alkyl group the solubility of PPP,[3] is enhanced, but steric repulsions of adjacent side chains twist the polymer backbone and decrease the lengths of conjugation chain along the polymer backbone[4]. In order to overcome this problem, the solubilising substituents can be used as bridges connecting two benzene rings together and thus planarising the system. Such types of phenylene bridged polymers include poly(dialkylfluorene)s (PDAF), poly(indenofluorene)s (PIF) and ladder-type poly(phenylene)s (LPPP), as shown in Figure 2.1.[5] In this chapter, we review the synthesis and properties of one class of such bridged polymers, polyfluorenes.

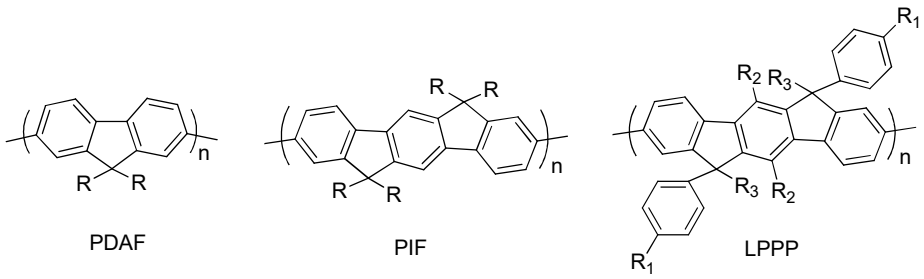

Figure 2.1 Bridged p-phenylene polymers.[5]

Polyfluorenes (PFs) are one of the most significant class of conjugated polymers[6,7,8] where fluorene is the building block unit that consists of two benzene rings linked by a methylene bridge making a planar structure. The methylene bridge not only locks the coplanar arrangement but also can be functionalised with solubilising groups without distorting the torsional angle between the benzene units. In polyfluorenes, electrophilic substitution takes place at positions 2 and 7 that allows the formation of the polymer chain linkage. Polyfluorenes themselves (homopolymers) are blue light emitters, but their copolymers can emit any colour through the entire visible region when fluorene building blocks are combined with more electron-rich or more electron-deficient conjugated building blocks. Polyfluorenes

are characterised by excellent chemical and thermal stabilities (for blue emitters) and have an exceptionally high quantum efficiency of emission, both in photoluminescence (PL) and in electroluminescence (EL) processes, not easily achieved by other classes of polymers.[9,10] Their photoluminescence quantum yields (PLQY), are typically of the order of 70–95% in solutions and 30–60% in the solid state. In addition to that, PFs show good charge mobility for both types of carriers, holes and electrons.[11,12] These features of PFs have made them prominent materials for light-emitting device fabrication.[13]

2.2 Substitution in fluorene and 9,9-dialkylsubstituted polyfluorenes

Substitution at carbon C-9 atom in fluorenes allows making polymers which are soluble (in common, but not in highly polar solvents) and easily processable while the intrachain interactions are not disturbed keeping the electronic structure of the backbone skeleton remain unchanged.[14,15] Such substituted (e.g. alkylated) homopolymers (**2.5**) are light yellow amorphous materials, which can form different morphological phases in the solid state depending on substituents R (R = alkyl, will be discussed in next sections). The developed methods of their synthesis allow to achieve high molecular weight of polymers (up to 400,000 Da in special conditions, while most common values of M_n are in the range of tens thousands to hundred thousands). Currently, polyfluorenes are generally prepared from the corresponding 9-substituted 2,7-dibromofluorene monomers **2.4** (R = Alk, Ar) by various polymerisation methods which will be discussed in the next section. In the case of dialkyl-derivatives, the monomers **2.4** can be prepared either by (i) bromination of fluorene **2.1** at positions 2,7 (to form **2.3**) following alkylation at C-9 atom, or to start first with alkylation with bromination of **2.2** in the next step (Scheme 2.1).

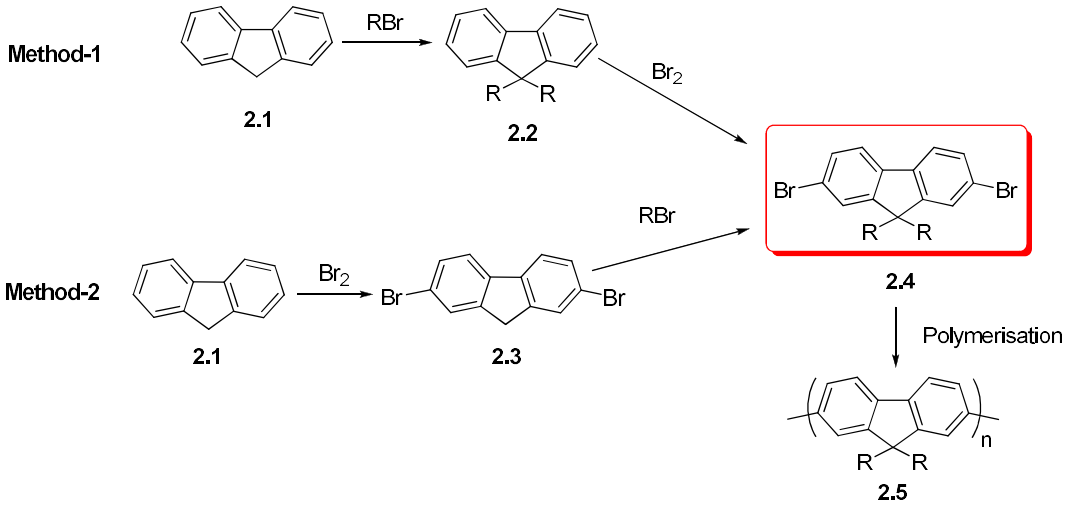

Scheme 2.1 Synthesis of dialkyl fluorene monomers by two common methods and their polymerisation.[14]

2.3 Synthetic methods to poly(9,9-dilakylfluorenes). Historical overview

Many synthetic methods to obtain polyfluorenes have been described in the literature. Being unable to describe all (or even a substantial part) of them we just give some historical overview on how these method were developed and introduced in synthesis of polyfluorenes, from old methods to the most recent and commonly methods used nowadays in chemistry laboratories (methods (1)–(9) below). We particularly focus on the synthesis of two of the most interesting and studied poly(9,9-dialkylfluorenes) with n-octyl and n-hexyl solubilising side groups, known as **PF8** and **PF6.**

(1) The first method reported by Rault-Berthelot in 1985, described the electrochemical anodic oxidation of fluorene to give unsubstituted polyfluorene.[16] Later on, chemical polymerisation of 9-substituted fluorene was studied for the first time by Yoshino's group who synthesised poly(9,9-dihexylfluorene), **PF6,** by oxidative polymerisation of monomer **2.6** by anhydrous iron chloride in chloroform (Scheme 2.2).[17, 18] The obtained polymer had relatively low molecular weight (M_n < 5,000 Da) and also low regioregularity due to a low selectivity of the oxidative coupling polymerisation that proceeds not regiospecifically, i.e. not only at positions 2,7 but also at the other atoms on the benzene rings leading to some degree of branching and non-conjugative linkages.

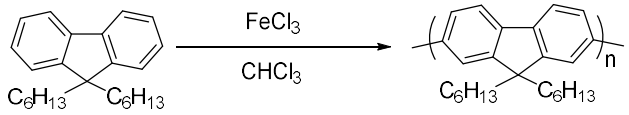

2.6 PF6

Scheme 2.2 Synthesis of polymer **PF6** by oxidative coupling of 9.9-dihexylfluorene (**2.6**).[18]

(2) Following to this, Yamamoto Ni(0) coupling reaction was used to polymerise various 2,9-dihalo-9,9-R^1,R^2-fluorenes. For example, Pei and Yang at UNIAX Corporation first synthesised polyfluorene **2.16** by the reductive polymerisation of 9,9-bis(3,6-dioxaheptyl)-fluorene (**2.15**) in DMF using zinc as a reductant and reactive Ni(0) as a catalyst (from $NiCl_2$ + Zn) (Scheme 2.3).[19] This method gave high molecular weight polymers (M_n ~ 94,000 Da) in spite of using a very polar solvent (DMF) and inorganic reagents insoluble in organic solvents. One reason for the success of this reaction (at least responsible for high M_n) might be the presence of hydrophilic groups in the monomer and polymer.

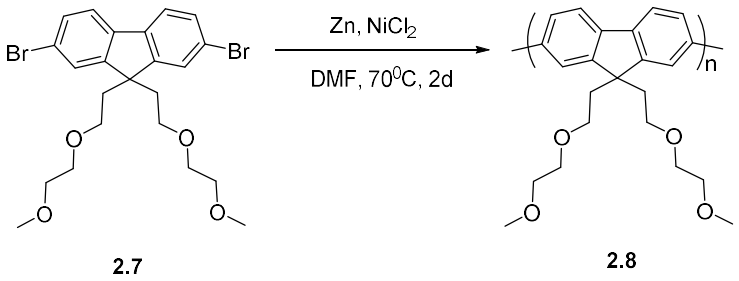

Scheme 2.3 Yamamoto synthesis of poly[9,9-bis(3,6-dioxaheptyl)fluorene] (**2.8**).[19]

(3) Later, Miller and coworkers synthesised polydihexylfluorene (**PF6**) through Yamamoto polycondensation method with monomer 2,7-dibromofluorene (**2.9**) using $Ni(COD)_2$/cyclooctadiene/bipyridyl in a toluene/DMF solvent mixture (Scheme 2.4).[20,21] By using this method of synthesis, polydialkylfluorenes with very high molecular weight (M_n ~250,000 Da) were obtained. This is now one of the common and successfully used method for synthesis of polyfluorenes, although one of its drawback is a high cost of $Ni(COD)_2$ from available suppliers.

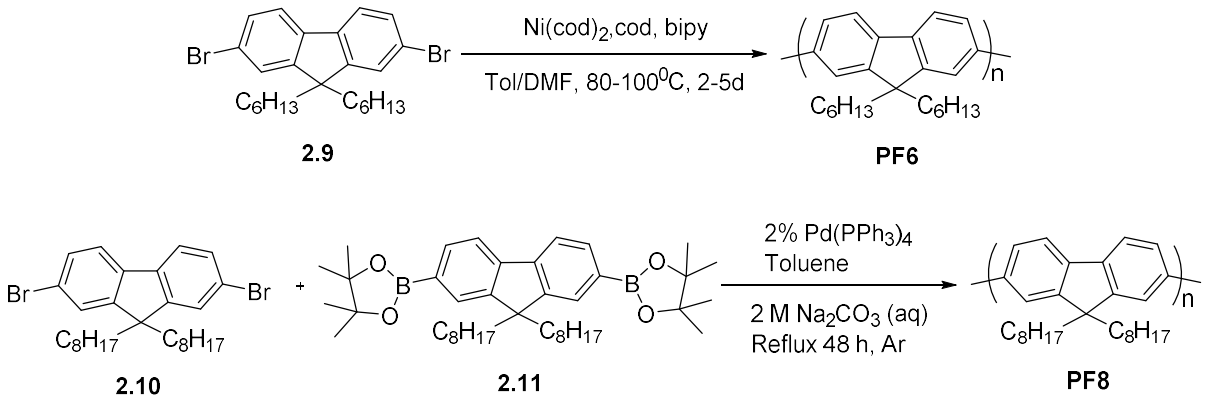

Scheme 2.4 Synthesis of polymers **PF6** by Yamamoto polymerisation of monomer **2.9** and polymer **PF8** by Suzuki coupling polymerisation of dibromide **2.10** with diborolane **2.11**.[21]

(4) Leclerc and co-workers then reported the use of Suzuki coupling polymerisation of dibromofluorene **2.10** and fluorenediborolane **2.11** to synthesise polymer **PF8** (Scheme 2.4).[21] In contrast to the Ni(0) Yamamoto method which requires equimolar amounts of the dihaloarene monomer and Ni(0) reagent, Suzuki coupling requires only catalytic amounts of $Pd(PPh_3)_4$ minimising metal contaminations in the resulting polymer. This is not critical for research laboratories, when the basic physical properties of novel polymers are studied but it becomes a critical issue for the industrial synthesis and implementation of materials in electronic devices, in which case metal impurities decrease the life time of OLED devices. Using a phase transfer catalyst in Suzuki coupling polycondensaton, Leclerc and co-workers

obtained high molecular weight **PF8** (M_n ~50,000).[22,23] Though Yamamoto coupling polymerisation achieved higher molecular weights than Suzuki reaction, in order to obtain such high molecular weights the reaction must be carefully controlled not only by the method of the coupling but also by careful purification of the monomers and by performing the reaction in a truly oxygen-free atmosphere. The solubility of resulting polymers in solvents used for polymerization also plays a critical role in achieving high molecular weights. Soon after that, Cambridge Display Technology (CDT) reported an improved technological procedure for Suzuki polymerisation to obtain the **PF8** polymer shown in Scheme 2.4.[24]

(5) More recently, Carter et al. reported a new method of synthesis of fluorene homopolymers. In this method, they synthesised **PF6** polymer in one step from monomer **2.9,** as one pot reaction on using the organolithium-activated nickel (OLAN) catalyst (Scheme 2.5).[25] This coupling reaction seems to be a very simple, convenient and attractive method compared to other polymerisation methods and may compete with Yamamoto or Suzuki polymerisation, although we have not found in the literature that it became popular in "polyfluorene community" for synthesis of this class of polymers. The advantage of the method is that it is performed at ambient temperature using t-BuLi and catalyst $Ni(dppp)Cl_2$ (which generate their OLAN catalyst) and the reaction is completed in 24 h. A rather high molecular weight **PF6** polymer (M_n = 33,400 Da) was obtained by this method, which is acceptable for research purposes but not high enough (compared to other methods) for technology transfer purposes. Also, the drawback of this method is that it cannot be used for the polymerisation of monomers having functional groups sensitive to the alkyllithium reagent.

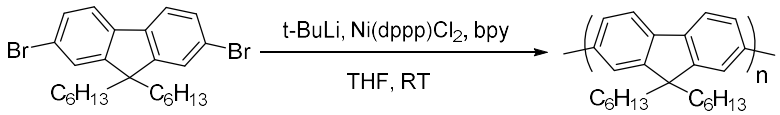

2.9 PF6

Scheme 2.5 Synthesis of polymer **PF6** by Ni-catalysed coupling of monomer **2.9** at room temperature.[25]

(6) Reynolds et al. reported one pot fluoride-mediated Suzuki-Miyaura polycondensation reaction of dibromofluorene **2.10** with diborolane using $Pd_2(dba)_3/HPCy_3BF_4/CsF$ system to synthesise **PF8** (Scheme 2.6).[26] Here fluoride ions effectively coordinate and activate aryl boronic ester (formed in the first step) for trans metalation with palladium catalyst. It is necessary and important to select properly the solvent because high molecular weight

polymers may get precipitated easily in poor solvents system. Phase transfer catalyst like tetrabutylammonium bromide (TBAB) was added to enhance the polymerisation reaction.

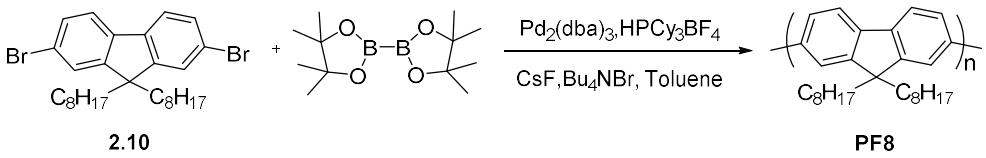

2.10 PF8

Scheme 2.6 One-pot reaction of Suzuki-Miyaura type polycondensation leading to polyfluorene **PF8**.[26]

(7) The McCullough group reported the synthesis of polymer **PF8** using a Grignard metathesis method (GRIM), which however, resulted in a moderate molecular weight polymer and copolymers.[27,28]

(8) Many transition metal polycondensations generally take 3–4 days to complete to achieve high molecular weights of polymers with reasonably low polydispersity index (PDI)., Many electronic properties depend on the structural parameters like end capping groups in the polymer, molecular weights, and the overall composition.[29,30,31] More recently, a new polymerisation protocol for polyfluorenes based on using a Kumada catalyst transfer polycondensation (KCTP) was investigated for controlled synthesis of conjugated polymers in very mild conditions.[32,33] So far, this type of reactions was mainly used for the synthesis of polythiophenes, polypyridines, polypyrroles and polyphenylenes. Geng et al. synthesised polymer **PF8** following the KCTP protocol by using $Ni(acac)_2$/phosphine ligands that gave high molecular weight (M_n = 62,200 Da) and low polydispersity polymer (PDI = 1.2), (Scheme 2.7).[34]

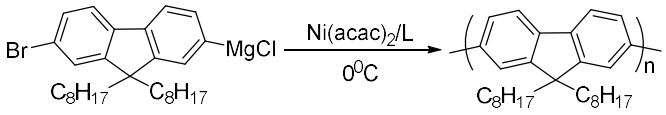

2.12 PF8

Scheme 2.7 Synthesis of polymer **PF8** using Kumada catalyst transfer polycondensation protocol (KCTP).[34]

From all the above methods, two main synthetic approaches are now the mostly used in chemistry laboratories for the synthesis of poly(9,9-dialkylfluorenes): Ni(0)-mediated Yamamoto polymerisation and Pd-catalysed Suzuki coupling polymerisation reactions. The polymers obtained according to Yamamoto are generally of high molecular weight, the

reaction is experimentally very simple (except the necessity of handling the reagents and performing the reaction in oxygen free and dry conditions). One disadvantage of the Yamamoto method is the necessity to use the Ni(0) reagent in stoichiometric amounts (in practice, to achieve very high molecular weight 1.5–2.0 eq. of the very expensive $Ni(COD)_2$ should be used). On the other hand, Suzuki coupling methodology require additional step(s) of preparation of the second coupling reagent (arenediboronic acid or its ester).

(9) Apart from "conventional methods", there is a well-recognised synthetic microwave-assisted method, which was first developed and introduced to organic synthesis in 1986. As we know, this method has more advantages such as reduced time, reduced amounts of by-products, inhibiting thermal decomposition of reagents/products and usage of confined energy. Basing on its recognised advantages in organic synthesis (including polymer synthesis), Zhang et al reported the microwave-assisted synthetic method for preparation of polymer **PF6**, exploiting Suzuki and Yamamoto polymerisation protocols.[35] This method was developed and optimised toward the reaction time, solvents, microwave power and catalysts. For Suzuki polymerisation, it was reported that optimal conditions were: 150 W microwave power/130 °C/14 min. In the case of Yamamoto polymerisation reaction, optimal reaction conditions were as 150 W/250 °C/60 min. Following these conditions, they prepared **PF6** polymer samples with quite high molecular weights (M_w = 37,200 Da, Suzuki and M_w = 43,400 Da, Yamamoto) comparable to that by the conventional methods (Scheme 2.8). However, it is obvious that the easier procedure and substantially shorter reaction time is a great advantage of this method.

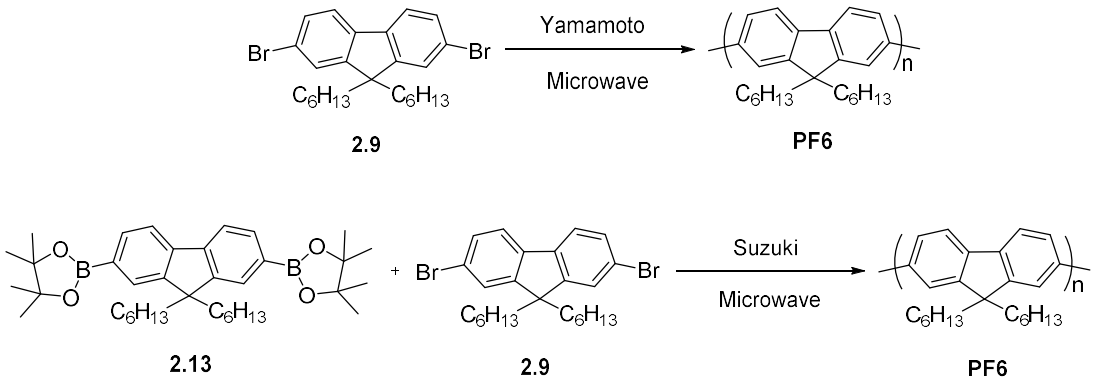

Scheme 2.8 Microwave-assisted Yamamoto and Suzuki polymerisation in synthesis of **PF6** polymer.[35]

2.4 Photophysical and electrochemical properties of polyfluorenes

The UV-Vis electron absorption spectrum of poly(9,9-dioctylfluorene), **PF8**, the most intriguing and the most studied fluorene polymer, in solutions shows the structureless band peaking at 285–390 nm, which is assigned to a π-π* electronic transition. In the solid state (thin films) it undergoes only a small red shift of ~5–10 nm due to intermolecular interactions between the chains (although some papers reported hyspochromic shifts of few nanometers). The optical band gap determined from the onset of the red edge of the absorption band is about 2.9 eV. Its photoluminescence (PL) emission spectrum shows three well-resolved vibronic bands peaked at 418 nm, 442 nm, and 472 nm corresponding to 0-0, 0-1, 0-2 intrachain singlet transitions, respectively (Figure 2.2).[36] This vibronic structure of PL spectrum arises from the rigid rod structure of the polymer and exact position and intensities of different vibronics are widely used to elucidate the intimate structure of polymer chains and morphology of the polyfluorene films in bulk solid state and in solutions. The photoluminescence quantum yields (PLQY) of polydialkylfluorenes are very high in solutions (ca. 80% for **PF8**) and remain high in films (normally, 20–40%).[37,38]

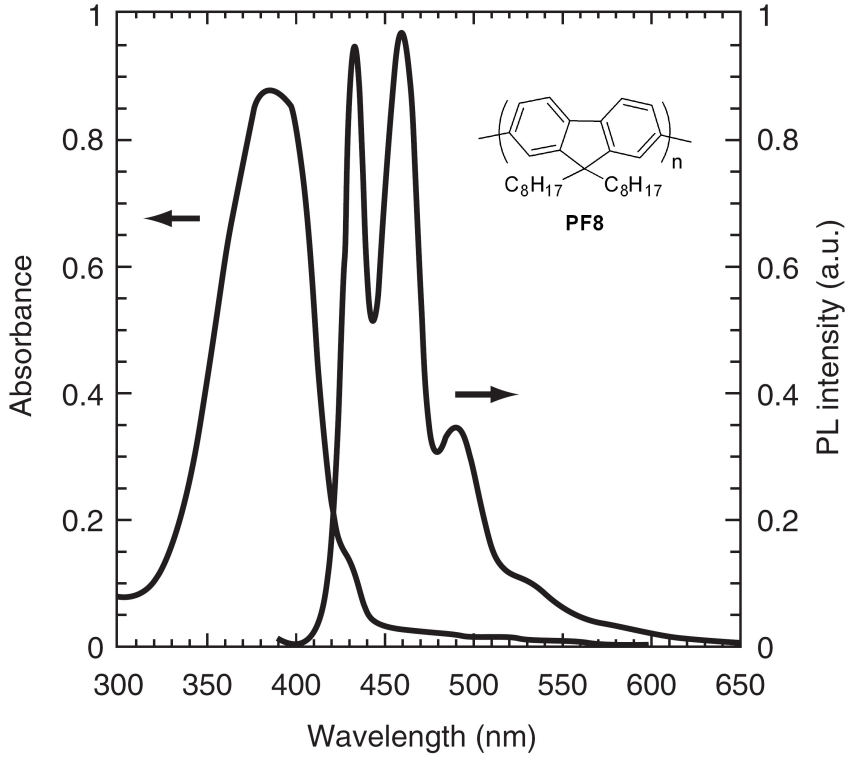

Figure 2.2 Absorption and emission spectra of poly(9,9-dioctylfluorene), **PF8**, in films.[39]

By the using cyclic voltammetry (CV) method, Janietz et al, estimated the ionisation potential (I_p = 5.8 eV) and the electron affinity (E_A = 2.12 eV) of **PF8**, that gave the band gap for this polymer E_g = 3.68 eV (Figure 2.3).[40] This value is very close to that estimated by Cao and coworkers (3.61 eV).[41] Both these values are substantially higher than the optical band gap estimates from UV-Vis spectroscopy (~2.9 eV, from the absorption onset).[42] One should keep in mind that electrochemical and optical methods measure different physical transitions and, frankly speaking, describe different phenomena, so the difference between the optical and electrochemical estimations of energy gaps in organic materials is a rather general observation.

Another method used for estimation of energy levels in **PF8** is an X-ray photoelectron spectroscopy (XPS), and XPS measurements gave energy of its HOMO = –5.6 ± 0.05 eV (I_p = –HOMO) and the band gap E_g = 3.1 ± 0.1 eV, which is comparable to an optical band gap of 2.9 eV.[43] Lee and coworkers[44] reported that the work function of ITO/PEDOT (–5.1 eV) and Ca electrode (–2.9 eV) are reasonably close to the energy levels in **PF8** that justify the use of this polymer as an electroluminescent active layer in polymer OLED in conjunction with these electrodes (it is very important to match the work function of used electrodes to the energy levels of active emissive material to minimize energy losses for charge injections in OLED operation).

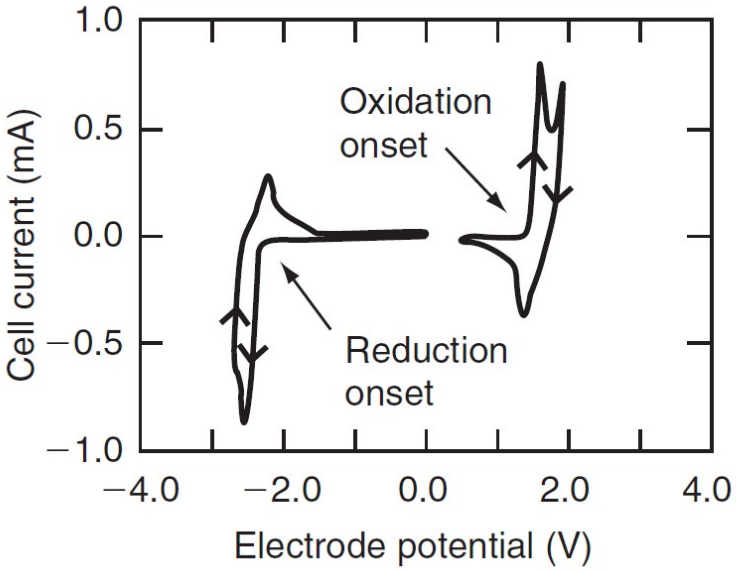

Figure 2.3 Cyclic voltammetry of **PF8** in thin films (potentials vs Ag/AgCl).[40]

2.5 Polyfluorene homopolymers with alkyl linear/branched and similar side chains

Section 2.3 has described various methods of synthesis of polyfluorenes. While this historical overview was exemplified mainly by two of the most popular poly(dialkylfluorenes) **PF8** and **PF6**, most of these methods can be applied (and are applied in practice) for the synthesis of other 9,9-disubstituted fluorene polymers (alkyl, aryl, etc). Apart of polyfluorenes having linear octyl and hexyl chains (and also widely studied polyfluorene with branched 2-ethylhexyl chain, **PF2/6**), many other groups have been introduced at C-9 fluorene position to prepare a wide range of polyfluorenes (e.g. **2.14–2.21**).[11,14,45] These variations in linear/branched alkyls, introduction of other functional groups in a side chain or substituents with stereogenic centres etc. were performed toward studies of basic physical, photophysical, morphological and other properties of polyfluorenes. For example, chiral polyfluorenes with side groups containing stereogenic centres **2.14-2.21** have been used in studies of chiroptical properties and polarised emission in materials (Figure 2.4).[46,47]

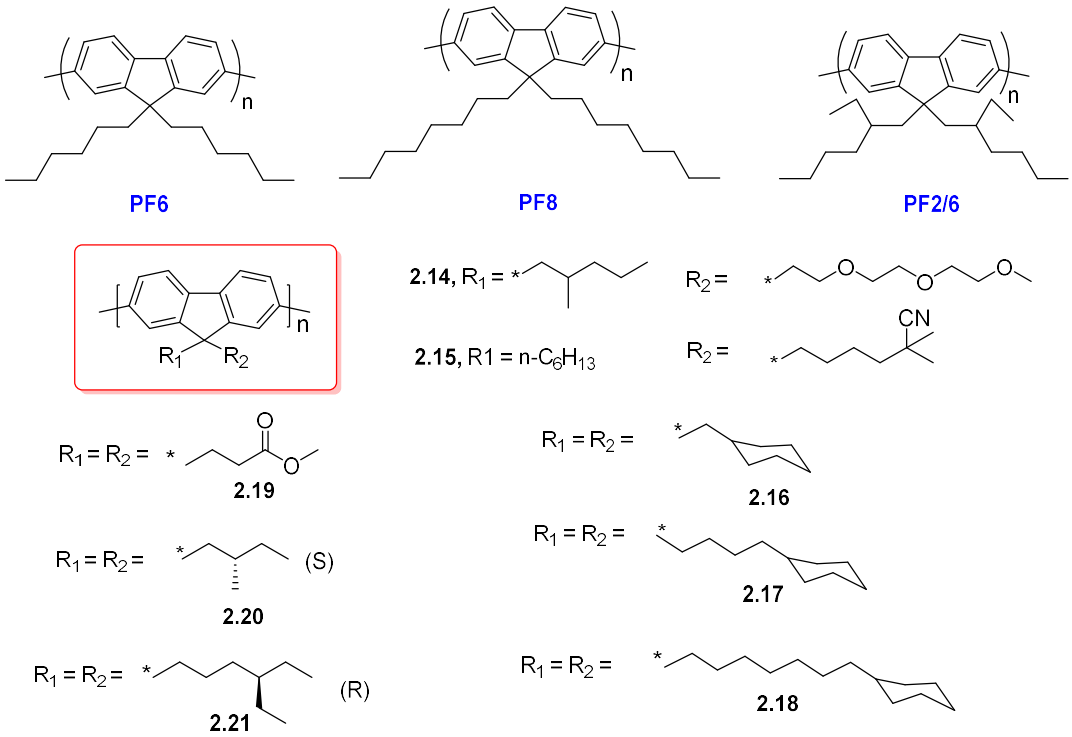

Figure 2.4 Polyfluorenes with different side chain groups (**2.14-21**).[46]

2.6 Blue-emitting dendronised polyfluorenes

Long bulky groups (working as well as solubilising groups) can be introduced as side groups or end-capping groups in conjugated polymers to minimise the interchain interaction. The IBM group synthesised and reported the Fréchet-type dendritic groups as end-cappers (generation from one to four) to **PF6** to obtain polyfluorene **2.22** (Figure 2.5).[48] Polymer **2.22** of ca. 80 fluorene units length prepared from an end capping ratio of 9:1 showed purely blue emission. For the third and fourth generation of dendrimers as the end groups, no degradation of polymers and no appearance of long wavelength emission was observed even after annealing at 200 °C. Using the Yamamoto polycondensation method, they also synthesised Fréchet-type dendrons of generations one to three as side chains (Figure 2.5).[49] High molecular weight random copolymers with 2-ethylhexyl side chains were synthesised, while it was found that an increase of dendron generation decreased an incorporation of the dendrimer fluorene moieties into the polymers **2.23** and **2.24**. In the Yamamoto polycondensation method, the monomers are less reactive, but in the Suzuki polymerisation conditions, they are more reactive giving copolymers **2.23** and **2.24** of the second generation with a high degree of polymerisation. Copolymers showed an intense blue emission, typical for polyfluorenes with high PLQY. No long wavelength emission was observed in PL and EL emission spectra in these copolymers in the case of second and third generation dendrimers as side chains confirming their higher stability compared to polyfluorenes with simpler alkyl chains (**PF6**, **PF8** or **PF2/6**). The work of Müllen and coworkers should also be noted, who reported on polyfluorenes with a first generation of polyphenylene dendron on the side chain.[50] Similarly to previous works, their polyfluorenes with dendritic side chains showed a blue emission and were much less susceptible to oxidation to fluorenone due to bulky groups that reduce interchain interactions and exciton diffusion to defect sites.

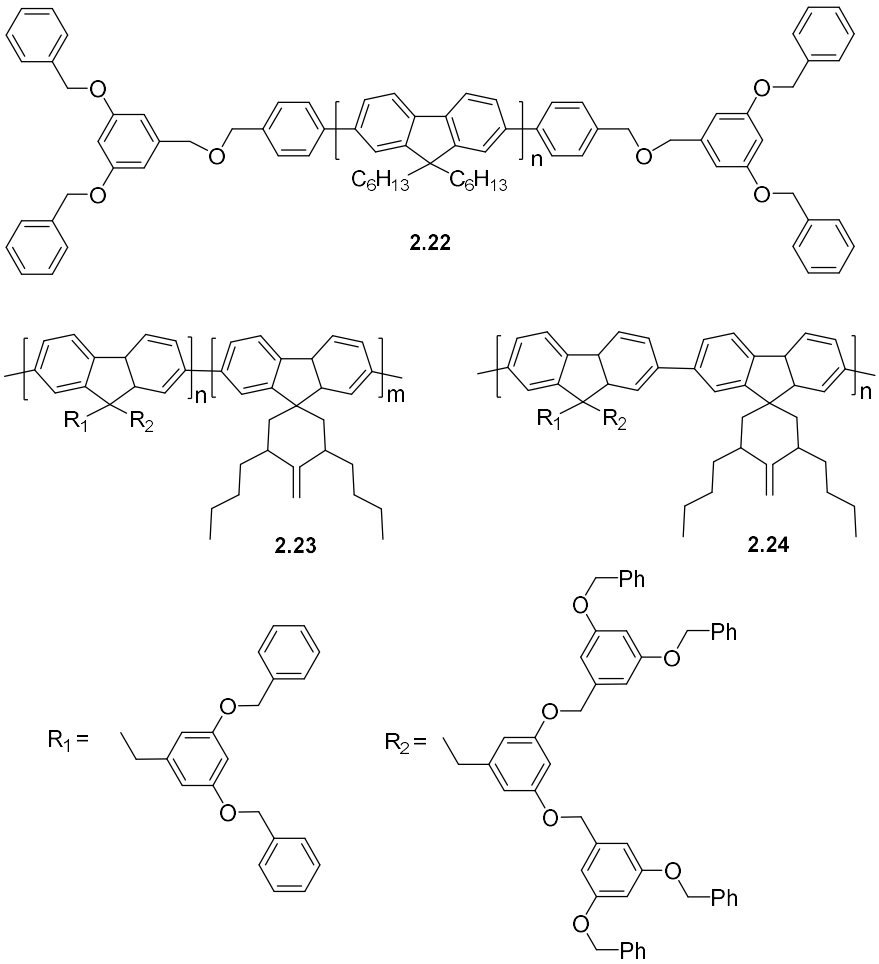

Figure 2.5 Polyfluorenes with Fréchet type dendrons as end-capping groups (**2.22**)[48] and as side chains (**2.23, 2.24**).[49]

2.7 Poly(9,9-diarylfluorenes)

Poly(diarylfluorenes) can be synthesised by several methods. Below we describe two common methods of their synthesis.

The first method starts from 2,7-dibromofluorenone (**2.25**), which can be easily obtained from commercially available fluorene, by its bromination to 2,7-dibromofluorene and following oxidation of CH_2 group into carbonyl C=O. On treatment of 2,7-dibromofluorenone (**2.25**) with KOH/Ph_2O at high temperature, 5-membered ring opening occurs and further treatment with MeOH in acidic conditions gives biphenyl-2-carboxylic acid methyl ester (**2.26**). Further arylation with aryl lithium results in a reaction at the carbonyl site to give compound **2.27**, which is cyclised in acidic conditions to 9,9-diaryfluorene monomer **2.28**. Such monomers can be then polymerised by various methods described in Section 2.3, e.g. by Ni(0) Yamamoto polymerisation to give poly(diarylfluorenes) **2.29** (Scheme 2.9).[50]

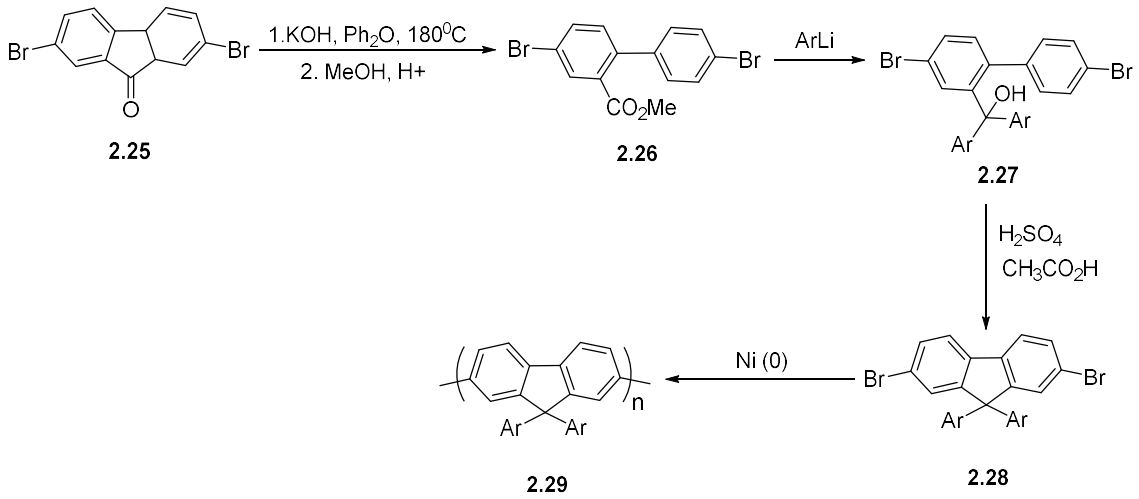

2.25 2.26 2.27 2.28 2.29

Scheme 2.9. Synthetic route to poly(9,9-diarylfluorenes) **2.29**.[50]

The second method starts again from of 2,7-dibromofluorenone (**2.25**) and it is based on nucleophilic substitution of the carbonyl group in acid-catalysed reaction with phenols, their ethers or *N,N*-disubstituted anilines (e.g. triphenylamine), which react in this case at their para-position (so, 4-unsubstituted phenols or anilines should be used). This condensation is often performed in the presence of mercaptoacetic acids, and results in 2,7-dibromo-9,9-diarylfluorene monomers **2.30**.[51] Here again, the monomers can be polymerised by various common methods (e.g. Ni(0)-mediated Yamamoto reaction) giving polymers **2.31** (Scheme 2.10).[52,53]

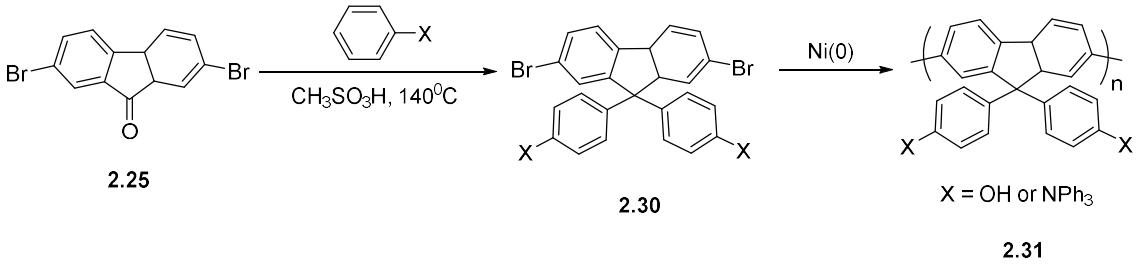

2.25 2.30 2.31

Scheme 2.10 Convenient method for the preparation of poly(9,9-diarylfluorenes) **2.31**.[52]

2.8 Morphology of poly(9,9-dioctylfluorene), PF8

Among the large number of polyfluorenes and fluorene-containing copolymers, and a huge number of publications on fluorene homopolymers (~3500, Web of Science database), poly(9,9-dioctylfluorene), **PF8**, is the most interesting and widely studied polymer due to its unique properties. **PF8** possesses excellent optical and electronic properties and widely used as light-emitting material in device fabrications.[54,55] Its unique properties are that it can exist in different conformational isomers and exhibits polymorphism with a number of different morphological phases, including crystalline phases, non-crystalline and liquid crystalline

phases (amorphous, nematic, glassy, crystalline α phase and meta stable α' phase, and β-phase).[56,66] Some of these phases exist for other poly(9.9-dialkyl fluorenes) as well. Thus, DSC analysis reveals mainly on amorphous nature of **PF6** and crystalline nature for **PF8** and **PF2/6**, with many other ordered morphological phases.[66] However, in **PF8** these different morphologies are more pronounced.

Depending on various thermal and other treatments, these phases can coexist.[57] In all of these phases, the β-phase plays a vital role due to its planar zigzag conformation with extended conjugation length of ~30 units (Figure 2.6),[58] tight molecular packing, and efficient excitation transfer due to large Förster radius. **PF8** with β-phase has stable blue light emission and represents an attractive morphology because of its excellent electric and optical properties, reduced triplet excitons formations and photobleaching, good hole mobility and high PL efficiency.[59,60]

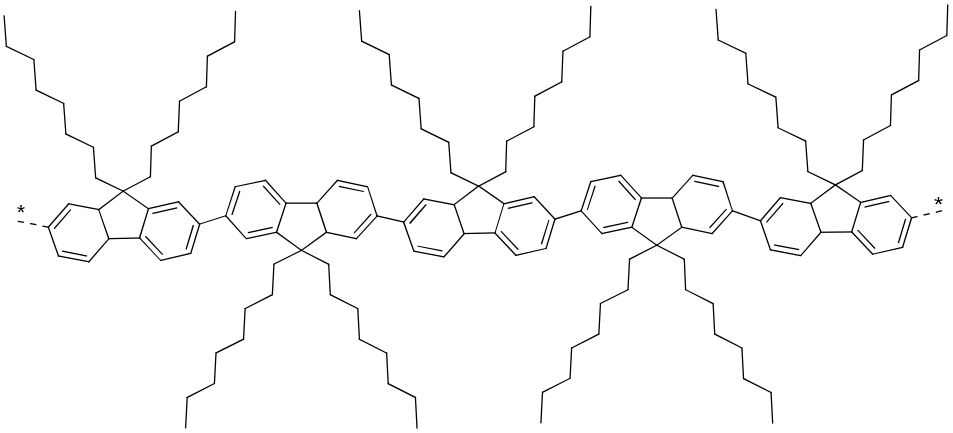

Figure 2.6 Planar zigzag structure of poly(9,9-dioctylfluorene), **PF8**.[58]

Because the β-phase is of special importance for electronic applications of **PF8** and because in this work we performed some investigations on an identification of β-phase in our novel 4-substituted polyfluorenes (Chapter 4), it makes sense to describe it in more details.

2.9 β-Phase in PF8

Grell and Bradley first observed the β-phase in **PF8**. The **PF8** in the net films, dispersed in polystyrene or in a solution of poor solvents exhibited a shoulder peak at 437 nm as the onset of the main absorption band at ~390 nm. It was also shown through many publications that the corresponding changes in PL spectra are also observed with the formation of β-phase.

When **PF8** film was exposed to solvents upon slow warming from very low temperature (–196 °C) to ambient temperature, the β-phase appears as a prominent peak (Figure 2.7).[58] This was explained according to X-ray fibre diffraction as the lower energy

state, which occurs due to extended **PF8** chain length and such a phase leads to a physical stress depending upon the quality of solvent or temperature. It was also concluded that the octyl is the optimum for the side chain length, which stabilises prominently the intra- and intermolecular interactions in solution compared to shorter hexyl or longer dodecyl side chains in the polymers.[61,62,63] The β-phase in **PF8** can be seen in some solutions, in films, in nanostructures and in gels.[64,65,66,67] In a poor solvent system like MCH, the β-phase appears as an additional peak next to the absorption π-π* transition and profoundly increases by slow warming of solution from 77 K to ambient temperature (Figure 2.7). Moreover, this small appearance of the β-phase peak considerably shows larger impact in the PL emission spectrum (not shown) with well-defined sharp and vibronic peaks which are red-shifted compared to the original emission of **PF8**, due to the efficient Förster resonance energy transfer from the excited state of the amorphous polymer onto the β-phase, from which the emission occurs. This was clearly demonstrated with time-resolved energy transfer measurements. [68]

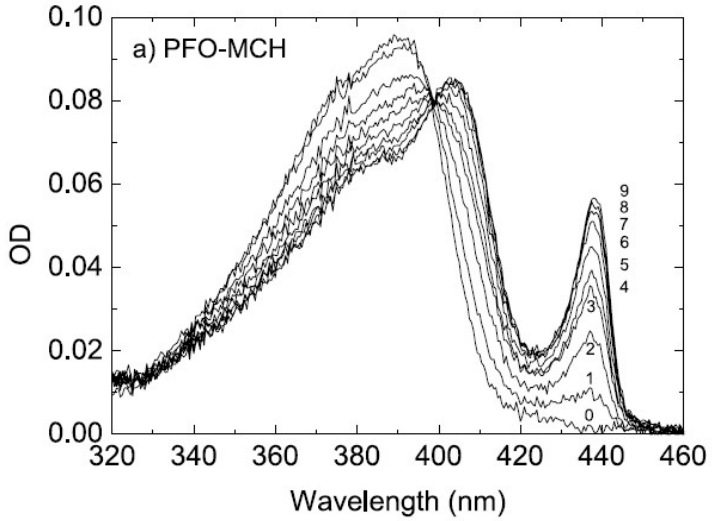

Figure 2.7 Changes in UV-Vis absorption spectra of **PF8** in MCH solution slowly warming from 77 K to room temperature.[58]

The β-phase is metastable, so many factors affect its formation (or not) in the films. Various methods have been used to attain the *β*-phase, for example using high boiling point solvents (toluene, 1,2-dichloroethane),[69,70] films exposing to solvent vapours (toluene, THF, hexane or cyclohexane), films dipping into "solvent/non-solvent" mixture (chloroform/methanol),[71] cyclic thermal annealing the polymer films, and end-capping the **PF8** chain with electron deficient moieties such as triazole, oxadiazole.

2.9.1 Solvent vapours effect on β-phase formation in PF8.

Polymer **PF8** exhibits *β*-phase with poor or high boiling point solvents by spin casting or else by drop cast method with slow solvent evaporation. This treatment leads to internal stresses in the material, which force some of the molecules to adopt a planar pattern orientation. Recently, Zhang et al. reported stable and efficient blue light emission from the *β*-phase of **PF8** polymer end-capped with phenyl groups (M_n = 69,400 Da, PDI = 1.33), in films prepared from the 1,2-dichloroethane (DCE, 5 mg/mL) on a quartz substrate.[72] UV-Vis absorption spectra showed two characteristic bands, one main band peaking at 398 nm and a shoulder at ca. 435 nm, assigned to main π-π* transition of an amorphous phase and to *β*-phase absorption, accordingly. PL emission spectra exhibited three bands peaking at 442, 467 and 496 nm corresponding to 0-0, 0-1 and 0-2 vibrational transition of the *β*-phase (Figure 2.8a).[72]

The absorption spectra of films prepared from toluene exhibit only one main peak at 385 nm, their PL emission spectra are peaked at 428 nm that clearly discloses the amorphous phase of **PF8** in this case.[73,74] Measured absolute PL quantum yields (PLQY, Φ_{PL}^{F}) of films using an integrating sphere gave Φ_{PL}^{F} = 45% for amorphous phase and Φ_{PL}^{F} = 58% for *β*-phase (at ambient temperature).[75] This increase in PLQY is explained by the increase of the effective conjugation length in *β*-phase and the reduction of radiation life time.

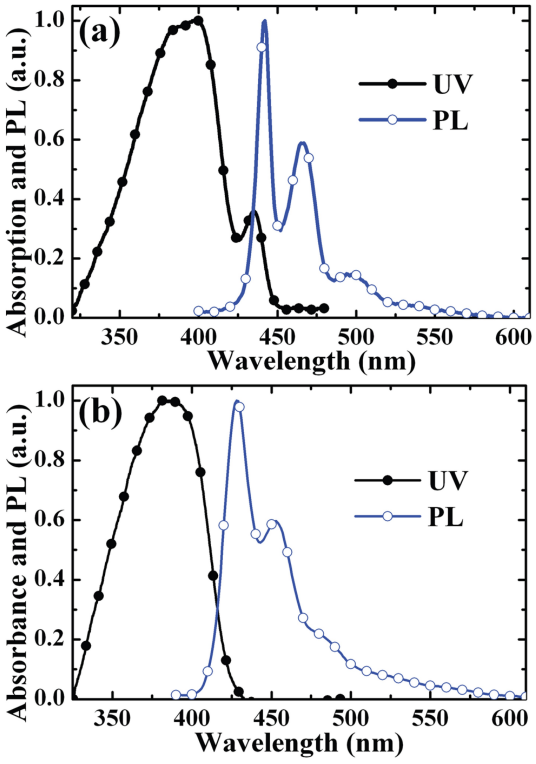

Figure 2.8 UV and PL spectra of **PF8**: (a) β-phase of **PF8** and (b) amorphous phase of **PF8**.[74]

2.9.2 Thermal cycling effect on β-phase formation in PF8

β-Phase is defined as a highly ordered structural planar orientation of polymer chain. On thermal heating, the polymer molecules of **PF8** can self-organise into a more stable planar configuration which extends the conjugation length and leads to the red-shifted peaks in absorption and PL spectra. This low energy phase traps easily the formed excitons through the FRET mechanism which then emits from the β-phase sites as red-shifted well resolved vibronic peaks. Recently, the Monkman group has reported β-phase formation in poly(9.9-didecylfluorene), **PF10**, thin film, which was observed in a thermal cycling process.[76] This procedure resulted in an appearance of a shoulder at 429 nm, and the bathochromic shift in PL spectra (0-0 transition) from 426 nm to 433 nm as a result of β-phase formation on thermal treatments (Figure 2.9).

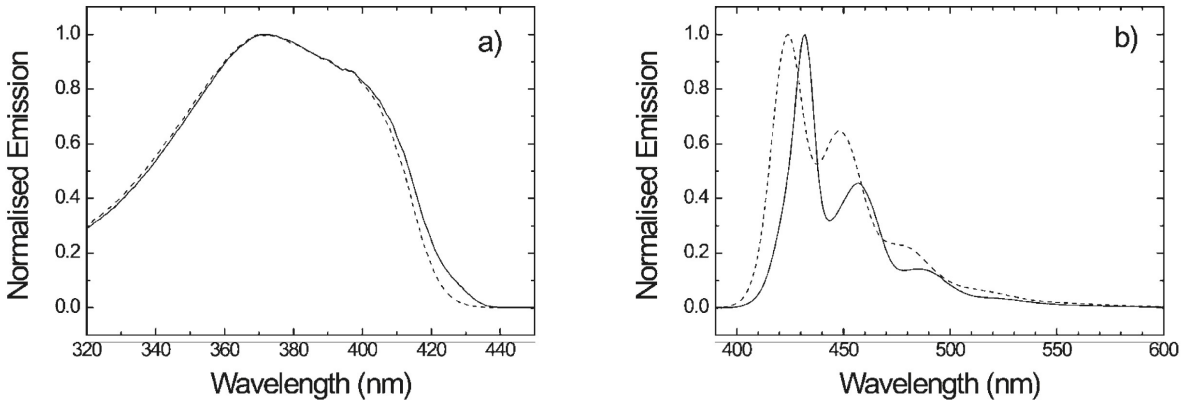

Figure 2.9 UV and PL spectra of poly(9,9-didecylfluorene), **PF10**, in thermal cycle process. Dashed and solid and dashed lines correspond to pristine **PF10** and β-phase in **PF10.** [76]

2.9.3 Alkyl chain length impact on β-phase formation in poly(9,9-dialkylfluorenes)

So far many studies were conducted on the existence of β-phase in **PF8**. Scherf, Monkman and coworkers reported on chain length dependence of the efficiency of β-phase formation for a series of polymers **PF6**, **PF7**, **PF8**, and **PF9** in MCH solution using optical spectroscopy.[77] **PF7** and **PF9** showed similar optical characteristics but blue-shifted by ~7 nm and the stabilities were different over time, whereas **PF8** clear showed stable β-phase formation (Figure 2.10). So, β-phase was more favourable in **PF8** compared to **PF7**, **PF9**, and much more stable than in **PF6.** The β-phase 2D sheet structures of **PF7**, **PF8**, and **PF9** were also observed in studies by X-ray and neutron scattering.[78,79] The side chain interaction between side-by-side polymers caused interchain zipping leading to a rigid planar backbone structure which was seen in X-ray experiments.

Formation of the β-phase mainly depends on two factors: (i) the dimer (from two polymer chains) and aggregate formation efficiency (for longer alkyl chains it becomes very low) and (ii) van der Waals bond energy to avoid steric repulsions and to adopt a polymer backbone in a planar conformation (this is the reason why shorter alkyl chains do not show β-phase).

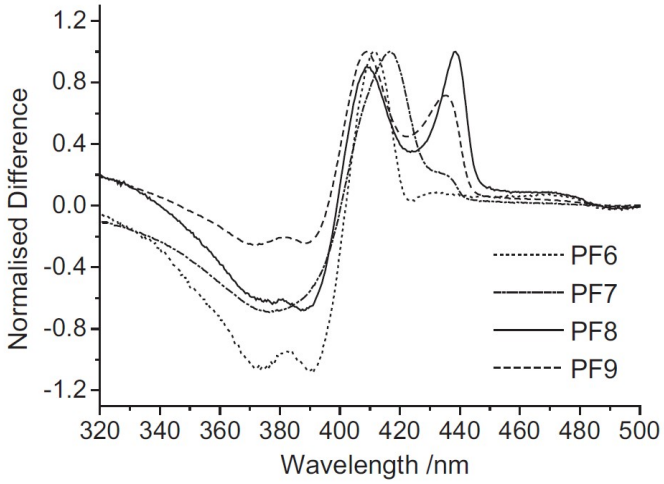

Figure 2.10 Differential absorption spectra of **PF6**, **PF7**, **PF8** and **PF9** in MCH solution.[80]

2.10 Degradation of polyfluorenes and fluorenone defects in poly(9,9-dialkylfluorene) chains

2.10.1 Excimers in polyfluorenes

Conjugated polymers have their own characteristics of excitations and excitation energy transfer, which relate to *intra*- and *inter*-chain packing order. The isolated conjugated polymer chain on photoexcitation of a chromophore produces an *intra*-chain exciton. Nevertheless, the situation is considerably more difficult when there are other chromophores in close proximity to the excited chromophore. The interaction between chromophores can enable the formation of *inter*-chain excitations. In the excited state, a commonly observed *inter*-chain excitation in which the two adjacent chromophores share their π-electrons (that does not occur in the ground state) is termed an excimer.[81,82] Excimers typically have a specific spectroscopic mark in the form of a red-shifted broad fluorescence peak compared to the emission of an isolated chromophore. Since the excimers are only weakly coupled to the ground state energy level, they feature long recombination lifetime and poor fluorescence quantum efficiency (low PLQY). One more type of interchain excitation, named as an aggregate, is the π-electron sharing in both the excited and ground states, which is delocalised over several chains and located at the adjacent polymer chains.[83] Aggregates also typically show relatively weak

absorption with shifts to longer wavelengths (red-shifted) in fluorescence. Aggregates of conjugated polymers are believed to be generally weakly emissive.[84,85] An aggregation of conjugated polymers are reported in many publications while the definition of an "aggregate" remains ambiguous. Clusters of polymer chains, whether the amorphous or possessing some degree of crystalline order, are often referred as aggregates regardless of whether they affect the optoelectronic properties to a substantial extent or not.[86,87]

2.10.2 Appearance of green emission in polyfluorenes

For polymers to be used in full-colour displays, materials with blue emission play a significant role. However, these materials are undeveloped compared to green and red emitters toward long-term stability of their emission in devices due to highly energetic transitions for photon emission (as well with respect to mobility of charges in the semiconducting polymer).

As mentioned in previous sections, polyfluorenes are promising blue emitters with high PLQY, good thermal stability and charge transport (among other classes of blue emitters). They can be blended (or patterned) with other conjugated polymers and dyes, enabling to achieve any colour of OLED device emission. However, it was recognised from early studies that with time their emission colour is changed and new, longer-wavelength band appears. In a device operation system, PLEDs from polyfluorenes showed a longer wavelength emission band (2.2–2.4 eV) appearing over time, gradually changing the colour from pure blue to blue-greenish and then to green. The same was observed in the PL spectra when polymer films were exposed to oxygen (or to air) at high temperature (Figure 2.11).[88,89] This new band appeared in poly(9,9-dialkylfluorenes) at ~535 nm is now called green band or *g*-band. Green emission is more intensely observed in EL rather than in PL spectra.[90]

In early studies this band was attributed to the formation of excimers (sometimes to aggregates) in polyfluorenes[91,92,93] (see previous section 2.10.1). The arguments for such an assignment were: (i) green band was observed for EL and for PL in the solid state, but not for solutions; (ii) in polyfluorene sample, films of which show green band, this band disappeared when the film was dissolved in a solvent, and appeared again when new film was prepared from this solution; (iii) new green emission was structureless, with no vibronic structure, which is commonly observed for excimers; (iv) total PLQY efficiency was decreased compared to pristine polyfluorene; (v) the band appeared after thermal annealing over the temperature of glass transition of polyfluorene.

Although the possibility of excimer formation can not be completely avoid and some studies indicate that they can be formed (for example Bard's work on electrogenerated

chemiluminescence in polyfluorenes,[94] or Teetsov and Bout studies on nanoscale ordering in thermally annealed films of polyfluorene by near-field scanning optical microscopy[95]), the general question is what is the origin of this *g*-band, and whether it appears due to excimer formation or has another origin. This question has been solved in the exciting works of List and Scherf.[14,90,96,,97,98] Many other research groups also have confirmed these conclusions in their independent researches and developed studies for a more intimate look into the mechanism and understanding of *g*-band formation.[39,99,100,101,102,103,104,105,106,107]

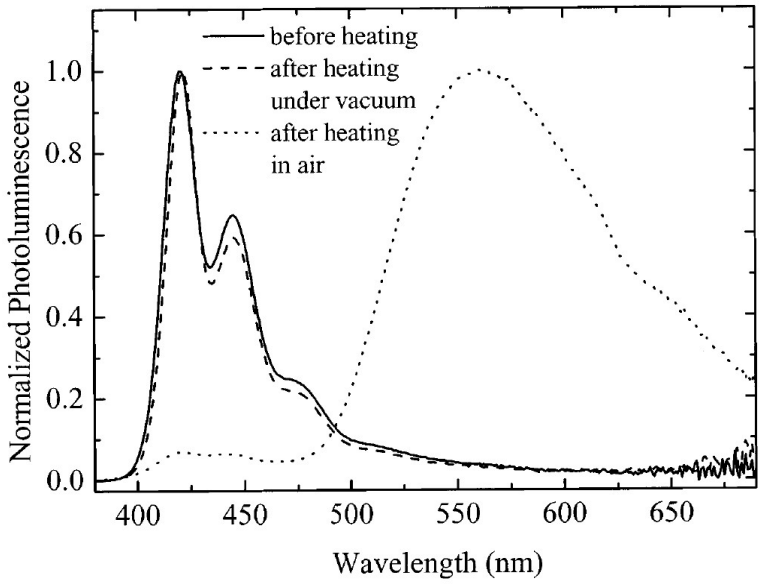

Figure 2.11 PL emission spectra of **PF8** before and after annealing at 200 °C in vacuum (10^{-4} mbar) and after annealing on air (the last quickly results in disappearance of blue emission from **PF8** and an appearance of new green emission band).[90]

2.10.3 Keto defects in polyfluorene chains

To address the issue regarding the origin of the *g*-band, Scherf and List have synthesised two polyfluorenes, **2.32** and **2.33**, from mono-alkylated and dialkylated fluorenes, respectively (Figure 2.12).[96] In solutions, both polymers showed expected and typical for polyfluorenes absorption and emission bands. In films, polymer **2.33** showed (apart of blue vibronic PL) a band in the green region around 533 nm (assigned to excimers in early works, see above). In contrast, monoalkylated polymer **2.32** did not show blue emission bands at all, but had a structureless band in the green region, similar to the additional green band in the case of dialkylated polymer **2.33**. Studies of IR spectra of these polymers showed a signal of a carbonyl group in monoalkylated polymer **2.32** at 1721 cm^{-1} (but not in dialkylated polymer **2.33**), which was assigned to the formation of fluorenone fragments in the polymer chain as a result of its oxidation during synthesis and workup. However, when polymer **2.33** was

irradiated with a 1000 W xenon lamp in air for several minutes, the same signal from the carbonyl group in its IR (as in monoalkylated polymer **2.32**) quickly appeared. So, the authors concluded that similar fluorenone defects are formed in polymer chains of **2.33** as a result of its oxidation in air.

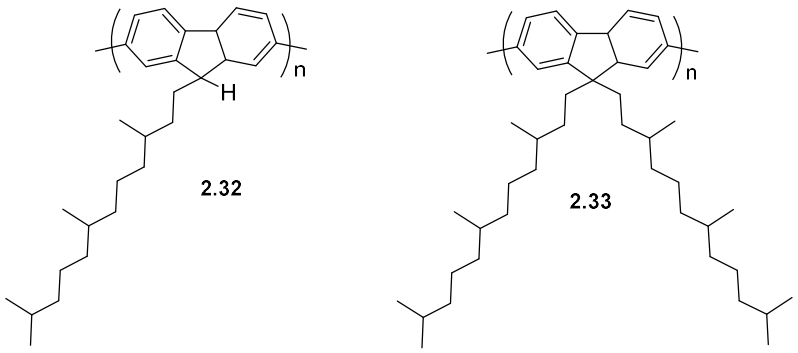

Figure 2.12 Mono- (**2.31**) and dialkylated (**2.32**) polyfluorenes.[96]

It was also demonstrated that the same longer wavelength emission band at 533 nm is observed not only in solid-state PL, but also in EL spectra, and it is even more pronounce in the electroluminescence process.[96] This can be understood from the viewpoint of fluorenone defects in polyfluorene chains, as these fluorenone units, having lower LUMO and HOMO energy levels can act as electron trapping sites in OLED device operation (when charges are traveling from electrodes to the emission sites), thus favoring charge recombination with photon expulsion at the defect sites (this was also supported by time-delayed experiments).

Formation of defect fluorenone sites in the pristine monoalkylated polymer was explained as ,the reduction of alkylfluorene by Ni(0) to form monoalkyl fluorenyl anion sites **2.34** during the polymerisation reaction, which are easily oxidised by air to form ketone fragments **2.36** in the polymer chain during the workup (Scheme 2.11).

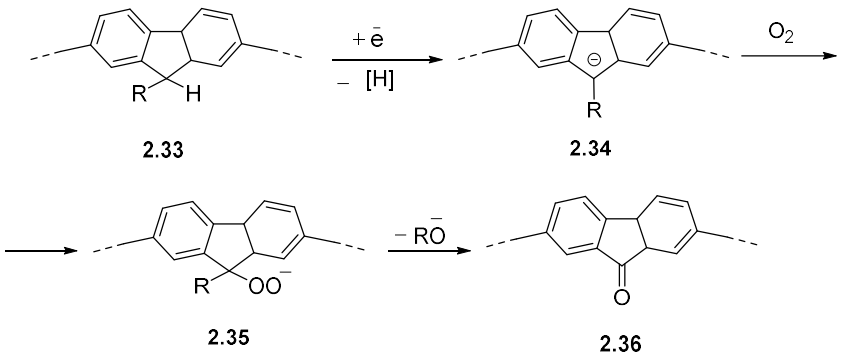

Scheme 2.11 Proposed mechanism of formation of keto-defects in polyfluorenes by an oxidation of monoalkylfluorene sites (**2.33–2.36**).[96]

The hypothesis and the mechanism were supported by List and Scherf by investigations of thermal annealing of **PF8** at high temperature of 200 °C.[90] In previous works, thermal annealing in the air above 140–160 °C quickly showed an appearance of a green band, but this band appeared slower on heating in vacuum (10^{-1}–10^{-2} mbar) as well. However, when such an annealing at 200 °C was performed in ultra-high vacuum (~10^{-4} mbar), no changes were observed, whereas heating the same sample at the same temperature in the air quickly resulted in the disappearance of the blue emission from **PF8** and an appearance of a new green emission band (Figure 2.13). These results have been confirmed by comparing PL emissions of **PF8** films heated under nitrogen and in air separately: a new green band quickly appeared only when the **PF8** sample was exposed to air at 190 °C, but not happened under nitrogen atmosphere (Figure 2.13).[39]

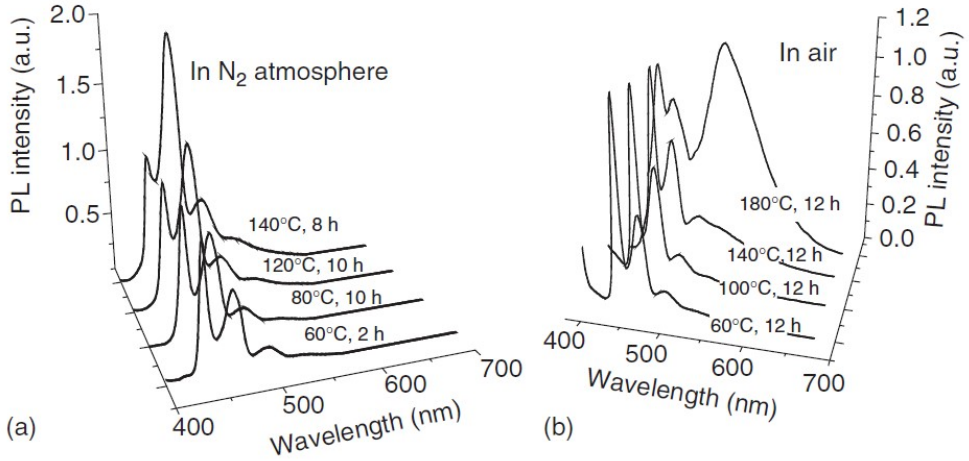

Figure 2.13 PL spectra of **PF8** films annealed at various temperatures: (a) in nitrogen atmosphere, (b) in an air atmosphere.[39]

Meijer and co-workers found that ultra-pure 2,7-dibromo-9,9-dialkylfluorene monomers give polyfluorene with much higher stability than "normal polyfluorene."[108] For that, they treated the monomer with the strong base potassium *tert*-butoxide in dry THF to deprotonate mono alkylated impurity and passed twice the solution through silica gel column eluting with petrol ether. The potassium salt of mono-alkylated fluorene, being highly polar, trapped on the silica column and eluted dialkylated monomer became "impurity-free" giving more stable polyfluorene on polymerisation. As seen from Figure 2.14, the substantially less intense green emission is observed in polyfluorene obtained from purified monomer compared to the unpurified one and also no further changes were observed in EL spectra after 60 h of OLED operation.[108]

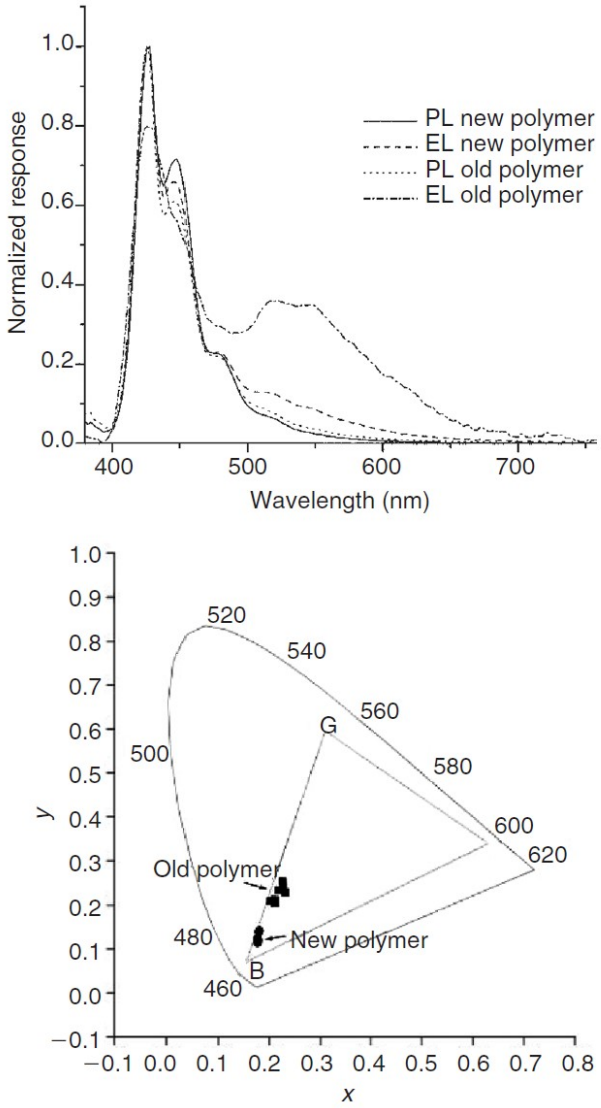

Figure 2.14 EL and PL spectra of **PF8** polymers obtained from purified monomer (new polymer) and unpurified monomer (old polymer) and their CIE x-y colour coordinates: old polymer – squares, new polymer – circles (for purification: the monomer was treated with tBuOK/THF and filtered through silica column).[108]

Holmes et al. also reported on poly(dialkylfluorenes) free from monoalkylated impurities.[109] In this case, dialkylfluorene monomer was prepared by the route similar to that shown in Scheme 2.9 through cyclisation of the tertiary alcohol (similar to **2.27**, but with alkyl groups instead of Ar groups) and further bromination at 2,7 positions. These dialkylated polyfluorenes showed higher stability toward degradation/oxidation and suppressed (but not completely avoided) emission in the green region (which is attributed to keto defects). Formation of *g*-band was not completely avoided indicating that dialkylated polyfluorenes can be oxidized as well (although they are much more stable) and that the changes in the emission

colour of polyfluorenes with an appearance of the green band is mainly due to the presence of very small amounts of monoalkylated impurities in the starting monomers (which can not be easily detected by common analytical methods, <0.5–1%).

g-Band emission is not simply emission from the fluorenone sites through *intra*-molecular exciton diffusion to them. This is cooperative effect involving *inter*-chain interactions and exciton migration to the defect sites. So, many efforts have done for the development of stable blue emission. Neher and coworkers reported on blends of fluorene copolymer with hole transporting molecules and obtained stable blue emission.[110] In this case dopants in the copolymer acted as hole traps facilitating formation of excitons and emissions just from these sites, thus reducing the number of charges trapped at defect sites. One more approach used to stabilise blue emission from polyfluorenes was toward reducing *inter*-chain interactions by cross-linking the polymers using the vinyl end groups or by attaching the bulky groups (e.g. dendritic solubilising groups or silsesquioxanes) as end-capping or side chain groups.

With this respect, poly(9,9-diarylfluorenes) obtained from fluorenone (Scheme 2.10) exhibited substantially better stability than poly(9.9-dialkylfluorenes) and this is normally explained in the literature as an effect of more bulky phenyl groups compared to linear alkyl chains. This might be right to certain extent, but we believe that there is another important reason for that. Namely, in the synthesis of diarylfluorenes from fluorenones by Scheme 2.10, the formation of mono-substituted product is impossible (it will then be decomposed on work-up back to fluorenone with easy removal of the later during work-up). This our point of view is supported by work of Holmes who showed higher stability of polyfluorenes obtained by Scheme 2.9.[109]

There is also another evidence: because highly active metals are normally used as cathodes in OLEDs, during the OLED operation reduction of fluorene (especially mono-alkylated sites) by calcium cathode may also result in the formation of keto-defects. It was shown that use of a buffer layer between the cathode and the polymer layer substantially suppress growing of *g*-band in device operation.

Another interesting and important work related to the above discussions is the synthesis of silicon analogues of polyfluorenes. Holmes et al. reported a stable blue light emission from poly(9,9-dihexyl-2,7-dibenzosiloles) (**2.39**) obtained through Suzuki polymerisation (Scheme (2.12).[111] This polymer showed extraordinary stability, with no green band in PL spectrum even after thermal heating in an air at 250 ^{o}C for 16 h (Figure 2.15). The stability of EL in fabricated OLED devices was also shown to be more stable with pure blue emission. The polymer **2.39** showed HOMO (–5.77 eV) and LUMO (–2.77 eV) energy levels

of ca. 0.1 eV lower than **PF8**, with the potential advantage of electron injection in OLED operation.

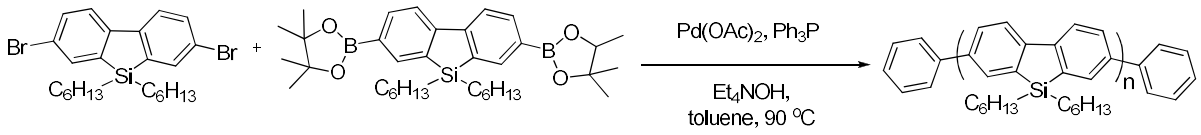

2.37 **2.38** **2.39**

Scheme 2.12 Suzuki polymerisation to poly(9,9-dihexyl-2,7-dibenzosilole) (**2.39**).[111]

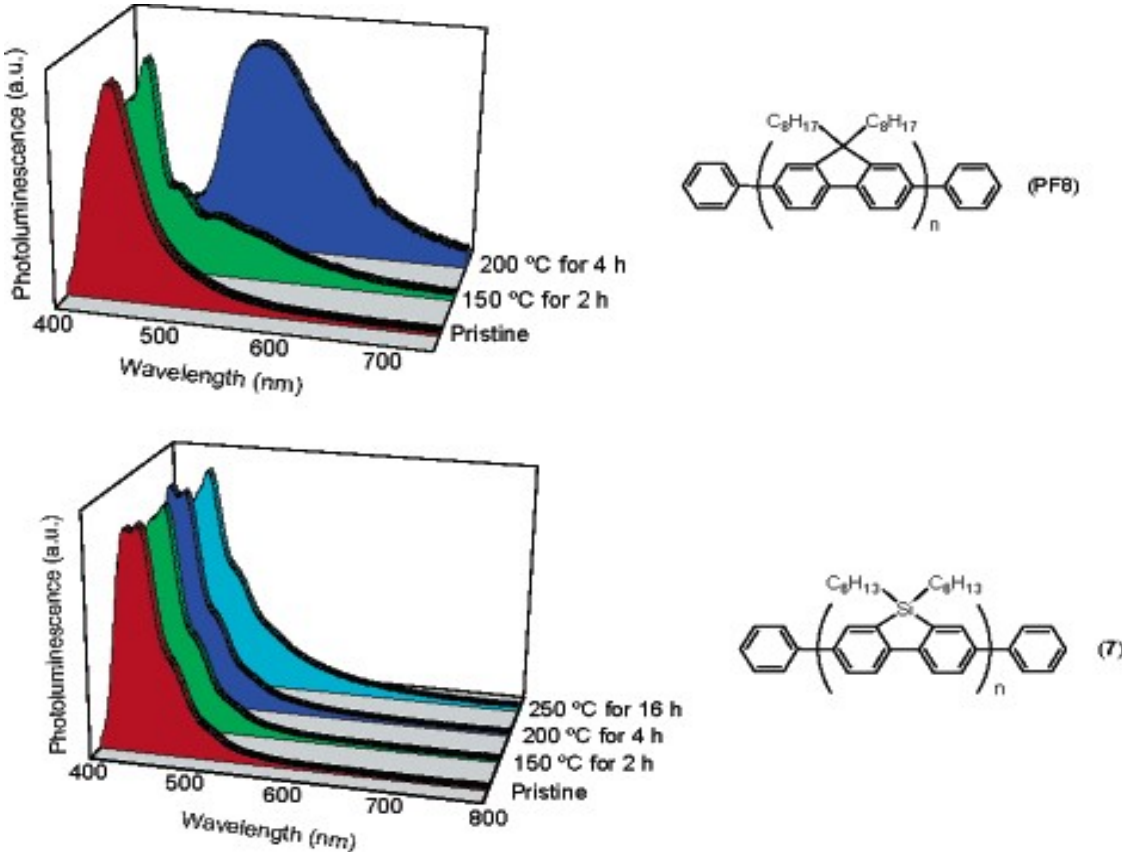

Figure 2.15. Effect of thermal annealing on PL spectrum of **2.39** (bottom, shown as **7** on a figure) and **PF8** (top) under air and ambient light.[111]

2.11 Polyfluorene copolymers

2.11.1. Blue-emitting polyfluorene copolymers

Miller and coworkers prepared copolymer **2.40** of dihexylfluorene with anthracene by Yamamoto coupling reaction.[112,113] These copolymers showed high molecular weights (M_w = 80,000 Da), glass transition temperature T_g = 135 °C, and stable blue emission with high PLQY (76% in film). The authors of the paper claimed that the stability of this blue emission is due to anthracene units which are perpendicular to fluorene π-system and thus they prevent slow contacts between chains and excimer formation. Now (after recognising the origin of *g*-

band) it is clear that anthracene fragments in such concentrations (~6:1) decrease the conjugation length of oligofluorene fragments and consequently decrease the HOMO energy level of the polymer (so it becomes more stable toward oxidation) and prevent migration of excitons to the defect sites.

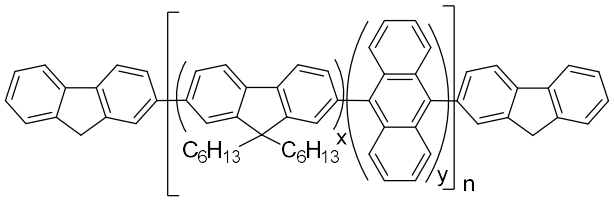

x = 0.85, y = 0.15

2.40

Huang group synthesised deep blue copolymers **2.42a-g** by Suzuki polymerisation method (Scheme 2.13).[114] These copolymers had band gaps ranging from 2.82 to 3.32 eV and emitted blue light in the region of 404–443 nm. The PLQY values of these copolymers varied in a wide range depending on aryl groups in the main chain (~10–88% in films). Their HOMO/LUMO energy levels were also tuned by varying from electron-rich to electron-deficient aryl groups in the backbone.

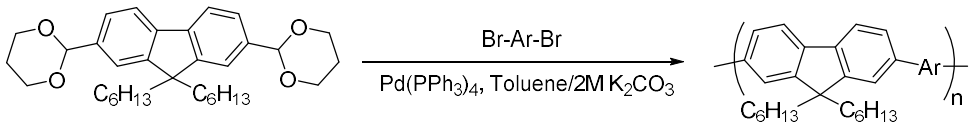

2.41 **2.42**

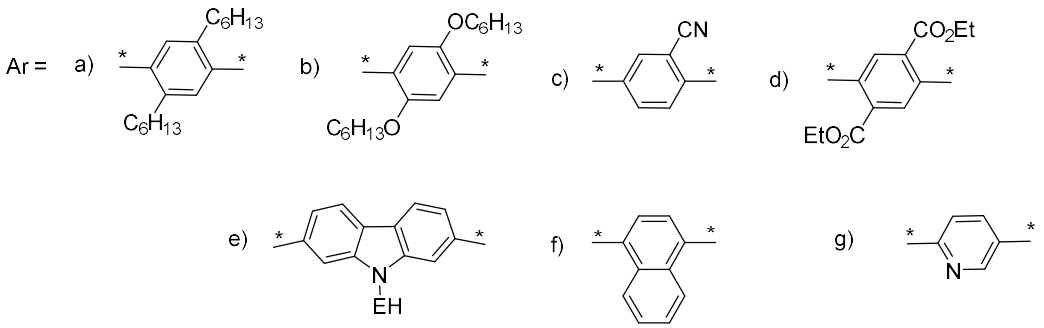

Scheme 2.13 Fluorene-arylene copolymers **2.42a-g**.[114]

Park et al. reported on a new series of T-shaped isophorone-containing fluorene-based copolymer **2.43** (Figure 2.16).[115] For the synthesis (by Suzuki coupling) of this T-shaped structure copolymer, they introduced triphenylamine as effective donor for charge transfer

with dicyanomethylene/isophorone end group through conjugated linkage. The copolymer **2.43** had moderate molecular weight, showed high thermal stability (450 °C) and T_g ~ 80 °C.

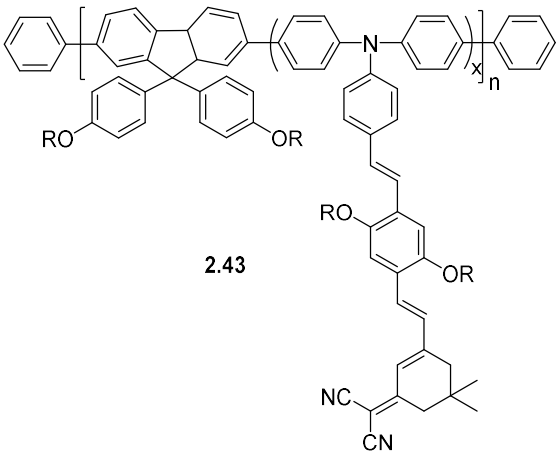

2.43

Figure 2.16 Fluorene-arylene copolymers **2.43**.[115]

2.11.2 Spiro-fluorene copolymers

Salbeck reported on spirobifluorenes as promising materials for blue OLEDs.[116] These spiro-units incorporated into polymers increased the T_g of materials and completely suppressed any aggregation in the solid state due to orthogonal (90º) geometry of the spirobifluorene units. As poly(diarylfluorenes) have known to be blue emitters it comes as no surprise that the polymers containing spirobifluorene fragments such as **2.44** and **2.45** (Figure 2.17) also produce stable blue emission. Polymer **2.44** with alkoxy group was soluble in common organic solvents and no green emission was observed in its films annealed in air at 200 ºC for 3 h.[117]

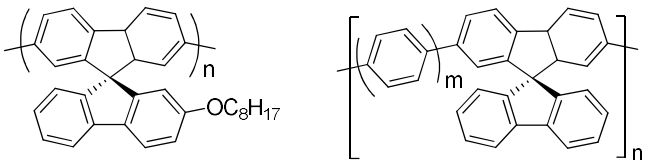

2.44 2.45

Figure 2.17 Spirofluorene polymer and copolymers **2.44** and **2.45**.[116]

Tseng et al. reported the synthesis of poly[spiro(fluorene-9,9'-xanthene)] by Suzuki coupling reaction (Scheme 2.14).[118] The polymer was prepared from 2,7-dibromofluorenone (**2.25**), which reacted with resorcinol in the presence of $ZnCl_2$/HCl as condensing agent to give spiro compound **2.46**. Subsequently, alkylation with 1-bromooctane/K_2CO_3 afforded spiro-monomer **2.47**. Diborolane monomer **2.48** was prepared by lithiation of **2.47** with

n-BuLi, treatment with tri-n-butyl borate, hydrolysis to diboronic acid and its esterification. Finally, the monomers **2.47** and **2.48** were co-polymerised through Suzuki coupling reaction to afford spiroxanthane polymer **2.49**. This polymer showed a high glass transition temperature, absorption at λ_{max} = 280 nm, and stable blue emission.

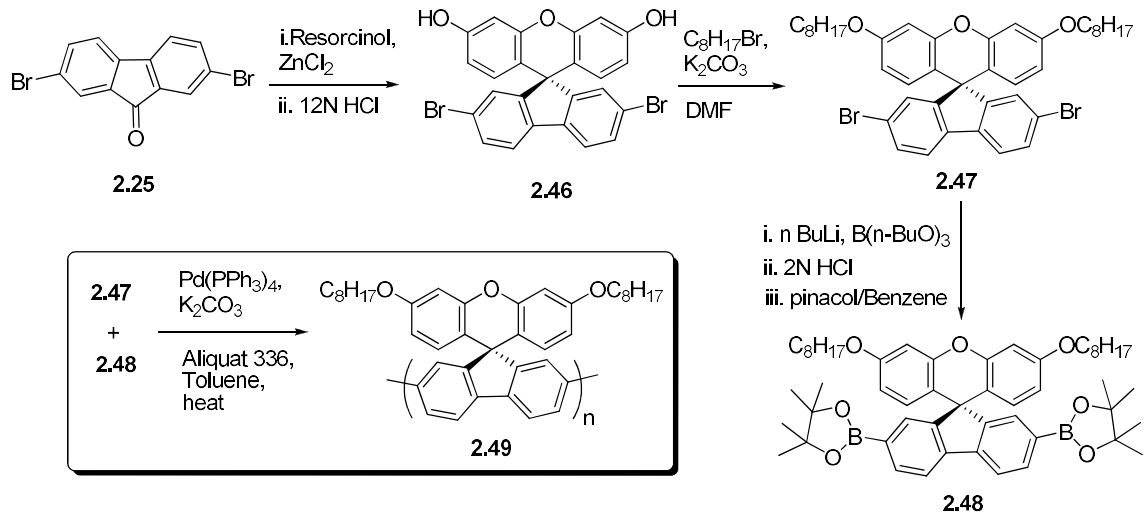

Scheme 2.14 Synthesis of spiro-xanthene polyfluorene **2.49**.[118]

Huang et al. synthesised copolymer **2.50** by Suzuki polymerisation (Figure 2.18).[119] It was well soluble in chlorobenzene but less soluble in THF and chloroform. The glass transition temperature of the polymer **2.50** was much higher than that of **PF6**. Upon on thermal annealing at 100 ºC, no longer wavelength emission band was observed, but above the glass transition temperature, it showed longer wavelength emission at 525 nm. Carter and coworkers synthesised random 3D branched copolymers **2.51–2.54** by Yamamoto coupling reaction (Figure 2.18).[120] These copolymers showed excellent thermal stability above 430 ºC and T_g was again higher than that of **PF6**. These copolymers revealed stable blue emission without any long wavelength band after annealing at 120 ºC for 30 minutes.

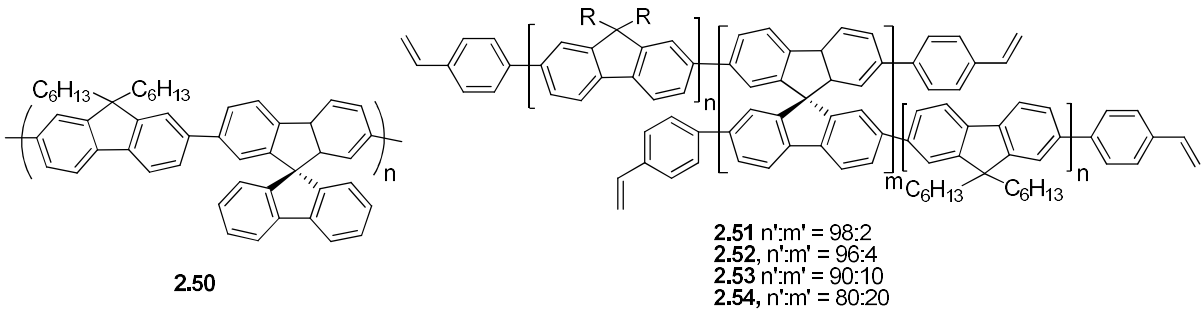

Figure 2.18 Polyfluorenes with spirobifluorene fragments **2.50–2.54**.[119,120]

2.11.3 Colour tuning in polyfluorene copolymers

In this section, we describe some approaches to the colour tuning in polyfluorene copolymers. Leclerc and coworkers synthesised a range of blue to red-emitting copolymers **2.59–2.62** having an alternation of fluorene units with phenylene, thiophenes, and phenylenevinylene units in the backbone.[121,122,123] Changing the nature of comonomer units, substantially changed the bandgap of copolymers and tuned the colour of their emission through the entire visible range spectrum (Figure 2.19).

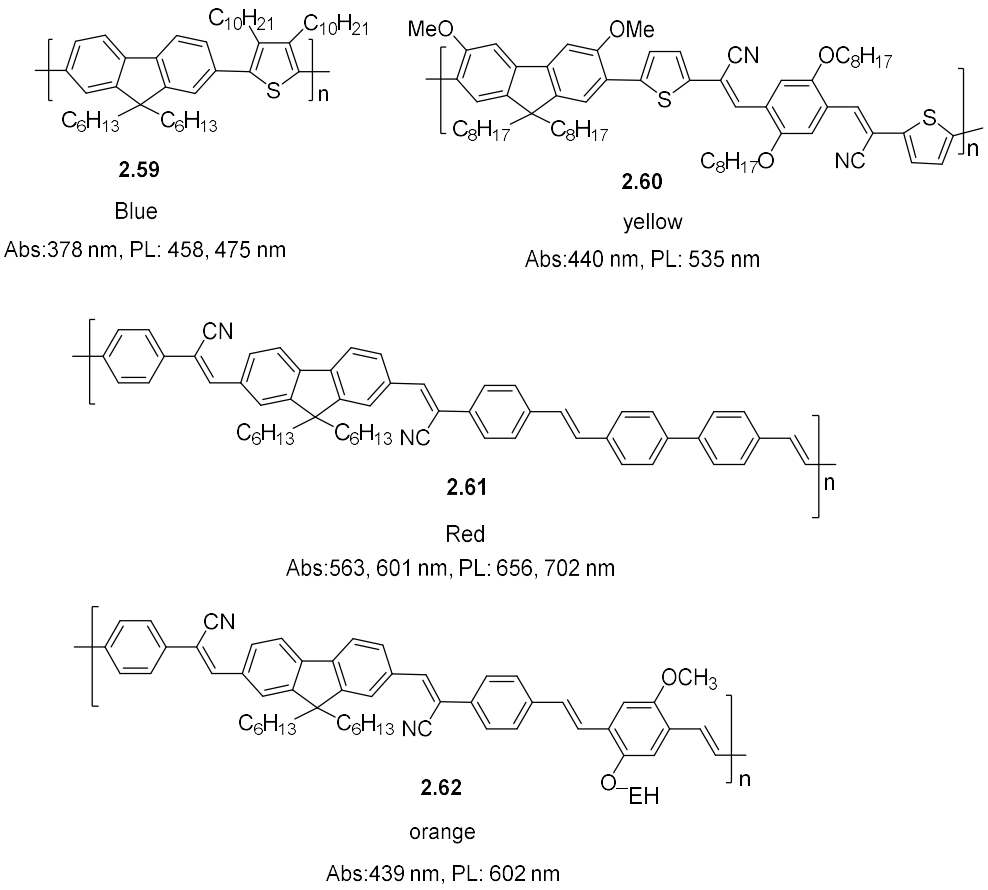

Figure 2.19 Various fluorene-containing copolymers **2.59-2.62** with tunable PL and EL colours.[121–123]

2.11.4 Hole and electron transporting polyfluorene copolymers

To decrease the energy barrier for hole injection from an anode into light-emitting polymers in OLED and to improve hole transporting properties of the polymer, electron-rich units such as carbazole and triphenylamine have been used. There are many examples now of such functionalisations in conjugated polymers, and in polyfluorenes this was done either by copolymerisation (**2.63)**, by attaching such groups in side chains (**2.64** and **2.65**) or end-capping (**2.66**) (Figure 2.20).[124,125,126] This functionalisation increased the HOMO energy level of the resulting copolymers facilitating hole injection and hole transport in OLEDs.

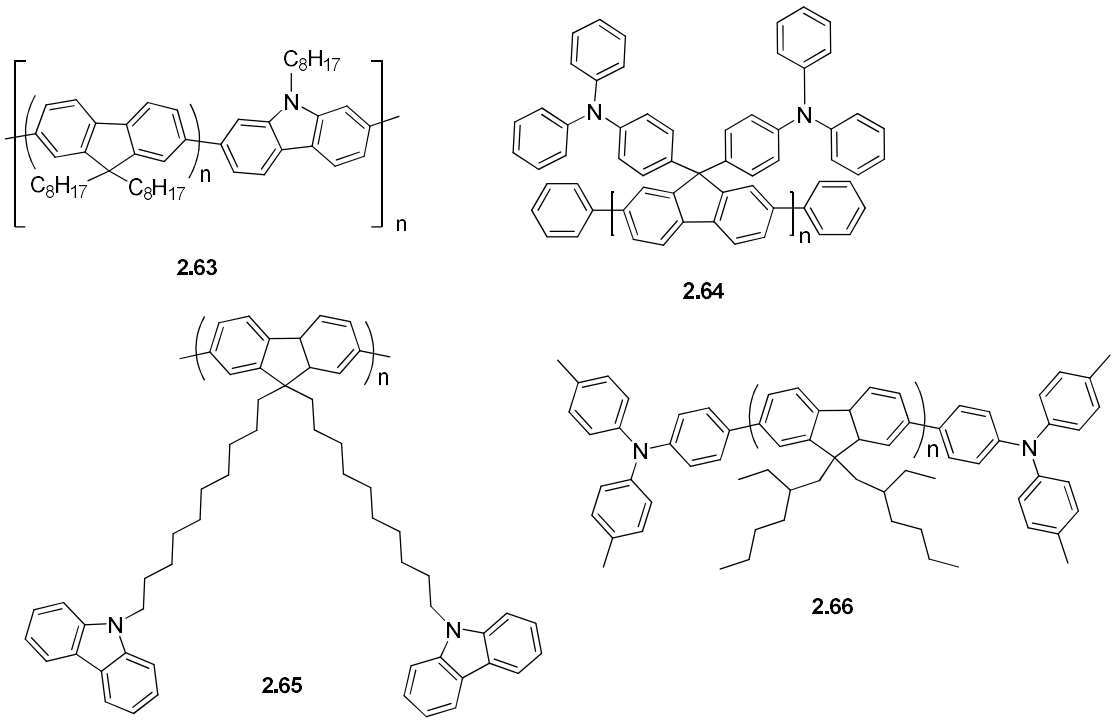

Figure 2.20 Hole transporting fluorene copolymers **2.63**–**2.66**.

In similar fashion, electron-deficient units in a conjugated copolymer decrease their LUMO energy thus decreasing the barrier of electron injection into the material and electron transport in it. Several examples of such fluorene-containing copolymers **2.68**–**2.71** having oxadiazole, quinoline, quinoxaline, and cyanophenylene or cyanovinylene moieties in the main chain are shown in Figure 2.21.[127,128]

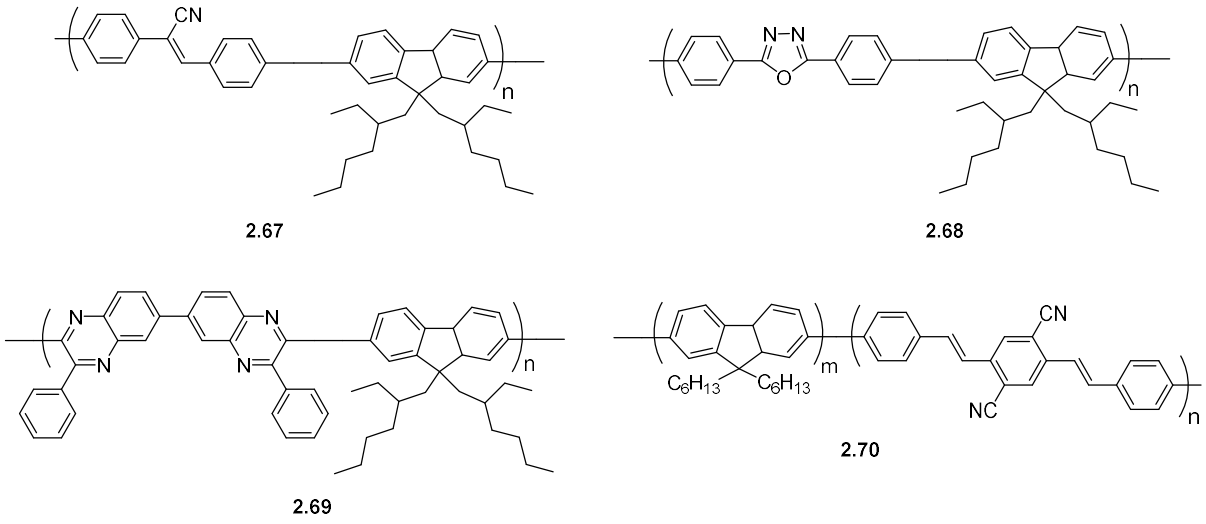

Figure 2.21 Electron transporting fluorene copolymers **2.67**–**2.70**.

References

1 U. Mitschke and P. Bäuerle, *J. Mater Chem*., **2000**, *10*, 1471–1507. (DOI: 10.1039/a908713c).

2 G. Grem, G. Leditzky, B. Ullrich, and G. Leising, *Adv Mater*., **1992**, *4*, 36–37. (DOI: 10.1002/adma.19920040107).

3 A. D. Schlüter and G.Wegner, *Acta Polymer.,* **1993**, *44,* 59–69. (DOI: 10.1002/actp.1993.010440201).

4 K. C. Park, L. R. Dodd, K. Levon, and T. K. Kwei, *Macromolecules*, **1996**, *29*, 7149–7154. (DOI: 10.1021/ma960607t).

5 A. C. Grimsdale and K. Müllen, in: *Polyfluorenes*, U. Scherf and D. Neher (Eds), Springer, 2008 – *Advances in Polymer Science,* **2008**, *212*, pp. 1–48. (DOI 10.1007/12_2008_137).

6 U. Scherf and D. Neher (Eds), *Polyfluorenes. – Advances in Polymer Science,* Springer, **2008**, *212*, 322 pp. (DOI 10.1007/978-3-540-68734-4).

7 M. T. Bernius, M. Inbasekaran, J. O'Brien, and W. S. Wu, *Adv. Mater*., **2000**, *12*, 1737–1750. (DOI: 10.1002/1521-4095(200012)12:23<1737).

8 M. Ranger, D. Rondeau, and M. Leclerc, *Macromolecules*, **1997**, *30*, 7686–7691. (DOI: 10.1021/ma970920a).

9 H.-H. Lu, C. -Y. Liu, C.-H. Chang, and S.-A. Chen, *Adv. Mater*., **2007**, *19*, 2574–2579. (DOI: 10.1002/adma.200602632).

10 B. K. Yap, R. Xia, M. Campoy-Quiles, P. N. Stavrinou, and D. D. C. Bradley, *Nature Mater*., **2008**, *7*, 376–380..(DOI:10.1038/nmat2165).

11 A. C. Grimsdale, K. L. Chan, R. E. Martin, P. G. Jokisz, and A. B. Holmes, *Chem. Rev*., **2009**, *109*, 897–1091. (DOI: 10.1021/cr000013v).

12 Q. Zhao, S. -J. Liu, W. Huang, *Macromol. Chem. Phys*., **2009**, *210*, 1580–1590. (DOI: 10.1002/macp.200900263).

13 A. Thangthong, D. Meunmart, T. Sudyoadsuk, S. Jungsuttiwong, N. Prachumrak, T. Keawin, and V. Promarak, *Chem. Commun.,* **2011**, *47*, 7122–7124. (DOI: 10.1039/C1CC11624J).

14 U. Scherf and E. J. W. List, *Adv. Mater*., **2002**, *14*, 477–487. (DOI: 10.1002/1521-4095(20020404)14).

15 A. J. Cadby, P. A. Lane, M. Wohlgenannt, C. An, Z. V. Vardeny, and D. D. C. Bradley, *Synth. Metals*, **2000**, *111*, 515–518. (DOI:10.1016/S0379-6779(99)00409-9).

16 J. Rault-Berthelot and J. Simonet, *J. Electrochem. Soc.*, **1985**, *182,* 187–192. (DOI:10.1016/0368-1874(85)85452-6).

17 M. Fukuda, K. Sawada, S. Morita, and K. Yoshino, *Synth Metals*, **1991**, *41*, 855–858. (DOI: 10.1016/0379-6779(91)91510-H).

18 M. Fukuda, K. Sawada, and K. Yoshino, *Jpn. J. Appl. Phys., Pt. 2 Letters*, **1989**, *28*, L1433–L1435. (DOI:http://dx.doi.org/10.1143/JJAP.28).

19 Q. Pei and Y. Yang, *J. Am. Chem. Soc.,* **1996**, *118*, 7416–7417. (DOI: 10.1021/ja9615233).

20 T. Yamamoto, *Prog. Polym. Sci.,* **1992**, *17*, 1153. (DOI: 10.1016/0079-6700(92)90009-N).

21 G. Klaerner and R. D. Miller, *Macromolecules*, **1998**, *31*, 2007–2009. (DOI: 10.1021/ma971073e).

22 M. Ranger and M. Leclerc, *Chem. Commun.,* **1997**, 1597–1598. (DOI: 10.1039/A703076B).

23 M. Ranger, D. Rondeau, and M. Leclerc, *Macromolecules,* **1997**, *30*, 7686–7691. (DOI: 10.1021/ma970920a).

24 C. R. Towns and R. O'Dell, PCT Patent WO 00/53656, **2000.**

25 S. B. Jhaveri, J. J. Peterson, and K. R. Carter, *Macromolecules*, **2008**, *41*, 8977–8979. (DOI: 10.1021/ma801243x).

26 R. M. Walczak, R. N. Brookins, A. M. Savage, E. M. vander Aa, and J. R. Reynolds, *Macromolecules*, **2009**, *42*, 1445–1447. (DOI: 10.1021/ma802462v).

27 M. C. Stefan, A. E. Javier, I. Osaka, and R. D. McCullough, *Macromolecules*, **2009**, *42*, 30–32. (DOI: 10.1021/ma8020823).

28 A. E. Javier, S. R. Varshney, and R. D. McCullough, *Macromolecules*, **2010**, *43*, 3233–3237. (DOI: 10.1021/ma100519g).

29 J. M. Frechet and P. M. Beaujuge, *J. Am. Chem. Soc*., **2011**, *133*, 20009–20029. (DOI: org/10.1021/ja2073643).

30 R. C. Coffin, J. Peet, J. Rogers, and G. C. Bazan. *Nature Chem*., **2009**, *1*, 657–661. (DOI:10.1038/nchem.403).

31 U. Scherf, A. Gutacker, and N. Koenen, *Acc. Chem. Res*., **2008**, *41*, 1086–1097. (DOI: 10.1021/ar7002539).

32 A. Kiriy, V. Senkovskyy, M. Sommer, *Macromol. Rapid Commun*., **2011**, *32*, 1503–1507. (DOI: 10.1002/marc.201100316).

33 K. Okamoto and C. K. Luscombe, *Polym. Chem*., **2011**, *2*, 2424–2434. (DOI: 10.1039/C1PY00171J).

34 A. Sui, X. Shi, S. Wu, H. Tian, Y. Geng, and F. Wang, *Macromolecules*, **2012**, *45*, 5436–5443. (DOI: 10.1021/ma3009299).

35 R. M. Walczak, R. N. Brookins, A. M. Savage, E. M. vander Aa, and J. R. Reynolds, *Macromolecules*., **2009**, *42*, 1445–1447. (DOI: 10.1021/ma802462v).

36 M. Fukuda, K. Sawada, and K. Yoshino, *J. Polym. Sci., Part A: Polym. Chem.,* **1993**, *31,* 2465–2471. (DOI: 10.1002/pola.1993.080311006).

37 Q. Pei and Y. Yang, *J. Am. Chem. Soc*., **1996**, *118*, 7416–7417. (DOI: 10.1021/ja9615233).

38 M. Kreyenschmidt, G. Klaerner, T. Fuhrer, J. Ashenhurst, S. Karg, W. D. Chen, V. Y. Lee, J. C. Scott, and R. D. Miller, *Macromolecules,* **1998**, *31,* 1099–1103. (DOI: 10.1021/ma970914e).

39 X. Gong, P. K. Iyer, D. Moses, G. C. Bazan, A. J. Heeger, and S. S. Xiao, *Adv. Funct. Mater.,* **2003**, *13*, 325–330. (DOI: 10.1002/adfm.200304279).

40 S. Janietz, D. D. C. Bradley, M. Grell, C. Giebeler, M. Inbasekaran, and E. P. Woo, *Appl. Phys. Lett.,* **1998***, 73,* 2453–2455. (DOI: org/10.1063/1.122479).

41 W. Yang, J. Huang, C. Liu, Y. Niu, Q. Hou, R. Yang, and Y. Cao, *Polymer*., **2004**, *45*, 865–872. (DOI:10.1016/j.polymer.2003.11.052).

42 T. Miteva, A. Meisel, W. Knoll, H. G. Nothofer, U. Scherf, D. C. Muller, K. Meerholz, A. Yasuda, and D. Neher, *Adv. Mater*., **2001**, *13*, 565–570. (DOI: 10.1002/1521-4095(200104)13).

43 L. S. Liao, M. K. Fung, C. S. Lee, S. T. Lee, M. Inbasekaran, E. P. Woo, W. W. Wu, *Appl. Phys. Lett.,* **2000**, *76*, 3582–3584. (DOI: org/10.1063/1.126713).

44 L. S. Liao, L. F. Cheng, M. K. Fung, C. S. Lee, S. T. Lee, M. Inbasekaran, E. P. Woo, and W. W. Wu, *Phys. Rev. B.*, **2000**, *62*, 10004–10007. (DOI: org/10.1103/PhysRevB.62.10004).

45 D. F. Perepichka, I. F. Perepichka, H. Meng, and F. Wudl, Chapter 2 in Book: *Organic Light-Emitting Materials and Devices*, Z. R. Li and H. Meng, Eds., CRC Press, Boca Raton, FL, **2006**, pp. 45–293.

46 E. P. Woo, W. R. Shiang, M. Inbasekaran, and G. R. Roof, U. S. Patent, **1999**, 5, 962, 631..

47 Y.-S. Suh, S. W. Ko, B.-J. Jung, and H.-K. Shim, *Opt. Mater*., **2002**, *21*, 109–118. (DOI:10.1016/S0925-3467(02)00122-2).

48 G. Klaerner and R. D. Miller, C. J. Hawker, *Polym. Prepr*., **1998**, *39*, 1006. (DOI: 10.1002/macp.201500510).

49 D. Marsitzky, R. Vestberg, P. Blainey, B. T. Tang, C. J. Hawker, and K. R. Carter, *J. Am. Chem Soc*., **2001**, *123*, 6965–6972. (DOI: 10.1021/ja010020g).

50 S. Setayesh, A. C. Grimsdale, T. Weil, V. Enkelmann, K. Müllen, F. Meghdadi, E. J. W. List, G. Leising, *J. Am. Chem. Soc*., **2001**, *123*, 946–953. (DOI: 10.1021/ja0031220).

51 M. Yamada, J. Sun, Y. Suda, and T. Nakaya, *Chem. Lett.,* **1998**, *28*, 1055–1056. (DOI: 10.1021/cm00054a004).

52 M. Leclerc, *J. Polym. Sci., Part A: Polym. Chem.,* **2001**, *39*: 2867–2873. (DOI: 10.1002/pola.1266).

53 C. Ego, A. C. Grimsdale, F. Uckert, G. Yu, G. Srdanov, and K. Müllen, *Adv. Mater.*, **2002**, *14*, 809–811. (DOI: 10.1002/1521-4095(20020605)14).

54 M. Grell, D. D. C. Bradley, G. Ungar, J. Hill, and K. Whitehead, *Macromolecules,* **1999**, *32*, 5810–5817. (DOI: 10.1021/ma990741o).

55 W. Chunwaschirasiri, B. Tanto, D. L. Huber, and M. J. Winokur, *Phys. Rev. Lett.,* **2005**, *94*, 107402–107405. (DOI: org/10.1103/PhysRevLett.94.107402).

56 M. Knaapila and M. J.Winokur, in: *Polyfluorenes*, U. Scherf and D. Neher (Eds), Springer, 2008 – *Advances in Polymer Science,* **2008**, *212,* 227–272. (DOI: 10.1007/12_2008_149).

57 S. H. Chen, A. C. Su, and S. A. Chen, *J. Phys. Chem. B.*, **2005**, *109*, 10067–10072. (DOI: 10.1021/jp044079w).

58 M. Grell, D. D. C. Bradley, X. Long, T. Chamberlain, M. Inbasekaran, E. P. Woo, *and* M. Soliman, *Acta Polym*., **1998**, *49*, 439–444. (DOI: 10.1002/(SICI)1521-4044(199808)49)..

59 K. Becker and J. M. Lupton, *J. Am. Chem. Soc*., **2005**, *127*, 7306–7307. (DOI: 10.1021/ja051583l).

60 A. Hayer, A. L. T. Khan, R. H. Friend, and A. Kohler, *Phys. Rev. B: Condens. Matter.Mater. Phys*., **2005**, *71*, 241302–241307. (DOI: org/10.1103/PhysRevB.71.241302).

61 J. Teetsov and M. A. Fox, *J. Mater. Chem*., **1999**, *9*, 2117–2122. (DOI: 10.1039/A902829C).

62 R. Zhu, J.-M. Lin, W.-Z. Wang, C. Zheng, W. Huang, Y.-H. Xu, J.-B. Peng, and Y. Cao, *J. Phys. Chem. B*, **2008**, *112*, 1611–1618. (DOI: 10.1021/jp076234n).

63 D. W. Bright, F. Galbrecht, U. Scherf, and A. P. Monkman, *Macromolecules*, **2010**, *43*, 7860–7863. (DOI: 10.1021/ma101570u).

64 C. Wu and J. McNeill, *Langmuir*, **2008**, *24*, 5855–5861. (DOI: 10.1021/la8000762).

65 Z.-Q. Lin, N.-E. Shi, Y.-B. Li, D. Qiu, L. Zhang, J.-Y. Lin, J.-F. Zhao, C. Wang, L.-H. Xie, and W. Huang, *J. Phys. Chem. C*, **2011**, *115*, 4418–4424. (DOI: 10.1021/jp109598y).

66 M. Knaapila and A. P. Monkman, *Adv. Mater*., **2013**, *25*, 1090–1108. (DOI: 10.1002/adma.201204296).

67 M. Knaapila, F. B. Dias, V. M. Garamus, L. Almásy, M. Torkkeli, K. Leppänen, F. Galbrecht, E. Preis, H. D. Burrows, U. Scherf, and A. P. Monkman, *Macromolecules*, **2007**, *40*, 9398–9405. (DOI: 10.1021/ma0715728).

68 M. Ariu, M. Sims, M. D. Rahn, J. Hill, A. M. Fox, D. G. Lidzey, M. Oda, J. Cabanillas-Gonzalez, and D. D. C. Bradley, *Phys Rev B*., **2003**, *67*, 195333–195343. (DOI: org/10.1103/PhysRevB.67.195333).

69 A. L. T. Khan, P. Sreearunothai, L. M. Herz, M. J. Banach, and A. Kohler, *Phys. Rev. B: Condens. Matter Mater. Phys.*, **2004**, *69*, 85201. (DOI: org/10.1103/PhysRevB.69.085201).

70 C. Y. Chen, C. S. Chang, S. W. Huang, J. H. Chen, H. L. Chen, C. I. Su, and S. A. Chen, *Macromolecules*, **2010**, *43*, 4346–4354. (DOI: 10.1021/ma100335c).

71 H. H. Lu, C. Y. Liu, C. H. Chang, and S. A. Chen, *Adv. Mater*., **2007**, *19*, 2574–2579. (DOI: 10.1002/adma.200602632).

72 X. Zhang, Q. Hu, J. Lin, Z. Lei, X. Guo, L. Xie, W. Lai, and W. Huang, *Appl. Phys. Lett*., **2013**, *103*, 153301–153304. (DOI: 10.1063/1.4824766).

73 H. H. Lu, C. Y. Liu, C. H. Chang, and S. A. Chen, *Adv. Mater*., **2007**, *19*, 2574. (DOI: 10.1002/adma.200602632).

74 C. C. Kitts and D. A. Vanden Bout, *Polymer*, **2007**, *48*, 2322–2330. (DOI:10.1016/j.polymer.2007.02.047).

75 A. J. Cadby, P. A. Lane, H. Mellor, S. J. Martin, M. Grell, C. Giebeler, D. D. C. Bradley, M. Wohlgenannt, C. An, and Z. V. Vardeny, *Phys. Rev. B*, **2000**, *62*, 15604–15609. (DOI: 10.1103/PhysRevB.62.15604).

76 D. W. Bright, F. Galbrecht, U. Scherf, and A. P. Monkman, *Macromolecules,* **2010**, *43*, 7860–7863. (DOI: 10.1021/ma101570u).

77 D. W. Bright, F. B. Dias, F. Galbrecht, U. Scherf, and A. P. Monkman, *Adv. Funct. Mater*., **2009**, *19*, 67–73. (DOI: 10.1002/adfm.200800313).

78 M. Knaapila, F. B. Dias, V. M. Garamus, L. Almasy, M. Torkkeli, K. Leppanen, F. Galbrecht, E. Preis, H. D. Burrows, U. Scherf, A. P. Monkman, *Macromolecules*, **2007**, *40*, 9398–9405. (DOI: 10.1021/ma0715728).

79 M. Knaapila, V. M. Garamus, F. B. Dias, L. Almasy, F. Galbrecht, A. Charas, J. Morgado, H. D. Burrows, U. Scherf, and A. P. Monkman, *Macromolecules*, **2006**, *39*, 6505–6512. (DOI: 10.1021/ma060886c).

80 D. W. Bright, F. B. Dias, F. Galbrecht, U. Scherf, and A. P. Monkman, *Adv. Funct. Mater*., **2009**, *19*, 67–73. (DOI: 10.1002/adfm.200800313).

81 V. N. Bliznyuk, S. A. Carter, J. C. Scott, G. Klärner, R. D. Miller, and D. C. Miller, *Macromolecules,* **1999,** *32*, 361–369. (DOI: 10.1021/ma9808979).

82 J.-L. Lee, G. Klärner, and R. D. Miller, *Synth. Metals,* **1999**, *101*, 126. (DOI:10.1016/S0379-6779(98)01365-4).

83 U. Lemmer, S. Heun, R. F. Mahrt, U. Scherf, M. Hopmeier, U. Siegner, E. O. Gobel, K. Müllen, and H. Bassler, *Chem. Phys. Lett.,* **1995**, *240*, 373–379. (DOI:10.1016/0009-2614(95)00512-3).

84 Y. N. Hong, J. W. Y. Lam, and B. Z. Tang, *Chem. Commun.,* **2009**, *29*, 4332–4353. (DOI: 10.1039/B904665H).

85 W. Z. Yuan, Z. -Q. Yu, Y. Tang, J. W. Y. Lam, N. Xie, P. Lu, E. -Q. Chen, and B. Z. Tang, *Macromolecules*, **2011**, *44*, 9618–9628. (DOI: 10.1021/ma2021979).

86 B. J. Schwartz, *Annu. Rev. Phys. Chem*., **2003**, *54*, 141–172. (DOI: 10.1146/annurev.physchem.54.011002.10381).

87 F. J. M. Hoeben, P. Jonkheijm, E. W. Meijer, and A. P. H. J. Schenning, *Chem. Rev*., **2005**, *105*, 1491–1546. (DOI: 10.1021/cr030070z).

88 F. Ukert, Y. H. Tak, K. Müllen, and H. Bassler, *Adv. Mater.,* **2000**, *12*, 905–908. (DOI: 10.1002/1521-4095(200006)12:12<905).

89 K. H. Weinfurtner, H. Fujikawa, S. Tokito, and Y. Taga, *Appl. Phys. Lett.,* **2000**, *76*, 2502–2504. (DOI: org/10.1063/1.126389).

90 M. Gaal, E. J. W. List, and U. Scherf, *Macromolecules,* **2003**, *36,* 4236–4237. (DOI: 10.1021/ma021614m).

91 V. N. Bliznyuk, S. Carter, J. C. Scott, G. Klärner, R. D. Miller, and D. C. Miller, *Macromolecules,* **1999**, *32*, 361–369. (DOI: 10.1021/ma9808979).

92 J. L. Lee, G. Klärner, R. D. Miller, .*Chem. Mater*., **1999**, *11*, 1083–1088. (DOI: 10.1021/cm981049v).

93 G. Zeng,W.–L. Yu, S.–J. Chua, and W. Huang,. *Macromolecules*, **2002**, *35*, 6907–6914. (DOI: 10.1021/ma020241m).

94 I. Prieto, J. Teetsov, M. A. Fox, D. A. V. Bout, and A. J. Bard, *J. Phys. Chem. A*, **2001**, *105*, 520–523. (DOI: 10.1021/jp003566i).

95 J. Teetsov and D. A. V. Bout, *Langmuir*, **2002,** *18*, 897–903. (DOI: 10.1021/la011302x).

96 E. W. J. List, R. Guentner, P. S. de Freitas, and U. Scherf, *Adv Mater.,* **2002**, *14*, 374–378. (DOI: 10.1002/1521-4095(20020304)14).

97 L. Romaner, A. Pogantsch, P. Scanducci de Freitas, U. Scherf, M. Gaal, E. Zojer, and E. J. W. List, *Adv. Funct. Mater.*, **2003**, *13*, 597–601. (DOI: 10.1002/adfm.200304360).

98 E. Zojera, A. Pogantsch, E. Hennebicq, D. Beljonne, J.-L. Brédas, P. Scandiucci de Freitas, U. Scherf, and E. J. W. List, *J. Chem. Phys.,* **2002**, *117*, 6794–6802. (DOI: doi: 10.1021/ma071659t).

99 M. Sims, D. D. C. Bradley, M. Ariu, M. Koeberg, A. Asimakis, M. Grell, and D. G. Lidzey, *Adv. Funct. Mater*., **2004**, *14*, 765–781. (DOI: 10.1002/adfm.200490024).

100 W. Zhao, T. Cao, and J. M. White, *Adv. Funct. Mater*., **2004**, *14*, 783–790. (DOI: 10.1002/adfm.200305173).

101 J. Y. Li, A. Ziegler, and G. Wegner, *Chem. Eur. J.,* **2005**, *11*, 4450–4457. (DOI: 10.1002/chem.200401319).

102 C. Chi, C. Im, V. Enkelmann, A. Ziegler, G. Lieser, and G. Wegner, *Chem. Eur. J.*, **2005**, *11*, 6833–6845. (DOI: 10.1002/chem.200500275).

103 A. P. Kulkarni, X. Kong, and S. A. Jenekhe, *J. Phys. Chem. B,* **2004**, *108*, 8689–8701. (DOI: 10.1021/jp037131h).

104 X. Chen, H.-E. Tseng, J.-L. Liao, and S.-A. Chen, *J. Phys. Chem. B*, **2005**, *109*, 17496–17502. (DOI: 10.1021/jp052549w).

105 K. L. Chan, M. Sims, S. I. Pascu, M. Ariu, A. B. Holmes, and D. D. C. Bradley, *Adv. Funct. Mater*., **2009**, *19*, 2147–2154. (DOI: 10.1002/adfm.200801792).

106 M. Kuik, G. -J. A. H. Wetzelaer, J. G. Laddé, H. T. Nicolai, J. Wildeman, J. Sweelssen, and P. W. M. Blom, *Adv. Funct. Mater*., **2011**, *21*, 4502–4509. (DOI: 10.1002/adfm.201100374).

107 B. Arredondo, B. Romero, A. Gutiérrez-Llorente, A. I. Martínez, A. L. Álvarez, X. Quintana, and J. M. Otón, *Solid-State Electronics*, **2011**, *61*, 46–52. (DOI:10.1016/j.sse.2011.02.004).

108 M. R. Craig, M. M. De Kok, J. W. Hofstraat, A. P. H. J. Schenning, and E. W. Meijer, *J. Mater. Chem.,* **2003**, *13*, 2861–2862. (DOI: 10.1039/B308402G).

109 S. Y. Cho, A. C. Grimsdale, D. J. Jones, S. E. Watkins, A. B. Holmes, *J. Am. Chem. Soc*., **2007**, *129*, 11910–1191. (DOI: 10.1021/ja074634i).

110 D. Sainova, T. Miteva, H.-G. Nothofer, U. Scherf, I. Glowacki, J. Ulanski, H. Fujikawa, and D. Neher, *Appl Phys Lett.,* **2000**, *76*, 1810–1812. (DOI: org/10.1063/1.126173).

111 K. L. Chan, M. J. McKiernan, C. R. Towns, and A. B. Holmes, *J. Am. Chem. Soc*., **2005**, *127*, 7662–7663. (DOI: 10.1021/ja0508065).

112 G. Klärner, M. H. Davey, W.-D. Chen, J. C. Scott, and R. D. Miller, *Adv. Mater*., **1998**, *10*, 993–997. (DOI: 10.1002/(SICI)1521-4095(199809)10).

113 G. Klärner, J.-I. Lee, M. H. Davey, and R. D. Miller, *Adv. Mater.,* **1999,** *11*, 115–119. (DOI: 10.1002/(SICI)1521-4095(199902)11).

114 B. Liu, W.-L. Yu, Y.-H. Lai, and W. Huang, *Chem. Mater.,* **2001**, *13*, 1984–1991. (DOI: 10.1021/cm0007048).

115 M.-J. Park, J. Lee, I. H. Jung, J.-H. Park, H. Kong, J.-Y. Oh, D.-H. Hwang, and H.-K. Shim, *J. Polym. Sci., Part A: Polym. Chem.*, **2010**, *48*, 82–90. (DOI: 10.1002/pola.23761).

116 J. Salbeck, B. Bunsenges, *Phys Chem*., **1996**, *100*,1666–1675. (DOI: 10.1021/jp952004+).

117 Y. Wu, J. Li, Y. Fu, and Z. Bo, *Org Lett*., **2004**, *6*, 3485–3487. (DOI: 10.1021/ol048709o).

118 Y. Tseng, P. Shih, C. Chien, A. Dixit, and C. Shu, *Macromolecules*, **2005**, *38*, 10055–10060. (DOI: 10.1021/ma051798f).

119 W.-L. Yu, J. Pei, W. Huang, and A. J. Heeger, *Adv. Mater.,* **2000**, *12*, 828–831. (DOI: 10.1002/(SICI)1521-4095(200006)12).

120 D. Marsitzky, J. Murray, J. C. Scott, and K. R. Carter, *Chem. Mater.,***2001**, *13*, 4285–4289. (DOI: 10.1021/cm010282h).

121 A. Donat-Bouillud, I. Levesque, Y. Tao, M. D'Iorio, S. Beaupré, P. Blondin, M. Ranger, J. Bouchard, and M. Leclerc, *Chem. Mater*., **2000**, *12*, 1931–1936. (DOI: 10.1021/cm0001298).

122 I. Lévesque, A. Donat-Bouillud, Y. Tao, M. D'Iorio, S. Beaupré, P. Blondin, M. Ranger, J. Bouchard, and M. Leclerc, *Synth. Met.,* **2001**, *122*, 79–81. (DOI:10.1002/macp.201600050).

123 S. Beaupré and M. Leclerc, *Macromolecules*, **2003**, *36*, 8986–8991. (DOI: 10.1021/ma035064j).

124 C. D. Muller, A. Falcou, N. Reckefuss, M. Rojahn, V. Wiederhirn, P. Rudati, H. Frohne, O. Nuyen, H. Becker, and K. Meerholz, *Nature*, **2003**, *421*, 829–833. (DOI:10.1038/nature01390).

125 Y. Li, J. Ding, M. Day, Y. Tao, J. Lu, and M. D'iorio, *Chem Mater.,* **2004,** *16*, 2165–2173. (DOI: 10.1021/cm030069g).

126 C. Ego, A. C. Grimsdale, F. Uckert, G. Yu, G. Srdanov, and K. Müllen, *Adv. Mater.,* **2002**, *14*, 809–811. (DOI: 10.1002/1521-4095(20020605)14).

127 M. S. Liu, X. Jiang, S. Liu, P. Herguth, and A. K.-Y. Jen, *Macromolecules,* **2002**, *35,* 3532–3538. (DOI: 10.1021/ma011790f).

128 X. Zhan, Y. Liu, X. Wu, S. Wang, and D. Zhu, *Macromolecules,* **2002**, *35,* 2529–2537. (DOI: 10.1021/ma011593g).

CHAPTER 3

Synthesis of 4-Substituted 2,7-Dibromo-9,9-dialkyl(diaryl)-fluorenes as Monomers for 4-Functionalised Polyfluorenes

3.1 Introduction

3.1.1 Substitution at C-9 in polyfluorenes

Polyfluorenes (Figure 3.1) are efficient blue light emitting polymers and they have been widely studied in many organic electronics applications, first of all in OLEDs for full colour displays, but also in lasing, organic field-effect transistors, photovoltaics etc.[1,2,3] Also, fluorene building blocks have been widely used to construct a wide range of conjugated copolymers with tunable properties. This has been reviewed in details in Chapter 2. However, most functionalisation of the fluorene core were made at the C-9 position of the fluorene moiety. Such functionalisation allowed the solubility of the polymers in common organic solvents, to change the morphology of the polymers films,[4] to bring some interesting properties to materials (e.g. liquid crystallinity, polarized emission),[5,6] to improve the stability of materials (e.g. when alkyl solubilising groups as in **3.1** have been replaced by aryl groups as in **3.3** the formation of fluorenone defects in polymers is decreased), to attach different side groups to make polymers water/alcohol-soluble (e.g. anionic or cationic ends in the side groups, **3.3)**[7,8,9,10,11] etc.

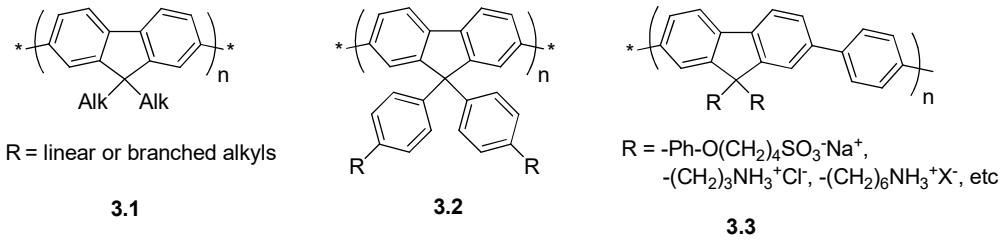

Figure 3.1 9,9-Disubstituted polyfluorenes (PFs) **3.1**–**3.3**.

However, all these functionalisations weakly affect the electronic energy levels of the backbone, because functionalisations have been performed at the sp^3-hybridised C-9 carbon atom with a weak transmission of electronic effects (mainly inductive effect). Moreover, because the aims of C-9 functionalisation were to make the polymers soluble and processable,

generally only alkyl/aryl groups have been used with weak electron donating effect (**3.1**, **3.2**). It was somewhat stronger in the case of e.g. 4-diarylaminophenyl-substituents at C-9 of fluorene and improved device performance has been demonstrated (see Chapter 2),[12] but in general, tunability of electronic properties through such functionalisation cannot be high. Of course, the characteristics of fluorene-based polymers can be efficiently changed by copolymerisation with other aromatic/heteroaromatic electron-rich or electron-deficient building blocks and this represents the main strategy of tuning frontier orbital energy levels, absorption-emission and other properties of copolymers for electronics.

On the other hand, it seems obvious that substitutions in the benzene ring of the fluorene moiety could be quite an efficient way of tuning the electronic state of the polymer backbone compared to substitution at the C-9 atom offering many new prospects of fluorene-based conjugated polymers for organic electronic applications. This not only includes the synthesis of novel families of polymers/copolymers, but also offer the way of fine tuning the properties of polymers already described in the literature with a great performance in one or another application, where further "ultra-fine" tuning the energy levels is required to achieve the highest performance in devices. Surprisingly, before our work, there was no attention paid to this opportunity, except one work from Leclerc's group[13] discussed below and in the introduction to Chapter 4.

3.1.2. 3,6-Disubstituted fluorenes for polyfluorenes functionalised in the benzene rings

So far, we have found very few examples in the literature on poly/oligofluorenes and fluorene dendrimers substituted in the benzene rings (see the introduction in Chapter 4). One of these is poly(3,6-dimethoxy-9,9-dihexylfluorene) (**3.8**, Scheme 3.1). In 2003, Leclerc *et al* reported the synthesis and properties of polyfluorene **3.8,** which was prepared by Yamamoto polymerisation of 2,7-dibromo-3,6-dimethoxy-9,9-dihexylfluorene (**3.7**).[13] The synthetic route for the monomer **3.7** and its polymerisation to homopolymer **3.8** are shown in Scheme 3.1.

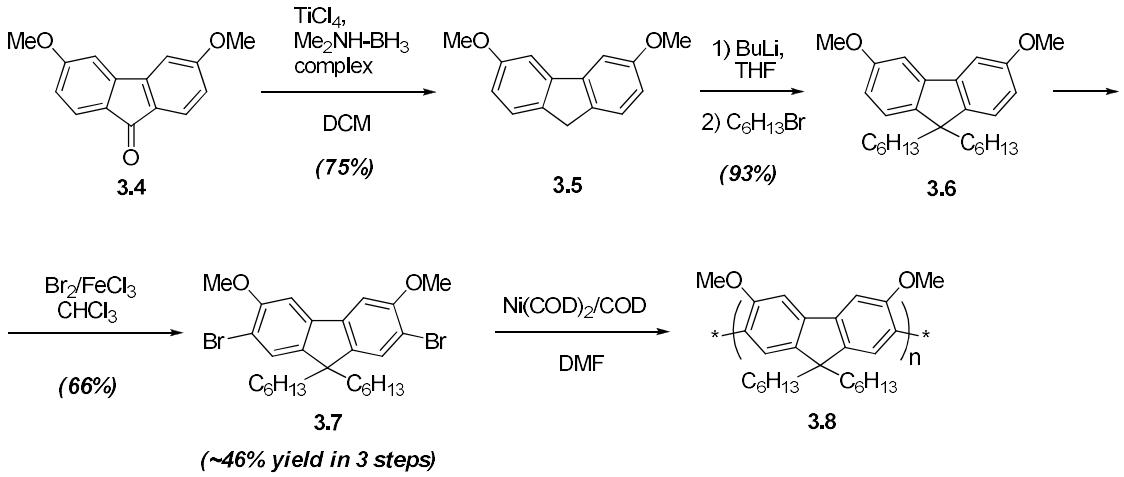

Scheme 3.1 Synthetic route to 2,7-dibromo-3,6-dimethoxy-9,9-dihexylfluorene (**3.7**) and its polymerisation to polymer **3.8**.[13]

The monomer **3.7** was prepared from 3,6-dimethoxyfluorenone (**3.4**) using common reactions of reduction of carbonyl fragment to **3.5**, alkylation at C-9 positions (**3.6**) and bromination of intermediate **3.6** to monomer **3.7**, which are the steps widely used in fluorene chemistry to obtain dibromo-monomers for polyfluorenes. However, starting 3,6-dimethoxyfluorenone cannot be obtained by direct functionalisation of commercially available fluorene (or fluorenone) cores, and it was synthesised by multi-step reactions from 2,4-dimethoxybenzoic acid as described by Schuster and co-workers (Scheme 3.2).[14] The key point in their synthesis was that they exploited the analogy of oxazoline chemistry of previous work of Meyer et al.[15] who showed the ortho-directing effect of oxazoline performing selective substitution of the ortho-methoxy group in aryloxazolines with aryllithium or arylmagnesium reagents.

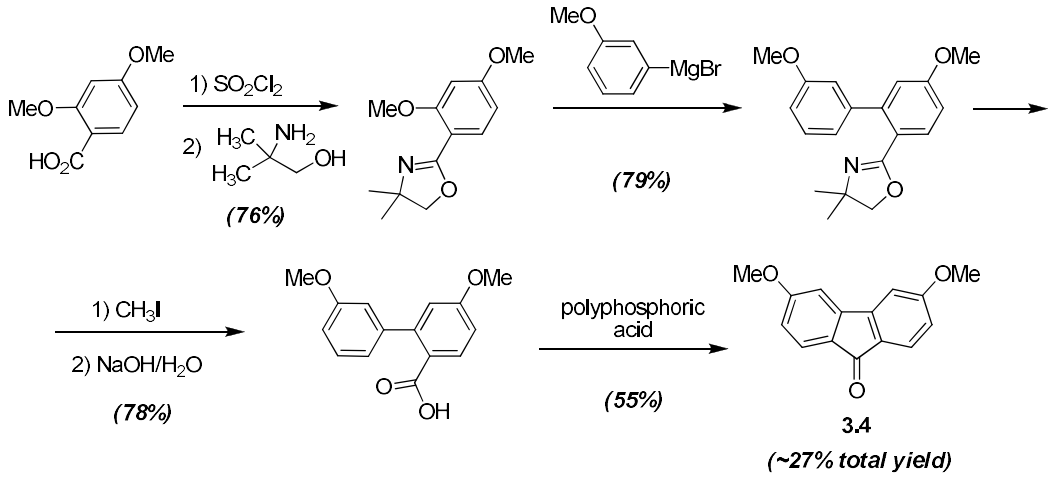

Scheme 3.2 Synthesis of 3,6-dimethoxyfluorenone (**3.4**).[14]

Introduction of two strong electron-donating methoxy-groups made monomer **3.**7 to be a stronger donor that increased the ionisation potential of the resulting polymer **3.8** by ca. 0.2 eV compared to corresponding poly(9,9-dihexylfluorene).[13] However, apart from the long multi-step way to monomer **3.7**, one problem with such substitution pattern at positions 3,6- of the fluorene moiety is that the MeO-substituents are in the ortho position of neighbouring fluorene moieties in the polymer chain, bringing an additional steric hindrance between the fluorene moieties of the polymer **3.8** (Figure 3.2). Such sterics exist even for unsubstituted polyfluorene (**3.1**, Alk = C_6H_{13}) for which the dihedral angles between fluorene moieties are ca. 37° that decrease the overlap of π-orbitals of neighbouring fluorene units and leads to a decrease in the conjugation length of the polymer. Additional introduction of two methoxy groups further increases this dihedral to ~54° (our calculations, Figure 3.2).

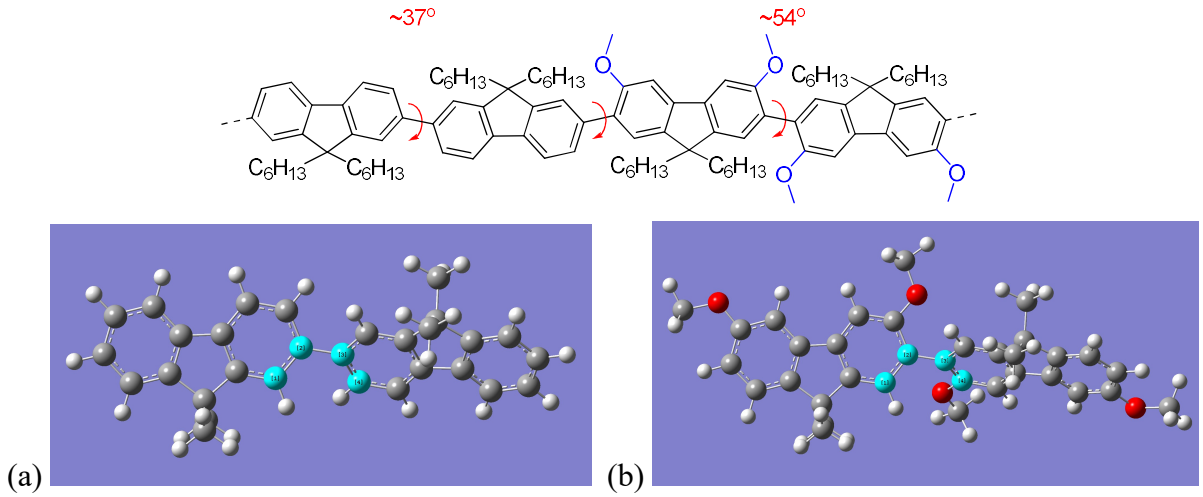

Figure 3.2 (top) Structural representation of polyfluorene, schematically showing the difference in the dihedral angles between the substituted and unsubstituted fluorene moieties, and (bottom) B3LYP/6-31G(d) calculations for the dimers of 9,9-dimethylfluorene (a) and 3,6-dimethoxy-9,9-dimethylfluorene (b). Dihedral angles (highlighted in cyan) are 36.9° (a) and 54.4° (b); (this work).

From this point of view, while substitution at positions 3,6 (as well as in positions 1,8) can be used to tune the electronic properties of polyfluorenes by introduction of corresponding electron-donating/electron-accepting substituents, they have the serious disadvantage of a steric effect on the polymer backbone. In contrast to that, positions 4 and 5 of the fluorene moiety are free from this drawback and they seem more suitable places for fluorene functionalisations to tune the electronic properties of polyfluorenes (Figure 3.3). It should also be mentioned that, while formally C-4 is a meta-position toward the polymer-link site at the same benzene ring (C-2), yet substituents at C-4 can effect the fluorene ring (and

the π-system of the polyfluorene main chain) by a mesomeric effect as well via resonance through the bridge between the benzene rings of the fluorene moiety (Figure 3.3), thus donor/acceptor effects of substituents at C-4 should be rather strong.

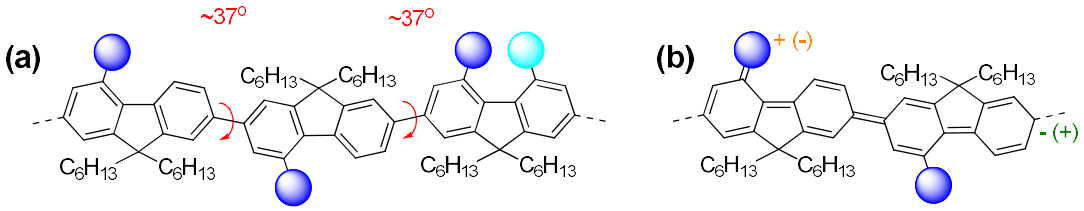

Figure 3.3 (a) Structural representation of polyfluorene, showing that substituents at positions 4 and 5 do not affect the dihedral angles between fluorene moieties; (b) structural representation of polyfluorene, showing the resonance effect of the substituents at position 4 on the polymer backbone.

3.1.3 Aims and research objectives: strategies to 4-substituted fluorenes

The aim of this work is a design, synthesis and studies of a novel family of polyfluorenes substituted at position 4. This novel type of functionalisation of fluorenes for conjugated polymers represents an interesting way to homopolymers with tunable properties. An introduction of electron withdrawing (EWG) or electron donating groups (EDG) in position 4 of the fluorene moiety should efficiently tune HOMO and LUMO energies of polymers, and synthetically a wide range of substituents can be introduced. Issues of the effects of these groups on the band gaps of polyfluorenes, their morphology and intermolecular interactions compared to unsubstituted poly(9,9-R_2-fluorenes) are also very important for materials applications. Consequently, we needed an elaboration of methods of synthesis of 2,7-dibromo-4-X-9,9-R_2-fluorenes, which can be used as starting monomers for the synthesis of polyfluorenes by Ni-promoted Yamamoto polymerisation or Pd-catalysed Suzuki coupling polymerisation. We considered three approaches for synthesis of 4-substituted 2,7-dibromofluorenes, which can be used as monomers for the synthesis of polyfluorenes **X-PF8** and **X-PF6/8,** as shown in Scheme 3.3. An importance of elaboration of synthetic methods for such monomers is more broad, as they can be used not only to access homopolymers (like **X-PF8** and **X-PF6/8**), but they also open the door to a large number of conjugated copolymers based on 4-substituted fluorenes.

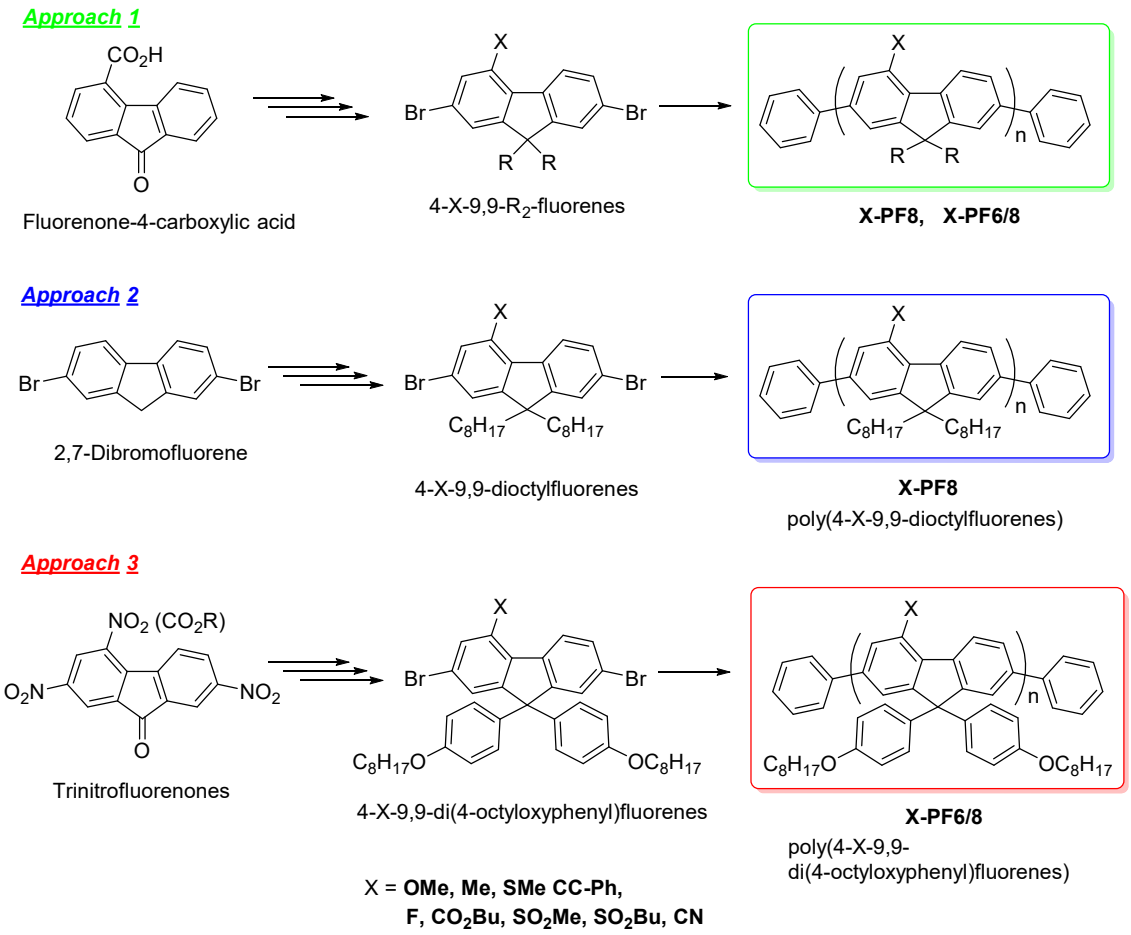

Scheme 3.3 Synthetic approaches to 4-substituted polyfluorenes.

Thus, the main objective of the research described in this chapter was developing synthetic methods to access 4-substituted 2,7-dibromofluorenes and below we describe in more details our strategic approaches to the monomers shown in Scheme 3.3.

The first approach was based on using fluorenone-4-carboxylic acid (**3.10**), which can be easily and quantitatively obtained by cyclisation of commercially available diphenic acid (**3.9**) in concentrated sulphuric acid. Previous attempts of its selective bromination at positions 2,7 were unsuccessful, giving a mixture of 2,7-dibromo- (**3.12**) and 2,6,7-tribromo-acids (**3.13**), which cannot be separated by either crystallisation or column chromatography (Scheme 3.4).[16] Obviously, the first bromination occurs at position 7. The second bromination can occur at position 2 (directing effect of the fluorene moiety), but due to the deactivation effect of the carboxy group at position 4, it competes with ortho-bromination at position 6 giving a mixture of non-separable products. Conversion of acid **3.10** into esters **3.11** with different R groups and attempts to brominate them, gave similar results (i.e. 4-CO_2R-2,7-dibromofluorenones (**3.12**) contaminated with 20–25% of tribromo-esters **3.13**.[16] While some esters have been separated by repetitive (4–5 times) flash chromatography on a ~100mg scale to obtain pure samples to prove their structures, the retention times of both products

(dibromo- and tribromo-) seems a contradiction for making synthesis of dibromo-derivatives (**3.12**) by this route to be inattractive and impractical.

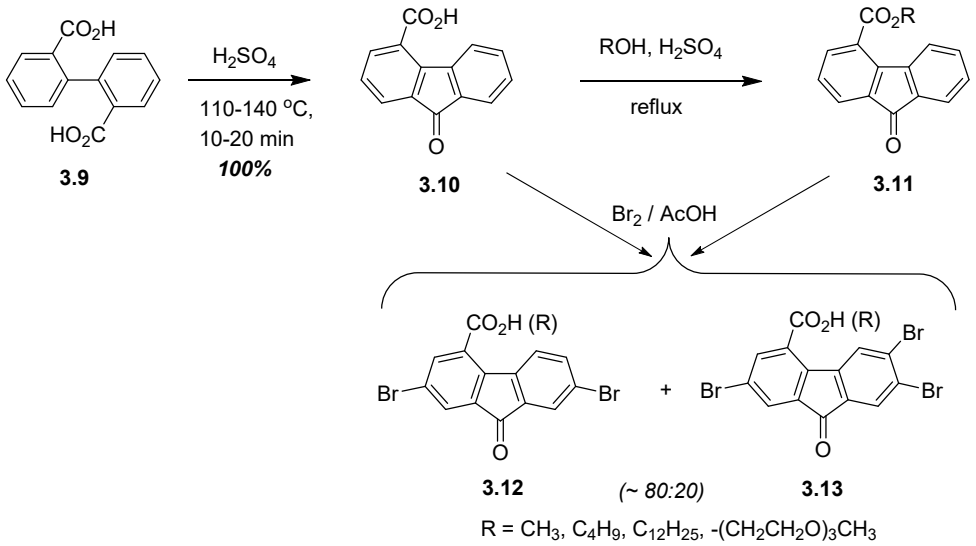

Scheme 3.4 Synthesis of 2,7-dibromo- and 2,6,7-tribromofluorenone-4-carboxylic acids and their esters.[16]

Therefore, continuing these studies, in our approach 1, we considered that iodination of fluorene-4-carboxylic acid (**3.14**) might work better because of less harsh conditions for the halogenation and be more selective because of larger size and lower reactivity of iodine compared to bromine (increased sterics in the case of iodination might decrease the second iodination in position 6). In the case of success of the key iodination step, this might be a convenient way for a wide range of 4-functionalised fluorenes (acid, esters, amides, nitrile etc) as depicted in Scheme 3.5.

The second approach is based on easily accessible 2,7-dibromofluorene. Electrophilic substitution in the fluorene moiety is known to occur at position 2, then 7, and then in position 4. So, starting from 2,7-dibromofluorene we could introduce a nitro group in position 4 of the fluorene moiety and, after its reduction to an amino group, the latter can be converted into a wide range of other groups using diazonium salts (Scheme 3.6).

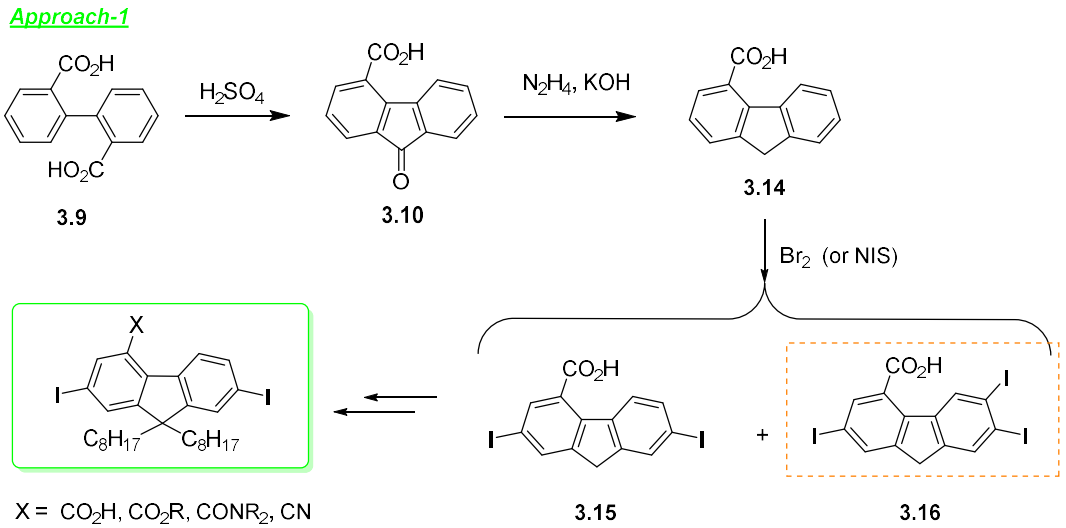

Scheme 3.5 *Approach 1* 4-substituted 2,7-diiodofluorenes from 4-fluorenone-4-carboxylic acid.

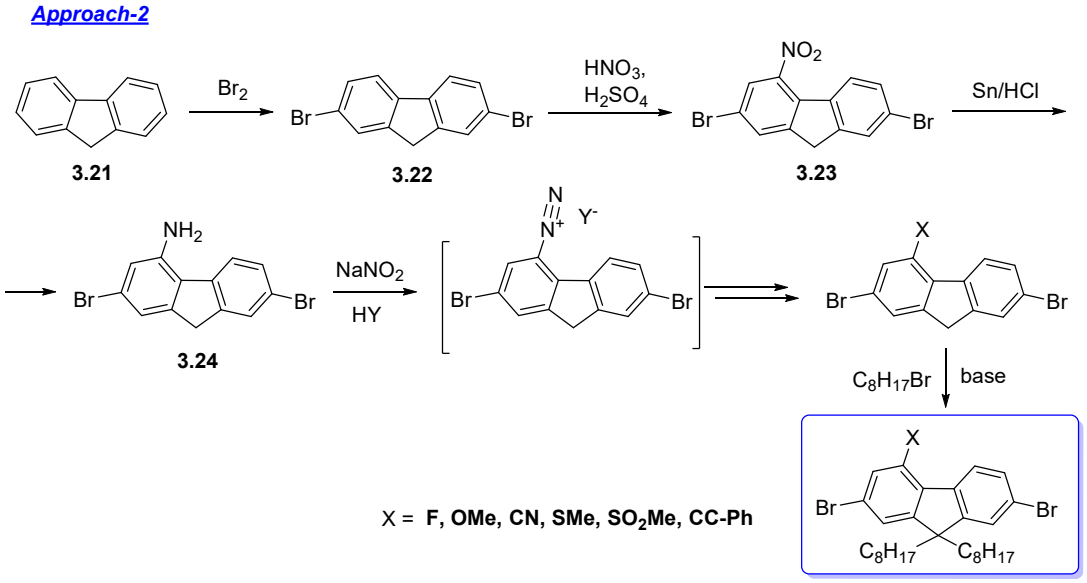

Scheme 3.6 *Approach 2* to 4-X-2,7-dibromofluorenes through nitration of 2,7-dibromofluorene at position 4 and further transformation of the NO_2 group in a wide range of other substituents.

The third approach is based on completely different chemistry. Instead of electrophilic substitution in the fluorene ring, it uses – as a key step – selective nucleophilic aromatic substitution in 2,4,7-trinitrofluorenone (**3.19**) at position 4 with O- or S-nucleophiles and transformation of 2,7-nitrogroups into Br groups (reduction and further transformation through diazonium salts as above) (Scheme 3.7). In addition, diphenic acid (**3.19**) can be cyclised and nitrated to give known 2,7-dinitrofluorenone-4-carboxylic acid (**3.17**), which can be converted into esters. Nitro groups in these esters can be converted into Br in a similar fashion (Scheme 3.7). When using alkyl thiol as a nucleophile for replacing the 4-nitrogroup,

the formed electron-donating alkylthio-group can also be oxidised into the electron-withdrawing alkyl sulfonyl group –SO_2R, expanding the range of functional groups at position 4 of the monomers. Potentially, intermediate 4-X-2,7-dibromofluorenones (**3.20**) can be reduced into the corresponding fluorenes and then alkylated to give a series of 9,9-dialkylated monomers, as in approach 2 (Scheme 3.6). However, as such 4-X-9,9-dialkylfluorenes can be available through approach 2, in this case, we have decided to use these fluorenone monomers **3.20** in the two last steps to make 9,9-diarylfluorenes expanding the library of 4-functionalised fluorene monomers (Scheme 3.7). The problem of relatively low stability of poly(9,9-dialkylfluorenes) due to their oxidation to form keto-defects in the polymer chain and the appearance of green emission have been discussed in Chapter 2. With this respect, 9,9-diaryl-substituted polyfluorenes show better stability toward oxidation (thermal, photochemical, in device operation) and more pure blue colour emission in OLED devices.[17]

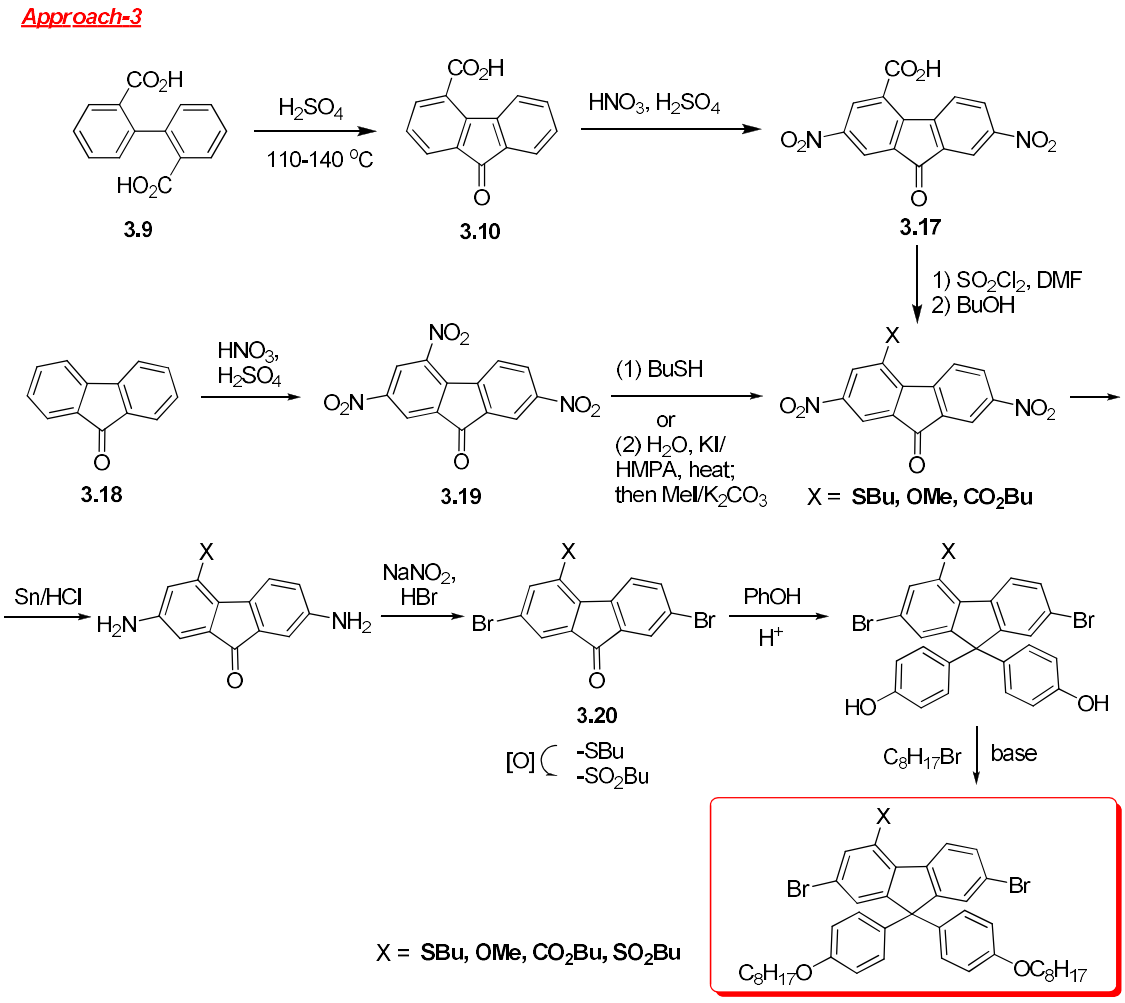

Scheme 3.7 Approach 3 to 4-X-2,7-dibromofluorenes from polynitrofluorenones exploiting selective nucleophilic aromatic substitution of the 4-NO_2 group and transformation of 2,7-NO_2 groups into Br (through reduction and diazotization reactions).

Synthesis and studies of polymers obtained from these monomers will be described in Chapter 4.

3.2 Results and Discussion

3.2.1 Approach-1: attempts to synthesise 4-substituted fluorene monomers by halogenation of fluorene-4carboxylic acid

The previous attempts of direct bromination of fluorenone-4-carboxylic acid (**3.10**) and its esters **3.11** gave the inseparable mixture of dibromo- and tribromo-derivatives **3.12** and **3.13** (Scheme 3.4). Therefore, we studied iodination of more reactive (consequently, milder conditions for the reaction) fluorene-4-carboxylic acid (**3.14**), which can be easily obtained by Kishner-Wolff reduction of acid **3.14** with hydrazine.[18]

We also hoped that this might be a more successful reaction, considering the lower reactivity of I^+ compared to Br^+ (from a general principle of reactivity-selectivity). Additionally, as iodine is a larger atom than bromine, this might further decrease the rate of iodination of the fluorene moiety at the ortho-position 6, after insertion of iodine at position 7 in the first step of the iodination reaction due to steric reasons. So, we performed two attempts of iodination of acid **3.14** using I_2/KIO_3/AcOH or *N*-iodosuccimide/H_2SO_4/AcOH. However, similarly to previous attempts, in both cases, the target diiodo-derivative **3.15** was substantially contaminated with triiodo by-product **3.16** and their separation was problematic (Scheme 3.8).

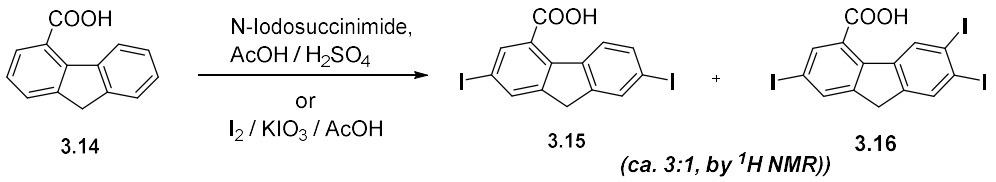

Scheme 3.8 Iodination of fluorene-4-carboxylic acid (**3.14**).

Because we were looking for reasonably good procedures scalable to ca. a ten-gram scale of these starting materials in a pure state, we decided not to continue optimisation of the reaction conditions by this route taking into account similarly bad results on selectivity of halogenation of fluorene- or fluorenone-4-carboxylic acids (or esters) and problems with the separation of dihalo/trihalo-compounds.

3.2.2 <u>Approach-2</u>: Synthesis of 4-substituted 2,7-dibromo-9,9-dioctylfluorene monomers from 2,7-dibromofluorene.

In this approach (Scheme 3.6), we started with 2,7-dibromofluorene (**3.22**), which was prepared from commercially available fluorene (**3.21**) in one batch on a 200 g scale following the literature procedure (Scheme 3.9).[19] The crude product was recrystallised from acetic acid giving 80 % yield of desired 2,7-dibromofluorene (**3.22**). In the second step, following the literature procedure,[20] 2,7-dibromofluorene (**3.22**) was nitrated by a mixture of HNO_3/H_2SO_4 (1:1, v:v) to give 2,7-dibromo-4-nitrofluorene (**3.23**). Here, we have slightly modified the literature procedure and used ethylacetate for recrystallisation of the crude product (instead of using toluene:EtOH, 1:1 as described in[20]) allowing to scale up the synthesis and increase the yield of pure product **3.23** from 63 to 72% (Scheme 3.9).

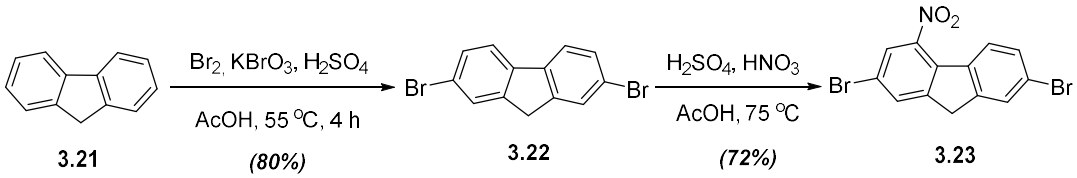

3.21 3.22 3.23

Scheme 3.9 Synthesis of 2,7-dibromo-4-nitrofluorene (**3.23**).[19,20]

Initial reduction of 2,7-dibromo-4-nitrofluorene (**3.23**) to 2,7-dibromo-4-aminofluorene (**3.24**) was done by powder tin with concentrated aqueous HCl in ethanol at reflux condition, as was reported by the Müllen group (Scheme 3.10).[21] However, we have found that the reaction works not as cleanly as described, at least on scaling up. Thus, in an attempt to follow this procedure on a 40 g scale batch we found that along with the required 2,7-dibromo-4-aminofluorene (**3.24**), ca. 20% of a second product was formed in the reaction, as was evidenced by ^{1}H NMR of the crude product. Thin layer chromatography (TLC) analysis showed two very close spots and all our attempts to purify the crude product by recrystallisation in various solvents (toluene, ethanol, dioxane, ethylacetate, chlorobenzene and THF, or their mixtures) were unsuccessful. After several attempts, we were able to separate these two products in a small amount (~100 mg) by flash chromatography in EA/PE (1:1, v/v), eluting first the target compound **3.24** followed by the undesired by-product, which was identified as the chlorinated amino compound **3.25** (Scheme 3.10).

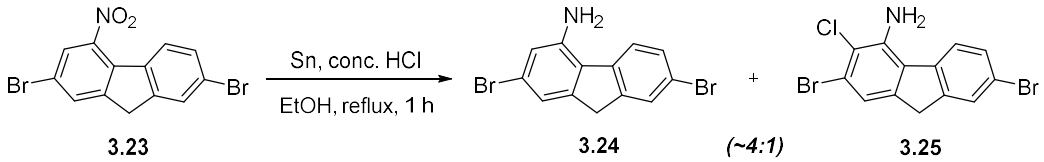

Scheme 3.10 Two products formed from a scale-up of the reduction reaction of 2,7-dibromo-4-nitrofluorene (**3.23**) by literature procedure (Sn/HCl/EtOH).[21]

The separated and purified by-product was analysed by ^{1}H NMR, ^{1}H-^{1}H COSY, ^{13}C NMR and MS proving its structure as 2,7-dibromo-3-chloro-4-aminofluorene (**3.25**). The ^{1}H NMR spectrum (Figure 3.4) indicates the presence of four non-equivalent protons in the benzene rings of the fluorene moiety (compared to 5 protons in **3.24**). Very close chemical shifts of protons at the 5 and 6 positions in compound **3.25** result in the disappearance of the H-H splitting of the signals to estimate their *J* coupling constants. Thus, we measured ^{1}H-^{1}H COSY NMR spectrum to look at interacting protons. ^{1}H-^{1}H COSY NMR clear showed a correlation between protons of H-5,6 with H-8, and H-8 with H-9 proton of the CH_2 group, indicating that this benzene ring remains unchanged during the reaction. H-9 of CH_2 group also shows a second correlation with H-1, thus it becomes clear that the substitution occurs at position C-3 (Figure 3.5). ^{13}C NMR spectrum showed the required number of carbons (1 CH_2 and 12 non-equivalent aromatic carbons, 4 of which are of higher intensity assuming C-H carbons). The mass spectrum showed the molecular ion with a mass (and isotope pattern), which corresponds to the replacement of one proton in the main product **3.24** by a chlorine atom (Figure 3.6). All these data confirmed the structure of this product as compound **3.25** chlorinated at position 3.

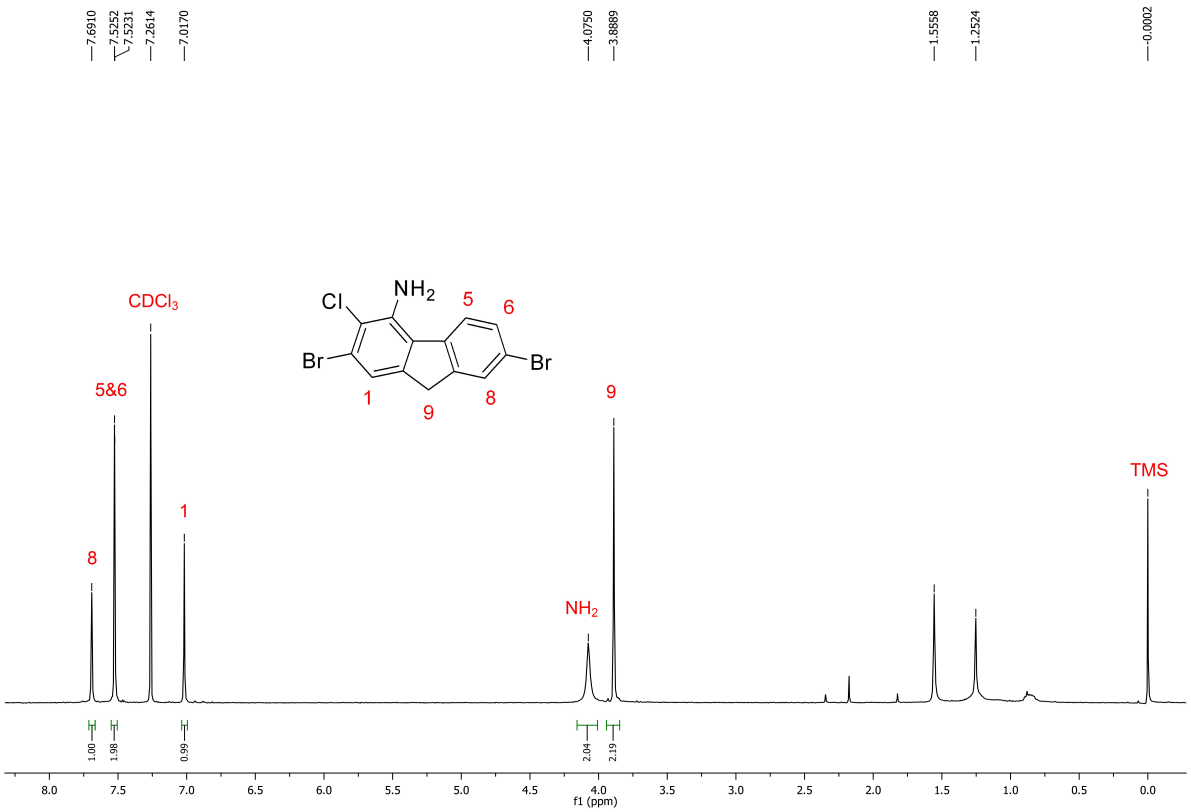

Figure 3.4 ^{1}H NMR spectrum of 2,7-dibromo-3-chloro-4-aminofluorene (**3.25**), with signals assignments.

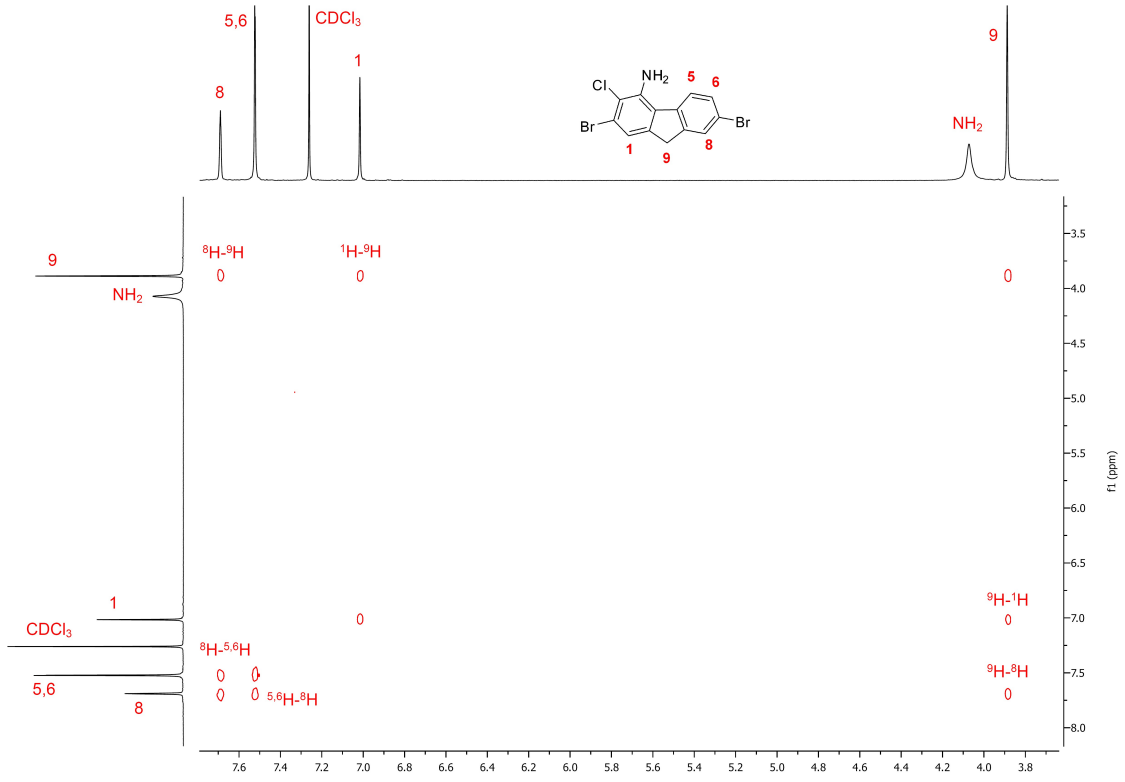

Figure 3.5 ^{1}H-^{1}H COSY spectrum of 2,7-dibromo-3-chloro-4-aminofluorene (**3.25**), showing correlations between the protons.

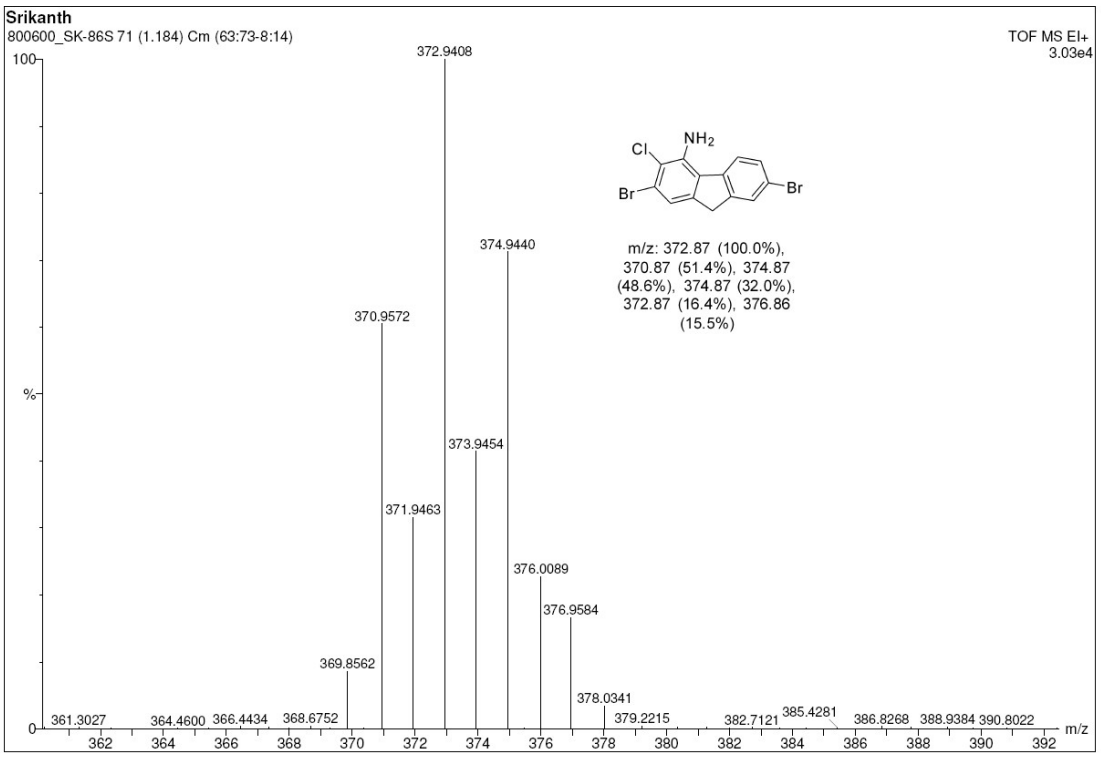

Figure 3.6 TOF EI+ mass spectrum of 2,7-dibromo-3-chloro-4-aminofluorene (**3.25**).

Formation of such a product is quite unusual and was surprising for us (i.e. electrophilic substitution at the benzene ring in the reductive reaction with Sn/H^+Cl^-, where chlorine is formally a nucleophile; we excluded nucleophilic substitution as the aromatic ring is not activated by an electron-withdrawing groups required for S_NAr substitution). So, we can speculate how this compound **3.25** can be formed as a by-product. It is well known that not only Sn but also $SnCl_2$/HCl is used in reductions of the nitro group into an amino group, and consequently, it is oxidised to $SnCl_4$ during this process. We assume that being a strong Lewis acid, stannous tetrachloride $SnCl_4$ can act as a chlorinating agent for highly activated aminofluorene **3.24** at high temperature electrophilically attacking compound **3.24** at the C-3 position to give by-product **3.25**.

Taking into account the difficulties in the separation of target compound **3.24** and by-product **3.25** on a large scale, we had been looking at reaction conditions, which would avoid the formation of by-product **3.25**. In optimising the reaction conditions, we considered that decreasing the temperature and diluting the reaction mixture with water (which might solvate and partly hydrolyse the $SnCl_4$ formed) might decrease or completely avoid the formation of by-product **3.25**. Really, performing the reduction reaction with tin and a mixture of concentrated HCl/H_2O (1:1) in ethanol at 60 °C for 3 h resulted in target 2,7-dibromo-4-aminofluorene **3.24** as a pure sample, with a high yield of 88% (Scheme 3.11).

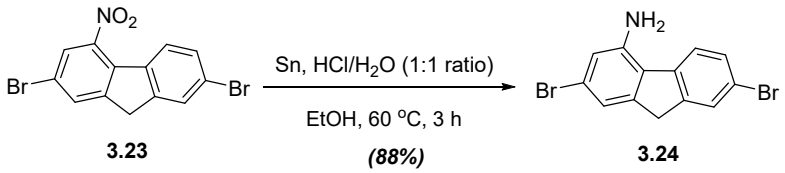

3.23 3.24

Scheme 3.11 Synthesis of 2,7-dibromo-4-aminofluorene (**3.24**).

Aminofluorene **3.24** was used as the key starting compound to access a series of 4-substituted 2,7-dibromofluorenes through diazonium chemistry. In the synthesis of iodofluorene **3.27**[21] and hydroxyfluorene **3.26**, diazotization with $NaNO_2$ was performed in sulfuric acid (instead of the more commonly used HCl, to avoid formation of 4-chloro by-products) at 0 ^oC and the formed diazonium salt was involved *in situ* in nucleophilic substitution reaction with water or KI at heating, resulting in the desired products 4-hydroxy- and 4-iodofluorenes, **3.26** and **3.27**, respectively.

For introducing the fluorine group, two-steps process was applied. Aminofluorene **3.24** was first diazotized using $NaNO_2$ in concentrated (48%) tetrafluoroboric acid to give the green coloured diazonium salt (**3.28**) which was precipitated from the reaction mixture and isolated by filtration. In the second step, following the Balz-Schiemann reaction,[22] the diazonium salt was heated to reflux in high boiling point solvent (xylene). Thermal decomposition of tetrafluoroborate compound **3.28** afforded the corresponding 2,7-dibromo-4-fluorofluorene (**3.29**) inwith a moderate yield (Scheme 3.12). Its structure was confirmed by ^1H NMR and ^{19}F NMR (the ^1H NMR shows nice F-4 coupling with adjacent H-3).

In a similar fashion, following the same conditions for diazotization of **3.24** as above ($NaNO_2/H_2SO_4$), and following the reaction of the formed diazonium salt with dimethyl disulphide, MeS-SMe, we hoped to get 2,7-dibromo-4-methylthiofluorene (**3.30**). However, the reaction failed and by flash chromatography of the crude mixture, we surprisingly isolated three different products. First, eluting with PE, two minor products have been isolated with low yields of 7.4% and 11.4%, for which we assigned the structures as methylthio-derivatives **3.31** and **3.32**, correspondingly (basing on their ^1H NMR spectra; particularly three doublets with J ~ 8 Hz in **3.31** indicated that MeS- group is at C-1 position). The third product was isolated by further elution in PE/EA (4:1, v:v) and, after repeated flash chromatography with gradient PE/EA solvents, its NMR and MS analysis indicated the structure **3.33** (Scheme 3.13).

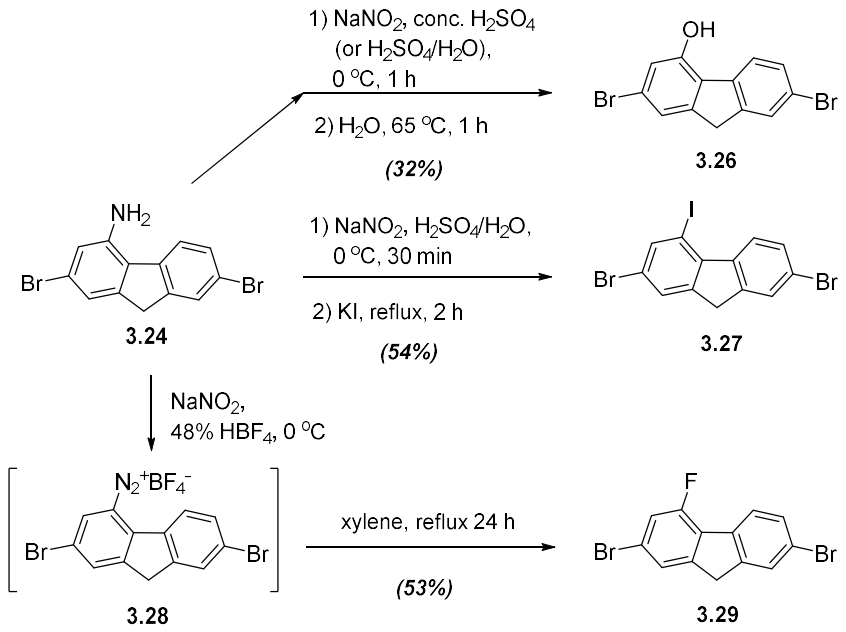

Scheme 3.12 Synthesis of 2,7-dibromo-4-X-fluorenes **3.26**, **3.27**[21] and **3.29** via diazonium chemistry.

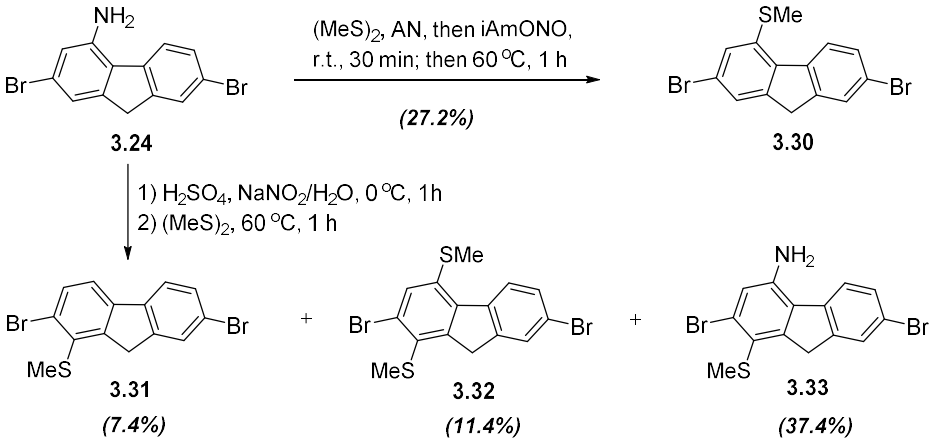

Scheme 3.13 Synthesis of 2,7-dibromo-4-methylthiofluorene (**3.30**) in nonaqueous neutral conditions and side products **3.31**–**3.33** forming in "usual" diazotization reaction.

We did not study this reaction in detail (as no target product **3.30** was obtained in this reaction), but we can speculate how these products can be formed (Scheme 3.14). Once diazonium salt **3.24a** is formed, it can react to give the target product **3.30**. On the other hand, it is well known that diazonium salts as N-electrophiles (and strong oxidising agents) can react with various nucleophiles at its terminal nitrogen atom (e.g. Ref.[23]). In the case of the reaction with dimethyl disulphide, this should give azo-product **3.24b** and generate strong electrophile species MeS^+ (this is a key point compared to the reaction of diazonium salts with O- or C-nucleophiles). Compound **3.24b** can be hydrolysed in the reaction mixture to

regenerate starting aminofluorene **3.24**, and both **3.24** and **3.24b** can undergo electrophilic attack by MeS^+ with substitution at position 1, to give compound **3.33** (in the case of **3.24c**, after hydrolysis of an intermediate **3.24c).** Also, compound **3.24c** can give compound **3.31**. Our target 4-methylthiofluorene **3.30**, if it is formed in the reaction mixture, can also be undergoing electrophilic attack by MeS^+ resulting in the disubstituted product **3.32**. We understand that this scheme is speculative and not free from criticism, but it seems, in general, it suggests possible pathways for the formation of these unexpected products (Scheme 3.14).

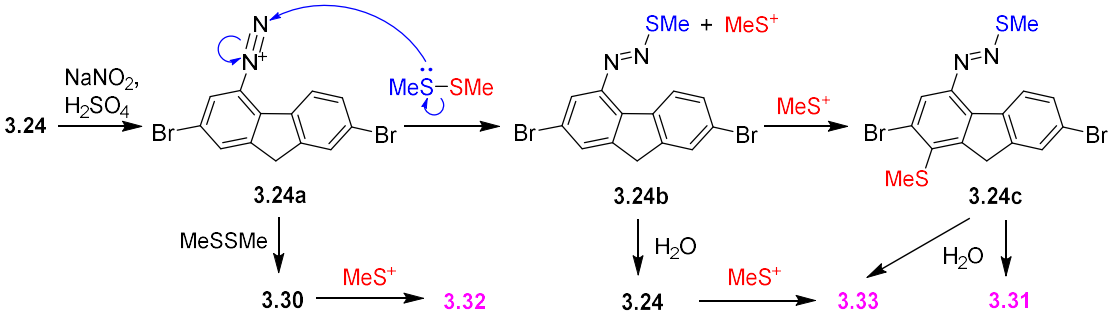

Scheme 3.14 Possible pathways for transformations of aminofluorene **3.24** into products **3.31**–**3.33** during diazotization / reaction with dimethyl disulphide.

Therefore, we tested another method for conversion of the amino group into a methylthio group, which is based on the reaction of aromatic/heteroaromatic amines with alkylnitrites and dialkyl disulphides in non-aqueous media in neutral conditions.[24,25,26,27] (It seems, that the mechanism of this reaction is not well understood yet, compared to classical diazotization reactions[24]). Adopting this method to aminofluorene **3.24**, we were able to obtain the desired 2,7-dibromo-4-methylthiofluorene (**3.30**) with 27% yield by reaction with a mixture of isopentylnitrite/dimethyl disulphide on gentle heating at 60 °C (Scheme 3.13).

2,7-Dibromo-4-hydroxyfluorene (**3.26**) obtained by Scheme 3.12 was then methylated with methyl iodide in presence of potassium carbonate in DMF to afford 2,7-dibromo-4-methoxyfluorene (**3.34**) in 47% yield (Scheme 3.15).

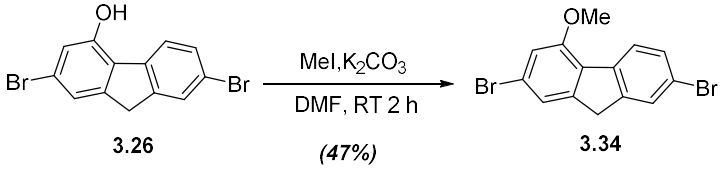

Scheme 3.15 Synthesis of 2,7-dibromo-4-methoxyfluorene (**3.34**).

For the introduction of the 4-CN group into the fluorene moiety, instead of diazotization of **3.24** and Sandmeyer reaction of formed diazonium salt **3.24a** with CuCN, we considered the replacement of I by CN in aryliodides, similar to approaches described in the literature. Synthesis of 2,7-dibromo-4-cyanofluorene (**3.35**) by Pd-catalysed coupling reaction of 2,7-dibromo-4-iodofluorene (**3.27**) with $Zn(CN)_2$ in DMF was straightforward and gave the desired product in a good yield of 63%. Pd-catalysed Sonogashira coupling reaction of iodofluorene **3.27** with phenylacetylene was also used to access 2,7-dibromo-4-phenylethynylfluorene (**3.36**) (Scheme 3.16).

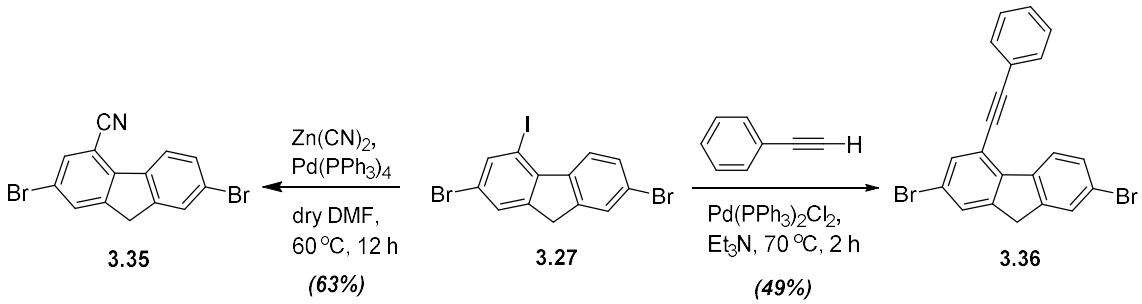

Scheme 3.16 Synthesis of 4-cyano- and 4-phenylethynyl-2,7-dibromofluorenes (**3.35** and **3.36**, respectively).

While the 4-ethynyl substituent (as in **3.36**) should weakly affect the electronic properties of polymers obtained from such monomers, the selective reaction at position 4 offers further structural variations in polyfluorenes with respect to their morphology, which can be changed by appropriately elongated alkynyl groups. This selective (at C-4) reaction is also important from the viewpoint of access to 4-alkyl-substituted polyfluorenes, because our attempts of direct alkylation of iodofluorene **3.27** with either Grignard reagent or tetramethyltin were unsuccessful (see below).

Several attempts have been performed for direct introduction of the methyl group at position 4. Taking into account high selectivity of substitution of the iodo-group in **3.27** (Scheme 3.11), we attempted to obtain 2,7-dibromo-4-methylfluorene (**3.38**) by coupling of compound **3.27** with the Grignard reagent MeMgBr catalysed by $Ni(dppp)Cl_2$, but observed the formation of 2,4,7-trimethylfluorene (**3.37**) as a major product (Scheme 3.17). Its structure was confirmed by ^1H NMR and MS spectral data (Figure 3.7). This could indicate that the Grignard reagent is too reactive in this coupling process and once the mono-alkylated product is formed (either at 4-, 2- or 7-positions), the reactivity of the obtained intermediate(s) is increased, so all halogens are substituted in the reaction.

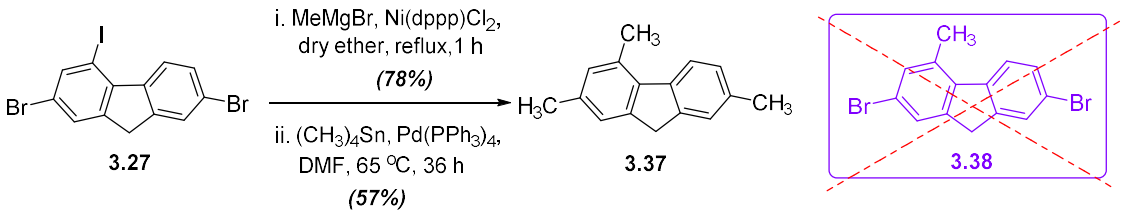

Scheme 3.17 Attempts of methylation of 2,7-dibromo-4-iodofluorene (**3.27**).

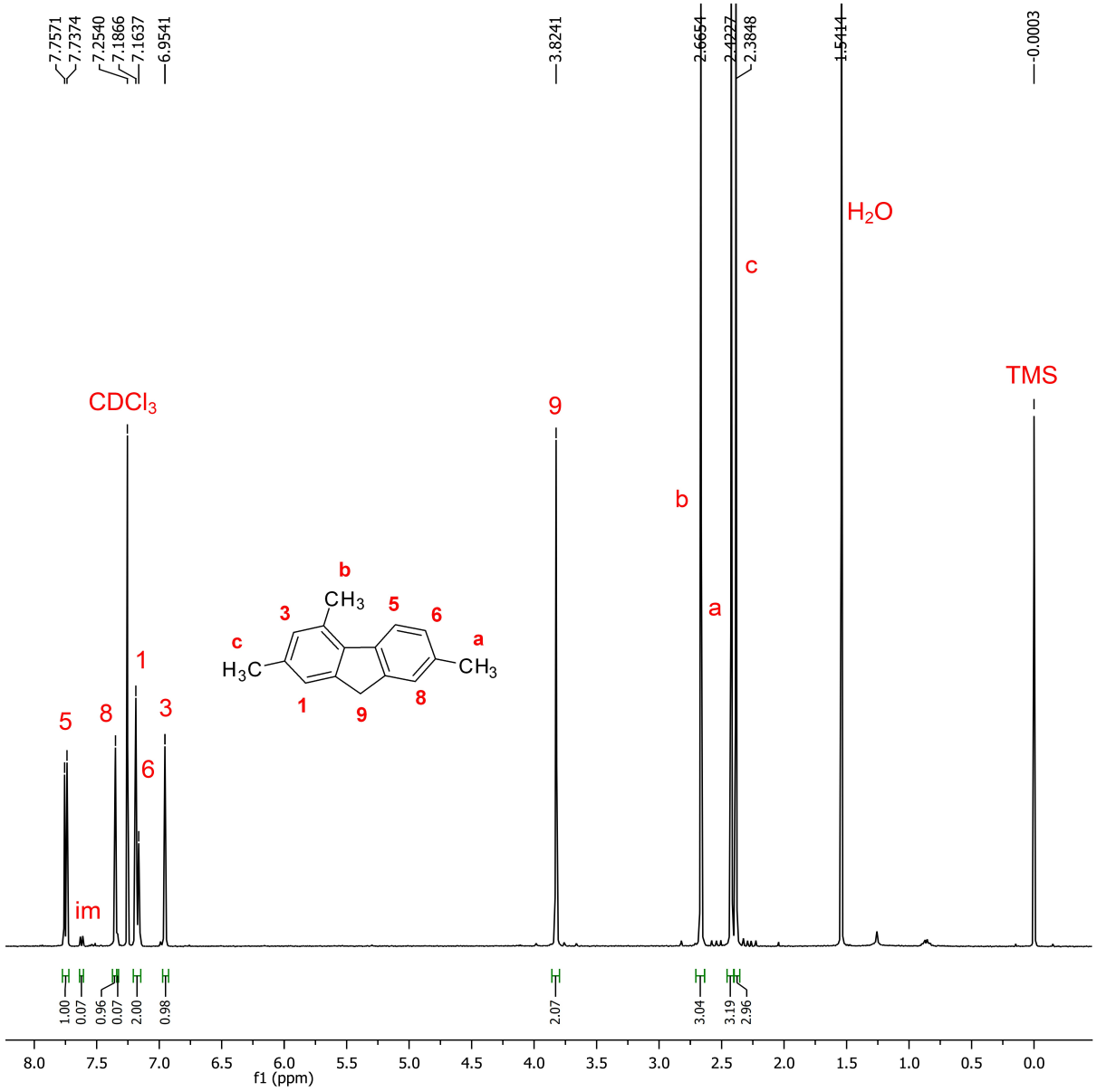

Figure 3.7 ^{1}H NMR spectrum of 2,4,7-trimethylfluorene (**3.37**).

So, we tried different reactions for coupling of compound **3.27** with tetramethyltin, Me_4Sn, catalysed by $(Pd(Ph_3)_4$ or $Pd(dppp)Cl_2$, but we also observed 2,4,7-trimethylfluorene (**3.37**) as a major product (with some starting material **3.27** recovered, but with no desired 2,7-dibromo-4-methylfluorene (**3.38**) in the mixture). As such, an alternative explanation is more grounded, namely, preferential oxidative addition in a catalytic cycle via a strictly intramolecular motion of the Pd(0) catalyst regenerated after the first addition step, resulting in polymethylation. A similar efficient intramolecular reaction resulting exclusively in the disubstitution product via Suzuki coupling between dibromofluorene and phenylboronic acid (in 1:1 ratio) was observed by Scherf and co-workers.[28] It is an even more common case for smaller aromatic moieties, e.g. Ni-catalysed Kumada polymerisation of thiophenes involving intramolecular catalyst transfer,[29,30] according to McCullough[31,32] and Yokozawa.[33,34]

Several different methods have been described in the literature for alkylation of fluorenes at the 9-CH_2 position by alkyl halides (R-X, X = Br, I). Some examples of fluorene alkylation in the literature in different conditions are: aq. NaOH/$BzNEt_3Cl$/R-X/DMSO, aq. NaOH/R-X/PTC, KOH/KI/R-X/DMSO, nBuLi/R-X/THF,[35,36,37,38] t-BuOK/R-X/THF.[39]

Widely used earlier methods of alkylation with alkyl halides with aqueous NaOH/KOH in the presence of phase-transfer catalysts (tertiary ammonium salts) have serious drawbacks because of incomplete alkylation and the presence in the resulting monomers of small impurities of mono-alkylated fluorenes (<0.1–2%,[40] which is difficult to detect by common analytical methods, e.g. by NMR). These have been shown to be the centers of oxidation of polyfluorenes obtained from such monomers, leading to the formation of fluorenone defects in the polymer chain and an appearance of an undesired green emission in their photoluminescence spectra on thermal annealing or UV-irradiation of polymers and green band in electroluminescence during the device operation.[41] This was particularly proved by treatment of synthesised 2,7-dibromo-9,9-dialkyfluorene with potassium tert-butoxide and filtration of the solution through silica gel, which absorbs the protonated form of mono-alkylated fluorene.[42,43] The stability of polyfluorene was substantially improved suppressing the green band appearance after such a treatment.[43]

Therefore, we performed an alkylation of our fluorenes by 1-bromooctane with t-BuOK as a strong base in non-aqueous conditions (DMSO or THF). Alkylation in THF is a particularly convenient method as it allows monitoring of the alkylation process.[39] During an addition of a solution of t-BuOK in THF to dibromofluorene/1-bromooctane solution in dry THF fluorene anion was generated as a slightly pink-coloured solution and the colour disappeared on alkylation. So, the completion of the process can be monitored visually when no colour change is observed after the next portion of t-BuOK (an excess of t-BuOK does not

affect the product, so using an excess of t-BuOK at the end of the process guaranteed no mono-octyl byproduct).

Two methods (alkylation in DMSO or in THF) have been successfully applied to the alkylation of 4-X-2,7-dibromofluorenes **3.29**, **3.35**, **3.34**, **3.30** and **3.36**, and corresponding 9,9-dioctylfluorenes **3.39–3.43** have been obtained in good yields of 52–91% (Scheme 3.18).

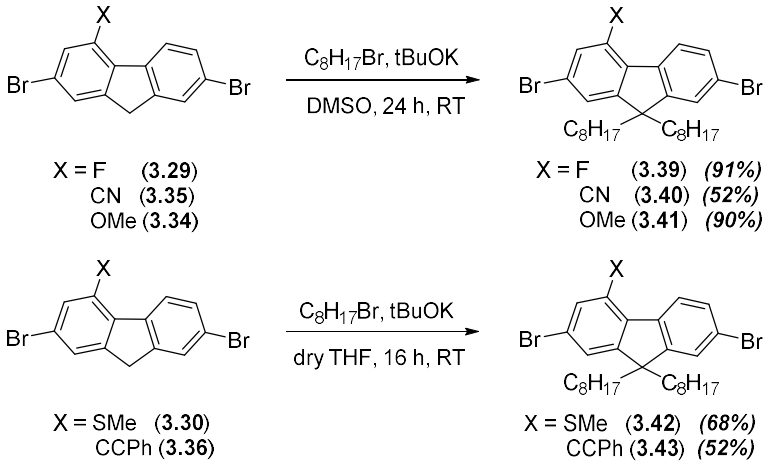

Scheme 3.18 Alkylation of 4-X-2,7-dibromofluorenes to obtain fluorene monomers **3.39–3.43**.

So far, we have successfully synthesised five 4-substituted 2,7-dibromo-9,9-dioctylfluorenes with electron-donating groups (**3.41**, **3.42** and **3.43**): OMe (strong EDG), SMe and CCPh (weak EDG) and electron-withdrawing groups (**3.39** and **3.40**): F (weak EWG) and CN (strong EWG). The sulfonyl group is another strong electron-withdrawing group, which might represent an interest (for strongly fluorescent sulfonyl-substituted polyphenylenes, see Chapter 2). Having in hand monomer **3.42** with the 4-SMe group, we decided to oxidise it to the 4-SO_2Me group (it cannot be done for 9-unsubstituted compound **3.30** as it can be oxidised to the corresponding fluorenone). Oxidation can be performed e.g. by hydrogen peroxide in acetic acid as it was demonstrated for oxidation of the butylthio-group into the butylsulphonyl-group in polynitrofluorenones.[44] Oxidation of alkylated fluorene **3.42** under the above conditions worked well to give methylsulfonyl-derivative **3.44** in a high yield of 83% (Scheme 3.19).

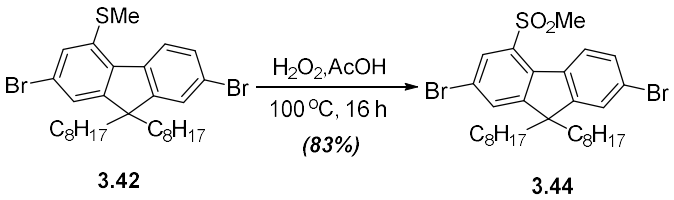

3.42 **3.44**

Scheme 3.19 Oxidation of methylthio-fluorene **3.42** into methylsufonyl-fluorene **3.44**.

3.2.3 Synthesis of 4-substituted 2,7-dibromo-9,9-di(4-octyloxyphenyl)fluorene monomers from polynitrofluorenones.

In this section, we present an alternative approach to the synthesis of 4-substituted 2,7-dibromofluorene monomers starting from polynitrated 9-fluorenones. Polynitrofluorenones have been widely studied as strong π-electron acceptors for charge-transfer complexes,[44,45,46,47] and have been used e.g. as sensitisers for photoconductive electron donors and for recording optical information.[48,49] So, their methods of synthesis are well elaborated and many reactions have been studied in the past. Electrophilic substitution in fluorenone (**3.18**) occurs at the 2,7-positions (similarly to fluorenes) and e.g. nitration of fluorenone gives 2,7-dinitrofluorenone and then 2,4,7-trinitrofluorenone (**3.19**). Therefore, we considered that they can also be convenient synthons, in which the nitro groups in positions 2,7 can be reduced to amino-groups and then converted into bromo-groups through diazonium chemistry to access new series of monomers for polyfluorenes.

First, we considered using starting materials with an alkoxycarbonyl group in position 4. This can be done from diphenic acid (**3.9**), which can be quantitatively cyclised into fluorenone-4-carboxylic acid (**3.10**) in sulphuric acid. The later can be converted, without isolation from the reaction mixture, into either ester **3.11** (by esterification) or into acid **3.17** (by nitration reaction). Performing nitration of ester **3.11** or esterification of acid **3.17** gave the target 2,7-dinitro-4-butoxycarbonylfluorenone (**3.45**),[50] which was used for further conversion of NO_2 groups into Br groups. While we have recently described this multi-step synthesis in our recent paper,[50] it is essentially based on some methods described in the old literature cited in this paper (Scheme 3.20). Nitration of acid **3.10** or ester **3.11** is more selective than their bromination/iodination described above [Scheme 3.3[16] and Scheme 3.4 (Section 3.2.1)] due to the strong deactivating effect of the NO_2 group, giving 2,7-dinitrated products **3.17** or **3.45.**

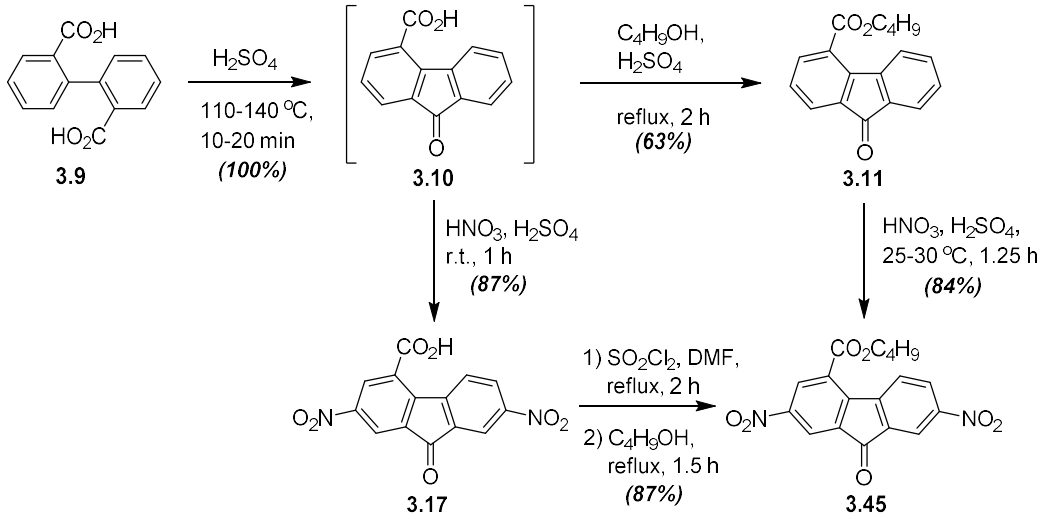

Scheme 3.20 Synthesis of 2,7-dinitro-4-butoxycarbonylfluorenone (**3.45**) from diphenic acid (**3.9**).[50]

To obtain other 4-substituted 2,7-dinitrofluorenones, we started from, 2,4,7-trinitro-9-fluorenone (**3.19**) which can be easily obtained by direct nitration of fluorenone (**3.18**) in the mixture of nitric and sulphuric acids.[51,52] Polynitrofluorenones being strong electron acceptors undergo nucleophilic substitution with O-,[53,54,55] S-,[44,56,55] and N-nucleophiles[57,55] with a replacement of a nitro group by a nucleophile, and several examples of such reactions have been described in the literature (although, generally, NO_2 is considered as a weak leaving group in nucleophilic substitution reactions). The position for nucleophilic substitution (2- or 4-) and selectivity of the reaction depend substantially on the type of nucleophile, the number of EWG in the fluorene moiety and the reaction conditions (solvent, temperature etc.). Thus, for 2,4,5,7-tetranitrofluorenone (**3.46**) (and some other tetrasubstituted polynitrated fluorenones), S_NAr nucleophilic substitution reactions with dialkylamines (to give **3.47**),[57,55] phenol (to give **3.48**)[55] and mercaptanes (to give **3.49–3.51**)[44] preferentially occur at 2-position. For the smaller HO^- nucleophile (from water) the 4-hydroxy-derivative (**3.52**) is mainly formed, apart from a minor amount of 2-substituted product (Scheme 3.21).[53,54]

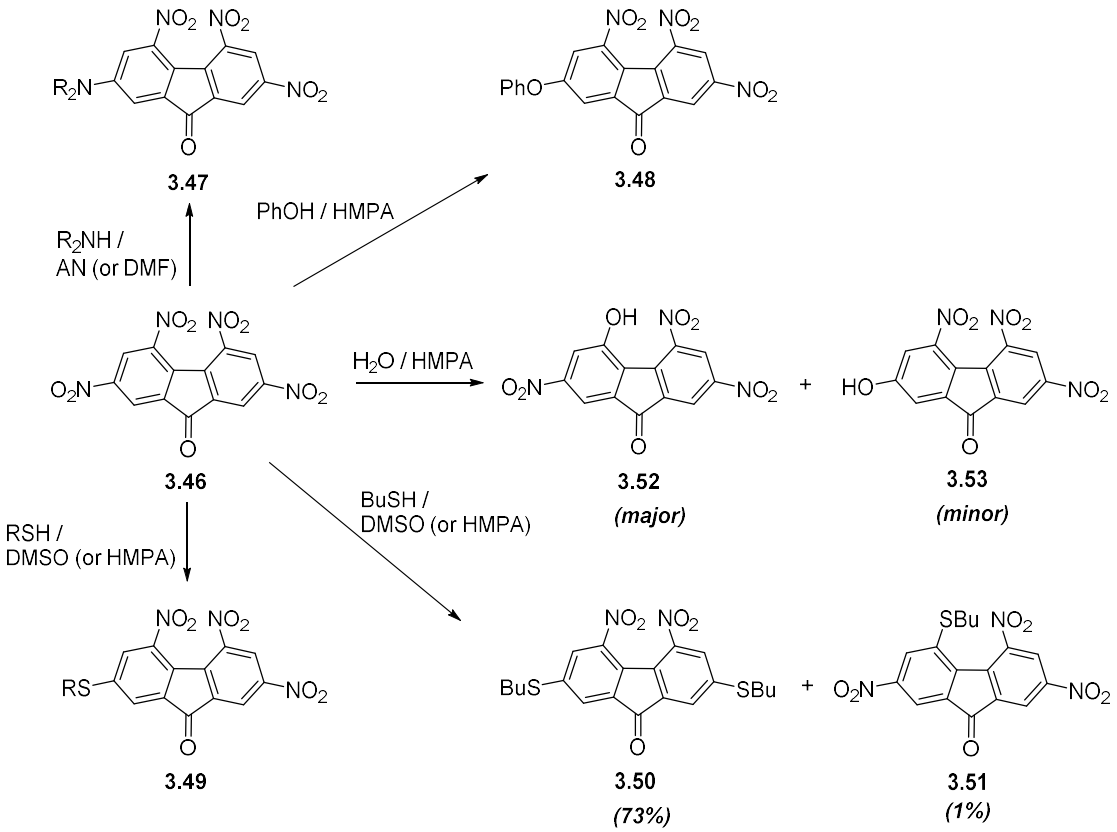

Scheme 3.21 Nucleophilic aromatic substitution in 2,4,5,7-tetranitrofluorenone (**3.46**).[44,53,54,55,57]

In the case of 2,4,7-trinitrofluorenone (**3.19**), the steric hindrance at positions 4,5 is smaller and S_NAr substitution occurs mainly at position 4, although some amount of 2-isomer is formed in the reaction as a minor product.[55,56] We have performed the reaction of 2,4,7-trinitrofluorenone (**3.19**) with butyl mercaptane in DMSO, which showed substitution of one NO_2 group by a BuS group, with formation of 4-BuS- and 2-BuS- isomers (**3.54** and **3.55**, respectively) in approximate ratio of (4–5):1 (according to NMR spectrum of the crude product). Two isomers showed very close spots on TLC, so their separation by flash chromatography on a gram scale was problematic, but fortunately, the desired 4-butylthio-2,7-dinitrofluorenone was successfully isolated by recrystallisation from ethylacetate (Scheme 3.22).

Substitution of the NO_2 group to an OH group in trinitrofluorenone **3.19** by water (as a smaller size nucleophile) in HMPA (traces of H_2O in a solvent) occurs more selectively, giving exclusively 4-hydroxy-2,7-dinitrofluorenone (**3.56**). The method, described in the old literature was performed at room temperature and required a very long time for the reaction (3 months). It was mentioned that an increase of the temperature resulted in the formation of a complex mixture of inseparable products.[53] More recent studies of this reaction have shown

that the reaction can be substantially accelerated by iodide ions, allowing to decrease the reaction time to ca 1 week at room temperature or to 1 day or several hours when heating at 60–100 °C.[58] So, we performed the reaction of 2,4,7-trinitrofluorenone (**3.19**) in wet HMPA and KI (2 eq.) at 100 °C on a 15 g scale batch and have isolated the desired 4-hydroxy-2,7-dinitrofluorenone (**3.56**) with a good yield of 80% after purification (Scheme 3.22). Further methylation of **3.56** under usual conditions for alkylation of phenols,[59] i.e. with methyl iodide in presence of potassium carbonate (K_2CO_3) in DMF gave 2,7-dinitro-4-methoxyfluorenone (**3.57**) in 57 % yield (Scheme 3.22).

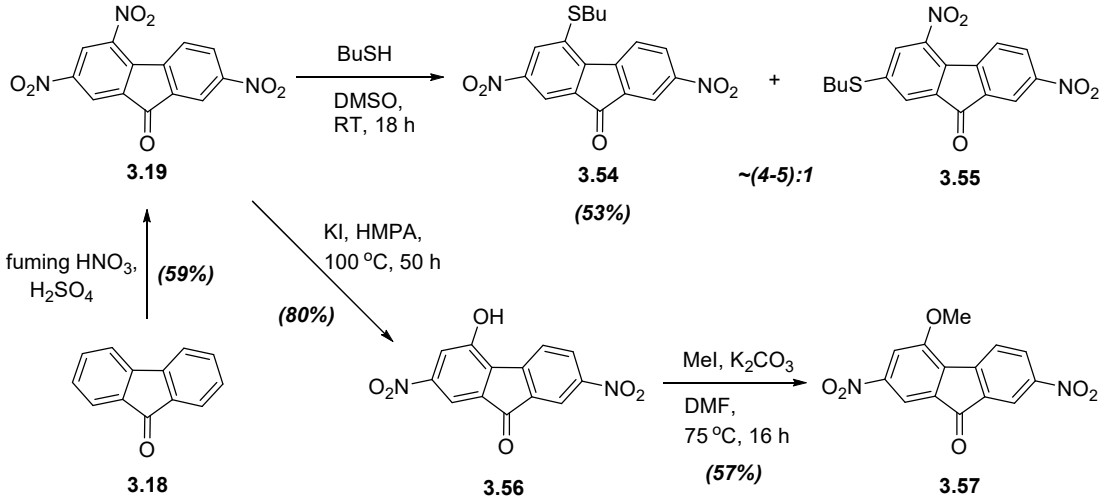

Scheme 3.22 Synthesis of 2,7-dinitro-4-butylthiofluorenone (**3.54**) and 2,7-dinitro-4-methoxyfluorenone (**3.57**).

Reduction of NO_2 groups in 2,7-dinitrofluorenones **3.54**, **3.57** and **3.45** was performed by Sn/HCl (37%) at 100 °C for 1–3 h and diaminofluorenes **3.58–3.60** have been isolated in 43–82 % yields (Scheme 3.23). Attempts to reduce 2,7-dinitro-4-butylthiofluorenone (**3.54**) by another method described in the literature for the reduction of nitro groups,[60] i.e. by $SnCl_2$/EtOAc at reflux for 24 h, was unsuccessful giving a complex mixture of products. We also tried to perform reduction of compound **3.54** by Pd/C in a hydrogen atmosphere (1 atm. H_2), commonly used for reduction of nitro groups,[61,62] and it worked well giving a high yield of 96% for crude unpurified product, which is still suitable for further transformations (Scheme 3.23).

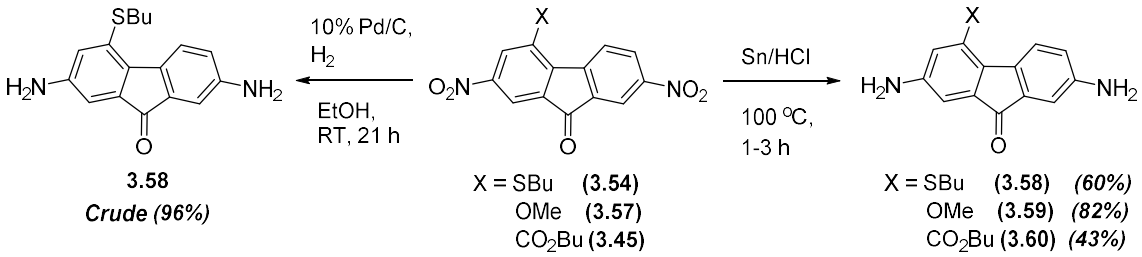

Scheme 3.23 Synthesis of 2,7-diamino-4-X-fluorenones **3.58-3.60** (X = SBu, OMe, CO_2Bu).

The three intermediate 2,7-diamino-4-X-fluorenones [X = SBu (**3.58**), OMe (**3.59**), CO_2Bu (**3.60)**] (Scheme 3.23) were converted to the corresponding dibromofluorenones **3.61–3.63** through diazotization reaction followed by Sandmeyer reaction with CuBr/HBr (Scheme 3.24). The butylthio-group in 2,7-dibromo-4-butylthiofluorenone (**3.61**) was also oxidised by hydrogen peroxide in acetic acid to obtain 2,7-dibromo-4-butylsuphonylfluorenone (**3.64**) in a good yield of 89%, to expand the series of 4-substituted fluorenones (Scheme 3.24).

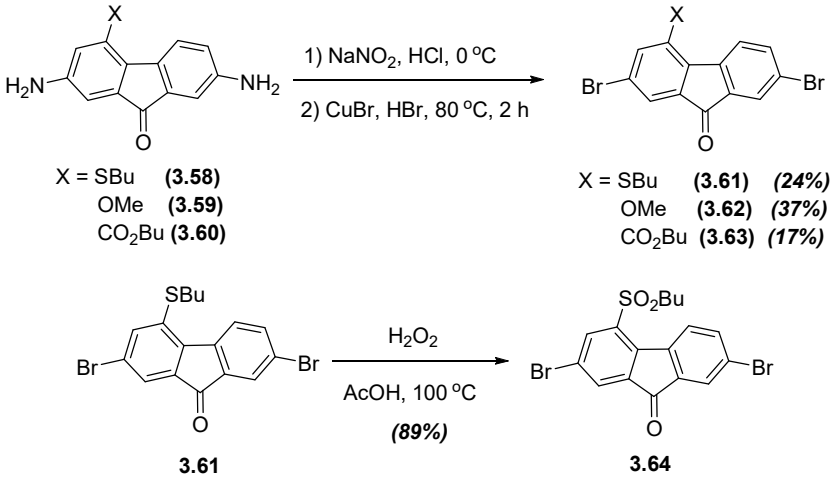

Scheme 3.24 Synthesis of 2,7-dibromo-4-X-fluorenones **3.61–3.64** (X = SBu, OMe, CO_2Bu, SO_2Bu).

In principle, fluorenones **3.61**–**3.64** can be reduced to the corresponding fluorenes (e.g. by Kishner-Wolff reaction through hydrazones or by $TiCl_4$ /dimethylamine-borane complex, as in Scheme 3.1), which can be then alkylated as described in section 3.4.2. However, as the synthesis of a number of such monomers have been already described in section 3.4.2 of this chapter, we considered to use fluorenones **3.61**–**3.64** for the synthesis of 9,9-diarylated fluorene monomers. This would extend a series of available 4-substituted polyfluorenes, and, for example, poly(9,9-di(4-octyloxyphenyl)fluorene) was used as a light-emitting polymer showing more pure blue emission compared to poly(9,9-dioctylfluorene).[17]

Various conditions of acid-catalysed (HCl or H_2SO_4 co-catalysed by β-mercaptopropionic acid) condensation of fluorenone with phenols[63,64] and its ethers,[65] as well as 2,7-dibromofluorenone with phenols[17,66,67] have already been described in the literature. We used conditions[64,68] of condensation of fluorenones **3.61**–**3.64** with phenol, catalysed by methanesulfonic acid and successfully synthesised fluorene bisphenols **3.65**–**3.68** in high yields of 73–86 % (Scheme 3.25). These were then alkylated with 1-bromooctane and potassium carbonate in DMF affording target monomers 2,7-dibromo-4-X-9,9-di(4-octyloxyphenyl)fluorenes **3.69–3.72** (Scheme 3.25).

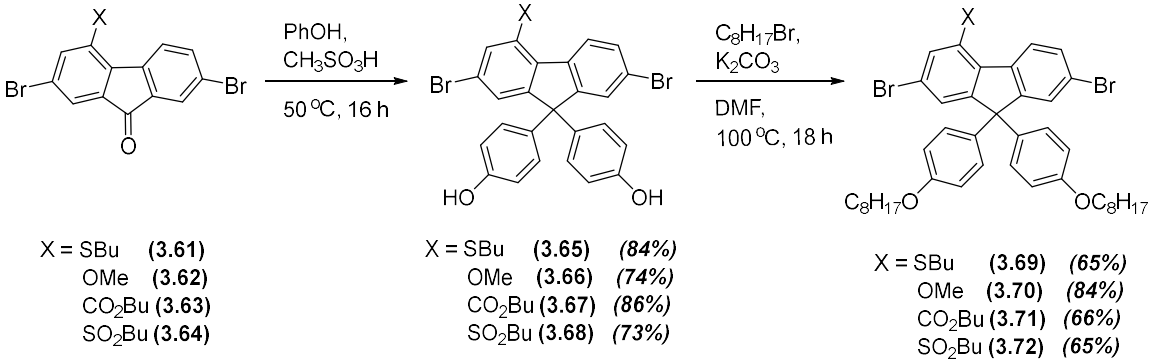

X = SBu **(3.61)**
OMe **(3.62)**
CO_2Bu **(3.63)**
SO_2Bu **(3.64)**

X = SBu **(3.65)** *(84%)*
OMe **(3.66)** *(74%)*
CO_2Bu **(3.67)** *(86%)*
SO_2Bu **(3.68)** *(73%)*

X = SBu **(3.69)** *(65%)*
OMe **(3.70)** *(84%)*
CO_2Bu **(3.71)** *(66%)*
SO_2Bu **(3.72)** *(65%)*

Scheme 3.25 Synthesis of 2,7-dibromo-4-X-9,9-di(4-octyloxyphenyl)fluorene monomers (X = SBu, OMe, CO_2Bu, SO_2Bu) (**3.69–3.72**).

3.3 Conclusion

Aiming to have an access to 4-substituted polyfluorenes with tunable electronic properties, we have elaborated methods of synthesis of two series of 2,7-dibromo-4-X-9,9-R,R-fluorene monomers with R = octyl and 4-octyloxyphenyl solubilising groups. Two main approaches have been realised to achieve this goal.

In the first approach, we started from 2,7-dibromofluorene (**3.22**), which was nitrated to 2,7-dibromo-4-nitrofluorene (**3.23**) and then reduced to 2,7-dibromo-4-aminofluorene (**3.24**). Further, the amino group was converted through diazonium chemistry (following further transformations in some cases) into a number of other functional groups: X = OH (**3.26**), OCH_3 (**3.34**), SCH_3 (**3.30**), C≡C–Ph (**3.36**), I (**3.27**), F (**3.29**), CN (**3.35**). 4-Functionalised 2,7-dibromofluorenes have been then alkylated with 1-bromooctane to afford a series of 4-substituted 2,7-dibromo-9,9-dioctylfluorene monomers for 4-functionalised polyfluorenes (described in Chapter 4), namely monomers with electron-donating groups (EDG): X = OCH_3 (**3.41**), SCH_3 (**3.42**), C≡C–Ph (**3.43**), I (**3.27**) and monomers with electron-withdrawing groups (EWG): X = F (**3.39**), CN (**3.40**), SO_2CH_3 (**3.44**).

Attempts of direct iodination of 4-fluorenecarboxylic acid (**3.14**) to access 2,7-diiodo-monomers with 4-carboxy-/alkoxycarbonyl groups were unsuccessful, resulting in the product being substantially contaminated with the 2,6,7-triodinated by-product, which was difficult to remove. Also, we were unable to achieve selective methylation of 2,7-dibromo-4-iodofluorene (**3.27**) at position 4 in either Ni-catalysed reaction with MeMgBr or Pd-catalysed reaction with Me_4Sn. In both cases, instead of target 2,7-dibromo-4-methylfluorene (**3.38**), we have isolated the polymethylated product, 2,4,7-trimethylfluorene (**3.37**). We also observed an unexpected by-product in the reduction reaction of 2,7-dibromo-4-nitrofluorene (**3.23**) when following the literature procedure (Sn/HCl/EtOH),[21] namely 2,7-dibromo-3-chloro-4-aminofluorene (**3.25**) and have rationalised its formation in the reduction reaction.

In the second approach, we used polynitrated fluorenones as starting compounds, which have two NO_2 groups at 2,7-positions. These have been reduced to amino groups, diazotized and then converted into Br groups by Sandmeyer reaction with CuBr/HBr. A series of 4-substituted 2,7-dibromofluorenones **3.69**–**3.72** have been obtained by this way. In the case of 4-butoxycarbonyl group (**3.69**), we started from 4-butoxycarbonyl-2,7-dinitrofluorenone (**3.45**), which was obtained as we published recently.[50] For others, we used 2,4,7-trinitrofluorenone (**3.19**) as starting materials and have selectively substituted the 4-nitrogroup by nucleophilic substitution reaction, S_NAr, by OH (which was then converted to OCH_3) or SBu (which then also converted to SO_2Bu), The obtained fluorenones have been subjected to condensation reaction with phenol to obtain fluorene-bisphenols **3.65**–**3.68**, which have been then alkylated to afford a new series of fluorene monomers, 4-X-2,7-dibromo-9,9-di(4-octyloxyphenyl)fluorenes **3.69**–**3.72**.

Finally, we have obtained and fully characterised two series of novel 4-substituted 2,7-dibromofluorenes as monomers for the synthesis of 4-functionalised polyfluorenes, with either n-octyl groups or 4-octyloxyphenyl groups at C-9 as solubilising substituents. In each case, functionalisation of position 4 was done with both EDG and EWG functional groups. Synthesis and studies of polyfluorenes prepared from these monomers will be described in the next Chapter 4.

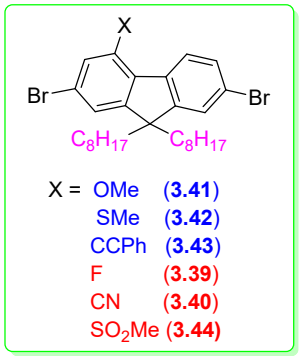

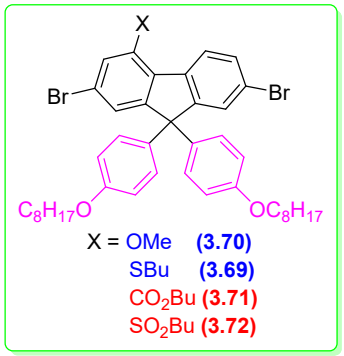

3.4 Experimental Section

3.4.1 Chemicals and instruments

All commercial chemicals and solvents were obtained from Aldrich, Acros, Apollo Scientific and Fisher suppliers, and were used in reactions without any further purification. Melting points were measured on a Büchi M-565 automatic melting point apparatus. ^{1}H, ^{13}C, ^{19}F and ^{1}H-^{1}H COSY NMR spectra were recorded on a Bruker Avance 400 spectrophotometer [operating at 400 MHz (for ^{1}H), 100 MHz (for ^{13}C), 376 MHz (for ^{19}F)] in deuterated solvents ($CDCl_3$, CD_3COCD_3 and DMSO-d_6) with tetramethylsilane (TMS) as an internal standard (δ = 0 ppm). Mass spectra were recorded on Thermo Scientific ITQ 900 mass-spectrometer (EI-TOF mode). For the monitoring the reactions and analysis of synthesised compounds, thin layer chromatography (TLC) on a standard precoated silica gel plates (Merck, 20 × 20 cm, silica gel F_{254}) was used [visualised by UV lamp (254/366 nm)]. Flash chromatography purification of synthesised compounds was performed on a Teledyne Isco Combiflash chromatograph model Rf-200 using silica gel (40–60 μm). Before running the flash chromatography purification, UV-Vis spectra of the crude products were measured on Shimadzu UV-Vis-NIR 3600 spectrophotometer to select the appropriate wavelengths for monitoring the purification process. VirTis Bench Top Pro 8L freeze dryer (SP Scientific) connected to the high vacuum pump (~10μbar) was used for the vacuum drying of the compounds.

3.4.2 Synthesis

2,7-Diiodofluorene-4-carboxylic acid (3.15) and 2,6,7-triiodofluorene-4-carboxylic acid (3.16)

Exp no: SK-11

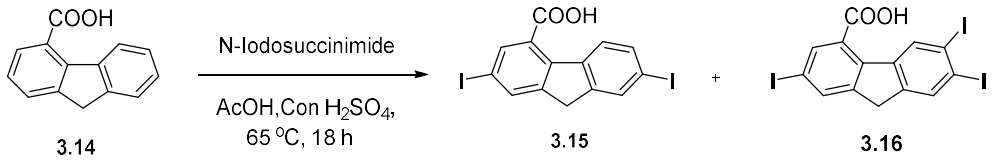

Fluorene-4-carboxylic acid (**3.14**) (0.502 g, 2.3 mmol), *N*-iodosuccinimide (1.0 g, 4.5 mmol), acetic acid and concentrated sulphuric acid mixture (5:1, v:v) (30 mL) were charged in 50 mL single neck round bottom flask. The mixture was heated to 65 °C for 18 h (the reaction progress was monitored by TLC) and cooled down to room temperature. The solid was filtered off, washed with water (2 × 15 mL) and dried *in vacuo* to afford a yellow solid (1.02

g, 107% basing on **3.15**). The crude product was purified by column chromatography on silica gel using MeOH/DCM (1:9, v/v) as eluent to afford compound **3.15** as a white solid (0.412 g, 37%). This compound, according to ^{1}H NMR is mainly diiodo-acid **3.15**, while it still contains 30% of impurity, presumably triiodo-acid **3.16**, which we were unable to separate further due to the very close R_f of the spots on TLC.

2,7-Diiodofluorene-4-carboxylic acid (3.4) (70% purity):

^{1}H NMR (400 MHz, $CDCl_3$) (**3.15**): δ (ppm) 9.27 (s, 1H), 8.41 (d, *J* = 6.6 Hz, 1H, H-5), 7.88 (d, *J* = 0.8 Hz, 1H), 7.77 (d, *J* = 1.3 Hz, 1H), 7.71 (d, *J* = 1.3 Hz, 1H), 7.60 (d, *J* = 1.2, 6.6 Hz, 1H, H-6), 3.86 (s, 2H).

***2,7-Dibromofluorene (3.22)*[19]**

Exp no: SK-84

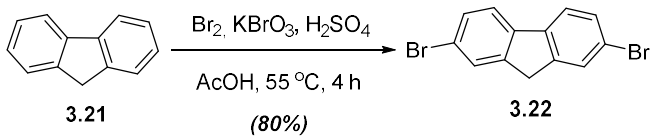

Fluorene (**3.21**) (204 g, 1.22 mol) was dissolved in acetic acid (1.8 L) at 70 °C and concentrated H_2SO_4 (17 mL) was added slowly to this solution. The reaction mixture was allowed to cool to 50 °C with stirring and a solution of bromine (104 mL, 2.02 mol) in acetic acid (120 mL) was added dropwise for 2–3 h, maintaining the temperature at 40–55 °C to avoid crystallisation of fluorene. On addition of half amount of bromine, 2,7-dibromofluorene started to crystallise. Second half of bromine and $KBrO_3$ (69.7 g, 0.417 mol) were added by turns in small portions at 40–55 °C with vigorous stirring, which resulted in the heavy precipitation of 2,7-dibromofluorene. The mixture was stirred for 3–4 h at 45–55 °C and left to cool to the room temperature. After cooling the mixture to 10 °C, the solid was filtered off, washed with 70% AcOH (330 mL), then with water until pH 7, and dried to give the crude product as a cream colour solid (348 g, 87 %). The crude product was stirred in acetic acid (700 mL) at reflux (no full dissolution) for 4 h, cooled down to room temperature, filtered off, washed with cold AcOH (100 mL) and dried *in vacuo* to afford 2,7-dibromofluorene (**3.22**) as a cream colour solid (318 g, 80%).

^{1}H NMR (400 MHz, $CDCl_3$): δ (ppm) 7.65 (m, 2H, H-1), 7.59 (d, *J* = 8.1 Hz, 2H, H-4), 7.49 (dd, *J* = 8.1, 1.6 Hz, 2H, H-3), 3.85 (s, 2H, CH_2).

^{13}C NMR (100 MHz, $CDCl_3$): δ (ppm) 144.79, 139.67, 130.14, 128.29, 121.18, 120.95, 36.55.

MS (TOF EI$^+$): *m/z* 321.79 (M^+, $^{79}Br/^{79}Br$, 100%), 323.77 (M^+, $^{79}Br/^{81}Br$, 98%), 325.82 (M^+, $^{81}Br/^{81}Br$, 90%). Calcd for $C_{13}H_8Br_2$: 321.90 (100%), 323.90 (51.4%), 325.90 (49.6%),

2,7-Dibromo-4-nitrofluorene (3.23)[20]

Exp no: SK-94

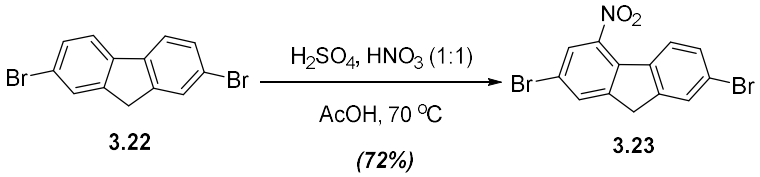

3.22 **3.23**

(72%)

2,7-Dibromofluorene (**3.22**) (50.0 g, 154 mmol) and glacial acetic acid (650 mL) were charged in 2 L round bottom flask. The reaction mixture was stirred at 35 °C and then a mixture of fuming HNO_3 (35 mL) and concentrated 96% H_2SO_4 (35 mL) solution was added dropwise for 10 minutes. The reaction mixture was stirred at 35 °C for 10 minutes, then at 70 °C for 15 minutes and left to cool down to room temperature. The yellow precipitate was filtered off, washed with water until pH 7 and dried *in vaccuo* to give crude product (61 g, 107%). The crude product was recrystallised from Tol/EtOH (1:1, 1.2 L) to afford compound **3.23** as a yellow solid (41.1 g, 72%), mp: 195–196 °C. Lit. mp: 194.5–195.5 °C.[69]

^{1}H NMR (400 MHz, $CDCl_3$): δ (ppm) 8.05 (d, *J* = 1.1 Hz, 1H), 7.94 (d, *J* = 8.6 Hz, 1H, H-5), 7.89 (d, *J* = 0.6 Hz, 1H), 7.72 (s, 1H), 7.54 (dd, *J* = 1.4, 8.6 Hz, 1H, H-6), 3.97 (s, 2H, CH_2).

^{13}C NMR (100 MHz, $CDCl_3$): δ (ppm) 147.66, 145.75, 145.00, 135.47, 132.76, 132.58, 130.81, 128.11, 126.24, 126.20, 123.52, 120.10, 36.59.

MS (TOF EI$^+$): *m/z* 366.77 (M^+, ^{79}Br/^{79}Br, 80%), 368.81 (M^+, ^{79}Br/^{81}Br, 100%), 370.82 (M^+, ^{81}Br/^{81}Br, 90%). Calcd for $C_{13}H_7Br_2NO_2$: 366.88 (51.4%), 368.88 (100%), 370.88 (48.7%).

2,7-Dibromo-4-aminofluorene(3.24) and 2,7-dibromo-4-amino-3-chlorofluorene(3.25):

Exp no: SK-86

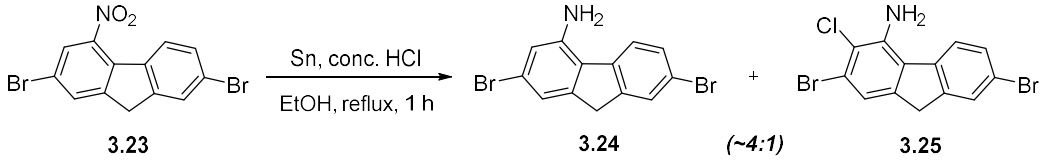

3.23 **3.24** *(~4:1)* **3.25**

*(On scale up the method described in Ref 21, apart of target product **3.24** chlorinated by-product **3.25** was formed).* 2,7-Dibromo-4-nitrofluorene (**3.23**) (41.4 g, 112 mmol), 37% HCl (200 mL), and EtOH (530 mL) were charged in a single neck round bottom flask. To the mixture, tin powder (52 g, 437 mmol) was slowly added and the reaction mixture (suspension) was stirred to reflux for 45 min. The reaction mixture was poured on ice (ca. 1 L) and pH was adjusted to basic (pH 9). Ethyl acetate (1.5 L) was added, the mixture was stirred for 4 h, the solid was filtered off and washed with ethylacetate. The organic layer was separated and the aqueous layer was washed with ethyl acetate (2 × 100 mL). The combined

ethyl acetate layer was dried over Mg_2SO_4, filtered off, the solvent was evaporated under reduced pressure and the residue was dried *in vacuo* to give pale yellow solid (47.5 g, 120%). The crude product showed 20% of the undesired compound according to ^{1}H NMR spectral analysis. The attempts of recrystallisation of the crude product from different solvents (toluene, ethylacetate, methanol, or 1,4-dioxan) were performed, but no pure product was obtained.. Therefore, 100 mg of the crude product was purified by flash chromatography on a large column (120 g silica gel, EA/PE (1:1, v/v) as eluent) to afford 2,7-dibromo-3-chloro-4-aminofluorene (**3.25**) as a light brown solid (0.018 g, 8%).

2,7-Dibromo-4-aminofluorene (3.24):

^{1}H NMR (400 MHz, $CDCl_3$): δ (ppm) 7.64 (s, 1H), 7.49 (d, J = 8.6 Hz, 1H, H-5), 7.50 (m, 1H), 7.12 (s, 1H), 6.86 (m, 1H), 4.08 (s, 2H, NH_2), 3.84 (s, 2H, CH_2).

2,7-Dibromo-4-amino-3-chlorofluorene(3.25):

^{1}H NMR (400 MHz, $CDCl_3$): δ (ppm) 7.69 (s, 1H, H-8), 7.52 (m, 2H, H-5,6), 7.01 (s, 1H, H-1), 4.07 (s, 2H, NH_2), 3.88 (s, 2H, H-9, CH_2).

Assignments of proton shifts have been made basing on ^{1}H-^{1}H COSY (400 MHz, $CDCl_3$), which which showed interatcions ^{5,6}H-^{8}H, ^{8}H-^{9}H, ^{9}H-^{1}H (Figure 3.5)

MS (TOF EI$^+$): *m/z* 370.95 (M$^+$, ^{79}Br/^{79}Br, 60%), 372.94 (M$^+$, ^{79}Br/^{81}Br, 100%), 374.94 (M$^+$, ^{81}Br/^{81}Br, 40%). Calcd for $C_{13}H_8Br_2ClN$: 370.87 (51.4%), 372.87 (100%), 374.87 (48.6%).

2,7-Dibromo-4-aminofluorene (3.24)

Exp no: SK-101

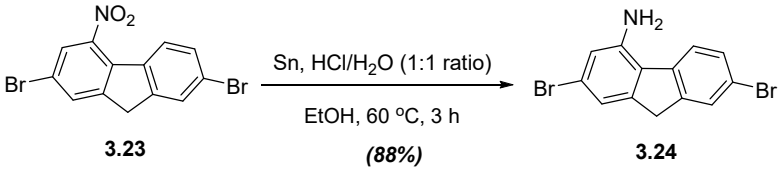

3.23 ***(88%)*** **3.24**

For the synthesis of compound **3.24**, we modified the procedure described in the literature.[21] 2,7-Dibromo-4-nitrofluorene (**3.23**) (26.7 g, 72.3 mmol), 37% HCl (50 mL), H_2O (80 mL) and EtOH (350 mL) were charged in 2 L flask. The mixture was stirred at room temperature for 10 minutes and then tin powder (34.0 g, 289 mmol) was slowly added portionwise with stirring. The mixture (suspension) was stirred at 60 °C for 3 h, cooled to room temperature, diluted with water (200 mL) and basified with 2 M NaOH (300 mL) to adjust to pH 9. The mixture was extracted with ethyl acetate (3 × 200 mL), the organic layer was dried over Mg_2SO_4, filtered off, evaporated to dryness and the residue was dried *in vacuo* to afford compound **3.24** as a cream colour solid (21.6 g, 88%).

^{1}H NMR (400 MHz, $CDCl_3$): δ (ppm) 7.64 (s, 1H), 7.51 (m, 1H), 7.50 (m, 1H), 7.12 (s, 1H), 6.86 (s, 1H), 4.08 (s, 2H, NH_2), 3.84 (s, 2H, CH_2).

^{13}C NMR (100 MHz, $CDCl_3$): δ (ppm) 146.25, 144.70, 143.17, 139.66, 129.88, 128.13, 125.49, 122.33, 121.48, 119.52, 118.89, 117.84, 36.91.

MS (TOF EI^+): *m/z* 336.90 (M^+/^{79}Br/^{79}Br, 50%), 338.89 (M^+, ^{79}Br/^{81}Br, 100%), 340.90 (M^+, ^{81}Br/^{81}Br, 49%), Calcd for $C_{13}H_9Br_2N$: 336.91 (51.4 %), 338.91 (100%), 340.91 (49.6 %).

2,7-Dibromo-4-hydroxyfluorene (3.26)

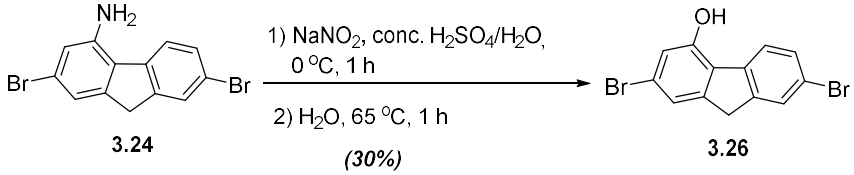

3.24 *(30%)* **3.26**

Method A. Exp no: SK-107

2,7-Dibromo-4-aminofluorene (**3.24**) (5.07 g, 15.0 mmol) was charged in a two neck round bottom flask, 95% concentrated H_2SO_4 (200 mL) was added and the mixture was stirred for 15 minutes to form a green colour solution. Upon dissolution, the mixture was cooled to 0 °C (internal temperature) and a solution of $NaNO_2$ (1.54 g, 22.4 mmol) in H_2O (10 mL) was added slowly with stirring over a period of 20 minutes maintaining the temperature of the reaction mixture at 0–2 °C (internal temperature). The excess nitrite ions was controlled by KI–starch paper. The mixture was stirred at –5 °C to 0 °C for 1 h, cold water (300 mL) was added and the mixture was heated to 65 °C for 1 h. The reaction mixture was cooled to room temperature, the precipitate was filtered off, washed with water (4 × 100 mL) and dried *in vacuo* to give brown solid (6.24 g, 122%). The crude product was purified by flash chromatography on silica gel using PE/EA (9:1–1:2, v/v) as gradient solvent eluent system to afford compound **3.26** as a yellow solid (1. 61 g, 32.1%).

Method B. Exp no: SK-121

2,7-Dibromo-4-aminofluorene (**3.24**) (5.10 g, 15.0 mmol) was charged in two neck round bottom flask. A mixture of concentrated H_2SO_4 (100 mL) and water (100 mL) was added stirred and the mixture was stirred for 15 minutes to form light green colour solution. The mixture was cooled down to 0 °C and a solution of $NaNO_2$ (1.50 g, 21.7 mmol) in H_2O (10 mL) was slowly added with steering over a period of 20 minutes maintaining the temperature of the reaction mixture at 0–2 °C (internal temperature). The excess nitrite ions was controlled by KI–starch paper. The mixture was stirred at –5 °C to 0 °C for 1 h, cold water (300 mL) was added and the mixture was heated to 65 °C for 1 h. The reaction mixture was cooled down to room temperature, the precipitate was filtered off, washed with water (4 × 100 mL) and dried

in vacuo to give yellow solid (6.34 g, 124%). The crude product was purified by flash chromatography on silica gel using PE/EA (9:1 to 1:2, v/v) as gradient solvent eluent system to afford compound **3.26** as a yellow solid (1. 54 g, 30.7%)

^{1}H NMR (400 MHz, $CDCl_3$): δ (ppm) 7.92 (d, *J* = 8.2 Hz, 1H, H-5), 7.63 (d, *J* = 0.8 Hz, 1H), 7.49 (dd, *J* = 1.7, 8.2 Hz, 1H, H-6), 7.26 (s, 1H), 6.92 (d, *J* = 0.6 Hz, 1H), 5.60 (br s, 1H, OH), 3.94 (s, 2H, CH_2).

^{1}H NMR (400 MHz, DMSO): δ (ppm) 10.65 (br s, 1H, OH), 7.91 (d, *J* = 8.2 Hz, 1H, H-5), 7.74 (d, *J* = 1.3 Hz, 1H), 7.54 (dd, *J* = 1.8, 8.2 Hz, 1H, H-6), 7.24 (d, *J* = 1.2 Hz, 1H), 7.00 (d, *J* = 1.4 Hz, 1H), 3.94 (s, 2H, CH_2).

^{13}C NMR (100 MHz, $CDCl_3$): δ (ppm) 151.75, 146.71, 144.11, 138.83, 130.14, 127.67, 127.08, 124.74, 120.98, 120.58, 120.19, 117.17, 37.07.

MS (TOF EI$^+$): *m/z* 337.86 (M^+, ^{79}Br/^{79}Br, 98%), 339.83 (M^+, ^{79}Br/^{81}Br, 100%), 341.89 (M^+, ^{81}Br/^{81}Br, 90%), Calcd for $C_{13}H_8Br_2O$: 337.89 (51.4%), 339.89 (100%), 341.89 (48.6%).

2,7-Dibromo-4-iodofluorene (3.27)

Exp no: SK-102

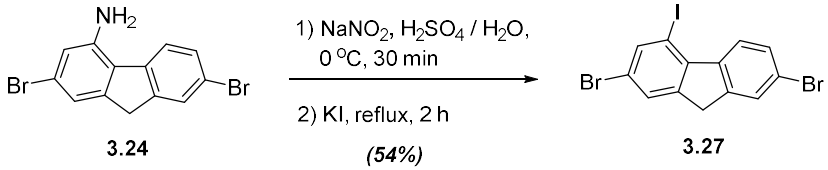

3.24 3.27

We have modified the procedure described in the literature.[21] 2,7-Dibromo-4-aminofluorene (**3.24**) (5.04 g, 14.9 mmol), H_2O (75 mL) and 95% concentrated H_2SO_4 (75 mL) were charged in 250 mL round bottom flask. The mixture was cooled to 0 °C, a solution of $NaNO_2$ (1.04 g (15.1 mmol) in H_2O (10 mL) was slowly added with stirring over a period of 10 minutes and the reaction mixture was stirred for 30 minutes maintaining the temperature at 0–2 °C (internal temperature). Solution of potassium iodide (5.30 g) in H_2O (10 mL) was added, the mixture was stirred at room temperature for 30 minutes and then heated to reflux for 2 h. The mixture was cooled down to room temperature, the brown precipitate was filtered off, washed with 2 M aqueous NaOH (2 × 50 mL), then with water (100 mL) and dried to give crude product (5.40 g, 81%). The crude product was purified by column chromatography on silica gel using PE as eluent to afford compound **3.27** as a pale yellow solid (3.61 g, 54.0%), mp: 170–171 °C.

^{1}H NMR (400 MHz, $CDCl_3$): δ (ppm) 8.64 (d, *J* = 8.4 Hz, 1H, H-5), 8.01 (d, *J* = 1.6 Hz, 1H), 7.67 (s, 1H), 7.64 (s, 1H), 7.58 (dd, *J* = 1.8, 8.4 Hz, 1H, H-6), 3.88 (s, 2H).

^{13}C NMR (100 MHz, $CDCl_3$): δ (ppm) 146.84, 145.48, 141.00, 140.78, 139.83, 129.26, 128.01, 127.87, 123.52, 121.94, 120.69, 87.79, 36.54.

MS (TOF EI$^+$): *m/z* 447.76 (M^+, $^{79}Br/^{79}Br$, 55%), 449.75 (M^+, $^{79}Br/^{81}Br$, 100%), 451.76 (M^+, $^{81}Br/^{81}Br$, 55%), Calcd for $C_{13}H_7Br_2I$: 447.80 (51.4 %), 449.79 (100%), 451.79 (48.6 %).

2,7-Dibromo-4-fluorofluorene (3.29)

Exp no: SK-134

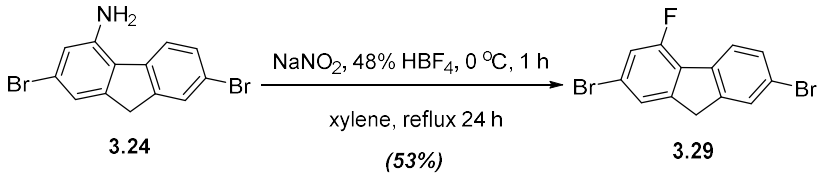

3.24 3.29

2,7-Ddibromo-4-aminofluorene (**3.24**) (3.04 g, 8.97 mmol) and 48% HBF_4 (300 mL) were charged in 500 mL of two-neck round bottom flask. The mixture was stirred for 20 minutes at room temperature to form yellow colour solution. The mixture was cooled down to 0 °C, a solution of $NaNO_2$ (1.80 g, 26.6 mmol) in H_2O (15 mL) was slowly added with stirring over a period of 20 minutes maintaining the temperature at –2 to 0 °C (internal temperature). The excess nitrite ions was controlled by KI–starch paper. The mixture was stirred at 0 °C for 1 h and then brought to room temperature (yellow solid was precipitated during the reaction). The solid was filtered off, washed with water (5 × 20 mL) and dried *in vacuo* at room temperature to obtain diazonium salt **3.28** (4.78 g, 155% by mass). The solid compound (salt **3.28**) was dissolved in xylene (*o-/m-/p*-mixture, 20 mL) and stirred at reflux for 24 h. The mixture was cooled to room temperature, water (100 mL) was added and the product was extracted with DCM (3 × 50 mL). The combined organic layer was dried over Mg_2SO_4, the solvent was evaporated under reduced pressure and the residue was dried *in vacuo* to give crude product (3.56 g, 117%). The crude product was purified by flash chromatography on silica gel using PE as eluent to afford compound **3.29** as a white solid (1.64 g, 53.5%), mp: 119–121 °C.

^{1}H NMR (400 MHz, $CDCl_3$): δ (ppm) 7.77 (d, *J* = 8.1 Hz, 1H, H-5), 7.66 (d, *J* = 0.6 Hz, 1H), 7.52 (dd, *J* = 1.4, 8.1 Hz, 1H, H-6), 7.46 (d, *J* = 1.0 Hz, 1H), 7.25 (d, $J_{H3\text{-}F4}$ = 8.1, Hz, 1H, H-3), 3.92 (s, 2H, CH_2).

^{19}F NMR (400 MHz, $CDCl_3$): δ (ppm) 117.79.

^{13}C NMR (100 MHz, $CDCl_3$): δ (ppm) 159.03, 156.50, 146.90, 146.83, 144.15, 137.00, 136.97, 130.55, 128.05, 127.47, 127.33, 124.56, 124.50, 124.28, 124.25, 121.30, 120.58, 120.50, 117.87, 117.64, 37.16.

MS (TOF EI$^+$): *m/z* 339.86 (M^+, $^{79}Br/^{79}Br$, 75%), 341.83 (M^+, $^{79}Br/^{81}Br$, 100%), 343.86 (M^+, $^{81}Br/^{81}Br$, 65%). Calcd for $C_{13}H_7Br_2F$: 339.89 (51.4%), 341.89 (100%), 343.89 (49.6%).

1-Methylthio-2,7-dibromofluorene (3.31), 1,4-di(methylthio)-2,7-dibromofluorene (3.32) and 1-methylthio-2,7-dibromo-4-aminofluorene (3.33):

Exp no: SK-105

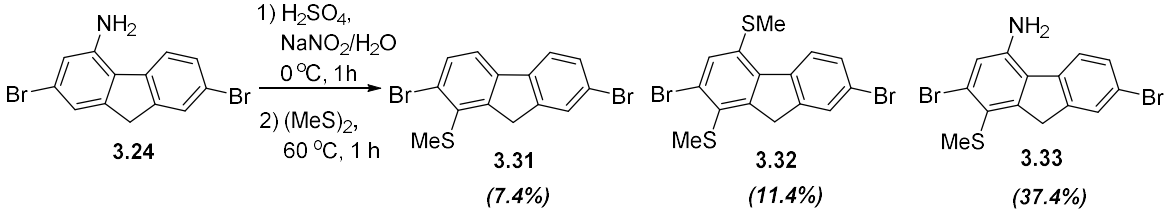

2,7-Dibromo-4-aminofluorene (**3.24**) (0.504 g, 1.49 mmol) was charged in 50 mL two-neck round bottom flask. Concentrated 95% H_2SO_4 (25 mL) was added slowly and the mixture was stirred for 10 minutes to form green solution. The mixture was cooled down to 0 °C, a solution of $NaNO_2$ (0.150 g (2.23 mmol) in H_2O (2 mL) was added slowly with stirring over a period of 10 minutes maintaining the temperature at 0–2 °C (internal temperature). The excess of nitrite ions was controlled by KI–starch paper. The mixture was stirred for 45 minutes, then dimethyl disulphide (0.20 mL, 2.23 mmol, 1.5 eq.) was added slowly, the temperature was brought to room temperature and then the mixture was stirred at 60 °C for 1 h. The reaction mixture was cooled down to room temperature, diluted with water (20 mL), the precipitate was filtered off, washed with water (2 × 10 mL) and dried *in vacuo* to afford crude product as a black solid (0.580 g). The crude product was purified by column chromatography on silica gel with PE as an eluent, eluting first 2,7-dibromo-1-methylthiofluorene (**3.31**) as a white solid (0.041 g, 7.4%) and then 2,7-dibromo-1,4-dimethylthiofluorene (**3.32**) (0.071 g, 11.4%). The column was further eluted with PE/EA (4:1, v/v) to afford crude compound **3.33** as dark brown solid (0.341 g, 59.6%). It was further purified by column chromatography on silica gel using the gradient solvent eluent system, from PE to PE/EA (4:1, v/v), to give pure compound **3.33** as a brown solid (0.214 g, 37.4%).

1-Methylthio-2,7-dibromofluorene (3.31):

^{1}H NMR (400 MHz, $CDCl_3$): δ (ppm) 7.70 (d, *J* = 0.8 Hz, 1H), 7.68 (d, *J* = 8.1 Hz, 1H, H-5), 7.59 (d, *J* = 8.1 Hz, 1H), 7. 54 (d, *J* = 8.0 Hz, 1H), 7.51 (dd, *J* = 8.2, 1.6 Hz, 1H, H-6), 4.05 (s, 2H, CH_2).

1,4-Di(methylthio)-2,7-dibromofluorene (3.32):

^{1}H NMR (400 MHz, $CDCl_3$): δ (ppm) 8.18 (d, *J* = 8.4 Hz, 1H, H-5), 7.69 (s, 1H), 7.53 (dd, *J* = 1.7, 8.4 Hz, 1H, H-6), 7.48 (s, 1H), 4.07 (s, 2H, CH_2), 2.61 (s, 3H, SCH_3), 2.47 (s, 3H, SCH_3).

1-Methylthio-2,7-dibromo-4-aminofluorene (3.33):

^{1}H NMR (400 MHz, $CDCl_3$): δ (ppm) 7.67 (s, 1H), 7.49 (m, 2H), 7.05 (s, 1H), 4.16 (s, 2H, NH_2), 4.02 (s, 2H, CH_2), 2.36 (s, 3H, SCH_3).

^{13}C NMR (100 MHz, $CDCl_3$): δ (ppm) 150.95, 144.71, 143.27, 139.91, 130.16, 129.89, 128.13, 125.86, 122.24, 122.10, 119.85, 119.75, 39.04, 18.91.

MS (TOF EI+): *m/z* 382.79 (M^+, ^{79}Br/^{79}Br, 98%), 384.75 (M^+, ^{79}Br/^{81}Br, 100%), 386.79 (M^+, ^{81}Br/^{81}Br, 95%),. Calcd for $C_{14}H_{11}Br_2NS$: 382.90 (51.4%), 384.90 (100%), 386.89 (48.6%).

2,7-Dibromo-4-methylthiofluorene (3.30)

Exp no: SK-171

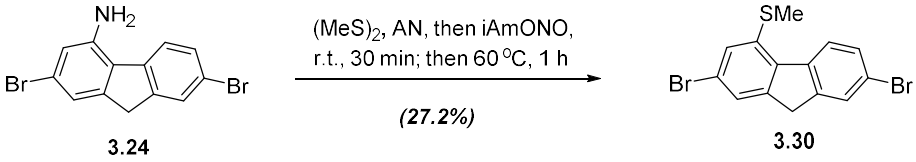

3.24 3.30

Under nitrogen atmosphere, the mixture of 2,7-dibromo-4-aminofluorene (**3.24**) (5.12 g, 15.1 mmol), dimethyl disulphide (10 mL, 105 mmol) and acetonitrile (50 mL) were stirred for 30 min (pale yellow colour suspension). After 30 minutes of stirring, isopentylnitrite (15 mL, 90.6 mmol) was slowly added and the mixture was stirred at 60 °C for 1 h to form dark brown colour precipitate. The reaction mixture was cooled to room temperature, the solid was filtered off, washed with water (3 × 10 mL) and dried *in vacuo* to give crude product as a brown solid (6.12 g, 109%). The crude product was first filtered through short silica gel column eluting with PE/DCM (1:1, v/v), solvent was evaporated and residue then was purified by flash chromatography on silica gel using PE/DCM (4:1, v/v) to afford compound **3.30** as a yellow solid (1.52 g, 27.2%), mp: 119–121 °C.

^{1}H NMR (400 MHz, $CDCl_3$): δ (ppm) 8.22 (d, *J* = 8.3 Hz, 1H, H-5), 7.65 (s, 1H), 7.53 (dd, *J* = 1.8, 8.4 Hz, 1H, H-6), 7.46 (d, *J* = 0.7 Hz, 1H), 7.33 (d, *J* = 1.0 Hz, 1H), 3.88 (s, 2H, CH_2), 2.60 (s, 3H, CH_3).

^{13}C NMR (100 MHz, $CDCl_3$): δ (ppm) 145.59, 144.99, 139.92, 136.78, 135.81, 129.94, 127.76, 126.69, 125.47, 124.58, 121.15, 120.72, 36.89, 15.75.

MS (TOF EI+): m/z 367.90 (M^+, ^{79}Br/^{79}Br, 65%), 369.91 (M^+, ^{79}Br/^{81}Br, 100%), 371.89 (M^+, ^{81}Br/^{81}Br, 60%),. Calcd for $C_{14}H_{10}Br_2S$: 367.89 (50.2 %), 369.88 (100 %), 371.88 (52.0 %).

2,7-Dibromo-4-methoxyfluorene (3.34)

Exp no: SK-130

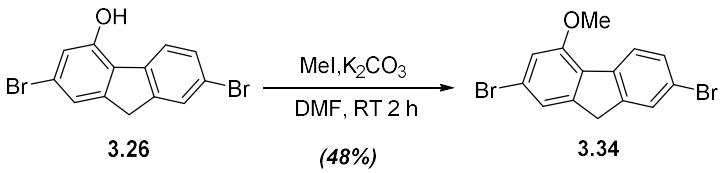

3.26 3.34

To a mixture of 2,7-dibromo-4-hydroxyfluorene (**3.26**) (1.308 g, 3.84 mmol) and potassium

carbonate (0.630 g, 4.61 mmol) in dry DMF (20 mL), methyl iodide (0.30 mL) was added dropwise and the mixture was stirred for 2 h at room temperature. The mixture was diluted with water (30 mL), the precipitate was filtered off, washed with water (3 × 10 mL) and dried *in vacuo* to give brown solid (1.53 g, 107%). The crude product was purified by flash chromatography on silica gel using PE as eluent to afford compound **3.34** as a white solid (0.681 g, 48%).

^{1}H NMR (400 MHz, DMSO): δ (ppm) 7.90 (d, *J* = 8.2 Hz, 1H, H-5), 7.77 (d, *J* = 1.3 Hz, 1H), 7.56 (dd, *J* = 1.8, 8.2 Hz, 1H, H-6), 7.42 (s, 1H), 7.22 (s, 1H), 3.99 (s, 3H, CH_3), 3.98 (s, 2H, CH_2).

^{13}C NMR (100 MHz, $CDCl_3$): δ (ppm) 155.99, 146.08, 144.14, 139.13, 129.98, 128.08, 127.51, 124.85, 121.24, 120.56, 120.04, 112.62, 55.66, 37.03.

MS (TOF EI$^+$): *m/z* 351.92 (M^+, ^{79}Br/^{79}Br, 65%), 353.93 (M^+, ^{79}Br/^{81}Br, 100%), 355.93 (M^+, ^{81}Br/^{81}Br, 60%), Calcd for $C_{14}H_{10}Br_2O$: 351.91 (51.3 %), 353.91 (100 %), 355.91 (49.9 %).

2,7-Dibromo-4-cyanofluorene (3.35)

Exp no: SK-133

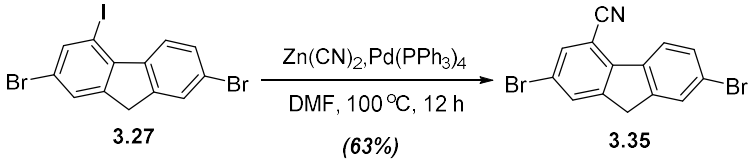

A mixture of 2,7-dibromo-4-iodofluorene (**3.27**) (2.55 g, 5.67 mmol), zinc cyanide (0.73 g, 6.24 mmol), $Pd(PPh_3)_4$ (0.32 g, 0.28 mmol) and dry DMF (30 mL) was purged with argon for 20 minutes and then stirred under argon at 100 °C for 12 h. The reaction mixture was cooled down to room temperature and diluted with water (20 mL). The precipitate was filtered off, washed with water (3 × 5 mL) and dried *in vacuo* to give pale yellow solid (2.41 g, 121%). The crude product was purified by flash chromatography on silica gel using PE/DCM (3:2, v/v) as eluent to afford compound **3.35** as a pale yellow solid (1.235 g, 63%).

^{1}H NMR (400 MHz, $CDCl_3$): δ (ppm) 8.23 (d, *J* = 8.3 Hz, 1H, H-5), 7.86 (d, *J* = 1.5 Hz, 1H), 7.76 (d, *J* = 1.6 Hz, 1H), 7.72 (d, *J* = 1.6 Hz, 1H), 7.58 (dd, *J* = 1.6, 8.3 Hz, 1H, H-6), 3.90 (s, 2H, CH_2).

^{13}C NMR (100 MHz, $CDCl_3$): δ (ppm) 145.89, 145.24, 141.29, 136.99, 133.85, 132.64, 130.95, 128.41, 123.54, 123.32, 120.19, 116.76, 105.67, 36.26.

MS (TOF EI$^+$): *m/z* 346.84 (M^+, ^{79}Br/^{79}Br, 98%), 348.81 (M^+, ^{79}Br/^{81}Br, 100%), 350.86 (M^+, ^{81}Br/^{81}Br, 85%). Calcd for $C_{14}H_7Br_2N$: 346.89 (51.4%), 348.89 (100%), 350.89 (48.7%).

2,7-Dibromo-4-phenylethynylfluorene (3.36)

Exp no: SA-009

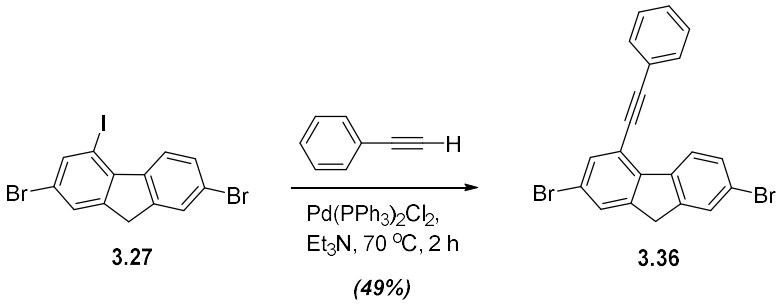

2,7-Dibromo-4-iodofluorene (**3.27**) (3.00 g, 6.6 mmol), phenylacetylene (0.68 g, 6.6 mmol), $Pd(PPh_3)_2Cl_2$ (0.093 g, 0.13 mmol), and triethylamine (3.0 mL) were charged in 25 mL glass tube. The reaction mixture was stirred at 70 °C for 2 h monitoring the progress of the reaction by TLC. The mixture was cooled to room temperature, pH was adjusted to neutral (pH 7) by adding diluted HCl and extracted with DCM (2 × 10 mL). The combined organic layer was dried over Mg_2SO_4, evaporated under reduced pressure and the residue was dried *in vacuo* to give crude product (3.39g, 120%). The crude product was purified by flash chromatography on silica gel using PE/DCM (9:1, v/v) as eluent to afford compound **3.36** as a cream colour solid (1.38 g, 49%), mp: 171–172.5 °C.

^{1}H NMR (400 MHz, $CDCl_3$): δ (ppm) 8.42 (d, J = 8.3 Hz, 1H), 7.66 (m, 2H), 7.61–7.59 (m, 3H), 7.55 (dd, J = 1.6, 8.3 Hz, 1H), 7.43–7.41 (m, 3H), 3.89 (s, 2H, CH_2).

^{13}C NMR (100 MHz, $CDCl_3$): δ (ppm) 145.14, 145.12, 139.60, 139.55, 133.86, 131.60 (2C), 130.21, 128.93, 128.63 (2C), 128.16, 127.96, 123.90, 122.76, 121.50, 120.08, 118.10, 95.13, 86.86, 36.36.

MS (TOF EI$^+$): *m/z* 425. 65 (M^+, ^{79}Br/^{79}Br, 52%), 421.34 (M^+, ^{79}Br/^{81}Br, 100%), 424.07 (M^+, ^{81}Br/^{81}Br, 50%). Calcd for $C_{21}H_{12}Br_2$: 425.93 (48.6%), 421.93 (100.4%), 423.93 (51.4%).

2,4,7-Trimethylfluorene (3.37)

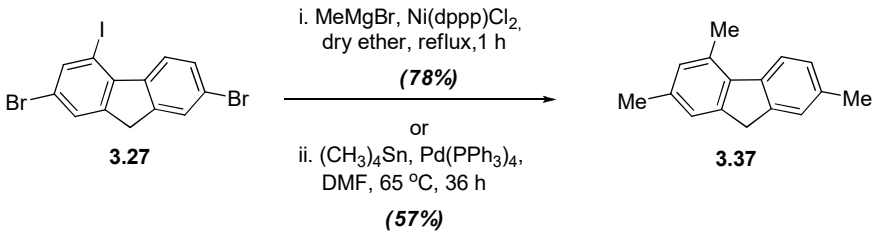

*Compound **3.37** was isolated in two unsuccessful attempts to synthesise 2,7-dibromo-4-methylfluorene (**3.38**).*

Method A.. Exp no: SK-140

Two neck round bottom flask was charged with 2,7-dibromo-4-iodofluorene (**3.27**) (0.085 g, 0.189 mmol), $Ni(dppp)Cl_2$ (6 mg), degassed by flushing with nitrogen for 25 minutes and

then dry diethyl ether (3 mL) was added. The reaction mixture was stirred under nitrogen for 5 minutes, MeMgBr (3 M solution in diethyl ether, 0.09 mL, 0.27 mmol) was added slowly dropwise and the mixture was stirred at reflux for 1 h. The reaction mixture was cooled down to room temperature, diluted with water (5 mL) and extracted with DCM (3 × 5 mL). The combined organic layer was dried over Mg_2SO_4, the solvent was evaporated under reduced pressure and the residue was dried *in vacuo* to give a brown liquid (0.041 g, 104%). The crude product was purified by column chromatography on silica gel using PE as eluent to afford compound **3.37** as a white solid (0.031 g, 78 %).

Method B. Exp no: SK-128

Two neck round bottom flask was charged with 2,7-dibromo-4-iodofluorene (**3.27**) (0.102 g, 0.22 mmol), tetramethyltin (0.03 mL, 0.27 mmol) and dry DMF (3 mL). The reaction mixture was purged with nitrogen for 20 minutes, $Pd(PPh_3)_4$ (0.01 g) was added and the mixture was stirred at 65 °C for 36 h. The mixture was cooled down to room temperature, diluted with water (5 mL) and extracted with ethylacetate (3 × 5 mL). The combined organic layer was dried over Mg_2SO_4, the solvent was evaporated under reduced pressure and the residue was dried *in vacuo* to give crude product (0.051 g, 108%). The crude product was purified by column chromatography on silica gel using PE, eluted first starting compound 2,7-dibromo-4-iodofluorene (**3.27**) (0.011 g, 13%) and then product **3.37** (0.041 g, 87%) as a colourless solid.

^{1}H NMR (400 MHz, $CDCl_3$): δ (ppm) 7.74 (d, *J* = 7.8 Hz, 1H), 7.35 (s, 1H), 7.17 (m, 2H), 6.95 (s, 1H), 3.82 (s, 2H), 2.66 (s, 3H, CH_3), 2.42 (s, 3H, CH_3), 2.38 (s, 3H, CH_3).

^{13}C NMR (400 MHz, $CDCl_3$): δ (ppm) 143.80, 143.73, 140. 06, 137.24, 135.75, 135.32, 132.25, 129.78, 127.33, 125.61, 123.08, 122.33, 36.76, 21.43, 21.31, 20.83.

MS (TOF EI$^+$): *m/z* 208.07 (M^+, 50%). Calcd for $C_{16}H_{16}$: 208.13.

2,7-Dibromo-4-fluoro-9,9-dioctylfluorene (3.39)

Exp no: SK-145

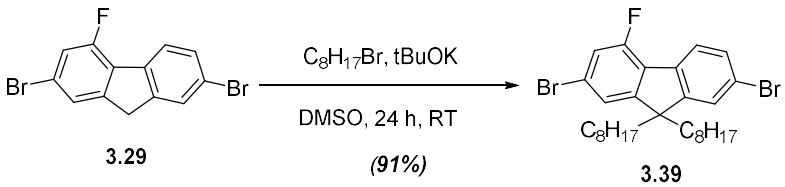

3.29 **3.39**

Under a nitrogen atmosphere, 2,7-dibromo-4-fluorofluorene (**3.29**) (0.404 g, 1.18 mmol) and DMSO (10 mL) was charged in 25 mL flask. The mixture was stirred for 10 minutes until full dissolution, then t-BuOK (0.294 g, 2.59 mmol) was added portionwise and the mixture was stirred for 30 minutes (violet colour was observed). 1-Bromooctane (0.8 mL) was added slowly dropwise and the mixture was stirred at room temperature for 24 h. The solution was

diluted with water (40 mL) and extracted with DCM (3 × 10 mL). The combined organic layer was dried over Mg_2SO_4, the solvent was evaporated and the residue was dried *in vacuo* to give yellow liquid (0.745 g, 111%). The crude product was purified by flash chromatography on silica gel using PE as eluent to afford compound **3.39** as a colourless plates (0.612 g, 91%), mp: 56–58 °C.

^{1}H NMR (400 MHz, $CDCl_3$): δ (ppm) 7.69 (d, J = 8.0 Hz, 1H, H-5), 7.47 (dd, J = 1.7, 8.0 Hz, 1H, H-6), 7.43 (d, J = 1.6 Hz, 1H), 7.23 (d, J = 1.4 Hz, 1H), 7.20 (dd, $J_{H3\text{-}F4}$ = 9.1 Hz, $J_{H3\text{-}H1}$ = 1.4 Hz, 1H, H-3), 1.92–1.88 (m, 4H, $CH_2C_7H_{15}$), 1.21–1.15 (m, 4H, $CH_2CH_2CH_2C_5H_{11}$) 1.13–1.05 (m, 16H, $C_3H_6C_4H_8CH_3$), 0.84 (t, J = 7.0 Hz, 6H, CH_3), 0.56 (m, 4H, $CH_2CH_2C_6H_{13}$).

^{19}F NMR (400 MHz, $CDCl_3$): δ (ppm) 117.72.

^{13}C NMR (100 MHz, $CDCl_3$): δ (ppm) 158.91, 156.37, 154.89, 154.84, 151.97, 136.34, 136.31, 130.54, 121.12, 120.97, 117.90, 117.67, 56.70, 40.25, 29.15, 29.12, 29.04, 23.58, 22.59, 14.06.

MS (TOF EI$^+$): *m/z* 564.15 (M^+, ^{79}Br/^{79}Br, 70%), 566.09 (M^+, ^{79}Br/^{81}Br, 100%), 568.11 (M^+, ^{81}Br/^{81}Br, 85%). Calcd for $C_{29}H_{39}Br_2F$: 564.14 (51.4%), 566.14 (100.0%), 568.14 (53.4%).

2,7-Dibromo-4-cyano-9,9-dioctylfluorene (3.40)

Exp no: SK-139

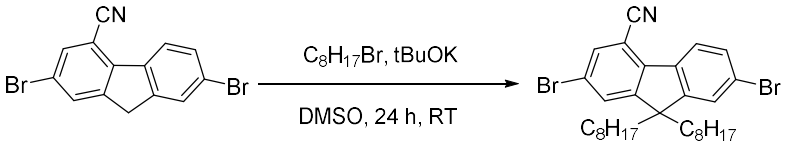

Under a nitrogen atmosphere, 2,7-dibromo-4-cyanofluorene (**3.35**) (1.210 g, 3.27 mmol) in DMSO (30 mL) was stirred for 15 minutes, then t-BuOK (1.40 g, 13.0 mmol) was added portionwise and the mixture was stirred for 30 minutes (violet colour was observed). 1-Bromooctane (1.7 mL) was added dropwise and the mixture was stirred at room temperature for 24 h. The mixture was diluted with water (50 mL) and extracted with DCM (3 × 10 mL). The organic layer was dried over Mg_2SO_4, the solvent was evaporated under reduced pressure and the residue was dried *in vacuo* to give brown liquid (2.19 g, 105%). The crude product was purified by flash chromatography on silica gel using PE/DCM (4:1–2:1, v/v) as a gradient solvent eluent system to afford compound **3.40** as a white solid (1.02 g, 52%), mp: 88–90 °C.

^{1} H NMR (400 MHz, $CDCl_3$): δ (ppm) 8.18 (d, J = 8.2 Hz, 1H, H-5), 7.72 (d, J = 1.6 Hz, 1H), 7.64 (d, J = 1.6 Hz, 1H), 7.55 (dd, J = 1.7, 8.2 Hz, 1H, H-6), 7.49 (d, J = 1.7 Hz, 1H), 1.95-1.91 (m, 4H, $CH_2C_7H_{15}$), 1.21–1.16 (m, 4H, $CH_2CH_2CH_2C_5H_{11}$) 1.14-1.05 (m, 16H, $C_3H_6C_4H_8CH_3$) 0.83 (t, J = 7.0 Hz, 6H, CH_3), 0.52 (m, 4H, $CH_2CH_2C_6H_{13}$).

^{13} C NMR (100 MHz, $CDCl_3$): δ (ppm) 153.88, 153.05, 140.80, 136.28, 133.78, 130.99, 130.40, 126.23, 123.93, 123.55, 120.67, 116.89, 105.64, 55.53, 39.94, 31.72, 29.71, 29.11, 29.07, 23.56, 22.58, 14.05.

MS (TOF EI^+): *m/z* 571.22 (M^+, $^{79}Br/^{79}Br$, 65%), 573.21 (M^+, $^{79}Br/^{81}Br$, 100%), 575.22 (M^+, $^{81}Br/^{81}Br$, 60%). Calcd for $C_{30}H_{39}Br_2N$: 571.14 (51.4%), 573.14 (100.0%), 575.14 (48.8%).

2,7-Dibromo-4-methoxy-9,9-dioctylfluorene (3.41)

Exp no: SK-146

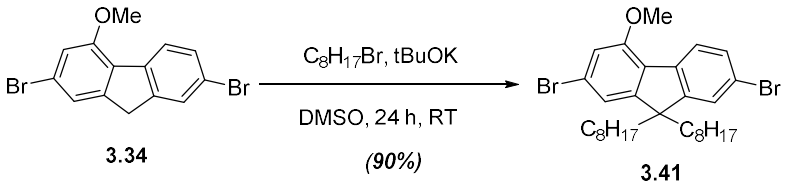

2,7-Dibromo-4-methoxyfluorene (**3.34**) (1.03 g, 2.91 mmol) in DMSO (30 mL) was stirred for 10 minutes, 1-bromooctane (2.0 mL) was added, then added t-BuOK (0.720 g, 6.41 mmol) portionwise and the mixture was stirred for 30 minutes. The solution became initially yellow and then changed to brown colour at the end of t-BuOK addition. The mixture was stirred at room temperature for 24 h, diluted with water (50 mL) and extracted with DCM (3 × 10 mL). The organic layer was dried over Mg_2SO_4, the solvent was evaporated under reduced pressure and the residue was dried *in vacuo* to give crude yellow liquid (1.785 g, 106%). The crude product was purified by flash chromatography on silica gel using PE as eluent to afford compound **3.41** as pale a yellow solid (1.52 g, 90 %), mp: 77.5–79 °C.

^{1}H NMR (400 MHz, $CDCl_3$): δ (ppm) 7.85 (d, *J* = 8.0 Hz, 1H, H-5), 7.41 (dd, *J* = 1.8, 8.0 Hz, 1H, H-6), 7.39 (d, *J* = 1.7 Hz, 1H), 7.06 (d, *J* = 1.3 Hz, 1H), 6.97 (d, *J* = 1.3 Hz, 1H), 3.97 (s, 3H, OCH_3), 1.91–1.84 (m, 4H, $CH_2C_7H_{15}$), 1.20–1.13 (m, 4H, $CH_2CH_2CH_2C_5H_{11}$), 1.11–1.03 (m, 16H, $C_3H_6C_4H_8CH_3$), 0.82 (t, *J* = 7.0 Hz, 6H, CH_3), 0.55 (m, 4H, $CH_2CH_2C_6H_{13}$).

^{13}C NMR (100 MHz, $CDCl_3$): δ (ppm) 155.81, 153.87, 151.93, 138.56, 130.01, 127.20, 125.41, 124.73, 121.76, 120.55, 118.46, 112.67, 56.04, 55.56, 40.26, 31.77, 29.86, 29.19, 29.15, 23.52, 22.60, 14.07.

MS (TOF EI^+): *m/z* 576.05 (M^+, $^{79}Br/^{79}Br$, 95%), 577.97 (M^+, $^{79}Br/^{81}Br$, 100%), 580.11 (M^+, $^{81}Br/^{81}Br$, 90%). Calcd for $C_{30}H_{42}Br_2O$: 576.16 (51.3%), 578.16 (100%), 580.16 (53.9%).

2,7-Dibromo-4-methylthio-9,9-dioctylfluorene (3.42)

Exp no: SK-172

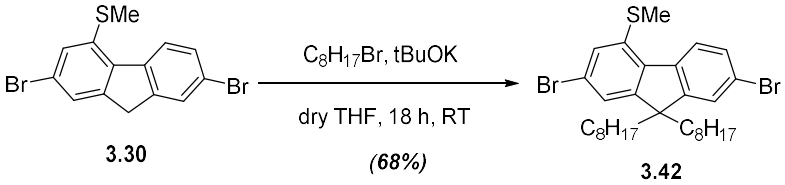

Under a nitrogen atmosphere, 2,7-dibromo-4-methylthiofluorene (**3.30**) (0.806 g, 2.17 mmol) and t-BuOK (1.2 g, 10.8 mmol) in dry THF (20 mL) were stirred at room temperature for 10 minutes. 1-Bromooctane (0.20 mL, 1.07 mmol) was slowly added dropwise and the mixture was stirred under nitrogen atmosphere at room temperature for 18 h. The precipitated KBr was filtered off and washed with DCM (2 × 10 mL). The combined filtrates were dried over Mg_2SO_4, the solvent was evaporated under reduced pressure and the residue was dried *in vacuo* to give crude product (1.321 g, 102%). The crude product was purified by flash chromatography on silica gel using PE as eluent to afford compound **3.42** as a white solid (0.889 g, 68%), mp: 88.5–90 °C.

^{1}H NMR (400 MHz, CD_3COCD_3): δ (ppm) 8.18 (d, *J* = 8.3 Hz, 1H, H-5), 7.69 (d, *J* = 1.8 Hz, 1H), 7.59 (dd, *J* = 1.8, 8.2 Hz, 1H, H-6), 7.47 (d, *J* = 1.6, Hz, 1H), 7.39 (d, *J* = 1.5 Hz, 1H), 2.69 (s, 1H, SCH_3), 2.08–2.05 (m, 4H, $CH_2C_7H_{15}$), 1.25–1.20 (m, 4H, $CH_2CH_2CH_2C_5H_{11}$) 1.18-1.07 (m, 16H, $C_3H_6C_4H_8CH_3$) 0.83 (t, *J* = 7.0 Hz, 6H, CH_3), 0.57 (m, 4H, $CH_2CH_2C_6H_{13}$).

^{13}C NMR (100 MHz, $CDCl_3$): δ (ppm) 153.39, 152.71, 139.35, 135.98, 135.74, 129.94, 126.34, 125.57, 125.36, 122.34, 121.67, 121.22, 55.45, 40.42, 31.75, 29.83, 29.18, 29.12, 23.47, 22.60, 15.59, 14.07,

MS (TOF EI$^+$): *m/z* 592.20 (M^+, ^{79}Br/^{79}Br, 65%), 594.14 (M^+, ^{79}Br/^{81}Br, 100%), 596.11 (M^+, ^{81}Br/^{81}Br, 65%). Calcd for $C_{30}H_{42}Br_2S$: 592.14 (50.0%), 594.14 (100%), 596.13 (51.7%).

2,7-dibromo-4-phenylethnylfluorene (3.43)

Exp no: SA-09

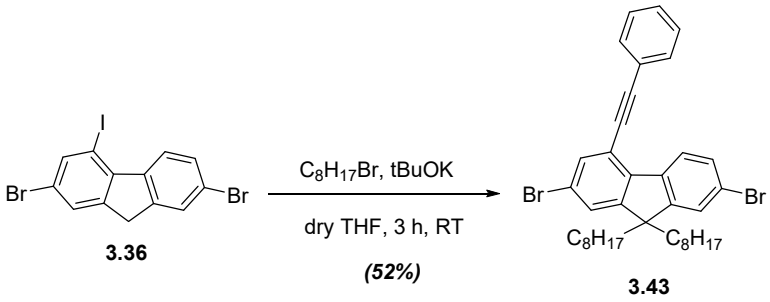

Under a nitrogen atmosphere, a mixture of 2,7-dibromo-4-iodofluorene (**3.36**) (1.02 g, 2.36 mmol) and t-BuOK (0.582 g, 5.19 mmol) in dry THF (45 mL) was stirred for 10 minutes, then 1-bromooctane (1.6 mL, 9.4 mmol) was added dropwise and the mixture was stirred at room temperature for 3 h. The precipitated KBr was filtered off and washed with DCM (2 × 10 mL). The combined organic layer was dried over Mg_2SO_4, the solvent was evaporated under reduced pressure and the residue was dried *in vacuo* to give the crude product, which was purified by flash chromatography on silica gel using PE as eluent to afford compound **3.43** as pale a yellow solid (0.801 g, 52%), mp: 85–87 °C.

^{1}H NMR (400 MHz, $CDCl_3$): δ (ppm) 8.34 (d, J = 8.2 Hz, 1H, H-5), 7.63–7.61 (m, 3H), 7.50–7.48 (m, 1H), 7.45–7.41 (m, 5H), 1.93–1.89 (m, 4H, $CH_2C_7H_{15}$), 1.21–1.05 (m, 20H, $C_2H_4C_5H_{10}CH_3$), 0.83 (t, J = 7.0 Hz, 6H, CH_3), 0.58 (m, 4H, $CH_2CH_2C_6H_{13}$).

^{13}C NMR (100 MHz, $CDCl_3$): δ (ppm) 152.95, 152.87, 139.06, 138.92, 133.86, 131.59, 130.26, 128.90, 128.63, 126.01, 125.78, 123.85, 122.80, 122.11, 120.59, 117.94, 95.02, 87.05, 55.20, 40.27, 31.78, 29.86, 29.20, 29.16, 23.57, 22.62, 14.10.

MS (TOF EI$^+$): *m/z* 646.33 (M^+, ^{79}Br/^{79}Br, 56%), 650. 21 (M^+, ^{79}Br/^{81}Br, 100%), 648.28 (M^+, ^{81}Br/^{81}Br, 49%). Calcd for $C_{37}H_{44}Br_2$: 646.18 (51.4%), 650.18 (100%), 648.18 (48.6%).

2,7-Dibromo-4-methylsulfonyl-9,9-dioctylfluorene (3.44)

Exp no: SK-173

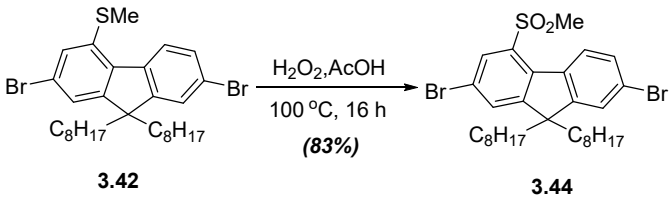

2,7-Dibromo-4-methylthio-9,9-dioctylfluorene (**3.42**) (2.08 g, 3.49 mmol) and 30% hydrogen peroxide (H_2O_2, 0.64 mL, 20.9 mmol) in acetic acid (50 mL) were stirred at 100 °C for 16 h. The mixture was diluted with water (30 mL), extracted with DCM (3 × 10 mL), the organic layer was washed with water (~20 mL) until pH 7 and dried over Mg_2SO_4. The solvent was

evaporated under reduced pressure and the residue was dried *in vacuo* to give crude product as a pale yellow liquid (2.34 g, 106%). The crude product was purified by flash chromatography on silica gel using PE/DCM (3:1, v/v) as eluent to afford compound **3.44** as a colourless solid (1.84 g, 83 %), mp: 86–88 °C.

^{1}H NMR (400 MHz, $CDCl_3$): δ (ppm) 8.46 (d, *J* = 8.5 Hz, 1H, H-5), 8.22 (d, *J* = 1.8 Hz, 1H), 7.70 (d, *J* = 1.8 Hz, 1H), 7.55 (dd, *J* = 1.8, 8.4 Hz, 1H, H-6), 7.50 (d, *J* = 1.8 Hz, 1H), 3.19 (s, 1H, SO_2CH_3), 1.99–1.91 (m, 4H, $CH_2C_7H_{15}$), 1.20–1.04 (m, 20H, $C_2H_4C_5H_{10}CH_3$) 0.82 (t, *J* = 7.0 Hz, 6H, CH_3), 0.52 (m, 4H, $CH_2CH_2C_6H_{13}$).

^{13}C NMR (100 MHz, $CDCl_3$): δ (ppm) 155.85, 153.72, 136.66, 135.72, 135.32, 131.24, 131.12, 130.96, 127.13, 126.17, 123.83, 121.34, 55.14, 42.28, 40.28, 31.71, 29.67, 29.12, 29.05, 23.44, 22.57, 14.05.

MS (TOF EI^+): *m/z* 624.13 (M^+, $^{79}Br/^{79}Br$, 50%), 626.04 (M^+, $^{79}Br/^{81}Br$, 100%), 628.04 (M^+, $^{81}Br/^{81}Br$, 55%). Calcd for $C_{30}H_{42}Br_2O_2S$: 624.13 (49.9%), 626.13 (100.0%), 628.12 (51.6%).

2,7-dinitro-4-butylthiofluorenone (3.54)

Exp no: SK-72

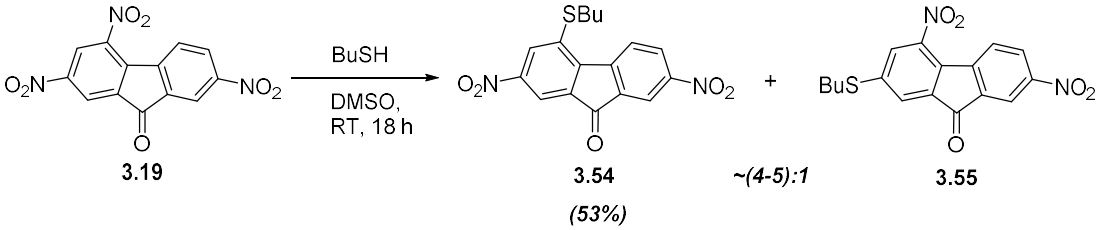

2,4,7-Trinitrofluorenone (**3.19**) (1.08 g, 3.42 mmol), 1-butanethiol (1.07 mL, 9.93 mmol) and DMSO (15 mL) were charged into a single neck round bottom flask. The reaction mixture was stirred at 80 °C for 40 h, cooled down to room temperature, diluted with a mixture of water (30 mL) and acetone (15 mL) and stirred for 30 minutes. The precipitate was filtered off and dried *in vacuo* to afford crude product (1.33 g, 113%) as a yellow solid. The crude product was recrystallised from ethyl acetate (20 mL) to afford pure compound **3.54** as a yellow solid (0.0.381 g, 31%). An additional portion of compound **3.54** (0.270 g, 22%) was isolated by recrystallisation of the residue from the mother liquor. The total yield of compound **3.54** is 0.651g (53%). TLC of the mother liquor showed two spots of comparable intensities and the second one is presumably the other isomer, 4,7-dinitro-2-butylthiofluorenone (**3.55**) (by analogy with literature data on substitution reactions in polynitrofluorenones; it was not isolated and not analysed).

Compound **3.54**: mp: 150–152 °C. Lit. mp: 151–152 °C.[55]

^{1}H NMR (400 MHz, $CDCl_3$): δ (ppm) 8.66 (m, 1H), 8.62 (m, 1H), 8.45 (m, 2H), 8.20 (d, *J* = 1.96 Hz, 1H), 3.42 (t, *J* = 7.31 Hz, 2H, S*CH*$_2$C$_3$H$_7$), 1.84 (m, 2H, SCH$_2$*CH*$_2$C$_2$H$_5$), 1.59 (m, 2H, SC$_2$H$_4$*CH*$_2$CH$_3$), 0.99 (t, *J* = 7.34 Hz, 3H, CH_3).

^{13}C NMR (400 MHz, $CDCl_3$): δ (ppm) 188.40 (C=O), 149.40, 148.87, 147.68, 143.73, 138.94, 136.88, 135.72, 130.17, 127.27, 126.39, 119.54, 115.65, 32.79, 30.39, 22.03, 13.58.

MS (TOF EI$^+$): *m/z* 358.00 (M^+, 100%). Calcd for $C_{17}H_{14}N_2O_5S$: 358.06.

2,7-Dinitro-4-hydroxyfluorenone (3.56)

Exp no: SK-55

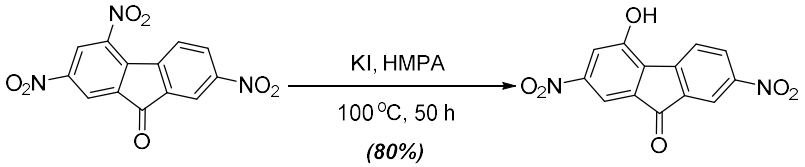

3.19 3.56

A mixture of 2,4,7-trinitrofluorenone (**3.19**) (15.04 g, 47.7 mmol) and potassium iodide (15.85 g, 95.5 mmol) in HMPA (75 mL) was stirred at 100 °C for 50 h to form deep brown solution. The mixture was cooled to room temperature, diluted with water (1.5 L) and stirred for 5 h. The brown precipitate was filtered off and dried *in vacuo* to give crude product (14.72 g, 108%). To the crude product acetone (60 mL) was added, the mixture (not full dissolution) was stirred for 1 h and the solid was filtered off to afford compound **3.56** (6.11 g, 45 %) as yellow crystals. The mother liquor was evaporated, acetone (25 mL) was added to the residue, the suspension was stirred at room temperature for 30 minutes, then filtered off and dried *in vacuo* to afford an additional portion of compound **3.56** (4.80 g, 35%) as a yellow solid. The total yield of compound **3.56** is 10.9 g (80%), mp: 147–149 °C (for the low melting point polymorph formed from acetone); on further heating, it is recrystallised to form a high melting point polymoprph with mp: 317–319 °C. Lit. mp: 309–310 °C (from AcOH).[53]

^{1}H NMR (400 MHz, $CDCl_3$): δ (ppm) 12.55 (s, 1H, OH), 8.50 (d, *J* = 2.0 Hz, 1H), 8.43 (dd, *J* = 2.1, 8.2 Hz, 1H, H-6), 8.23–8.21(m, 2H), 8.04 (d, *J* = 1.8 Hz, 1H).

^{13}C NMR (100 MHz, $CDCl_3$): δ (ppm) 189.65 (C=O), 156.23, 150.46, 148.30, 148.23, 136.78, 135.08, 132.66, 130.25, 125.52, 119.30, 118.79, 110.25.

MS (TOF EI$^+$): *m/z* 285.99 (M^+, 100%). Calcd for $C_{13}H_6N_2O_6$: 286.02 (100.0%).

2,7-Dinitro-4-methoxyfluorenone (3.57)

Exp no: SK-62

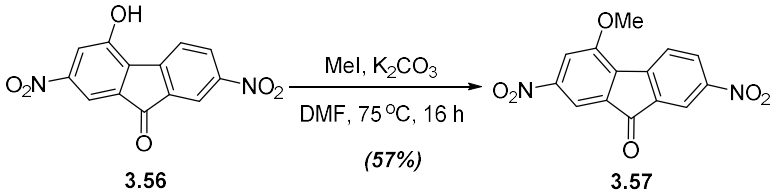

3.56 **3.57**

To the stirred mixture of 4-hydroxy-2,7-dinitrofluorenone (**3.56**) (10.6 g, 37.1 mmol), and potassium carbonate (25.6 g, 185.0 mmol) in DMF (100 mL), methyl iodide (13.0 mL) was added and the mixture was stirred at 75 °C for 16 h. The mixture was diluted with cold water (200 mL), extracted with ethyl acetate (3 × 20 mL), the organic layer was separated and dried over $MgSO_4$. The solvent was evaporated under reduced pressure and the residue was dried *in vacuo* to give crude product (10.4 g, 93%). The crude product was purified by column chromatography on silica gel using PE/EA (1:1, v/v) as eluent to afford compound **3.57** as an orange solid (6.46 g, 57%).

^{1}H NMR (400 MHz, $CDCl_3$): δ (ppm) 8.53 (d, *J* = 2.0, Hz, 1H), 8.46 (dd, *J* = 8.2, 2.1 Hz, 1H, H-6), 8.22 (d, *J* = 1.7 Hz, 1H), 8.15 (d, *J* = 8.2 Hz, 1H, H-5), 8.05 (d, *J* = 1.7 Hz, 1H), 4.17 (s, 3H, OCH_3).

^{13}C NMR (100 MHz, CD_3COCD_3): δ (ppm) 190.37 (C=O), 158.44, 152.81, 150.78, 148.66, 138.47, 136.92, 136.19, 132.33, 127.74, 120.50, 115.61, 112.84, 58.52.

MS (TOF EI+): *m/z* 299.95 (M^+, 100%), Calcd for $C_{14}H_8N_2O_6$: 300.04 (100.0%).

2,7-Diamino-4-butylthiofluorenone (3.58)

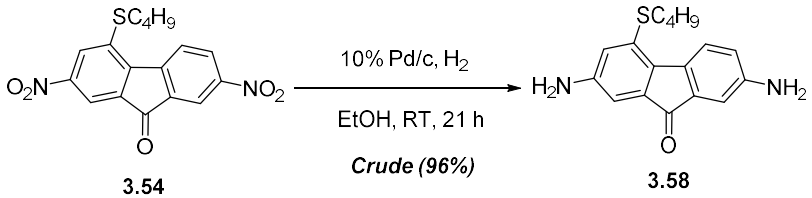

3.54 **3.58**

Metod A. Exp no: SK-75

2,7-Dinitro-4-butylthiofluorenone (**3.54**) (0.103 g, 0.28 mmol) in ethanol (4 mL) was stirred in 25 mL round bottom flask. To this heterogeneous solution, purged with nitrogen, 10% Pd/C (0.10 g) was added and the mixture was stirred under hydrogen atmosphere (1 atm) for 21 h. The mixture was filtered through celite bed, washed with ethylacetate (2 × 10 mL), the solvent was evaporated under reduce pressure and the residue was dried *in vacuo* to afford crude compound **3.58** as a black solid (0.082 g, 96%), mp: 136–138 °C.

^{1}H NMR (400 MHz, $CDCl_3$): δ (ppm) 7.82 (d, *J* = 8.3 Hz, 1H, H-5), 6.92 (d, *J* = 2.3 Hz, 1H), 6.78 (d, *J* = 2.1 Hz, 1H), 6.69 (dd, *J* = 2.4, 8.0 Hz, 1H, H-6), 6.62 (d, *J* = 2.0 Hz, 1H) 3.76 (s,

4H, NH_2) 2.92 (t, *J* = 7.3 Hz, 2H, SCH_2), 1.67 (m, 2H, $SCH_2CH_2C_2H_5$), 1.47 (m, 2H, $SCH_2CH_2CH_2CH_3$), 0.93 (t, *J* = 7.3 Hz, 3H, CH_3).

Method B. Exp no: SK-13

A mixture of 2,7-dinitro-4-butylthiofluorenone (**3.54**) (12.0 g, 33.5 mmol), tin powder (21.7 g, 184 mmol) and 37% of HCl (100 mL) was stirred at 100 °C for 1 h. The mixture was cooled to room temperature, diluted with water (20 mL) and basified to pH 9 by addition of 4 M NaOH solution (~800 mL). Ethyl acetate (200 mL) was added, the mixture was stirred for 2 h and filtered off. The organic layer was separated, dried over Mg_2SO_4, the solvent was evaporated under reduced pressure and the residue was dried *in vacuo* to give crude compound (8.70 g, 87%). The crude product was purified by column chromatography on silica gel using PE/EA (4:1, v/v) as eluent to afford compound **3.58** as a brown solid (6.12 g, 60%).

^{1}H NMR (400 MHz, $CDCl_3$): δ (ppm) 7.82 (d, *J* = 8.3 Hz, 1H, H-5), 6.92 (d, *J* = 2.3 Hz, 1H), 6.78 (d, *J* = 2.1 Hz, 1H), 6.69 (d, *J* = 2.2, 8.0 Hz, 1H, H-6), 6.62 (d, *J* = 2.0 Hz, 1H), 3.76 (s, 4H, NH_2) 2.93 (t, *J* = 7.3 Hz, 2H, SCH_2), 1.67 (m, 2H, $SCH_2CH_2C_2H_5$), 1.47 (m, 2H, $CH_2CH_2CH_2CH_3$), 0.93 (t, *J* = 7.3 Hz, 3H, CH_3).

^{13}C NMR (100 MHz, $CDCl_3$): δ (ppm) 146.034, 145.80, 136.70, 136. 10, 135.80, 134.60, 132.30, 124.33, 120.20, 119.74, 111.16, 109, 54, 50.20, 33.32, 22.04, 22.04, 13.70.

MS (TOF EI$^+$): *m/z* 298.10 (M^+, 100%). Calcd for $C_{17}H_{18}N_2OS$: 298.11 (100.0%).

2,7-Diamino-4-methoxyfluorenone (3.59)

Exp no: SK-91

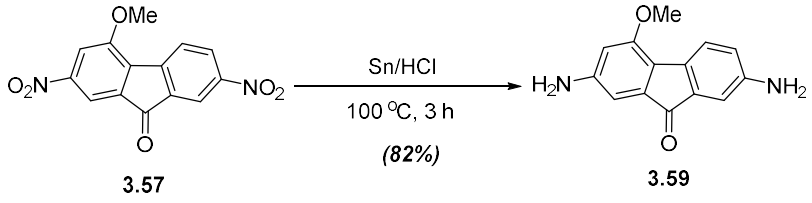

3.57 3.59

A mixture of 2,7-dinitro-4-methoxyfluorenone (**3.57**) (15.8 g, 52.8 mmol), tin powder (41.0 g, 343 mmol) and 37% of HCl (100 mL) was stirred at 100 °C for 3 h. The mixture was cooled to room temperature, diluted with water (20 mL) and pH was adjusted to pH 9 by addition of 4 M NaOH solution (~800 mL). Ethyl acetate was added (600 mL), the mixture was stirred for 4 h and filtered off. The organic layer was separated, dried over Mg_2SO_4, the solvent was evaporated under reduced pressure and the residue was dried *in vacuo* to give the crude product (14.5 g, 112%). The crude product was purified by column chromatography on silica gel using PE/EA (1:1, v/v) as eluent to afford compound **3.59** as a black solid (10.5 g, 82%).

^{1}H NMR (400 MHz, DMSO-d_6): δ (ppm) 7.14 (d, *J* = 7.9 Hz, 1H, H-5), 6.70 (d, *J* = 2.1 Hz, 1H), 6.55 (dd, *J* = 2.2, 7.9 Hz, 1H, H-6), 6.36 (d, *J* = 1.6 Hz, 1H), 6.32 (d, *J* = 1.6 Hz, 1H), 5.40 (s, 2H, NH_2) 5.22 (s, 2H, NH_2) 3.79 (s, 3H, OCH_3).

^{13}C NMR (100 MHz, DMSO-d_6): δ (ppm) 195.48 (C=O), 155.15, 150.49, 147.79, 136.11, 134.38, 133.14, 122.97, 120.26, 118.93, 110.44, 102.97, 102.82, 55.60.

MS (TOF EI$^+$): *m/z* 239.98 (M^+, 100 %). Calcd for $C_{14}H_{12}N_2O_2$: 240.09.

2,7-Diamino-4-butoxycarbonylfluorenone (3.60)

Exp no: SK-12

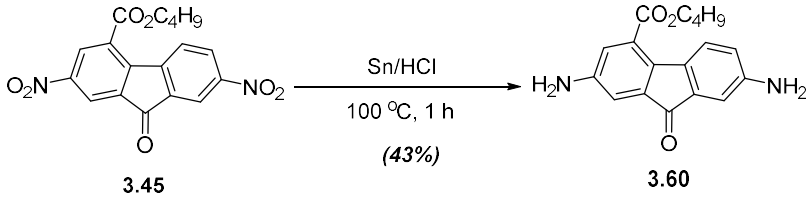

3.45 3.60

A mixture of 2,7-dinitro-4-butoxycarbonylfluorenone (**3.45**)[50] (5.09 g, 13.5 mmol), tin powder (8.7 g, 74.3 mmol) and 37% of HCl (26 mL) was stirred at 100 °C for 1 h. The mixture was cooled to room temperature, diluted with water (20 mL) and neutralised with saturated aqueous $NaHCO_3$ solution. Ethyl acetate (200 mL) was added, the mixture was stirred for 2 h and filtered off. The organic layer was dried over Mg_2SO_4, the solvent was evaporated under reduced pressure and the residue was dried *in vacuo* to give crude product (4.60 g, 112%). The crude product was purified by column chromatography on silica gel using PE/EA (4:1, v/v) as eluent to afford compound **3.60** as a brown solid (1.80 g, 43%), mp: 158–162 °C.

^{1}H NMR (400 MHz, $CDCl_3$): δ (ppm) 7.69 (d, *J* = 8.4 Hz, 1H, H-5), 7.05 (d, *J* = 2.3 Hz, 1H), 6.98 (d, *J* = 2.5 Hz, 1H), 6.82 (d, *J* = 2.3 Hz , 1H), 6.66 (dd, *J* = 2.4, 8.3 Hz, 1H, H-6), 5.68 (s, 2H, NH_2), 5.61 (s, 2H, NH_2), 4.32 (t, *J* =7.0 Hz, 2H), 1.75 (m, 2H), 1.51-1.43 (m, 2H), 0.97 (t, 3H).

^{13}C NMR (100 MHz, $CDCl_3$): δ (ppm) 194.25 (C=O), 167.22, 149.25, 148.24, 136.75, 135.67, 132.43, 131.94, 125.82, 125.47, 118.94, 118.61, 113.51, 109.69, 64.95, 30.69, 19.22, 14.07.

MS (TOF EI$^+$): *m/z* 310.13 (M^+, 100%). Calcd for $C_{18}H_{18}N_2O_3$: 310.13.

2,7-Dibromo-4-butylthiofluorenone (3.61)

Exp no: SK-15

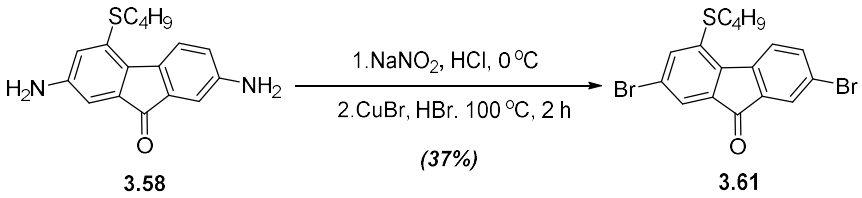

3.58 **3.61**

A suspension of 2,7-diamino-4-butylthiofluorenone (**3.58**) (6.0 g, 14.0 mmol) in 37 % HCl (12 mL) was stirred for 20 minutes at room temperature and then cooled down to 0 °C. A solution of sodium nitrite (3.6 g, 42.2 mmol) in water (18 mL) was added dropwise maintaining the temperature of the reaction mixture at –2/0 °C (internal temperature). The excess of nitrite ions was monitored by KI-starch paper. The mixture was stirred for 1 h at 0°C, copper (I) bromide (5.70 g) and 48% HBr (74 mL) were added and the mixture was stirred at 100 °C for 2 h. The mixture was cooled to room temperature, diluted with water (40 mL), neutralised with 4 M NaOH (20 mL) and extracted with ethyl acetate (3 × 100 mL). The combined organic layer was dried over Mg_2SO_4, the solvent was evaporated under reduced pressure and the residue was dried *in vacuo* to give crude product (8.5 g, 102%). The crude product was purified by column chromatography on silica gel using PE/EA (4:1, v/v) as eluent to afford compound **3.61** as a yellow solid (3.2 g, 37 %), mp: 92–94 °C.

^{1}H NMR (400 MHz, $CDCl_3$): δ (ppm) 8.05 (d, *J* = 8.7 Hz, 1H, H-5), 7.77 (d, *J* = 1.7 Hz, 1H), 7.64 (dd, *J* = 1.6, 8.1 Hz, 1H, H-6), 7.59 (d, *J* = 1.4 Hz, 1H), 7.51 (d, *J* = 1.3 Hz, 1H) 3.04 (t, *J* = 7.3 Hz, 2H), 1.73 (m, 2H), 1.50 (m, 2H), 0.96 (t, J = 7.3 Hz, 3H, CH_3).

^{13}C NMR (100 MHz, $CDCl_3$): δ (ppm) 190.80 (C=O), 142.52, 139.80, 137.33, 136.31, 135.95, 135.78, 135.18, 127.45, 126.14, 124.41, 123.27, 122.93, 33.02, 30.69, 22.03, 13.63.

MS (TOF EI$^+$): *m/z* 423.91 (M^+, ^{79}Br/^{79}Br, 40%), 425.91 (M^+, ^{79}Br/^{81}Br, 100%), 427.90 (M^+, ^{81}Br/^{81}Br, 15%), Calcd for $C_{17}H_{14}Br_2OS$: 423.91 (50.2%), 425.91 (100%), 427.91 (52.1%).

2,7-Dibromo-4-methoxyfluorenone (3.62)

Exp no: SK-98

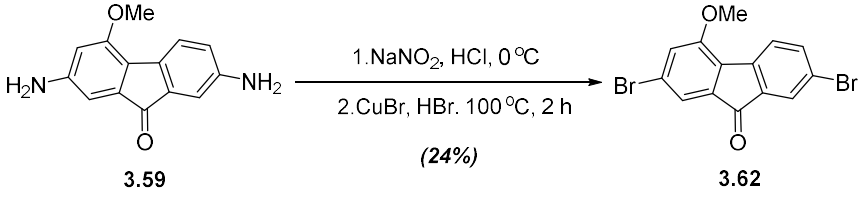

3.59 **3.62**

2,7-Diamino-4-dodecyloxyfluorenone (**3.59**) (7.21 g, 30.0 mmol) and 95% concentrated H_2SO_4 (150 mL) were stirred in 1 L flask for 20 minutes at room temperature and then, cooled down to 0 °C. A solution of sodium nitrite (4.10 g, 60.0 mmol) in water (30 mL) was

added dropwise maintaining the temperature of the reaction mixture at –2/0 °C (internal temperature). The excess of nitrite ions was monitored by KI-starch paper. The mixture was stirred for 1 h at 0 °C, copper (I) bromide (8.60 g) and 48% HBr (30 mL) were added and the mixture was stirred at 100 °C for 2 h. The mixture was cooled to room temperature, diluted with water (400 mL), neutralised with 4 M NaOH (200 mL) and extracted with ethyl acetate (3 × 100 mL). Combined extracts were dried over Mg_2SO_4, the solvent was evaporated under reduced pressure and the residue was dried *in vacuo* to give crude product (13.1 g, 118%). The crude product was purified by column chromatography on silica gel using PE/Tol (1:1, v/v) as eluent to afford compound **3.62** as a brown solid (2.54 g, 24%), mp: 168–170 °C.

^{1}H NMR (400 MHz, $CDCl_3$): δ (ppm) 7.72 (d, J = 1.8, Hz, 1H, H-8), 7.64 (d, J = 7.9 Hz, 1H, H-5), 7.57 (dd, J = 1.8, 7.9 Hz, 1H, H-6), 7.40 (d, J = 1.4 Hz, 1H, H-3), 7.17 (d, J = 1.3 Hz, 1H, H-1), 3.98 (s, 3H, OCH_3).

^{13}C NMR (100 MHz, $CDCl_3$): δ (ppm) 191.35 (C=O), 155.70, 141.74, 137.41, 136.13, 134.62, 129.66, 127.41, 125.55, 123.85, 122.24, 120.87, 119.99, 56.05.

MS (TOF EI$^+$): *m/z* 365.79 (M^+, ^{79}Br/^{79}Br, 55%), 367.51 (M^+, ^{79}Br/^{81}Br, 100%), 369.26 (M^+, ^{81}Br/^{81}Br, 55%). Calcd for $C_{14}H_8Br_2O_2$: 365.89 (51.3%), 367.89 (100%), 369.89 (50.0%).

2,7-Dibromo-4-butoxycarbonylfluorenone (3.63)

Exp no: SK-31

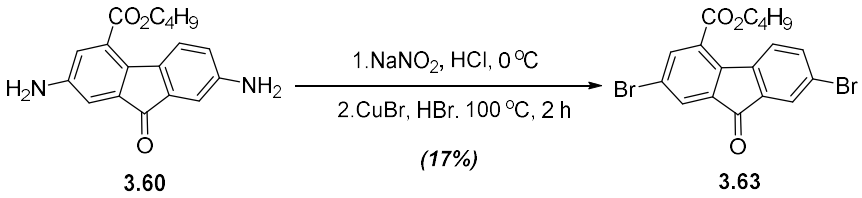

A stirred suspension of 2,7-diamino-4-butoxycarbonylfluorenone (**3.60**) (9.0 g, 32.9 mmol) in water (28 mL) and 37% HCl (19 mL) was cooled down to 0 °C and a solution of sodium nitrite (3.6 g, 42.2 mmol) in water (8 mL) was added dropwise maintaining the temperature of the reaction mixture –2/0 °C (internal temperature). The excess of nitrite ions was monitored by KI-starch paper. The mixture was stirred for 1 h at 0 °C, copper (I) bromide and 48% HBr (116 mL) were added and the mixture was stirred at 100 °C for 2 h. The mixture was cooled down to room temperature, diluted with water (50 mL) and extracted with ethyl acetate (2 × 50 mL). The combined extracts were dried over Mg_2SO_4, the solvent was evaporated under reduced pressure and the residue was dried *in vacuo* to give crude product (14.3 g, 112%). The crude product was purified by column chromatography on silica gel using PE/EA (4:1, v/v) as eluent to afford compound **3.63** as a yellow solid (2.2 g, 17%), mp: 125–127 °C.

^{1}H NMR (400 MHz, $CDCl_3$): δ (ppm) 8.31 (d, *J* = 8.4 Hz, 1H, H-5), 8.10 (d, *J* = 2.0 Hz, 1H), 7.93(d, *J* = 2.0 Hz, 1H), 7.81 (d, *J* = 1.6 Hz, 1H), 7.64 (dd, *J* = 2.1, 8.3 Hz, 1H, H-6) 4.41 (t, *J* = 6.7 Hz, 2H), 1.81(m, 2H), 1.51 (m, 2H), 1.01(t, *J* = 7.3 Hz, 3H, CH_3).

^{13}C NMR (100 MHz, $CDCl_3$): δ (ppm) 190.22 (C=O), 165.18, 142.10, 141.26, 138.60, 137.83, 136.71, 135.05, 130.55, 128.56, 128.12, 127.45, 124.34, 122.70, 66.04, 30.62, 19.24, 13.74.

MS (TOF EI$^+$): *m/z* 435.93 (M^+, ^{79}Br/^{79}Br, 20%), 437.93 (M^+, ^{79}Br/^{81}Br, 100%), 439.92 (M^+, ^{81}Br/^{81}Br, 18%). Calcd for $C_{18}H_{14}Br_2O_3$: 435.93 (51.4%), 437.93 (100%), 439.93 (49.3%).

2,7-Dibromo-4-butylsulfonylfluorenone (3.64)

Exp no: SK-38

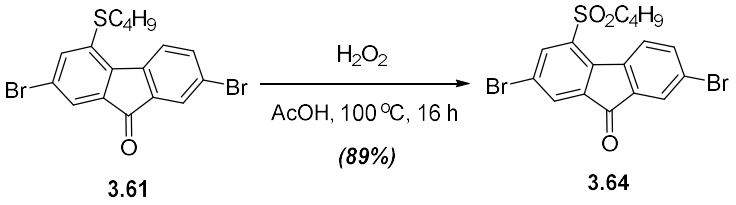

A mixture of 2,7-dibromo-4-butylthiofluorenone (**3.61**) (1.49 g, 3.51 mmol) and hydrogen peroxide (0.64 mL) and acetic acid (46 mL) was stirred at 100 °C for 16 h. The mixture was cooled to room temperature and diluted with water (100 mL). The solid was filtered off, washed with water (2 × 5 mL) and dried *in vacuo* to afford compound **3.64** as a yellow solid (1.421 g, 89%).

^{1}H NMR (400 MHz, $CDCl_3$): δ (ppm) 8.34 (d, *J* = 8.65 Hz, 1H), 8.29 (d, *J* = 1.54 Hz, 1H), 8.04 (d, *J* = 1.44 Hz, 1H), 7.89 (d, *J* = 1.25 Hz, 1H), 7.74 (dd, *J* = 7.88 Hz, 1H), 3.23 (t, *J* = 8.15 Hz, 2H O*CH*$_2$C$_3$H$_7$,), 1.78 (m, 2H, *CH*$_2$C$_2$H$_5$), 1.43 (m, 2H, *CH*$_2$CH$_3$), 0.91 (t, *J* = 7.22 Hz, 3H, CH_3).

^{13}C NMR (100 MHz, $CDCl_3$): δ (ppm) 189.03 (C=O), 140.33, 139.41, 138.51, 138.12, 137.31, 135.62, 135.41, 132.13, 127.83, 125.42, 125.52, 123.84, 54.22, 24.14, 21.52, 13.52.

MS (TOF EI$^+$): *m/z* 455.90 (M^+, ^{79}Br/^{79}Br, 35%), 457.88 (M^+, ^{79}Br/^{81}Br, 100%), 459.89 (M^+, ^{81}Br/^{81}Br, 25%). Calcd for $C_{17}H_{14}Br_2O_3S$: 455.90 (50.2%), 457.90 (100%), 459.90 (52.1%).

2,7-Dibromo-4-butylthio-9,9-di(4-hydroxyphenyl)fluorene (3.65)

Exp no: SK-40

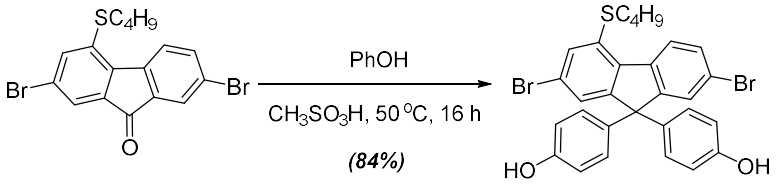

3.61 3.65

A mixture of 2,7-dibromo-4-butylthiofluorenone (**3.61**) (1.40 g, 3.29 mmol), phenol (1.79 g, 19.0 mmol), and methanesulfonic acid (6 mL) was stirred at 50 °C for 16 h. The mixture was cooled down to room temperature, diluted with water (20 mL) and extracted with ethyl acetate (3 × 15 mL). The organic layer was dried over Mg_2SO_4, evaporated at reduced pressure and the residue was dried *in vacuo* to give dark brown crude product (4.9 g, 252%). The crude product was purified by column chromatography on silica gel using PE/EA (9:1, v/v) as eluent to afford compound **3.65** as a yellowish solid (1.65 g, 84%), mp: 125–127 °C.

^{1}H NMR (400 MHz, DMSO): δ (ppm) 9.43 (s, 2H, OH), 8.25 (d, *J* = 8.6 Hz, 1H, H-5), 7.63 (dd, *J* = 8.5 Hz, 1H, H-5), 7.48 (s, 1H), 7.45 (s, 1H), 7.27 (s, 1H), 6.87 (m, 4H, C_6H_4), 6.66 (m, 4H, C_6H_4), 3.18 (t, *J* = 7.2 Hz, 2H, S*CH*$_2$C$_3$H$_7$), 1.71–1.64 (m, 2H, SCH$_2$*CH*$_2$C$_2$H$_5$), 1.52–1.43 (m, 2H, SCH$_2$CH$_2$*CH*$_2$CH$_3$), 0.92 (t, *J* = 7.3 Hz, 3H, CH_3).

^{13}C NMR (100 MHz, $CDCl_3$): δ (ppm) 154.62, 153.92, 138.15, 136.75, 136.71, 135.71, 135.20, 130.55, 129.40, 129.32, 128.78, 126.07, 126.06, 121.67, 121.62, 115.33, 64.04, 33.09, 30.73, 22.09, 13.67.

MS (TOF EI$^+$): *m/z* 593.97 (M$^+$, ^{79}Br/^{79}Br, 15%), 595.96 (M$^+$, ^{79}Br/^{81}Br, 100%), 597.96 (M$^+$, ^{81}Br/^{81}Br, 12%), Calcd for $C_{29}H_{24}Br_2O_2S$: 593.99 (50.2%), 595.98 (100%), 597.98 (52.0%).

2,7-Dibromo-4-methoxy-9,9-di(4-hydroxyphenyl)fluorene (3.66)

Exp no: SK-43

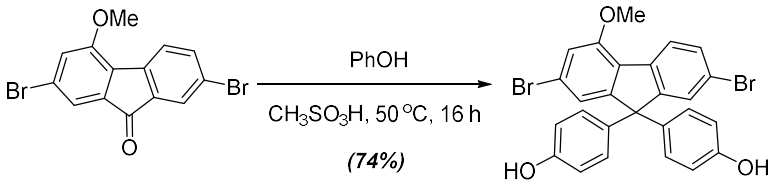

3.62 3.66

A mixture of 2,7-dibromo-4-methoxyfluorenone (**3.62**) (0.955 g, 2.59 mmol), phenol (1.41 g, 15.0 mmol), and methanesulfonic acid (5.0 mL) was stirred at 50 °C for 16 h. The mixture was cooled down to room temperature, diluted with water (15 mL) and extracted with ethyl acetate (3 × 10 mL). The organic layer was dried over Mg_2SO_4, the solvent was evaporated under reduced pressure and the residue was dried *in vacuo* to give crude product (1.86 g,

134%). The crude product was purified by column chromatography on silica gel using PE/EA (9:1, v/v) as eluent to afford compound **3.66** as a light brown solid (1.02 g, 74%), mp: 263–265 °C.

^{1}H NMR (400 MHz, DMSO): δ (ppm) 9.45 (s, 2H, OH), 7.97 (d, *J* = 8.4 Hz, 1H, H-5), 7.60 (dd, *J* = 8.1 Hz, 1H, H-6), 7.50 (d, *J* = 1.3 Hz, 1H), 7.26 (s, 1H), 7.11 (s, 1H), 6.93 (m, 4H, C_6H_4), 6.71 (m, 4H, C_6H_4), 4.06 (s, 3H, OCH_3).

^{13}C NMR (100 MHz, $CDCl_3$): δ (ppm) 157.13, 156.84, 155.88, 154.46, 137.81, 135.62, 130.88, 129.44, 128.93, 126.24, 125.89, 122.30, 121.63, 120.81, 115.70, 113.61, 65.21, 56.08.

MS (TOF EI$^+$): *m/z* 535.96 (M^+, ^{79}Br/^{79}Br, 20%), 537.95 (M^+, ^{79}Br/^{81}Br, 100%), 539.95 (M^+, ^{81}Br/^{81}Br, 18%), Calcd for $C_{26}H_{18}Br_2O_3$: 535.96 (51.4%), 537.96 (100%), 539.96 (49.3%).

2,7-Dibromo-4-butoxycarbonyl-9,9-di(4-hydroxyphenyl)fluorene (3.65)

Exp no: SK-41

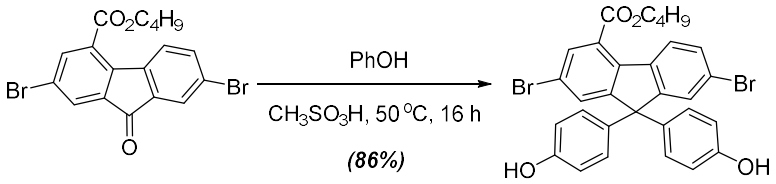

3.63 3.65

A mixture of 2,7-dibromo-4-butoxycarbonylfluorenone (**3.63**) (2.40 g, 5.48 mmol), phenol (2.99 g, 31.8 mmol) and methansulfonic acid (11 mL) was stirred at 50 °C for 16 h. The mixture was cooled down to room temperature, diluted with water (30 mL) and extracted with ethyl acetate (3 × 20 mL). The combined extracts were dried over Mg_2SO_4, the solvent was evaporated under reduced pressure and the residue was dried *in vacuo* to give crude product (6.5 g, 196%). The crude product was purified by column chromatography on silica gel using PE/EA (9:1, v/v) as eluent to afford compound **3.65** as a white solid (2.87 g, 86 %), mp: 167-169 °C.

^{1}H NMR (400 MHz, DMSO): δ (ppm) 9.16 (s, 2H, OH), 8.73 (d, *J* = 8.3 Hz, 1H), 8.38 (d, *J* = 1.8 Hz, 1H), 8.19 (d, *J* = 1.8 Hz, 1H), 8.01–7.97 (m, 2H), 7.52–7.47 (m, 4H), 7.29–7.22 (m, 4H), 4.92 (t, *J* = 6.6 Hz, 2H, $OCH_2C_3H_7$), 2.22–1.98 (m, 2H, $OCH_2CH_2C_2H_5$), 1.97–1.91 (m, 2H, $CH_2CH_2CH_2CH_3$), 1.44 (t, *J* = 7.3 Hz, 3H, CH_3).

^{13}C NMR (100 MHz, $CDCl_3$): δ (ppm) 166.61, 157.32, 156.93, 156.01, 137.20, 137.33, 137.30, 135.32, 135.24, 131.01, 129.54 (4C), 129.33, 129.31, 127.41, 127.32, 123.33, 123.24, 121.01, 116.32 (4C), 66.45, 64.22, 31.22, 19.52, 13.64.

MS (TOF EI$^+$): *m/z* 605.99 (M^+, ^{79}Br/^{79}Br, 25%), 607.99 (M^+, ^{79}Br/^{81}Br, 100%), 609.99 (M^+, ^{81}Br/^{81}Br, 18%). Calcd for $C_{30}H_{24}Br_2O_4$: 606.00 (51.4%), 608.00 (100%), 610.00 (48.6%).

2,7-Dibromo-4-butylsulfonyl-9,9-di(4-hydroxyphenyl)fluorene (3.68)

Exp no: SK-42

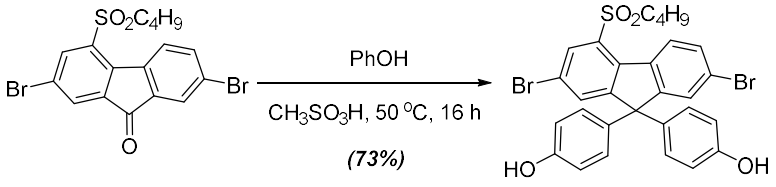

3.64 3.68

A mixture of 2,7-dibromo-4-butylsulfonylfluorenone (**3.64**) (1.39 g, 3.04 mmol), phenol (1.66 g, 17.6 mmol) and methanesulfonic acid (6 mL) was stirred at 50 °C for 16 h. The mixture was cooled down to room temperature, diluted with water (15 mL) and extracted with ethyl acetate (2 × 15 mL). The organic layer was dried over Mg_2SO_4, the solvent was evaporated under reduced pressure and the residue was dried *in vacuo* to give crude product (2.2 g, 118%). The crude product was purified by column chromatography on silica gel using PE/EA (9:1, v/v) as eluent to afford compound **3.68** as a white solid (1.39 g, 73 %), mp: 229–231 °C.

^{1}H NMR (400 MHz, DMSO): δ (ppm) 9.48 (s, 2H, OH), 8.43 (d, J = 8.5 Hz, 1H), 8.01 (d, J = 1.19 Hz, 1H), 7.89 (d, J = 1.4 Hz, 1H), 7.70 (dd, J = 8.6 Hz, 1H), 7.55 (d, J = 1.59 Hz, 1H), 6.91 (m, 4H, C_6H_4), 6.68 (m, 4H, C_6H_4), 3.53–3.49 (t, J = 7.7 Hz, 2H, $SO_2CH_2C_3H_7$), 1.71–1.63 (m, 2H, $CH_2CH_2C_2H_5$), 1.37–1.32 (m, 2H, $CH_2CH_2CH_2CH_3$), 0.80 (t, J = 7.58 Hz, 3H, CH_3).

^{13}C NMR (100 MHz, $CDCl_3$): δ (ppm) 136.18, 136.04, 135.23, 134.77, 134.74, 134.65, 132.44, 131.59, 129.65, 129.58, 128.48, 123.76, 121.48, 115.90, 64.34, 53.73, 24.56, 21.51, 13.31.

MS (TOF EI$^+$): *m/z* 625.97 (M^+, ^{79}Br/^{79}Br, 15%), 627.97 (M^+, ^{79}Br/^{81}Br, 100%), 629.97 (M^+, ^{81}Br/^{81}Br, 20%). Calcd for $C_{29}H_{24}Br_2O_4S$: 625.98 (50.2%), 627.97 (100%), 629.97 (52.0%).

2,7-Dibromo-4-butylthio-9,9-di(4-octyloxyphenyl)fluorene (3.69)

Exp no: SK-47

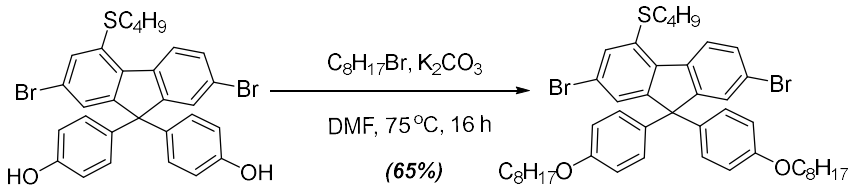

3.65 3.69

A mixture of 2,7-dibromo-4-butylthio-9,9-di(4-hydroxyphenyl)fluorene (**3.65**) (1.41 g, 2.36 mmol), potassium carbonate (0.979 g, 7.09 mmol), 1-bromooctane (1.02 mL, 5.91 mmol) and DMF (25 mL) was stirred at 75 °C for 16 h. The mixture was cooled down to room

temperature, diluted with water (30 mL), extracted with ethyl acetate (3 × 15 mL) and dried over Mg_2SO_4. The solvent was evaporated under reduced pressure and the residue was dried *in vacuo* to give yellow liquid (2.89 g, 152%). The crude product was purified by column chromatography on silica gel using PE as eluent to afford compound **3.69** as a colourless liquid (1.25 g, 65 %), which is slowly solidified with a time, mp: 60–62 °C.

^{1}H NMR (400 MHz, $CDCl_3$): δ (ppm) 8.31 (d, *J* = 8.3 Hz, 1H, H-5), 7.47 (dd, *J* = 1.8, 8.3 Hz, 1H, H-6), 7.43 (d, *J* = 1.7 Hz, 1H), 7.34 (d, *J* = 1.4 Hz, 1H), 7.25 (d, *J* = 1.4 Hz, 1H), 7.02 (m, 4H, C_6H_4), 6.75 (m, 4H, C_6H_4), 3.89 (t, 4H, O*CH*$_2$$C_7H_{15}$), 3.03 (t, 2H, S*CH*$_2$$C_3H_7$), 1.77–1.70 (m, 6H) 1.42–1.38 (m, 4H), 1.31–1.26 (m, 18H), 0.96 (t, 3H, $SCH_2CH_2CH_2$*CH*$_3$), 0.87 (m, 6H, CH_3).

^{13}C NMR (100 MHz, $CDCl_3$): δ (ppm) 158.24, 154.81, 154.23, 138.15, 136.27, 136.23, 135.75, 135.07, 130.45, 129.13, 128.82, 127.57, 126.15, 126.01, 125.91, 125.67, 121.63, 121.59, 114.31, 114.13, 67.96, 64.09, 33.10, 33.02, 31.82, 30.74, 29.35, 29.27, 29.24, 26.06, 22.66, 22.10, 14.11, 13.68.

MS (TOF EI$^+$): *m/z* 818.23 (M$^+$, ^{79}Br/^{79}Br, 40%), 820.21 (M$^+$, ^{79}Br/^{81}Br, 100%), 822.22 (M$^+$, ^{81}Br/^{81}Br, 15%). Calcd for $C_{45}H_{56}Br_2O_2S$: 818.24 (50.2%), 820.23 (100%), 822.23 (52.0%).

2,7-Dibromo-4-methoxy-9,9-di(4-octyloxyphenyl)fluorene (3.70)

Exp no: SK-46

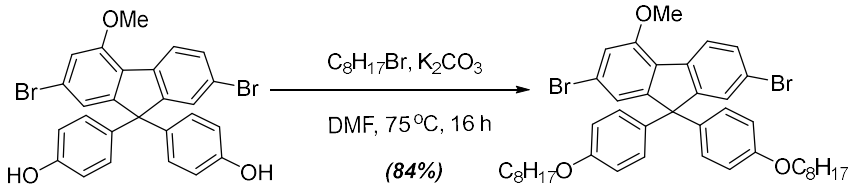

3.66 3.70

A mixture of 2,7-dibromo-4-methoxy-9,9-di(4-hydroxyphenyl)fluorene (**3.66**) (0.952 g, 1.76 mmol), potassium carbonate (0.732 g, 5.30 mmol), 1-bromooctane (0.77 mL, 4.42 mmol) and DMF (20 mL) was stirred at 75°C for 16 h. The mixture was cooled down to room temperature, diluted with water (30 mL), extracted with ethyl acetate (3 × 15 mL) and dried over Mg_2SO_4. The solvent was evaporated under reduced pressure and the residue was dried *in vacuo* to give crude product (1.57, 117%). The crude product was purified by column chromatography on silica gel using PE as eluent to afford compound **3.70** as a colorless liquid (1.110 g, 84%), which is slowly solidified with a time.

^{1}H NMR (400 MHz, $CDCl_3$): δ (ppm) 7.91 (d, *J* = 8.11 Hz, 1H, H-5), 7.43–7.41 (m, 2H), 7.13–7.11 (m, 1H), 7.02–6.96 (m, 4H, C_6H_4), 6.97 (m, 1H), 6.76–6.71 (m, 4H, C_6H_4), 3.97 (s, 3H, OCH_3), 3.89 (t, *J* = 6.48 Hz, 4H, O*CH*$_2$$C_7H_{15}$) 1.77–1.170 (m, 4H, OCH_2*CH*$_2$$C_6H_{13}$),

1.42–1.38 (m, 4H, $O(CH_2)_2CH_2C_5H_{11}$), 1.29–1.27 (m, 16H, $O(CH_2)_3(CH_2)_4CH_3$), 0.87 (m, 6H, CH_3).

^{13}C NMR (100 MHz, $CDCl_3$): δ (ppm) 158.18, 156.01, 154.90, 153.24, 137.27, 136.32, 136.28, 130.55, 129.07, 128.57, 126.09, 125.29, 122.02, 121.46, 120.88, 114.28, 113.07, 67.94, 64.67, 55.75, 31.81, 29.27, 29.18, 26.06, 22.66, 14.11.

MS (TOF EI$^+$): *m/z* 760.55 (M^+, ^{79}Br/^{79}Br, 15%), 762.20 (M^+, ^{79}Br/^{81}Br, 100%), 764.19 (M^+, ^{81}Br/^{81}Br, 15%). Calcd for $C_{42}H_{50}Br_2O_3$: 760.21 (51.4%), 762.21 (100%), 764.21 (49.3%).

2,7-Dibromo-4-butoxycarbonyl-9,9-di(4-octyloxyphenyl)fluorene (3.71)

Exp no: SK-44

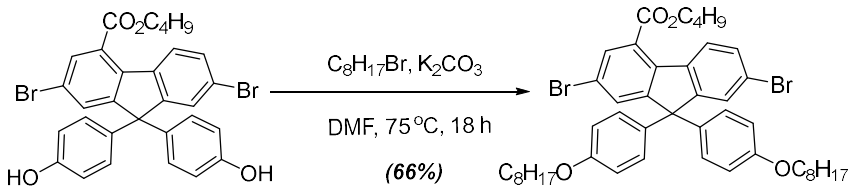

3.67 **3.71**

A mixture of 2,7-dibromo-4-butoxycarbonyl-9,9-di(4-hydroxyphenyl)fluorene (**3.67**) (2.52 g, 4.14 mmol), potassium carbonate (1.71 g, 12.4 mmol), 1-bromooctane (1.69 mL, 10.3 mmol) and DMF (50 mL) was stirred at 75 °C for 18 h. The mixture was cooled down to room temperature, diluted with water (30 mL) and extracted with ethyl acetate (3 × 20 mL). The combined extracts were dried over Mg_2SO_4, the solvent was evaporated under reduced pressure and the residue was dried *in vacuo* to give crude product (3.70 g, 110%). The crude product was purified by column chromatography on silica gel using PE as eluent to afford pure compound **3.71** as a colorless liquid (2.28 g, 66 %), which is slowly solidified with a time, mp: 67–69 °C.

^{1}H NMR (400 MHz, $CDCl_3$): δ (ppm) 8.22 (d, *J* = 8.96 Hz, 1H, H-5), 7.87 (d, *J* = 1.8 Hz, 1H), 7.57 (d, *J* = 1.8 Hz, 1H), 7.44–7.42 (m, 2H), 7.02 (m, 4H, C_6H_4), 6.76 (m, 4H, C_6H_4), 4.42 (t, *J* = 6.64 Hz, 2H), 3.90 (t, *J* = 6.4 Hz, 4H), 1.84–1.72 (m, 4H), 1.49–1.45 (m, 2H), 1.42–1.38 (m, 4H), 1.29–1.27 (m, 18H), 1.01 (t, *J* = 7.44 Hz , 3H), 0.876 (t, *J* = 6.68 Hz, 6H).

^{13}C NMR (100 MHz, $CDCl_3$): δ (ppm) 166.69, 158.33, 158.80, 154.78, 137.27, 136.40, 135.93, 135.89, 132.46, 132.26, 130.72, 129.14, 128.89, 128.31, 126.82, 122.89, 120.85, 114.39, 67.98, 65.71, 63.60, 31.82, 30.70, 29.35, 29.26, 29.24, 26.06, 22.66, 19.28, 14.11, 13.78.

MS (TOF EI$^+$): *m/z* 830.24 (M^+, ^{79}Br/^{79}Br, 15%), 832.24 (M^+, ^{79}Br/^{81}Br, 100%), 833.24 (M^+, ^{81}Br/^{81}Br, 10%). Calcd for $C_{46}H_{56}Br_2O_4$: 830.25 (51.4%), 832.25 (100.0%), 833.26 (51.7%).

2,7-Dibromo-4-butylsulfonyl-9,9-di(4-octyloxyphenyl)fluorene (3.72)

Exp no: SK-45

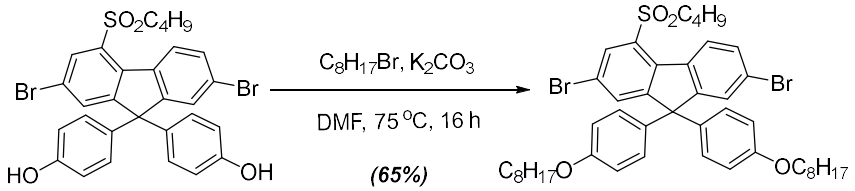

3.68 **3.72**

A mixture of 2,7-dibromo-4-butylsulfonyl-9,9-di(4-hydroxyphenyl)fluorene (**3.68**) (1.136 g, 1.81 mmol), potassium carbonate (0.750 g, 5.45 mmol), 1-bromooctane (0.64 mL, 3.34 mmol) and DMF (25 mL) was stirred at 75 °C for 16 h. The mixture was cooled down to room temperature, diluted with water (30 mL), extracted with ethyl acetate (3 × 20 mL) and dried over Mg_2SO_4. The solvent was evaporated under reduced pressue and the residue was dried *in vacuo* to give crude product (2.05 g, 134%). The crude product was purified by column chromatography on silica gel using PE as eluent to afford compound **3.72** as a colourless liquid (0.980 g, 65 %), which is slowly solidified with a time, mp: 71–73 °C.

^{1}H NMR (400 MHz, $CDCl_3$): δ (ppm) 8.50 (d, *J* = 8.5 Hz, 1H, H-5), 8.19 (d, *J* = 1.8 Hz, 1H), 7.71 (d, *J* = 1.7 Hz, 1H), 7.53 (d, *J* = 9.0, 1.8 Hz, 1H), 7.49 (m, 1H), 7.00 (m, 4H, C_6H_4), 6.77 (m, 4H, C_6H_4), 3.90 (t, *J* = 6.48 Hz, 4H), 3.29 (t, *J* = 7.80 Hz, 2H) 1.75 (m, 4H), 1.40–1.27 (m, 22H), 0.87 (m, 10H, $3CH_3$).

^{13}C NMR (100 MHz, $CDCl_3$): δ (ppm) 158.57, 157.13, 157.05, 155.30, 155.18, 155.04, 135.75, 135.19, 135.15, 134.62, 134.56, 134.53, 134.43, 134.10, 133.90, 132.52, 131.48, 129.43, 129.04, 127.45, 127.19, 124.00, 123.90, 121.61, 114.56, 68.02, 63.75, 53.66, 31.81, 29.33, 29.23, 26.05, 24.16, 22.65, 21.47, 14.10, 13.49.

MS (TOF EI$^+$): *m/z* 850.22 (M^+, ^{79}Br/^{79}Br, 12%), 852.21 (M^+, ^{79}Br/^{81}Br, 100%), 854.20 (M^+, ^{81}Br/^{81}Br, 15%). Calcd for $C_{45}H_{56}Br_2O_4S$: 850.23 (50.2%), 852.22 (100.0%), 854.22 (52.0%).

References

1 A .C. Grimsdale, K. L. Chan, R. E. Martin, P. G. Jokisz, and A. B. Holmes, *Chem. Rev.*, **2009**, *109*, 897–1091. (DOI: 10.1021/cr000013v).

2 U. Scherf and D. Neher (Eds), *Polyfluorenes. – Advances in Polymer Science,* Springer, **2008**, *212*, 322 pp. (DOI 10.1007/978-3-540-68734-4).

3 D. F. Perepichka, I. F. Perepichka, H. Meng, and F. Wudl, Light-emitting polymers. Chapter 2 in Book: *Organic Light-Emitting Materials and Devices*, Z. R. Li and H. Meng (Eds), CRC Press, Boca Raton, FL, **2006**, pp. 45–293.

4 M. Knaapila and A. P. Monkman, *Adv. Mater*., **2013**, *25*, 1090–1108. (DOI: 10.1002/adma.201204296).

5 D. Neher, *Macromol. Rapid Commun*., **2001**, *22*, 1365–1385. (DOI: 10.1002/1521-3927(20011101)22:17<1365).

6 H. Cheun, X. Liu, F. J. Himpsel, M. Knaapila, U. Scherf, M. Torkkeli, and M. J. Winokur, *Macromolecules*, **2008**, *41*, 6463–6472. (DOI: 10.1021/ma702579r).

7 A. Garcia, J. Z. Brzezinski, and T.-Q. Nguyen, *J. Phys. Chem. C*, **2009**, *113*, 2950–2954. (DOI: 10.1021/jp806374s).

8 R. C. Evans, A. G. Macedo, S. Pradhan, U. Scherf, L. D. Carlos, and H. D. Burrows, *Adv. Mater*., **2010**, *22*, 3032–3037. (DOI: 10.1002/adma.200904377).

9 B. Zhu, Y. Han, M. Sun, and Z. Bo, *Macromolecules*, **2007**, *40*, 4494–4500. (DOI: 10.1021/ma062246f).

10 A. Gutacker, C.-Y. Lin, L. Ying, T.-Q. Nguyen, U. Scherf, and G. C. Bazan, *Macromolecules,* **2012**, *45*, 4441−4446. (DOI: .org/10.1021/ma202738t).

11 H. D. Burrows, V. M. M. Lobo, J. Pina, M. L. Ramos, J. S. D. Melo, A. J. M. Valente, M. J. Tapia, S. Pradhan, and U. Scherf, *Macromolecules*, **2004**, *37*, 7425–7427. (DOI: 10.1021/ma048780+).

12 C. Ego, A. C. Grimsdale, F. Uckert, G. Yu, G. Srdanov, and K. Müllen, *Adv. Mater*., **2002**, *14*, 809–811. (DOI: 10.1002/1521-4095(20020605)14:11<809).

13 S. Beaupre and M. Leclerc, *Macromolecules*, **2003**, *36*, 8986–8991. (DOI: 10.1021/ma035064j).

14 C. Chuang, S. C. Lapin, A. K. Schrock, and G. B. Schuster, *J. Am. Chem. Soc*., **1985**, *107*, 4238–4243. (DOI: 10.1021/ja00300a027).

15 A. I. Meyers, R. Gabel, and E. Milhelich, *J. Org. Chem.,* **1978**, *43*, 1372–1379. (DOI: 10.1021/jo00401a018).

16 I. F. Perepichka, unpublished results.

17 J. H. Ahn, C. Wang, I. F. Perepichka, M. R. Bryce, and M. C. Petty, *J. Mater. Chem.*, **2007**, *17*, 2996–3001. (DOI: 10.1039/b700047b).

18 M. E. Furrow and A. G. Myers, *J. Am. Chem. Soc*., **2004**, *126*, 5436-5445. (DOI: 10.1021/ja049694s),

19 I. I. Perepichka, I. F. Perepichka, M. R. Bryce, and L. O. Pålsson, *Chem. Commun*., **2005**, 3397–3399. (DOI: 10.1039/B417717G),

20 D. W. Price, Jr., and J. M. Tour, *Tetrahedron*, **2003**, *59*, 3131–3156. (DOI: 10.1016/S0040-4020(03)00334-X),

21 L. Oldridge, M. Kastler, and K. Müllen, *Chem. Commun*., **2006**, 885–887. (DOI: 10.1039/b516078b).

22 J. T. Repine, D. S. Johnson, A. D. White, D. A. Favor, M. A. Stier, J. Yip, T. Rankin, Q. Ding, and S. N. Maiti, *Tetrahedron Lett*., **2007**, *48*, 5539–5541. (DOI:10.1016/j.tetlet.2007.05.156).

23 M. Wang, K. Funabiki, and M. Matsui, *Dyes Pigments,* **2003***, 57*, 77–86. (DOI: 10.1016/S0143-7208(03)00011-1).

24 G. Liu, J. Xu, K. C. Park, N. Chen, S. Zhang, Z. Ding, F. Wang, and H. Du, *Tetrahedron*, **2011**, *67*, 5156–5160. (DOI: 10.1016/j.tet.2011.05.056).

25 C. S. Giam and K. Kikukawa, *J. Chem. Soc., Chem. Commun*., **1980**, 756–757. (DOI: 10.1039/C39800000756).

26 A. H. Ingall, J. Dixon, A. Bailey, M. E. Coombs, D. Cox, J. I. McInally, S. F. Hunt, N. D. Kindon, B. J. Teobald, P. A. Willis, R .G. Humphries, P. Leff, J. A. Clegg, J. A. Smith, and W. Tomlinson, *J. Med. Chem*., **1999**, *42*, 213–220. (DOI: 10.1021/jm981072s).

27 F. S. Allaire and J. W. Lyga, *Synth. Commun.*, **2001**, *31*, 1857–1861. (DOI:10.1081/SCC-100104335).

28 S. K. Weber, F. Galbrecht, and U. Scherf, *Org. Lett*., **2006**, *8*, 4039–4041. (DOI: 10.1021/ol061476b).

29 V. Senkovskyy, N. Khanduyeva, H. Komber, U. Oertel, M. Stamm, D. Kuckling, and A. Kiriy, *J. Am. Chem. Soc*., **2007**, *129*, 6626–6632. (DOI: 10.1021/ja0710306).

30 N. Khanduyeva, V. Senkovskyy, T. Beryozkina, V. Bocharova, F. Simon, M. Nitschke, M. Stamm, R. Grötzschel, and A. Kiriy, *Macromolecules*, **2008**, *41*, 7383–7389. (DOI: 10.1021/ma800889c).

31 E. E. Sheina, J. Liu, M .C. Iovu, D. W. Laird, R .D. McCullough, *Macromolecules*., **2004**, *37*, 3526–3528 (DOI: 10.1021/ma0357063).

32 M. C. Iovu, E. E. Sheina, R. R. Gil, and R .D. McCullough, *Macromolecules*, **2005**, *38*, 8649–8656. (DOI: 10.1021/ma051122k).

33 A. Yokoyama, R. Miyakoshi, and T. Yokozawa, *Macromolecules*, **2004**, *37*, 1169–1171. (DOI: 10.1021/ma035396o).

34 R. Miyakoshi, A. Yokoyama, T. Yokozawa, *J. Am. Chem. Soc*., **2005**, *127*, 17542–17547. (DOI: 10.1021/ja05568800).

35 H.-C. Su, H.-F. Chen, C.-C. Wu, and K.-T. Wong, *Chem. Asian J.*, **2008**, *3*, 1922–1928. (DOI: 10.1002/asia.200800020).

36 M. Ranger and M. Leclerc, *Chem. Commun*., **1997**, 1597–1598. (DOI: 10.1039/A703076B).

37 G. Saikia and P. K. Iyer, *J. Org. Chem*., **2010**, *75*, 2714–2717. (DOI: 10.1021/jo100028d).

38 D. K. Belfield, K. J. Schafer, W. Mourad, and B. A. Reinhardt, *J. Org. Chem*., **2000**, *65*, 4475–4481. (DOI: 10.1021/jo991950+).

39 I. I. Perepichka, I. F. Perepichka, M. R. Bryce, and L. Pålsson, *Chem. Commun.*, **2005,** 3397–3399. (DOI: 10.1039/b417717g).

40 M. Gaal, E. J. W. List, and U. Scherf, *Macromolecules*, **2003**, *36*, 4236–4237. (DOI: 10.1021/ma021614m).

41 E. J. W. List, R. Guentner, P. S. de Freitas, and U. Scherf, *Adv. Mater.*, **2002**, *14*, 374–378. (DOI: 10.1002/1521-4095(20020304)14:5<374).

42 T.-P. Liu, C.-H. Xing, and Q.-S. Hu, *Angew. Chem. Int. Ed.*, **2010**, *122*, 2971–2974. (DOI: 10.1002/ange.201000327).

43 M. R. Craig, M. M. de Kok, J. W. Hofstraat, A. P. H. J. Schenning, and E. W. Meijer, *J. Mater. Chem.*, **2003**, *13*, 2861–2864. (DOI: 10.1039/b308402g).

44 I. F. Perepichka, A. F. Popov, T. V. Orekhova, M. R. Bryce, M. A. M. Andrievskii, S. A. Batsanov, J. A. K. Howard, and N. I. Sokolov, *J. Org. Chem.*, **2000**, *65*, 3053–3063. (DOI: 10.1021/jo991796r).

45 I. F. Perepichka, L. G. Kuz'mina, D. F. Perepichka, M. R. Bryce, L. M. Goldenberg, A. F. Popov, and J. A. K. Howard, *J. Org. Chem.*, **1998**, *63***,** 6484–6493. (DOI: 10.1021/jo9803481).

46 I. F. Perepichka, D. F. Perepichka, S. B. Lyubchik, M. R. Bryce, A. S. Batsanov, and J. A. K. Howard, *J. Chem. Soc., Perkin Trans. 2*, **2001**, 1546–1551. (DOI: 10.1039/b103392c).

47 V. G. Pavelyev, O. D. Parashchuk, M. Krompiec, T. V. Orekhova, I. F. Perepichka, P. H. M. van Loosdrecht, D. Y. Paraschuk, and M. S. Pshenichnikov, *J. Phys. Chem. C*, **2014**, *118*, 30291–30301. (DOI: 10.1021/jp510543c).

48 I. F. Perepichka, in: *"Multiphoton and Light Driven Multielectron Processes in Organics: Materials, Phenomena, Applications", NATO Science Series: 3. High Technology – Vol. 79,* F. Kajzar and M. V. Agranovich (Eds), Kluwer Academic Publishers, Dordrecht, **2000**, p. 371–386.

49 D. F. Perepichka, I. F. Perepichka, M. R. Bryce, N. I. Sokolov, and A. J. Moore, *J. Mater. Chem.*, **2001**, *11*, 1772–1774. (DOI: 10.1039/b102081l).

50 A. Y. Sosorev, O. D. Parashchuk, S. A. Zapunidi, G. S. Kashtanov, I. V. Golovnin, S. Kommanaboyina, I. F. Perepichka, and D. Y. Paraschuk, *Phys. Chem. Chem. Phys.*, **2016**, *18*, 4684–4696. (DOI: 10.1039/C5CP05266A).

51 M. Orchin and E. O. Woolfolk, *J. Am. Chem. Soc*., **1946**, *68*, 1727–1729. (DOI: 10.1021/ja01213a014).

52 M. Orchin, L. Reggel, and E. O. Woolfolk, *J. Am. Chem. Soc*., **1947**, *69*, 1225–1227. (DOI: 10.1021/ja01197a519).

53 A. M. Andrievskii, N. G. Grekhova, N. A. Andronova, R. R. Shifrina, V. N. Aleksandrov, and K. M. Dyumaev, *J. Org. Chem. USSR*, **1982**, *18*, 1719–1723 (Engl. Translation); *Zh. Org. Khim.*, **1982**, *18*, 1961–1966 (in Russian). (DOI: 10.1039/P29960002453).

54 O. V. Semidetko, L. A. Chetkina, V. K. Belskii, D. D. Mysyk, I. F. Perepichka, A. M. Andrievskii, *J. General Chem. USSR*, **1987**, *52*, 415–421 (Engl.Translation). (DOI: 10.1016/0032-3861(92)90113-B).

55 A. M. Andrievskii, M. K. Grachev, and O. V. Chelysheva, *Russ. J. Org. Chem.*, **2013**, *49*, 228–232 (*Zh. Org. Khim.*, **2013**, *49*, 232–237 (in Russian)). (DOI: 10.1134/S1070428013020097)..

56 O. V. Chelysheva, L. A. Chetkina, V. K. Bel'skii, and A. M. Andrievskii, *Kristallografiya,* **1989**, *34*, 1020–1022 (in Russian). (DOI: 10.1039/P29960002453).

57 I. F. Perepichka, A. F. Popov, T. V. Orekhova, M. R. Bryce, A. N. Vdovichenko, A. S. Batsanov, L. M. Goldenberg, J. A. K. Howard, N. I. Sokolov, and J. L. Megson, *J. Chem. Soc., Perkin Trans. 2*, **1996**, 2453–2469. (DOI: 10.1039/p29960002453).

58 I. F. Perepichka and T. V. Artyomova, unpublished results.

59 L. J. Lindgren, X. Wang, O. Inganas, and M. R. Andersson, *Synth. Metals*, **2005**, *154*, 97–100. (DOI:10.1016/j.synthmet.2005.07.025).

60 J. G. Rodríguez, L. J. Tejedor, T. La Parra, and C. Díaz, *Tetrahedron*, **2006**, *62*, 3355–3361. (DOI: org/10.1016/j.tet.2006.01.032).

61 S. P. Hollinshead, M. L. Trudell, P. Skolnick, and J. M. Cook, *J. Med. Chem.,* 1990, *33*, 1062-1069. (DOI: 10.1021/jm00165a028).

62 P. Ren, O. Vechorkin, K. V. Allmen, R. Scopelliti, and X. Hu, *J. Am. Chem. Soc.,* **2011**, *133*, 7084–7095. (DOI: 10.1021/ja200270k).

63 P. W. Morgan, *Macromolecules*., **1970**, *3*, 536–544. (DOI: 10.1021/ma60017a013).

64 W. Orth, E. Pastorek, W. Weiss, and H. W. Kleffner, US Patent 5, 149, 886 (22.09.**1992**).

65 M. Yamada, J. Sun, Y. Suda, and T. Nakaya, *Chem. Lett*., **1998**, 1055–1056. (DOI: 10.1021/cm00054a004).

66 C. H. Chou and C. F. Shu, *Macromolecules*, **2002**, *35*, 9673–9677. (DOI: 10.1021/ma0210271).

67 K.-Y. Pu, B. Zhang, Z. Ma, P. Wang, X.-Y. Qi, R.-F. Chen, L.-H. Wang, Q.-L. Fan, and W. Huang, *Polymer*, **2006**, *47*, 1970–1978. (DOI:10.1016/j.polymer.2006.01.006).

68 K. Ono, T. Yanase, M. Ohkita, K. Saito, Y. Matsuhita, S. Naka, K. Okada, and H. Onnagawa, *Chem. Lett.*, **2004**, *33*, 276–277. (DOI: 10.1246/cl.2004.276).

69 H.-L. Pan and T. L. Fletcher, *J. Med. Chem.*, **1965**, *8*, 491–497.

CHAPTER 4

Synthesis and Characterisation of 4-Substituted Functionalised Polyfluorenes

---

4.1 Introduction

The discovery of electroluminescent (EL) properties in polymer semiconductors, laid terrific intensive quality of research in conjugated polymers. There are several numbers of exciting features like solution processability, tuning of bandgap energy levels by chemical structural modifications and self-organisation, which make them attractive for the replacement of conventional inorganic materials.[1] Hitherto a huge number of conjugated polymers were synthesised, characterised and used in wide varieties of light-emitting and other optoelectronic applications.[2,3] Among them, polyfluorenes (PFs), which can be considered as bridged polyphenylenes, are one of the most important class of conjugated polymers,[4] (the second most important class of conjugated polymers are polythiophenes and thiophenes-based copolymers).[5] The possibilities of structural modifications and property relationships of polyfluorene homopolymers and copolymers made them very attractive as unique functional materials.[6,7.8,9]

Just a simple search in the Web of Science, using the keywords "polyfluorene or polyfluorenes" gives over 3700 papers in total, with over 200 papers appearing each year in the past decade, which collected over 137,000 total citations (Figure 4.1). This search does not take into account publications on fluorene-containing copolymers or oligomers, which don't use the above keywords in the topics, so the total number of publications on fluorene-containing conjugated systems is well above that.

In spite of such enormous interest of researchers (chemists, physicists, materials scientists and engineers) from academia and industry to this class of conjugated materials, till now very few modifications have been made on the benzene rings of the fluorene moiety in conjugated polyfluorenes. This is contrasting to other classes of semiconducting polymers, e.g. polythiophenes or poly(p-phenylene vinylenes) where functionalisation at the aromatic/heteroaromatic rings is a common and widely used approach to expanding the number of available building blocks and polymers for tuning their properties to use them in organic electronics. Some of such functionalised polyfluorenes are highlighted in this introduction, before presenting the results of our own research on 4-substituted polyfluorenes.

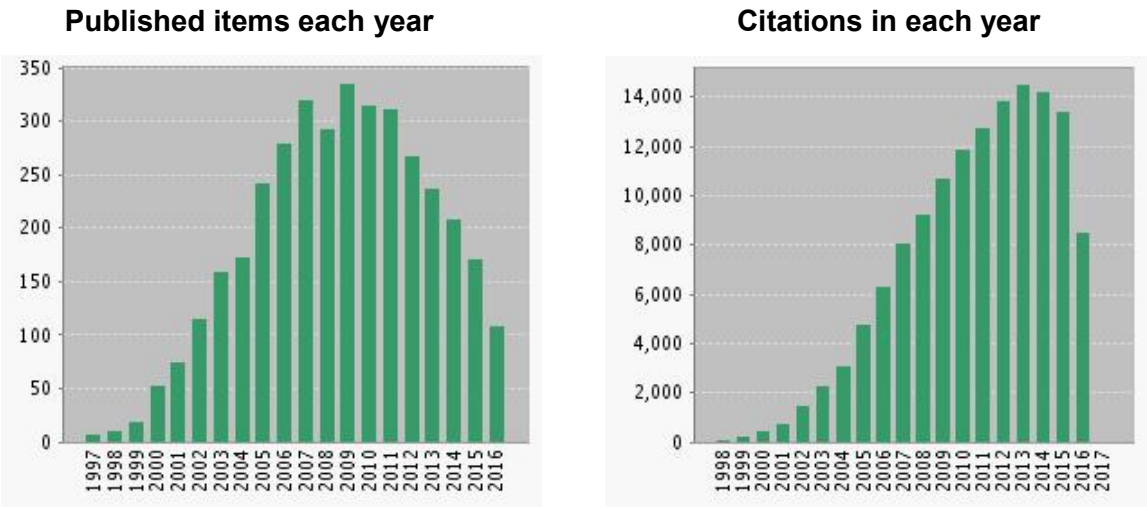

Figure 4.1 Number of publications and citations in each year with the topic "polyfluorene or polyfluorenes" from Web of Science ™ (Thomson Reuters ™) as of 15 October, 2016.

4.1.1 3,6-Dimethoxyfluorene-based polymers

In 2003, Leclerc and co-workers reported the synthesis and properties of poly(3,6-dimethoxy-9,9-dihexylfluorene) (**4.1**) and some copolymers (**4.2–4.6**).[10] The synthesis of the monomer 2,7-dibromo-3,6-dimethoxy-9,9-dihexylfluorene (**3.7**) used for the preparation of these polymers is described in Chapter 3. The homopolymer **4.1** and copolymers with various conjugated moieties (**4.2–4.6**) were synthesised by Yamamoto or Suzuki coupling polymerisation methods, respectively (Figure 4.2). These polymers were well soluble in common organic solvents and had wide variations of their molecular weights (M_w = 3,100–176,000 Da, M_n = 2,400–41,200 Da), with low molecular weights for copolymers **4.3** and **4.4**. Copolymers **4.4** and **4.5** showed thermal decompositions at 224 and 260 °C, respectively, while the rest of the polymers stabilities were higher (388–412 °C). All polymers are amorphous materials with glass transition temperatures (T_g) varying in the range of 60–130 °C.

The "polyphenylene-type" polymers **4.1, 4.2** and **4.4** have absorption bands in the range of 374–388 nm in chloroform solution and 366–392 nm in the films (Figure 4.3). Homopolymer **4.1** (**P1**) has an absorption peak at 374 nm in chloroform solution, with a hypsochromic shift in the film (366 nm), which is lower than in unsubstituted polyfluorenes (385–390 nm in solutions and 5–10 nm bathochromic shifts in films) and an opposite trend of absorption maxima from the solutions to films. Copolymer **4.2** (**P2**) with alternating dimethoxyfluorene/"unsubstituted" fluorene units in the chain shows intermediate spectral characteristics (388 nm in chloroform, 380 nm in films) between **4.1** and **PF8**.

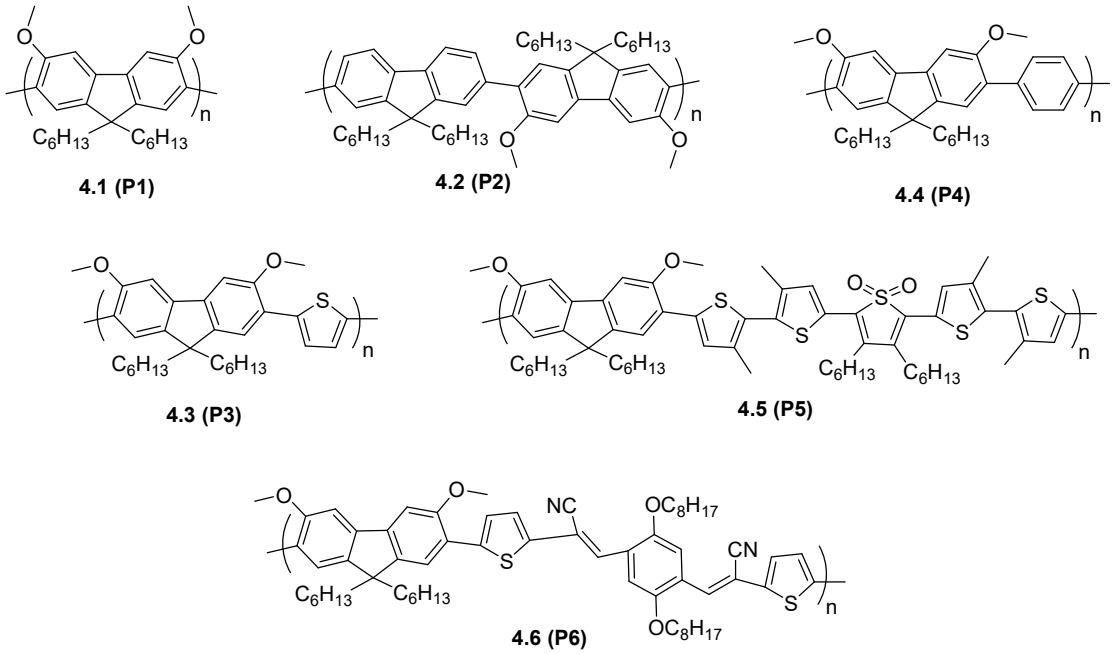

Figure 4.2 3,6-Dimethoxyfluorene-based homopolymer **4.1 (P1**) and copolymers **4.2-4.6 (P2-P6**).[10]

The homopolymer **4.1** (**P1**) shows PL emission at 412 with a shoulder at 436 nm in chloroform, so its emission is quite similar to that for unsubstituted polyfluorenes, although the vibronic feature is less resolved, perhaps due to a larger dihedral angle between the fluorene units due to sterics of the MeO group (see Figure 3.2 in Chapter 3).[11] It also shows a somewhat lower photoluminescence quantum yield (PLQY) of 48% compared to e.g. **PF6** (PLQY = 82%). The copolymer **4.4** (**P4**) has no substantial difference of absorption (374 nm) and PL emission (415, 438 nm) as compared to unsubstituted dihexylfluorene-*alt*-phenylene copolymer (**PFP**, **4.8**) (λ_{abs} = 370 nm, λ_{PL} = 408, 431 nm).

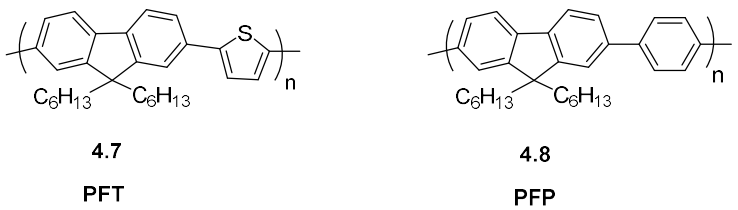

The copolymers **4.3**, **4.5** and **4.6** with electron-donating/electron-accepting moieties demonstrate intramolecular charge transfer resulting in bathochromic shifts in their absorption and emission spectra, giving thus the materials with green (**4.3**: λ_{PL} = 498 nm) and red (**4.5**: λ_{PL} = 645 nm; **4.6**: λ_{PL} = 616 nm) emissions (Figure 4.3).

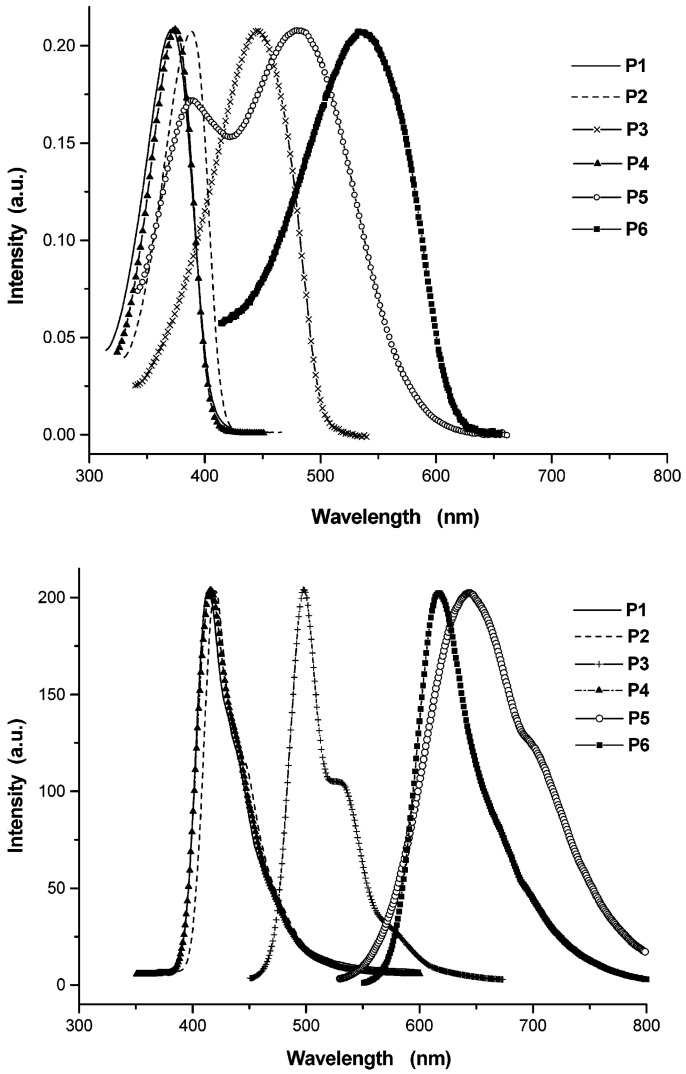

Figure 4.3 UV-Vis electron absorption (top), photoluminescence (bottom) spectra of 3,6-dimethoxyfluorene-based polymers **4.1 (P1), 4.2 (P2), 4.3 (P3), 4.4 (P4), 4.5 (P5),** and **4.5 (P6**) in chloroform solution.[10]

All 3,6-dimethoxyfluorene-based homo- and copolymers (**4.1–4.6**) can be p- or n-doped and exhibit quasi-reversible or irreversible oxidation and reduction waves in cyclic voltammetry experiments (Figure 4.4). Homopolymer **4.1** (**P1**) and copolymer **4.2** (**P2**) show oxidation onsets at 1.25 and 1.28 V, and reductions onsets at –2.02 and –2.10 V, respectively (vs SCE). Recalculation of redox potentials to frontier orbital energies gives the following energies for HOMO: –5.65 eV (**4.1**) and 5.67 eV (**4.2**), and for LUMO: –2.38 eV (**4.1**) and 2.30 eV (**4.2**). Janietz et al. reported HOMO/LUMO energy levels for unsubstituted polyfluorene **PF8** (HOMO = 5.80 eV, LUMO = 2.12 eV).[12] Thus, electron-donating methoxy groups increase both energy levels by ca. 0.15–0.2 eV.

Similar effect of methoxy groups is observed when copolymers **4.3** and **4.4** are compared with their unsubstituted analogs poly(2,7-(9,9-dihexylfluorene)-*alt*-(2,5-thienylene (**PFT**) and poly(2,7-(9,9-dihexylfluorene)-*alt*-(1,4-phenylene) (**PFP**).[13,10]

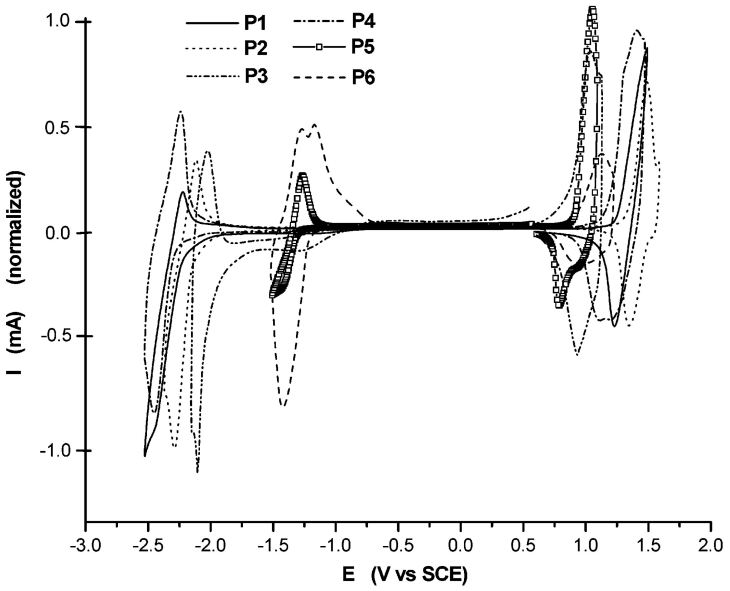

Figure 4.4 Cyclic voltammogram of 3,6-dimethoxyfluorene-based polymers **4.1 (P1), 4.2 (P2), 4.3 (P3), 4.4 (P4), 4.5 (P5),** and **4.5 (P6).**[10]

4.1.2 2,4,7-Hyperbranched and cross-linked polyfluorene-vinylenes and related conjugated materials

A number of fluorene-vinylene small conjugated molecules and hyperbranched polymers have been developed for organic electronic applications based on the 2,4,7-substitution pattern, exploiting accessibility of 2,4,7-tris(bromomethyl)fluorene **4.11** and corresponding phosphonim salt **4.12a** (or phosphonate **4.12b**) and tris(vinyl)fluorene **4.13** (Scheme 4.1).

Compound **4.12b** was used in the synthesis of fluorene-bridged tris-imidazole derivative **4.14** decorated with polyaromatic moieties as blue-emitting materials (λ_{PL} = 440–456 nm, Φ_{PL} = 59–88% in toluene) used in solution-processed OLEDs (Figure 4.5).[14] Another example of solution-processable hole-transporting triphenylamine-terminated tris(vinylene)fluorene **4.15** (λ_{PL} = 474 nm ($CHCl_3$), 504 nm (film), prepared from phosphonium salt **4.12a** was reported by the Chen group.[15] Its incorporation in Alq_3 or polyfluorene-based OLEDs gave an increase in the brightness of devices by 30–50%, to 9390 and 4040cd/m^2, respectively. Triphenylamine-end-capped branched compound **4.16** based on 2,4,7-tris(vinyl)fluorene and prepared by Horner-Emmons coupling from phosphonate **4.12b** (and tris-aldehyde synthesised from **4.11**), was also used as the material for non-linear

optics.[16] The compound was highly fluorescent (λ_{PL} = 488 nm, Φ_{PL} = 88% in cyclohexane) and showed very high two-photon absorption (cross-section value of 4195 GM at 570 nm).

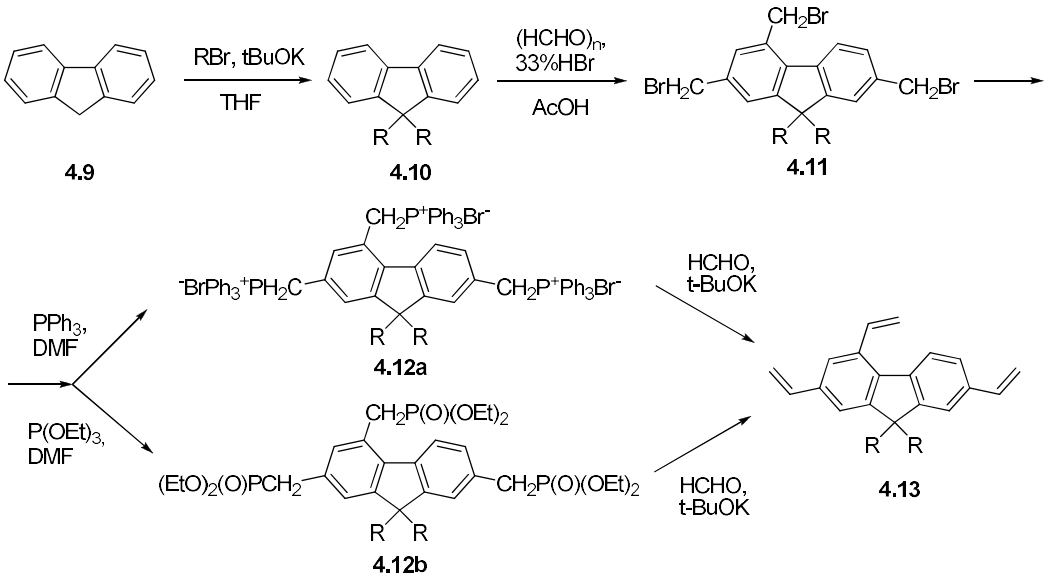

Scheme 4.1 Synthesis of 2,4,7-trisubstituted fluorenes **4.11–4.13** for hyperbranched polymers.

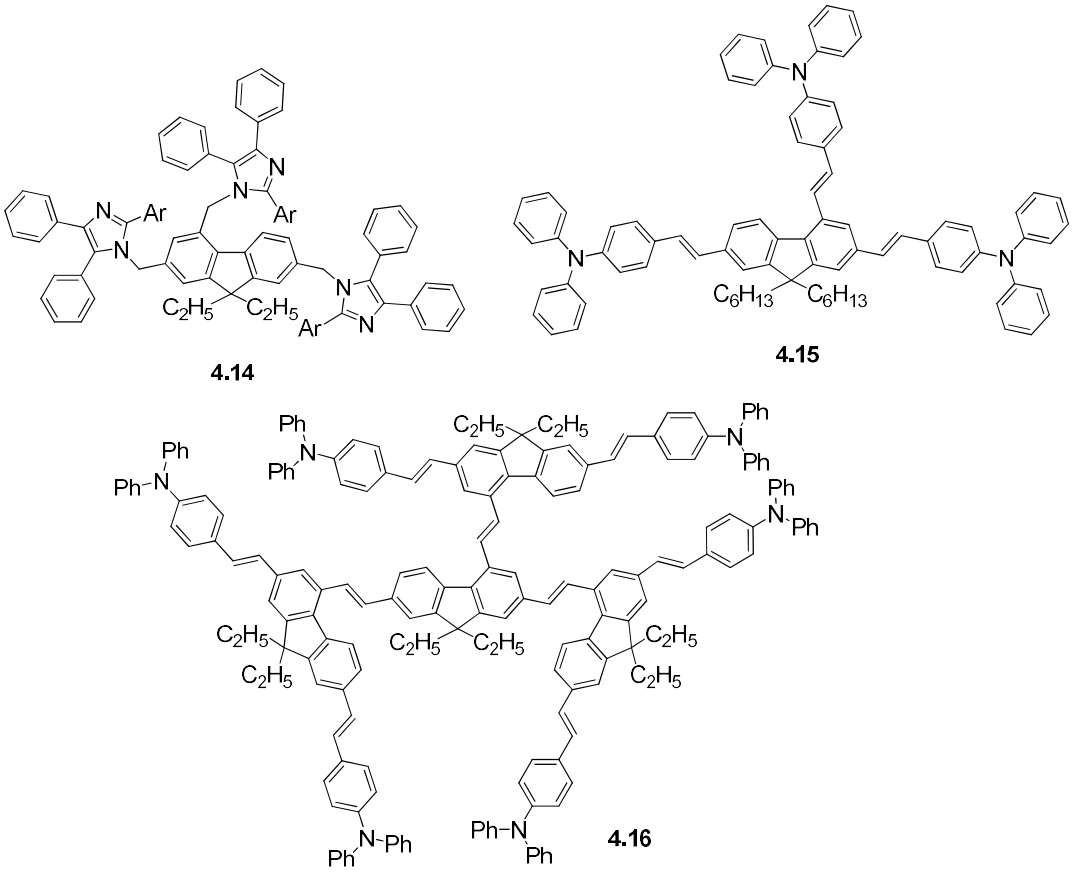

Figure 4.5 2,4,7-Trisubstituted fluorene small molecules **4.14–4.16** for organic electronics.[14,15,16]

The Chen group have also synthesised hyperbranched fluorene-cored polymers **4.17** and **4.18** containing triphenylamine moieties (Figure 4.6).[17,18] Polymer **4.17** was prepared by coupling of tris(vinyl)fluorene **4.13** with 4-carbaldehydo-4'-vinyl-triphenylamine following thermal curing (at 160 ^{o}C) on terminal alkene groups to produce soluble in common solvent cross-linked material emitting at λ_{PL} = 485, 509 nm (film).[17] Its HOMO energy (–5.19 eV) was lower than PEDOT:PSS (–5.0) and MEH-PPV (–5.02), whereas LUMO energy (–2.46 eV) was higher than that of MEH-PPV (–2.70 eV). So, it was successfully used in MEH-PPV based OLED for simultaneous reduction of hole injection barrier from PEDOT:PSS to MEH-PPV and blocking of electron transport from MEH-PPV to the anode.

Cross-linkable hyperbranched polymers **4.18** were prepared by Heck coupling of monomer **4.13** and 4,4'-dibromotriphenylamines.[18] Its thermal curing (210 ^{o}C, 30 min) gave cross-linked material, readily soluble in common solvents (chloroform, toluene) which emit in the bluish region (λ_{PL} = 483–494 in films). Similar to **4.17**, it was used as hole-transporting layer in OLED devices.

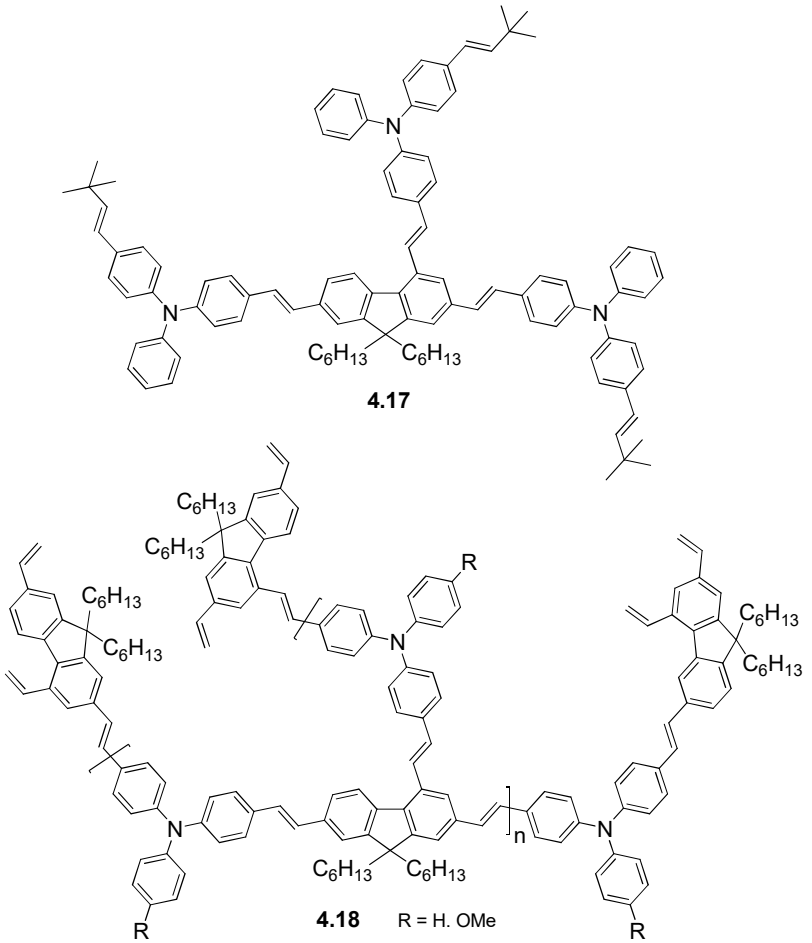

Figure 4.6 Hyperbranched polymers with 2,4,7,-tris(vinylene)fluorene core **4.17** and **4.18**.

Optically active poly(fluorenevinylene) polymer **4.20** obtained by tBuOK-promoted polymerisation of 2,4,7-tris(bromomethyl)fluorene **4.19** (Scheme 4.2) demonstrated circularly polarised light emission with a broad band in the range of 400–700 nm.[19] It showed an intense CD spectrum in solution with a similar CD shape in the film, suggesting that the chiral structure of the polymer does not largely change on film fabrication.

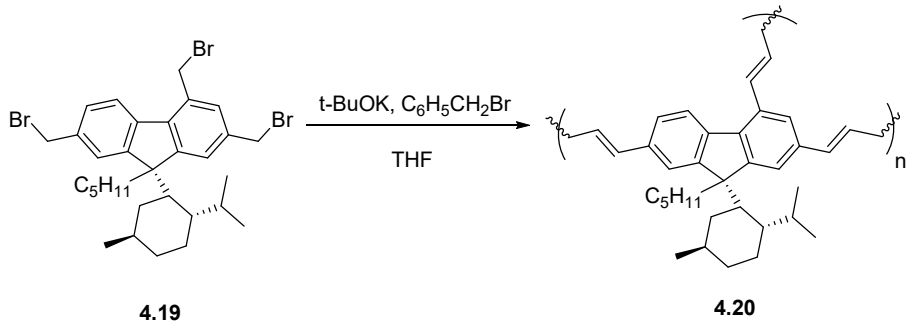

4.19 **4.20**

Scheme 4.2 Synthesis of an optically active hyperbranched polymer **4.20**.

4.1.3 4-Substituted polyfluorenes

While branched molecules and polymers described in the previous section successfully used position 4 in the fluorene moiety, for linear polyfluorenes functionalisation at this position is very rare. Actually, there were no works on that strategy at the time we started our studies, only one paper has appeared recently describing the synthesis and properties of such a polymer **4.26** and this is depicted in Scheme 4.3.[20]

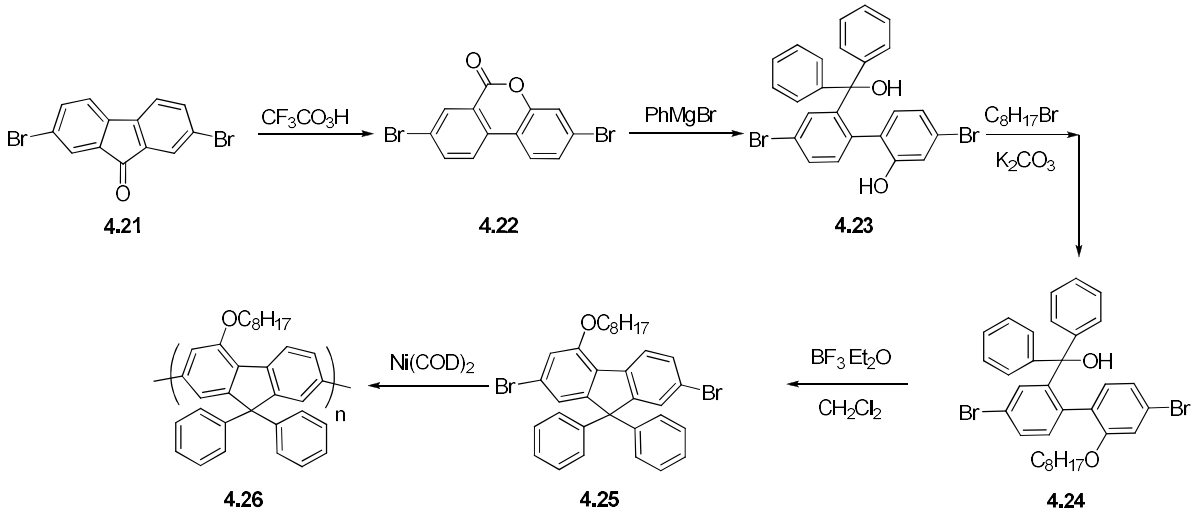

4.21 **4.22** **4.23** **4.26** **4.25** **4.24**

Scheme 4.3 Synthesis of 4-substituted poly(9,9-diphenylfluorene) **4.26**.[20]

Actually, the design of this polymer was not aimed to electronically tune the polymer backbone but as another approach for β phase stabilisation through in-plane noncovalent

attraction between hydrophobic linear alkyl chains. Polymer **4.26** showed an absorption peak located at 390 nm in different states (solution, gels, films) attributed to main-chain backbones, typical for polyfluorenes, with the shoulder peaks at 444 nm (similar to 436 nm in **PF8**) growing from solution to gels and to differently prepared films confirming the formation of β phase. Its PL spectra in toluene showed three well-resolved emission bands at 432, 456, and 468 nm (Figure 4.7a). Some bathochromic shifts and quenching the shortest vibronics at 432 nm was observed in gels and in films (prepared from toluene solution) clearly indicating the formation of β phase (Figure 4.7b). Films prepared from $CHCl_3$ solution did not show the β phase, however, thermal annealing of the films resulted in the evolution of their UV-Vis and PL spectra indicating the formation of this planar phase (Figure 4.7c). Moreover, on annealing on an air, no obvious changes was observed for low-energy green bands at 530–550nm indicating on high spectral and antioxidation stability of this polymer (Figure 4.7d).

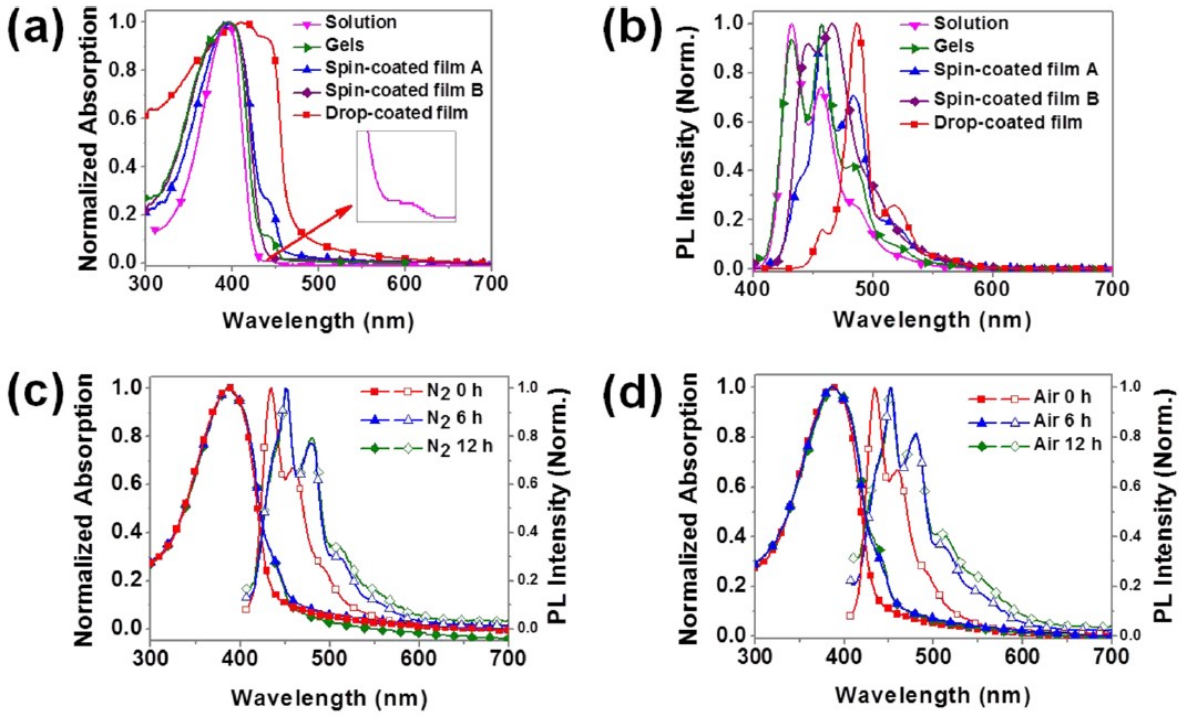

Figure 4.7. Optical properties of polyfluorene **4.26** in various states. UV−Vis (a) and PL spectra (b) in toluene solution, organogels, and films (spin-coated from toluene(A) and $CHCl_3$ (B)). UV−Vis and PL spectra of films spin-coated from $CHCl_3$ solution after thermal annealing at 200 °C in N_2 (c) and in air (d) for 0, 6, and 12 h.[20]

Grazing-incidence-X-ray scattering (GIXD) analysis suggested that the featuring peak at Q = 0.48 A^{-1} corresponds to the interdigitation distance of 13.09 Å, suggesting a possible chain arrangement of face-on packing relative to the silicon substrates (peak at 1.51 A^{-1} (4.16

Å) in the in-plane direction is from a stacked π–π plane) (Figure 4.8). Amplified spontaneous emission (ASE) and lasing (1D DFB laser) at 460 nm was also demonstrated for this polymer.

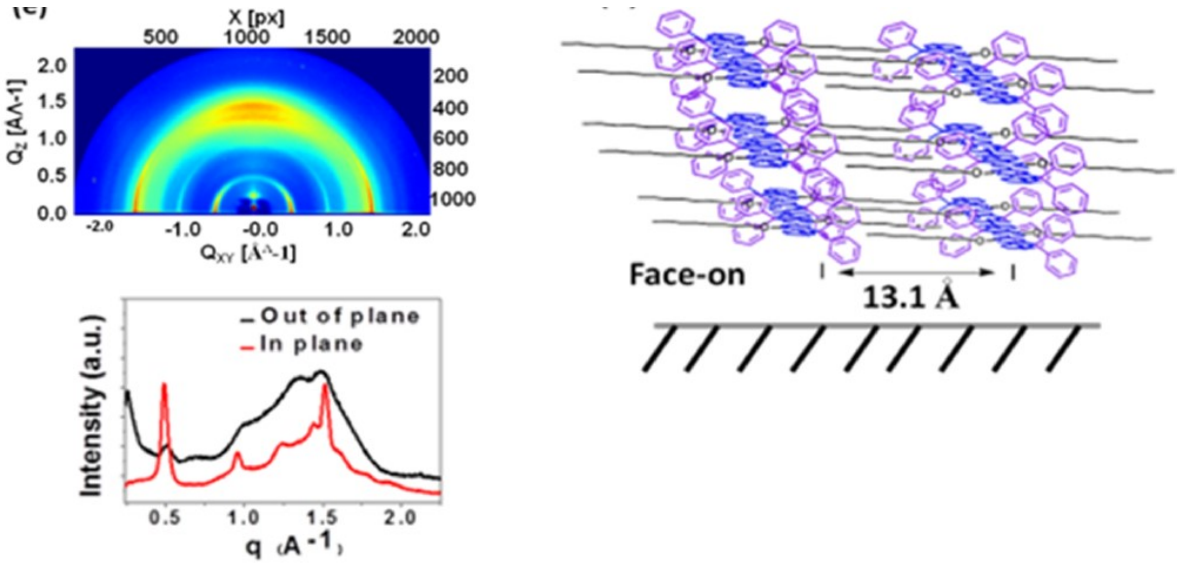

Figure 4.8 Grazing-incidence-X-ray scattering (GIXD) image (top left), X-ray profile (bottom left), and schematic models (right) of polyfluorene **4.26** films drop-coated on the Si substrate showing face-on orientation in the out-of-plane in the β-phase domain.[20]

It should also be mentioned one recent patent from Cambridge Display Technology Ltd (CDT) describing the synthesis of dibromofluorene **4.33** with a branched alkyl chain at position 4 (Scheme 4.4), which was claimed to be used for the synthesis of conjugated copolymers,[21] although the details of the synthesis and the properties of the polymers have not been disclosed.

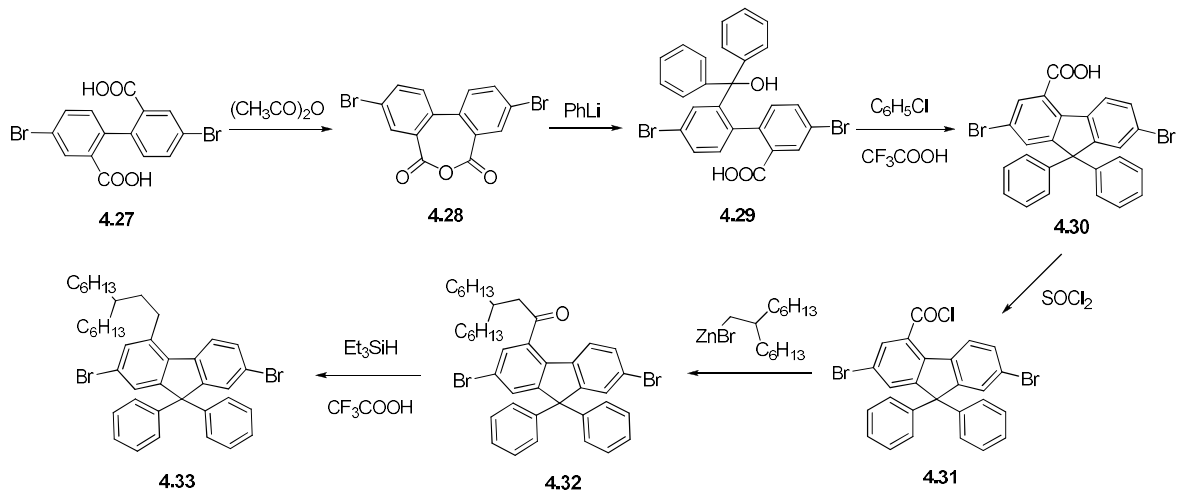

Scheme 4.4 Synthesis of 4-alkyl-2,7-dibromofluorene **4.33**.[21]

4.1.4 Aims and research objectives

Having elaborated new synthetic methods to access 4-substituted 2,7-dibromofluorenes described in Chapter 3, we aimed to develop novel functionalised polyfluorenes and to study their structure-property relationships. In this Chapter, we describe the design, synthesis, characterisation and studies of two series of 4-substituted fluorene homopolymers from monomers described in Chapter 3. For both series of polymers, EDG and EWG groups at position 4 have been used to look at their effect on the optical, electrochemical and other properties of novel polymers **X-PF8** and **X-PF6/8** compared to their "unsubstituted" analogues **PF8 and PF6/8**.

4.2 Results and Discussion

4.2.1 Synthesis of 4-substituted poly(9,9-dioctylfluorenes) X-PF8 and poly(9,9-di(4-octyloxyphenyl)fluorenes) X-PF6/8

The synthesis of 4-substituted 2,7-dibromo-9,9-R,R-fluorenes (**3.39–3.44** and **3.69–3.72**) has been described in Chapter 3. Polymerisation of dibromofluorene monomers **3.39–3.44** and **3.69–3.72** have been performed by Ni-promoted Yamamoto coupling polycondensation,[22] widely used for the synthesis of polyfluorenes and other conjugated polymers. Miller and co-workers have demonstrated an efficiency of the $Ni(COD)_2$/COD/bipy system in a mixture of toluene/DMF for the polymerisation process,[23,24] and Scherf[25] and List[26] have noted the convenience of this method on a lab scale to achieve high molecular weight polymers.

We first used this polymerisation method to obtain poly(9,9-dihexylfluorene) (**PF6**) to gain an experience in Yamamoto-type polymerisation and to obtain 4-unsubstituted polymer for comparison with 4-substituted analogues (Scheme 4.5a). Although its molecular weight was not very high (see below), it was still above the conjugation lengths of polyfluorenes of n~11–14), so the sample was suitable for comparison with other polymers. In a similar fashion, we have performed polymerisation of dibrominated dioctylfluorenes **3.39–3.44** and di(4-octyloxyphenylfluorenes) **3.69–3.72** (Scheme 4.5b,c). A deep blue-violet Ni complex was obtained from $Ni(COD)_2$ in DMF solution, then toluene solutions of fluorene monomers were added and polymerisation was carried out at 80 ^{o}C for 4 days with end-capping of the resulting polymers by addition of bromobenzene and heating at 80 ^{o}C for additional 12–16 h. After precipitation into methanol, the crude polymer was Soxhlet extracted from impurities and low-molecular weight fractions by methanol and acetone, then extracted with chloroform with re-precipitation of the chloroform-soluble fraction into methanol to afford two series of polymers, **X-PF8** and **X-PF6/8** (*here, the numbers 8 and 6/8 in the abbreviations of the polymers denote 9.9-dioctyl and 9,9-di(4-octyloxyphenyl) groups*) (Schemes 4.5b,c). Two

series of polymers were thus synthesised, **X-PF8** and **X-PF6/8,** and were well soluble in chloroform and toluene, and less soluble in THF.

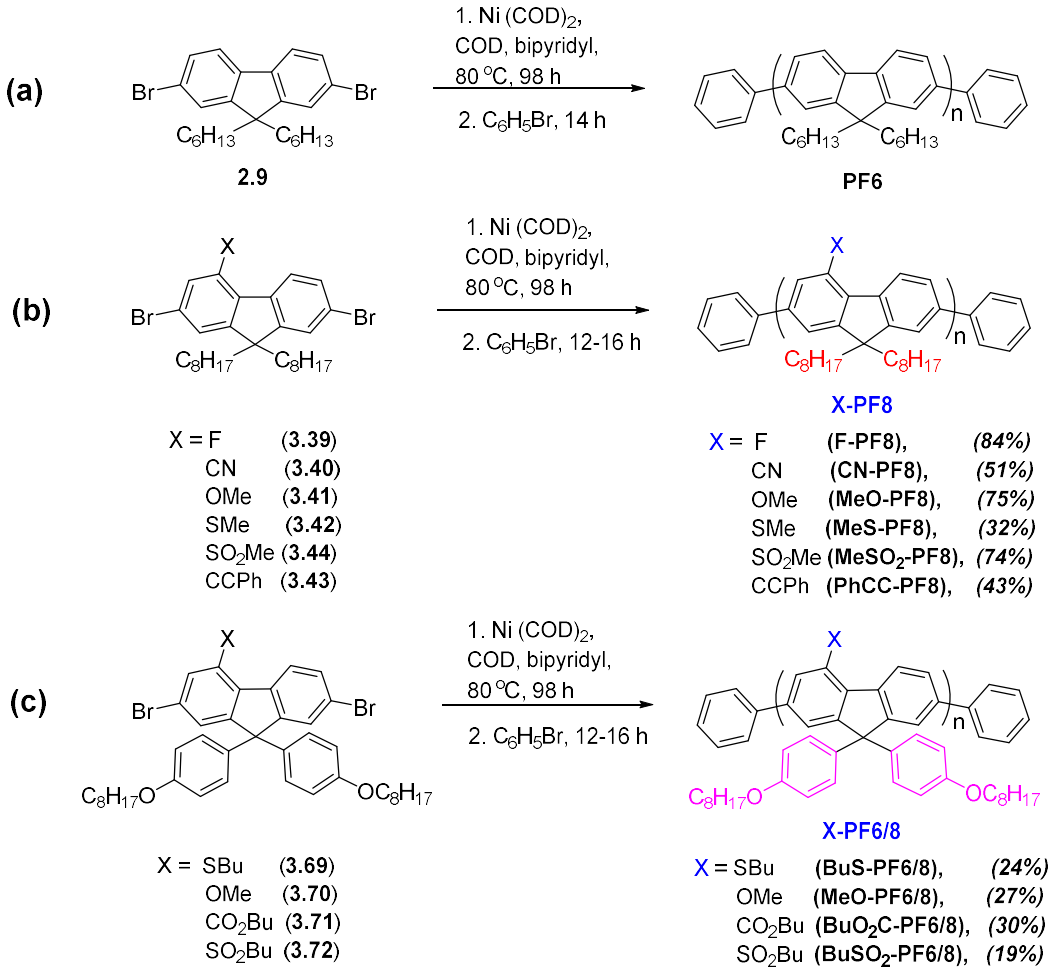

Scheme 4.5 Yamamoto polymerisation of 4-substituted functionalised 2,7-dibromofluorenes.

4.2.2 Characterisation of 4-substituted poly(9,9-dioctylfluorenes) X-PF8 and poly(9,9-di(4-octyloxyphenyl)fluorenes) X-PF6/8 by ^{1}H NMR, FT-IR and GPC methods

The synthesised homopolymers **X-PF8** and **X-PF6/8** were characterised by ^{1}H NMR spectroscopy. Because NMR spectroscopy gives limited information about the polymer structure (compared to small molecule NMRs) due to slight non-equivalency of protons of repeating building blocks and – as a result – broadening of the peaks (which normally appear as broad signals without spin-spin coupling), we compared the NMRs of the obtained polymers with those of the corresponding monomers to ensure the structure of the obtained polymer samples matched with our expectations.

For example, Figure 4.9 shows the ^{1}H NMR spectra for 4-methylsulfonyl-containing monomer **3.44** (X = SO_2Me) and the corresponding polymer **$MeSO_2$-PF8**, with complete assignments of observed signals to the corresponding protons.

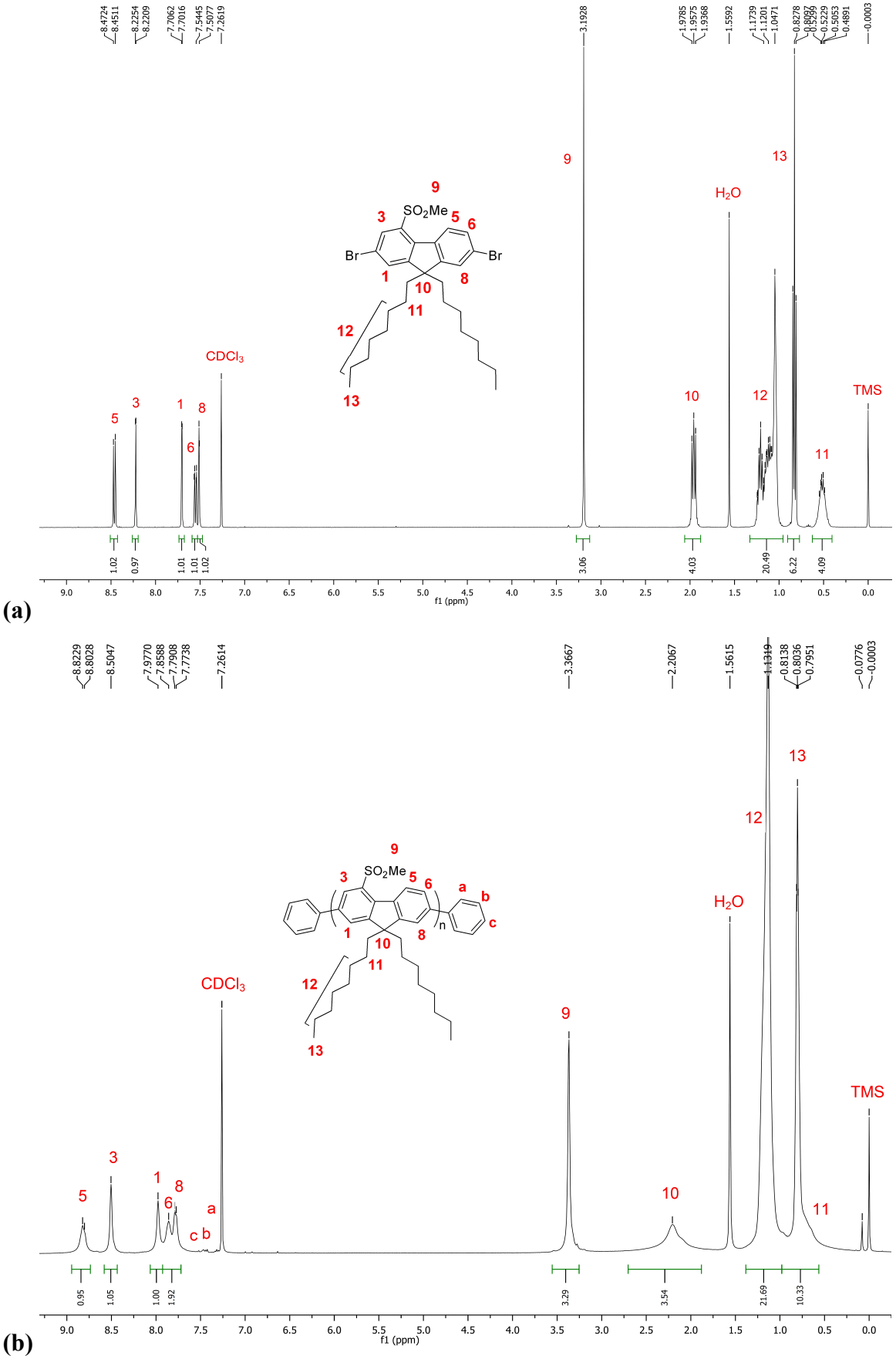

Figure 4.9 ^{1}H NMR spectra of 4-methylthio-2,7-dibromo-9,9-dioctylfluorene monomer (**3.44**, X = SO_2Me) and **$MeSO_2$-PF8** polymer obtained from it by Yamamoto polymerisation.

As one can see, polymer **$MeSO_2$-PF8** shows a very similar pattern of proton signals as its monomer **3.44**, with some shifts of the resonance proton signals on polymerisation. Compared to the monomer **3.44**, in polymer **$MeSO_2$-PF8** aromatic protons are down field shifted: the largest shift is observed for H-5 proton (0.36 ppm) and other protons are shifted by 0.28–0.31 ppm. Methyl protons of $MeSO_2$ group and methylene protons of CH_2 group at C-9 are also shifted to down field, but the shift is smaller (0.18 ppm) (the second CH_2 is probably also shifted by a similar value and overlaps with CH_3 group), whereas other aliphatic protons of octyl groups are weakly sensitive to polymerisation (*cf.* Figures 4.9a and 4.9b). NMR spectrum of the polymer also shows small signals of end phenyl groups in the region of ~7.3–7.6 ppm (marked as "a,b,c" on Figure 4.9b), which are very weak due to high molecular weight of the polymer.

For polymer **CN-PF8,** apart from ^{1}H NMR characterisation, we have recorded its FT-IR spectrum to prove that cyano-group in monomer **3.40** (X = CN) is not affected by polymerisation process and remain unchanged in the resulting polymer. FT-IR data presented on Figure 4.10 clear demonstrate strong signal of CN stretching mode at 2225 cm^{-1}, supporting the structure of **CN-PF8**. ^{1}H NMR spectrum of this polymer shows similar features as for above discussed polymer **$MeSO_2$-PF8**, i.e. down field shifts of protons on polymerisation, with larger shifts for aromatic protons (again, H-5 proton shows the largest shift of 0.34 ppm) (figures for this and others monomer/polymer pairs are not shown, but one can compare ^{1}H NMR data for them from the experimental parts in Chapters 3 and 4).

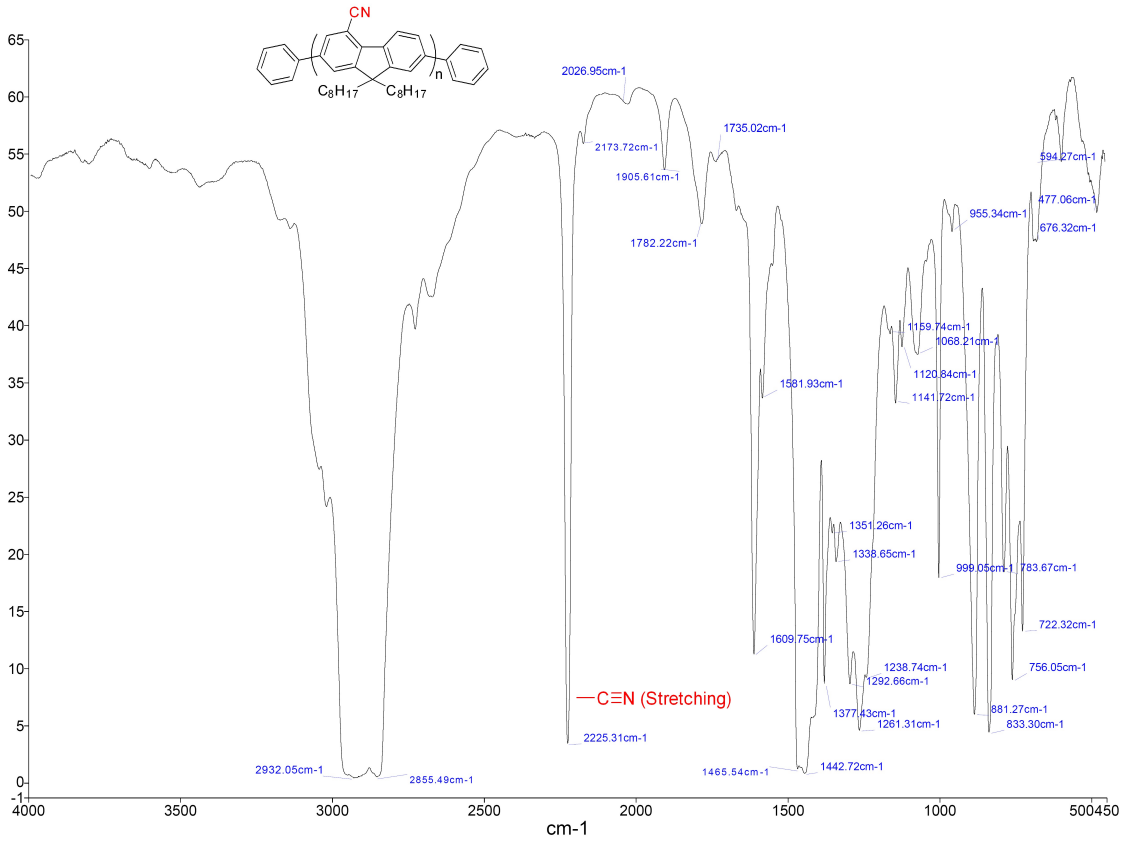

Figure 4.10 FT-IR spectrum of **CN-PF8** polymer in films.

Molecular weights of the synthesised polymers have been estimated by gel permeation chromatography (GPC) in THF solutions with calibration the column versus polystyrene standards, estimating their weight average molecular weight (M_w), number average molecular weight (M_n) and polydispersity index PDI = M_w/M_n. An example of a GPC trace is shown in Figure 4.11 for the **F-PF8** polymer.

All synthesised **X-PF8** polymers showed high molecular weights (M_w = 45,100–185,000 Da; M_n =10,300-78,700 Da; PDI = 2.17–4.37), from which the average chain length can be estimated as n = 18–126. For **X-PF6/8** series of polymers, the molecular weights were somewhat lower (M_w = 24,700–85,400 Da; M_n = 9,700–56,500 Da), but still quite high, with more narrow polydispersity PDI = 1.51–2.54. Estimations from their molecular weights give average lengths of polymer chains of 15–168. Thus, in all the cases, the molecular weight is substantially higher then the conjugation length in polyfluorenes (estimated in the literature as n = 11–14).

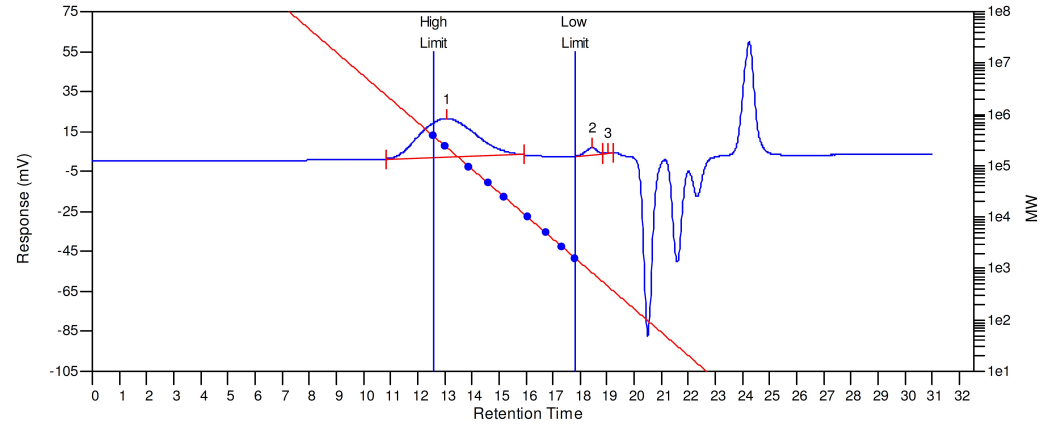

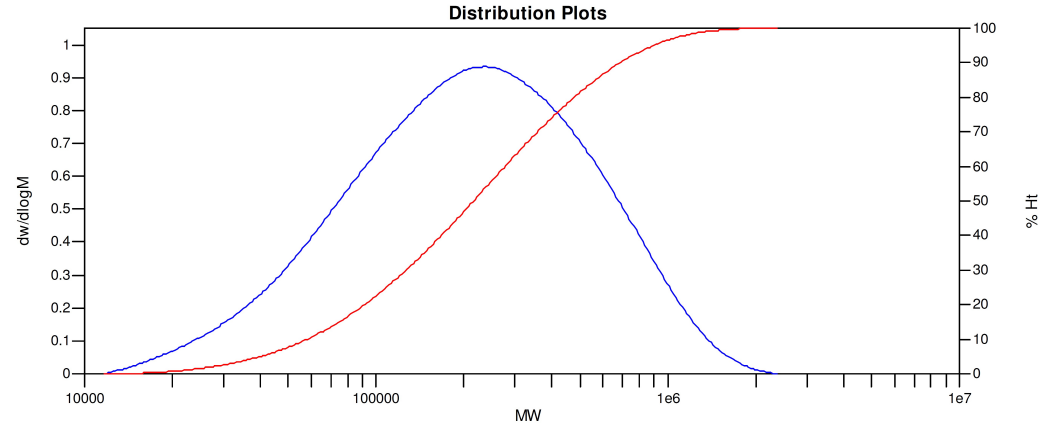

MW Averages

Peak No	Mp	Mn	Mw	Mz	Mz+1	Mv	PD
1	238124	129492	304652	565032	833328	272779	2.35267
2	841	850	883	917	953	878	1.03882
3	465	478	482	485	489	481	1.00837

Figure 4.11 GPC trace for the **F-PF8** polymer in THF.

4.2.3 Thermal analyses of 4-substituted poly(9,9-dioctylfluorenes) X-PF8 and poly(9,9-di(4-octyloxyphenyl)fluorenes) X-PF6/8

The thermal stabilities of polymers have been studied by thermogravimetric analysis (TGA). Estimating their thermal decomposition in a nitrogen atmosphere at a level of 5% mass loss with a heating rate of 10 ^{o}C/min. All polymers showed good stability, with decomposition temperatures of T_d = 392–426 ^{o}C, typical for polyfluorenes (e.g. for **PF8** it was reported as T_d = 385 °C[27]) (Figure 4.12). From TGA data in the region of ~400–500 ^{o}C with ca 45–55% mass loss, it seems that major mass losses on decomposition are due to cleavage of the octyl groups in both series of polymers, **X-PF8** and **X-PF6/8**.

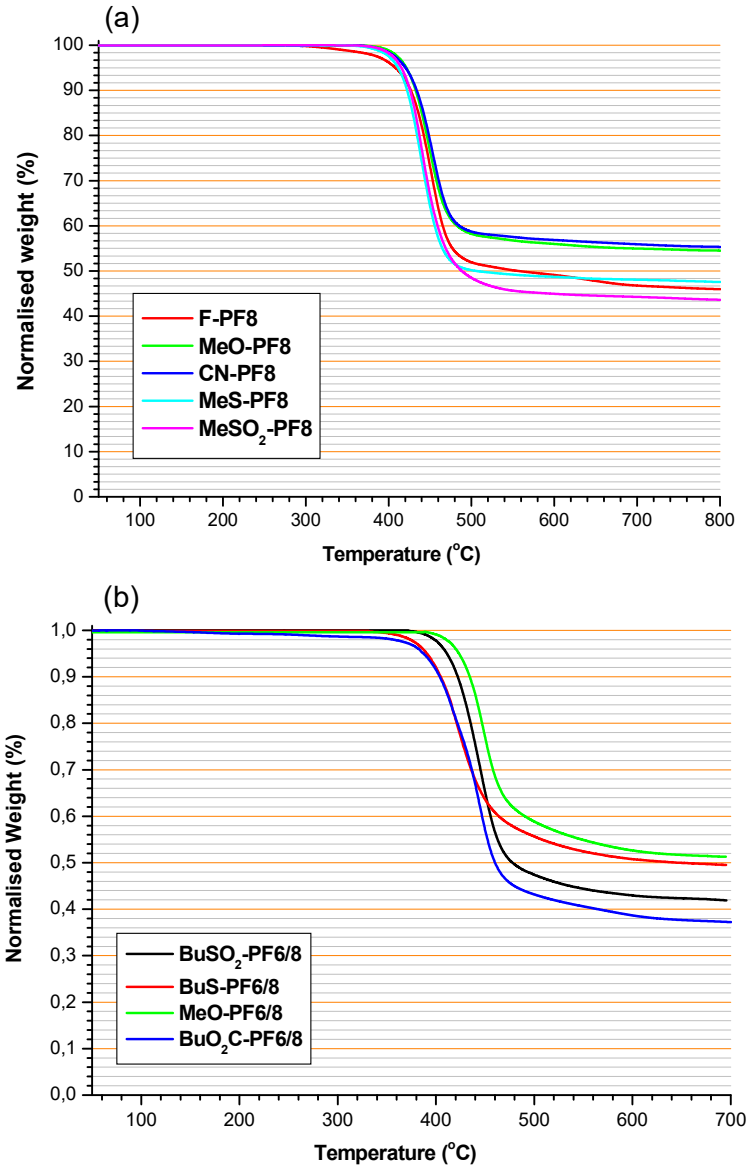

Figure 4.12. Thermogravimetric analysis (TGA) curves of **X-PF8** (a) **X-PF6/8** (b) polymers under a nitrogen atmosphere at a heating rate of 10 °C/min.

The differential scanning calorimetry (DSC) was used to measure the glass transition temperatures of **X-PF8** polymers (T_g). The **X-PF8** polymers glass transition temperatures are in the range of 57–86 °C, which is comparable to that for "unsubstituted" PFs. The data of GPC, TGA and DSC results are presented in Table 4.1.

Table 4.1 GPC, TGA and DSC data for **X-PF8** and **X-PF6/8** polymers.

Polymer	M_w,[a] (Da)	M_n,[b] (Da)	PDI[c]	T_d,[d] (^oC)	T_g,[e] (^oC)
F-PF8	124,000	40,100	3.09	398	86
MeO-PF8	75,000	34,500	2.17	409	61
CN-PF8	45,100	10,300	4.37	402	63
MeS-PF8	120,000	32,400	3.70	402	57
$MeSO_2$-PF8	185,000	78,700	2.35	413	79
PhCC-PF8	99,800	23,200	4.30	–	–
PF6	25,000	9,700	2.57	–	–
BuO_2C-PF6/8	28,600	18,500	1.54	392	–
MeO-PF6/8	34,400	23,400	1.47	426	–
BuS-PF6/8	24,700	9,700	2.54	393	–
$BuSO_2$-PF6/8	85,400	56,500	1.51	409	–

[a] M_w is weight average molecular weight. [b] M_n is number average molecular weights, [c] Polydispersity index, PDI = M_w/M_n. [d] T_d is decomposition temperature measured at 5 % weight loss under N_2. [e] T_g is glass transition temperature.

4.2.4 DFT calculations of electronic properties of 4-substituted polyfluorenes

For estimation of HOMO and LUMO energy levels of synthesised 4-substituted polyflyuorenes **(X-PF8** and **X-PF6/8)** we have performed density functional theory (DFT) computations of corresponding oligomers (from n = 1 to n = 13–20) and extrapolated the evolution of their HOMO and LUMO energy levels to the infinite length chain (i.e. to polymers). Computations have been performed for isolated molecules in a gas phase at the B3LYP/6-31G(d) level of theory, at which the geometries of oligomers have been optimised and the energy levels have been calculated for the optimised geometries. We used this very time-consuming approach for calculations (instead of using PBC method (periodic boundary conditions) often used for "direct" calculations of electronic structures of conjugated polymers) as it not only gives the predictions of the energy levels of the polymers, but also allows to look on the evolution of frontier orbital energy levels and the HOMO–LUMO gaps with an increase of the oligomer chain.

To minimise the computation time and because substituents at position 9 have little effect on the electronic state of oligomers, we have performed calculations for 9,9-dimethylfluorene oligomers **X-OFMe_2** (the same for the chains in the substituent X, methyl

groups was used for sulfones, ketones and esters in all calculations). In these calculations, apart of substituents X, present in our synthesised monomers/polymers, we have performed calculation for some other groups, to have a more general picture of the effect of substituents in position 4, which might be a useful insight for expansion of this work and the synthesis of other 4-substituted polymers. Namely, we have additionally calculated oligofluorenes with EDG groups X = NMe_2, NPh_2, Me, and with EWG groups X = COMe, CF_3.

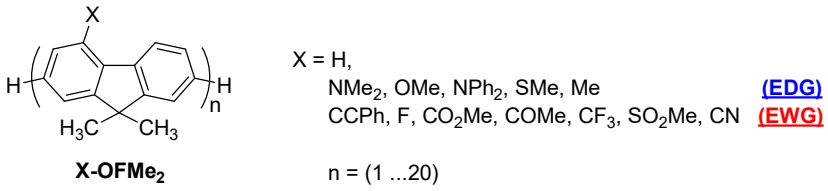

Figure 4.13 shows changes in HOMO and LUMO energy levels for the studied **X-OFMe$_2$** oligomers depending on the number of repeating units in the chain (n) and Figure 4.14 shows the evolution of the energy gap, E_g = LUMO–HOMO, for them. With an increase of n, the HOMO is exponentially growing and the LUMO is exponentially decreasing. The effect of substituents X on both the HOMO and the LUMO is very strong: for the studied series of oligomers the variations in both HOMO and LUMO levels are about 1 eV, from the strongest donor X = OMe to the strongest acceptor X = CN (at n ~16–20, when n is higher than the conjugation length in polyfluorenes, ~11–14 units). However, an effect of substituents X on the HOMO–LUMO energy gaps is substantially smaller and variations in E_g are of ~0.28 eV only (~0.15–0.18 eV for most oligomers, with somewhat smaller HOMO–LUMO gaps for X = C≡CPh and COMe) (Figure 4.14).

These theoretical calculations predict that by changing the substituents X in polyfluorenes, one can efficiently tune their HOMO and LUMO energy levels (e.g. to match them with the work function of electrodes or other layers in OLED applications), whereas the band gap of polymers will be weakly affected by this functionalisation. This is an important prediction, because it tells us that 4-functionalised polyfluorenes should absorb and emit the light near in the same region as “unsubstituted” polyfluorenes, that is to be blue-emitting materials.

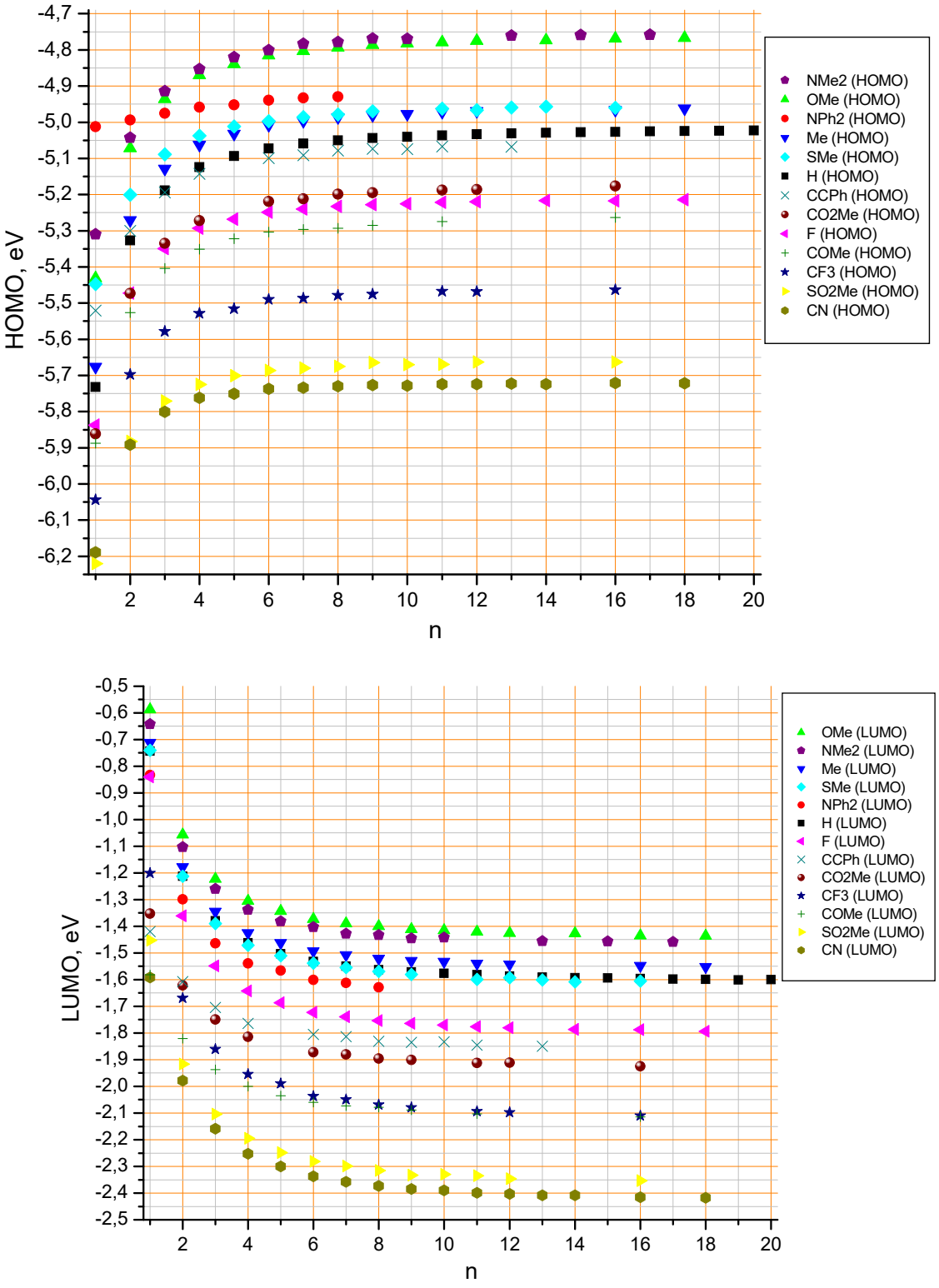

Figure 4.13 HOMO (top) and LUMO (bottom) energy levels for **X-OFMe$_2$** oligomers as a function of the oligomers chain length (n), from DFT B3LYP/6-/31G(d) calculations in the gas phase.

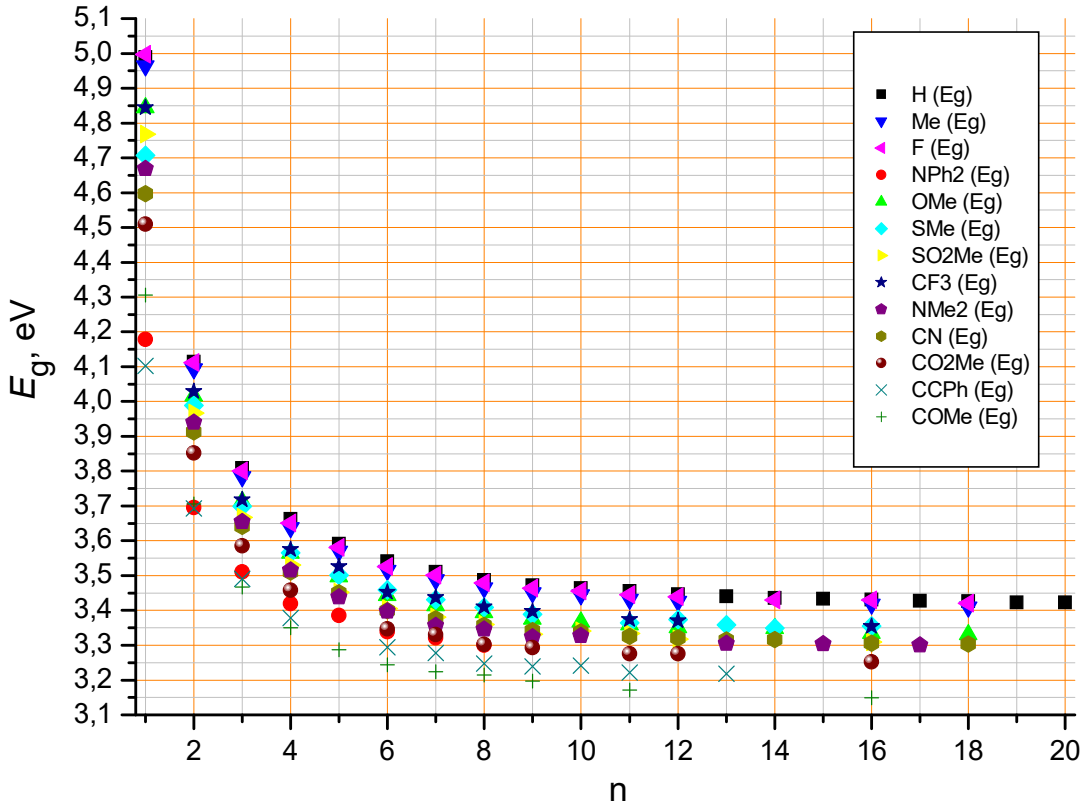

Figure 4.14 HOMO-LUMO energy gaps, E_g, for **X-OFMe$_2$** oligomers as a function of the oligomers chain length (n), from DFT B3LYP/6-/31G(d) calculations in the gas phase.

We have re-plotted graphs presented in Figures 4.13 and 4.14 as functions of a reciprocal number of repeating units, 1/n, the procedure which is commonly used to linearise exponential dependencies "Energy *versus* n" (Figures 4.15 and 4.16). As seen, reasonable linear dependencies are observed, although for longer oligomers (n > 10) the dependencies deviate from linearity with a tendency to saturation. This is a common feature for both experimental data for conjugated oligomers[28,29,30 31], and for computational values as well.[28,32,33] Namely, experimental values of HOMOs for polymers are always somewhat lower and LUMOs are higher than the linear extrapolations of *E* vs 1/n predict (band gaps, E_g, are larger than those obtained from linear extrapolation, as well). Deviation of experimentally measured energy values (electrochemical potentials, absorption-emission maxima, $E_{0\text{-}0}$ transitions etc) from linearity (*E* vs 1/n) for large n is commonly attributed to the conjugation length of polymers. At n close to or higher than conjugation length of particular oligomers, no further changes are observed with the further increase of the length of the oligomer chain (so-called "polymer limit"). Similar deviations from 1/n are also observed for computed values and it particularly explained by "empirical" nature of plots vs 1/n.

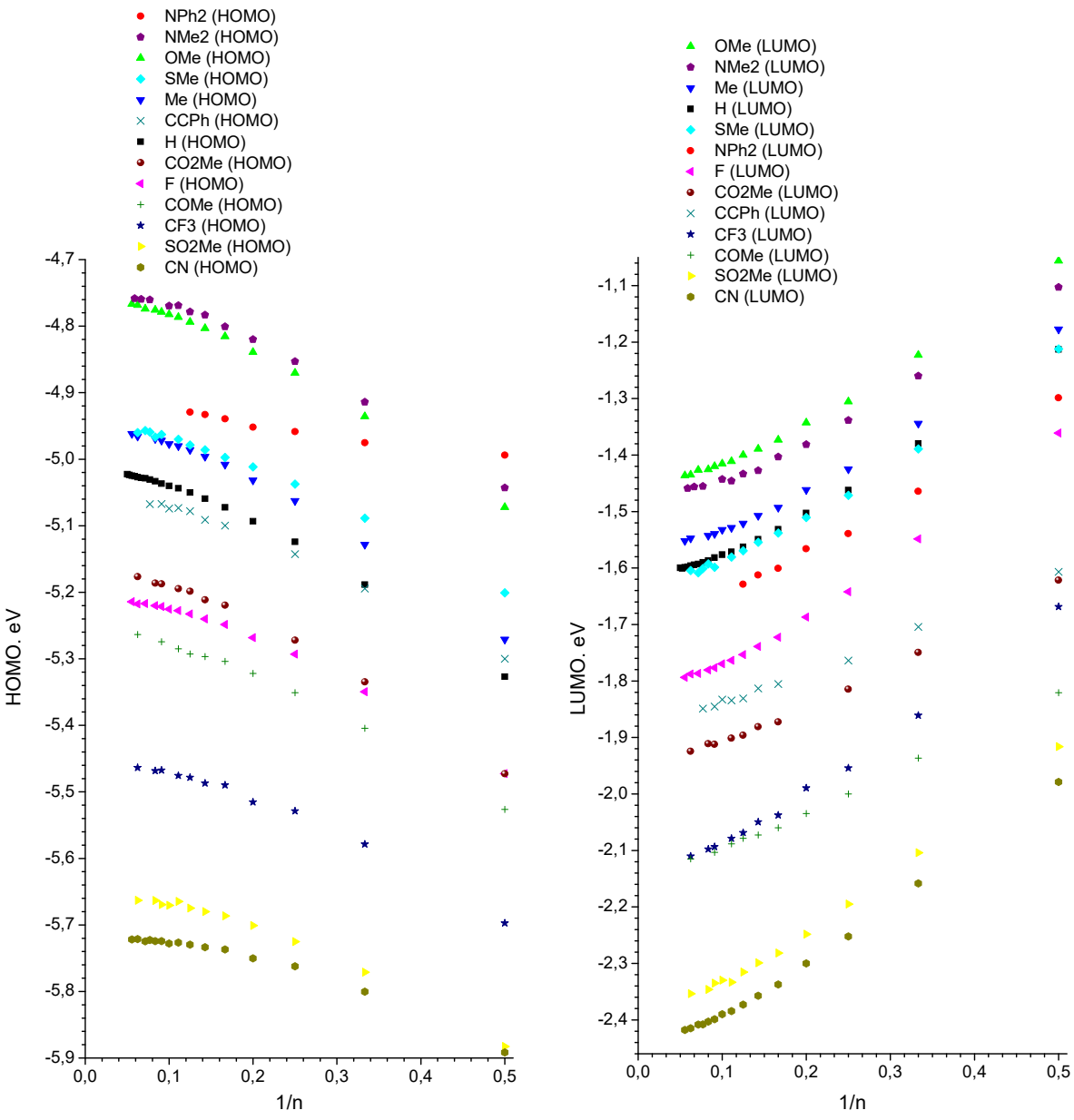

Figure 4.15 HOMO (left) and LUMO (right) energy levels for **X-OFMe$_2$** oligomers as a function 1/n, from DFT B3LYP/6-/31G(d) calculations in the gas phase.

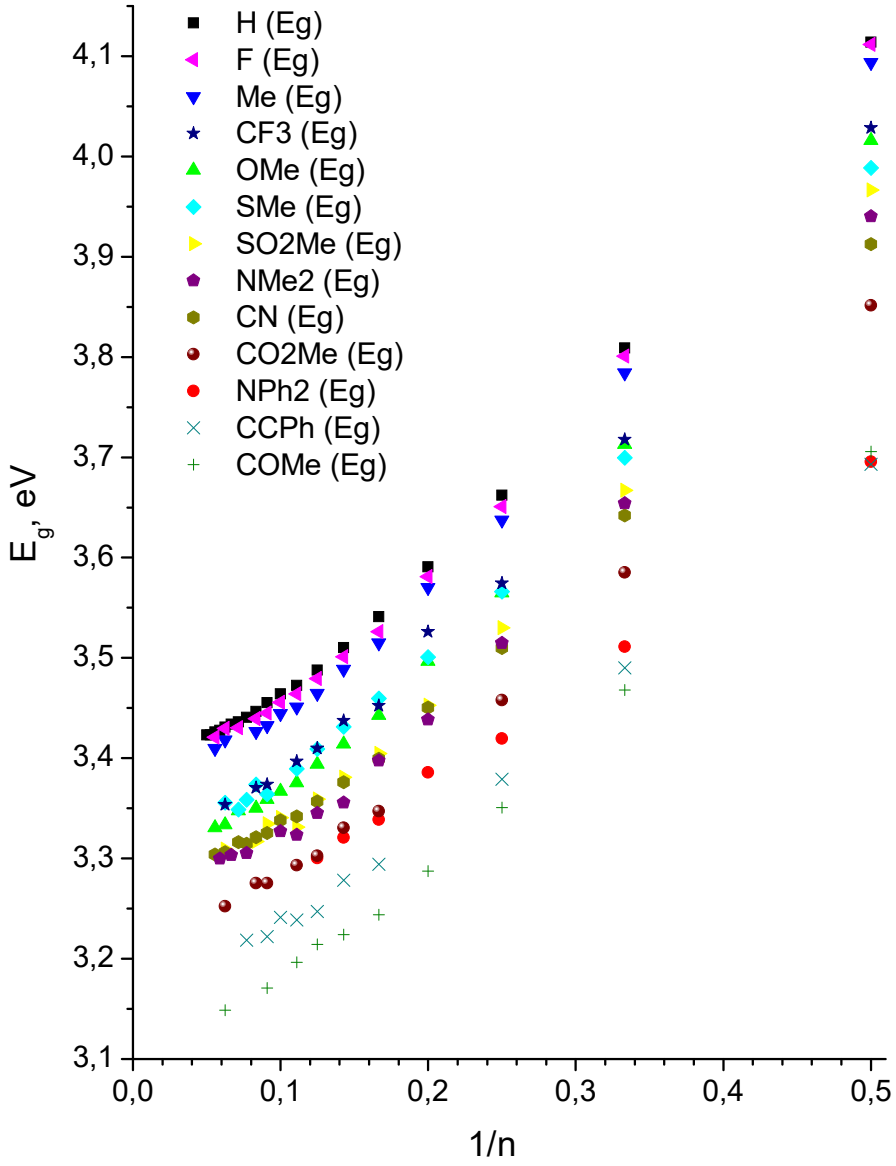

Figure 4.16 HOMO-LUMO energy gaps, E_g, for **X-OFMe$_2$** oligomers as a function of 1/n, from DFT B3LYP/6-/31G(d) calculations in the gas phase.

Different (semi) empirical extrapolation methods (1/n) have been proposed in the literature, some of them have been reviewed by Meijer et al.[34] Several models (e.g. free-electron model, coupled oscillator model, excitonic model) have been described in the literature to fit the energies of π-conjugated systems depending on their length.[31,35] W. Kuhn,[36] based on the early work of Lewis and Calvin,[37] have proposed an equation (1) for the description of excitation energies of systems with N identical oscillators:[28,35]

$$E = E_0\sqrt{1 + 2\frac{k'}{k_0}\cos\frac{\pi}{N+1}} \qquad (1)$$

where N is a number of adjacent double bonds coupled with a force constant k', $E_0 = (k_0/4\pi^2\mu_0)^{1/2}$ is the frequency of an isolated oscillator unit; k'/k_0 is usually on the order of ≈ −0.45. So, we have-re-calculated exponential dependencies presented in Figures 4.12 and 4.13 by the Kuhn equation (1), and the results are shown in Figures 4.17 and 4.18.

Good linear dependencies have been obtained for HOMO, LUMO and E_g versus the Kuhn function and these have been extrapolated to n = ∞ (corresponding to the Kuhn value = 0.3162) to estimate the energy levels for polymers. The results of DFT-predicted energies are collated in Table 4.2, which also contains data on changes in HOMO, LUMO and E_g energies of 4-substituted polyfluorenes relative to unsubstituted polymer.

Absolute values of HOMO, LUMO and E_g from DFT calculations are expectedly different from experimental energies (from electrochemistry or spectroscopy, see next sections) because calculations have been done for the gas phase and because of the prediction ability of the chosen functional. However, for the chosen series of structurally similar molecules, they all should deviate similarly from experiments and therefore relative changes in their energies due to groups X should be estimated with quite a high accuracy. As expected, electron-donating groups increase both HOMO and LUMO energy levels and electron-withdrawing groups decrease them; the quantitative estimations of the degree of the effect of groups X is given in Table 4.2: ΔHOMO and ΔLUMO (relative to X = H). More interesting results arising from these DFT calculations are that the highest HOMO–LUMO energy gap, E_g, is observed for "unsubstituted" polyfluorene (X = H) and for fluorinated polymer (X = F) (X = Me also gives very close E_g values), whereas other 4-substituted polymers show somewhat smaller E_g energy gaps, for both EDG and EWG substituents. This band gap contraction is not high, for most of the studied polymers it is < 0.2 eV, and for polymers which we have synthesised in this work, ΔE_g is only 0.07–0.15 eV (Figure 4.18 and Table 4.2). These seem to be interesting results on the prediction of the electronic properties of 4-substituted polyfluorenes, both for their frontier orbital energy levels and band gaps (and consequently the wavelengths of their absorption and emission).

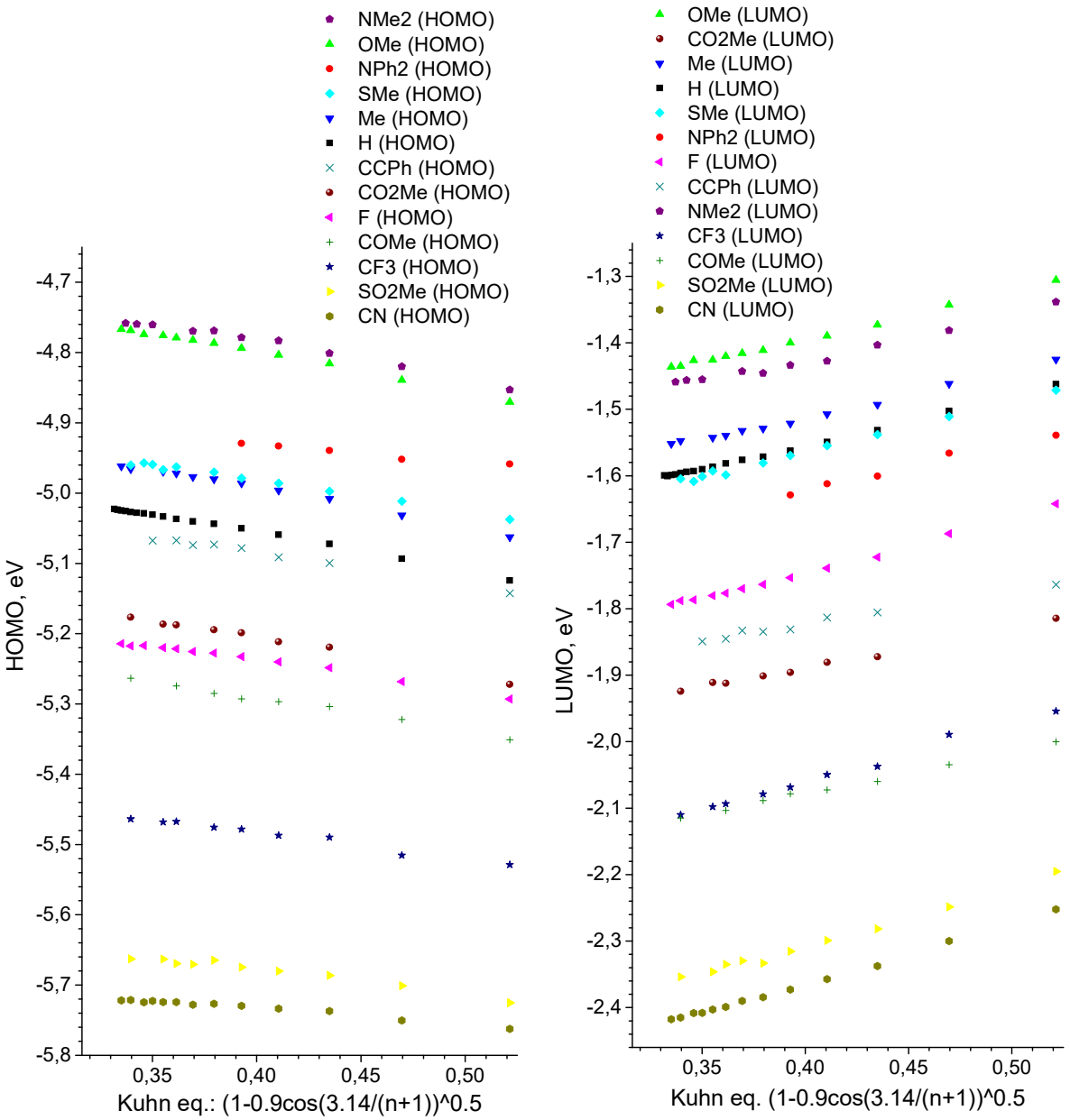

Figure 4.17 HOMO (left) and LUMO (right) energy levels for **X-OFMe$_2$** oligomers versus the Kuhn function $(1 - 0.9\cos(3.14/(n+1)))^{0.5}$; DFT B3LYP/6-/31G(d) calculations in the gas phase. Graphs for oligomers with $n \geq 4$ are shown (the X axis starts from the point "Kuhn" = 0.3162, which corresponds to $n = \infty$; the largest points on the X axes correspond to the tetramers, $n = 4$ ("Kuhn function" = 0.5214).

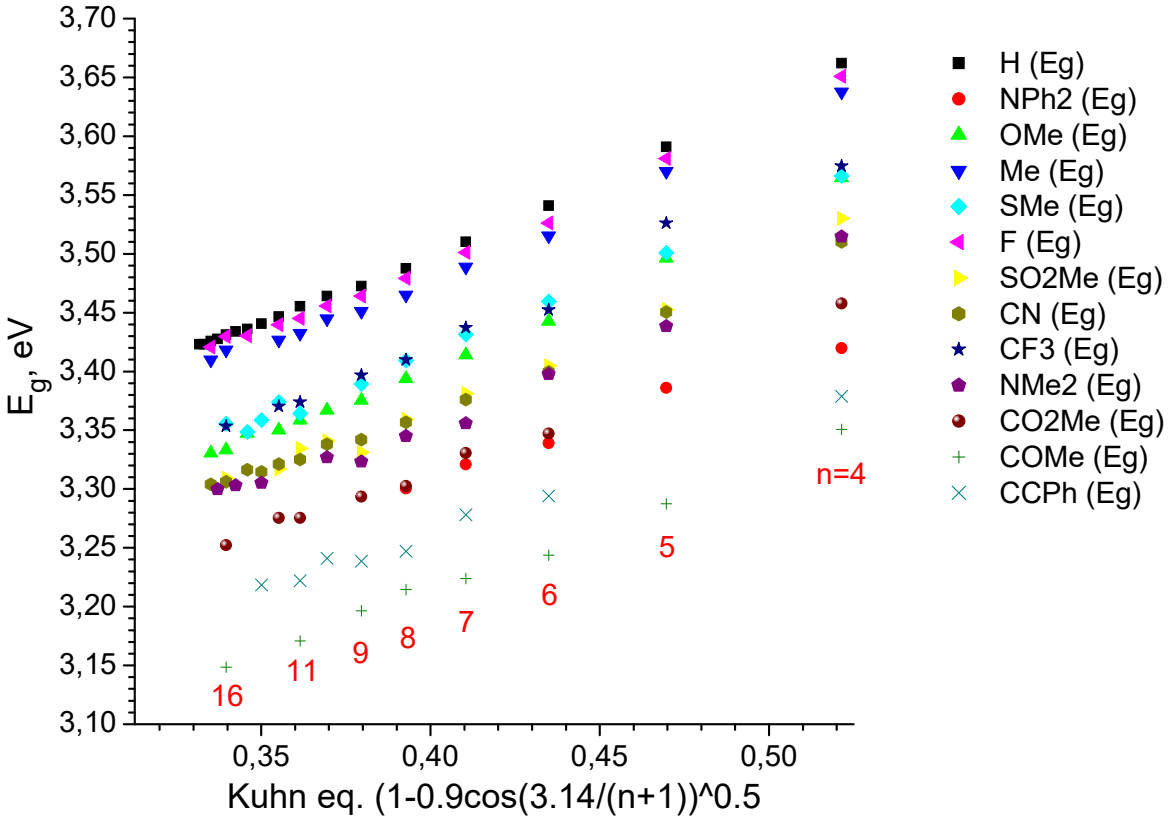

Figure 4.18 HOMO-LUMO energy gaps, E_g, for **X-OFMe$_2$** oligomers versus Kuhn function $(1 - 0.9\cos(3.14/(n+1)))^{0.5}$; DFT B3LYP/6-/31G(d) calculations in the gas phase. Graphs for oligomers with $n \geq 4$ are shown (the X axis starts from the point "Kuhn" = 0.3162, which corresponds to $n = \infty$; the largest points on the X axis correspond to the tetramers, $n = 4$ ("Kuhn function" = 0.5214).

Table 4.2 HOMO and LUMO energy levels, and the band gaps (E_g) of 4-substituted polyfluorenes, extrapolated from B3LYP/6-31G(d) calculations of their oligomers **X-OFMe$_2$** by the Kuhn equation (1), and effects of groups X on their energies relative to unsubstituted polyfluorene (X =H).

X	HOMO, eV	LUMO, eV	E_g, eV	ΔHOMO,[b] eV	ΔLUMO,[c] eV	ΔE_g,[d] eV
NMe_2	–4.74	–1.48	3.365	+0.27	+0.13	+0.035
OCH_3	–4.76	–1.45	3.300	+0.25	+0.16	+0.100
NPh_2	–4.92	–1.68	3.225	+0.09	–0.07	+0.175
SMe	–4.95	–1.62	3.315	+0.06	–0.01	+0.085
Me	–4.95	–1.56	3.385	+0.06	+0.05	+0.015
H	**–5.01**	**–1.61**	**3.400**	**0**	**0**	**0**
C≡CPh	–5.05	–1.86	3.180	–0.04	–0.25	+0.220
F	–5.21	–1.81	3.395	–0.20	–0.20	+0.005
CO_2Me	–5.16	–1.94	3.225	–0.15	–0.33	+0.175
COMe	–5.25	–2.13	3.120	–0.24	–0.52	+0.280
CF_3	–5.45	–2.13	3.315	–0.44	–0.52	+0.085
SO_2Me	–5.65	–2.38	3.275	–0.64	–0.77	+0.125
CN	–5.72	–2.44	3.280	–0.71	–0.83	+0.120

[a] E_g values have been calculated by extrapolation of linear dependencies from Figure 4.8g, and not as a difference in HOMO and LUMO from columns 2 and 3 of this table.

[b] ΔHOMO = HOMO(X=H) – HOMO(X). [c] ΔLUMO = LUMO(X=H) – LUMO(X).

[d] $\Delta E_g = E_g(X=H) - E_g(X)$.

4.2.5 Electrochemical studies of 4-substituted polyfluorenes X-PF8 and X-PF6/8

The electrochemical behaviour of **X-PF8** and **X-PF6/8** polymers has been studied by cyclic voltammetry (CV) in films drop-cast from solution onto glassy carbon electrodes. Measurements have been done in acetonitrile with 0.1 M Bu_4NPF_6 as supporting electrolyte at a scan rate of 100 mV/s. The results of CV experiments are shown in Figures 4.19 and 4.20, demonstrating that all polymers are electroactive and undergo oxidation (p-doping) with onsets in the region of +(0.77–1.54) V and reduction (n-doping) with onsets in the region of –(1.89–2.71) V, i.e. with pronounced effect of substituents 4-X- on their redox potentials.

From these CV measurements, we have estimated the HOMO/LUMO energy levels of **X-PF8** and **X-PF6/8** polymers using general formulas (2, 3), where 4.8 eV is an estimation of the potential of Fc/Fc^+ couple versus vacuum.[38]

$$E_{HOMO} = -e(E^{ox}_{onset} + 4.8)\ eV \quad (2)$$

$$E_{LUMO} = -e(E^{red}_{onset} + 4.8)\ eV. \quad (3)$$

Onsets of redox potentials (E^{ox}_{onset} and E^{red}_{onset}), together with frontier orbital energies (HOMO and LUMO) and electrochemical band gaps (E_g^{CV}) are collated in Table 4.3. The results of CV experiments show that HOMO/LUMO energy levels of polyfluorenes can be efficiently tuned by substituents in the position 4 of the fluorene ring. Thus, for the **X-PF8** series of polymers, from the strongest EDG (X = OMe) to the strongest EWG (X = CN, SO_2Me), HOMO and LUMO energy levels can be tuned by 0.38 eV and 0.67 eV, respectively. These tunings of frontier orbital energies are somewhat lower than those obtained from DFT calculations for isolated molecules in the gas phase (tuning both HOMO and LUMO by ~1 eV, Table 4.2), which can be expected as DFT calculations do not take into account solvation and solid state effects. Nevertheless, the strong effect itself and the trends are in good agreement with DFT predictions.

Another important conclusion from CV measurements is that the effect of substituents on the band gap of polymers, E_g^{CV}, is weaker. Unsubstituted polymer **PF8** is among the highest band gap polymers in the series and an introduction of either EDG or EWG in position 4 generally results in some band gap contraction. Taking into account the irreversibility of redox processes (especially for reduction at highly negative potentials below –2 V), accuracies of their onset potential estimations are not high enough to look at good correlations with DFT predictions. Yet, the trend is clear.

Table 4.3 also presents optical band gaps, E_g^{opt}, estimated from the red edge of absorption spectra of the studied polymers (see next section for detailed studies). These values are lower than electrochemical band gaps (E_g^{CV}) estimated from CV experiments. It is not surprising as optical and electrochemical energy gaps belong to different physical processes, and such differences are well documented in the literature. However, similar to E_g^{CV} values, E_g^{opt} are weakly affected by 4-X-substituents.

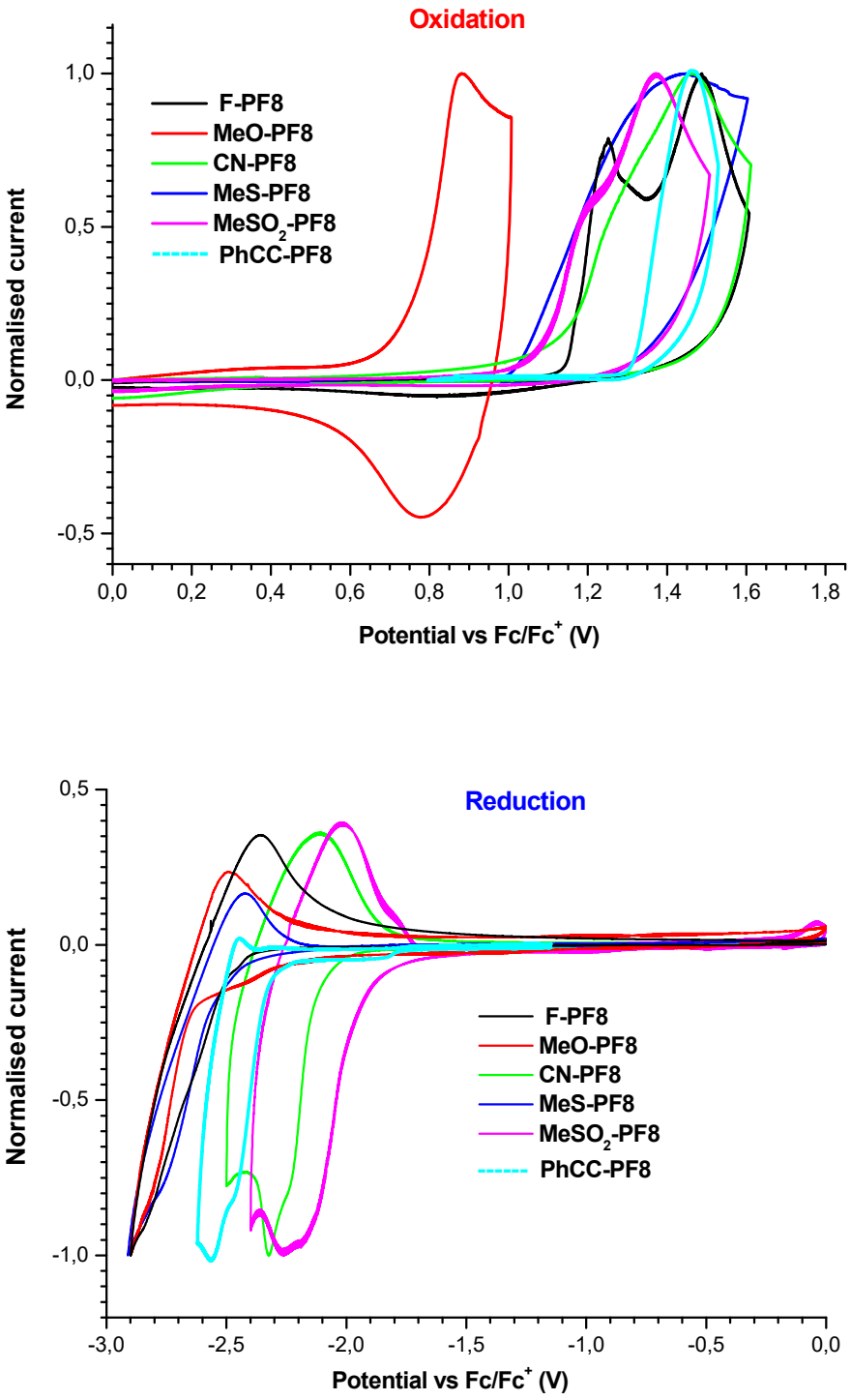

Figure 4.19 Cyclic voltammograms of **X-PF8** polymers films on glassy carbon electrode in 0.1 M of Bu_4NPF_6 / CH_3CN, scan rate 100 mV/s (for convenience, CV data are presented with normalisation to the current maximum of an oxidation / reduction processes. Measured peak currents were in the range of ~20–50 μA).

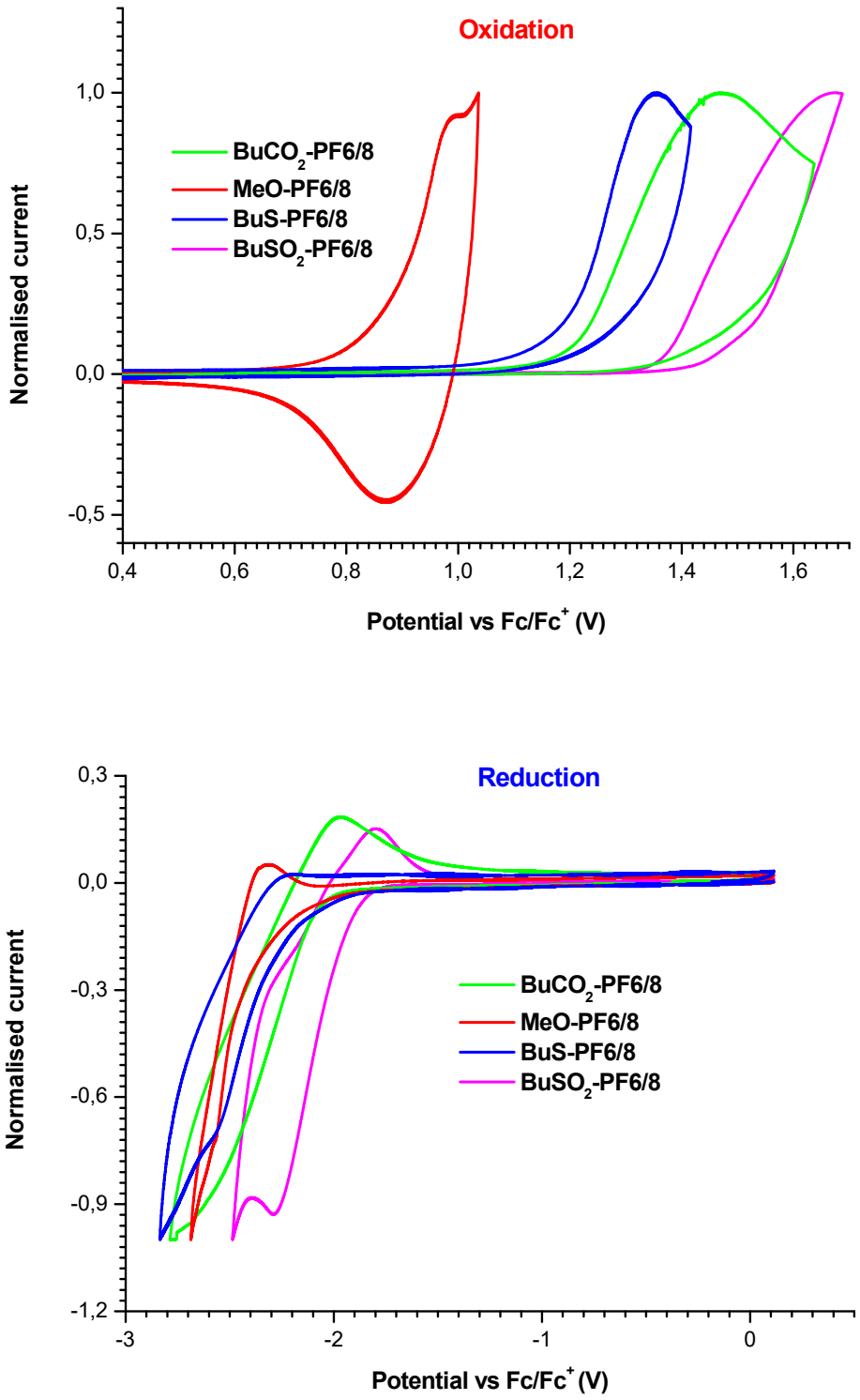

Figure 4.20.Cyclic voltammograms of **X-PF6/8** polymers films on glassy carbon electrode in 0.1 M of Bu_4NPF_6 / CH_3CN, scan rate 100 mV/s (for convenience, CV data are presented with normalisation to the current maximum of an oxidation / reduction processes. Measured peak currents were in the range of ~20–50 μA).

Table 4.3 Cyclic voltammetry data, HOMO/LUMO energy levels and band gaps of **X-PF8** and **X-PF6/8** polymers.

Polymer	E_g^{opt},[a] (eV)[a]	E^{ox}_{onset},[b] (V)	E^{red}_{onset},[b] (V)	HOMO[c] (eV)	LUMO[c] (eV)	E_g^{CV},[d] (eV)
F-PF8	2.86	1.14	–2.46	–5.94	–2.34	3.60
MeO-PF8	2.85	0.76	–2.62	–5.56	–2.18	3.38
CN-PF8	2.72	1.13	–2.12	–5.93	–2.68	3.25
MeS-PF8	2.83	1.02	–2.52	–5.82	–2.28	3.54
$MeSO_2$-PF8	2.75	1.08	–1.95	–5.88	–2.85	3.03
PhCC-PF8	2.64	1.12	–2.42	–5.92	–2.38	3.54
***PF8*[39]**	–	*0.97*[e]	*–2.64*[e]	*–5.77*	*–2.16*	*3.61*
$BuCO_2$-PF6/8	2.78	1.20	–2.06	–6.00	–2.74	3.26
MeO-PF6/8	2.85	0.87	–2.40	–5.67	–2.40	3.27
BuS-PF6/8	2.87	1.19	–2.23	–5.99	–2.57	3.42
$BuSO_2$-PF6/8	2.89	1.36	–1.92	–6.16	–2.88	3.28

[a] E_g^{opt} are optical band gaps estimated from the red edge of UV–Vis specta of polymer films (see next section). [b] E^{ox}_{onset} and E^{red}_{onset} are the onset potentials of oxidation and reduction of polymer films measured versus Fc/Fc^+ couple. [c] HOMO and LUMO energies calculated from empirical formulas (2) and (3): HOMO (eV) = –e(E^{ox}_{onset} + 4.8) and LUMO = –e(E^{red}_{onset} + 4.8). [d] Electrochemical band gap E_g^{CV} = LUMO – HOMO. [e]CV data in ref. 39 are given versus Ag/AgCl electrode; we have recalculated them to Fc/Fc^+ as $E(Fc/Fc^+) = E(Ag/AgCl) – 0.4$ V.

4.2.6 Photophysical studies of 4-substituted polyfluorenes X-PF8 and X-PF6/8

4.2.6.1 Electron absorption and photoluminescence spectra of X-PF8 polymers

The electron absorption spectra of 4-substituted **X-PF8** polymers in toluene solution show absorption with peaks in the region of 385–410 nm, which can be assigned to the π-π* transition of delocalised electrons on the backbone of the polymer (Figure 4.21), a typical region for polyfluorenes. Their λ_{abs} maxima (except X = F) are slightly red-shifted compared to unsubstituted **PF8** (λ_{abs} = 389 nm[40]) with the largest shift of 21 nm observed for **$MeSO_2$-PF8** (λ_{abs} = 410 nm). In the solid state (spin-coated films from toluene solution), some bathochromic shifts (3–12 nm) of absorption maxima are observed (Figure 4.21, Table 4.4).

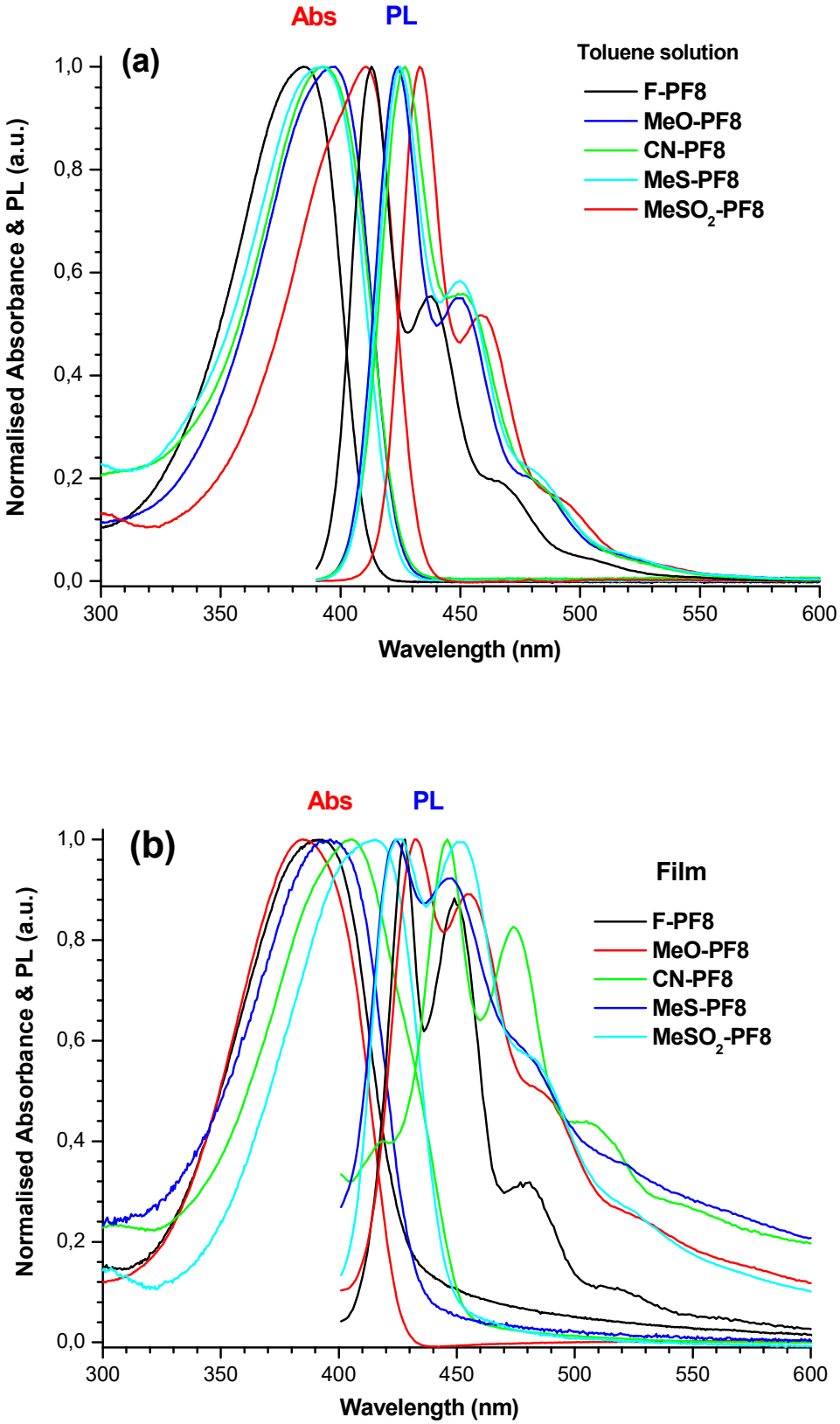

Figure 4.21 UV-Vis absorption and PL spectra of **X-PF8** polymers (a) in toluene solution and (b) in films (spin-coated from toluene solution).

All synthesised **X-PF8** (and **X-PF6/8**) are highly emissive materials emitting blue bright light (both in solution and the solid state) typical for polyfluorenes. For example, Figure 4.22 shows emission from a solution of the **MeSO$_2$-PF8** polymer under UV irradiation. Their photoluminescence spectra have been recorded with an excitation at the maxima of their absorbance. Photoluminescence spectra of **X-PF8** polymers show well-resolved vibronic structure, characteristic for polyfluorenes (as rigid-rod conjugated structures),[40,41,39] with 3 major peaks corresponding to 0-0, 0-1, 0-2 transitions (Figure 4.21). In toluene solution, **F-PF8** polymer shows a small hypsochromic shift compared to the unsubstituted polymer **PF8**, whereas the others demonstrate bathochromic shifts of their PL by 7–16 nm. Similar to **PF8**, the PL maxima of 4-substituted polymers in films are slightly bathochromically shifted compared to solution PL (Figure 4.21a,b and Table 4.4).

Figure 4.22 Blue light emission of **MeSO$_2$-PF8** polymer solution under UV irradiation.

4-Phenylethynyl-substituted polymer **PhCC-PF8** shows somewhat different spectral characteristics. First, its absorption maximum in solution is hypsochromically shifted (compared to other **X-PF8**, including **PF8** itself) to 371 nm, with a more pronounced bathochromic shift of 23 nm when going to the solid state (394 nm) compared to other **X-PF8** polymers (Figure 4.23, Table 4.4) (smaller peaks are also observed at 274/297 nm, which can be attributed to the contribution of the phenylacetylene moiety). Second, its PL spectra (both in solution and in films) don't show separate vibronic transitions, but some shoulders and non-symmetry of PL indicate weakly-resolved vibronics. The reason for that is not fully clear (might be due an effect of PhCC- group on the rigidity of the system or changing the dipole of the transition due to elongated π-substituent) and requires more detailed studies.

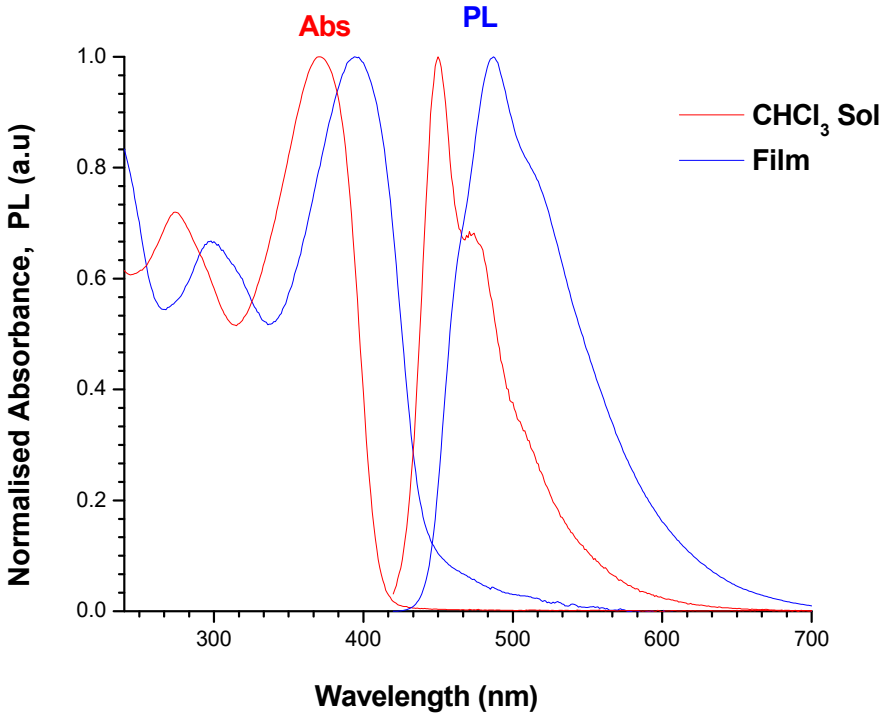

Figure 4.23 UV-Vis absorption and PL spectral data of **PhCC-PF8** in chloroform solution and as a film (spin-coated from chloroform solution).

4.2.6.2 Electron absorption and photoluminescence spectra of X-PF6/8 polymers

Electron absorption spectra of 4-substituted poly(9,9-di(4-octyloxyphenyl)fluorenes) **X-PF6/8** are similar to those of the **X-PF8** series, although with smaller "solid state effects", i.e. the shifts from solution to films are only a few nanometers (–2/+4 nm) (Figure 4.24, Table 4.4). This is understandable, because the more bulky 4-octyloxyphenyl groups at the C-9 atom (compared to octyl groups in **X-PF8**) prevent closer packing of the polymers in the solid state. In toluene solution, their PL spectra are vibronically resolved, similar to the **X-PF8** polymers and lie in the same region**.** So, there are no significant differences between these two series of polymers in solutions. In films, **BuS-PF6/8** and **BuSO$_2$-PF6/8** polymers show the expected PL spectra (some increased peaks at 535 nm are observed for **MeO-PF6/8**). However for **BuO$_2$C-PF6/8** polymer (which showed "nothing unusual" in solution), the PL in films, apart from vibronic peaks in the blue region, strong emission peak is observed in the green region at 509 nm. Considering the method of the synthesis of **X-PF6/8** polymers, for which mono-arylation is impossible (in contrast to monoalkylated impurities in poly(dialkylfluorenes), discussed previously), and taking into account literature reports that **PF6/8** is more stable than **PF8**,[42] this band cannot be attributed to "fluorenone defects". It is more likely that in this case

the charge transfer occurs from the fluorene backbone onto the carbonyl fragment of the butoxycarbonyl group, resulting in simultaneous dual emission from both the locally excited (LE) state and the intramolecular charge transfer state (ICT) resulting in broad emission in the region of 400–600 nm. Similar broadened LE/ICT emission was previously observed in fluorene–dibenzothiophene-*S,S*-dioxide copolymers in both photoluminescence and electroluminescence processes,[43,44] and was shown to be an efficient approach toward the design of white-light emitting polymers for solid state lighting.

4.2.6.3 Photoluminescence quantum yields (PLQY) of X-PF8 and X-PF6/8 polymers

Both series of polymers, **X-PF8** and **X-PF6/8**, show bright blue emission in solution (see Figures 4.21, 4.24). We have estimated their photoluminescence quantum yields (PLQY, Φ_{PL}) in solution using 9,10-diphenylanthracene (DPA) as a reference (Φ_{PL}^{R} = 90% in ethanol[75,76]). In toluene, all polymers demonstrate very high PLQY values of Φ_{PL}^{S} ~63–93%, comparable to the values reported in the literature for other polyfluorenes (Table 4.4). Solid state PLQY has been measured for spin coated films on a quartz substrate (from toluene solution) by an absolute method using an integrating sphere. The values are expectedly lower (as usually for solid state PLQY compared to the solution) but still reasonably high, 12–41% (values of 25–40% are reported in the literature for many other 9,9-disubstituted polyfluorenes).

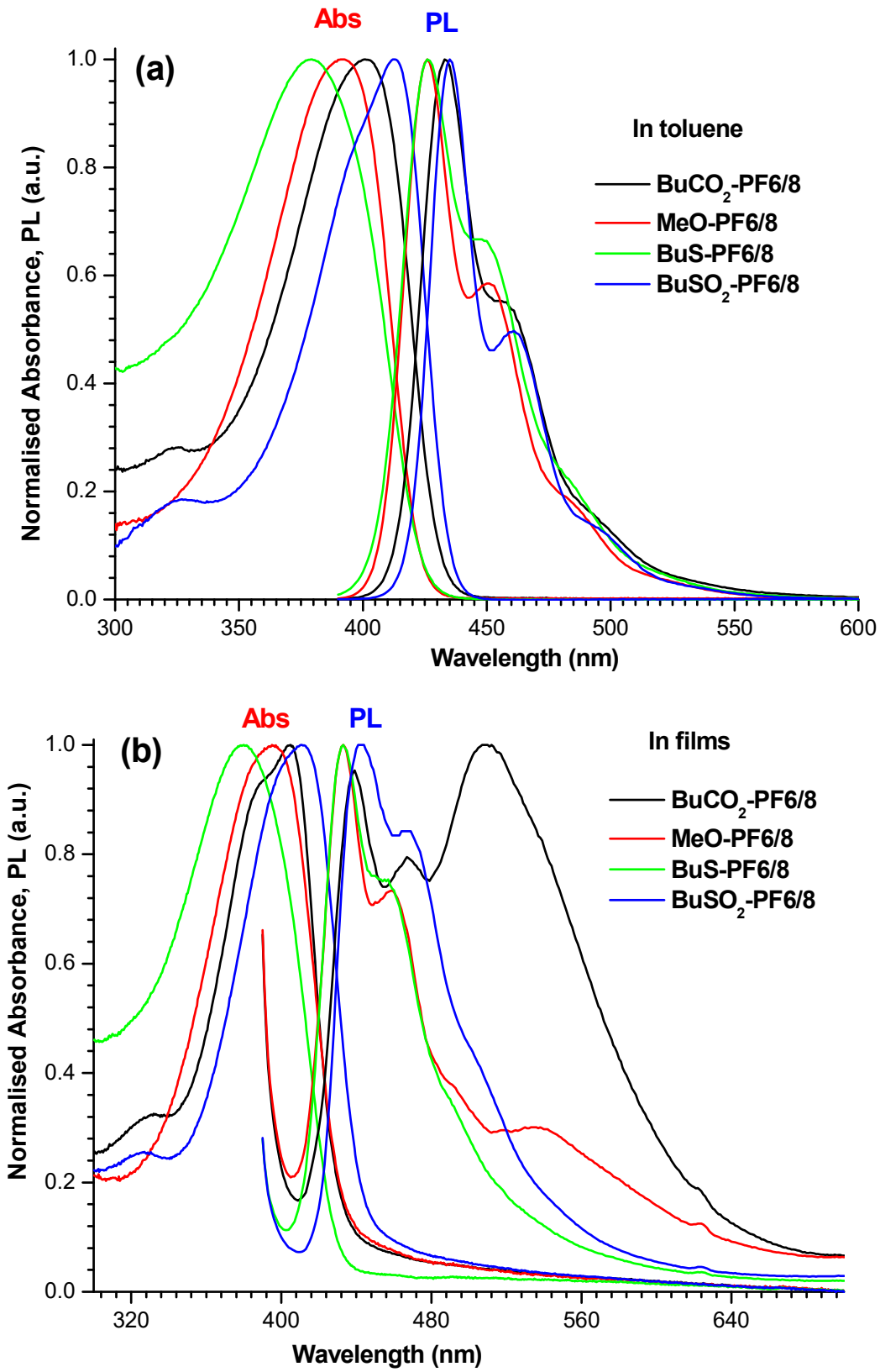

Figure 4.24 UV-Vis absorption and PL spectra of **X-PF6/8** polymers (a) in toluene solution and (b) in films (spin-coated from toluene solution).

Table 4.4 UV-Vis electron absorption and photoluminescence spectral data for **X-PF8**, **X-PF6/8** polymers in solutions and in films.[a]

Polymers	λ_{abs}^{S} toluene (nm)	λ_{abs}^{F} film (nm)	λ_{PL}^{S} toluene (nm)	λ_{PL}^{F} film (nm)	Φ_{PL}^{S} toluene (%)[b]	Φ_{PL}^{F} film (%)[c]	CIE (x,y) coordinates, film
F-PF8	385	391	415, 439, 468sh	428, 447, 480	87	24	0.15, 0.03
MeO-PF8	397	395	424, 450, 481sh	433, 455, 487sh	85	22	0.15, 0.06
CN-PF8	393	403	426, 451, 483sh	445, 473, 505	88	41	0.15, 0.10
MeS-PF8	391	395	425, 449, 480sh	433, 457, 489sh	87	24	0.17, 0.13
$MeSO_2$-PF8	410	415	433, 458, 490sh	445, 471, 502sh	88	31	0.14, 0.09
CCPh-PF8	274, 371[d]	297, 394	442sh, 460[d]	444sh, 471	62	(3)	0.18, 0.22
PF8[40]	389	383 (384[45])	417, 439	425, 447, 520	78	40	
BuO_2C-PF6/8	401	390sh, 404	433, 457, 493sh	438, 467, 508sh	93	20	0.23, 0.39
MeO-PF6/8	391	395	425, 451, 482sh	433, 459, 490sh, 536	80	13	0.20, 0.20
BuS-PF6/8	379	380	426, 449, 484sh	433, 456, 491sh	63	12	0.16, 0.11
$BuSO_2$-PF6/8	413	411	435, 461, 495sh	442, 466, 502sh	73	36	0.14, 0.15
PF6/8[42]		388		422, 446[e]			

[a] Photoluminescence spectra have been recorded with excitations at maxima of absorptions, λ_{abs}^{max}. [b] Φ_{PL}^{S} is PLQY measured in toluene solution using DPA as reference (Φ_{PL}^{R} = 90 %).[46] [c] Φ_{PL}^{F} is an absolute PLQY in film measured using an integrating sphere. [d] In chloroform solution. [e] EL spectra for ITO/PEDOT:PSS/**PF6/8**/Ca/Al device: λ_{EL}^{max} = 426, 453, 483, 517 nm.[47]

4.2.6.4. Effects of thermal annealing on UV-Vis and PL spectra of X-PF8 polymers: formation of keto-defects

In Chapter 2 we have mentioned that poly(9,9-dialkylfluorenes), being bright blue emitting materials can undergo thermal (heating above 140–160 ^{o}C) or photochemical degradation (irradiation with UV light in an air atmosphere) with an appearance and growth of an additional peak in their emission spectra at ca. 535 nm[48] that results in a change of the colour of their emission from pure blue to greenish-blue. The same band appears under device operation when these polymers are used as active layers in OLEDs. This band is now well known in the literature as the *g*-band ("green band"). Initial studies at the end of 1990s/beginning of 2000s attributed this phenomenon to the formation of aggregates or excimers and the band at 535 nm was assigned to excimer emission.[49,50,51,52,53] Later works of List, Scherf et al. have shown that it is due to on-chain defects of the polymer backbone as a result of oxidation of the fluorene moiety at its C-9 carbon atom to fluorenone.[54,55,56,57,58] This phenomenon is more complex than simply the formation of fluorenone molecular defects in the polyfluorene chain, as the 535 nm band appears in the solid state PL spectra, whereas the same polymer in solution still shows usual polyfluorene emission. It was intensively studied by many groups to understand deeply the nature of green emission in polyfluorenes, including intramolecular charge transfer, intermolecular interactions etc.[45,48,59,60,61,62,63,64,65,66] Now this is a commonly accepted concept, and apart from its negative effect toward the use of polyfluorenes as blue emitters in OLEDs, this was exploited to shift the emission of materials to the green/yellow region or to expand the emission over the visible region (through combination of blue PF emission with long wavelength emission from fluorene-fluorenone sites) to achieve white-light emitting OLEDs.[67,68,69,70]

Apriori, we expected that thermal annealing of 4-substituted polyfluorenes **X-PF8** with exposure to an air atmosphere should show spectral changes of their solid state PL similar to that commonly observed for **PF8** (see Chapter 2). The effect might be more or less pronounced, depending on substituent X, but the general behaviour was expected to be similar. So, we have conducted thermal annealing experiments on three 4-substituted polymers, **CN-PF8**, **MeSO$_2$-PF8,** and **MeS-PF8,** at high temperature (180 ^{o}C and 200 ^{o}C) monitoring the change of their absorption and PL spectra (in films) with time intervals. In these experiments, we were trying to use polymer films of similar thicknesses (roughly estimated by absorption intensities) to avoid misinterpretation of the results.

The results of measurements are shown in Figures 4.25–4.27. For all three polymers, thermal annealing in the air only slightly changes their absorption spectra. As seen from Figures 4.26 and 4.28, **MeSO$_2$-PF8** and **MeS-PF8** show a small decrease in absorption

intensities, without shifts of maxima or broadening/narrowing of the spectra. This decrease of intensities, however, can be due to a change of film morphology and/or thickness during heating at the temperatures well above their T_g. For the **CN-PF8** polymer (Figure 4.25), annealing at 180 ^oC for 1 h results in more "structured absorbance" with a bathochromic shift of the blue side of the spectrum and appearance of a shoulder at 430 nm (although λ_{max} = 405 nm remains unchanged). The spectrum remains unchanged after the next 12 h of heating. We assume that this might be attributed to morphological changes in the film, for example, more ordered phase domains formation; potentially, it could be due to β-phase or other phase formation, although no changes in PL were observed in parallel to changes in the absorption spectra as one would expect. So, we think, this behaviour requires more detailed studies (Figure 4.25).

In the PL spectra of **CN-PF8** and **$MeSO_2$-PF8** films, on thermal annealing a new band at 510 nm appear, which is progressively growing with annealing time. Similar growth of the long-wavelength band was observed for the **MeS-PF8** film, but the maximum of the growing peak in this case was at 530 nm, close to that observed on thermal degradation of unsubstituted polymer **PF8**. A shorter wavelength of the growing green band in **CN-PF8** and **$MeSO_2$-PF8** compared to **MeS-PF8** can be due to the electron-withdrawing character of the CN and $MeSO_2$ groups, slightly increasing the ICT energy, and consequently blue-shift in PL wavelength. On the other hand, **MeS-PF8** seems somewhat more stable toward oxidation compared to **CN-PF8** and **$MeSO_2$-PF8** (one can compare, for example, the intensities of the green bands after 10–12 h annealing at 180 ^oC, relative to the blue 0-0 transition for these polymers).

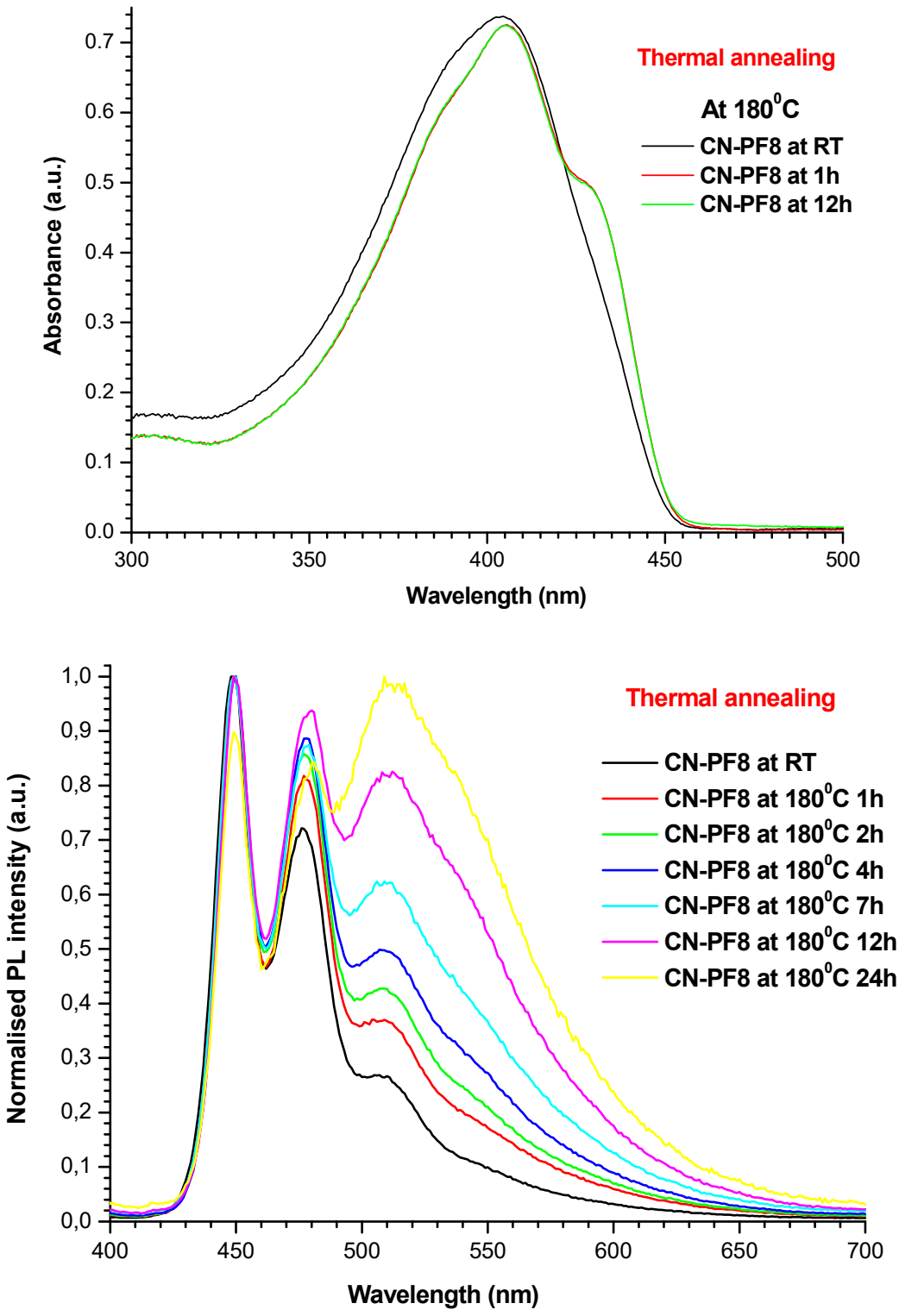

Figure 4.25 Evolution of UV-Vis absorption and photoluminescence spectra of **CN-PF8** films on thermal annealing (PL spectra have been normalised at the shortest wavelength maxima; absorption spectra are not normalised).

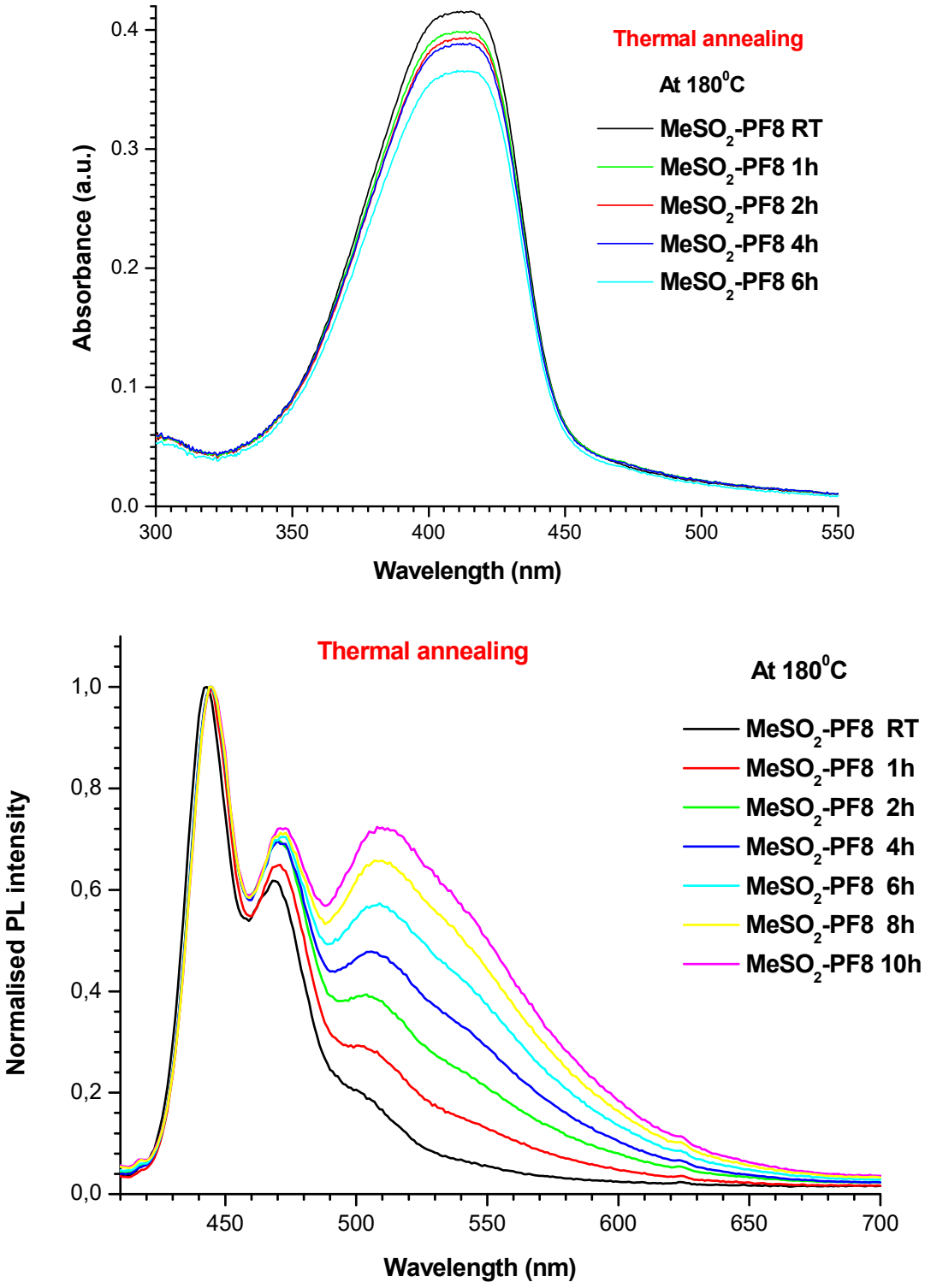

Figure 4.26 Evolution of UV-Vis absorption and photoluminescence spectra of **$MeSO_2$-PF8** films on thermal annealing (PL spectra have been normalised at the shortest wavelength maxima; absorption spectra are not normalised).

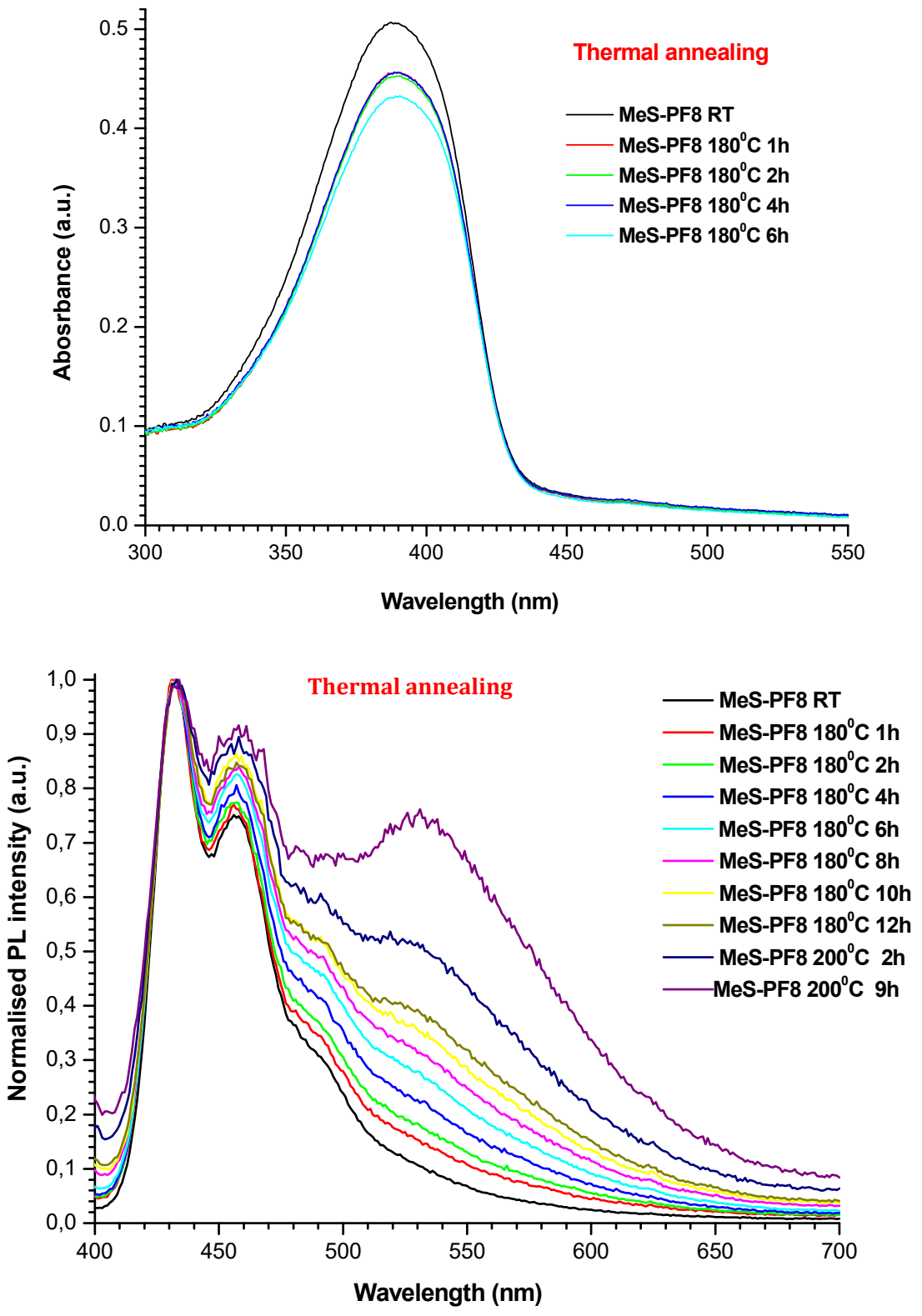

Figure 4.27 Evolution of UV-Vis absorption and photoluminescence spectra of **MeS-PF8** films on thermal annealing (PL spectra have been normalised at the shortest wavelength maxima; absorption spectra are not normalised).

4.2.6.5 β-Phase studies of X-PF8: solvent effects on UV-Vis spectra

Formation of ordered β-phase with the alternating orientation of neighbouring fluorene units is one of the intriguing properties of polyfluorenes and some fluorene-based copolymers. This ordered β-phase often appears as a red-shifted band in the UV-Vis and PL spectra of polyfluorenes (additional peak or shoulder in UV-Vis or shift in PL spectra). It has not only academic interest for a deeper understand of the morphology of polymers, but also of practical importance, it was also shown that lasing or electroluminescent properties of this phase are substantially improved compared to amorphous polyfluorenes.

Many factors affect the ability of polymers to form this phase and its thermodynamic stability, such as (i) structure of polyfluorene (e.g. length and branching of the solubilising groups), (ii) solvent used for films deposition, (iii) films preparation (drop-cast, spin-coating etc), (iv) temperature (annealing around glass transition temperature, quick quenching with liquid nitrogen etc) and others.[71] Poly(9,9-dioctylfluorene), **PF8**, is the most known to easily form stable β-phase, which is easily formed in films deposited from low polar solvents (toluene, chlorobenzene, methylcyclohexane). It was also shown that for **PF8** this phase can exist in solution, in "poor solvents" (e.g. methylcyclohexane or THF). The reason for good stability of β-phase in **PF8** is an appropriate length of side alkyl chains, which are orthogonal to the polymer backbone, and linear C_8H_{17}-groups facilitate good interdigitating of side chains thus connecting together neighbouring polymer molecules. Shorter or branched chains and copolymers with other conjugated units make β-phase less stable or not formed at all.

Therefore, in this and the next two sections, we consider the ability of the new family of 4-substituted polyfluorenes **X-P8** to form this ordered β-phase. We tried different approaches to generate and observe this phase (solvent effects, thickness of the films and thermal annealing, with UV-Vis and PL monitoring of β-phase formation). For that, we used analogies with some different literature procedures.[72,73,74]

Our first attempt was to study the changes in UV-Vis absorption spectra in all **X-PF8** polymer films (**F-PF8**, **CN-PF8**, **MeO-PF8, MeS-PF8**, and **$MeSO_2$-PF8**) deposited by drop-cast (DC) and spin-coating techniques (SC) from their solutions in different solvents. Generally, the probability of β-phase formation by the drop-cast method is higher, as the polymer chains have more time for re-ordering and self-organisation before the solvent is evaporated. The solvent also has an effect on the process of β-phase formation and in "poor solvents" (very non-polar solvents like cyclohexane or too polar, e.g. THF, where the solubility of the polymer is lower with a greater probability of polymer chain aggregation) is higher.

The results of these studies are shown in Figure 4.28. Among all the studied polymers, **CN-PF8** has shown the clear formation of the β-phase, which appeared as a shoulder at ca. 437 nm. For films deposited from a chloroform solution, this phase was observed for deposition by DC, but not by SC method, whereas for the "poor solvent" THF it was clearly observed for both deposition methods. It seemed that **F-PF8** polymer also formed the β-phase, although less stable, which appeared as a red-shifted absorbtion band for DC deposition from THF. It also seemed that some signature on the possible formation of the β-phase was observed for other polymers, but the results were not very conclusive, because the absorption bands changed their width for films deposited under different conditions (Figure 4.28, **MeO-PF8** and **MeS-PF8** polymers) or a red-shift was also observed for the blue tail of their absorption bands (Figure 4.28, **$MeSO_2$-PF8** polymer). So, these changes could be due to film qualities (different scattering of the films deposited by DC or SC methods from different solvent). Therefore, we decided to perform more extended experiments using simultaneously UV-Vis absorption and PL emission monitoring the possible β-phase formation.

4.2.6.6 β-Phase studies of X-PF8 polymers: solvent effects on UV-Vis and PL spectra. Extended experiments

In simultaneous studies of **X-PF8** film morphologies by UV-Vis and PL spectroscopy, we used a wider range of studied solvents and DC and SC method of depositions. Also, for spin-coating, we used films of different thicknesses (thick films, labelled as SC-L on Figures 4.29 and 4.30, and 10–20 times thinner films, labelled as SC-L, estimated by absorbance of the films) (Figures 4.29–4.31).

These studies clearly showed β-phase formation in the **CN-PF8** polymer (Figure 4.30). While changes for the films deposited from chloroform were rather small, there were substantial changes in the PL spectra for the films deposited by different methods (many studies in the literature on β-phase indicate that PL is a more sensitive method than UV-Vis absorption in this case). It is even more evident for the films deposited from THF, where both UV-Vis and PL undergo substantial changes. It should be mentioned that films prepared here show somewhat different features compared to that shown in Figure 4.28 (more pronounced bathochromic shift with more structured absorption bands), but such results are sometimes observed as temperature, humidity etc may also effect on the probability of formation of ordered phase in the films.

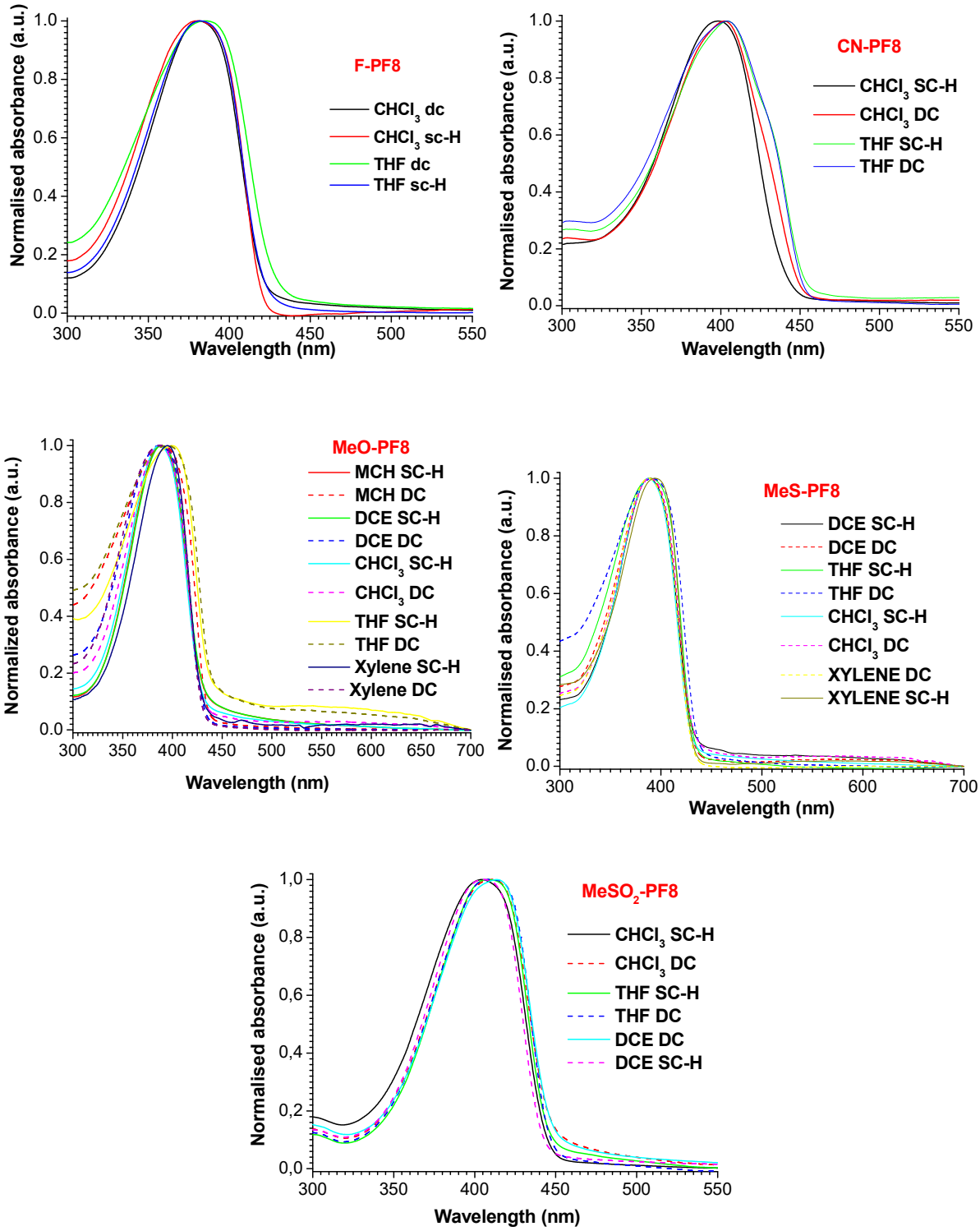

Figure 4.28 UV absorption spectra of **X-PF8** polymer films (X = F, CN, OMe, SMe, SO_2Me) deposited from various solvents by spin-coating (SC) and drop-casting (DC) techniques. The film thicknesses were prepared to have optical densities around 0.5–1.0 a.u. (all spectra are normalised to their maxima).

For the **F-PF8** polymer (Figure 4.29), changes in absorption spectra were substantially smaller (similar to what we observed in previous experiments, Figure 4.28). However, their PL spectra underwent substantial changes as well, not only in changes of relative intensities of the PL vibronic bands, but also in their shift toward lower energies. The effect was less pronounced compared to **CN-PF8**, but still evident for the formation of the β-phase in this polymer.

Three other polymers, **MeO-PF8**, **MeS-PF8** and **MeSO$_2$-PF8**, did not show β-phase formation in our experiments (Figure 4.31), in spite of studying a wider number of solvents to find evidence for it. Similar to previous experiments, shown in Figure 4.29, we saw some minor changes in their UV-Vis absorption spectra, but no clear shoulder at the red tail or an additional low energy peak was observed. So, these minor changes in absorption could be attributed to solvatochromism, i.e. to small energetic changes by solvations. Really, the PL spectra of all these polymers do not show changes in their emission maxima and PL spectra normalised to the first vibronic 0-0 transition (shortest peak) nicely coincide, with only minor changes in intensities of other vibronics (0-1, 0-2, …), but no red shifts in PL spectra were observed. As such, we conclude that these polymers did not form β-phase in our experiments. It should be also mentioned, that for some polyfluorenes, the formation of the β-phase does not lead to substantial red shifts in PL spectra. This depends on its stability and on the concentration of domains of this ordered phase in the bulky material. Nevertheless, the formation of this phase leads to changes in relative intensities of 0-0 and 0-1 vibronics and the intensity of 0-1 transition is increased with an increase of the concentration of the β-phase dominating the 0-0 transition. However, as one can see from Figure 4.30, in all the cases (for all polymers, **MeO-PF8**, **MeS-PF8** and **MeSO$_2$-PF8**, all solvents and all deposition methods), the PL intensities of the first 0-0 vibronics are higher than the 0-1 transitions.

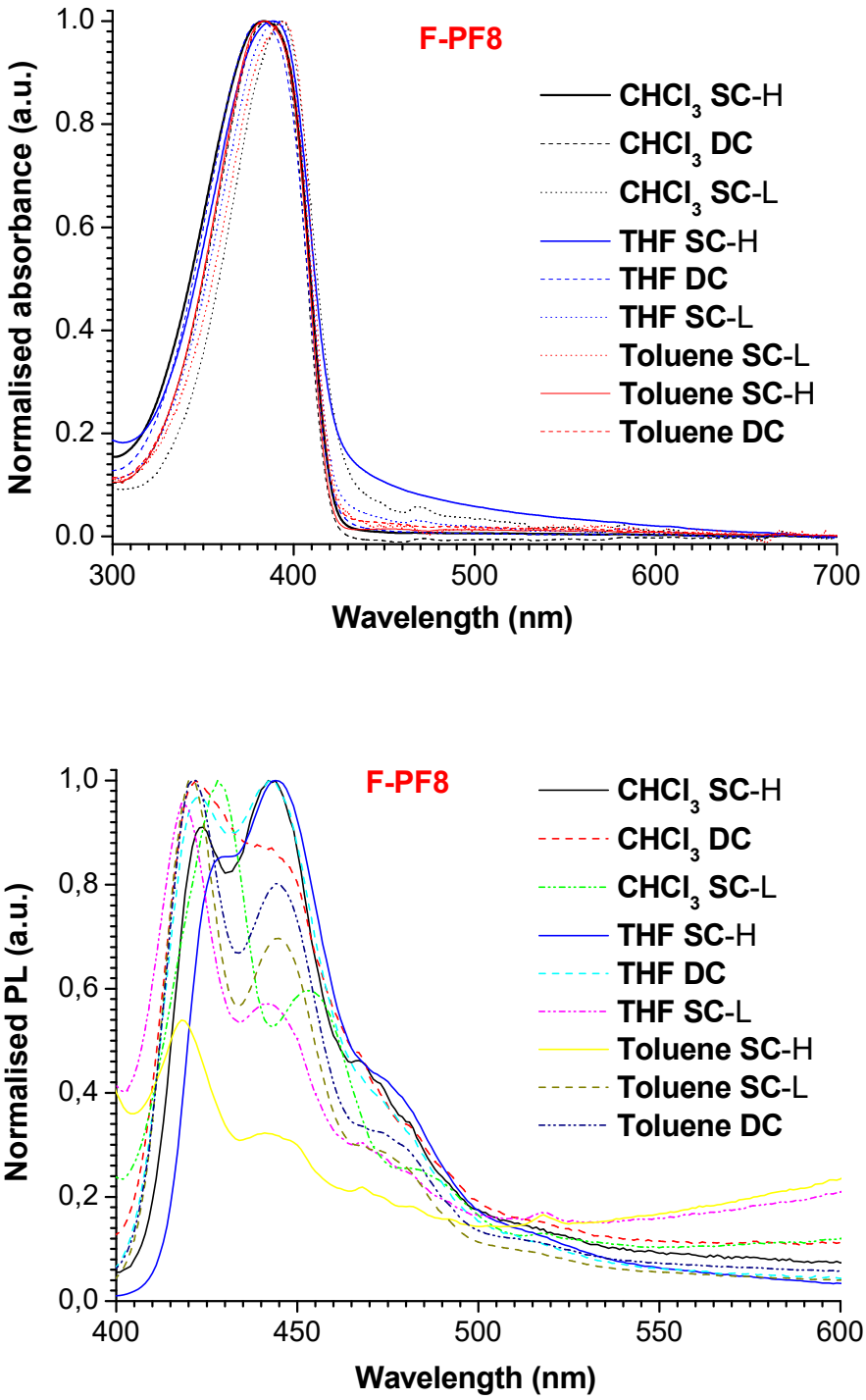

Figure 4.29 UV-Vis absorption (top) and PL spectra (bottom) of **F-PF8** polymer films prepared from different solvents by drop-cast (DC) and spin-coating methods (SC-H: thick films, OD = 0.5–1 a.u.; SC-L: thin films, OD = 0.02–0.1 a.u.). (SC-H film from toluene became too scattered giving unreliable PL spectrum).

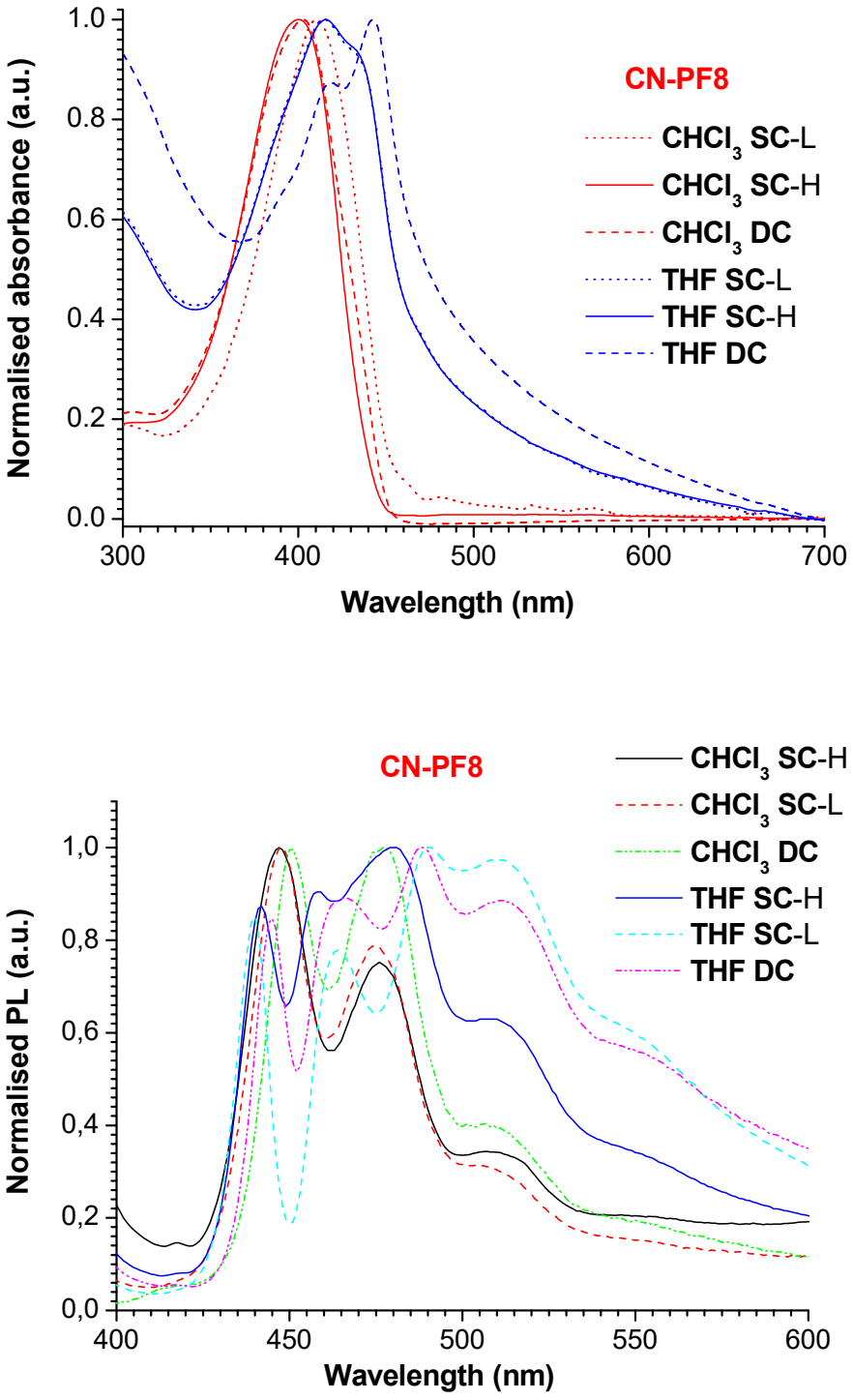

Figure 4.30 UV-Vis absorption (top) and PL spectra (bottom) of **CN-PF8** polymer films prepared from different solvents by drop-cast (DC) and spin-coating methods (SC-H: thick films, OD = 0.5–1 a.u.; SC-L: thin films, OD = 0.02–0.1 a.u.).

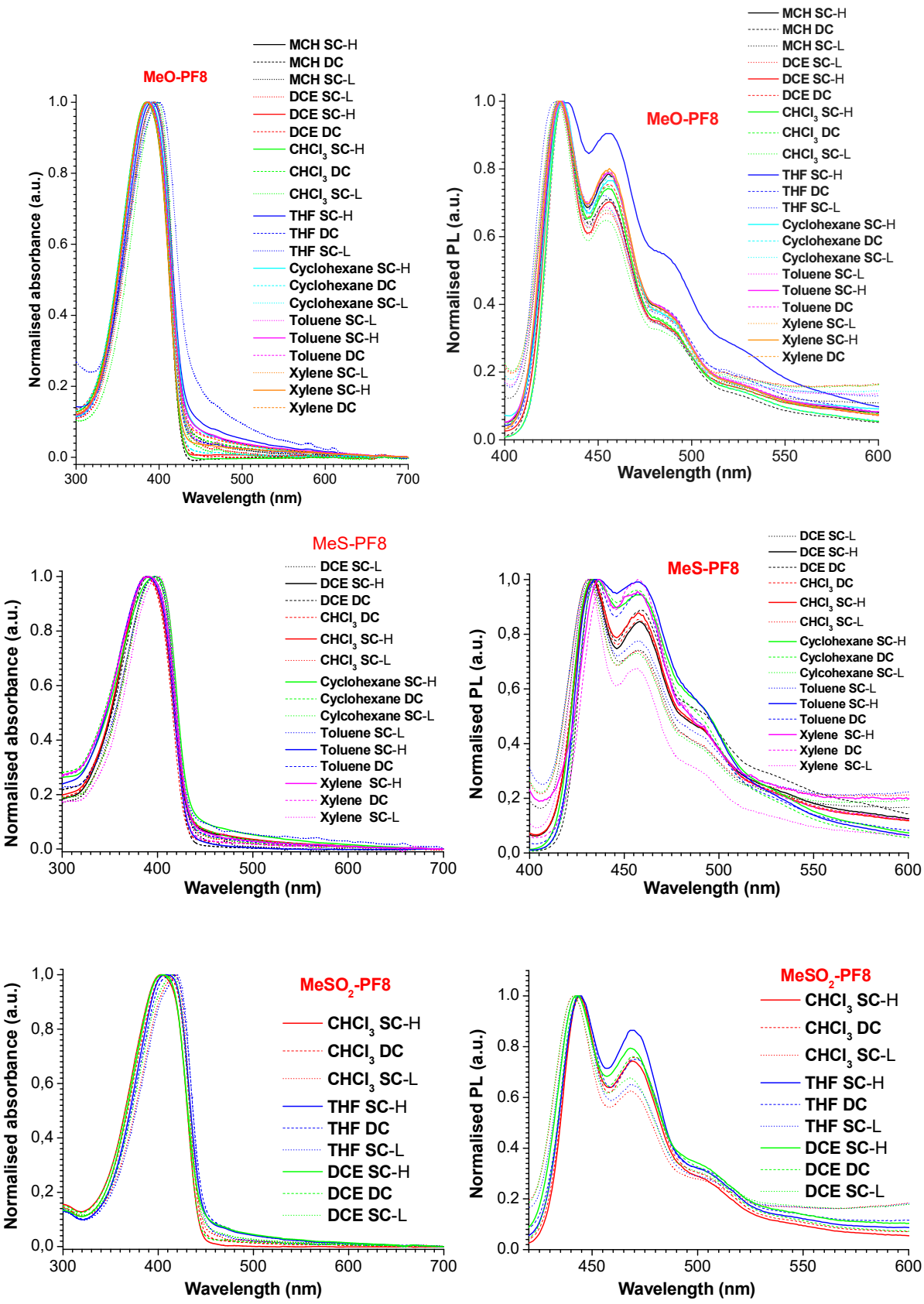

Figure 4.31 UV-Vis absorption (left) and PL spectra (right) of **MeO-PF8, MeS-PF8** and **$MeSO_2$-PF8** polymer films prepared from different solvents by drop-cast (DC) and spin-coating methods (SC-H: thick films, OD = 0.5–1 a.u.; SC-L: thin films, OD = 0.02–0.1 a.u.).

4.2.6.7 β-Phase studies of F-PF8 polymer: effect of thermal annealing on UV-Vis and PL spectra

As changes in UV-Vis spectra of **F-PF8** polymer were quite small to be evident for β-phase formation (Figure 4.28), but its PL spectra showed clear changes, i.e. bathochromic shifts in PL and an increase of intensity of the 0-1 transition compared to the 0-0 vibronic peak (Figure 4.29), we have performed additional experiments on the thermal annealing of **F-PF8**. Thermal annealing experiments have been performed at 60–100 ^{o}C, i.e. at temperatures well below the temperature of thermal degradation of **F-PF8** and thus spectral changes cannot be attributed to the formation of keto-defects in the polymer chains in this case.

Figure 4.32 shows the changes of UV-Vis and PL spectra of **F-PF8** films deposited by the spin-coating method (thick films, SC-H) from chloroform solution. Even for this "good solvent" (i.e. high solubility of polymer in chloroform, so less probability for self-organisation to form β-phase), annealing of the films at 100 ^{o}C (i.e. at the temperatures above the glass transition of this polymer T_g = 86 ^{o}C, Table 4.1) for 30–120 min resulted in a slight bathochromic shift of the absorption band and more clear bathochromic shifts in PL, with an increase of the second 0-1 vibronics relatively to the 0-0 vibronics.

In less polar toluene, the picture becomes even more evident already after annealing at 60 ^{o}C for 30 min, the maximum of absorbance is bathochromically shifted from 386 nm to 392 nm and a new clear shoulder is formed on the red tail of the absorption spectra at 437 nm. Simultaneously, its PL spectrum is strongly shifted to the red by 14 nm, from 422 nm to 436 nm (first 0-0 vibronic band, Figure 4.33). Further annealing at 100 ^{o}C for 30 min and 2 h result in additional small red shifts to 437 and 438 nm. For the second, 0-1 vibronic transitions, these shifts are 445 nm → 459 nm → 460 nm → 461.5 nm. Moreover, the intensity of the 0-1 transition is increased relative to the 0-0 peak. These results give clear evidence of the formation of the β-phase in **F-PF8** films, especially pronounced for deposition from toluene solution.

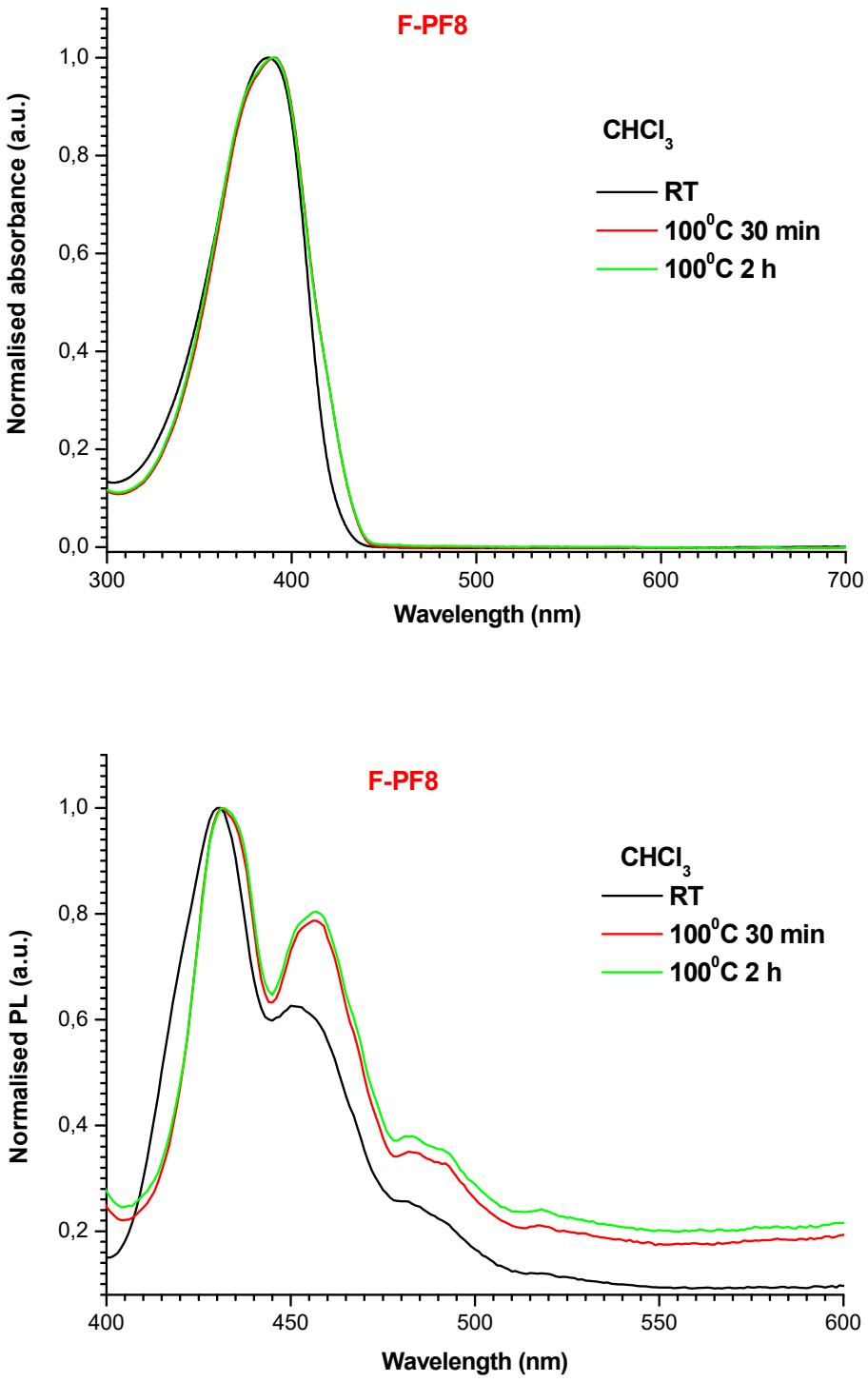

Figure 4.32 UV-Vis absorption and PL emission spectra of **F-PF8** polymer films spin-coated from chloroform solution (OD ~0.5–1.0 a.u.) on thermal annealing around the glass transition temperature.

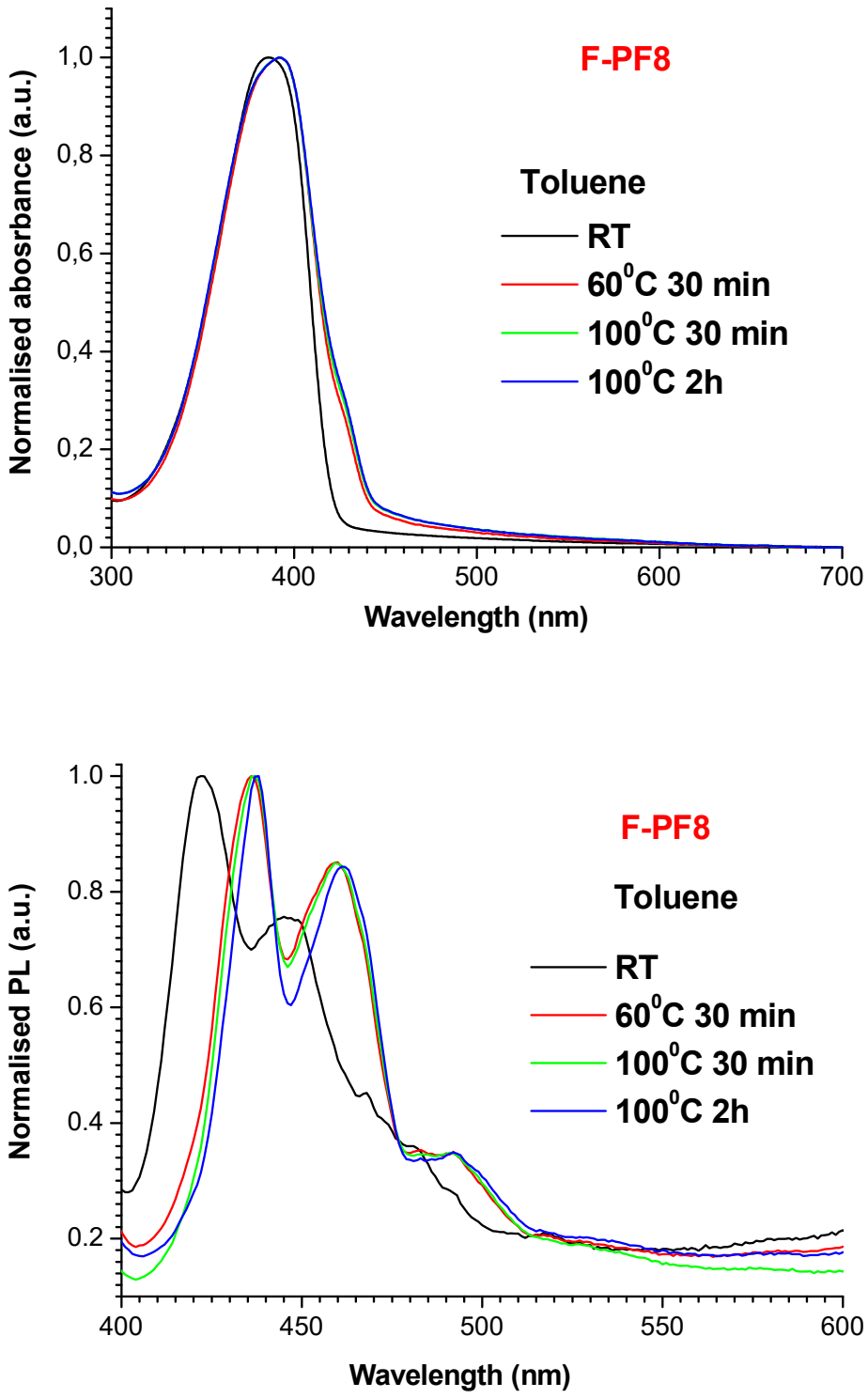

Figure 4.33 UV-Vis absorption and PL emission spectra of **F-PF8** polymer films spin-coated from toluene solution (OD ~ 0.5–1.0 a.u.) on thermal annealing around the glass transition temperature.

4.3 Conclusion

Two novel families of 4-substituted polyfluorenes, **X-PF8** and **X-PF6/8**, functionalised with various electron-donating and electron-withdrawing groups have been synthesised by Ni-mediated Yamamoto polymerisation of the corresponding 2,7-dibromofluorene monomers (here "8" and "6/8" denote 9,9-di(n-octyl)- and 9,9-di(4-octylloxyphenyl)- solubilising groups). For the **X-PF8** series, 4-substituents were X = -OMe, SMe, -C≡CPh, -F, -CN and -SO_2Me and for **X-PF6/8** polymers X = -OMe, -SBu, -CO_2Bu and -SO_2Bu.

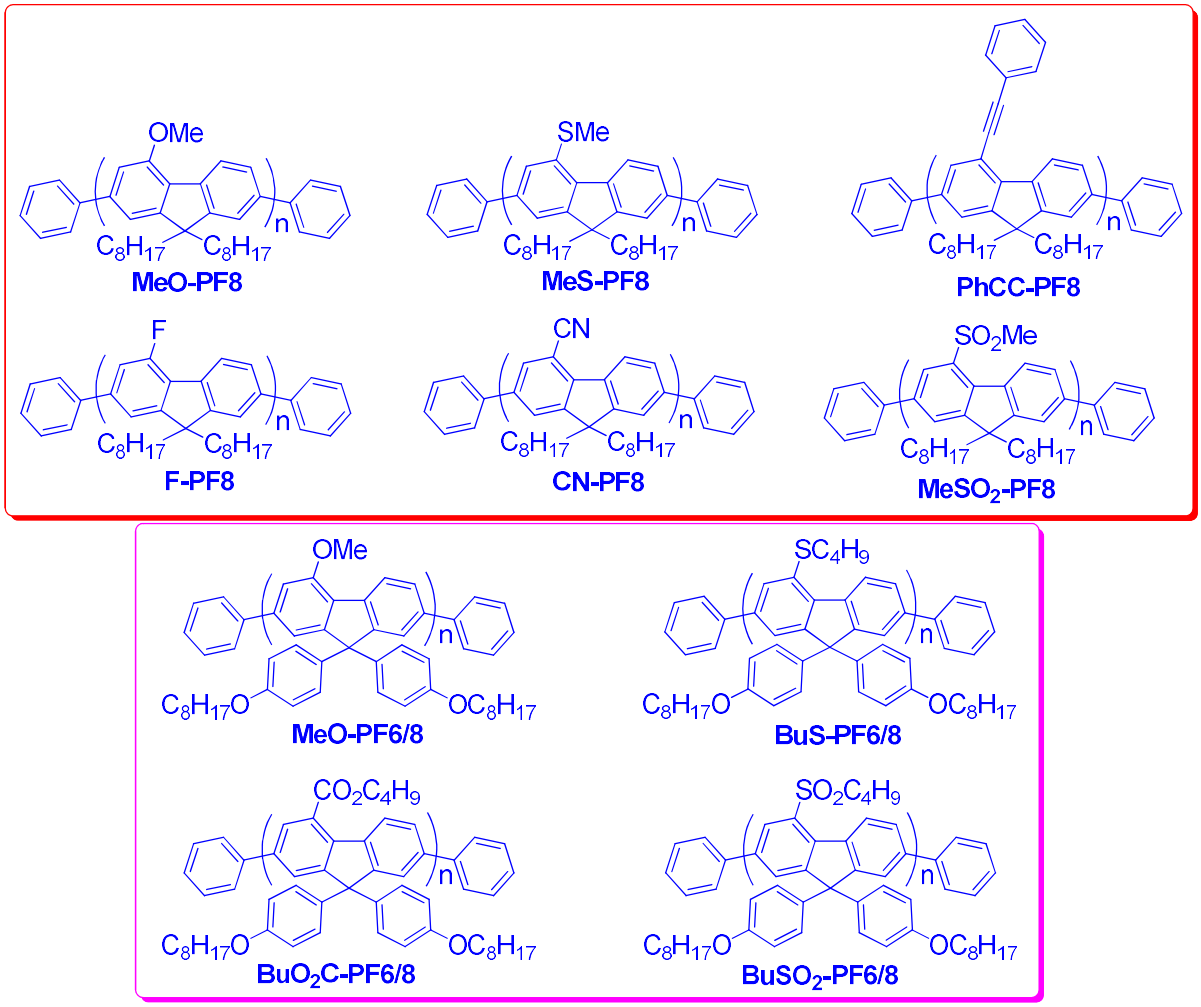

The polymers have been obtained with high molecular weights (M_w = 24,700–185,000 Da, M_n = 9,700–78,700 Da) and showed excellent thermal stabilities (T_d = 398–413 °C). Cyclic voltammetry studies of polymer films showed that they can be electrochemically oxidised and reduced (p-doped and n-doped) and from their redox potential onsets, the HOMO and LUMO energies of these polymers have been estimated (HOMO = –6.16 to –5.56 eV; LUMO = –2.88 to –2.18 eV). Analysis of these data clear shows the strong effect of the 4-substituents on the energy levels of the synthesised polymers: an introduction of the EDG

results in increasing and an introduction of the EWG results in decreasing of both HOMO and LUMO, respectively.

DFT calculations at the B3LYP/6-31G(d) level of theory have been performed for model 4-substituted oligofluorenes (from 1 to 20 repeating fluorene units) and the data have been extrapolated to the polymer limit. The HOMO and LUMO energy levels derived for 4-substituted polyfluorenes, fit well with CV data showing a pronounced effect of the substitution at position 4 on the frontier orbital energies of polyfluorenes.

UV-Vis electron absorption and photoluminescence spectral data have been obtained for **X-PF8** and **X-PF6/8** polymers in both solution and the solid state. All these polymers are characterised by structureless absorption bands in the region of λ_{abs} = 379–411 nm, and bathochromically shifted emissions at λ_{PL} = 415–435 nm (for 0-0 transition) with finely resolved vibronic structure of the photoluminescence spectra.. There is an obvious effect of the substituents on the wavelengths of both absorption and photoluminescence spectra. However, as the substituents simultaneously change the HOMO and LUMO energies in the same direction (as follows from CV and DFT data), the band gaps of polymers are changed only slightly. So all the polymers emit in the blue region (some band gap contraction and bathochromic shift in emission are observed for all but the fluoro-substituted polymer). The emission from the polymers is very bright and the photoluminescence quantum yields estimated for solutions and for the solid state are Φ_{PL}^{S} = 63–93% and Φ_{PL}^{F} = 12–41%, respectively.

Thermal annealing studies of **X-PF8** polymer films have been performed at high temperature (180–200 ^{o}C) on an air to investigate their stability toward oxidation. The polymers show some degradation at or above 180 ^{o}C to form keto-defects (fluorenone fragments) in their backbone that results in an appearance of a broad structureless band in the green region (peaking at 510–530 nm for different polymers). The stability of the studied **X-PF8** polymers toward oxidation is similar to that reported in the literature for the unsubstituted **PF8** polymer. Among the studied polymers, **MeS-PF8, CN-PF8,** and **$MeSO_2$-PF8,** showed the best stability, perhaps due to the lower acidity of its C-9 atom.

Formation of the ordered β-phase in **X-PF8** polymers have been studied for films of different thicknesses, deposited from different solvents and by different coating techniques (drop-casting or spin-coating methods). These studies have shown that the **CN-PF8** polymer easily forms the β-phase, as evidenced by UV-Vis absorption and PL emission spectral changes. The β-phase has been also registered for the **F-PF8** polymer, but it is less stable and is formed when the films are deposited from "poor solvents" or after thermal annealing near the glass transition temperature of the polymer.

Finally, a new class of functionalised blue-emitting polyfluorenes have been developed, in which the substituents at position 4 of the fluorene ring directly affect the frontier energy levels of polymers. These have been exemplified by two new families of **X-PF8** (6 polymers) and **X-PF6/8** (4 polymers) with different solubilizing groups. The polymers represent a new step forward in light-emitting polymers and offer many exciting prospects for further functionalisation in fluorene homo- and copolymers for electroluminescent and other organic electronic applications.

4.4 Experimental Section

4.4.1 Chemicals

The chemicals and solvents were received from Aldrich, Alfa Aesar and Fisher, and used without further purifications. Dry solvents for water-sensitive reactions or measurements either were commercial dry solvents or have been dried in a still (reflux over Na for THF and toluene).

4.4.2 Instrumentation and measurements

Details on ^{1}H NMR measurements are the same as mentioned in Chapter 3.

4.4.2.1 GPC measurements

The polymers weight average molecular weights (M_w), number average molecular weights (M_n) and polydispersity indices (PDI) were measured on Varian PL-GPC 50 plus gel permeation chromatograph (GPC) at room temperature in THF solution with calibration of the column by polystyrene standards. In a typical procedure, the polymer sample in THF (2 mg/mL) was stirred for 30–45 minutes using the rotamixer until full dissolution, filtered through 0.2 μm membrane filter and used for GPC analysis.

4.4.2.2 TGA and DSC measurements

The thermal stabilities of polymers (5–7 mg samples) were measured by thermogravimetry analysis (TGA) on TA-SDT-Q600 instrument in a nitrogen atmosphere with a heating rate of 10 ^{o}C/min. The decomposition temperatures (T_d) of the samples were estimated at the level of 5% mass loss. The glass transition temperatures (T_g) of polymers (4–5 mg) were measured by differential scanning calorimetry (DSC) on TA-Q 20 instrument. The experiments were done in a nitrogen atmosphere, with a heating rate of 10 ^{o}C/min.

4.4.2.3 UV-Vis absorption and photoluminescence spectra measurements

General. Electron absorption spectra were recorded on Shimadzu UV-3600 spectrophotometer. For the solution measurements, quartz cells of 10 mm path length were used. For the solid state measurements, thin films of polymers have been deposited on d = 12.5 mm quartz ring windows by spin-coating method and measurements were done in the transmission mode. Generally, the absorbances of the samples for the UV-Vis measurements were kept at around 0.5–1.0 a.u. (~0.2–1.5 a.u in some cases).

Photoluminescence spectra were recorded on Horiba Jobin Yvon Fluromax-4 spectrofluorimeter. The solution measurements were performed in fluorescence quartz cells of 10 mm path length. The solid state measurements were performed for spin-coated films (or, when necessary, for drop-casted films, as mentioned in the experiments' descriptions) on d = 12.5 mm quartz ring windows. For the PL measurements in both solution and the solid state, the concentration (for solutions) or the thickness of the films was kept to be such to give an absorbance of the sample in the range of ~0.02–0.10 a.u.

Spin-coating of polymer films for UV-Vis and PL studies. Programmed spin coater Laurell Technologies model WS-650Mz-23NPP/LITE was used for polymer thin films preparation (on an air). Thin polymer films were prepared by spin-coating from toluene or chloroform solutions. The concentrations of ca. 1.0 mg/mL were for the absorbtion spectra measurements to have optical densities of the samples of ~0.5–1.0 a.u.. More diluted concentrations of ca. 0.1–0.2 mg/mL were used for the preparation of the films used for PL measurements (to give absorbances of ~0.02–0.1 a.u.). Thin films were prepared from these solutions by dropping their solutions on d = 12.5 or 25 mm quartz ring windows placed on the spin-coater and rotating at 4000 rpm for 30 seconds. After that, the polymer films were dried *in vacuo* (~20–50 μbar) for 0.5–2 h before the measurements.

Thermal annealing (thermal stability) experiments. For the thermal annealing measurements, a quartz ring windows (d = 12.5 mm) were used, on which the polymer films were deposited from a solution by spin-casting method. The polymers in chloroform solution (2 mg/mL) were dropped on a quartz window placed in the Laurell spin-coater and spun at 4000 rpm for 30 seconds. The spin-casted films were then dried in a freeze dyer (~20–50 μbar) for 30 minutes. For studies of their thermal stabilities, the films were placed in a preheated oven at 180 °C for a fixed time, then taken out from an oven and their UV-Vis and PL spectra were recorded. The experiments were repeated with a time intervals measuring the spectra of the samples

after 1 h, 2 h, 4 h, … 24 h. For some polymers, the experiments were also performed at 180 °C. The thickness of the films for the thermal stability experiments was kept to have the optical densities of ~0.4–0.7 a.u.

UV-Vis and PL studies on β-phase of X-PF8 polymers. The possibility of formation of ordered β-phase for the synthesised polymers **X-PF8** in films was studied for their deposition from different solvents by drop-cast and spin-coat methods. For spin-coating methods, two sets of films of different thicknesses have been prepared and studied. Abbreviations "DC" (drop-casting), "SC-H" (spin-coating, high absorbance – thick films), and "SC-L" (spin-coating, low absorbance – thin films) are used in corresponding graphs in the Results and Discussion section. The concentration of polymers used for the film preparation was ~ 0.5–1 mg/mL for DC films (OD ~ 0.5–1 a.u.), ~ 5 mg/mL for SC-H films (OD ~ 0.5–1.0 a.u.) and ~ 0.5 mg/mL for SC-L films (OD ~ 0.02–0.1 a.u.). The films were deposited fom the following solvents: cyclohexane, methylcyclohexane (MCH), dichloroethane (DCE), chloroform, toluene, xylene and tetrahydrofuran (THF). The solutions of the polymers in corresponding solvents were spin-coated on d = 12.5 mm quartz ring windows at a spin rate of 4000 rpm for 30 seconds and then dried for ~5 minutes *in vacuo*. In the case of drop-cast deposition, the films were left at ambient temperature for ~10 minutes and then dried *in vacuo* (~20–50 μbar) for ~30 minutes.

4.4.2.4 Photoluminescence quantum yields (PLQY) measurements

The photoluminescence quantum yields, PLQY, of the polymers ($\Phi_{PL(p)}$) in solutions were estimated using 9,10-diphenylanthracene (DPA) as a reference emitter (PLQY, Φ_R = 90%[75,76]). The reference sample solutions of the DPA were prepared in ethanol in concentrations between OD = 0.10–0.02 a.u. and carefully degassed (*Important:* bubbling nitrogen in DPA solution for 30 minutes). The quantum yields of **X-PF8** and **X-PF6/8** polymers ($\Phi_{PL(p)}$) were calculated by the following equation:

$$\Phi_{PL(p)} = \Phi_R \times (I_p/I_R) \times (OD_p/OD_R) \times (n_p/n_R)^2. \quad (4)$$

where $\Phi_{PL(p)}$ is the quantum yield of the polymer, Φ_R quantum yield of the reference (standard), I_p, I_R are integrated emission intensities, OD_p, OD_R are optical densities and n_p, n_R are refractive indices of the polymer sample and the reference.

Measurements of absolute PLQY values in the solid state were done using an integrating sphere Horiba F-3018 on Horiba Jobin Yvon Fluromax-4 spectrofluorimeter. The

film thickness for these measurements was varied to have OD = 0.02–0.10 a.u. Normally, 3–5 measurements were done for the different film thickness in the above OD range and the obtained PLQY values were averaged (unless obvious deviation of one measurement from the others was observed, in which case additional measurements were performed).

4.4.2.5 Cyclic voltammetry measurements

Cyclic voltammetry experiments have been done for the polymer films on Metrohm Autolab PGSTAT-302N potentiostat/galvanostat. The measurements have been done on a three-electrode scheme (Figure 4.33) in spectroscopic grade acetonitrile (dry acetonitrile for CV reduction measurements) with 0.1 M Bu_4NPF_6 as supporting electrolyte. Ag/Ag^+ (0.01 M $AgNO_3$ with 0.1 M Bu_4NPF_6 in dry acetonitrile) was used as the reference electrode. The thin polymer films were prepared by drop-casting of the chloroform solutions (~5mg/mL) on glassy carbon working electrode (d = 2 mm). The films were first dried in an air for 5–10 minutes and then under vacuum (~10^{-2} mbar) for 1 h before CV measurements. Cyclic voltammetry measurements have been done at ambient temperature under argon atmosphere with a scan rate 100mV/s, from which oxidation and reduction potentials of the polymers have been estimated. The potentials measured versus Ag/Ag^+ were then calibrated against ferrocene/ferrocenium redox couple (Fc/Fc^+) as an internal standard, and recalculated to Fc/Fc^+ scale.

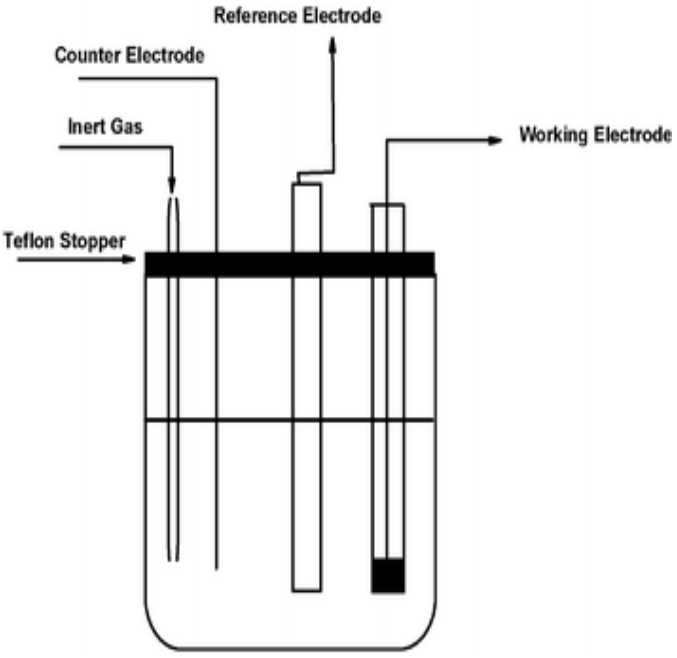

Figure 4.34 Cyclic voltammetry cell representation.

4.4.3 Computational procedures.

DFT computations of the geometries of studied oligofluorenes were carried out with the Gaussian 09[77] package of programs using Pople's 6-31G split valence basis set supplemented by d-polarization functions and diffusion functions for the heavy atoms. Becke's three-parameter hybrid exchange functional[78,79] with the Lee–Yang–Parr gradient-corrected correlation functional (B3LYP)[80] were employed. The restricted Hartree-Fock formalism was used and calculations were performed for the isolated molecules in a gas phase. No constraints of bonds/angles/dihedral angles were applied in the calculations and all the atoms were free to optimise. Generally, for decreasing the time of calculations, the first optimisation was performed for the longest oligomers (n = 16–20), then shorter oligomers structures have been generated by removal of one to "n–1" fluorene moieties and obtained structures have been used as input <*.gjf> files for the re-optimisation. Thus, the geometries of all oligomers were optimised at the B3LYP/6-31G(d) level of theory and the electronic structures were calculated at the same level of theory for the estimation of frontier orbital energies (HOMO and LUMO). The treatment of the calculated data and plotting the graphs of energies versus the size of the molecules were done with Origin Pro7.0 software.

4.4.4 Synthesis

Poly(9,9-dihexylfluorene), PF6

Exp no: SK-149

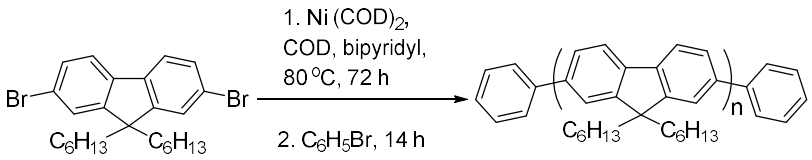

4.34 **PF6**

Under an argon atmosphere, a mixture of bis(1,5-cylcooctadiene)nickel(0) $Ni(COD)_2$, (96 mg, 0.34 mmol), 1,5-cyclooctadiene (37 mg, 0.34 mmol), and 2,2'-bipyridyl (54 mg, 0.34 mmol) in dry DMF (1.5 mL) was stirred at 80 °C for 30 min to form dark violet colour solution. To this solution, a solution of 2,7-dibromo-9,9-dihexylfluorene (**4.34**) (0.158 g, 0.32 mmol) in dry toluene (3.0 mL) was added and the mixture was stirred at 80 °C for 72 h. Then bromobenzene (0.03 mL) was added as end-capper and the mixture was stirred at 80° C for additional 14 h. The mixture was cooled down to room temperature and poured dropwise into a vigorously stirred solution of methanol:acetone:concentrated HCl (1:1:1, v/v) (75 mL) to form a cream colour semi-solid. Due to difficulties of its separation from milky-like solution, after stirring for 4 h, it was extracted with chloroform (20 mL), the chloroform layer washed with water (2 × 10 mL) concentrated to a small volume (ca. 4 mL) and poured dropwise into vigorously stirred methanol (75 mL) to form cream colour precipitate. After stirring for 2 h, the solid was filtered off, washed with methanol (5 mL) and dried *in vacuo* to give cream colour solid. It was transferred into Soxhlet apparatus and extracted with methanol (18 h) and then with acetone (18 h) to remove by-products and low molecular weight fractions. The residue was then extracted with chloroform (16 h), chloroform extract was concentrated to a small volume (~4 mL) and poured dropwise into stirred methanol (75 mL). The precipitate was filtered off, washed with methanol (5 mL) and dried *in vacuo* to afford polymer **PF6** as a cream colour solid (87 mg, 81.5%).

^{1}H NMR (400 MHz, $CDCl_3$): δ (ppm) 7.85–7.83 (m, 2H), 7.75–7.69 (m, 4H), 2.12 (m, 4H), 1.13 (m, 16H), 0.77 (m, 6H, CH_3).

GPC (THF): M_w = 25,000 Da, M_n = 9,700 Da, PDI = 2.57.

Poly(4-fluoro-9,9-dioctylfluorene), F-PF8

Exp no: SK-155

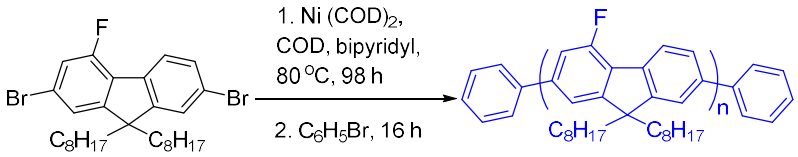

3.39 **F-PF8**

Under an argon atmosphere, a mixture of bis(1,5-cylcooctadiene)nickel(0) Ni(COD)$_2$, (0.426 g, 1.55 mmol), 1,5-cyclooctadiene (0.167 g, 1.55 mmol), and 2,2'-bipyridyl (0.243 g, 1.55 mmol) in dry DMF (3.4 mL) was stirred at 80 °C for 30 min to form dark violet colour solution. To this solution, a solution of 2,7-dibromo-4-fluoro-9,9-dioctylfluorene (**3.39**) (0.502 g, 0.88 mmol) in dry toluene (10.2 mL) was added slowly and the mixture was stirred at 80 °C for 98 h. Then bromobenzene (0.09 mL) was added as end-capper and the mixture was stirred at 80 °C for additional 16 h. The mixture was cooled down to room temperature and poured dropwise into vigorously stirred solution of methanol:acetone:concentrated HCl (1:1:1, v/v) (150 mL) and stirred for 2 h to form cream colour semi-solid and milky-like suspension. It was extracted with chloroform (50 mL), the chloroform layer was washed with water (2 × 10 mL), concentrated to a small volume (~6 mL) and poured dropwise into stirred methanol (100 mL). The mixture was stirred for 2 h, the precipitate was filtered off, washed with methanol (5 mL) and dried *in vacuo* to give cream colour solid. The solid was transferred into Soxhlet apparatus and extracted with methanol (18 h) and then with acetone (18 h) to remove by-products and low molecular weight fractions. The residue was extracted with chloroform (8 h), chloroform solution was concentrated to a small volume (~10 mL) and slowly poured into stirred methanol (100 mL). The precipitate was filtered off, washed with methanol (10 mL) and dried *in vacuo* to afford polymer **F-PF8** as a cream colour solid (0.305 g, 84%).

^{1}H NMR (400 MHz, $CDCl_3$): δ (ppm) 8.02 (m, 1H), 7.71 (m, 1H), 7.64 (m, 1H), 7.45 (m, 1H), 7.38 (m, 1H), 2.12 (m, 4H), 1.25–1.14 (m, 20H), 0.83-0.79 (m, 10H).

GPC (THF): Mw = 124,000 Da, Mn = 40,100 Da, PDI = 3.09.

Repeated synthesis, Exp no: SK-153: Monomer **3.39** (0.102 g), Ni (COD)$_2$ (86 mg, 0.31 mmol), 1,5-cyclooctadiene (34 mg, 0.31 mmol), 2,2'-bipyridyl (49 mg, 0.31 mmol), dry DMF (0.7 mL), dry toluene (2.1 mL), bromobenzene (0.01 mL). Yield: 56 mg (76 %).

GPC (THF): M_w = 304,000 Da, M_n = 129,000 Da, PDI = 2.35.

Poly(4-methoxy-9,9-dioctylfluorene,) MeO-PF8

Exp no: SK-156

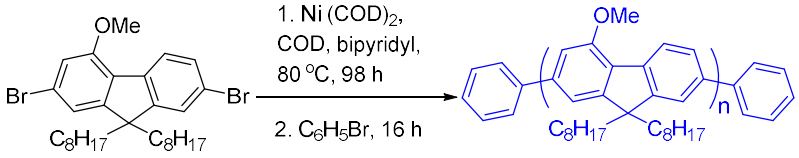

3.41 **MeO-PF8**

Under an argon atmosphere, a mixture of bis(1,5-cylcooctadiene)nickel(0) $Ni(COD)_2$, (0.414 g, 1.50 mmol), 1,5-cyclooctadiene (0.162 g, 1.50 mmol), and 2,2'-bipyridyl (0.235 g, 1.50 mmol) in dry DMF (3.4 mL) was stirred at 80 °C for 30 min to form dark violet colour solution. To this solution, a solution of 2,7-dibromo-4-methoxy-9,9-dioctylfluorene (**3.41**) (0.498 g, 0.86 mmol) in dry toluene (10.2 mL) was added slowly and the mixture was stirred at 80 °C for 98 h. Then bromobenzene (0.09 mL) was added as end-capper and the mixture was stirred at 80 °C for additional 16 h. The mixture was cooled down to room temperature and poured dropwise into a stirred solution of methanol:acetone:concentrated HCl (1:1:1, v/v) (150 mL) to form yellow colour semi-solid. After stirring for 1 h, it was extracted with chloroform (50 mL), the chloroform layer was washed with water (2 × 10 mL), concentrated to a small volume (~6 mL) and poured dropwise into methanol (100 mL) with vigorous stirring. The precipitate was stirred for 2 h, filtered off, washed with methanol and dried *in vacuo* to give yellow colour solid. This solid was extracted in a Soxhlet apparatus with methanol (18 h) and then with acetone (18 h) to remove by-products and low molecular weight fractions. The residue was extracted with chloroform (8 h), concentrated to a small volume (~10 mL) and poured dropwise into methanol (100 mL) with stirring. The precipitate was filtered off, washed with methanol (10 mL) and dried *in vacuo* to afford polymer **MeO-PF8** as a yellow solid (0.272 g, 75%).

^{1}H NMR (400 MHz, $CDCl_3$): δ (ppm) 8.16 (m, 1H), 7.68–7.62 (m, 2H), 7.29–7.25 (m, 1H), 7.17–7.16 (m, 1H), 4.11 (br.s, 3H), 2.10 (m, 4H), 1.25–1.14 (m, 20H), 0.83–0.79 (m, 10H).

GPC (THF): M_w = 75,000 Da, M_n = 34,500 Da, PDI = 2.17.

Poly(4-cyano-9,9-dioctylfluorene), CN-PF8

Exp no: SK-157

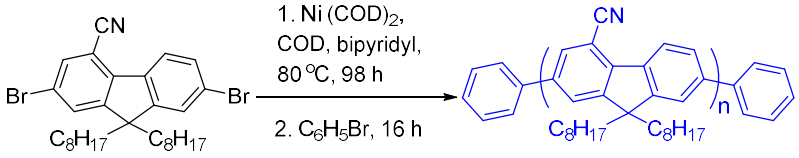

3.40 **CN-PF8**

Under an argon atmosphere, a mixture of bis(1,5-cylcooctadiene)nickel(0) Ni(COD)$_2$, (424 mg, 1.54 mmol), 1,5-cyclooctadiene (167 mg, 1.54 mmol), and 2,2'-bipyridyl (241 mg, 1.54 mmol) in dry DMF (3.4 mL) was stirred at 80 °C for 30 min to form dark violet colour solution. To this, a solution of 2,7-dibromo-4-cyano-9,9-dioctylfluorene (**3.40**) (506 mg, 0.88 mmol) in dry toluene (10.2 mL) was added slowly and the mixture was stirred at 80 °C for 98 h. Then bromobenzene (0.09 mL) was added as end-capper and the mixture was stirred at 80 °C for additional 16 h. The mixture was cooled down to room temperature, poured dropwise into a stirred solution of methanol:diluted HCl (9:1, v/v) (100 mL) and stirred for 2 h to form greenish-yellow semi-solid and milky-like suspension. After stirring for 4 h, it was extracted with chloroform (50 mL), the chloroform layer was washed with water (2 × 10 mL), concentrated to a small volume (~8 mL) and poured dropwise into methanol (100 mL) with vigorous stirring to form green colour precipitate. The mixture was stirred for 2 h, the solid was filtered off, washed with methanol and dried *in vacuo* to give green solid (333 mg, 91%). This was extracted in a Soxhlet apparatus with methanol (18 h) and then with acetone (18 h) to remove by-products and low molecular weight fractions. The residue was then extracted with chloroform (12 h), the solution was concentrated to a small volume (~8 mL) and poured dropwise into stirred methanol (100 mL). The precipitate was filtered off, washed with methanol (10 mL) and dried *in vacuo* to afford polymer **CN-PF8** as a green solid (0.186 g, 51%).

^{1}H NMR (400 MHz, $CDCl_3$): δ (ppm) 8.54 (m, 1H), 7.95 (m, 1H), 7.88–7.76 (m, 1H), 7.73–7.67 (m, 2H), 2.17 (m, 4H), 1.25–1.13 (m, 20H), 0.81 (m, 10H).

GPC (THF): M_w = 45,100 Da, M_n = 10,300 Da, PDI = 4.37.

Poly(4-thiomethyl-9,9-dioctylfluorene), MeS-PF6/8

Exp no: SK-174

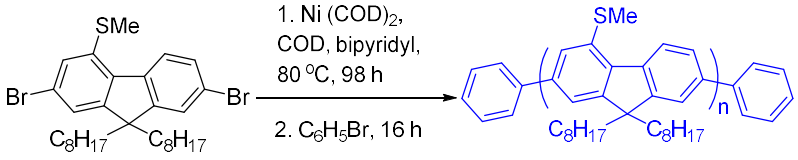

3.42 **MeS-PF8**

Under an argon atmosphere, a mixture of bis(1,5-cylcooctadiene)nickel(0) Ni(COD)$_2$, (432 mg, 1.57 mmol), 1,5-cyclooctadiene (170 mg, 1.50 mmol), and 2,2'-bipyridyl (245 mg, 1.57 mmol) in dry DMF (3.4 mL) was stirred at 80 °C for 30 min to form dark violet colour solution. To this, a solution of 2,7-dibromo-4-thiomethyl-9,9-dioctylfluorene (**3.42**) (534 mg, 0.89 mmol) in dry toluene (10.2 mL) was added slowly and the mixture was stirred at 80 °C for 98 h. Bromobenzene (0.09 mL) was added as end-capper and the mixture was stirred at 80 °C for additional 16 h. The mixture was cooled down to room temperature and poured dropwise into a stirred solution of methanol:acetone:concentrated HCl (1:1:1, v/v) 100 mL to form yellow colour semi-solid and milky-like suspension. The mixture was stirred for 4 h, extracted with chloroform (50 mL), the chloroform layer was washed with water (3 × 20 mL), concentrated to a small volume (~6 mL) and poured dropwise into stirred methanol (75 mL). The precipitate was filtered off, washed with methanol (5 mL) and dried *in vacuo* to give pale yellow solid (294 mg, 75 %). This solid was extracted in a Soxhlet apparatus first with methanol (20 h) to give (after evaporation of methanol) pale yellow liquid (34 mg). Then it was extracted with acetone (24 h) to remove low-molecular weight by-products that gave (after solvent evaporation) pale yellow liquid (86 mg). (*Isolations of these two products were aimed to see how much materials are extracted by methanol and acetone, and which products are extracted*). Finally, the residue was extracted with chloroform for 16 h, the solution was concentrated to a small volume (~5 mL) and poured dropwise into stirred methanol (75 mL). The precipitate was filtered off, washed with methanol (5 mL) and dried *in vacuo* to afford polymer **MeS-PF8** as a pale yellow solid (124 mg, 32%).

^{1}H NMR (400 MHz, $CDCl_3$): δ (ppm) 8.50 (m,1H), 7.73 (m, 1H), 7.68 (m, 1H), 7.54 (m, 1H), 7.47 (m, 1H), 2.72 (br s, 3H), 2.11 (m, 4H), 1.14 (m, 20H), 0.81 (m, 10H).

GPC (THF): M_w = 120,000 Da M_n = 32,400 Da, PDI = 3.70.

Poly(4-methylsulfonyl-9,9-dioctylfluorene), $MeSO_2$-PF8

Exp no: SK-175

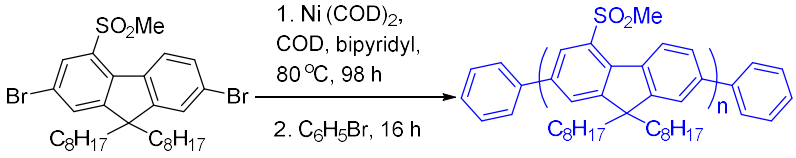

3.44 **$MeSO_2$-PF8**

Under an argon atmosphere, a mixture of bis(1,5-cylcooctadiene)nickel(0) $Ni(COD)_2$, (487 mg, 1.77 mmol), 1,5-cyclooctadiene (186 mg, 1.77 mmol), and 2,2'-bipyridyl (276 mg, 1.77 mmol) in dry DMF (6.0 mL) was stirred at 80 °C for 30 minutes to form dark violet colour solution. To this, a solution of 2,7-dibromo-4-methylsulfonyl-9,9-dioctylfluorene (**3.44**) (555 mg, 0.88 mmol) in dry toluene (14.0 mL) was added slowly and the mixture was stirred at 80 °C for 98 h. Then bromobenzene (0.09 mL) was added as end-capper and the mixture was stirred at 80 °C for additional 16 h. The mixture was cooled down to room temperature and poured dropwise into a stirred solution of methanol:acetone:concentrated HCl (1:1:1, v/v) (120 mL) to form semi-solid and milky-like suspension. The mixture was stirred for 4 h, extracted with chloroform (50 mL), the chloroform layer was washed with water (3 × 20 mL) concentrated to a small volume (~8 mL) and poured dropwise into stirred methanol (120 mL) to form yellow precipitate. The solid was filtered off, washed with methanol (5 mL) and dried *in vacuo* to give yellow solid (374 mg, 92%). This solid was extracted in a Soxhlet apparatus with methanol (18 h) and then with acetone (18 h) to remove by-products and low molecular weight fractions, which gave (after solvent evaporation) yellow liquid (68 mg). The residue in the Soxhlet apparatus was extracted with chloroform for 12 h, the solution was concentrated to a small volume (~6 mL) and poured dropwise into stirred methanol (100 mL). The precipitate was filtered off, washed with methanol (5 mL) and dried *in vacuo* to afford polymer **$MeSO_2$-PF8** as a yellow solid (303 mg, 74%).

^{1}H NMR (400 MHz, $CDCl_3$): δ (ppm) 8.82 (m, 1H), 8.50 (br s, 1H), 7.97 (br s, 1H), 7.85–7.79 (m, 2H), 3.36 (br s, 3H), 2.20 (m, 4H), 1.13 (m, 20H), 0.80 (m, 10H).

GPC (THF): M_w = 185,000 Da, M_n = 78,700 Da, PDI = 2.34.

Poly(4-phenylacetylene-9,9-dioctylfluorene), PhCC-PF8

Exp no: SK-176

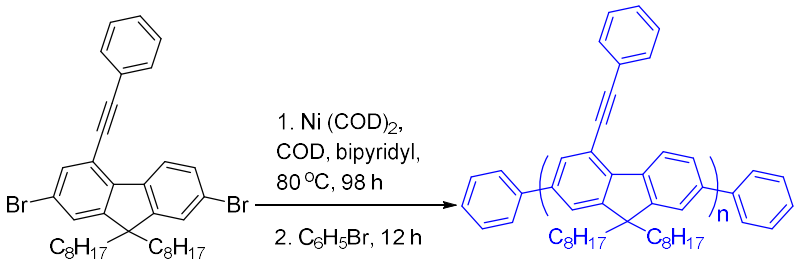

3.43 **PhCC-PF8**

Under an argon atmosphere, a mixture of bis(1,5-cylcooctadiene)nickel(0) $Ni(COD)_2$, (348 mg, 1.25 mmol), 1,5-cyclooctadiene (137 mg, 1.25 mmol), and 2,2-bipyridyl 200mg, 1.25 mmol) in dry DMF (4.4.0 mL) was stirred at 80 °C for 30 min to form dark violet colour solution. To this, a solution of 2,7-dibromo-4-phenylethynyl-9,9-dioctylfluorene (**3.43**) (408 mg, 0.62 mmol) in dry toluene (10.2 mL) was added slowly and the mixture was stirred at 80 °C for 98 h. Then bromobenzene (0.07 mL) was added as end-capper and the mixture was stirred at 80 °C for additional 12 h. The mixture was cooled down to room temperature and poured dropwise into a stirred solution of methanol:acetone:concentrated HCl (1:1:1, v/v) (120 mL) to form semi-solid and milky-like suspension. It was stirred for 4 h, extracted with chloroform (50 mL), the chloroform layer was washed with water (3 × 20 mL), concentrated to a small volume (~6 mL) and poured dropwise into stirred methanol (120 mL). The precipitate was filtered off, washed with methanol (5 mL) and dried *in vacuo* to give yellow solid (221 mg, 71%). This solid was extracted in a Soxhlet apparatus with methanol (18 h) and then with acetone (18 h) to remove by-products and low molecular weight fractions that gave (after solvent evaporation) yellow liquid (33 mg). Finally, the residue in the Soxhlet apparatus was extracted with chloroform for 12 h, the solution was concentrated to a small volume (~6 mL) and poured dropwise into stirred methanol (100 mL). The precipitate was filtered off, washed with methanol (5 mL) and dried *in vacuo* to give polymer **PhCC-PF8** as a yellow solid (108 mg, 35%).

^{1}H NMR (400 MHz, $CDCl_3$): δ (ppm) 8.65 (m, 1H), 7.74 (m, 3H), 7.43 (m, 3H), 7.10–6.99 (m, 2H), 6.74–6.63 (m, 1H), 3.36 (s, 4H), 2.20 (m, 4H), 1.13 (m, 16H), 0.80 (m, 10H).

GPC (THF): M_w = 185,000 Da, M_n = 78,700 Da, PDI = 2.34.

Poly(4-methoxy-9,9-diphenyloxyfluorene), MeO-PF6/8

Exp no: SK-177

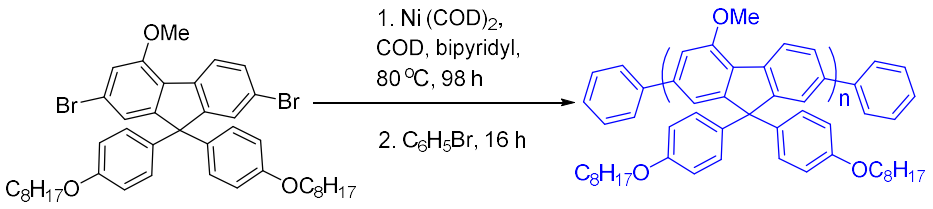

3.70 **MeO-PF6/8**

Under an argon atmosphere, a mixture of bis(1,5-cylcooctadiene)nickel(0), $Ni(COD)_2$, (289 mg, 1.04 mmol), 1,5-cyclooctadiene (112 mg, 1.04 mmol), and 2,2'-bipyridyl (160 mg, 1.04 mmol) in dry DMF (4.4 mL) was stirred at 80 °C for 30 minutes to form dark violet colour solution. To this solution, a solution of 2,7-dibromo-4-methoxy-9,9-dioctylphenoxyfluorene (**3.70**) (397 mg, 0.52 mmol) in dry toluene (10.2 mL) was added slowly and the mixture was stirred at 80 °C for 98 h. Bromobenzene (0.07 mL) was added as end-capper and the mixture was stirred at 80 °C for additional 16 h. The mixture was cooled down to room temperature and poured dropwise into stirred solution of methanol:acetone:concentrated.HCl (1:1:1, v/v) (120 mL) to form yellow colour semi-solid. It was stirred for 4 h, extracted with chloroform (50 mL), the chloroform layer was washed with water (3 × 40 mL), concentrated to a small volume (~6 mL) and poured dropwise into stirred methanol (150 mL). The precipitate was filtered off, washed with methanol (5 mL) and dried *in vacuo* to give yellow solid (224 mg, 71 %). This solid was extracted in a Soxhlet apparatus with methanol (18 h) (17 mg of pale yellow liquid after solvent evaporation) and then with acetone (18 h) (89 mg of pale yellow liquid after solvent evaporation) to remove by products and low molecular weight fractions. Finally, the residue in the Soxhlet apparatus was extracted with chloroform for 16 h, the solution was concentrated to a small volume (~5 mL) and poured dropwise into stirred methanol (50 mL). The precipitate was filtered off, washed with methanol (5 mL) and dried *in vacuo* to afford polymer **MeO-PF6/8** as a yellow solid (86 mg, 27 %).

^{1}H NMR (400 MHz, $CDCl_3$): δ (ppm) 8.09 (br s, 1H), 7.51 (br s, 1H), 7.48 (br s, 1H), 7.15–7.13 (m, 5H), 6.97 (m, 1H), 6.74–6.72 (m, 4H), 4.03 (s, 3H), 3.87 (m, 4H), 1.74–1.71 (m, 4H), 1.41 (m, 4H), 1.28–1.26 (m, 16H), 0.86–0.84 (m, 6H).

GPC (THF): M_w = 34,400 Da, M_n = 23,400 Da, PDI = 1.47.

Poly(4-thiomethyl-9,9-dioctylphenoxyfluorene), BuS-PF6/8

Exp no: SK-178

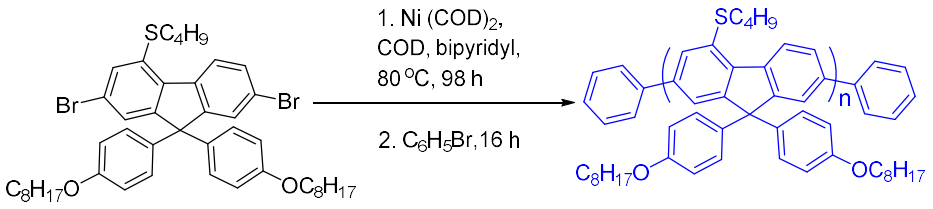

3.69 **BuS-PF6/8**

Under an argon atmosphere, a mixture of bis(1,5-cylcooctadiene)nickel(0) $Ni(COD)_2$, (275 mg, 1.01 mmol), 1,5-cyclooctadiene (110 mg, 1.01 mmol), and 2,2'-bipyridyl (156 mg, 1.01 mmol) in dry DMF (4.4 mL) was stirred at 80 °C for 30 min to form violet colour solution. To this, a solution of 2,7-dibromo-4-thiomethyl-9,9-dioctylphenoxyfluorene (**3.69**) (416 mg, 0.86 mmol) in dry toluene (10.2 mL) was added slowly and the mixture was stirred at 80 °C for 98 h. Bromobenzene (0.07 mL) was added as end-capper and the mixture was stirred at 80 °C for additional 16 h. The mixture was cooled down to room temperature and poured dropwise into stirred solution of methanol:acetone:concentrated HCl (1:1:1, v/v) (120 mL) to form yellow colour semi-solid. The mixture was stirred for 4 h, extracted with chloroform (50 mL), the chloroform layer was washed with water (3 × 20 mL), concentrated to a small volume (~6 mL) and poured dropwise into stirred methanol (75 mL). The precipitate was filtered off, washed with methanol (5 mL) and dried *in vacuo* to give yellow colour solid (296 mg, 88%). This solid was extracted in a Soxhlet apparatus with methanol (18 h) (24 mg of pale yellow liquid after solvent evaporation) and then with acetone (18 h) (182 mg of pale yellow liquid, after solvent evaporation) to remove by products and low molecular weight fractions. Finally, the residue in the Soxhlet apparatus was extracted with chloroform for 16 h, the solution was concentrated to a small volume (~4 mL) and poured dropwise into stirred methanol (50 mL). The precipitate was filtered off, washed with methanol (5 mL) and dried *in vacuo* to afford polymer **BuS-PF6/8** as a cream colour solid (81 mg, 24%).

^{1}H NMR (400 MHz, $CDCl_3$): δ (ppm) 8.42 (m, 1H), 7.53–7.51 (m, 2H), 7.40–7.31 (m, 2H), 7.11–7.08 (m, 4H), 6.72 (br s, 4H), 3.87 (br s, 4H), 3.02 (br s, 2H), 1.72 (br s, 4H), 1.56–1.39 (br s, 6H), 1.26 (br s, 18H), 0.86 (m, 9H).

GPC (THF): M_w = 24,700 Da, M_n = 9,690 Da, PDI = 2.54.

Poly(4-butylsulfonyl-9,9-dioctylphenoxyfluorene), BuSO$_2$-PF6/8

Exp no: SK-179

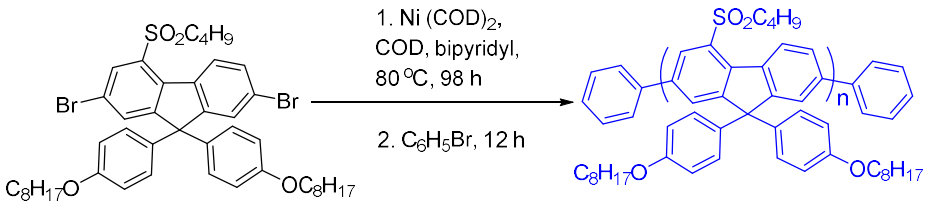

3.72 **BuSO$_2$-PF6/8**

Under an argon atmosphere, a mixture of bis(1,5-cylcooctadiene)nickel(0) Ni(COD)$_2$, (255 mg, 0.92 mmol), 1,5-cyclooctadiene (103 mg, 0.92 mmol), and 2,2'-bipyridyl (145 mg, 0.92 mmol) in dry DMF (4.4 mL) was stirred at 80 °C for 30 min to form dark violet colour solution. To this, a solution of 2,7-dibromo-4-butylsulfonyl-9,9-dioctylphenoxyfluorene (**3.72**) (394 mg, 0.46 mmol) in dry toluene (10.2 mL) was added slowly and the mixture was stirred at 80 °C for 98 h. Bromobenzene (0.07 mL) was added as end-capper and the mixture was stirred at 80 °C for additional 12 h. The mixture was cooled down to room temperature and poured dropwise into a stirred solution of methanol:acetone:concentrated HCl (1:1:1, v/v) (90 mL) to form greenish colour semi-solid. It was stirred for 4 h, extracted with chloroform (60 mL), the chloroform layer was washed with water (3 × 20 mL), concentrated to a small volume (~6 mL) and poured dropwise into stirred methanol (120 mL). The precipitate was filtered off, washed with methanol (5 mL) and dried *in vacuo* to give green solid (207 mg, 64%). This solid was extracted in a Soxhlet apparatus with methanol (18 h) (17 mg of a pale greenish-yellow liquid, after solvent evaporation) and then with acetone (18 h) (97 mg of a greenish-yellow liquid, after solvent evaporation) to remove by products and low molecular weight fractions. Finally, the residue in the Soxhlet apparatus was extracted with chloroform for 12 h, the solution was concentrated to a small volume (~4 mL) and poured dropwise into methanol (50 mL). The precipitate was filtered off, washed with methanol (5 mL) and dried *in vacuo* to afford polymer **BuSO$_2$-PF6/8** as a green solid (62 mg, 19%).

^{1}H NMR (400 MHz, $CDCl_3$): δ (ppm) 8.69–8.67 (br s, 1H), 8.24 (m, 1H), 7.78 (m, 1H), 7.59 (m, 2H), 7.10–7.09 (m, 4H), 6.78–6.76 (m, 4H), 3.89 (br s, 4H), 3.36 (br s, 2H), 1.83 (br s, 2H), 1.73 (br s, 4H), 1.41 (br s, 6H), 1.28–1.26 (m, 16H), 0.86 (m, 9H).

GPC (THF): M_w = 85,400 Da, M_n = 56,500 Da, PDI = 1.51.

Poly(2,7-dibromo-4-butoxycarbonyl-9,9-(dioctylphenoxy)fluorene), BuO_2C-PF6/8

Exp no: SK-161

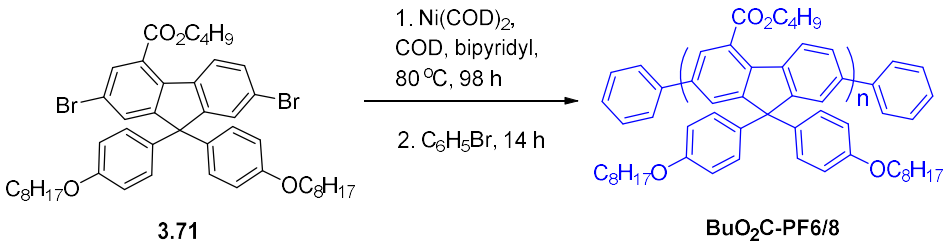

3.71 **BuO_2C-PF6/8**

Under an argon atmosphere, a mixture of bis(1,5-cylcooctadiene)nickel(0), $Ni(COD)_2$, (295 mg, 1.07 mmol), 1,5-cyclooctadiene (116 mg, 1.07 mmol), and 2,2'-bipyridyl (167 mg, 1.07 mmol) in dry DMF (3.4 mL) was stirred at 80 °C for 30 min to form dark violet colour solution. To this, a solution of 2,7-dibromo-4-butoxycarbonyl-9,9-(dioctylphenoxy)fluorene (**3.71**) (511 mg, 0.61 mmol) in dry toluene (10.2 mL) was added slowly and the mixture was stirred at 80 °C for 98 h. Bromobenzene (0.09 mL) was added as end-capper and the mixture was stirred at 80 °C for additional 14 h. The mixture was cooled down to room temperature and poured dropwise into a stirred solution of methanol:acetone:concentrated HCl (1:1:1, v/v) (150 mL) to form pale yellow colour semi-solid. The mixture was stirred for 1 h, extracted with chloroform (50 mL), the chloroform layer was washed with water (2 × 10 mL), concentrated so a small volume (~6 mL) and poured dropwise into stirred methanol (100 mL). The precipitate was filtered off, washed with methanol (10 mL) and dried *in vacuo* to give pale yellow solid (0.386 g, 93%). This solid was extracted in a Soxhlet apparatus with methanol (18 h) and acetone (18 h) to remove by products and low molecular weight fractions. The residue was extracted with chloroform (12 h), concentrated to a small volume (~6 mL) and poured dropwise into stirred methanol (75 mL). The precipitate was filtered off, washed with methanol (5 mL) and dried *in vacuo* to afford polymer **BuO_2C-PF6/8** as a pale yellow solid (124 mg, 30 %).

^{1}H NMR (400 MHz, $CDCl_3$): δ (ppm) 8.29 (m, 1H), 7.85 (m, 1H), 7.65 (m, 1H), 7.51 (m, 2H), 7.13–7.06 (m, 4H), 6.75–6.73 (m, 4H), 4.45 (br s, 2H), 3.88 (br s, 4H), 1.81–1.71 (m, 4H), 1.47–1.41 (m, 6H), 1.25 (m, 18H), 0.98 (m, 3H), 0.86 (m, 6H).

GPC (THF): M_w = 28,600 Da, M_n = 18,500 Da, PDI = 1.54.

References

1 M. S. AlSalhi, J. Alam, L. A. Dass, and M. Raja, *Int. J. Mol. Sci*., **2011**, *12*, 2036–2054. (DOI:10.3390/ijms12032036).

2 A .C. Grimsdale, K. L. Chan, R. E. Martin, P. G. Jokisz, and A. B. Holmes, *Chem. Rev.*, **2009**, *109*, 897–1091. (DOI: 10.1021/cr000013v).

3 D. F. Perepichka, I. F. Perepichka, H. Meng, and F. Wudl, Light-emitting polymers. Chapter 2 in Book: *Organic Light-Emitting Materials and Devices*, Z. R. Li and H. Meng (Eds), CRC Press, Boca Raton, FL, **2006**, pp. 45–293.

4 U. U. Scherf and D. Neher (Eds), *Polyfluorenes. – Advances in Polymer Science,* Springer, **2008**, *212*, 322 pp. (DOI 10.1007/978-3-540-68734-4).

5 I. F. Perepichka and D. F. Perepichka (Eds), *Handbook of Thiophene-Based Materials: Applications in Organic Electronics and Photonics* (*Vol. 1: Synthesis and Theory, Vol. 2: Properties and Applications)*, Wiley, **2009**, 910 pp.

6 D. Neher, *Macromol. Rapid Commun*., **2001**, *22*, 1365–1385. (DOI: 10.1002/1521-3927(20011101)22:17<1365).

7 B. Tsuie, J. L. Reddinger, G. A. Sotzing, J. Soloducho, A. R. Katritzky, and J. R. Reynolds, *J. Mater. Chem.*, **1999**, *9*, 2189–2200. (DOI:10.1039/A903374B).

8 D. Marsitzky, R. Vestberg, P. Blainey, B. T. Tang, C. J. Hawker, and K. R. Carter, *J. Am. Chem. Soc*., **2001**, *123*, 6965–6972. (DOI: 10.1021/ja010020g).

9 U. Scherf and E. J. List, *Adv. Mater*., **2002**, *14*, 477–487. (DOI: 10.1002/1521-4095(20020404)14:7<477).

10 S. Beaupre and M. Leclerc, *Macromolecules*, **2003**, *36*, 8986–8991. (DOI: 10.1021/ma035064j).

11 B. Liu, W.-L. Yu, Y.-H. Lai, and W. Huang, *Chem. Mater*., **2001**, *13*, 1984–1991. (DOI: 10.1021/cm0007048).

12 S. Janietz, D. D. C. Bradley, M. Grell, C. Giebeler, M. Inbasekaran, and E. P. Woo, *Appl. Phys. Lett*., **1998**, *73*, 2453–2455. (DOI: org/10.1063/1.122479).

13 A. Charas, N. Barbagallo, J. Morgado, and L. Alcacer, *Synth. Metals*, **2001**, *122*, 23–25. (DOI:10.1016/S0379-6779(00)01328-X).

14 D. Kumar, K. R. J. Thomas, Y.-L. Chen, Y.-C. Jou, and J.-H. Jou, *Tetrahedron*, **2013**, *69*, 2594–2602. (DOI: org/10.1016/j.tet.2013.01.046).

15 H.-F. Yang, W.-F. Su, and Y. Chen, *New J. Chem*., **2011**, *35*, 1219–1225. (DOI: 10.1039/c0nj00886a).

16 S. Yao and K. D. Belfield, *J. Org. Chem.,* **2005**, *70*, 5126–5132. (DOI: 10.1021/jo0503512).

17 C.-S. Wu, Y.-J. Yang, S.-W. Fang, and Y. Chen, *J. Polym. Sci. A: Polym. Chem*., **2012**, *50*, 3875–3884. (DOI: 10.1002/pola.26184).

18 J.-M. Yu and Y. Chen, *Polymer*, **2010**, *51*, 4484–4492. (DOI: 10.1016/j.polymer.2010.08.001).

19 J. -M. Yu, T. Sakamoto, K. Watanabe, S. Furumi, N. Tamaoki, Y. Chen, and T. Nakano, *Chem. Commun*., **2011**, *47*, 3799–3801. (DOI: 10.1039/c0cc05564f).

20 J.-Y. Lin, W.-S. Zhu, F. Liu, L.-H. Xie, L. Zhang, R. Xia, G.-C. Xing, and W. Huang, *Macromolecules*, **2014**, *47*, 1001−1007. (DOI: dx.doi.org/10.1021/ma402585n).

21 J. Pillow and J. Morey, Patent WO 2013/114068 A2 (08.08.**2013**).

22 T. Yamamoto, *Prog. Polym. Sci*., **1992**, *17*, 1153–1205. (DOI: 10.1039/c3py00166k).

23 G. Klaerner and R. D. Miller, *Macromolecules*, **1998**, *31*, 2007–2009. (DOI: 10.1021/ma971073e).

24 M. Kreyenschmidt, G. Klaerner, T. Fuhrer, J. Ashenhurst, S. Karg, W. D. Chen, V. Y. Lee, J. C. Scott, and R. D. Miller, *Macromolecules*, **1998**, *31*, 1099–1103. (DOI: 10.1021/ma970914e).

25 H.-G. Nothofer, A. Meisel, T. Miteva, D. Neher, M. Forster, M. Oda, G. Liester, D. Sainova, A. Yasude, D. Lupo, W. Knoll, and U. Scherf, *Macromol. Symp*., **2000**, *154*, 139–148. (DOI: 10.1002/1521-3900(200004)154:1<139).

26 U. Scherf and E. J. W. List, *Adv. Mater.*, **2002**, *14*, 477–487. (DOI: 10.1002/1521-4095(20020404)14:7<477).

27 E. Wang, C. Li, Y. Mo, Y. Zhang, G. Ma, W. Shi, J. Peng, W. Yang, and Y. Cao, *J. Mater. Chem*., **2006**, *16*, 4133–4140. (DOI: 10.1039/B609250K).

28 J. Gierschner, J. Cornil, and H.-J. Egelhaaf, *Adv. Mater.,* **2007**, *19*, 173–191. (DOI: 10.1002/adma.200600277).

29 G. Klaerner and R. D. Miller, *Macromolecules*, **1998**, *31*, 2007–2009. (DOI: 10.1021/ma971073e).

30 T. Izumi, S. Kobashi, K. Takimiya, Y. Aso, and T. Otsubo, *J. Am. Chem. Soc.*, **2003**, *125*, 5286–5287. (DOI: 10.1021/ja034333i).

31 J. Gierschner, H.-G. Mack, H.-J. Egelhaaf, S. Schweizer, B. Doser, and D. Oelkrug, *Synth. Metals*, **2003**, *138*, 311–3115. (DOI:10.1016/S0379-6779(03)00030-4).

32 P. Tavan and K. Schulten, *J. Chem. Phys.*, **1986**, *85*, 6602–6609. (DOI: org/10.1063/1.451442).

33 A. Pogantsch, G. Heimel, and E. Zojer, *J. Chem. Phys.*, **2002**, *117*, 5921–5928. (DOI: 10.1063/1.1502244).

34 H. Meier, U. Stalmach, and H. Kolshorn, *Acta Polym.*, **1997**, *48*, 379–384. (DOI: 10.1002/actp.1997.010480905).

35 J. Torras, J. Casanovas, and C. Alemán, *J. Phys. Chem. A*, **2012**, *116*, 7571−7583. (DOI: dx.doi.org/10.1021/jp303584b).

36 W. Kuhn, *Helv. Chim. Acta*, **1948**, *31*, 1780−1799. (DOI: 10.1002/hlca.19480310644).

37 G. N. Lewis and M. Calvin, *Chem. Rev*., **1939**, 25, 273−328. (DOI: 10.1021/cr60081a004).

38 C. M. Cardona, W. Li, A. E. Kaifer, D. Stockdale, and G. C. Bazan, *Adv. Mater*., **2011**, *23*, 2367–2371. (DOI: 10.1002/adma.201004554).

39 W. Yang, J. Huang, C. Liu, Y. Niu, Q. Hou, R. Yang, and Y. Cao, *Polymer*, **2004**, *45*, 865–872. (DOI: 10.1016/j.polymer.2003.11.052).

40 C. Xia and R. C. Advincula, *Macromolecules*, **2001**, *34*, 5854–5859. (DOI: 10.1021/ma002036h).

41 Y. Zhu, K. M. Gibbons, A. P. Kulkarni, and S. A. Jenekhe, *Macromolecules*, **2007**, *40*, 804–813. (DOI: 10.1021/ma062445z).

42 J.-H. Lee and D.-H. Hwang, *Chem. Commun*., **2003**, 2836–2837. (DOI: 10.1039/B309006J).

43 F. B. Dias, S. King, A. P. Monkman, I. I. Perepichka, M. A. Kryuchkov, I. F. Perepichka, and M. R. Bryce, *J. Phys. Chem. B*, **2008**, *112*, 6557–6566. (DOI: 10.1021/jp800068d).

44 S. M. King, I. I. Perepichka, I. F. Perepichka, F. B. Dias, M. R. Bryce, A. P. Monkman, *Adv. Funct. Mater*., **2009**, *19*, 586–591. (DOI: 10.1002/adfm.200801237).

45 X. Gong, P. K. Iyer, D. Moses, G. C. Bazan, A. J. Heeger, and S. S. Xiao, *Adv. Funct. Mater*., **2003**, *13*, 325–330. (DOI: 10.1002/adfm.200304279).

46 A. M. Brouwer, *Pure Appl. Chem.*, **2011**, *83*, 2213–2228. (DOI:10.1351/PAC-REP-11-11-12).

47 J. H. Ahn, C. Wang, I. F. Perepichka, M. R. Bryce, and M. C. Petty, *J. Mater. Chem*., **2007**, *17*, 2996–3001. (DOI: 10.1039/b700047b).

48 M. Sims, D. D. C. Bradley, M. Ariu, M. Koeberg, A. Asimakis, M. Grell, and D. G. Lidzey, *Adv. Funct. Mater*., **2004**, *14*, 765–781. (DOI: 10.1002/adfm.200490024).

49 A. W. Grice, D. D. C. Bradley, M. T. Bernius, M. Inbasekaran, W. W. Wu, and E. P. Woo, *Appl. Phys. Lett*., **1998**, *73*, 629–998. (DOI: 10.1002/marc.200600786).

50 V. N. Bliznyuk, S. Carter, J. C. Scott, G. Klärner, R. D. Miller, and D. C. Miller, *Macromolecules,* **1999**, *32*, 361–369. (DOI: 10.1021/ma9808979).

51 J. I. Lee, G. Klärner, and R. D. Miller, *Chem. Mater.*, **1999**, 11, 1083–1088. (DOI: 10.1021/cm981049v).

52 D. Sainova, T. Miteva, H. G. Nothofer, U. Scherf, I. Glowacki, J. Ulanski, H. Fujikawa, and D. Neher, *Appl. Phys. Lett*., **2000**, *76*, 1810–1812. (DOI.org/10.1063/1.126173).

53 G. Zeng, W.-L. Yu, S.-J. Chua, and W. Huang, *Macromolecules*, **2002**, *35*, 6907–6914. (DOI: 10.1021/ma020241m).

54 M. Gaal, E. J. W. List, and U. Scherf, *Macromolecules*, **2003,** *36*, 4236–4237. (DOI: 10.1021/ma021614m).

55 L. Romaner, A. Pogantsch, P. Scanducci de Freitas, U. Scherf, M. Gaal, E. Zojer, and E. J. W. List, *Adv. Funct. Mater.*, **2003**, *13*, 597–601. (DOI: 10.1002/adfm.200304360).

56 E. J. W. List, R. Guentner, P. Scanducci de Freitas, and U. Scherf, *Adv. Mater*., **2002**, *14*, 374–378. (DOI: 10.1002/1521-4095(20020304)14).

57 U. Scherf and E. J. W. List, *Adv. Mater*., **2002**, *14*, 477–487. (DOI: 10.1002/1521-4095(20020404)14).

58 E. Zojera, A. Pogantsch, E. Hennebicq, D. Beljonne, J.-L. Brédas, P. Scandiucci de Freitas, U. Scherf, and E. J. W. List, *J. Chem. Phys.,* **2002**, *117*, 6794–6802. (DOI: 10.1021/ma071659t. PMCID: PMC2567116).

59 W. Zhao, T. Cao, and J. M. White, *Adv. Funct. Mater*., **2004**, *14*, 783–790. (DOI: 10.1002/adfm.200305173).

60 J. Y. Li, A. Ziegler, and G. Wegner, *Chem. Eur. J.,* **2005**, *11*, 4450–4457. (DOI: 10.1002/chem.200401319).

61 C. Chi, C. Im, V. Enkelmann, A. Ziegler, G. Lieser, and G. Wegner, *Chem. Eur. J*., **2005**, *11*, 6833–6845. (DOI: 10.1002/chem.200500275).

62 A. P. Kulkarni, X. Kong, and S. A. Jenekhe, *J. Phys. Chem. B,* **2004**, *108*, 8689–8701. (DOI: 10.1021/jp037131h).

63 X. Chen, H.-E. Tseng, J.-L. Liao, and S.-A. Chen, *J. Phys. Chem. B*, **2005**, *109*, 17496–17502. (DOI: 10.1021/jp052549w).

64 M. Kuik, G. -J. A. H. Wetzelaer, J. G. Laddé, H. T. Nicolai, J. Wildeman, J. Sweelssen, and P. W. M. Blom, *Adv. Funct. Mater*., **2011**, *21*, 4502–4509. (DOI: 10.1002/adfm.201100374).

65 K. L. Chan, M. Sims, S. I. Pascu, M. Ariu, A. B. Holmes, and D. D. C. Bradley, *Adv. Funct. Mater.*, **2009**, *19*, 2147–2154. (DOI: 10.1002/adfm.200801792).

66 B. Arredondo, B. Romero, A. Gutiérrez-Llorente, A. I. Martínez, A. L. Álvarez, X. Quintana, and J. M. Otón, *Solid-State Electronics*, **2011**, *61*, 46–52. (DOI:10.1016/j.sse.2011.02.004).

67 Q. J. Sun, B. H. Fan, Z. A. Tan, C. H. Yang, and Y. F. Lia, and Y. Yang, *Appl. Phys. Lett*., **2006**. *88*, 163510. (DOI: org/10.1063/1.2197318).

68 S. Panozzo, J. -C. Vial, Y. Kervella, and O. Stéphan, *J. Appl. Phys*., **2002**, *92*, 3495–3502. (DOI:10.1063/1.1502920).

69 J.-R. Wu, Y. Chen, and T.-Y. Wu, *J. Appl. Polym. Sci*., **2011**, *119*, 2576–2583. (DOI 10.1002/app.32705).

70 H. Wang, J. Yang, J. Sun, Y. Xu, Y. Wu, Q. Dong ,W.-Y. Wong, Y. Hao, X. Zhang, and H. Li, *Macromol. Chem. Phys*., **2014**, *215*, 1060−1067. (DOI: 10.1002/macp.201400070).

71 M. Knaapila and A. P. Monkman, *Adv. Mater*., **2013**, *25*, 1090–1108. (DOI: 10.1002/adma.201204296)

72 A. Perevedentsev, S. Aksel, K. Feldman, P. Smith, P. N. Stavrinou, and D. D. C. Bradley, *J. Polym. Sci. B: Polym. Phys*., **2015**, *53*, 22–38. (DOI: 10.1002/polb.23601).

73 C. Wu and and J. McNeill, *Langmuir*, **2008**, *24*, 5855–5861. (DOI: 10.1021/la8000762).

74 L. Huang, L. Zhang, X. Huang, T. Li, B. Liu, and D. Lu, *J. Phys. Chem. B*, **2014**, *118*, 791–799. (DOI: 10.1021/jp406598x).

75 A. M. Brouwer, *Pure. Appl. Chem*., **2011**, *83*, 2213–2228. (DOI:10.1351/PAC-REP-10-09-31).

76 W-J. Li, B. Liu, Y. Qian, L-H. Xie, J. Wang, S-B. Li, and W. Huang, *Polym. Chem*., **2013**, *4*, 1796–1802. (DOI: 10.1039/C2PY20971C).

77 Gaussian 09, Revision A02, M. J. Frisch, G. W. Trucks, H. B. Schlegel, G. E. Scuseria, M. A. Robb, J. R. Cheeseman, G. Scalmani, V. Barone, B. Mennucci, G. A. Petersson, H. Nakatsuji, M. Caricato, X. Li, H. P. Hratchian, A. F. Izmaylov, J. Bloino, G. Zheng, J. L. Sonnenberg, M. Hada, M. Ehara, K. Toyota, R. Fukuda, J. Hasegawa, M. Ishida, T. Nakajima, Y. Honda, O. Kitao, H. Nakai, T. Vreven, J. A. Montgomery Jr., J. E. Peralta, F. Ogliaro, M. J. Bearpark, J. Heyd, E. N. Brothers, K. N. Kudin, V. N. Staroverov, R. Kobayashi, J. Normand, K. Raghavachari, A. P. Rendell, J. C. Burant, S. S. Iyengar, J. Tomasi, M. Cossi, N. Rega, N. J. Millam, M. Klene, J. E. Knox, J. B. Cross, V. Bakken, C. Adamo, J. Jaramillo, R. Gomperts, R. E. Stratmann, O. Yazyev, A. J. Austin, R. Cammi, C. Pomelli, J. W. Ochterski, R. L. Martin, K. Morokuma, V. G. Zakrzewski, G. A. Voth, P. Salvador, J. J. Dannenberg, S. Dapprich, A. D. Daniels, Ö. Farkas, J. B. Foresman, J. V. Ortiz, J. Cioslowski, and D. J. Fox, Gaussian, Inc., Wallingford CT, 2009.

78 A. D. Becke, *Phys. Rev. A*, **1988**, *38*, 3098–3100. (DOI: org/10.1103/PhysRevA.38.3098).

79 A. D. Becke, *J. Chem. Phys.,* **1993**, *98*, 5648–5652. (DOI: 10.1063/1.464913).

80 C. Lee, W. Yang, and R. G. Parr, *Phys. Rev. B*, **1988**, *37*, 785–789. (DOI: org/10.1103/PhysRevB.37.785).

CHAPTER 5

Direct Sulfonylation of 2,7-Dibromofluorene and 4-Sulfonyl-substituted Polyfluorenes

5.1 Introduction

In previous Chapters 3 and 4 we have described the functionalisation of the fluorene moiety with different groups at position 4 and the preparation of polymers from such fluorenes. One of the approaches in Chapter 3 was based on the nitration of 2,7-dibromofluorene (**3.22**) as a first step in the multi-step reaction to the target monomers, following transformation of the NO_2 group into other functional groups. It might be interesting to look at other reactions of electrophilic aromatic substitution (S_EAr reactions) for functionalisation of the fluorene moiety at position 4. From these, direct introduction of the sulfonyl substituent might represent an interest because SO_2 is quite a strong electron-withdrawing group for tuning the LUMO/HOMO energies of the molecules and many conjugated materials (from small molecules to polymers) with sulfonyl functionality show highly efficient photoluminescence (in contrast, e.g. to the nitro group or carbonyl group, which often increase contributions from non-radiative pathways of an excited state relaxation and therefore quench the emission). Therefore, we have decided to study the reaction of 2,7-dibromofluorenes with chlorosulfonic acid to expand the methods of functionalisation of fluorene monomers at position 4. The choice of this reaction was, particularly, dictated by possibilities of further functionalisation of the introduced 4-SO_2Cl substituent with many other functional groups by replacing the chlorine atom and thus expanding the range of available functionalities at position 4.

Before we start the description of our work in this field, here is presented a brief overview on some fluorescent polymers and small conjugated molecules containing the sulfonyl group, -SO_2R, in their structures and applications of these materials in organic electronics. Considering a large number of such works and structures in the literature, this is not aiming to present a comprehensive review on the subject but rather to give some taste toward such kind of materials and functionalisation.

5.1.1 Thiophene-S,S-dioxide oligomers and polymers

Barbarella and co-workers first performed a range of pioneering studies to introduce thiophene-*S,S*-dioxides as electron-deficient building blocks into conjugated oligomers and polymers in materials for organic electronics.[1,2,3,4] In contrast to the parent oligothiophenes, which are electron-rich and thus easily oxidised materials, oligomers with thiophene-*S,S*-dioxides are easily reduced materials. They widely studied oligothiophene-S,S-dioxides and have also shown that these materials possess substantially higher photoluminescence (and electroluminescence) efficiency compared to the parent oligothiophenes.[5,6,7] Also, for some of those materials an interesting phenomenon of substantially higher PLQY in the solid state compared to the solution was demonstrated (Figure 5.1).[5,6,8]

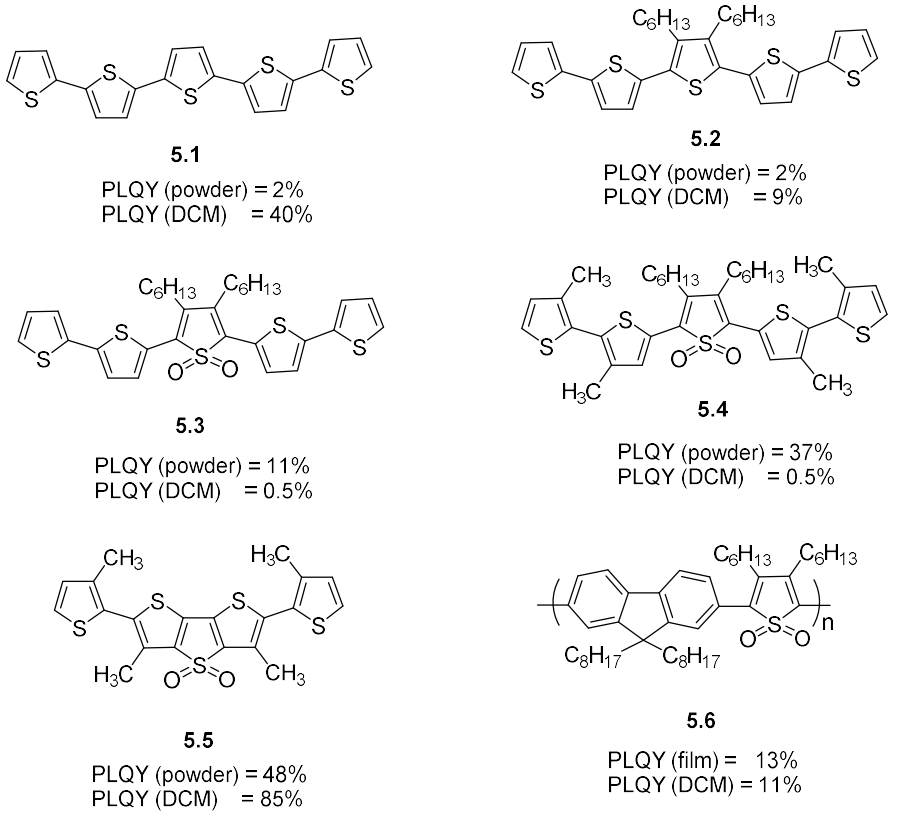

Figure 5.1 Comparison of PLQY in solution and in the solid state for selected oligomers and polymers with thiophene-S,S-dioxide units (**5.1**–**5.6**).[5,6,8]

Moreover, their emission can be efficiently tuned through the visible range from blue to deep red (or even near infrared) by a combination of electron-rich building blocks (thiophenes and others) with electron-deficient thiophene-*S,S*-dioxides (Figure 5.2).[8]

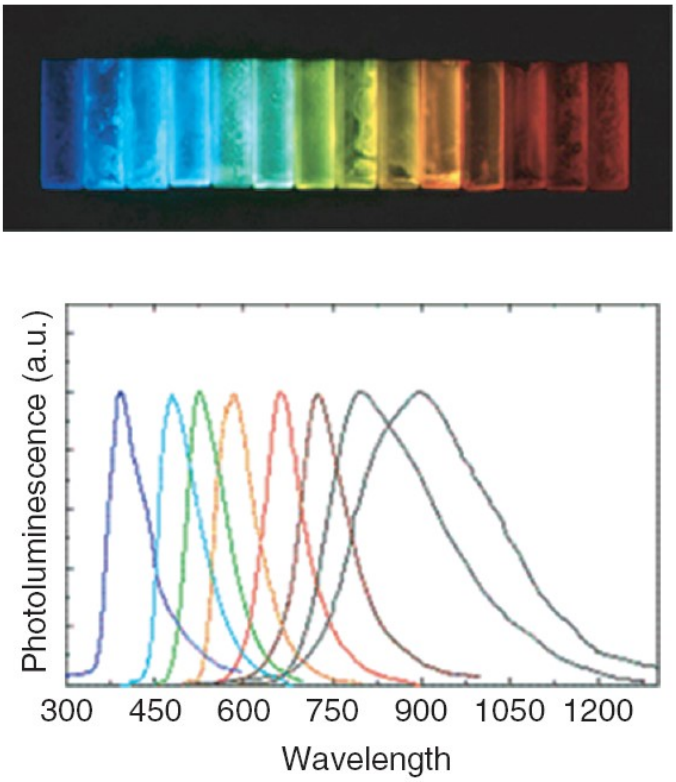

Figure 5.2 Colour emissions of different oligomers and polymers containing thiophene-S,S-dioxide building blocks (top) and normalised PL emission spectra of cast films from $CHCl_3$ obtained by irradiation with a single light source, λ_{exc} = 364 nm (bottom). Each colour in the visible region corresponds to different oligomers (all compounds emitting at wavelengths greater than 700 nm are polymers).[8]

5.1.2 Blue-emitting phenylene copolymers with sulfonyl groups

Wegner et al. introduced sulfonyl substituents into fluorene-phenylene copolymers and reported that the sulfonyl groups facilitate the anti-oxidation of the materials and improve the spectral stability of these blue light emitting materials.[9] Copolymers **5.7** and **5.8** were synthesised by Suzuki polycondensation reaction (Figure 5.3). They are well soluble in common organic solvents, absorb light at 350 nm and emit at ~410–413 nm (Figure 5.3).

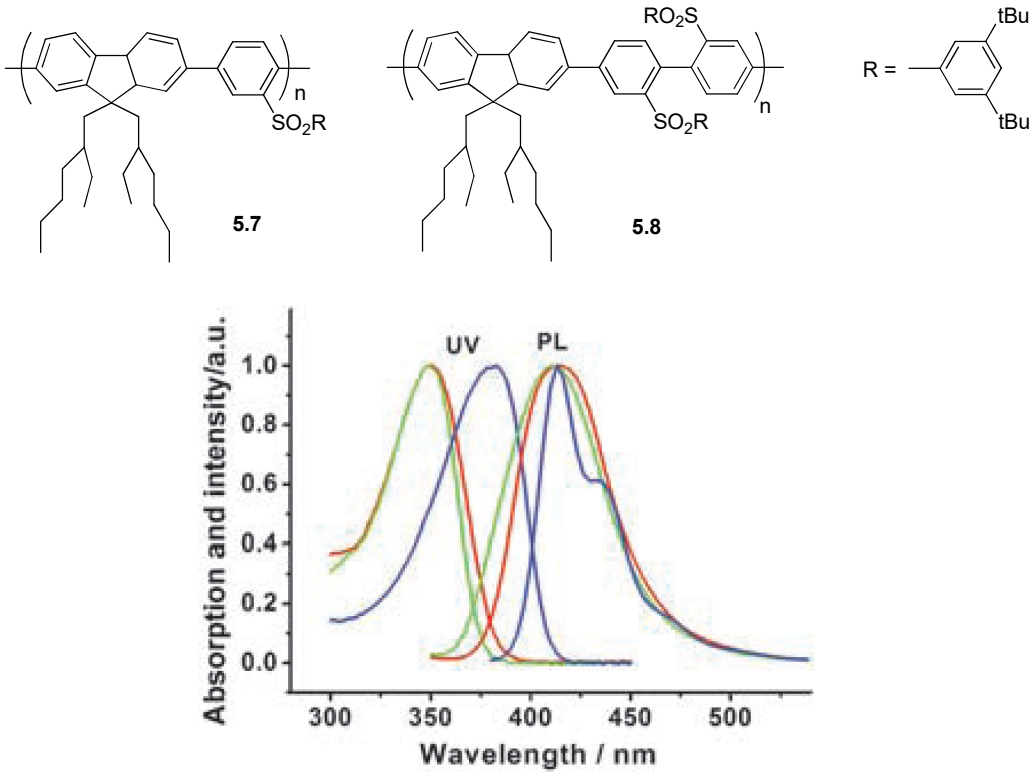

Figure 5.3 (top) Fluorene-phenylene copolymers **5.7** and **5.8** with sulfonyl groups in the side chains and (bottom) UV absorption and PL emission spectra of these copolymers (**5.7** is shown by the red line, **5.8** by the green line and **PF8** by the blue line).[9]

Polymers **5.7** and **5.8** exhibited a nematic liquid crystalline phase and have higher energy band gaps compared to poly(9,9-dioctylfluorene) (**PF8**) (*cf* their absorptions (red edge energies) in Figure 5.3). Also, they showed improved spectral stabilities compared to **PF8** (this issue in **PF8** has been discussed in Chapter 2), with no spectral change on annealing the films of polymers **5.7** and **5.8** even at high temperature (Figure 5.4).

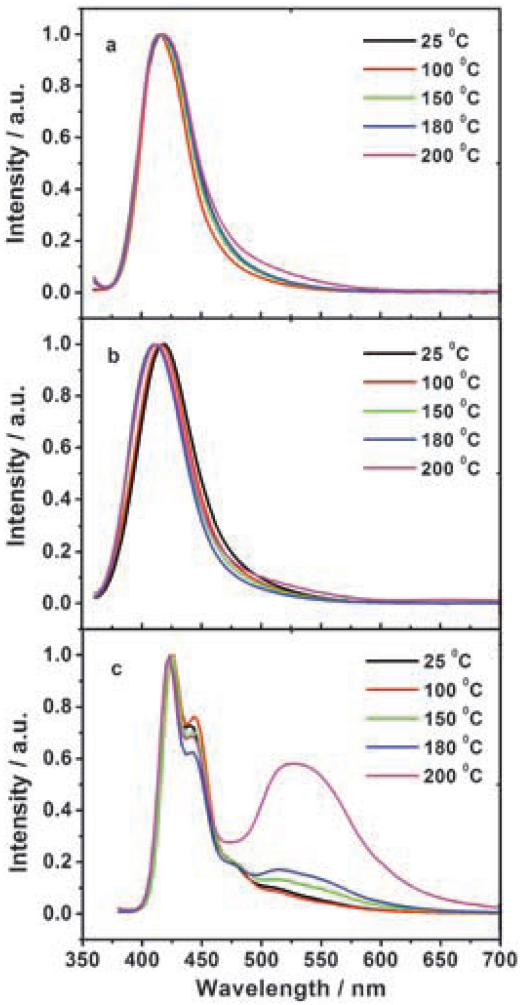

Figure 5.4 PL emission spectra of copolymers **5.7** (a) and **5.8** (b) on thermal annealing of their films in the air, in comparison with that for **PF8** (c).[9]

5.1.3 Dibenzothiophene-S,S-dioxide–containing oligomers and polymers

In 2005, Perepichka and Bryce introduced dibenzothiophene-*S,S*-dioxide (**5.9**) as a prominent building block for organic electronic materials.[10] The idea was that it was topologically similar to the fluorene moiety, in which the $C(R_2)$ bridge between the phenylene moieties is replaced by an electron-deficient SO_2 bridge, thereby decreasing the LUMO energy and giving the materials a higher electron affinity (by 1.04 eV for the monomer **5.9** and by ~0.5–0.6 eV for the co-oligomers **5.10, 5.11**). Some of these oligomers are shown in (Figure 5.5).

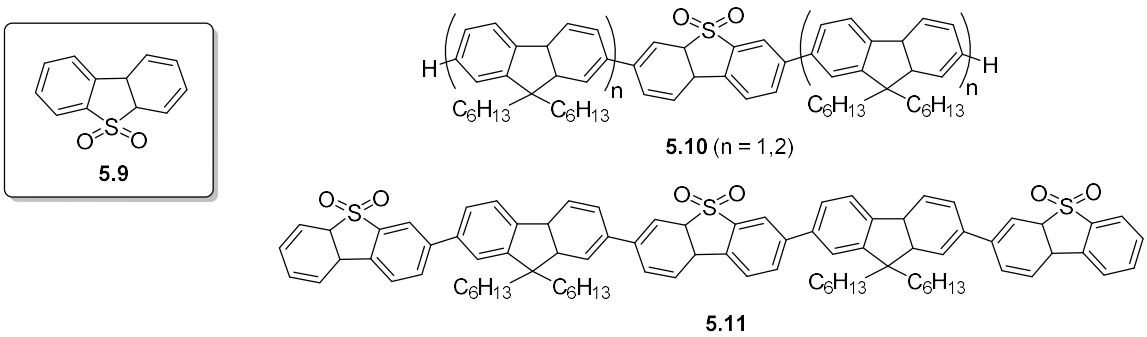

Figure 5.5 Dibenzothiophene-*S,S*-dioxide – fluorene co-oligomers.[10]

Moreover, these oligomers have been shown to be highly emissive (PLQY 65–67% in chloroform solution, 44–65% in the solid state),[10] so the dibenzothiophene-S,S-dioxide electron-deficient moiety did not quench the emission compared to the fluorenone moiety. It was also shown that in such oligomers and copolymers of compound **5.9** with the 9,9-dioctylfluorene building blocks, simultaneous emission from both the locally excited states (LE) and the intramolecular charge-transfer state (ICT) is observed,[11,12] which was used for the design of electroluminescent materials with a broadened emission as a novel approach towards white-light emitting electroluminescent polymer devices (WPLED).[13]

Many other research groups have used building block **5.9** for the construction of a wide range of emissive conjugated materials. Cao et al. reported on a series of fluorene – dibenzothiophene-*S,S*-dioxide copolymers **5.12–5.20** (Figure 5.6) as highly efficient and spectrally stable blue light emitters with decreased LUMO energy levels and enhanced electron transport in the materials.[14]

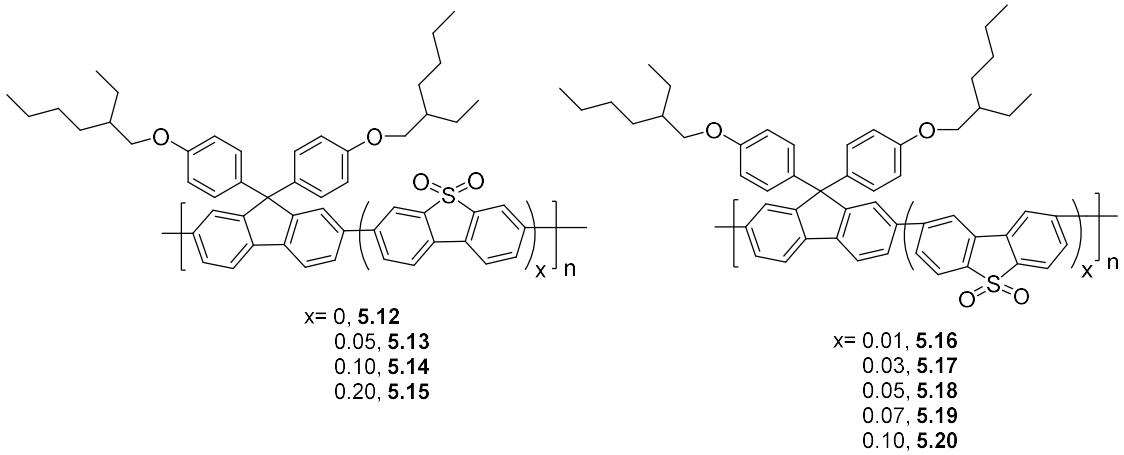

Figure 5.6 Dibenzothiophene-*S,S*-dioxide related polyfluorenes (**5.12**–**5.20**).[14]

The copolymers **5.13–5.20** were readily soluble in common organic solvents and showed a higher thermal stabilities compared to the polyfluorene **5.12**, which increased the number of **5.9** units in the main chain. Decreasing their LUMO energy levels due to **5.9** fragments made them more stable toward oxidation, giving stable PL emission with an absence of the green band appearing on thermal annealing, as was often observed for the polyfluorenes. More stable EL emission was observed for the fabricated OLED devices (Figure 5.7).

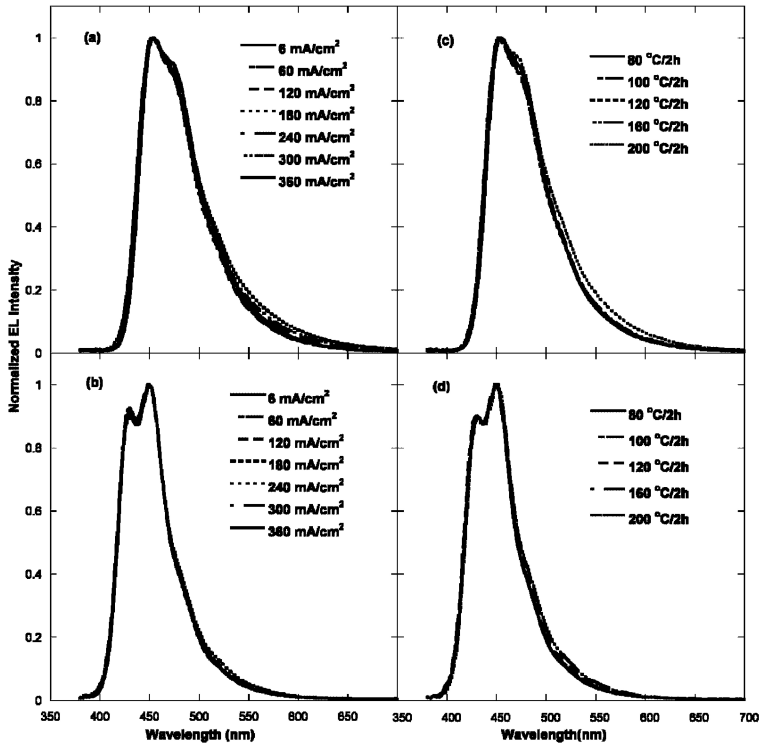

Figure 5.7 Electroluminescence (EL) spectra of copolymers (**5.15**–**5.18)** with thermal annealing at various temperatures under different applied current densities.[14]

Similar copolymers have been reported by Bryce et al, in which alkyl groups have been inserted in moiety **5.9**, thereby slightly increasing the dihedral angle between units in the backbone and allowing a higher content of dihexyldibenzothiopehene-*S,S*-dioxide units into the polymer chain (Figure 5.8).[15] This gave materials with more deep blue emission (e.g. λ_{PL} = 420 nm for **5.23** compared to 450–46-nm for "non-alkylated" analogues) and increased PLQY (~50%).

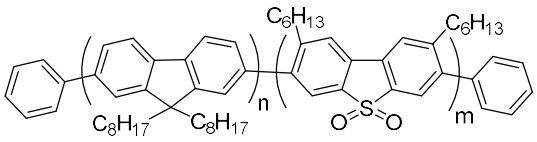

n:m 85:15, **5.21**
n:m 70:30, **5.22**
n:m 50:50, **5.23**

Figure 5.8 2,8-Dialkyldibenzothiophene-*S,S*-dioxide–fluorene copolymer **5.21–5.23**.[15]

Another example of similar types of materials are deep blue fluorescent copolymers **5.24–5.30**, which have been studied as active layers in polymer OLEDs (Figure 5.9).[16] Here the effect of conjugated ("para") / non-conjugated ("meta") linkages has been studied on the emission properties and device efficiencies.

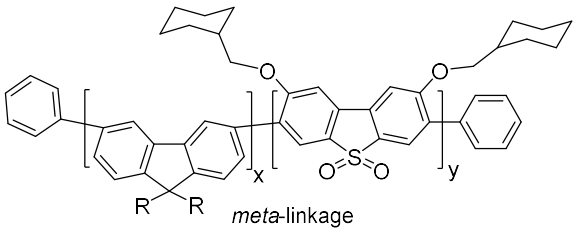

meta-linkage

x = 50: y = 50, **5.24**
x = 70: y = 30, **5.25**
x = 85: y = 15, **5.26**
R = n-C_6H_{13}

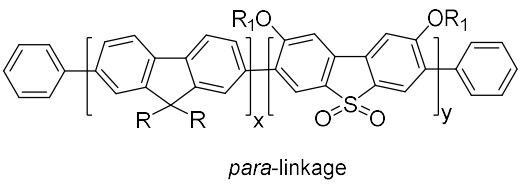

para-linkage

R = n-C_6H_{13}, R_1 = CH_2Cy, x = 50: y = 50, **5.27**
n-C_6H_{13}, R_2 = CH_2Cy, x = 70: y = 30, **5.28**
R, R_1= n-C_6H_{13} x = 50: y = 50, **5.29**
R, R_1= n-C_6H_{13} x = 70: y = 30, **5.30**

Figure 5.9 Dibenzothiophene-*S,S*-dioxide copolymers with "meta" (**5.24**–**5.26**) and "para" linkage (**5.27**–**5.30**) at the fluorene sites.[16]

Yang et al. reported an improved spectral stability of dibenzothiophene-*S,S*-dioxide – carbazole and – benzothiadiazole copolymers **5.31**–**5.39** which were synthesised by Suzuki polycondensation (Figure 5.10).[17,18] These copolymers showed higher thermal stability (T_d = 440 °C) compared to related polycarbazoles (T_d = 385 °C). Their HOMO and LUMO energy levels were gradually reduced with an increase of **5.9** units in the main chain. OLED devices based on these materials have been tested.

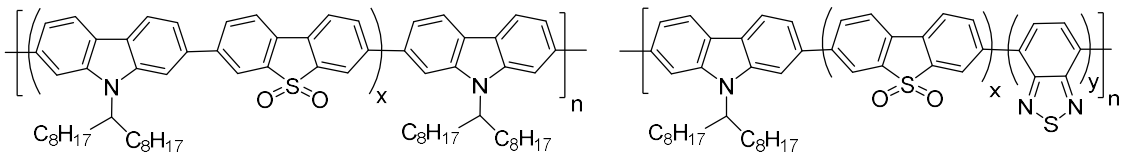

Figure 5.10 Dibenzothiophene-*S,S*-dioxide–carbazole and –benzothiadiazole copolymers **5.31**–**5.39**.[17]

Dias, Bryce and Monkman reported dibenzothiophene-S,S-dioxide-containing molecules **5.40** and **5.41** as ambipolar donor-acceptor-donor systems for tuning the intramolecular charge transfer emission from deep blue to red upon manipulation of conjugation and strength of the electron donor units (Figure 5.11).[19] Here the molecules **5.40** and **5.41** on the substitution of carbazole and arylamine units shift the emission from the blue to the red region. Such compounds have been studied and confirmed as extremely efficient (100%) triplet energy harvesters for thermally activated delayed fluorescence (TADF).

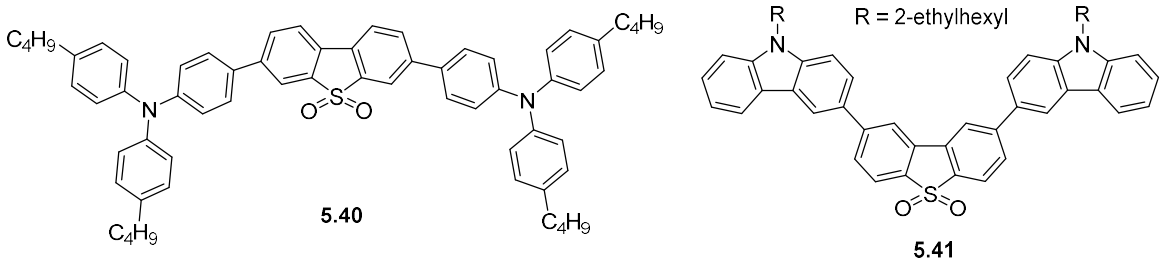

Figure 5.11 Dibenzothiophene-*S,S*-dioxide derivatives **5.40** and **5.41**).[19]

Huang et al. reported another series of dibenzothiophene–based phosphine oxide compounds to be used as host and electron transporting materials for the construction of efficient blue TADF materials.[20] The Patel group synthesised and compared two fluoroanthene derivatives **5.42** and **5.43** (consisting dibenzothiophene-*S,S*-dioxide and diphenylsulfone bridges) (Figure 5.12). Both materials showed extremely high thermal stability (>500 °C), emitting in the blue region (454–460 nm) and have been used as light emitting and electron transporting materials.[21]

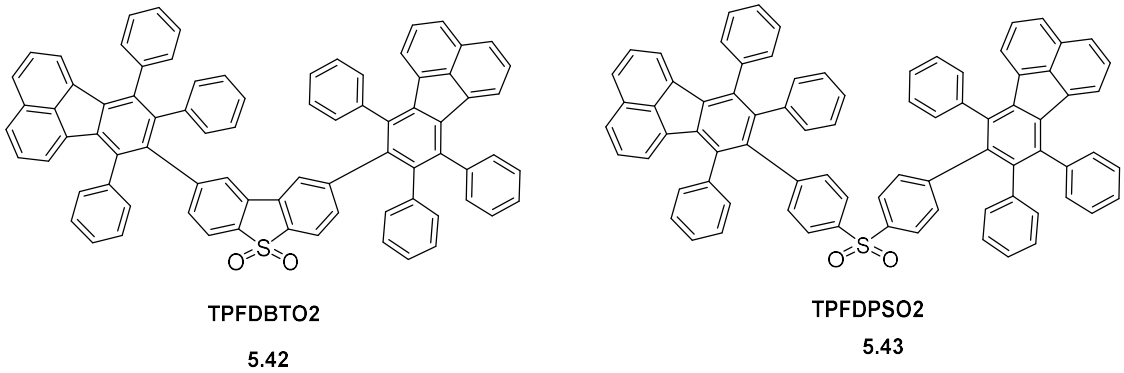

Figure 5.12 Sulfonyl derivatives **5.42** and **5.43**.[21]

Many other structural variations in dibenzothiophene-*S,S*-dioxide based novel copolymers and co-oligomers have been reported in the past decade for OLED and other organic electronic applications (e.g. in photovoltaics) (see e.g. Ref.[22,23,24,25,26,27,28,29,30,31,32,33,34,35] in the past two years).

5.1.4 Aims and research objectives

In Chapters 3 and 4, 4-substituted fluorene monomers and polymers with various EDG and EWG (OMe, SR, CCPh, F, CN, SO_2R, CO_2Bu) were described. Polymers with alkylsulfonyl groups showed bright blue emissions with high PLQY in both solution (Φ_{PL} = 73–88%) and solid state (Φ_{PL} = 31–36%) with improved electron affinity (decrease of LUMO by 0.77 eV (from DFT calculations) or ~0.5–0.6 eV (from CV data). Thus, sulfonyl groups on the fluorene core seemed a promising type of functionalisation for polyfluorenes resulting in the polymers with an improved electron affinity (low-lying LUMO energy orbitals) and blue emission with high PLQY values.

Therefore, we decided to extend the functionalisation of the fluorene moiety with an SO_2 group and perform studies on the direct introduction of the SO_2Cl substituent in position 4 of the fluorene monomers aiming to develop new convenient method to novel 4-substituted fluorene monomers. We also explored the possibility of the replacement of the reactive chlorine atom by a range of other functional groups, thus expanding the series of available 4-functionalised polyfluorenes. In this Chapter the reactions of 2,7-dibromofluorene (and its 9,9-dialkylated analogue) with chlorosulfonic acid are described together with the synthesis of some functional monomers (diethyl amide, phenyle ester), their polymerisation and studies of the properties of the resulting polymers **X-PF6** (X = SO_2NEt, SO_2OPh).

5.2 Results and Discussion

5.2.1 Synthesis of 2,7-dibromo-4,6-di(chlorosulfonyl)fluorene.

Aiming to introduce the 4-chlorosulfonyl group into the fluorene moiety to obtain the target compound **5.46**, the electrophilic substitution of 2,7-dibromo-9.9-dihexylfluorene (**5.45**) in the reaction with chlorosulfonic acid (using it as both the reagent and the solvent) were studied. Heating **5.45** in chlorosulfonic acid at 120 °C resulted in a fast reaction and the formation a dark brown mixture and an intense gas evolution (presumably HCl and/or SO_2), indicating that the reaction proceeded not only on the aromatic rings but also on the alkyl chains to give a complex mixture of products and a tag.

Therefore we studied the chlorosulfonation of non-alkylated fluorene **3.22** under the same conditions. The reaction worked well and in 30 minutes a white product started to precipitate. However, the product isolated after 2 h with a low yield (31%) was not the mono-substituted compound 2,7-dibromo-4-chlorosulfonylfluorene, but 4,6-di(chlorosulfonyl) derivative **5.44** (Scheme 5.1). The same product **5.44** was isolated in the reaction at 80–100 ^{o}C, with a better yield of 67%. Its structure was confirmed by ^{1}H and ^{13}C NMR and MS spectra. Bacause the signals in the ^{1}H NMR were broadened with no clear J values (even for meta-coupling), The ^{1}H-^{1}H COSY experiments were performed to assign the 4 different types of protons in the aromatic region. These experiments clearly showed that after chlorosulfonation at position 4, the second chlorosulfonyl group is introduced at the other benzene ring in position 6 (Figure 5.13). Basing on these experiments, the reaction was then performed in less harsh conditions hoping to achieve selective mono-chlorosulfonation at the desired position 4. However, performing the experiments at room temperature or at 0 ^{o}C, dilution of chlorosulfonic acid with chloroform (up to 6× times dilution), as well as experiments with decreased amount of chlorosulfonic acid (from 40 eq. to 5 eq) and performing the reaction at room temperature for 64 h, in all cases gave disubstituted compound **5.44** as a major product in the crude material (70–80% purity). From these experiments, we concluded that chlorosulfonic acid is extremely reactive in this electrophilic substitution in 2,7-dibromofluorene, and selective mono-substitution requires even more gentle conditions (see discussions in the next section).

Considering that disubstitution worked well under very mild conditions, we checked again the chlorosulfonation of dialkylated fluorene **5.45** at room temperature and successfully isolated di(chlorosulfonyl) fluorene **5.47** (Scheme 5.1).

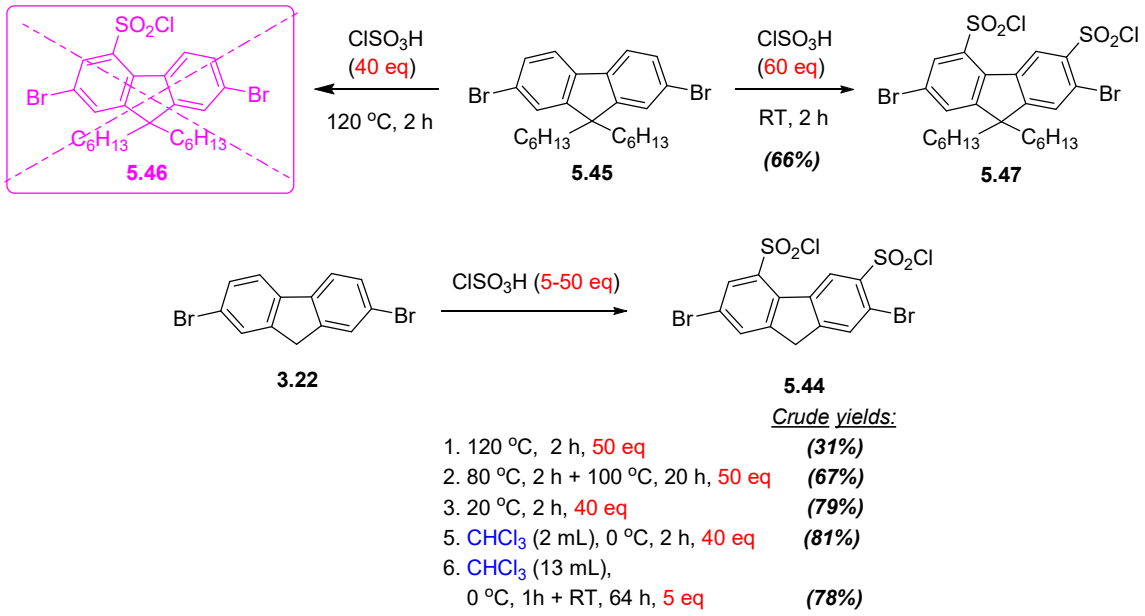

Scheme 5.1 Chlorosulfonation of 2,7-dibromofluorenes **3.22** and **5.45** with chlorosulfonic acid to yield 4,6-di(chlorosulfonyl)-substituted products **5.44** and **5.47**

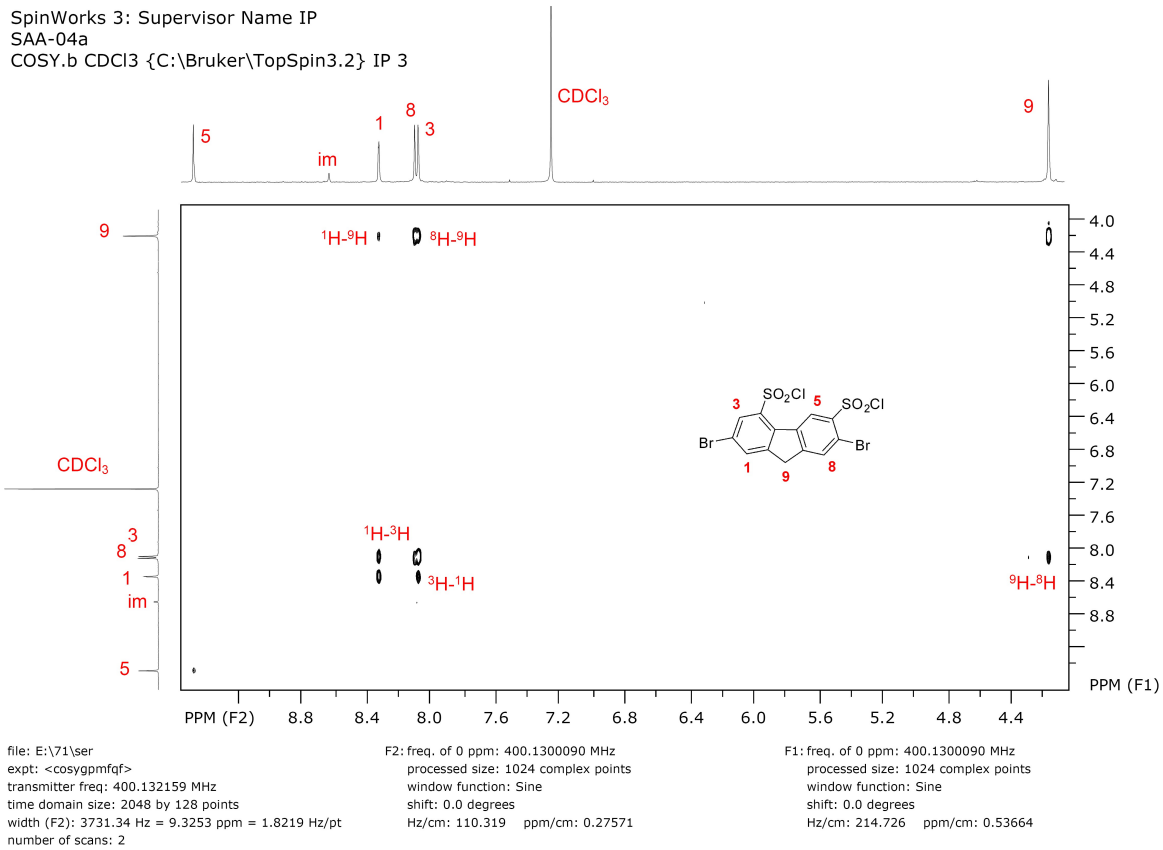

Figure 5.13 ^{1}H-^{1}H COSY spectrum of 2,7-dibromo-4,6-di(chlorosufonyl)fluorene (**5.44**) showing proton correlations.

5.2.2 Synthesis of 2,7-dibromo-4-chlorosulfonylfluorene and other 4-sulfonyl-substituted 2,7-dibromofluorenes

Considering that disubstitution occurred under very mild conditions, selective mono-substitution with just 1.0–1.2 equivalents of chlorosulfonic acid was performed. This, however, gave not the target chlorosulfonyl-fluorene **5.49**, but the acid **5.48** as a mixture with the starting compound **3.22** (from NMR data of the crude product). In a further optimisation of the reaction, selective monosubstitution succeeded at position 4 using 5 equivalents of chlorosulfonic acid diluted with chloroform at 0 °C for 2 h, but again, instead of the expected chlorosulfonyl derivative **5.49**, fluorenesulfonic acid **5.48** was isolated with the 80% yield (Scheme 5.2). Therefore, in the next step the acid **5.48** was converted into its chloroanhydride **5.49** by treatment with $PCl_5/POCl_3$. Chlorosulfonyl-fluorene **5.49** was then converted into diethylamide **5.50**, which was then alkylated at position 9 with 1-bromooctane, similarly to the methodology used in Chapter 3 for other 4-substituted fluorenes, to obtain monomer **5.51** (Scheme 5.2)

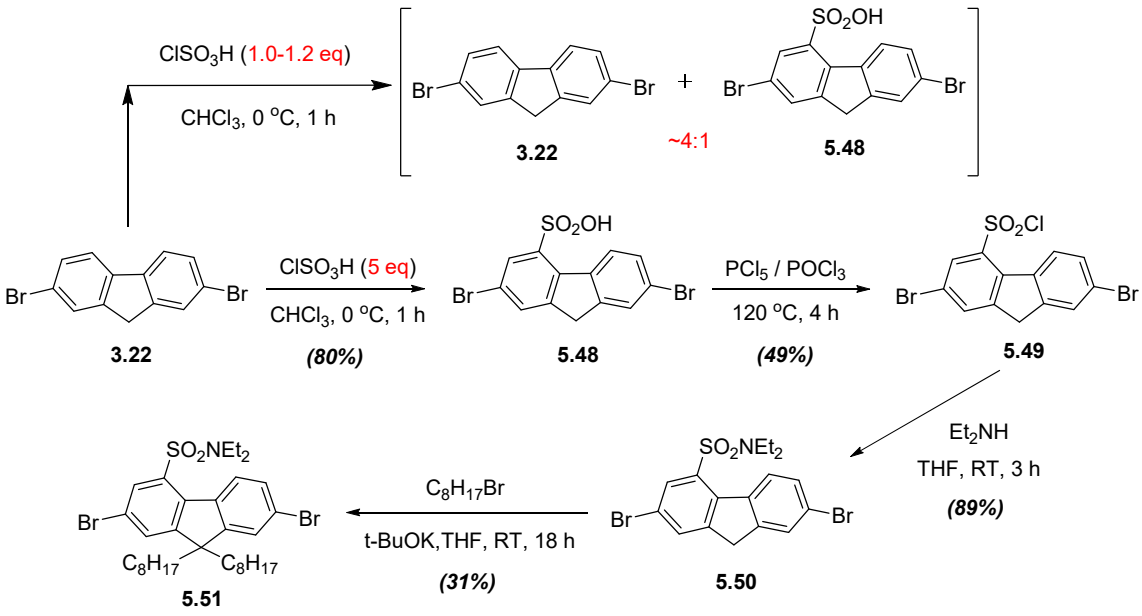

Scheme 5.2 Monosulfonation of dibromofluorene **3.22** and further reactions to access derivatives **5.48–5.51**.

Considering that chlorosulfonation of 2,7-dibromo-9,9-dihexylfluorene (**5.45**) to afford the disubstituted compound **5.47** at ambient temperature worked well, with no reaction on the alkyl chains (Scheme 5.1), we performed its mono-chlorosulfonation in conditions similar to those shown in Scheme 5.2 for the synthesis of compound **5.48** and obtained a similar fluorene-4-chlorosulfonic acid **5.52** (Scheme 5.3). Due to the inconvenience of

purifying the crude product, obtained with a yield >100% (by weight), we converted it into the sodium salt **5.53** and on further reacting with $PCl_5/POCl_3$, the target key intermediate for 4-sulfonyl-substituted fluorene monomers, i.e. 2,7-dibromo-4-chlorosulfonyl-9,9-dihexylfluorene (**5.54**), was isolated with a yield of 65% in 3 steps. This product was then used to replace nucleophilically the chlorine atom and to prepare two derivatives, with phenoxy- (**5.55**) and diethylamino-groups (**5.56**), both with high yields of 84–85% (Scheme 5.3). These two compounds have been used as monomers for the synthesis of 4-sulfonyl-functionalised fluorene polymers.

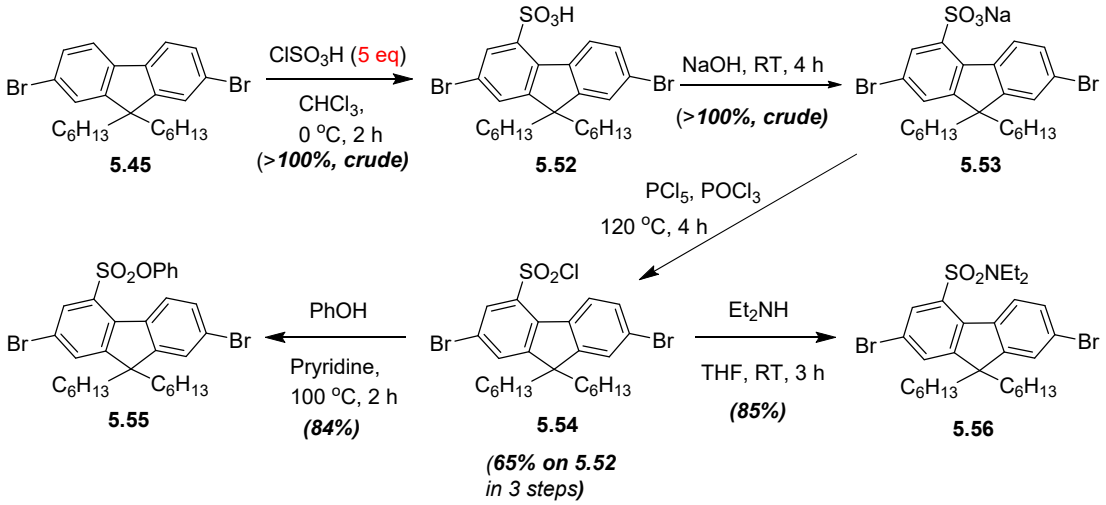

Scheme 5.3 Synthetic route to 4-sulfonyl-substituted fluorene monomers **5.55** and **5.56** from 2,7-dibromo-9,9-dihexylfluorene **5.45.**

5.2.3 Synthesis and characterisation of 4-sulfonyl-substituted polyfluorenes XSO_2-PF6 (X = Et_2N, $PhOSO_2$)

Synthesis of polyfluorenes with Et_2NSO_2- and $PhOSO_2$- functionalities at position 4 was performed by Ni-mediated Yamamoto polycondensation, similar to that used in the synthesis of other 4-substituted polyfluorenes in Chapter 4. The reaction is presented in Scheme 5.4.

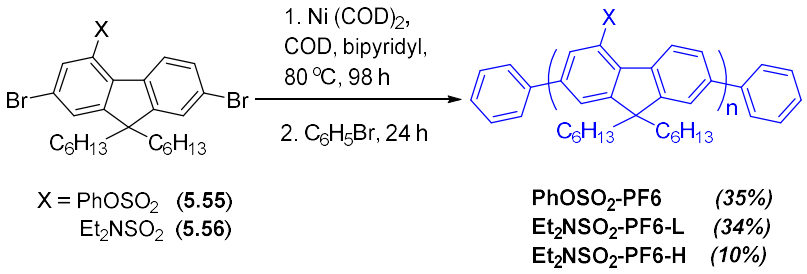

Scheme 5.4 Synthesis of poly(4-sulfonyl-9,9-dihexylfluorenes) **Et_2NSO_2-PF6** and **$PhOSO_2$-PF6**

One specific feature here is that polymer **Et_2NSO_2-PF_6** obtained from monomer **5.56** was more soluble in polar solvents compared to the other polymers synthesised in this work and the other unsubstituted polyfluorenes **PF8/PF6**. The reason for that is the presence of highly polar and hydrophilic diethylaminosulfonyl substituent (and, possibly, partly the shorter alkyl chain on the C-9 atom, thus their hydrophobic effect is less expressed compared to the octyl groups). On extraction of the crude polymer in Soxhlet apparatus, a substantial amount of the product was extracted with acetone (which was normally used in the previous purifications of polyfluorenes to remove low molecular weight fractions from the polymer). However, GPC analysis showed rather high molecular weight for the acetone soluble fraction (M_n = 16,000 Da). Further extraction of the acetone-insoluble residue in a Soxhlet apparatus using chloroform gave another, higher molecular weight fraction (M_n = 27,000 Da, Table 5.1). Hence, two fractions of **Et_2NSO_2-PF_6** polymer with different molecular weights have been isolated.

For the obtained polymer **$PhOSO_2$-PF6**, the molecular weight was even lower (M_n = 8,700 Da). Considering that other **X-PF8** polymers described in Chapter 4 have been obtained with higher molecular weights, we assumed that it was not due to the $PhOSO_2$ group but more likely an effect of the reaction conditions, and on further optimisation this polymer can be obtained with substantially higher molecular weight. Nevertheless, calculation of an average length of polymer chains from their M_n values and the molecular weight of repeating units gave the values of n = 18, 34 and 58 fluorene units for polymers **$PhOSO_2$-PF6**, **Et_2NSO_2-PF-L**, and **Et_2NSO_2-PF-H,** respectively. Thus, in all the cases the length of the polymer chain is higher than the effective conjugation length limit in polyfluorenes (n ~12[36]) and therefore the properties of all synthesised materials should characterise the polymeric properties of these structures.

The structures of **Et_2NSO_2-PF6** and **$PhOSO_2$-PF6** polymers have also been confirmed by ^{1}H NMR spectroscopy, which (similar to other polymers described in Chapter 4) have been compared to the corresponding ^{1}H NMR spectra of the parent monomers. As expected, **Et_2NSO_2-PF6** and **$PhOSO_2$-PF6** polymers showed broadened signals of the aromatic and aliphatic protons in the predicted regions, which are slightly shifted down field compared to the parent monomers (shifts for aromatic protons are higher).

One thing that should be mentioned is the somewhat unexpectedly good solubility of the relatively high molecular weight (M_n = 16,000 Da) polymer fraction **Et_2NSO_2-PF6-L** in acetone. There is much interest in non-ionic light-emitting conjugated polymers soluble in highly polar solvents. Because most efficient conjugated polymers for OLEDs are hydrophobic and soluble in low polar solvents like toluene, chloroform and chlorobenzene,

there is a need for materials with orthogonal solubility (in polar, hydrophilic solvents) to prevent mixing the polymer layers in the preparation of multi-layer devices. In this respect, the results on the solubility of **Et_2NSO_2-PF6-L** in acetone might be a starting point for further design and developments of related polymers with improved solubility in polar solvents.

Table 5.1 GPC and TGA data for poly(4-sulfonyl-9,9-dihexylfluorenes) **XSO_2-PF6**

Polymer	M_w,[a] (Da)	M_n,[b] (Da)	PDI[c]	T_d,[d] (^oC)
$PhOSO_2$-PF6	12,600	8,700	1.44	404
Et_2NSO_2-PF6-L[e]	26,000	16,000	1.62	388
Et_2NSO_2-PF6-H[f]	43,000	27,000	1.59	390

[a] M_w is a weight average molecular weight; [b] M_n is a number average molecular weight. [c] Polydispersity index, PDI = M_w/M_n. [d] T_d is decomposition temperature measured at 5 % mass loss by TGA under N_2 atmosphere at heating rate 10 ^{o}C/min. [e] Low molecular fraction of polymer, soluble in acetone. [f] High molecular fraction of polymer, soluble in chloroform.

5.2.4 Thermal stability of Et_2NSO_2-PF6 and $PhOSO_2$-PF6 polymers

The thermal properties of the synthesised **XSO_2-PF6** polymers were estimated by TGA, showing their high stability, with decomposition temperatures of 388–390 ^{o}C for **Et_2NSO_2-PF6** and 404 °C for **$PhOSO_2$-PF6** (Figure 5.14). The thermal properties of these polymers are quite similar to those for other 4-substituted polyfluorenes described in Chapter 4 and are typical for other polyfluorenes reported in the literature.

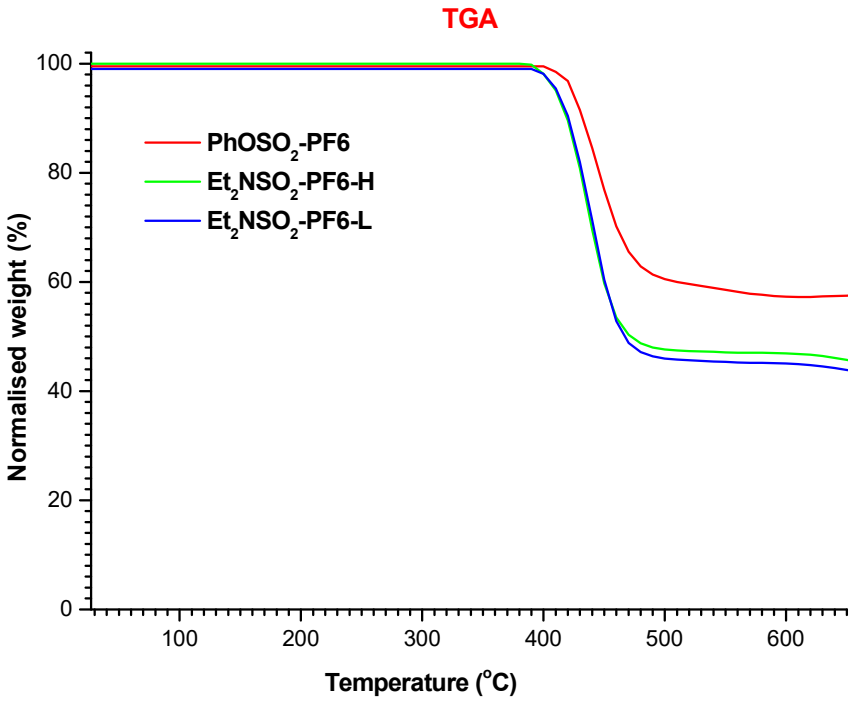

Figure 5.14 TGA traces of poly(4-X-sulfonyl-9,9-dihexylfluorenes) **Et_2NSO_2-PF6** and **$PhOSO_2$-PF6.**

5.2.5 Electron absorption and PL emission spectra of Et_2NSO_2-PF6 and $PhOSO_2$-PF6 polymers

In chloroform solution, both polymers absorb in the blue region, typical for polyfluorenes, with a bathochromic shift of 19–23 nm from **$PhOSO_2$-PF6** (λ_{max} = 385 nm) to **Et_2NSO_2-PF6** (λ_{max} = 404–408 nm) (Figure 5.15a). There are no, or relatively small (3–5 nm), shifts in their absorbances from solution to films (Figure 5.15b, Table 5.2).

Their emission spectra are also typical for polyfluorenes, while they are bathochromically shifted compared to unsubstituted **PF8** by 15–17 nm in solution and by 9–16 nm in films (*cf.* data in Tables 5.2 and 4.4). In chloroform solution, the first emission peak for all the polymers appears at near the same wavelength of λ_{PL} = 432–434 nm (Table 5.2; *cf.* with λ_{PL} = 433 nm for **$MeSO_2$-PF8** in toluene, Table 4.4), i.e. no bathochromic shift from **$PhOSO_2$-PF6** to **Et_2NSO_2-PF6** is observed in the PL in contrast to that observed for absorption spectra (from 385 to 408 nm, Table 5.2). Similar behaviour is observed for the films: a very small difference between **$PhOSO_2$-PF6** emissions (λ_{PL} = 436 nm) and **Et_2NSO_2-PF6** (λ_{PL} = 438–441 nm), with only a small bathochromic shift from solution to the solid state (4–8 nm, Table 5.2; *cf.* with a shift for **$MeSO_2$-PF8** of 12 nm, Table 5.2).

There are some differences in the relative intensities of PL vibronics of **Et_2NSO_2-PF6** polymers with different molecular weights: for higher molecular weight polymer **Et_2NSO_2-PF6-H,** the intensity of the 0-1 vibronic peak is slightly increased with respect to the 0-0 transition compared to the lower molecular weight polymer **Et_2NSO_2-PF6-H.** As this is observed for both solution and films, it is not an effect of the solid state packing, but an internal characteristics of the individual polymer chains.

The photoluminescence quantum yields for these polymers in solution are very high (Φ_{PL} = 88–91%), and are similar to those for other polyfluorenes studied in this work and to the unsubstituted polymers **PF8** and **PF6**.

Table 5.2 Absorption and PL maxima and PLQY values for **XSO_2-PF6** polymers in chloroform solution and in films,[a] and CIE coordinates of their PL emission in films.

Polymer	λ_{abs} $CHCl_3$ (nm)	λ_{abs} film (nm)	$\lambda_{PL,}$[b] $CHCl_3$ (nm)	$\lambda_{PL,}$[b] film (nm)	Φ_{PL}^{S},[c] $CHCl_3$ (%)[a]	Φ_{PL}^{F},[c] film (%)	CIE (x,y) coordinates, Films
$PhOSO_2$-PF6	296, 385	299, 382	432, 455sh	436, 460	88	(4)	0.18, 0.18
Et_2NSO_2-PF6-L[d]	404	404	433, 461, 493sh	441, 467, 496sh	90	14	–
Et_2NSO_2-PF6-H[d]	408	403	434, 461, 493sh	438, 465, 496sh	91	23	0.19, 0.22

[a] Spin-coated films from chloroform solution. [b] Samples have been excited at maxima of their absorption bands, λ_{abs}. [c] Φ_{PL}^{S} is PLQY measured in chloroform solution using DPA as reference (Φ_R = 90 %), Φ_{PL}^{F} is an absolute PLQY in film measured using an integrating sphere. [d] Letters L and H denote low-molecular weight (acetone-soluble) and high molecular weight (chloroform-soluble) fractions of this polymer.

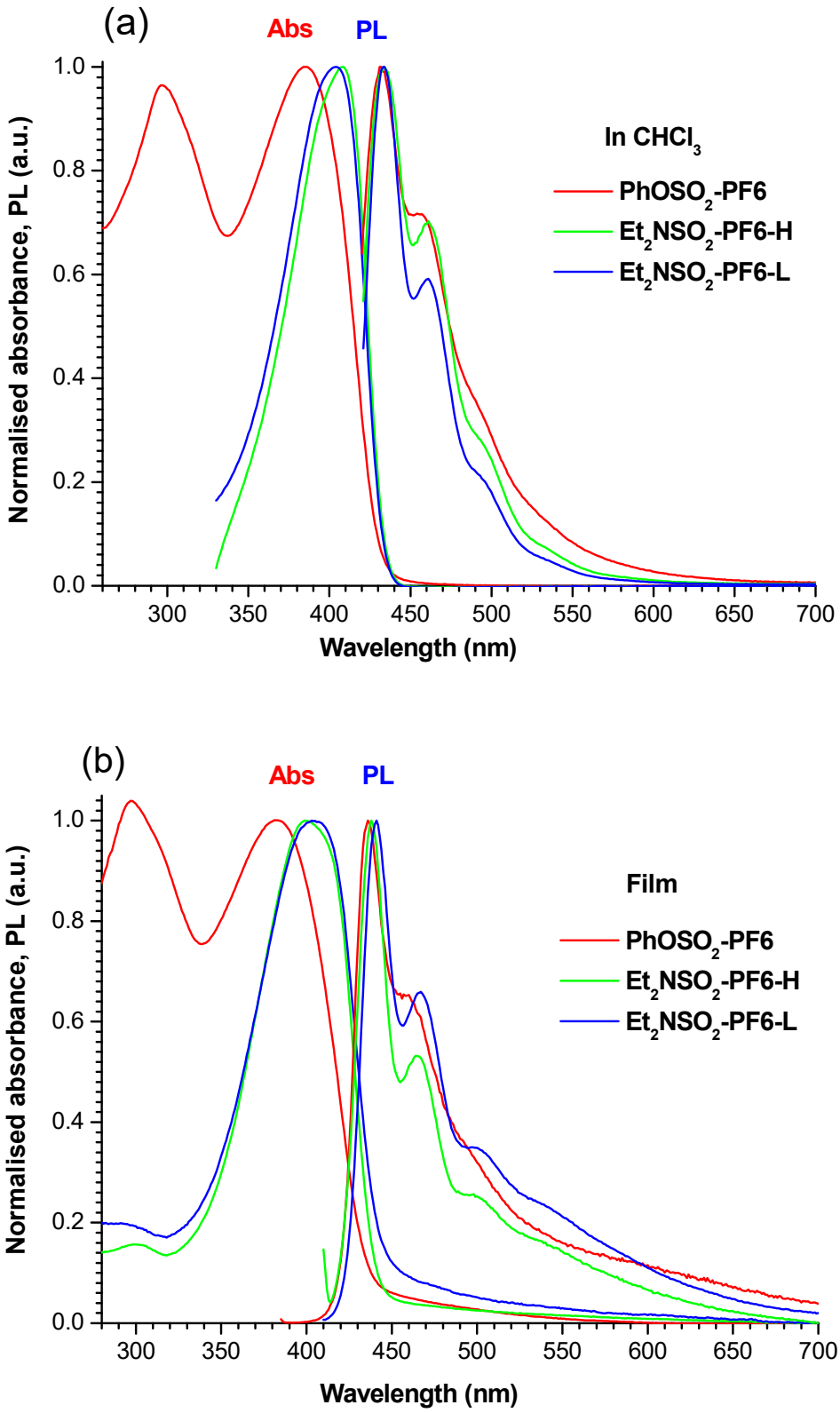

Figure 5.15 Normalised UV absorption and PL emission spectra of **XSO_2-PF6** polymers in chloroform solutions (a) and in films (b). For PL spectra, the samples have been excited at the maxima of their absorptions.

5.2.6 Electrochemical studies of Et_2NSO_2-PF6 and $PhOSO_2$-PF6

Cyclic voltammetry (CV) was used to assess the oxidation and the reduction potentials of the synthesised **XSO_2-PF6** (X = Et_2N, PhO) polymers for estimation of their HOMO/LUMO energy levels and the band gaps. The measurements have been done for the polymer films (deposited by drop casting on a glassy carbon electrode) in 0.1 M Bu_4NPF_6/CH_3CN under nitrogen. Both polymers exhibited elecroactivity in the p- and n-doping processes. In both cases, the doping processes were irreversible. For oxidation, clear peaks were observed in p-doping, whereas n-doping was observed at highly negative potentials as an increase of the cathodic currents. Due to the presence of the EWG groups, the **Et_2NSO_2-PF6** and **$PhOSO_2$-PF6** polymers showed the onsets of their reductions at less negative potentials (–2.35 and –2.25 V, respectively) compared to the unsubstituted polymer **PF8** (–2.64/–2.68 V vs Fc/Fc^+). They were also oxidised at more positive potentials (1.17 and 1.06 V, respectively) than **PF8** (0.96/1.00 V) (Figure 5.16, Table 5.3).

Table 5.3 Cyclic voltammetry data, HOMO/LUMO energy levels and band gaps of **XSO_2-PF6** (X = Et_2N, PhO) polymers

Polymer	E_g^{opt},[a] (eV)[a]	E^{ox}_{onset},[b] (V)	E^{red}_{onset},[b] (V)	HOMO[c] (eV)	LUMO[c] (eV)	E_g^{CV},[d] (eV)
Et_2NSO_2-PF6	2.76	1.17	–2.35	–5.97	–2.45	3.52
$PhOSO_2$-PF6	2.80	1.06	–2.25	–5.86	–2.55	3.31
PF8[37]	–	*0.97*[e]	*–2.64*[e]	*–5.77*	*–2.16*	*3.61*
PF8[38]	*2.95*	*1.00*[e]	*–2.68*[e]	*–5.8*	*–2.12*	*3.68*

[a] E_g^{opt} are optical band gaps estimated from the red edge of UV–Vis specta of polymer films. [b] E^{ox}_{onset} and E^{red}_{onset} are the onset potentials of oxidation and reduction of polymer films measured versus Fc/Fc^+ couple. [c] HOMO and LUMO energies calculated from empirical formulas HOMO (eV) = –e(E^{ox}_{onset} + 4.8) and LUMO = –e(E^{red}_{onset} + 4.8). [d] Electrochemical band gap E_g^{CV} = LUMO – HOMO. [e] CV data in Refs.[37,38] are given versus Ag/AgCl electrode; we have recalculated them to Fc/Fc^+ as $E(Fc/Fc^+) = E(Ag/AgCl) – 0.4$ V.

The HOMO and LUMO energy levels estimated from the onsets of their redox potentials, indicate that **Et_2NSO_2-PF6** and **$PhOSO_2$-PF6** are stronger acceptors (by 0.29–0.39 eV) and weaker donors (by 0.09–0.20 eV) compared to the unsubstituted **PF8** polymer[37] (Table 5.3). These new polymers also show some contraction of their electrochemical band gap compared to **PF8** (by 0.09–0.30 eV). Comparison of the optical energy gaps (E_g^{opt}) of **Et_2NSO_2-PF6** and **$PhOSO_2$-PF6** (estimated from the onsets of their absorptions in films)

with those for **PF8** also shows some band gap contraction due to an introduction of $PhOSO_2$ or Et_2NSO_2 groups into the polymers (by 0.15–0.19 eV), which is in good agreement with CV data. Optical energy gaps (E_g^{opt}) are lower than those from the electrochemical experiments (E_g^{CV}), but this is a commonly observed phenomenon discussed in previous sections, which is well documented in the literature (*cf.* literature data on E_g^{opt} and E_g^{CV} for **PF8** in Table 5.3).

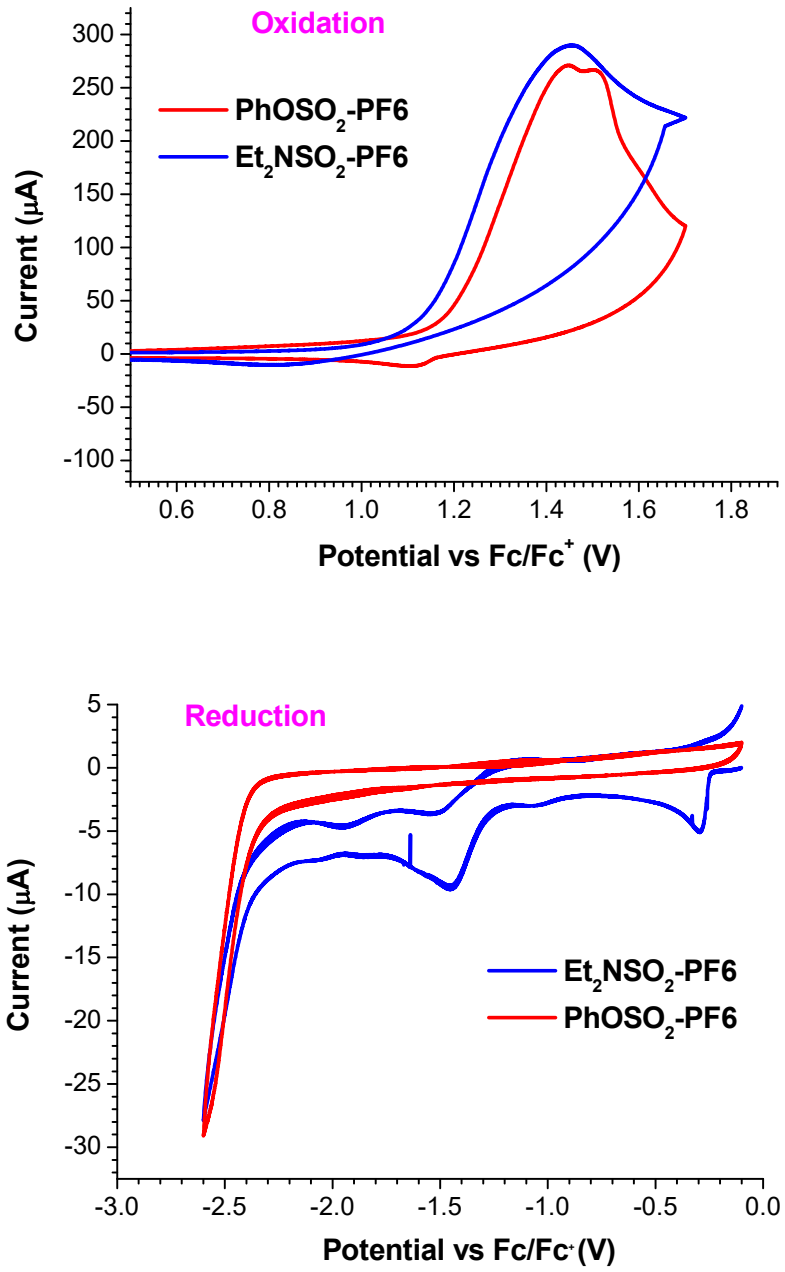

Figure 5.16. Cyclic voltammograms of the **Et_2NSO_2-PF6** and **$PhOSO_2$-PF6** polymers in films deposited onto glassy carbon electrodes in acetonitrile / 0.1 M of Bu_4NPF_6, scan rate 100 mV/s. Potentials were measured versus Ag/Ag^+ and calibrated versus Fc/Fc^+.

5.3 Conclusion

Chlorosulfonation of 2,7-dibromofluorene (**3.22**) with chlorosulfonic acid gives fluorene-4,6-disulfonylchlorides. Under milder conditions (chloroform solution, 0 °C, 2 h) mono-substitution occurs, but both **3.22** and its 9,9-dihexylated analogue **5.45** give corresponding fluorene-4-sulfonic acids **5.48** and **5.52**, respectively, and not chlorosulfonyl derivatives **5.49** and **5.54**. These acids have been successfully converted into sulfonylchlorides **5.49** and **5.54** with $POCl_3/PCl_5$. Compound **5.54** was used to prepare phenoxy- and diethylamino-derivatives **5.55** and **5.56**, respectively, which were successfully polymerised by Ni(0)-mediated Yamamoto polycondensation to obtain polymers **PhOSO$_2$-PF6** and **Et$_2$N SO$_2$-PF6**. Both polymers had moderate to high molecular weights (M_n = 8,700–27,000 Da) and showed good thermal stability (T_d = 388–404 °C). **PhOSO$_2$-PF6** and **Et$_2$N SO$_2$-PF6** are bright blue-emitting polymers with absorption and emission characteristics typical for polyfluorenes, which are quite close to those observed for **MeSO$_2$-PF6** studied in Chapter 4, namely λ_{PL} = 432–434 nm in solution (Φ_{PL} = 88–91%) and λ_{PL} = 436–441 nm in films.

Thus, we have elaborated a new and convenient method for the functionalisation of 2,7-dibromofluorene with chlorosulfonyl groups at position 4. This new method offers many other opportunities for further modifications at the sulfonyl site to access a wider range of light-emitting 4-functionalised polyfluorenes. This approach has been demonstrated by making and characterising two novel blue-emitting polymers with $PhOSO_2$- and Et_2NSO_2-groups at position 4 of the fluorene moiety.

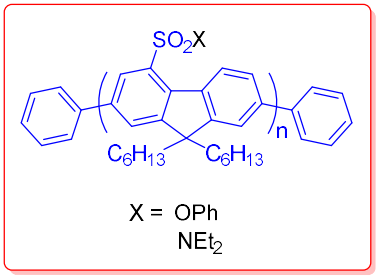

5.4 Experimental Section

5.4.1 Chemicals and instrumentation

All chemicals and solvents were obtained from commercial suppliers like Aldrich, Acros, Apollo Scientific and Fisher companies and used in the reactions with no further purification. Instruments (NMR and MS spectrometers, UV-Vis and PL spectrophotoometers, GPC and flash chromatographs, freeze dryer, TGA and melting point instruments) are described in the Chapters 3 and 4.

5.4.2 Synthesis

2,7-Dibromo-4,6-di(chlorosulfonyl)fluorene (5.54)

Exp no: 14SAA-04

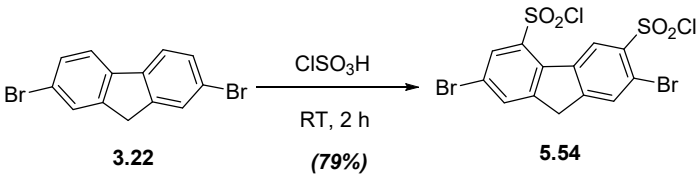

3.22 **5.54**

2,7-Dibromofluorene (**3.22**) (0.501 g, 1.55 mmol) was charged into 50 mL single neck round bottom flask. Chlorosulfonic acid (4.0 mL, 60 mmol) was added slowly and the reaction mixture was stirred for 2 h at ambient temperature. Green precipitate was filtered off, washed with water (5 mL), and dried *in vacuo* to afford crude product **5.54** as a white solid (0.638 g, 79%), mp: 250–253 °C.

^{1}H NMR (400 MHz, $CDCl_3$): δ (ppm) 9.49 (s, 1H), 8.33 (d, J = 1.6 Hz, 1H), 8.11 (s, 1H), 8.09 (s, 1H), 4.15 (s, 2H, CH_2).

^{13}C NMR (100 MHz, $CDCl_3$): δ (ppm) 151.36, 148.17, 142.87, 139.82, 136.68, 134.99, 134.91, 132.59, 131.03, 129.23, 122.17, 121.18, 37.13

MS (TOF EI$^+$): *m/z* 517.86 (M^+, ^{79}Br/^{81}Br, 45%), 521.82 (M^+, ^{79}Br/^{81}Br, 100%), 519.82 (M^+, ^{81}Br/^{81}Br, 98%). Calcd for $C_{13}H_6Br_2Cl_2O_4S_2$: 517.75 (51.4%), 521.74 (100%), 519.74 (63.9%).

Other experiments:

In a similar fashion, several other experiments have been performed for this chlorosulfonation reaction at different conditions:

14SAA-01: **3.22** (1. 00 g, 3.08 mmol), $ClSO_3H$ (10 mL, 150.3 mmol), 120 ^{o}C, 2 h.
Yield: 0.497 g (31%), ~70 % purity by ^{1}H NMR.

14SAA-03: **3.22** (0.500 g, 1.54 mmol), $ClSO_3H$ (5 mL, 75.2 mmol), 80 °C, 2 h + 100 °C, 20 h. Yield: 0.546 g (67%), ~70 % purity by ^{1}H NMR.

14SAA-05: **3.22** (0.501 g, 1.54 mmol), $ClSO_3H$ (4 mL, 60. 2 mmol), $CHCl_3$ (2 mL), 0 °C, 2 h. Yield: 0.654 g (81%).

14SAA-10: **3.22** (0.502 g, 1.54 mmol), $ClSO_3H$ (0.5 mL, 7.53 mmol), $CHCl_3$ (13 mL), 0 °C – RT, 64 h. Yield: 0.636 g (78%).

2,7-Dibromofluorene-4-sulfonic acid (5.48)

Exp no: 14SAA-11

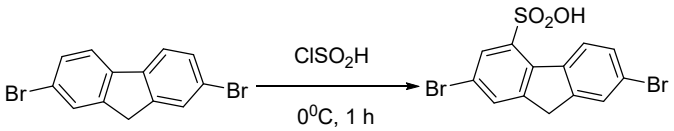

3.22 ***(80%)*** **5.48**

2,7-Dibromofluorene (**3.22**) (0.503 g, 1.54 mmol) and chloroform (13 mL) were charged in 25 mL two neck round bottom flask. The mixture was stirred until full dissolution and cooled down to 0 °C. Chlorosulphonic acid (0.5 mL, 7.53 mmol, 5.0 eq.) was added dropwise and the mixture was stirred at 0 °C for 1 h. During the reaction, white solid was precipitated. It was filtered off and (without further washing) was dried *in vacuo* to afford the crude product as a white solid (1.022 g, 163%). This sample was stirred under reflux in dioxane (2 mL) for 1 h, cooled down to room temperature, the solid was filtered off, washed with hexane (2 mL) and dried to give crude product (0.713 g, 114%; ~80% purity by ^{1}H NMR). Further purification was carried out by flash chromatography on silica gel using DCM/MeOH (9:1, v/v) as eluent to afford **5.48** as a cream coloured solid (0.476 g, 80 %), mp: 198–200 °C.

^{1}H NMR (400 MHz, $CDCl_3$): δ (ppm) 8.66 (d, J = 8.6 Hz, 1H, H-5), 8.11 (d, J = 1.2 Hz, 1H), 8.01 (s, 1H), 7.82 (s, 1H), 7.61 (dd, J = 8.5, 1.9 Hz, 1H, H-6), 4.08 (s, 2H, CH_2).

^{13}C NMR (100 MHz, $(CD_3)_2CO$): δ (ppm) 147.39, 146.37, 143.97, 138.74, 136.01, 129.74, 129.43, 128.82, 128.71, 127.37, 120.78, 119.30, 36.67.

MS (TOF EI^{+}): *m/z* 405.85 (M^{+}, ^{79}Br/^{79}Br, 55%), 402.00 (M^{+}, ^{79}Br/^{81}Br, 100%), 403.91 (M^{+}, ^{81}Br/^{81}Br, 50%). Calcd for $C_{13}H_8Br_2O_3S$: 405.85 (48.6%), 401.86 (100%), 403.85 (51.4%).

Other experiments:

14SAA-13: **3.22** (1.00 g, 3.09 mmol), $ClSO_3H$ (0.361 g, 3.09 mmol), $CHCl_3$ (30 mL), 0 °C, 1 h. Yield: 1.130 g (90%); ^{1}H NMR analysis: **5.48** (~30%) and **3.22** (~70%).

14SAA-17: **3.22** (1.00 g, 3.09 mmol), $ClSO_3H$ (0.432 g, 3.708 mmol), $CHCl_3$ (30 mL), 0 °C, 1 h. Yield: 1.216 g (97%); ^{1}H NMR analysis: **5.48** (~20%) and **3.22** (~80%).

2,7-Dibromo-4-chlorosulfonylfluorene (5.49)

Exp no: 14SAA-020

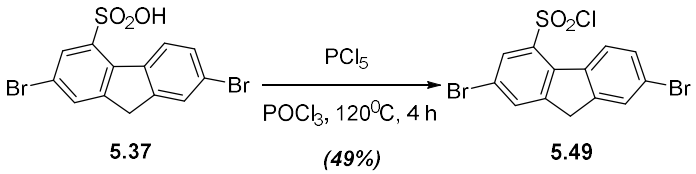

5.37 *(49%)* **5.49**

2,7-Dibromofluorene-4-sulphonic acid (**5.37**) (0.50 g, 1.23 mmol), PCl_5 (0.32 g, 1.54 mmol), and phosphorous oxychloride, $POCl_3$(2.06 g, 7.53 mmol) were charged in 50 mL single neck round bottom flask. The reaction mixture was stirred at 120 °C for 4 h, an excess of $POCl_3$ was evaporated to dryness under reduced pressure and the residue was dried *in vacuo* to give brown coloured crude product (0.42 g, 80%). The crude product was purified by flash chromatography on silica gel with PE/DCM (1:1, v/v) as eluent to afford compound **5.49** as a yellow solid (0.257 g, 49%), mp: 228–230 °C.

^{1}H NMR (400 MHz, $CDCl_3$): δ (ppm) 8.49 (d, *J* = 8.6 Hz, 1H, H-5), 8.27 (d, *J* = 1.2 Hz, 1H), 8.00 (d, *J* = 0.8 Hz, 1H), 7.77 (d, *J* = 0.8 Hz, 1H), 7.65 (dd, *J* = 8.6, 1.7 Hz, 1H, H-6), 4.02 (s, 2H, CH_2, H-9).

^{13}C NMR (100 MHz, $CDCl_3$): 148.50, 145.99, 139.17, 137.15, 135.49, 134.62, 131.12, 130.34, 128.64, 128.12, 123.95, 120.02, 36.90.

MS (TOF EI$^+$): *m/z* 419.80 (M^+, ^{79}Br/^{79}Br, 45%), 423.81 (M^+, ^{79}Br/^{81}Br, 100%), 421.80 (M^+, ^{81}Br/^{81}Br, 80%). Calcd for $C_{13}H_7Br_2ClO_2S$: 419.82 (43.3%), 423.82 (100%), 421.82 (72.8%).

2,7-Dibromo-4-diethylaminosulfonylfluorene (5.50)

Exp no: 14SAA-022

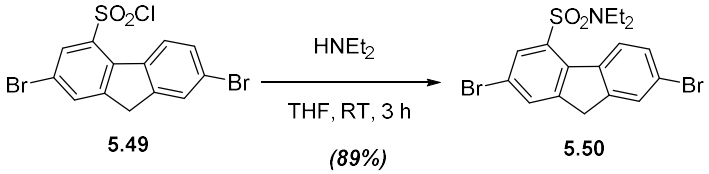

5.49 *(89%)* **5.50**

To a stirred solution of 2,7-dibromo-4-chlorosulfonylfluorene (**5.49**) (0.255 g, 0.60 mmol) in THF (20 mL), diethylamine (0.22 g, 3.01 mmol) was added and the mixture was stirred at ambient temperature for 3 h. The mixture was diluted with water (75 mL) and stirred for 15 min. The precipitate was filtered off, washed with water (2 × 3 mL) and dried *in vacuo* to afford compound **5.50** as a yellow solid (0.248 g, 89%).

^{1}H NMR (400 MHz, $CDCl_3$): δ (ppm) 8.49 (d, *J* = 8.6 Hz, 1H, H-5), 7.84 (s, 1H), 7.83 (s, 1H), 7.68 (s, 1H), 7.55 (dd, *J* = 8.6, 1.8 Hz, 1H, H-6), 3.92 (s, 2H, CH_2), 3.42 (q, *J* = 7.1 Hz, 4H, NCH_2CH$_3$), 1.22 (t, *J* = 7.1 Hz, 6H, NCH$_2$$CH_3$).

^{13}C NMR (100 MHz, $CDCl_3$): δ (ppm) 148.13, 145.49, 137.33, 136.87, 135.58, 131.78, 130.46, 129.40, 127.77, 127.68, 122.67, 119.85, 53.42, 42.03, 36.71, 30.92, 14.06.

MS (TOF EI$^+$): *m/z* 456.84 (M^+, ^{79}Br/^{79}Br, 53%), 460.84 (M^+, ^{79}Br/^{81}Br, 100%), 458.85 (M^+, ^{81}Br/^{81}Br, 55%). Calcd for $C_{17}H_{17}Br_2NO_2S$: 456.93 (50.2%), 460.93 (100%), 458.93 (52%).

2,7-Dibromo-4-diethylaminosulfony-9,9-dihexylfluorene (5.51)

Exp no: 14SAA-031

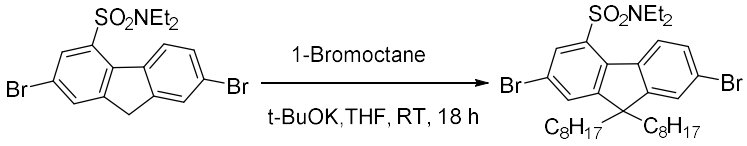

5.50 **5.51**

Under a nitrogen atmosphere, a solution of 2,7-dibromo-4-diethylaminosulfonylfluorene (**5.50**) (0.100 g, 0.21 mmol) and t-BuOK (0.06 g) in dry THF (5 mL) was stirred for 10 minutes, then 1-bromooctane (0.188 g, 0.85 mmol) was added dropwise and the mixture was stirred at ambient temperature for 18 h. The precipitated KBr was filtered off, washed with DCM (2 × 10 mL), the solvent was evaporated under reduced pressure and the residue was dried *in vacuo* to give crude product (0.164 g, 112%). The crude product was purified by flash chromatography on silica gel using PE/DCM (1:1, v/v) as eluent to afford compound **5.51** as a colourless plates (51 mg, 31%).

^{1}H NMR (400 MHz, $CDCl_3$): δ (ppm) 8.38 (d, *J* = 8.5 Hz, 1H, H-5), 7.91 (d, *J* = 1.7 Hz, 1H), 7.61 (d, *J* = 1.7 Hz, 1H), 7.49 (dd, *J* = 8.5, 1.8 Hz, 1H, H-6), 7.44 (d, *J* = 1.7 Hz, 1H), 3.37 (q, *J* = 7.16 Hz, 4H, N*CH*$_2$CH$_3$), 1.93 (m, 4H, *CH*$_2$C$_7$H$_{15}$), 1.20–1.03 (m, 26H), 0.82 (t, *J* = 7.2 Hz, 6H, CH_3), 0.52–0.47 (m, 4H, CH_2*CH*$_2$C$_6$H$_{13}$).

^{13}C NMR (100 MHz, $CDCl_3$): δ (ppm) 156.04, 153.15, 136.93, 136.32, 135.12, 130.43, 129.65, 127.82, 125.44, 123.30, 120.46, 55.03, 53.42, 41.50, 40.42, 31.73, 29.71, 29.07, 23.45, 22.58, 14.05, 13.71.

MS (TOF EI$^+$): *m/z* 680.92 (M^+, ^{79}Br/^{79}Br, 50%), 684.89 (M^+, ^{79}Br/^{81}Br, 100%), 682.90 (M^+, ^{81}Br/^{81}Br, 55%). Calcd for $C_{33}H_{49}Br_2NO_2S$: 681.19 (50.2%), 685.18 (100%), 683.18 (52.1%).

2,7-Dibromo-4,6-di(chlorosulfonyl)fluorene (5.47)

Exp no: 14CB-01

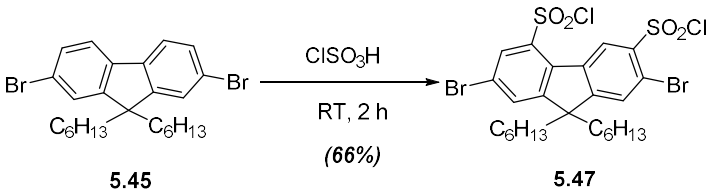

5.45 **5.47**

2,7-Dibromo-9,9-dihexylfluorene (**5.45**) (20.0 g, 40.6 mmol) and chlorosulphonic acid (160 mL, 2.35 mol) were charged into 500 mL round bottom flask. The mixture was stirred at ambient temperature for 2 h. The reaction mixture was diluted with water (40 mL), brown precipitate was filtered off, washed with water (3 × 100 mL) and dried *in vacuo* to afford the crude product (29.07 g, 103%). The crude product was purified by column chromatography on silica gel using PE/DCM (2:1, v/v) as eluent to afford compound **5.47** as a colourless solid (18. 57 g, 66%), mp: 155–159 °C.

^{1}H NMR (400 MHz, $CDCl_3$): δ (ppm) 9.41 (s, 1H), 8.27 (d, *J* = 1.7 Hz, 1H), 7.84 (s, 2H), 2.10–1.98 (m, 4H, $CH_2C_5H_{11}$), 1.09–1.03 (m, 12H, $CH_2CH_2C_3H_6CH_3$), 0.77 (br.s, 6H, CH_3), 0.63–0.47 (m, 4H, $CH_2CH_2C_4H_9$).

^{13}C NMR (100 MHz, $CDCl_3$): δ (ppm) 159.46, 156.35, 142.73, 139.84, 135.86, 134.12, 132.53, 131.02, 130.34, 129.24, 122.69, 121.81, 56.34, 39.92, 31.23, 29.29, 23.59, 22.49, 13.92.

MS (TOF EI$^+$): *m/z* 685.82 (M^+, ^{79}Br/^{79}Br, 40%), 689.51 (M^+, ^{79}Br/^{81}Br, 100%), 687.50 (M^+, ^{81}Br/^{81}Br, 98%). Calcd for $C_{25}H_{30}Br_2Cl_2O_4S_2$ 685.93 (37.4%), 689.93 (100%), 687.93 (95.1%).

Sodium 2,7-dibromo-9,9-dihexylfluorene-4-sulfonate (5.53)

Exp no: 14SAA-040

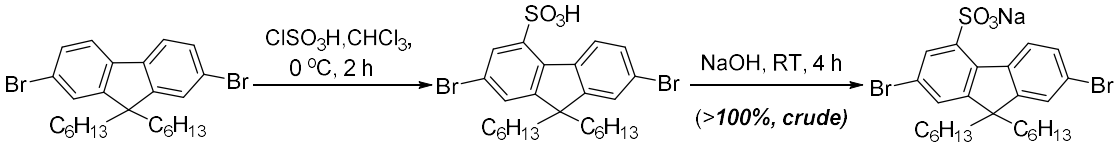

5.45 **5.52** **5.53**

2,7-Dibromo-9,9-dihexylfluorene (**5.45**) (20.0 g, 74.1 mmol) in chloroform (600 mL) was stirred in 1.0 L two neck round bottom flask for 15 minutes at room temperature until full dissolution and then cooled down to 0 °C (internal temperature). To this solution, chlorosulphonic acid (15.5 mL, 235.6 mmol) was added slowly and the mixture was stirred at 0 °C for 2 h. The reaction mixture was diluted with water (10 mL) and a white coloured solid was precipitated. The mixture was evaporated at reduced pressure and the residue was dried *in*

vacuo at room temperature to afford compound **5.52** as an off-white solid (47.3 g, 203 % by weight). In the next step, the crude product was diluted with water (1.0 L), stirred for 4 h (full dissolution), then NaOH solution (110 g in 400 mL of H_2O) was added and the mixture was stirred for 10 h to form white precipitate. It was filtered off and dried *in vacuo* to afford crude compound **5.53** as a white solid (30.7 g, 131% by weight, thus assuming that it contains some NaCl as an impurity).

^{1}H NMR (**5.53**) (400 MHz, $CDCl_3$): δ (ppm) 8.65 (d, *J* = 8.5 Hz, 1H, H-5), 8.08 (d, *J* = 1.7 Hz, 1H), 7.90 (d, *J* = 1.6 Hz, 1H), 7.70 (d, *J* = 1.8 Hz, 1H), 7.56 (dd, *J* = 8.4, 1.9 Hz, 1H, H-6), 2.15 (m, 4H, $CH_2C_5H_{11}$), 1.14–1.00 (m, 12H, $CH_2CH_2C_3H_6CH_3$), 0.76 (t, *J* = 6.8 Hz, 6H, CH_3), 0.62–0.52 (m, 4H, $CH_2CH_2C_4H_9$).

^{13}C NMR (**5.53**) (100 MHz, $CDCl_3$) δ (ppm) 155.30, 155.11, 153.16, 136.48, 136.40, 136.37, 135.95, 130.58, 130.48, 129.60, 129.32, 128.94, 127.30, 125.50, 122.90, 120.52, 54.87, 40.33, 31.36, 31.31, 29.54, 29.48, 23.49, 22.55, 13.94.

MS (TOF EI$^+$) (**5.53**): *m/z* 573.92 (M^+, ^{79}Br/^{79}Br, 65%), 572.00 (M^+, ^{79}Br/^{81}Br, 100%), 5.70.88 (M^+, ^{81}Br/^{81}Br, 35%), Calcd for $C_{25}H_{32}Br_2O_3S$: 574.04 (48.6%), 572.04 (100.0%), 570.04 (51.4%).

2,7-Dibromo-4-chlorosulphonyl-9,9-dihexylfluorene (5.54)

Exp no: 14SAA-043

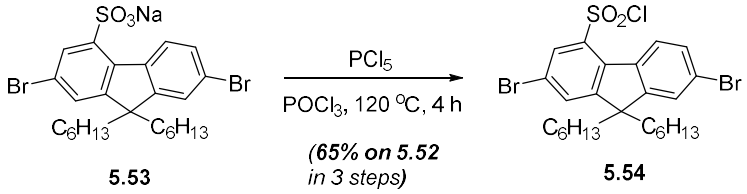

Sodium 2,7-dibromo-9,9-dihexylfluorene-4-sulfonate (**5.53**) (29.6 g, 50.0 mmol), PCl_5 (13.0 g, 62.5 mmol), and $POCl_3$ (60 mL) were charged into 500 mL single neck round bottom flask. The reaction mixture was stirred at 120 °C (oil bath temperature) for 4 h. $POCl_3$ was evaporated under reduced pressure and the residue was dried *in vacuo* to give a yellow crude product (52.9 g, 175%). The crude product was purified by flash chromatography on silica gel using PE as eluent to afford compound **5.54** as a yellow solid (15.0 g, 74%), mp: 66–68.5 °C.

^{1}H NMR (400 MHz, $CDCl_3$): δ (ppm) 8.41 (d, *J* = 8.6 Hz, 1H, H-5), 8.20 (d, *J* = 1.6 Hz, 1H), 7.76 (d, *J* = 1.6 Hz, 1H), 7.58 (dd, *J* = 8.6, 1.8 Hz, 1H, H-6), 7.51 (d, *J* = 1.7 Hz, 1H), 1.97 (m, 4H, $CH_2C_5H_{11}$), 1.14–1.09 (m, 12H, $CH_2CH_2C_3H_6CH_3$), 0.78 (t, *J* = 7.0 Hz, 6H, CH_3), 0.62–0.44 (m, 4H, $CH_2CH_2C_4H_9$).

^{13}C NMR (100 MHz, $CDCl_3$): δ (ppm) 156.67, 153.73, 139.15, 136.60, 134.77, 132.25, 131.11, 130.31, 128.66, 125.91, 124.57, 120.55, 55.50, 53.42, 40.22, 31.32, 29.37, 23.44, 22.51, 13.94.

MS (TOF EI$^+$): *m/z* 587.82 (M^+, ^{79}Br/^{79}Br, 36%), 591.87 (M^+, ^{79}Br/^{81}Br, 100%), 589.87 (M^+, ^{81}Br/^{81}Br, 60%). Calcd for $C_{25}H_{31}Br_2ClO_2S$: 588.01 (48.6%), 592.01 (100%), 590.01 (51.4%).

2,7-Dibromo-4-diethylaminosulfonyl-9,9-dihexylfluorene (5.56)

Exp no: 14SAA-044

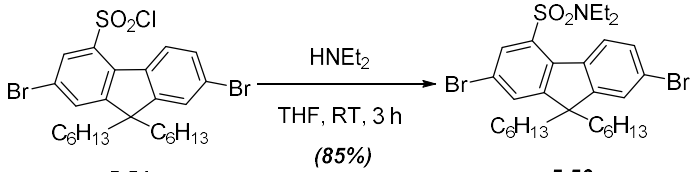

5.54 **5.56**

2,7-Dibromo-4-chlorosulfonyl-9,9-dihexylfluorene (**5.54**) (2.05 g, 3.38 mmol) and THF (15 mL) were stirred in 50 mL single neck round bottom flask. To the stirred solution, diethylamine (1.7 mL) was added and the mixture was stirred at ambient temperature for 3 h. The solvent was evaporated and the residue was dried *in vacuo* to give crude product (2.89 g, 132%). The crude product was purified by flash chromatography on silica gel using PE/DCM (1:1, v/v) as eluent to afford compound **5.56** as a white solid (1.86 g, 85%).

^{1}H NMR (400 MHz, $CDCl_3$): δ (ppm) 8.38 (d, *J* = 8.5 Hz, 1H, H-5), 7.91 (d, *J* = 1.8 Hz, 1H), 7.61 (d, *J* = 1.8 Hz, 1H), 7.49 (dd, *J* = 8.5, 1.9 Hz, 1H, H-6), 7.44 (d, *J* = 1.8 Hz, 1H), 3.37 (q, *J* = 7.1 Hz, 4H, N*CH*$_2$CH$_3$), 1.93 (t, *J* = 7.8 Hz, 4H, *CH*$_2$C$_5$H$_{11}$), 1.14–0.98 (m, 18H, CH$_2$CH$_2$*C*$_3$*H*$_6$CH$_3$ + NCH$_2$*CH*$_3$), 0.77 (t, *J* = 16.3 Hz, 6H, CH$_3$), 0.54–0.45 (m, 4H, CH$_2$*CH*$_2$C$_4$H$_9$).

^{13}C NMR (100 MHz, $CDCl_3$): δ (ppm) 156.04, 153.14, 136.93, 136.32, 135.13, 130.44, 130.40, 129.65, 127.83, 125.44, 123.30, 120.45, 55.03, 41.51, 40.46, 31.36, 29.44, 23.48, 22.51, 13.95, 13.71.

MS (TOF EI$^+$): *m/z* 629.95 (M^+, ^{79}Br/^{79}Br, 15%), 624.97 (M^+, ^{79}Br/^{81}Br, 100%), 626.94 (M^+, ^{81}Br/^{81}Br, 39%). Calcd for $C_{29}H_{41}Br_2NO_2S$: 629.12 (48.6%), 625.12 (100%), 627.12 (51.4%).

2,7-Dibromo-4-phenyloxysulfonyl-9,9-dihexylfluorene (5.55)

Exp no: 14SAA-045

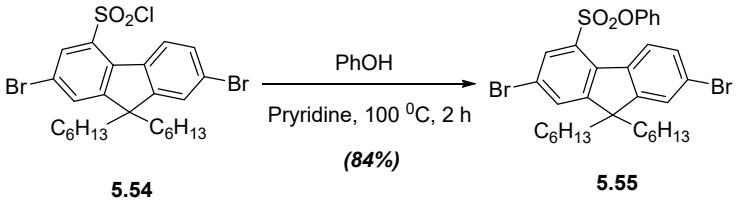

5.54 **5.55**

2,7-Dibromo-4-chlorosulfonyl-9,9-dihexylfluorene (**5.54**) (2.52 g, 4.26 mmol) and phenol (2.42 g, 4.2 mmol) were charged into 25 mL single neck round bottom flask. The reaction mixture was stirred at 100 °C for 30 minutes. The mixture was cooled down to room temperature, pyridine (1.5 mL) was added and the mixture was stirred at 100 °C for 2 h. The reaction mixture was diluted with water (20 mL) and extracted with DCM (4 × 20 mL). The combined extracts were evaporated at reduced pressure and the residue was dried *in vacuo* to give a crude product (3.54 g, 128%). The crude product was purified by flash chromatography on silica gel using PE/DCM (2:1, v/v) as eluent to afford compound **5.55** as a white solid (2.23 g, 84%).

^{1}H NMR (400 MHz, $CDCl_3$): δ (ppm) 8.59 (d, J = 8.5 Hz, 1H, H-5), 7.91 (d, J = 1.8 Hz, 1H), 7.66 (d, J = 7.5 Hz, 1H) 7.59 (dd, J = 8.6, 1.8 Hz, 1H, H-6), 7.52 (d, J = 1.8 Hz, 1H), 7.16–7.13 (m, 3H), 6.88–6.85 (m, 2H), 2.05–1.92 (m, 4H, $CH_2C_5H_{11}$), 1.18–1.05 (m, 12H, , $CH_2CH_2C_3H_6CH_3$), 0.79 (t, J = 6.9 Hz, 6H, CH_3), 0.59–0.40 (m, 4H, $CH_2CH_2C_4H_9$).

^{13}C NMR (100 MHz, $CDCl_3$): δ (ppm) 155.61, 153.48, 149.47, 137.53, 135.46, 132.41, 131.29, 131.14, 129.69, 129.58, 127.76, 127.44, 125.72, 124.23, 121.85, 120.71, 55.19, 40.48, 31.44, 29.41, 23.50, 22.52, 13.96.

MS (TOF EI$^+$): *m/z* 645.95 (M^+, ^{79}Br/^{79}Br, 46%), 649.88 (M^+, ^{79}Br/^{81}Br, 100%), 647.92 (M^+, ^{81}Br/^{81}Br, 48%). Calcd for $C_{31}H_{36}Br_2O_3S$: 646.08 (50.2%), 650.07 (100%), 648.07 (52%).

Poly(4-phenyloxysulfonyl-9,9-dihexylfluorene), PhOSO$_2$-PF6

Exp no: SK-184

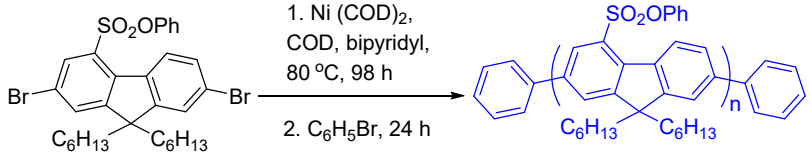

5.55 **PhOSO$_2$-PF6**, ***(35%)***

Under an argon atmosphere, a mixture of bis(1,5-cylcooctadiene)nickel(0), $Ni(COD)_2$ (338 mg, 1.23 mmol), 1,5-cyclooctadiene (133 mg, 1.23 mmol), and 2,2'-bipyridyl (191 mg, 1.23 mmol) in dry DMF (4.4 mL) were stirred at 80 °C for 30 min to form a dark violet solution. To this, a solution of 2,7-dibromo-4-phenyloxysulfonyl-9,9-dihexylfluorene (**5.55**) (399 mg,

0.61 mmol) in dry toluene (10.2 mL) was added slowly and the mixture was stirred at 80 °C for 98 h. Bromobenzene (0.09 mL) was added as the end-capper and the mixture was stirred at 80 °C for additional 16 h. The mixture was cooled to room temperature and poured dropwise into a stirred solution of methanol:acetone:conc. HCl (1:1:1, v/v; 100 mL) to give a yellow semi-solid and milky-like suspension. The mixture was stirred for 4 h and extracted with chloroform (50 mL). Chloroform extracts were washed with water (3 × 20 mL), the organic layer was concentrated to a low volume (~6.0 mL) and slowly poured dropwise into methanol (50 mL) with vigorous stirring. A brown precipitate was filtered off, washed with methanol (5.0 mL) and dried *in vacuo* to give crude produc as a brown solid (258 mg, 85 %). This solid was extracted in a Soxhlet apparatus with methanol (18 h) and then with acetone (18 h) to remove by-products and low molecular weight fractions. Finally, it was extracted with chloroform for 16 h. The chloroform solution was concentrated to a small volume (~5.0 mL) and slowly added dropwise to a vigorously stirred methanol (50 mL) to form a light brown precipitate, which was filtered off, washed with methanol (5.0 mL) and dried *in vacuo* to afford **PhOSO$_2$-PF6** as a light brown solid (106 mg, 35%).

^{1}H NMR (400 MHz, $CDCl_3$): δ (ppm) 8.60 (m, 1H), 8.40 (m, 1H), 7.82 (m, 1H), 7.69–7.63 (m, 2H), 7.50–7.36 (m, 5H) 2.03–1.93 (m, 4H, $CH_2C_5H_{11}$), 1.25–1.13 (m, 12H, $CH_2CH_2(CH_2)_3CH_3$), 0.84–0.69 (m, 10H, $CH_2CH_2(CH_2)_3CH_3$).

GPC (THF): M_w = 12,600 Da, M_n = 8,700 Da, PDI = 1.44.

Poly(4-diethylaminosulfonyl-9,9-dihexylfluorene) Et$_2$NSO$_2$-PF6

Exp no: SK-185

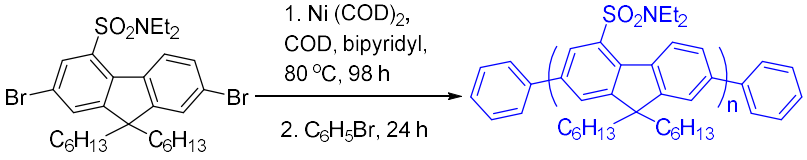

5.56

NEt$_2$SO$_2$-PF6-L ***(34%)***

NEt$_2$SO$_2$-PF6-H ***(10%)***

Under an argon atmosphere, a mixture of bis(1,5-cylcooctadiene)nickel(0), Ni(COD)$_2$ (403 mg, 0.64 mmol), 1,5-cyclooctadiene (138 mg, 1.28 mmol), and 2,2-bipyridyl (200 mg, 1.28 mmol) in dry DMF (4.4 mL) were stirred at 80 °C for 30 min to form a dark violet solution. To this, a solution of 2,7-dibromo-4-diethylaminosulfonyl-9,9-dihexylfluorene (**5.56**) (403 mg, 0.64 mmol) in dry toluene (10.2 mL) was added slowly and the mixture was stirred at 80 °C for 98 h. Bromobenzene (0.09 mL) was added as the end-capper and the mixture was stirred at 80 °C for additional 16 h. The mixture was cooled to room temperature and poured dropwise into a stirred solution of methanol:acetone:con.HCl (1:1:1, v/v) 100 mL to form a

yellow coloured semi-solid and milky like suspension. After stirring for 4 h, it was extracted with chloroform (50 mL), the chloroform layer was washed with water (3 × 20 mL), concentrated to a small volume (~6.0 mL) and added slowly to methanol (75 mL) with vigorous stirring. The presipitate was filtered off, washed with methanol (5.0 mL) and dried *in vacuo* to afford crude product as yellow solid (217 mg, 72 %). This solid was extracted in a Soxhlet apparatus with methanol (18 h) and then with acetone (18 h). The acetone fraction was evaporated under reduced pressure to give the polymer fractions **Et_2NSO_2-PF6-**L as yellow solid (104 mg, 34 %). The residue in the Soxhlet apparatus was extracted with chloroform for 16 h, the chloroform solution was concentrated to a small volume (~5 mL) and slowly added dropwise to methanol (50 mL) with vigorous stirring. The precipitate was filtered off, washed with methanol (5.0 mL) and dried *in vacuo* to afford the polymer fraction **Et_2NSO_2-PF6-H** as a yellow solid (29 mg, 10%).

Acetone-soluble fraction, **Et_2NSO_2-PF6-L**:

GPC (THF): M_w = 26,000 Da, M_n = 16,000 Da, PDI = 1.62.

Chloroform-soluble fraction, **Et_2NSO_2-PF6-H**:

^{1}H NMR (400 MHz, $CDCl_3$): δ (ppm) 8.70 (m, 1H), 8.22 (m, 1H), 7.87 (m, 1H), 7.77 (br s, 1H), 7.68 (m, 1H), 3.54–3.46 (m, 4H, N*CH_2*CH_3), 2.17 (m, 4H, *CH_2*C_5H_{11}), 1.25–1.11 (m, 18H, CH_2CH_2(*CH_2)$_3$*CH_3 + NCH_2*CH_3*), 0.85–0.76 (m, 10H, CH_2*CH_2*$(CH_2)_3$*CH_3*).

GPC (THF): M_w = 43,000 Da, M_n = 27,000 Da, PDI = 1.59.

References

1 G. Barbarella, L. Favaretto, M. Zambianchi, O. Pudova, C. Arbizzani, A. Bongini, and M. Mastragostino, *Adv. Mater*., **1998**, *10*, 551–554. (DOI: 10.1002/(SICI)1521-4095(199805)10:7<551).

2 G. Barbarella, L. Favaretto, G. Sotgiu, M. Zambianchi, L. Antolini, O. Pudova, and A. Bongini, *J. Org. Chem*., **1998**, *63*, 5497–5506. (DOI: 10.1021/jo980507g).

3 G. Barbarella, L. Favaretto, G. Sotgiu, M. Zambianchi, C. Arbizzani, A. Bongini, and M. Mastragostino, *Chem. Mater*., **1999,** *11*, 2533–2541. (DOI: 10.1021/cm990245e).

4 A. Bongini, G. Barbarella, M. Zambianchi, C. Arbizzania, and M. Mastragostino, *Chem. Commun*., **2000**, 439–440. (DOI: 10.1039/a909390g).

5 G. Barbarella, L. Favaretto, G. Sotgiu, M. Zambianchi, V. Fattori, M. Cocchi, F. Cacialli, G. Gigli, and R. Cingolani, *Adv. Mater*., **1999**, *11*, 1375–1379. (DOI: 10.1002/(SICI)1521-4095(199911)11).

6 G. Barbarella, L. Favaretto, G. Sotgiu, L. Antolini, G. Gigli, R. Cingolani, and A. Bongini, *Chem. Mater.*, **2001**, *13*, 4112–4122. (DOI: 10.1021/cm010436t).

7 L. Antolini, E. Tedesco, G. Barbarella, L. Favaretto, G. Sotgiu, M. Zambianchi, D. Casarini, G. Gigli, and R. Cingolani, *J. Am. Chem. Soc*., **2000,** *122*, 9006–9013. (DOI: 10.1021/ja000834h).

8 G. Barbarella and M. Melucci, Chapter 4 in Book: *Handbook of Thiophene-Based Materials: Applications in Organic Electronics and Photonics*, I. F. Perepichka and D. F. Perepichka (Eds), *Vol. 1*, Wiley, **2009**, pp. 255–292.

9 J. Y. Li, A. Ziegler, and G. Wegner, *Chem. Eur. J*., **2005**, *11*, 4450–4457. (DOI: 10.1002/chem.200401319)

10 I. I. Perepichka, I. F. Perepichka, M. R. Bryce, and L. O. Pålsson. *Chem. Commun*., **2005**, 3397–3399. (DOI: 10.1039/B417717G).

11 I. I. Perepichka, I. F. Perepichka, M. Tavasli, and M. R. Bryce, *J. Phys. Chem. B*, **2006**, *110*, 19329–19339. and (DOI: 10.1021/jp0643653).

12 F. B. Dias, S. King, A. P. Monkman, I. I. Perepichka, M. A. Kryuchkov, I. F. Perepichka, and M. R. Bryce, *J. Phys. Chem. B*, **2008**, *112*, 6557–6566. (DOI: 10.1021/jp800068d).

13 S. M. King, I. I. Perepichka, I. F. Perepichka, F. B. Dias, M. R. Bryce, and A. P. Monkman, *Adv. Funct. Mater.*, **2009**, *19*, 586–591. (DOI: 10.1002/adfm.200801237).

14 J. Liu, J. Zou, W. Yang, H. Wu, C. Li, B. Zhang, J. Peng, and Y. Cao, *Chem. Mater*., **2008**, *20*, 4499–4506. (DOI: 10.1021/cm800129h).

15 K. T. Kamtekar, H. L. Vaughan, B. P. Lyons, A. P. Monkman, S. U. Pandya, and M. R. Bryce, *Macromolecules*, **2010**, *43*, 4481–4488. (DOI: 10.1021/ma100566p).

16 J. H. Cook, J. Santos, H. Li, H. A. Al-Attar, M. R. Bryce, and A. P. Monkman, *J. Mater. Chem. C*, **2014**, *2*, 5587–5592. (DOI: 10.1039/C4TC00896K).

17 R. He, S. Hu, J. Liu, L. Yu, B. Zhang, N. Li, W. Yang, H. Wu, and J. Peng, *J. Mater. Chem*., **2012**, *22*, 3440–3446. (DOI: 10.1039/C2JM14926E).

18 R. He, J. Xu, Y. Xue, D. Chen, L. Ying, W. Yang, and Y. Cao, *J. Mater. Chem. C*, **2014**, *2*, 7881–7890. (DOI: 10.1039/C4TC01089B).

19 F. B. Dias, K. N. Bourdakos, V. Jankus , K. C. Moss, K. T. Kamtekar, V. Bhalla, J. Santos, M. R. Bryce, and A. P. Monkman, *Adv. Mater*., **2013**, *25*, 3707–3714. (DOI: 10.1002/adma.201300753).

20 C. Fan, C. Duan, Y. Wei, D. Ding, H. Xu, and W. Huang, *Chem. Mater*., **2015**, *27*, 5131–5140. (DOI: 10.1021/acs.chemmater.5b02012).

21 S. Kumar and S. Patil, *J. Phys. Chem. C*, **2015**, *119*, 19297–19304. (DOI: 10.1021/acs.jpcc.5b03717).

22 S. Fujii, Z. Duan, T. Okukawa, Y. Yanagi, A. Yoshida, T. Tanaka, G. Zhao, Y. Nishioka, and H. Kataura, *Phys. Status Solidi B*, **2012**, *249*, 2648–2651. (DOI 10.1002/pssb.201200439).

23 L. Ying, Y.-H. Li, C.-H. Wei, M.-Q. Wang, W. Yang, H.-B. Wu, and Y. Cao, *Chinese J. Polym. Sci*., **2013**, *31*, 88–97. (DOI: 10.1007/s10118-013-1199-6).

24 L. Yu, J. Liu, S. Hu, R. He, W. Yang, H. Wu, J. Peng, R. Xia, and D. D. C. Bradley, *Adv. Funct. Mater*., **2013**, *23*, 4366–4376. (DOI: 10.1002/adfm.201203675).

25 R. He, J. Xu, Y. Yang, P. Cai, D. Chen, L. Ying, W. Yang, and Y. Cao, *Org. Electronics*, **2014**, *15*, 2950–2958. (DOI: dx.doi.org/10.1016/j.orgel.2014.08.026).

26 J. Zhang, S. Dong, K. Zhang, A. Liang, X. Yang, F. Huang, and Y. Cao, *Chem. Commun*., **2014**, *50*, 8227–8230. (DOI: 10.1039/c4cc03080j).

27 H. Xiao, J. Miao, J. Cao, W. Yang, H. Wub, and Y. Cao, *Org. Electronics*, **2014**, *15*, 758–774. (DOI: org/10.1016/j.orgel.2014.01.006).

28 S. Liu, C. Zhong, S. Dong, J. Zhang, X. Huang, C. Zhou, J. Lu, L. Ying, L. Wang, F. Huang, and Y. Cao, *Org. Electronics*, **2014**, *15*, 850–857. (DOI: org/10.1016/j.orgel.2014.01.016).

29 Y. Yang, L. Yu, Y. Xue, Q. Zou, B. Zhang, L. Ying, W. Yang, J. Peng, and Y. Cao, *Polymer*, **2014**, *55*, 1698–1706. (DOI: org/10.1016/j.polymer.2014.02.032).

30 N. Lin, J. Qiao, L. Duan, L. Wang, and Y. Qiu, *J. Phys. Chem. C*, **2014**, *118*, 7569−7578. (DOI: org/10.1021/jp412614k).

31 J. Yang, L. Zhao, X. Wang, S. Wang, J. Ding, L. Wang, X. Jing, and F. Wang, *Macromol. Chem. Phys*., **2014**, *215*, 1107−1115. (DOI: 10.1002/macp.201400046).

32 X. Wang, L. Zhao, S. Shao, J. Ding, L. Wang, X. Jing, and F. Wang, *Macromolecules*, **2014**, *47*, 2907−2914. (DOI: org/10.1021/ma500407m).

33 Y. Wang, Y. Gao, L. Chen, Y. Fu, D. Zhu, Q. He, H. Cao, J. Cheng, R. Zhang, S. Zheng, and S. Yan, *RSC Adv*., **2015**, *5*, 4853–4860. (DOI: 10.1039/c4ra12966k).

34 T. Guo, L. Yu, B. Zhao, L. Ying, H. Wu, W. Yang, and Y. Cao, *J. Polym. Sci. A: Polym. Chem*., **2015**, *53*, 1043–1051. (DOI: 10.1002/pola.27532).

35 X. Zhan, Z. Wu, Y. Lin, S. Tang, J. Yang, J. Hu, Q. Peng, D. Ma, Q. Lia, and Z. Li, *J. Mater. Chem. C*, **2015**, *3*, 5903–5909. (DOI: 10.1039/c5tc01028d).

36 G. Klaerner and R. D. Miller, *Macromolecules*, **1998**, *31*, 2007–2009. (DOI: 10.1021/ma971073e).

37 W. Yang, J. Huang, C. Liu, Y. Niu, Q. Hou, R. Yang, and Y. Cao, *Polymer*, **2004**, *45*, 865–872. (DOI: 10.1016/j.polymer.2003.11.052).

38 S. Janietz, D. D. C. Bradley, M. Grell, C. Giebeler, M. Inbasekaran, and E. P. Woo, *Appl. Phys. Lett*., **1998**, *73*, 2453–2455. (DOI: org/10.1063/1.122479).

CHAPTER 6

Soluble 4-Substituted Functionalised Polyfluorenones

6.1 Introduction

Most semiconducting conjugated polymers are electron-rich systems, which possess high HOMO energy levels (e.g polythiophenes, poly(*p*-phenylenevinylenes), polyfluorenes).[1,2,3,4] They show higher hole mobility in the materials compared to electron mobility, can be more easily p-doped to form positive polarons than n-doped to form negative polarons and their p-doped state is generally more stable. Historically, p-type semiconductors have been developed more than n-type, although a number of organic electronic applications require electron-deficient n-type semiconductors (e.g. n-type transistors for full logic circuits, photovoltaics (plastic solar cells), cathode materials, charge-transfer materials etc).[5,6,7,8,9,10,11] To decrease the LUMO of organic semiconductors, particularly in conjugated polymers several approaches are used, e.g. (i) implementation of electron-deficient heterocyclic systems in polymer chain (oxadiazoles, benzothiadiazoles, pyridines, quinoxalines, thiophenes-S,S-dioxides etc) or (ii) construction of conjugated polymers on electron-deficient heterocyclic building blocks, (iii) using electron-withdrawing substituents on the side chains, (iv) combination of electron-withdrawing/electron-donating building blocks in the construction of the polymer backbone to achieve a narrow band gap and a low LUMO level of polymers etc.[12,13,14,15,16]

The importance of n-type conjugated polymers was understood soon after the progress of other, electron-rich classes of polymers, and the field started to be developed in the 90s of last century.[17,18,19,20] Electron deficient conjugated polymers can increase the performance of OLEDs in two ways: (i) by improved electron injection from the metal cathode and (ii) by blocking the holes in the emitting layer from a cathode thus equalising the electrons and holes in the material, hence increasing the probability of exciton formation. In recent years, significant efforts have been made for charge transfer (CT) type polymers with the use of electron accepting and electron donating units.[21]

Fluorenone, in contrast to fluorene is an electron-deficient compound due to the electron-withdrawing character of the carbonyl group and from this point of view it represents an interesting building block for the construction of conjugated systems. Müllen et al. first

reported the electron deficient polymer 2,7-poly(fluorenone) (**PFon**) to be used as an electron injection material for multilayer OLED.[22] Lee et al. reported the electron mobility as 0.06 cm^{-2} V^{-1} s^{-1} for perfluorohexylcarbonyl-substituted fluorenone-based acceptors.[23] Facchetti, Marks et al. reported on the design of a series of bis(indeno)fluorenone-based polymers as n-channel and ambipolar semiconductors for OFETs.[24]

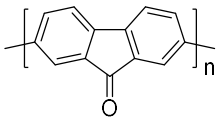

Polyfluorenone (PFon)

In the next sections, we highlight the history of the introduction of polyfluorenones as electron-deficient polymers and electron-transporting materials and give some examples of using fluorenone building blocks in the construction of low-LUMO lying and donor-acceptor conjugated polymers.

6.1.1 Unsubstituted polyfluorenone: electrochemical synthesis and synthetic approach through soluble precursor polymer

Zotti and co-workers first described the unprocessable films deposited on an electrode by electrochemical polymerisation from the cathodic coupling of fluorenone as early as 1986.[25] They also reported that anodic oxidative polymerisation of fluorenone was impossible. Electrochemically prepared polyfluorenone (**PFon**) without solubilising groups, was an insoluble material and was only characterised by cyclic voltammetry toward its redox potentials, with no evidence of its linear 1D structure and an absence of other types of couplings during electropolymerisation.

Later on, however, Onal et al. reported on the preparation of **PFon** by electrochemical oxidative polymerisation of fluorenone in DCM.[26] The obtained **PFon** films deposited on an anode have been characterised by cyclic voltammetry, FTIR and ESR. CV of polymer films showed a quasi-reversible oxidation and reduction peaks, similar to the material reported by Zotti and co-workers (Figure 6.1).[25] The UV-Vis spectrum was, however, unclear. It showed absorption bands at 440 and 860 nm. The longest one was assigned to polarons (which, however, was not completely removed by applying corresponding potentials). The shortest might correspond to the π-π* of the polymer chain, but it was weakly resolved and appeared as a shoulder, indicating poor quality polymer film.

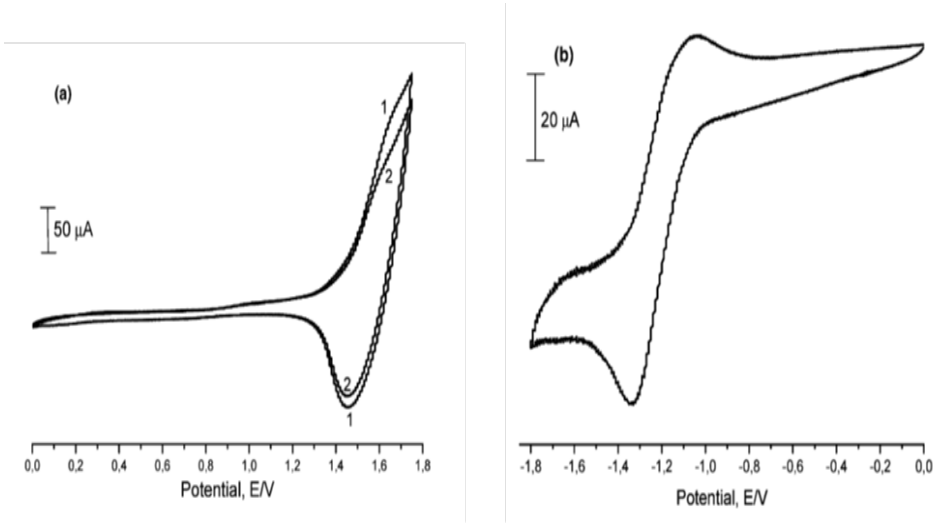

Figure 6.1 Cyclic voltammetry of **PFon** films obtained by electropolymerisation method: (a) anodic oxidation traces and (b) cathodic reduction traces.[26]

The first reportof the chemical synthesis of **PFon** was published by Müllen and co-workers who reported the synthesis of insoluble 2,7-poly(9-fluorenone) (**PFon**) through a soluble precursor polyfluorene **6.6** (Scheme 6.1).[27] The idea of the work was to functionalise the carbonyl group by converting it into a ketal with a long-chain solubilising group and to cleave it back to the keto group in an acidic condition to get **PFon**. For that, the authors coupled 2,7-dibromofluorenone (**6.4**) with diol **6.3** (obtained from malonic acid diethyl ester (**6.1**) by Knoevenagel reaction with 1-iodooctane following reduction of diester **6.2** with $LiAlH_4$) in acidic conditions to obtain monomer **6.5**. This monomer was polymerised through the Yamamoto reaction to obtain the precursor polymer **6.6**.

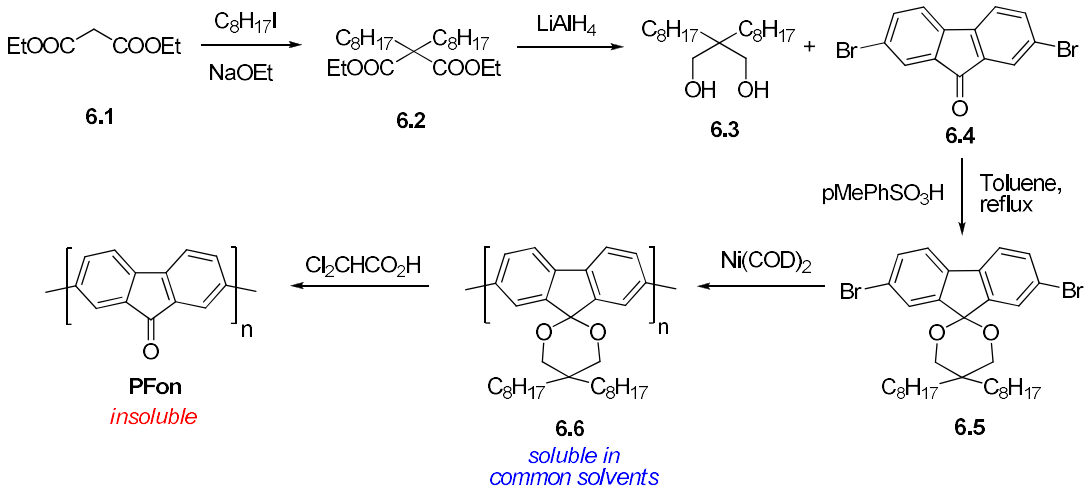

Scheme 6.1 First synthetic method to polyfluorenone **PFon** from precursor polymer **6.6**.[27]

The precursor polyfluorene **6.6** showed good solubility in general organic solvents and was fully characterised by ^{1}H NMR (Figure 6.2) and other methods. This polymer was obtained with high molecular weights (M_w = 200,000 Da, M_n = 76,000 Da) and demonstrated thermal decomposition at 314 °C. It was characterised as an amorphous material with no phase transitions in the range of –100 °C to +200 °C (DSC). Polymer **6.6** showed an absorption maximum at 384 nm and PL emission at 414 nm in chloroform solution and 456 nm in thin film (typical for polyfluorenes, although a more pronounced shift in PL from solution to the solid state was observed).

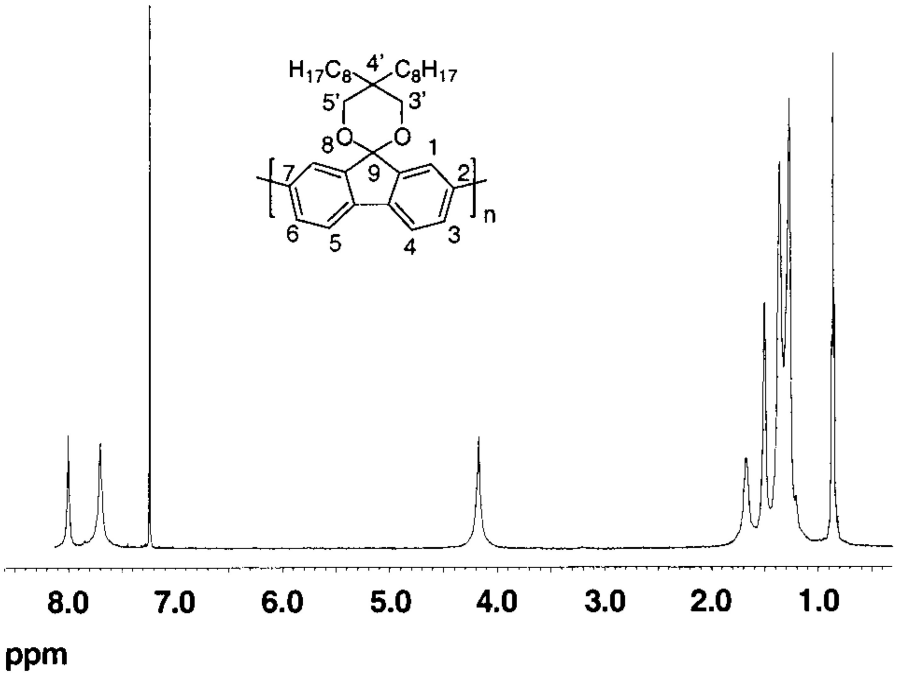

Figure 6.2 ^{1}H NMR spectrum of precursor polyfluorene **6.6**.[27]

The precursor polymer **6.6** thin film was heated at 50 °C and exposed to a dichloroacetic acid atmosphere resulting in a change of its colour from yellow (typical for polyfluorenes) to red (expected for polyfluorenones). The film was washed with acetone and the insoluble film of **PFon** was characterised (in particular, the IR spectrum evidently showed the carbonyl group appeared at 1716 cm^{-1}). The insoluble thin film of **PFon** polymer showed three absorption bands at 306, 374 and 480 nm, respectively (Figure 6.3). The peak at 374 nm, close to that in polyfluorenes, assigned as the π-π* transition of the delocalised electrons on the polymer backbone while the longest wavelength peak at 480 nm is due to the n-π* forbidden transition of the carbonyl group of **PFon**. A thin **PFon** film on indium/ITO can be electrochemically reduced showing the quasi-reversible reduction at –1.48 eV vs Fc/Fc^+ that corresponds to its LUMO energy level of – 3.3 V (Figure 6.3). This value is in the

order of the magnesium work function (–3.7 eV), used as an electrode in OLEDs, thus making **PFon** a promising electron injection/electron transport and hole blocking material. The Müllen group have further studied this polymer in OLEDs and have shown that it emits red light with a peak at 580 nm for both photoluminescence and electroluminescence processes.[18] Analysis of current-electrical field characteristics for ITO/**6.6**/Mg and ITO/**PFon**/Mg devices showed that the current in **PFon**-based devices is of 4–7 orders of magnitude higher than that in polymer **6.6**, and the electron mobility in **PFon** estimated from these characteristics was on the order of 10^{-6} cm^2 $V^{-1}s^{-1}$.

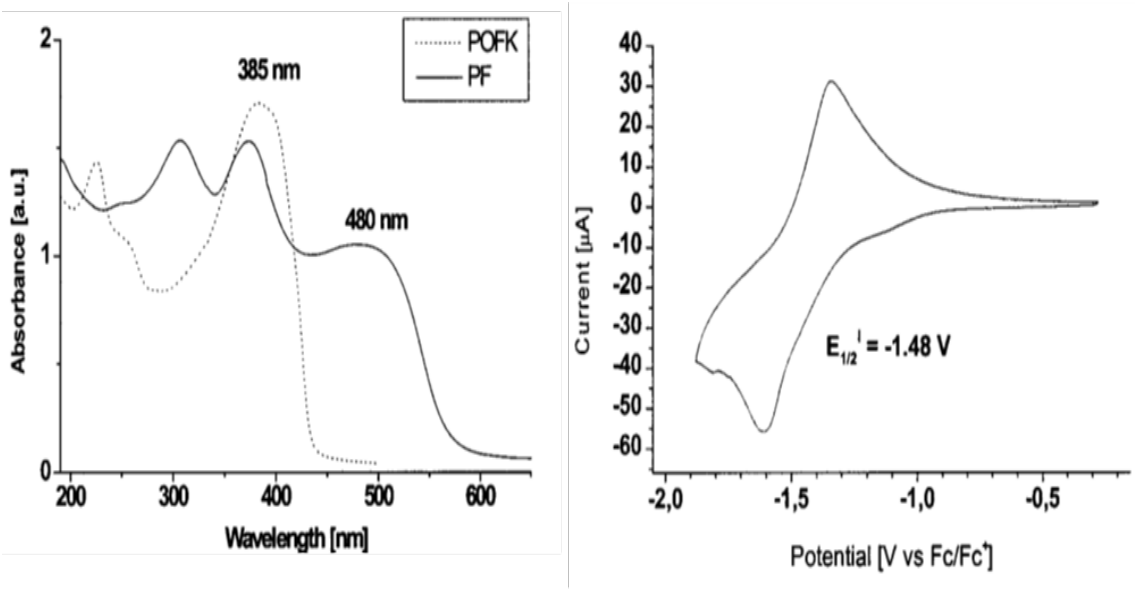

Figure 6.3 UV-Vis absorption spectra of precursor polymer **6.6** (POFK) and polyfluorenone **PFon** (PF on a graph) (left) and cyclic voltammogram of **PFon (**right).[27]

6.1.2 Soluble 4-arylsubstituted polyfluorenone (Ar-PFon)

After seven years of their initial report on insoluble **PFon**, Müllen and co-workers reported the first synthesis of soluble polyfluorenone with a bulky aryl substituent at position 4, **Ar-PFon**.[28] The synthetic route to polymer **Ar-PFon** is outlined in Scheme 6.2. Starting from commercially available 2,7-dibromofluorene (**3.22**), in several steps they prepared 2,7-dibromo-4-ethynylfluorenone (**6.8**), which underwent Diels-Alder reaction with R-functionalised tetraphenylcyclopentadiene to give monomer **6.9** with a bulky polyaryl substituent at position 4, decorated with branched solubilising alkyl groups. Ni-mediated Yamamoto polycondensation gave the target polymer **Ar-PFon** (Scheme 6.2).

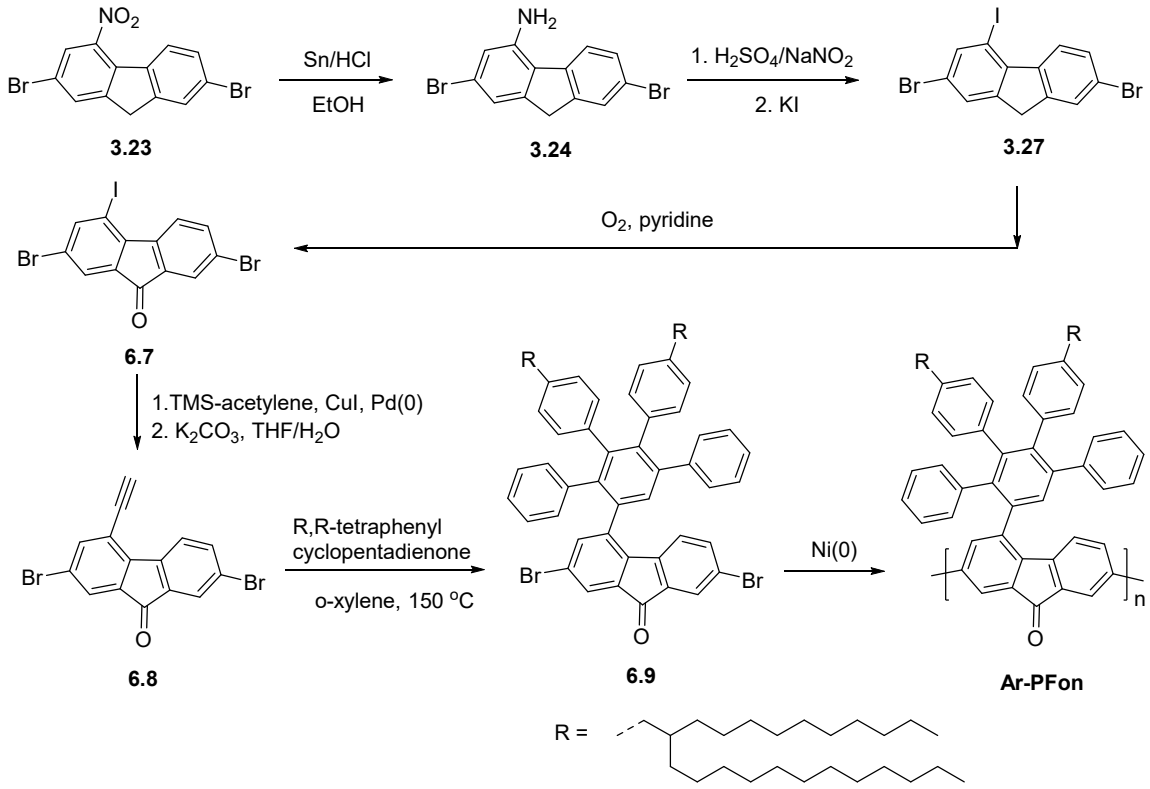

Scheme 6.2 Synthetic route to dendronised 4-substituted polyfluorenone **Ar-PFon**.[28]

The synthesised **Ar-PFon** was well soluble in common organic solvents such as toluene or THF, and showed high thermal stability (T_d = 400 °C from TGA analysis). According to GPC data, it had M_n = 26, 000 Da that corresponds to ca. 20 repeating units. The polymer was amorphous, with no phase transitions in the range of –100 °C to 350 °C. The UV-Vis absorption spectra in toluene showed two peaks at 367 nm (π-π* transition of polyphenylene backbone) and 456 nm (n-π* forbidden transition of the carbonyl group), that is close to that observed in previously reported work on substituted **PFon** (Figure 6.4).[27] Some bathochromic shift was observed in the films. The PL emissions of **Ar-PFon** polymer in solution and in thin films were 524 nm and 554 nm, respectively, i.e. hypsochromically shifted compared to **PFon** (*cf.* Figures 6.3 and 6.4). The electron affinity (LUMO energy level) of this polymer estimated from differential pulse voltammetry (DPV) gave the value of –3.0 eV, that is **Ar-PFon** is somewhat weaker as an electron acceptor compared to unsubstituted **PFon** (–3.3 eV).

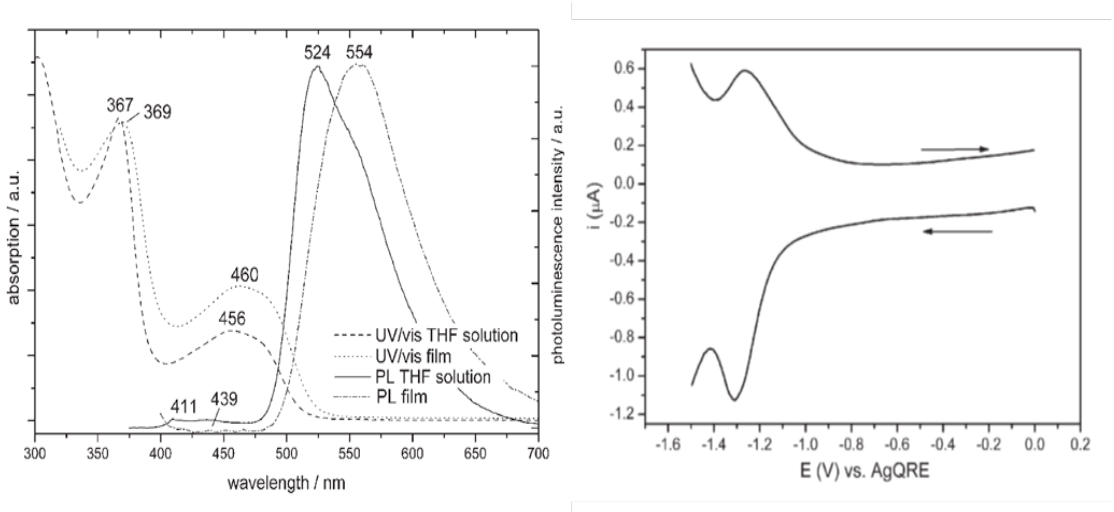

Figure 6.4 Normalised UV-Vis absorption and PL emission spectra of **Ar-PFon** in THF solution and in films (left) and reduction potential graph from DPV experiments (right).[28]

6.1.3 Fluorenone-containing copolymers

While oxidation of polyfluorenes (thermal, photo- or in device operation) resulting in an appearance of fluorenone defects in the polymer backbone is a very undesired process (see Chapter 2), fluorenone has been successfully used as a building block in the synthesis of various conjugated copolymers for organic electronic applications. Structures of some such copolymers are shown in Figure 6.5. Panozzo et al. reported the synthesis and studies of fluorene-fluorenone copolymer **6.10** as a stable and efficient material for EL devices with yellow emission.[29] This red shifted emission (compared to polyfluorenes) was attributed to excimers or aggregates and an involvement of the fluorenone segment in the exciton transfer between non aggregated fluorene and aggregates of fluorenones. Recently, Sonar et al. reported fluorenone–thiophene-based copolymer **6.11** with a small band gap of 1.62 eV, which was used as high mobility OFET material.[30] Ying-ping et al. reported two red emissive PPV-type copolymers with a fluorenone moiety in the backbone, **6.12** and **6.13**.[31] These copolymers were very soluble in organic solvents and showed good thermal stability (T_d = 410 °C). Polymers **6.12** and **6.13** absorbed at 428 and 445 nm, and were emissive with PL peaking at 633 and 620 nm, respectively. They demonstrated rather high electron affinity, showing reversible reduction potentials at –1.54 eV and –1.57 eV that correspond to LUMO energy levels of –3.17 eV and –3.14 eV, respectively (HOMO energy levels are –5.21 eV and –5.31 eV, with band gaps of 2.04 eV and 2.17 eV, respectively).

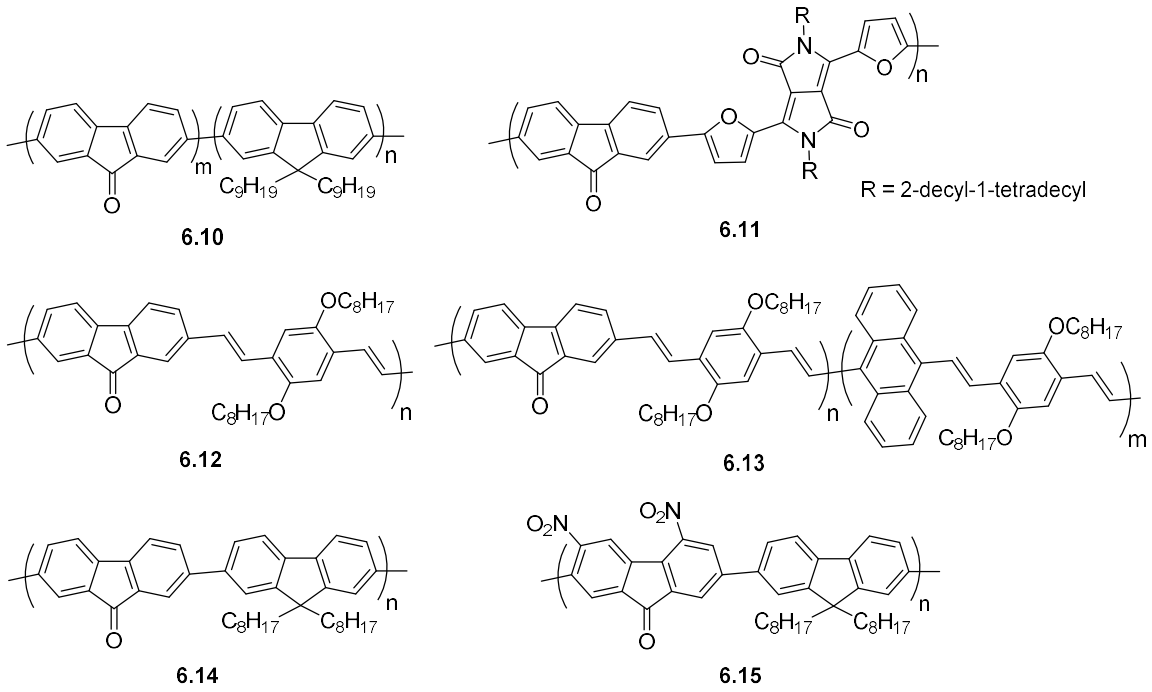

Figure 6.5 Examples of fluorenone-containing copolymers.[29,30,31, 32]

Hayashi et al. reported the synthesis and comparative studies of two fluorenone-containing copolymers, **6.14** and **6.15** (Figure 6.5).[32] Due to the presence of two nitro groups at positions 3 and 5, polymer **6.15** containing a 3,5-dinitro-fluorenone moiety showed high electron affinity, 1.18 eV higher than that of polymer **6.14** (reduction potentials are –0.84 V and –2.02 V, respectively) (Figure 6.6). The thermal stability of polymer **6.15** was somewhat lower than commonly observed for polyfluorenes or its copolymers, but was still high (T_d = 326 °C). The UV-Vis absorption showed three overlapped bands peaking at 312 nm (unassigned transition), 392 nm (π-π* transition), and 468 nm (n-π* transition). The n-π* transition was much more intense than that of polymer **6.14**, although this might be due to overlap with nitro aromatic absorption. In films, polymer **6.15** also showed a bathochromic shift in emission compared to **6.14** (~600 nm and ~550 nm, respectively, Figure 6.6), but in both cases the PLQY were very low (0.1% for **6.14** and even lower for **6.15**).

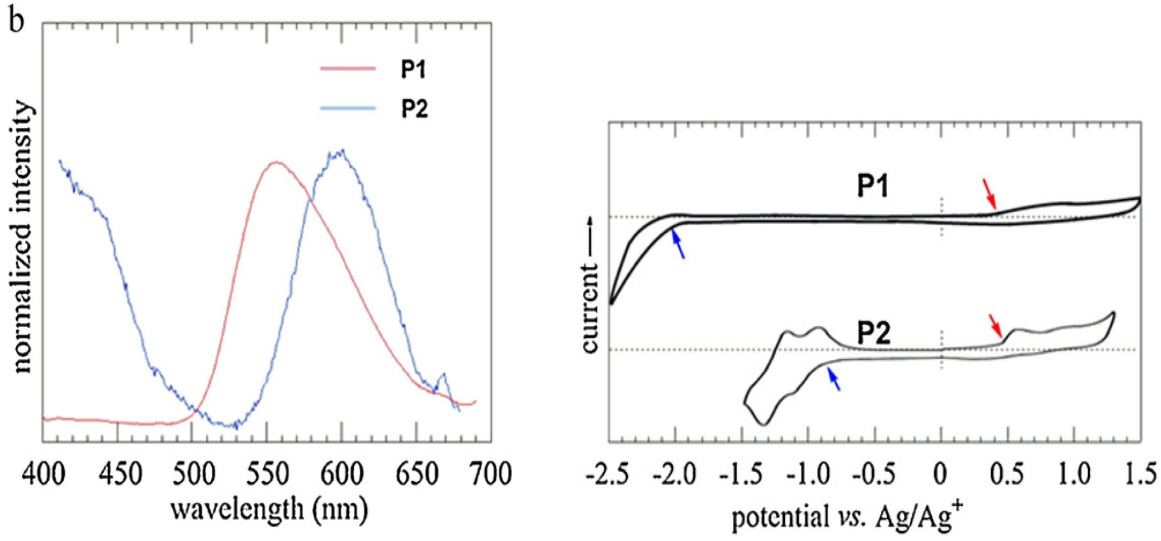

Figure 6.6 Normalised PL emission spectra (left) and cyclic voltammetry traces (right) for films of polymers **6.14** (P1) and **6.15** (P2).[32]

6.1.4 Aims and research objectives

The aim of the research described in this chapter was to synthesise and characterise soluble 4-substituted polyfluorenones as electron-deficient polymers. We considered to insert linear alkyl chains as solubilising groups because such a motif represents an interest in a sense that the solubilising group can lie in the plane of the aromatic fluorene ring, allowing closer π-π interactions between neighbouring polymer chains in the solid state. For this goal we decided to use chemistry developed in Chapter 3, in which we described synthetic approaches to 2,7-dibromofluorenones with EDG and EWG groups OBu, SBu and SO_2Bu (which were used in the case for the synthesis of **X-PF6/8** series of polymers). We considered that the dodecyl chain should be long enough to bring solubility to the polymers and as such we expected to obtain information on the electronic effects of 4-substituents on the properties of soluble polyfluorenones **X-PFon**. So here we describe the synthesis of 4-substituted polyfluorenones **X-PFon** (X = $OC_{12}H_{25}$, $SC_{12}H_{25}$, $SO_2C_{12}H_{25}$) and their characterisation by electrochemical and spectroscopic methods.

6.2 Results and Discussion

6.2.1 Synthesis of 4-substituted 2,7-dibromofluorenone monomers

Similar to the reaction route described in Chapter 3, for the synthesis of 4-substituted 2,7-dibromofluorenes with long-chain solubilising groups (X = $C_{12}H_{25}$, $SC_{12}H_{25}$ and $SO_2C_{12}H_{25}$), we started from 2,4,7-trinitrofluorenone (**3.19**). 2,7-Dinitro-4-hydroxyfluorenone (**3.56**) obtained from **3.19** was alkylated with 1-bromododecane /potassium carbonate in DMF to afford 2,7-dinitro-4-dodecyloxyfluorenone (**6.16**) (Scheme 6.3). Nucleophilic aromatic substitution in **3.19** with dodecylmercaptane gave a mixture of two isomers **6.17** and **6.18** in the approximate ratio of (3–4):1 (from the NMR spectrum of the crude product). Two spots on TLC for the crude product had very close R_f in many solvents we tested, so their separation by column chromatography was problematic. We were able to isolate in low yields two pure samples of **6.17** and **6.18** to prove their structures, but the method was impractical for larger scale. Therefore, we performed several recrystallisation attempts of crude materials from various solvent systems such as acetonitrile, acetone, methanol, cyclohexane, 1-butanol, heptane and ethyl acetate. Fortunately, we were able to recrystallise it successfully from 1,4-dioxane to obtain the desired 2,4-dinitro-4-dodecylthiofluorenone (**6.17**) in a pure state in 65% yield.

Regarding the second product, its structure was confirmed as **6.18** by its ^{1}H NMR shifts/couplings and ^{1}H-^{1}H COSY spectra (Figure 6.7). The ^{1}H-^{1}H COSY spectrum showed correlations between interaction protons as one would expect for structure **6.18** (Figure 6.7).

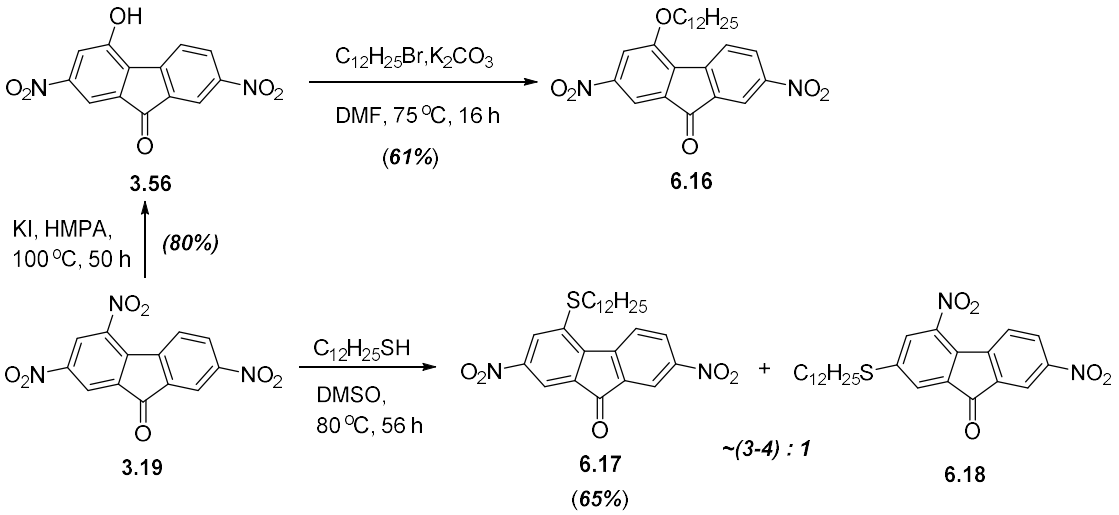

Scheme 6.3 Synthesis of 2,7-dinitro-X-fluorenones **6.16** and **6.17**.

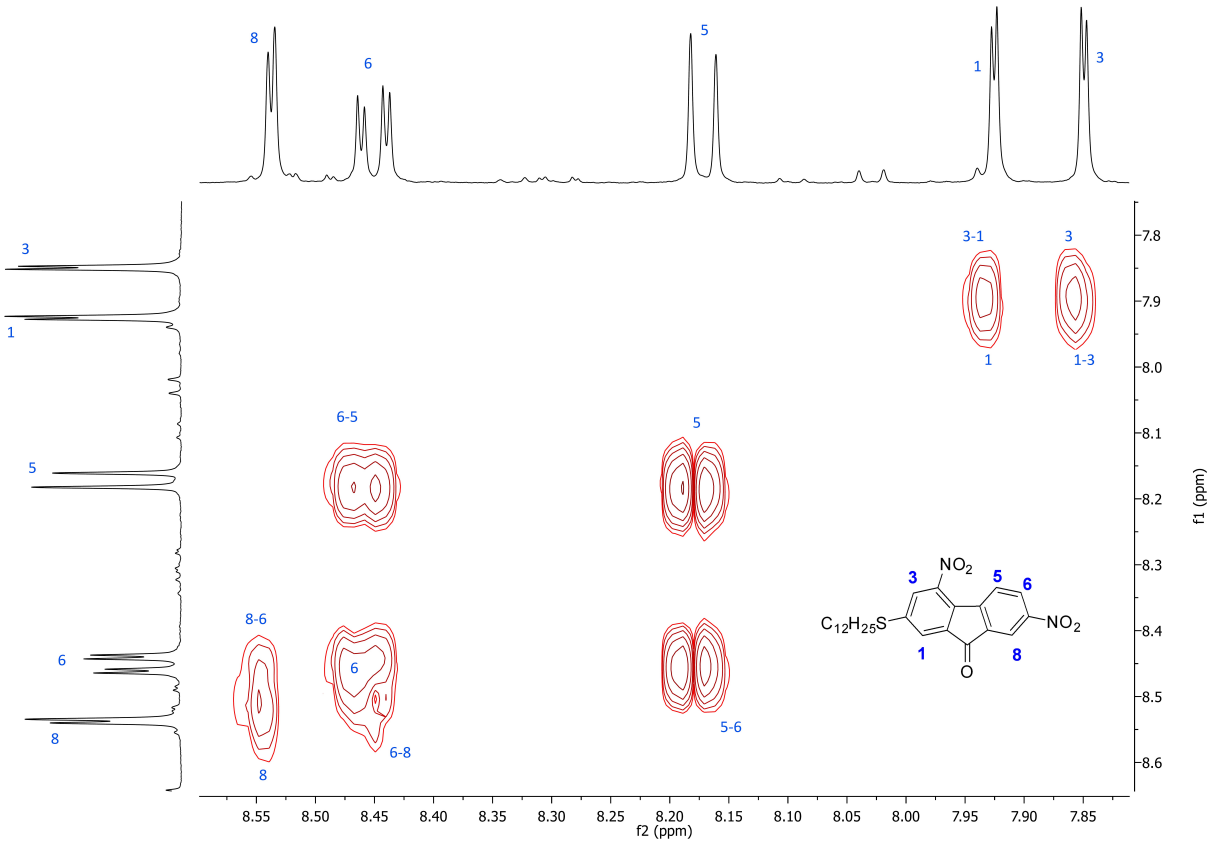

Figure 6.7 ^{1}H-^{1}H-COSY NMR of 2-dodecylthio-4,7-dinitrofluorenone (**6.18**) in $CDCl_3$ with assignments of proton signals.

We tried to reduce two 2,7-nitrogroups by hydrogen (1 atm) using 10% Pd/C.[33] However, our trials using different solvents (EtOH, toluene, THF) were not very successful. The reaction did not work well in EtOH and toluene (mainly starting materials on TLC after 54 h), perhaps due to the low solubility of the starting compound **6.17** in these solvents. In THF, the solubility was somewhat better, but nevertheless the reduction process was very slow and conversion was too far from completion after 55 h at room temperature. Therefore we turned to a classical reduction by Sn/HCl (37%), successfully used for the reduction of other 2,7-dinitrofluorenones in Chapter 3. In this case, the nitro groups in **6.16** and **6.17** were readily reduced to amino groups at 100 °C for 3 h to give compounds **6.19** and **6.20** in reasonably high yields of 59–84%. (Scheme 6.4).

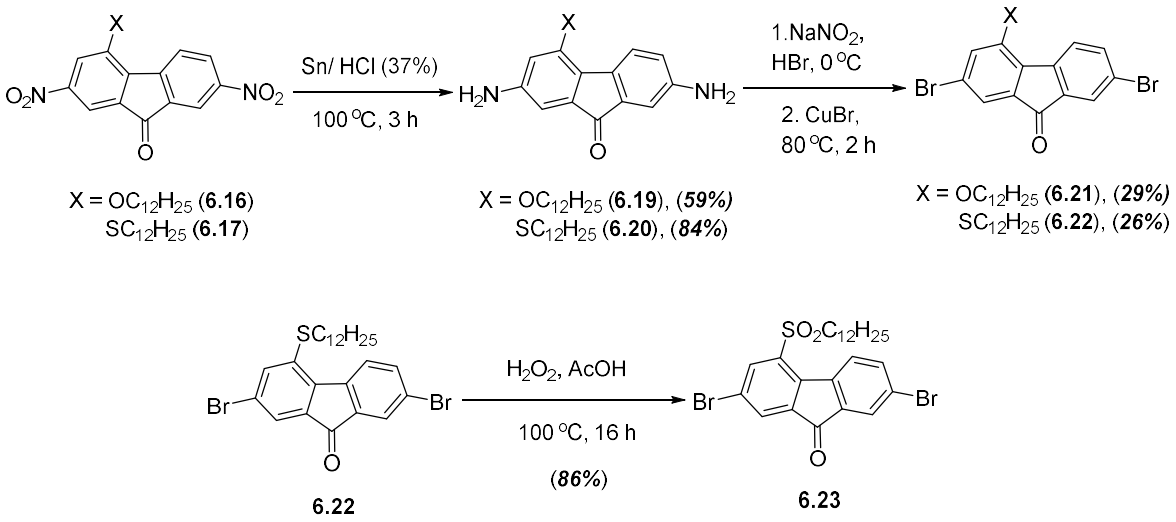

Scheme 6.4 Synthesis of X-2,7-dibromofluorenones (X = $OC_{12}H_{25}$, $SC_{12}H_{25}$) **6.21**–**6.23.**

These 2,7-diamino compounds **6.19** and **6.20** were then converted into the corresponding 2,7-dibromofluorenones **6.21** and **6.22** by diazotization with $NaNO_2$/HBr and Sandmeyer reaction *in situ* in the presence of copper(I) bromide (CuBr) at 80 °C. The obtained 2,7-dibromo-4-dodecylthiofluorenone (**6.22**) was oxidised with hydrogen peroxide in acetic acid, similar to the procedure described in Ref. 34 which we used in Chapter 3 for 4-butylthiofluorenone **3.61** to afford 4-dodecylsulphonyl-derivative **6.23** in high yield. Thus, we have obtained three 4-substituted fluorenone monomers with strong EDG (**6.21**, X = $OC_{12}H_{25}$), weak EDG (**6.22**, X = $SC_{12}H_{25}$) and strong EWG (**6.23**, X = $SO_2C_{12}H_{25}$), (Scheme 6.4).

Initially, we considered two methods of synthesis of polyfluorenones, i.e Ni(0)-mediated Yamamoto polycondensation and Miyara-Suzuki coupling polymerisation of dibromofluorenones with fluorenone-diborolanes. The aims were (i) to expand the synthetic methods to polyfluorenones and (ii) to realise combinations of fluorenone building blocks with different EDG/EWG groups at position 4 in coupling polymerisation. Therefore, using the common Miyaura borylation protocol of the Pd-catalysed reaction of arylbromides with diborolanes,[35] we synthesised fluorenone-2,7-diboronic acid dipinacol ester **6.24** from 2,7-dibromo-4-dodecyloxyfluorenone **6.21** (Scheme 6.5). However, in the future studies we did not use this monomer for the synthesis of polymers, because we faced a problem of solubility of the high molecular weight 4-substituted polyfluorenones, synthesised by Yamamoto polymerisation (see next section).

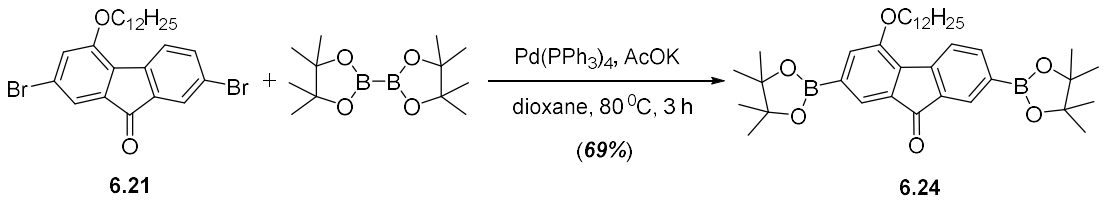

Scheme 6.5 Synthesis of 4-dodecyloxyfluorenone-2,7-diboronic acid dipinacol ester (**6.24**).

6.2.2 Optimisation of polymerisation of 2,7-dibromo-4-X-fluorenones and analysis of 4-substituted poly- / oligo-fluorenones

For the preparation of 4-substituted polyfluorenones, **X-PFon**, from monomers **6.21–6.23**, we initially attempted to use common conditions of the Yamamoto polymerisation with ca. 2 eq. of $Ni(COD)_2$ in a mixture of DMF/toluene system at 80 °C for 98 h.[36,37] These conditions worked well when **X-PF8** and **X-PF6/8** polymers were prepared (Chapter 4). However, polymerisation of the 4-dodecylsulfonyl-substituted monomer **6.23** using these common conditions gave an insoluble red material in near quantitative yield (Scheme 6.6a).

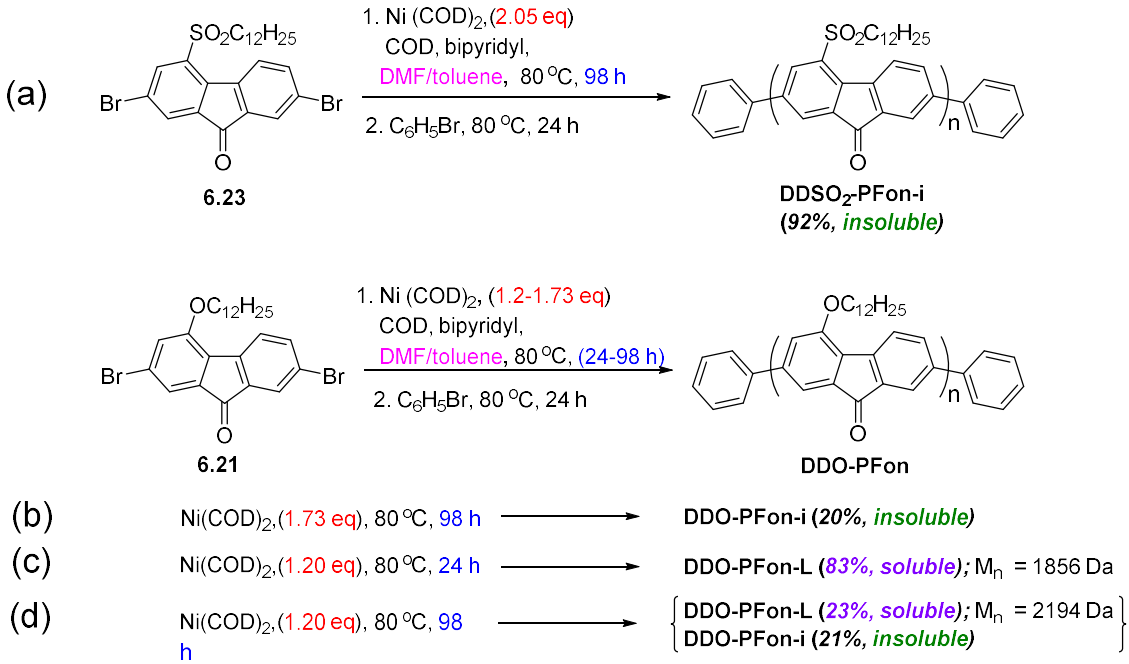

Scheme 6.6 Initial attempts to synthesise soluble **X-PFon** polymers by Yamamoto polymerisation.

The UV-Vis spectrum of this insoluble material (presumably polyfluorenone **$DDSO_2$-PFon-i**) in the solid state on an integrating sphere in a reflectance mode showed a shoulder around 380–410 nm, with some small peaks on the red side of this absorbance band at ca. 440 and 480 nm (Figure 6.8a). By stirring/extracting of this sample with chloroform for 24 h,

some soluble fraction was obtained after filtration through a 0.2 μm membrane filter. The solution had a slightly reddish colour and its UV-Vis spectrum showed peaks at 308, 386, 477 and 501 nm. By the shape and the spectral region it was very similar to the insoluble unsubstituted **PFon** (cf. Figure 6.8b and 6.3). The peak at 386 nm was assigned to the π-π* transition and peaks at 477/501 nm to the n-π* excitation.

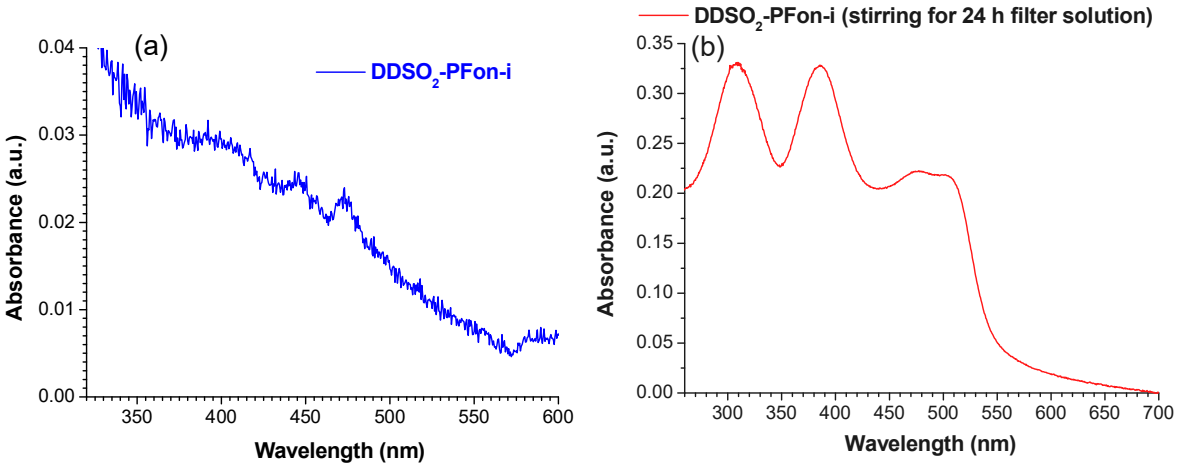

Figure 6.8 UV-Vis electron absorption spectra for insoluble polymer **DDSO$_2$-PFon-i** synthesised by Scheme 6.6a: (a) solid-state UV-Vis spectrum on an integrating sphere in reflectance mode (versus $BaSO_4$ background), (b) UV-Vis spectrum of chloroform fraction extracted from the solid material (after filtration through 0.2 μm membrane filter).

Scanning electron microscopy (SEM) did not show highly ordered material (as one would expect from "as precipitated" polymer), however some layered structure was observed (Figure 6.9). Therefore, we performed powder X-ray diffraction (XRD) analysis of the sample (Figure 6.10). Two broad peaks were observed in the XRD indicating some ordering in the material. The first peak at $2\theta = 19.2^{o}$ corresponds to a distance of 4.61 Å, a typical distance of π-π stacking in organic materials. Hence it can be assigned to the π-π distance between the neighbouring chains of **DDSO$_2$-PFon-i** polymer. The second broad signal at $2\theta = 25.7^{o}$ corresponds to 3.46 Å. This value is smaller than the doubled value of polymer "width" (i.e. the dimension of fluorenone unit in the perpendicular direction to the main chain, ~2.3 Å). As such, we can assign it to the in-plane distance between polyfluorenone chains, in which case linear dodecylsulfanyl groups (which are orthogonal to the main polymer chain direction) are interdigitated, decreasing the "in-plane" distance between the polymers chains.

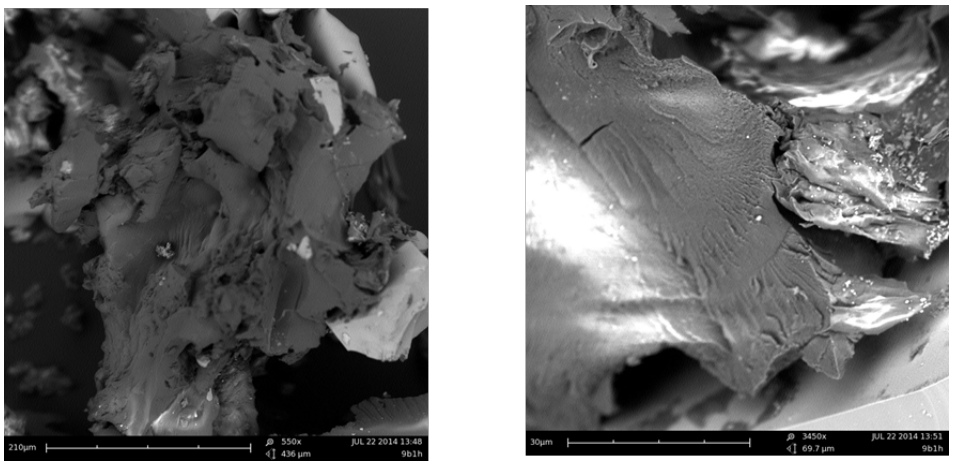

Figure 6.9 Scanning electron microscopy (SEM) image of **DDSO$_2$-PFon-i** (insoluble polymer, synthesised by Scheme 6.6a).

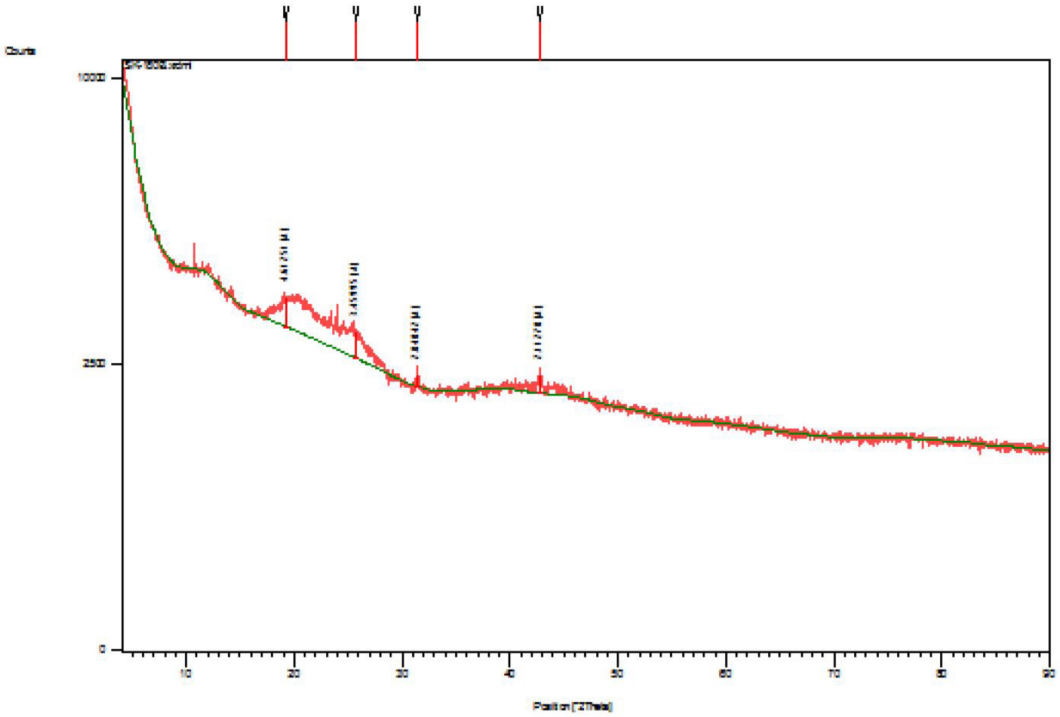

Peak List

Pos.[°2Th.]	Height[cts]	FWHM[°2Th.]	d-spacing[Å]	Rel.Int.[%]
19.2432	589.01	1.0706	4.61251	100.00
25.7491	480.14	1.3382	3.45995	81.52
31.4064	175.10	0.4015	2.84842	29.73
42.7646	283.94	0.4896	2.11278	48.21

Figure 6.10 Powder X-ray diffraction (XRD) of **DDSO$_2$-PFon-I** synthesised by Scheme 6.6a. The broad peak at 2θ = 19.2^o (4.61 Å) corresponds to a π-π distance between polyfluorenone chains and the smaller peak at 2θ = 25.7^o (3.46 Å) corresponds to the in-plane distance between the chains with interdigitating dodecylsulfonyl side groups.

So, it seems that Yamamoto polymerisation works well for fluorenones, but the solubilising effect of a linear dodecyl chain is not enough to make the material soluble. Therefore, we considered to optimise the reaction conditions to obtain lower molecular weight polymers (but with M_n to be high enough, close to the effective conjugation length of the materials). These experiments have been performed on 4-dodecyloxyfluorene **6.21** and we decreased the amount of $Ni(COD)_2$ to obtain a soluble polymer with a lower molecular weight. When 1.73 eq. of $Ni(COD)_2$ was used, 20% of insoluble fraction **DDO-PFon-i** was isolated along with a small amount of soluble polymer (analysed by ^1H NMR) (Scheme 6.6a) together with a substantial amount of methanol/acetone soluble fractions (short oligomers). Decreasing the amount of $Ni(COD)_2$ to 1.2 eq. and reducing the time of the reaction from 4 days to 1 day resulted in a mixture of short oligomers in the crude product (Scheme 6.6c). GPC analysis of this material showed elution of short oligomers of a few thousands Daltons, followed by three well-resolved peaks for hexamer/trimer/monomer (Figure 6.11) (see also the details in the experimental part for the synthesis of **DDO-PFon-L** in Exp. SK-181). Similar results were obtained when the reaction time was increased to 96 hours (83% yield, with very close GPC analysis data (Experimental part, synthesis of **DDO-PFon-L,** Exp. SK-182). The combined crude products were extracted by MeOH (18% yield) and then acetone (15% yield) to remove the monomers and short oligomers (dimer and maybe partly trimer), and the chloroform-soluble fraction **DDO-PFon-L** (22% yield) from the residue. This was analysed by MALDI-TOF, showing that the material represented a mixture of oligomers from trimer to octamer (Figure 6.12). There was also an insoluble polymer isolated within the yield of 21% (presumably formed mainly in the longer 96 h experiment, Scheme 6.6d).

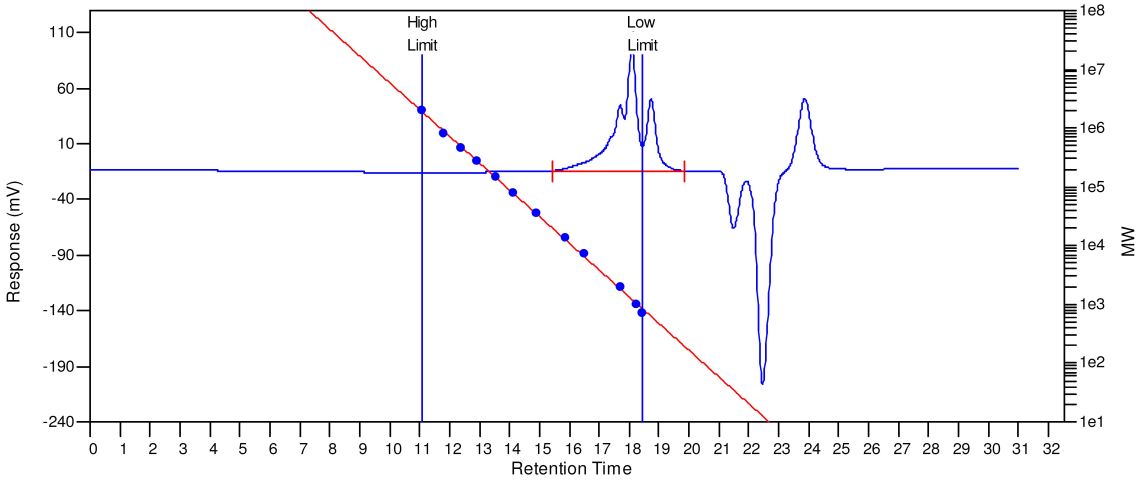

Distribution Plots

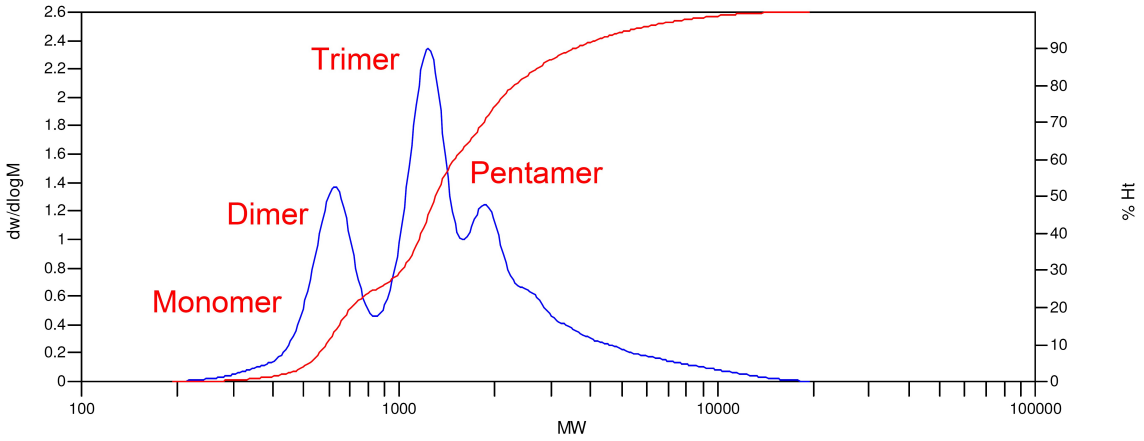

MW Averages

Peak No	Mp	Mn	Mw	Mz	Mz+1	Mv	PD
1	1234	1110	1818	3565	6592	1658	1.63784

Processed Peaks

Peak No	Name	Start RT (mins)	Max RT (mins)	End RT (mins)	Pk Height (mV)	% Height	Area (mV.secs)	% Area
1		15.45	18.08	19.85	110.732	0	6213.41	100

Figure 6.11 GPC data for low molecular weight **DDO-PFon-L** polymer (chloroform-soluble fraction from synthesis in Scheme 6.6c).

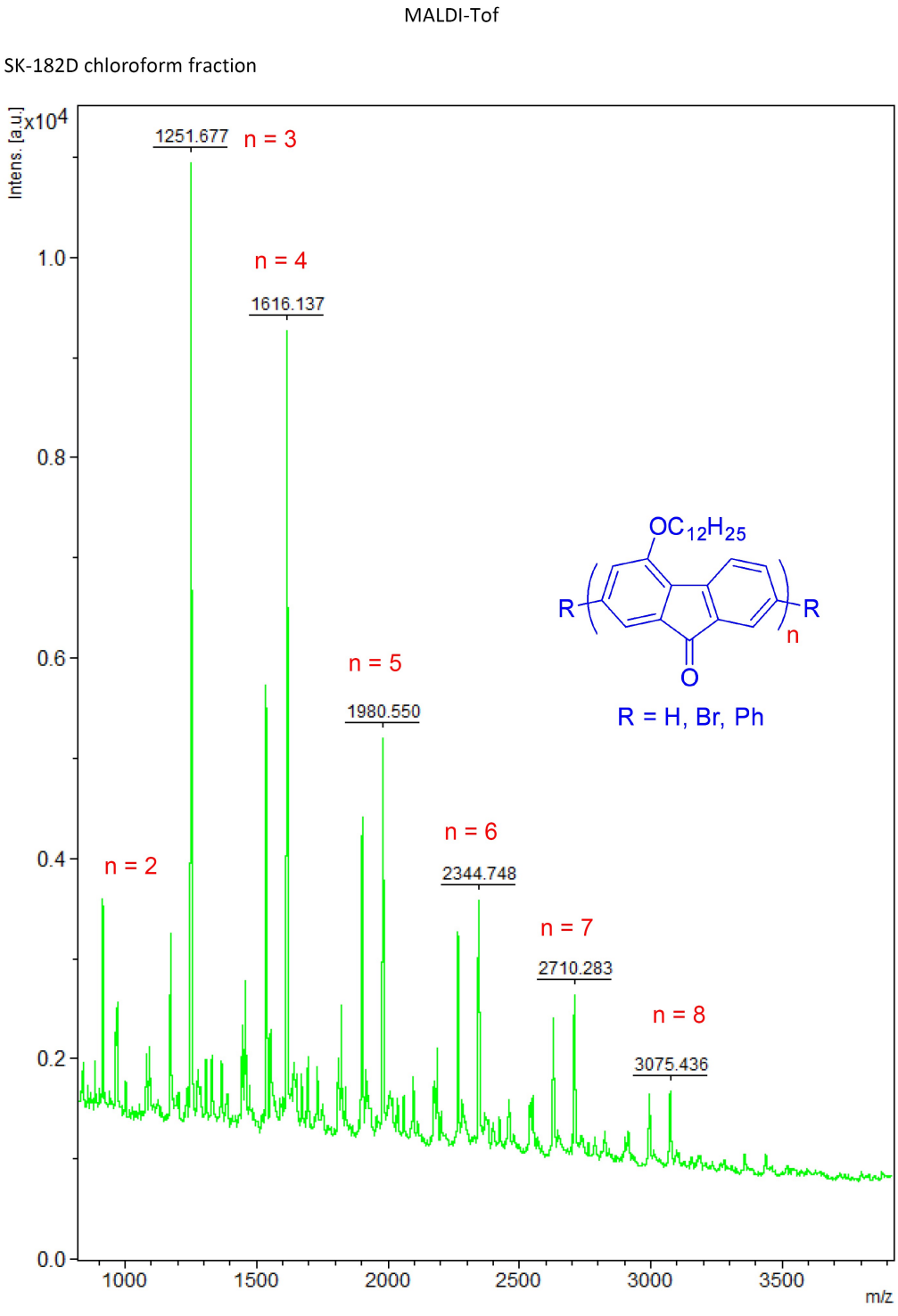

Figure 6.12 MALDI-TOF mass spectrum for low molecular weight polymer **DDO-PFon-L** polymer (chloroform-soluble fraction from synthesis in Scheme 6.6c).

6.2.3 Synthesis and characterisation of soluble 4-substituted polyfluorenones X-PFon

Considering the data obtained in the previous section for the formation of insoluble **X-PFon** polymers and short oligomers, depending on the reaction conditions, we have taken out an additional step forward to obtain soluble **X-PFon** polymers. First, we aimed to generate soluble materials and, secondly, to obtain materials with molecular weights high enough to "classify the materials as polymers" (i.e to have polymer chain lengths close or slightly above the effective conjugation length in the related class of polymers, i.e. polyfluorenes (n ~ 12)). Therefore we have considered two points. First, to use pure DMF as a reaction medium for polymerisation (instead of the usual DMF/toluene mixture) hoping that limited solubility of the polymers in polar DMF will control at some extent the molecular weights of the formed materials, thus preventing their further polymerisation to higher molecular weight insoluble polymers. Second, to decrease slightly the amount of $Ni(COD)_2$ to 1.1 eq. and to start the polymerisation reaction in an "unusual way" by mixing all components together (instead of the preparation of the Ni(0) reactive complex followed by addition of dibromoarene, as commonly used).

Polymerisation reactions for all three monomers **6.21–6.23** have been performed under these conditions (Scheme 6.7). After normal workup, i.e. quenching the crude products with methanol:concentrated HCl, removal of the short oligomers and by-products by Soxhlet extraction, the final polymers have been isolated from the residual chloroform-soluble fraction with reasonable yields (33–51%) as red solid materials.

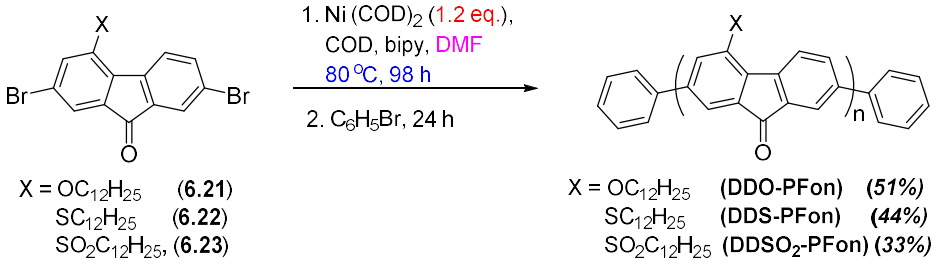

X = $OC_{12}H_{25}$ (**6.21**)
$SC_{12}H_{25}$ (**6.22**)
$SO_2C_{12}H_{25}$, (**6.23**)

X = $OC_{12}H_{25}$ (DDO-PFon) ***(51%)***
$SC_{12}H_{25}$ (DDS-PFon) ***(44%)***
$SO_2C_{12}H_{25}$ (**$DDSO_2$-PFon**) ***(33%)***

Scheme 6.7 Synthesis of **X-PFon** polyfluorenones (X = $OC_{12}H_{25}$, $SC_{12}H_{25}$, $SO_2C_{12}H_{25}$). Yields are given for soluble fractions, purified from low-molecular weight oligomers

The synthesised polymers have been characterised by ^1H NMR spectroscopy and their spectra have been compared to that of the parent monomers. For example, Figure 6.13 shows the ^1H NMR spectra for both monomer **6.2 h** (X = $SO_2C_{12}H_{25}$) and polymer **$DDSO_2$-PFon**. All the required signals, present in the monomers, are observed in **$DDSO_2$-PFon** and slightly downfield shifted, as we observed for series of **X-PF8** and **X-PF6/8** polymers (with additional small peaks of phenyl-end-cappers), confirming the structure of the polymer.

GPC analysis of the synthesised **X-PFon** polymers showed that they have molecular weights in the range of M_n = 4.700–5,800 Da with a quite narrow polydispersity of PDI = 1.05–1.12 (Table 6.1). For example, (Figure 6.14) shows a smooth GPC trace of **DDS-PFon** polymer which corresponds to an average polymer chain length of n = 11.7–16.0. This is close to or above the effective conjugation lengths reported in the literature for structurally related polyfluorenes. As such, their electrochemical and spectroscopic parameters should be characteristic values for polyfluorenone polymers.

TGA analysis shows rather high thermal stability of all **X-PFon** polymers with decomposition temperatures above 340 ^oC, although slightly lower than polyfluorene materials (Figure 6.15 and Table 6.1).

Table 6.1 GPC and TGA data for soluble poly(4-X-fluorenones) **X-PFon** (X = $OC_{12}H_{25}$, $SC_{12}H_{25}$, $SO_2C_{12}H_{25}$).

Polymer	M_w,[a] (Da)	M_n,[a] (Da)	n[b]	PDI[c]	T_d,[d] (^oC)
DDO-PFon	6,100	5,800	16.0	1.05	377
DDS-PFon	6,200	5,600	14.8	1.10	358
DDSO$_2$-PFon	5,300	4,700	11.4	1.12	351
Ar-PFon[28]	70,000	27,000	22.1	2.6	400

[a] M_w is weight average molecular weight and M_n is number average molecular weights versus polystyrene standards. [b] n is an average number of repeating monomer units in the polymer chain, estimated as $n = M_n/M_W$, where M_W is molecular weight of the monomer unit (presence of end group, H, Br or Ph have not been taken in these estimations); [c] Polydispersity index, $PDI = M_w/M_n$. [d] T_d is an onset decomposition temperatures measured at 5 % weight loss by TGA under N_2 atmosphere.

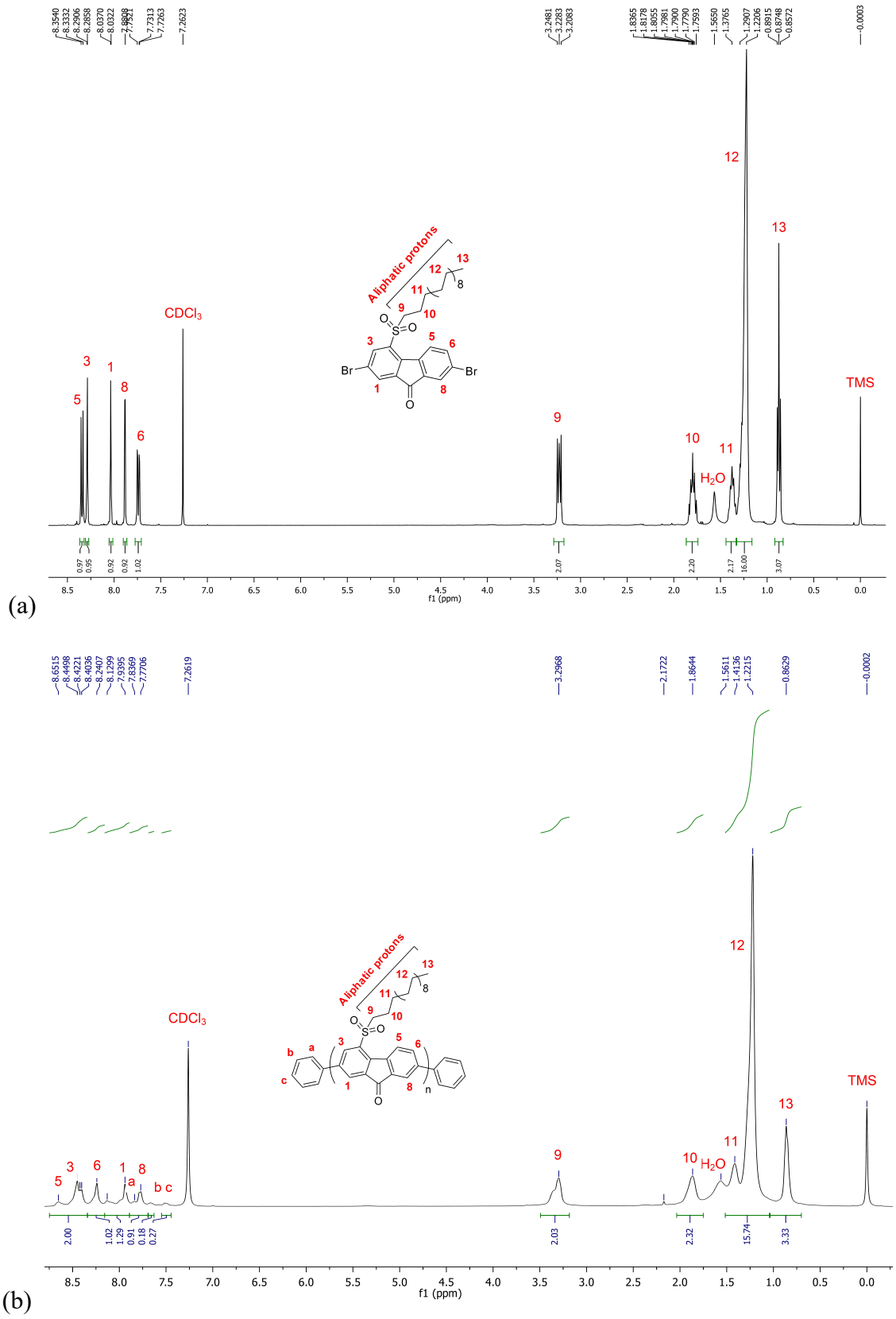

Figure 6.13 ^{1}H NMR spectra of 2,7-dibromo-4-dodecylsulfonylfluorenone (**6.23**) and **DDSO$_2$-PFon** polymer obtained by Yamamoto polymerisation (from conditions shown in Scheme 6.7).

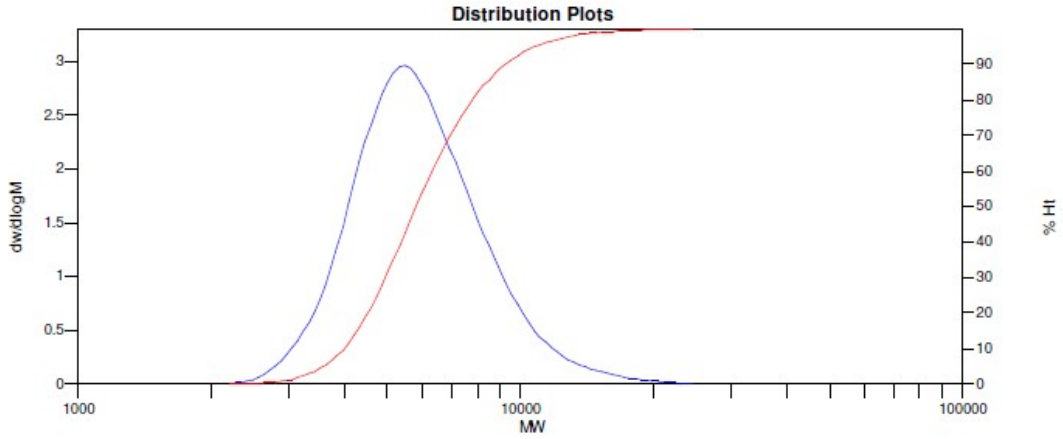

Figure 6.14 GPC trace of **DDS-PFon** polymer in THF.

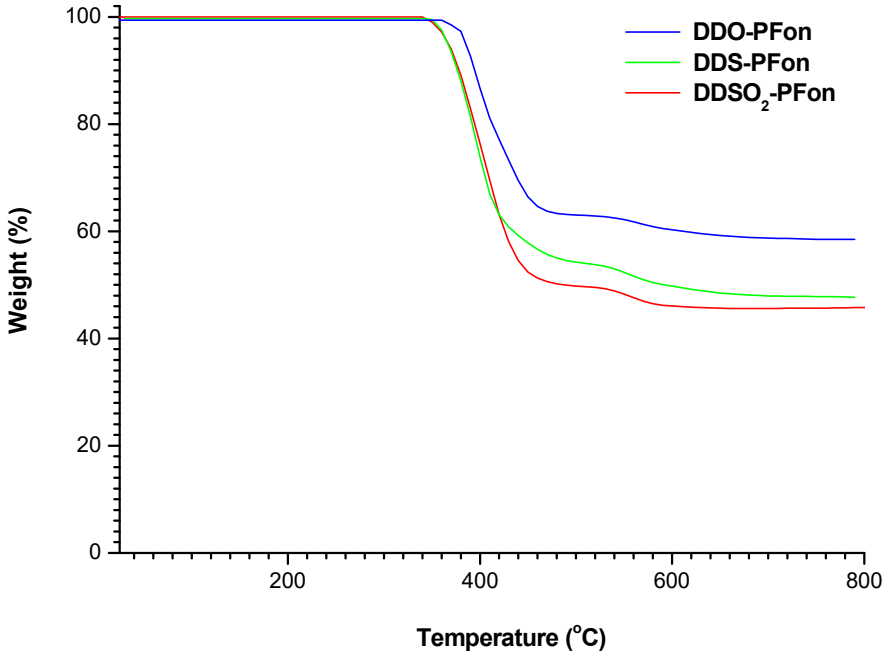

Figure 6.15 TGA curves for **X-PFon** polyfluorenones (X = $OC_{12}H_{25}$, $SC_{12}H_{25}$, $SO_2C_{12}H_{25}$).

6.2.4 UV-Vis electron absorption and photoluminescence spectral studies of X-PFon polymers

The UV-Vis absorption spectra of 4-substituted polyfluorenones **DDSO$_2$-PFon**, **DDS-PFon,** and **DDO-PFon** in chloroform solution showed three major absorption peaks in the ranges of (296–299 nm), (332–345 nm) and (433–474 nm), (Figure 6.16). The second peaks are assigned to the π-π* transition of delocalised electrons on the polymer backbone, while the third series i.e., the longest wavelength bands belong to the n-π* forbidden transition

involving the carbonyl group. These absorptions are somewhat blue-shifted compared to the **Ar-PFon** polymer with a bulky group at position 4 reported in the literature,[28] although they have been measured in different solvents (Table 6.2). There are very small red shifts in absorption spectra from chloroform solution to films (except **DDS-PFon**, in which case 57 nm shift was observed).

All **X-PFon** polymers are weakly emissive materials emitting from orange to red light. Their PL spectra show structureless bands with maxima in the range of λ_{PL}^{S} = 557–629 nm in chloroform solution that are bathochromically shifted by 26–41 nm to λ_{PL}^{F} = 583–655 nm in films (Figure 6.16 and Table 6.2). For all polymers, the emission is observed at longer wavelengths than for **Ar-PFon** (524 nm in THF solution and 554 nm in films). Because in our series of **X-PFon** polymers we used both EDG and EWG groups, these differences can not be attributed to electronic effects of the substituents and are more likely due to the linear nature of substituents X (in contrast to bulky branched (tetraphenyl)phenyl groups in **Ar-PFon**) facilitating slight planarisation of the polymer chain in the excited state. Photoluminescence spectra show a clear effect of substituents X on the emission wavelengths of **X-PFon** polymers with bathochromic shifts of PL maxima from EWG to EDG units. Being a strong electron acceptor, the polyfluorenone chain is involved in a charge-transfer with the EDG in the excited state, resulting in the observed PL shifts. Considering that there are no differences in this effect for the solution and the solid state (*cf.* PL for **DDSO$_2$-PFon** and **DDO-PFon**: $\Delta\lambda_{PL}^{S} = \Delta\lambda_{PL}^{F}$ = 71–72 nm, Table 6.2) we assign it to an intramolecular process on the polymer chain, with negligible (or completely absent) intermolecular CT interactions.

It should also be noted that for the PL spectra of **Ar-PFon** in THF a shoulder at 550 nm was observed after the main PL peak at 524, which the authors have attributed to excimer emission (basing on its coincidence with the PL in films at 554 nm).[28] We think that this might be not a well justified assumption, as we did not see any long-wavelength shoulders for our **X-PFon** polymers, which have more planar (linear) substituents and as such should more likely tend to aggregate and form the excimers.

The optical band gaps of the synthesised polymers **X-PFon,** estimated from the red edge of their absorption spectra in films lie in the range of 2.28–2.32 eV in solution and 2.17–2.27 eV in the solid state (Table 6.2).

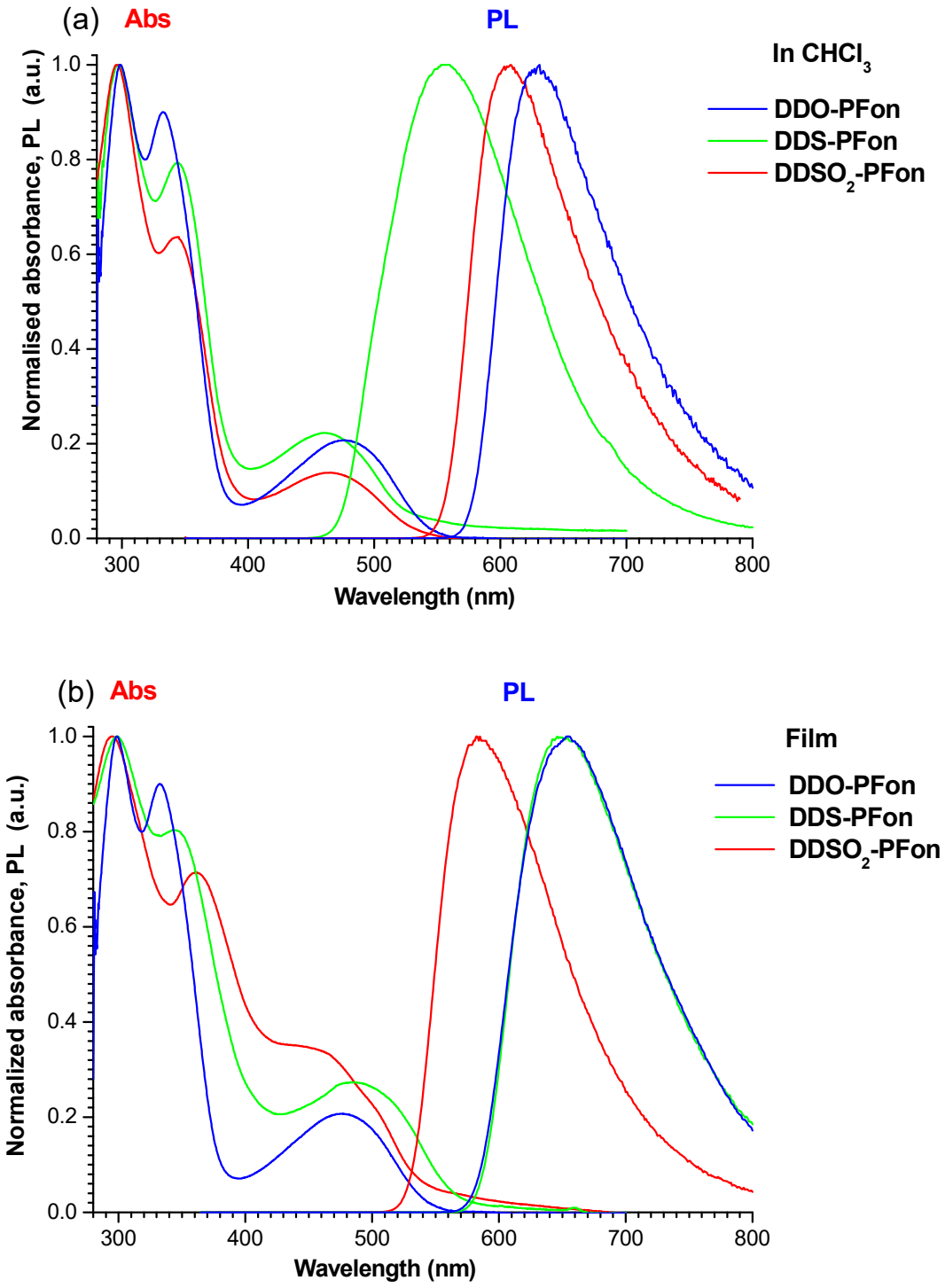

Figure 6.16 UV-Vis absorption and PL emission spectra of polymers **X-PFon** (X = $OC_{12}H_{25}$, $SC_{12}H_{25}$, $SO_2C_{12}H_{25}$) in chloroform (a) and in films (b). PL spectra have been recorded with excitations at the maxima of the longest wavelength absorptions of the corresponding samples.

Table 6.2 UV-Vis Absorption and PL emission data for 4-substituted polyfluorenones **X-PFon** (X = $OC_{12}H_{25}$, $SC_{12}H_{25}$, $SO_2C_{12}H_{25}$) in chloroform solution and films.

Polymer	λ_{abs} $CHCl_3$ (nm)	λ_{abs} film[a] (nm)	E_g^{opt},[a] $CHCl_3$ (nm)	E_g^{opt},[a] film (nm)	λ_{PL} $CHCl_3$ (nm)	λ_{PL} film[a] (nm)[b]	Φ_{PL}^{S},[b] $CHCl_3$ (%)[c]
DDO-PFon	299, 331, 478	299, 333, 476	2.28	2.27	629	655	0.9
DDS-PFon	296, 334, 465	299, 344, 483	2.31	2.18	608	648	1.05
DDSO$_2$-Fon	297, 335, 460	295, 361, 455sh	2.32	2.26	557	584	6.9
ArP-Fon[28]	367, 456[c]	369, 460	–	–	524[c]	554	–

[a] Films are spin-coated from chloroform solution. [b] Φ_{PL}^{S} is PLQY measured in toluene solution using DPA as a reference (Φ_{PL}^{R} = 90 %). [c] Measured in THF solution.

6.2.5 Electrochemical studies of X-PFon polymers

Cyclic voltammetry (CV) was used to assess the reduction potentials of the synthesised **X-PFon** polymers for the estimation of their LUMO energy levels, which characterise the electron affinities of the materials. CV measurements have been done for polymer films deposited by drop casting on a glassy carbon electrode in 0.1 M Bu_4NPF_6/CH_3CN under nitrogen. All polymers can be easily n-doped. Polymers **DDO-PFon** and **DDS-PFon** show partly reversible reductions peaking at –1.90 V and –1.85 V vs Fc/Fc^+ (Figure 6.17, Table 6.3). Polymer **DDSO$_2$-PFon** is oxidised more easily (at less negative potentials), with two closely-spaced reduction waves peaking at E^{red}_{pc} = –1.45 and –1.54 V. These reductions are quasi-reversible, showing back re-oxidation peaks with differences of cathodic/anodic potentials of $\Delta E^{red}_{pc\text{-}pa}$ = 130–140 mV (Table 6.3).

LUMO energy levels of polymers were estimated from the onsets of their reduction potentials, by addition of ferrocene with a known energy level of the Fc/Fc^+ couple versus vacuum. They vary in the range of 0.4 eV by substituents in position 4, from –3.11 eV for the weakest acceptor **DDO-PFon** to –3.51 eV for the strongest acceptor **DDSO$_2$-PFon.** So, there is an obvious trend of decreasing LUMO energy levels with an increase of electron-accepting character of the 4-substituent. The estimated LUMO energies are close to those reported in the literature for unsubstituted **PFon** and **Ar-Phon** (Table 6.3).

So, one could expect that the **X-PFon** can easily permit facile electron injection from the cathode and promote electrons as a very good electron transporting material for OLEDs.[22] In this respect **DDSO$_2$-PFon**, whose LUMO energy level is very low (–3.51 eV) is of particular interest, as this energy is quite close to the work function of magnesium (–3.7 eV),[38] a common cathode in OLEDs. Thus **DDSO$_2$-PFon** might be an exceptionally promising candidate as an electron injection/electron transporting material with low energy losses in electron injections in OLEDs. Another important property of **DDSO$_2$-PFon** is that it shows the reversible (quasi-reversible) reduction, that is its n-doping state is highly stable. Many other electron deficient polymers that have been synthesised in the past and studied as electron injection/electron transporting layers lack redox stability. For example, widely studied cyano-substituted poly(*p*-phenylenevinylene) (CN-PPV) has been successfully used as the electron transporting layer in OLED, but it shows an irreversible reduction.[39,40]

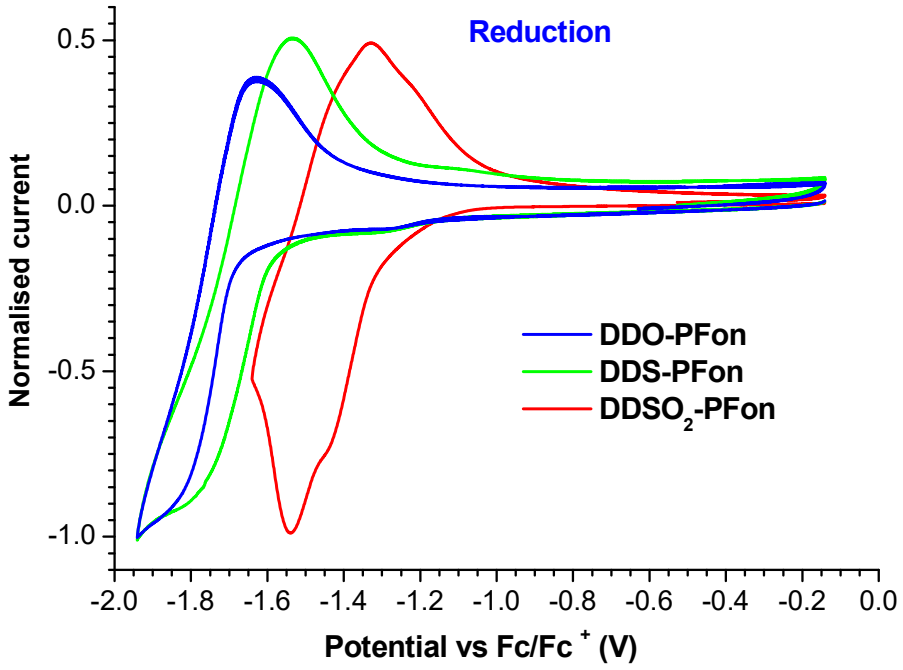

Figure 6.17.Cyclic voltammograms of **X-PFon (**X = $OC_{12}H_{25}$, $SC_{12}H_{25}$, $SO_2C_{12}H_{25}$**)** polymer films on glassy carbon electrode in 0.1 M of Bu_4NPF_6/CH_3CN, scan rate 100mV/s. Potentials were measured versus Ag/Ag^+ and calibrated versus Fc/Fc^+.

Table 6.3 CV Reduction potentials and LUMO energy levels for **X-PFon** polymers in films.

Polymer	E^{red}_{pc}, [a] (V)	E^{red}_{pa}, [a] (V)	$\Delta E^{red}_{pc\text{-}pa}$, [a] (mV)	E^{red}_{onset}, [a] (V)	LUMO, [b] (eV)
DDO-PFon	–1.90	–1.63	270	–1.69	–3.11
DDS-PFon	–1.85	–1.54	310	–1.58	–3.22
DDSO$_2$-PFon	–1.45, –1.54	–1.31, –1.41	140, 130	–1.29	–3.51
Ar-PFon[28]					–3.0
PFon[22]				–1.48	–3.32

[a] E^{red}_{pc} is cathodic peak potential, E^{red}_{pa} is anodic peak potential for re-oxidation process, $\Delta E^{red}_{pc\text{-}pa}$ is a difference between the cathodic and anodic peak potentials, E^{red}_{onset} is an onset of reduction potential (all are measured vs Fc/Fc^{+}). [b] LUMO energy levels calculated as LUMO = $-e(E^{red}_{onset} + 4.8)$ eV.

6.3 Conclusion

A new series of soluble 4-substituted functionalised polyfluorenones **X-PFon** with EDG and EWG have been synthesised by Ni-mediated Yamamoto polymerisation reaction. All polymers, **DDO-PFon** (X = $OC_{12}H_{25}$), **DDS-PFon** (X = $SC_{12}H_{25}$), **DDSO$_2$-PFon** (X = $SO_2C_{12}H_{25}$), have been characterised by ^{1}H NMR, GPC, TGA, CV, UV-Vis absorption and photoluminescence spectroscopies.

The solubilising effect of the $C_{12}H_{25}$ linear side groups, which lie in the plane of the fluorenone π-system is not strong enough and the usual Yamamoto polymerisation conditions gave insoluble (presumably too high molecular weight) polymers. So, different conditions for the Yamamoto polymerisation have been developed to obtain soluble **X-PFon** with M_n close or above the effective conjugation length (4,700–5,800 Da) and with very narrow polydispersity of PDI = 1.05–1.12.

The optical properties of the synthesised polymers have been studied in both chloroform solution and in films. The polymers have optical band gaps of ca. 2.2–2.3 eV and emit light in the orange-red region (557–629 nm in solution, 584–655 in films). Solution photoluminescence quantum yields of emission of **X-PFon** polymers vary from 1 to 7%. There is a clear electronic effect of the groups in position 4 on the emission energies, with ~70 nm bathochromic shift in PL from **DDSO$_2$-PFon** to **DDO-PFon**, as well as a bathochromic shift in PL of 26–41 nm from solution to the solid state. **X-PFon** polymers show quasi-reversible reductions in cyclic voltammetry experiments, from which their LUMO energies have been estimated as: –3.11 eV (**DDO-PFon**), –3.22 eV (**DDS-PFon**), –3.51 eV (**DDSO$_2$-PFon**). The strong electron-accepting character of the synthesised **X-PFon** polymers

and the stability of their doped states make them attractive candidates for organic electronic applications. In particular, the high electron affinity (low-lying LUMO energy level) of the **DDSO$_2$-PFon** polymer (–3.51 eV) is quite close to the Mg work function, making it promising for its use as an electron injecting and electron transport layer for OLED devices.

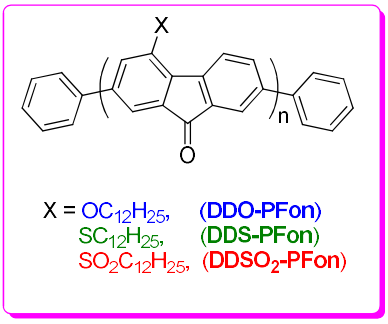

6.4 Experimental Section

6.4.1 Chemicals and instrumentation

All chemicals and solvents were received from the suppliers Aldrich, Acros, Apollo Scientific, Fisher and used without any further purification. Instruments (NMR, EI-MS, flash chromatograph, freeze dryer, GPC, TGA, UV-Vis and PL) are the same as mentioned in Chapters 3 and 4. Scanning electron microscopy images were obtained on SEM Phenom Pro model. Matrix-assisted laser desorption/ionisation time of flight (MALDI-TOF) mass spectra were recorded on a Bruker Reflex IV mass-spectrometer operating at 20 kV acceleration voltage in positive ion reflectron mode with pulsed ion extraction (200 ns). The insoluble polymer was analysed by powder X-ray-diffraction on a Phillips Xpert Pro instrument.

6.4.2 Synthesis

2,7-Dinitro-4-dodecyloxyfluorenone (6.16)

Exp no: SK-58

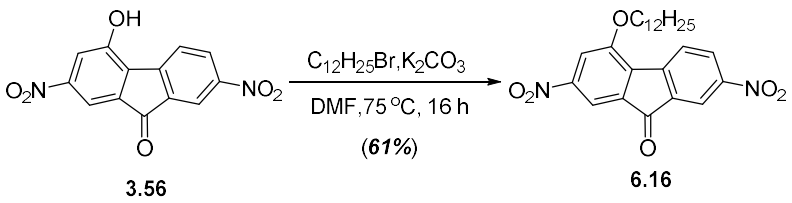

3.56 6.16

A mixture of 4-hydroxy-2,7-dinitrofluorenone (**3.56**) (10.5 g, 36.6 mmol), dodecyl bromide (13.3 mL) and potassium carbonate (25.3 g, 183 mmol) in DMF (100 mL) were stirred at 75 °C for 16 h. The reaction mixture was cooled to room temperature and diluted with cold water (200 mL). Green precipitate was filtered off, washed with water and dried *in vacuo* to give crude product (17.3 g, 104%). The crude product was purified by column chromatography on

silica gel using PE/EA (4:1, v/v) as eluent to afford compound **6.16** as a brown solid (10.2 g, 61 %), mp: 89–90 °C.

^{1}H NMR (400 MHz, $CDCl_3$): δ (ppm) 8.51 (d, *J* = 1.99, Hz, 1H), 8.47 (dd, *J* = 2.22, 8.21 Hz, 1H), 8.18 (d, J = 1.63 Hz, 1H), 8.11 (d, J = 8.17 Hz, 1H), 8.01 (d, J = 1.63 Hz, 1H), 4.30 (t, J = 6.4 Hz, 2H, $OCH_2C_{11}H_{23}$), 2.01 (m, 2H, $OCH_2CH_2C_{10}H_{21}$), 1.57 (m, 2H), 1.45 (m, 2H), 1.26 (s, 14H), 0.87 (t, J = 7.0 Hz, 3H).

^{13}C NMR (100 MHz, $CDCl_3$): δ (ppm) 188.76, 155.79, 150.75, 148.81, 147.03, 136.74, 135.10, 134.56, 130.39, 125.56, 119.58, 113.77, 111.93, 70.03, 31.90, 29.64, 29.57, 29.52, 29.34, 29.25, 28.94, 26.01, 22.68, 14.10.

MS (TOF EI+): *m/z* 454.99 (M^+, 100%). Calcd for $C_{25}H_{30}N_2O_6$: 454.21.

2,7-Dinitro-4-dodecylthiofluorenone (6.17) and 2-dodecyl-4,7-dinitrofluorenone (6.18)

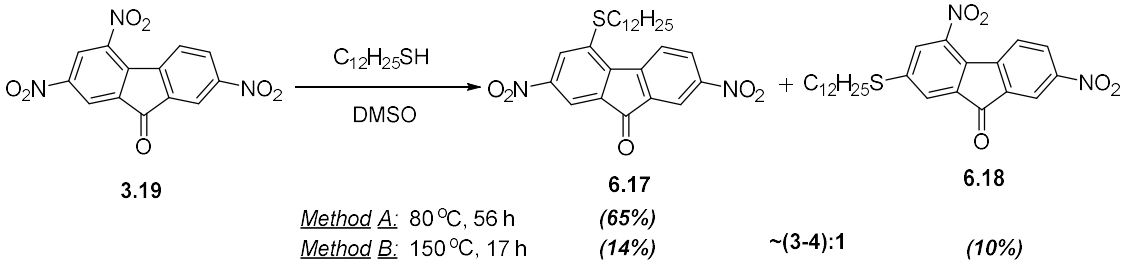

Method A (6.17). Exp no: SK-74

A mixture of 2,4,7-trinitrofluorenone (**3.19**) (20.0 g, 63.7 mmol) and 1-dodecanethiol (44 mL, 184 mmol) in DMSO (250 mL) was stirred at 80 °C for 56 h. The reaction mixture was cooled to room temperature, diluted with water (650 mL) and stirred for 2 h. An orange precipitate was filtered off, washed with water (4 × 500 mL) and dried *in vacuo* to give crude product (34.5 g, 115%). It was purified by recrystallisation from 1,4-dioxane (300 mL): the mixture was stirred under reflux for 2 h and left to stay at ambient temperature for 4 h. The solid was filtered off, washed with dioxane (2 × 50 mL) and dried *in vacuo* to afford pure compound **6.17** as a yellow solid (19.5 g, 65 %), mp: 104–106° C.

^{1}H NMR (400 MHz, acetone-d_6): δ (ppm) 8.65–8.58 (m, 2H), 8.43 (s, 2H), 8.18 (s, 1H), 3.41 (t, *J* = 7.2 Hz, 2H, $SCH_2CH_2C_{10}H_{21}$), 1.89–1.83 (m, 2H, $SCH_2CH_2C_{10}H_{21}$), 1.60–155 (m, 2H) 1.29 (m, 16H), 0.88 (t, *J* = 6.60 Hz, 3H, CH_3).

^{13}C NMR (100 MHz, $CDCl_3$): δ (ppm) 188.41, 149.41, 148.88, 147.69, 143.75, 138.94, 136.89, 135.74, 130.16, 127.31, 126.40, 119.55, 115.67, 67.09, 33.12, 31.90, 29.61, 29.54, 29.43, 29.33, 29.07, 28.85, 28.38, 22.68, 14.11.

MS (TOF EI^+): *m/z* 469.92 (M^+, 100%). Calcd for $C_{25}H_{30}N_2O_5S$: 470.19.

TLC analysis of the filtrate showed a mixture of compounds **6.17** and **6.18**, but with a substantial amount of the **6.17**. The compounds were not separated in this experiment.

Method B (6.17 + 6.18). Exp no: SK-50

A mixture of 2,4,7-trinitrofluorenone (**3.19**) (1.020 g, 3.23 mmol), 1-dodecanethiol (0.90 mL, 3.88 mmol) in DMSO (10 mL) was stirred at 150°C for 17 h. The reaction mixture was cooled to room temperature, diluted with water (20 mL) and extracted with DCM (3 × 10 mL). The organic layer was dried over Mg_2SO_4, the solvent was evaporated under reduced pressure and the residue was dried *in vacuo* to give crude product (1.89 g, 121%). The crude product was purified by column chromatography on silica gel using PE/DCM (9:1, v/v) eluted first compound **6.18** (0.098 g, 10%) and then compound **6.17** (0.210 g, 14%).

Analytical data for 2,7-dinitro-4-dodecylthiofluorenone (**6.17**) were the same as in method A.

2-Dodecylthio-4,7-dinitrofluorenone (6.18): mp: 106–108° C.

^{1}H NMR (400 MHz, $CDCl_3$) (**6.18**): δ (ppm) 8.53 (d, 1H), 8.45 (dd, *J* = 8.5, 2.3 Hz, 1H), 8.17 (d, *J* = 8.5 Hz, 1H), 7.92 (d, 1H), 7.84 (d, 1H), 3.08 (t, *J* = 7.3 Hz, 2H, $SCH_2CH_2C_{10}H_{21}$), 1.74 (m, 2H, $SCH_2CH_2C_{10}H_{21}$), 1.48 (m, 2H) 1.26 (m, 16H), 0.87 (t, *J* = 6.60 Hz, 3H, CH_3).

2,7-Diamino-4-dodecyloxyfluorenone (6.19)

Exp no: SK-59

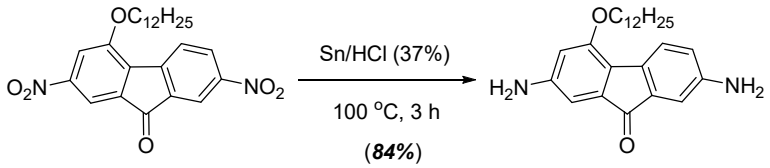

6.16 **6.19**

To a stirred mixture of 2,7-dinitro-4-dodecyloxyfluorenone (**6.16**) (9.30 g, 20.6 mmol) and 37% HCl (60 mL), tin powder (15.9 g, 134 mmol) was added slowly portionwise at room temperature (*Caution! Intense gas evolution and foaming the reaction mixture occurs*). The mixture was stirred at 100 °C for 3 h, cooled to room temperature, diluted with water (20 mL) and basified to pH 9 by adding saturated $NaHCO_3$ solution (~150 mL). Ethyl acetate (750 mL) was added and the mixture was stirred for 4 h. The inorganic solid (stannous hydroxide) was filtered off and washed with ethyl acetate. The organic layer was separated and the aqueous layer was extracted twice with ethylacetate. The combined organic layer was dried over $MgSO_4$, the solvent was evaporated under reduced pressure and the residue was dried *in vacuo* to give a crude product (9.50 g, 116 %). The crude compound was purified by column chromatography on silica gel using ethyl acetate as eluent to afford compound **6.19** as a black solid (6.80 g, 84%), mp: 96–98 °C.

^{1}HNMR (400 MHz, DMSO): δ (ppm) 7.14 (d, *J* = 7.89 1H, H-5), 6.71 (d, *J* = 2.31 Hz, 1H, H-8), 6.55 (dd, *J* = 2.13, 7.88 Hz, 1H, H-6), 6.36 (d, *J* = 1.62 Hz, 1H), 6.30 (d, *J* = 1.67 Hz, 1H),

5.29 (s, 4H, NH_2), 3.95 (t, J = 6.3 Hz, 2H, $OCH_2C_{11}H_{23}$), 1.75 (m, 2H), 1.44 (m, 2H), 1.22 (m, 16H), 0.83 (t, J = 4.5 Hz, CH_3).

^{13}C NMR (100 MHz, $CDCl_3$): δ (ppm) 195.48, 154.56, 150.37, 147.72, 136.13, 134.46, 133.34, 122.78, 120.44, 118.90, 110.47, 103.73, 102.84, 67.79, 61.19, 33.00, 31.76, 29.50, 29.43, 29.40, 29.19, 29.11, 25.98, 22.56, 14.40.

MS (TOF EI+): *m/z* 394.18 (M^+, 100%). Calcd for $C_{25}H_{34}N_2O_2$: 394.26.

2,7-Diamino-4-dodecylthiofluorenone (6.20)

Exp no: SK-85

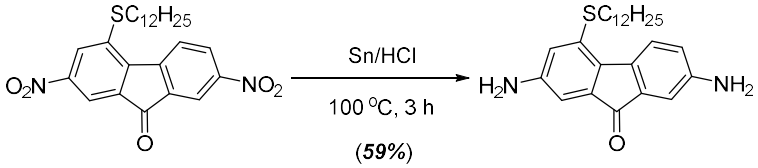

6.17 **6.20**

To a stirred mixture of 2,7-dinitro-4-dodecylthiofluorenone (**6.17**) (18.0 g, 38.4 mmol) in 37% of HCl (150 mL), tin powder (29.6 g, 249 mmol) was added slowly portionwise at room temperature (*Caution! Intense gas evolution and foaming the reaction mixture*). The mixture was stirred at 100 °C for 3 h, cooled down to room temperature, diluted with water (100 mL) and basified to pH 9 by additing 4 M NaOH solution (~800 mL). Ethyl acetate (600 mL) was added and the mixture was stirred for 4 h. The inorganic solid (stannous hydroxide) was filtered off and washed with ethyl acetate. The organic layer was separated and the aqueous layer was extracted twice with ethylacetate. The combined organic layer was dried over $MgSO_4$, the solvent was evaporated under reduced pressure and the residue was dried *in vacuo* to give a crude product. It was purified by column chromatography on silica gel using PE/EA (1:1, v/v) as eluent to afford compound **6.20** as a black solid (9.4 g, 59 %), mp: 89–91 °C.

^{1}H NMR (400 MHz, $CDCl_3$): δ (ppm) 7.82 (d, J = 8.0 Hz, 1H, H-5), 7.26 (s, 1H), 6.92 (d, J = 2.32 Hz, 1H), 6.69 (dd, J = 2.4, 8.0 Hz, 1H, H-6), 6.62 (d, J = 2.1 Hz, 1H), 3.77 (s, 4H, NH_2) 2.91 (t, J = 7.4 Hz, 2H), 1.68 (m, 2H), 1.41 (m, 2H), 1.29 (m, 16H), 0.87 (t, J = 6.6 Hz, 3H, CH_3).

^{13}C NMR (100 MHz, DMSO): δ (ppm) 194.36, 146.05, 145.80, 136.68, 136.04, 135.74, 134.50, 132.28, 124.32, 120.15, 119.72, 111.54, 109.51, 33.61, 31.91, 29.65, 29.63, 29.59, 29.51, 29.34, 29.17, 29.09, 28.91, 22.69, 14.12.

MS (TOF EI+): *m/z* 410.16 (M^+, 100%), Calcd for $C_{25}H_{34}N_2OS$: 410.24.

2,7-Dibromo-4-dodecyloxyfluorenone (6.21)

Exp no: SK-61

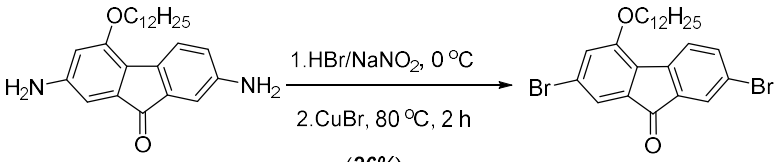

6.19 **6.21**

A suspension of 2,7-diamino-4-(dodecyloxy)fluorenone (**6.19**) (5.70 g, 14.5 mmol) in 48% HBr (28 mL) was stirred for 20 minutes at ambient temperature and cooled down to 0 °C. A solution of sodium nitrite (2.50 g, 36.2 mmol) in H_2O (10 mL) was added dropwise maintaining the temperature of the reaction mixture at –2/0 °C (internal temperature). The excess of nitrite ions was controlled by KI-starch paper. The mixture was stirred at 0 °C for 45 min and then copper (I) bromide (5.20 g) was added portionwise. The mixture was stirred at 80 °C for 2 h, cooled to room temperature, diluted with water (20 mL), neutralised with saturated $NaHCO_3$ (50 mL) and extracted with DCM (3 × 100 mL). The combined DCM extracts were dried over Mg_2SO_4, the solvent was evaporated under reduced pressure and the residue was dried *in vacuo* to give a crude compound as a brown solid . The crude product was dissolved in DCM and filtered through a silica gel column (d ~ 5–6 cm, L = 6-8 cm) eluting with PE/DCM (1:1, v/v). After solvent evaporation, the residue was purified by column chromatography on silica gel using PE/toluene (1:2, v/v) as eluent to afford compound **6.21** as a yellow solid (1.97 g, 26 %), mp: 94–96 °C.

^{1}H NMR (400 MHz, $CDCl_3$): δ (ppm) 7.65 (d, *J* = 1.3 Hz, 1H, H-8), 7.56 (d, *J* = 7.8 Hz, 1H, H-5), 7.50 (dd, *J* = 1.6, 7.8 Hz, 1H, H-6), 7.31 (d, *J* = 0.8 Hz, 1H), 7.09 (d, *J* = 0.8 Hz, 1H), 4.10 (t, *J* = 6.4 Hz, 2H, $CH_2C_{11}H_{23}$), 1.83 (m, 2H, $CH_2CH_2C_{10}H_{21}$), 1.44 (m, 2H, $(CH_2)_2CH_2C_9H_{19}$), 1.19 (m, 16H, $(CH_2)_3(CH_2)_8CH_3$), 0.88 (t, *J* = 7.0 Hz, 3H, CH_3).

^{13}C NMR (100 MHz, $CDCl_3$): δ (ppm) 191.46, 155.29, 141.95, 137.45, 136.12, 134.69, 129.63, 127.42, 125.42, 123.80, 122.14, 121.59, 119.80, 69.02, 31.92, 29.66, 29.57, 29.53, 29.36, 29.26, 29.09, 26.03, 22.70, 14.12.

MS (TOF EI+): *m/z* 523.85 (M^+, ^{79}Br/^{79}Br, 60%), 521.79 (M^+, ^{79}Br/^{81}Br, 100%), 519.85 (M^+, ^{81}Br/^{81}Br, 60%), Calcd for $C_{25}H_{30}Br_2O_2$: 524.06 (49.0%), 522.06 (100%), 520.06 (51.4%).

UV-Vis ($CHCl_3$): λ_{max} = 264, 273, 304, 316, 336sh, 442 nm.

2,7-Dibromo-4-dodecylthiofluorenone (6.22)

Exp no: SK-88

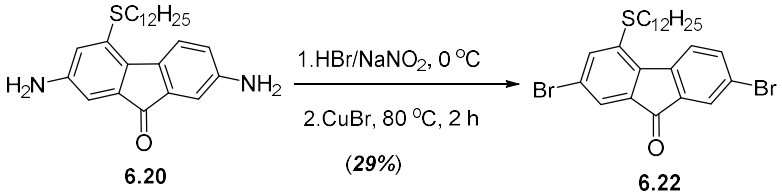

A suspension of 2,7-diamino-4-dodecylthiofluorenone (**6.20**) (7.8 g, 19.1 mmol) in 48% HBr (50 mL) was stirred for 30 min at ambient temperature and cooled down to 0 °C. A solution of sodium nitrite (3.2 g, 47.7 mmol) in H_2O (20 mL) was added dropwise maintaining the temperature of the reaction mixture at –2/0 °C (internal temperature). The excess of nitrite ions was controlled by KI-starch paper. The mixture was stirred at 0 °C for 45 minutes and then copper(I) bromide (6.8 g) was added portionwise. The mixture was stirred at 80 °C for 2 h, cooled to room temperature, diluted with water (20 mL), neutralised with saturated $NaHCO_3$ (50 mL) and extracted with ethyl acetate (3 × 100 mL). The combined EA extracts were dried over Mg_2SO_4, the solvent was evaporated under reduce pressure and the residue was dried *in vacuo* to give a crude brown product (11.4 g, 111%). The crude product was dissolved in DCM and filtered through a silica gel column (d ~ 5–6 cm, L = 6–8 cm) eluting with PE/DCM (4:1, v/v). The solvent was evaporated and the residue was purified by column chromatography on silica gel using toluene as eluent to afford compound **6.22** as an orange solid (2.97 g, 29%), mp: 70–71 °C.

^{1}H NMR (400 MHz, $CDCl_3$): δ (ppm) 8.04 (d, J = 8.12 Hz 1H, H-5), 7.76 (d, J = 1.8 Hz, 1H), 7.63 (dd, J = 1.92, 8.12 Hz, 1H, H-6), 7.57 (d, J = 1.68 Hz, 1H), 7.49 (d, J = 1.68 Hz, 1H), 3.02 (t, J = 7.3 Hz, 2H, $CH_2C_{11}H_{23}$), 1.72 (m, 2H, $SCH_2CH_2C_{10}H_{21}$), 1.45 (m, 2H, $(CH_2)_2CH_2C_9H_{19}$), 1.25 (s, 16H, $(CH_2)_3(CH_2)_8CH_3$), 0.87 (t, J = 7.0 Hz, 3H, CH_3).

^{13}C NMR (100 MHz, $CDCl_3$): δ (ppm) 190.87, 142.57, 139.87, 137.36, 136.31, 135.97, 135.88, 135.20, 127.48, 126.18, 124.46, 123.26, 122.95, 33.34, 31.92, 29.64, 29.57, 29.46, 29.36, 29.10, 28.84, 28.64, 22.71, 14.15

MS (TOF EI+): *m/z* 535.91 (M^+, ^{79}Br/^{79}Br, 60%), 537.87 (M^+, ^{79}Br/^{81}Br, 100%), 539.97 (M^+, ^{81}Br/^{81}Br, 60%),. Calcd for $C_{25}H_{30}Br_2OS$: 536.04 (51.3%), 538.04 (100%), 540.03 (53.1%).

2,7-Dibromo-4-dodecylsulfonylfluorenone (6.23)

Exp no: SK-89

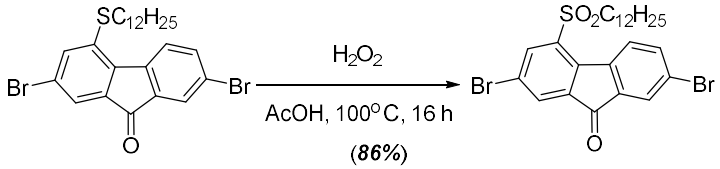

6.22 **6.23**

2,7-Dibromo-4-dodecylthiofluorenone (**6.22**) (1.506 g, 2.79 mmol), 30% hydrogen peroxide (0.5 mL) and acetic acid (50 mL) were stirred at 100° C for 16 h. The reaction mixture was cooled down to room temperature and diluted with water (50 mL). The precipitate was filtered off, washed with water (2 × 10 mL) and dried *in vacuo* to afford compound **6.23** as a yellow solid (1.362 g, 86%), mp: 101–103 °C.

^{1}H NMR (400 MHz, ($CDCl_3$): δ (ppm) 8.34 (d, *J* = 8.3 Hz, 1H, H-5), 8.28 (d, *J* = 1.8 Hz, 1H), 8.03 (d, *J* = 1.8 Hz, 1H), 7.88 (d, *J* = 1.9 Hz, 1H), 7.74 (dd, *J* = 2.0 Hz, 8.3 1H, H-6), 3.23 (t, *J* = 7.9 Hz, 2H, $CH_2C_{11}H_{23}$), 1.78 (m, 2H, $CH_2CH_2C_{10}H_{21}$), 1.35 (m, 2H, $(CH_2)_2CH_2C_9H_{19}$), 1.27 (m, 16H, $(CH_2)_3(CH_2)_8CH_3$), 0.87 (t, *J* = 7.0 Hz, 3H, CH_3).

^{13}C NMR (100 MHz, $CDCl_3$): δ (ppm) 189.07, 140.29, 139.37, 138.47, 137.30, 135.55, 135.41, 132.10, 128.23, 128.08, 125.42, 123.80, 54.42, 31.89, 29.57, 29.56 (2C by peak intensity), 29.45, 29.31, 29.18, 28.90, 28.18, 22.68, 22.16, 14.13.

MS (TOF EI+): *m/z* 567.67 (M^+, $^{79}Br/^{79}Br$, 50%), 569.66 (M^+, $^{81}Br/^{81}Br$, 100%), 571.87 (M^+, $^{79}Br/^{81}Br$, 55%), Calcd for $C_{25}H_{30}Br_2O_3S$: 568.03 (50.3%), 570.03 (100%), 572.02 (52.0%).

4-Dodecyloxyfluorenone-2,7-diboronic acid dipinacol ester (6.24)

Exp no: SK-73

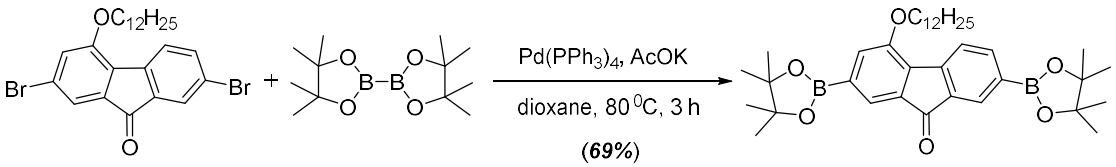

6.21 **6.24**

2,7-Dibromo-4-(dodecyloxy)fluorenone (**6.21**) (0.506 g, 0.96 mmol), bis(pinacolato)diboron (0.817 g, 3.10 mmol) and potassium acetate (0.285 g, 2.90 mmol) in dry dioxane (20 mL) were stirred and purged with nitrogen for 25 min. Tetrakis(triphenylphosphine) palladium(0), $Pd(PPh_3)_4$, (0.033 g, 0.029 mmol) was added and the mixture was stirred and purged with nitrogen for additional 15 min. The mixture was then stirred under nitrogen at 80 °C for 3 h, cooled down to room temperature, diluted with water (30 mL) and extracted with DCM (3 × 10 mL). The combined DCM extracts were dried over Mg_2SO_4, the solvent was evaporated under reduced pressure and the residue was dried *in vacuo* to give a crude product. It was

purified by column chromatography on silica gel using Et_2O/toluene (1:9, v/v) as eluent to afford compound **6.24** as a yellow oil (0.412 g, 69%).

^{1}H NMR (400 MHz, $CDCl_3$): δ (ppm) 8.09 (m, 1H), 7.92 (dd, J = 0.9, 7.4 Hz, 1H, H-6), 7.85 (d, J = 7.4 Hz, 1H, H-5), 7.75 (m, 1H), 7.45 (m, 1H), 4.19 (t, J = 6.3 Hz, 2H, $CH_2C_{11}H_{23}$), 1.91 (m, 2H, $CH_2CH_2C_{10}H_{21}$), 1.58–1.50 (m, 2H, $(CH_2)_2CH_2C_9H_{19}$) 1.43–1.38 (m, 2H, $(CH_2)_3CH_2C_8H_{17}$), 1.34 (s, 24H, CH_3 borolane), 1.30–1.26 (m, 14H, $(CH_2)_4(CH_2)_7CH_3$), 0.87 (t, J = 6.6 Hz, 3H, CH_3).

^{13}C NMR (100 MHz, $CDCl_3$): δ (ppm) 194.13, 154.79, 146.28, 141.54, 135.33, 133.53, 133.10, 130.04, 124.46, 123.80, 122.66, 84.14 (2C), 84.00 (2C), 68.49, 31.91, 29.67, 29.65, 29.61, 29.59, 29.37, 29.35 (3C), 26.18, 25.02, 24.87 (8C), 22.69, 14.12.

MS (TOF EI+): *m/z* 616.24 (M^+, 100%), Calcd for $C_{37}H_{54}B_2O_6$: 616.41.

Insoluble poly(4-dodecylsulfonylfluorenone), DDSO$_2$-PFon-i

Exp no: SK-180

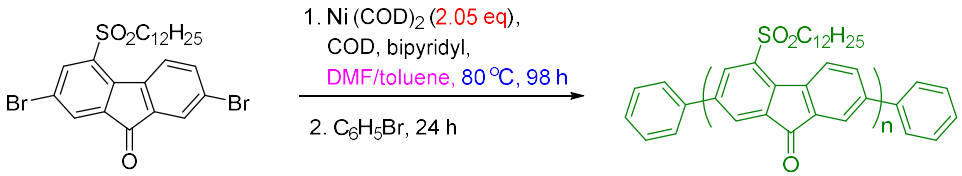

6.23 DDSO$_2$-PFon-i

Under an argon atmosphere, mixture of bis(1,5-cylcooctadiene)nickel(0), $Ni(COD)_2$, (98 mg, 0.35 mmol), 1,5-cyclooctadiene (44 mg, 0.35 mmol) and 2,2'-bipyridyl (64 mg, 0.35 mmol) in dry DMF (1.0 mL) were stirred at 80 °C for 30 minutes to form a dark violet solution. A solution of 2,7-dibromo-4-dodecylsuphonylfluorenone (**6.23**) (102 mg, 0.17 mmol) in dry toluene (1.75 mL) was added slowly to the Ni (0) complex solution and the mixture was stirred at 80° C for 98. After 24 h, the reaction mixture became viscous, with the formation of suspension that decreased the rate of stirring. The heating at 80 °C was continued additional 74 h, occasionally shaking the flask. The mixture was cooled down to room temperature and poured dropwise into a stirred solution of methanol:concentrated HCl (4:1, v/v) (50 mL) to form a red precipitate. The mixture was stirred at room temperature for 4 h, the precipitate was filtered off, washed with water (3 × 10 mL) and dried *in vacuo* to afford a red solid (68 mg, 92%). This polymer **DDSO$_2$-PFon-i** appeared as an amorphous red solid, which was almost insoluble in any solvent (THF, benzene, toluene, 1,4-dioxane, 1,2-dichlorobenzene, acetone, chloroform and ethylacetate were tested). The sample was analysed by the following techniques: reflectance UV-Vis absorption in the solid state on $BaSO_4$ surface using an

integrating sphere, solution UV-Vis absorption for some chloroform extracts, SEM and XRD (see Results and Discussion section).

Low molecular weight and insoluble poly(4-dodecyloxyfluorenones), DDO-PFon-L and DDO-PFon-i

Exp no: SK-64

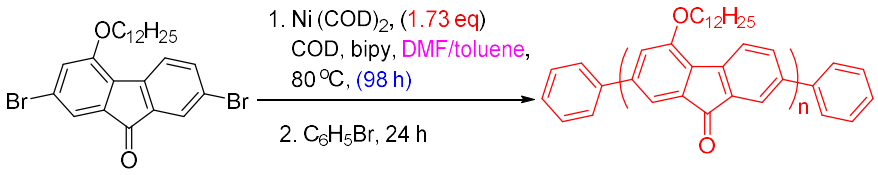

6.21 **DDO-PFon**

Under an argon atmosphere, bis(1,5-cylcooctadiene)nickel(0), $Ni(COD)_2$, (91 mg, 0.33 mmol), 1,5-cyclooctadiene (0.04 mL, 0.33 mmol), 2,2'-bipyridyl (52 mg, 0.33 mmol) in dry DMF (0.5 mL) were stirred at 80 °C for 30 minutes to form a dark violet solution. To this, a solution of 2,7-dibromo-4-dodecyloxyfluorene (**6.21**) (104 mg, 0.19 mmol) in dry toluene (1.5 mL) was added and the mixture was stirred at 80 °C for 96 h. Bromobenzene (0.01 mL) was added as an end-capper and the mixture was stirred at 80 °C for additional 18 h. The mixture was cooled down to room temperature and poured dropwise into a stirred solution of methanol:concentrated HCl:acetone (1:1:1, v/v) (30 mL) to form a yellow precipitate. Toluene (20 mL) was added to extract and dissolve the solid, the organic layer was separated and dried over Mg_2SO_4. The solvent was evaporated under reduced pressure and the residue was dried *in vacuo* to give the crude product as a brown solid (84 mg, 115%). The crude product was extracted in a Soxhlet apparatus with methanol (16 h) and then with acetone (18 h) to remove by-products and low molecular weight fractions to give (after solvent evaporation) an orange solid (45 mg, 62%). The residue in a thimble was extracted with chloroform for 12 h, the solution was concentrated to a small volume (~ 2 mL) and poured dropwise into stirred methanol (7 mL). The precipitate was filtered off, washed with methanol and dried *in vacuo* to afford **DDO-PFon-L** as a red solid (5 mg, 7%). The insoluble material in the thimble was a red powder solid of **DDO-PFon-i** (15 mg, 20%).

DDO-PFon-L: ^{1}H NMR (400 MHz, ($CDCl_3$): δ (ppm) 7.71 (m, 1H), 7.62 (br d, J = 7.7 Hz, 1H), 7.57 (br d, J = 7.8 Hz, 1H), 7.37 (m, 1H), 7.16 (m, 1H, $CH_2C_{11}H_{23}$), 4.10 (m, 2H, $CH_2CH_2C_{10}H_{21}$), 1.90 (m, 2H, $(CH_2)_2CH_2C_9H_{19}$), 1.27 (m, 16H, $(CH_2)_3(CH_2)_8CH_3$), 0.88 (m, 3H, CH_3).

Low molecular weight poly(4-dodecyloxyfluorenone), DDO-PFon-L

Exp no: SK-181

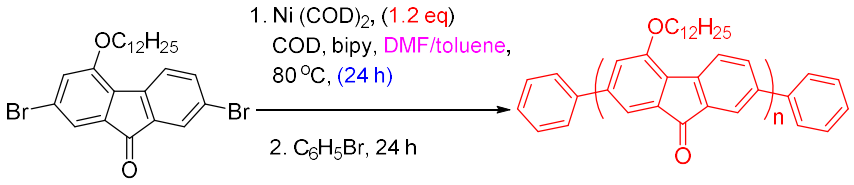

6.21 DDO-PFon-L

Under an argon atmosphere, a mixture of bis(1,5-cylcooctadiene)nickel(0), $Ni(COD)_2$, (68 mg, 0.24 mmol), 1,5-cyclooctadiene (26 mg, 0.24 mmol), and 2,2'-bipyridyl (38 mg, 0.24 mmol) in dry DMF (1.0 mL) were stirred at 80 °C for 30 minutes to form a dark violet solution. To this, a solution of 2,7-dibromo-4-dodecyloxyfluorenone (**6.21**) (108 mg, 0.20 mmol) in dry toluene (6.0 mL) was added slowly and the mixture was stirred at 80 °C for 24 h. The mixture was cooled down to room temperature and poured dropwise into a stirred solution of methanol:concentrated HCl (4:1, v/v) (50 mL) to form a red precipitate. It was filtered off, washed with water (3 × 10 mL) and dried *in vacuo* to give **DDO-PFon-L** as a red solid (62 mg, 83%), (sample SK-181A).

Analysis: The unpurified sample SK-182A was analysed by GPC using THF and chloroform as eluents. GPC analyses showed that the material represented a mixture of the monomer, trimer, pentamer and some longer oligomers. The sample preparation for the GPC analysis: a sample 2 mg/1.0 mL THF (or chloroform) was stirred for 24 h, centrifuged for 3 h, filtered through a membrane filter (0.5 μm) and the filtrate was submitted for the GPC analysis.

GPC (THF): M_w = 1,818 Da, M_n = 1,110 Da, PDI = 1.64. Detailed analysis: broad unresolved signal at M_n > 2,300 Da, then Peak 1 (M_w = 2,301 Da, M_n = 2,194 Da, pentamer), Peak 2 (M_w = 1,205 Da, M_n = 1,194 Da, trimer), Peak 3 (M_w = 624 Da, M_n = 615 Da, monomer).

GPC (chloroform): broad unresolved signal at M_n > 2,300 Da, then Peak 1 (M_w = 1,979 Da, M_n = 1,966 Da, pentamer), Peak 2 (M_w = 1,236 Da, M_n = 1,226 Da, trimer), Peak 3 (M_w = 531, M_n = 523 Da, monomer).

Low molecular weight and insoluble poly(4-dodecyloxyfluorenones), DDO-PFon-L and DDO-PFon-i

Exp no: SK-182

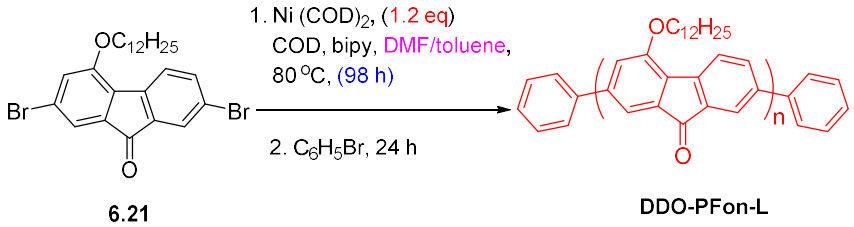

6.21 DDO-PFon-L

Under an argon atmosphere, a mixture of bis(1,5-cylcooctadiene)nickel(0), $Ni(COD)_2$, (68 mg, 0.24 mmol), 1,5-cyclooctadiene (26 mg, 0.24 mmol), and 2,2'-bipyridyl (38 mg, 0.24 mmol) in dry DMF (1.0 mL) was stirred at 80 °C for 30 minutes to form a dark violet solution. To this, a solution of 2,7-dibromo-4-dodecyloxyfluorenone (**6.21**) (108 mg, 0.20 mmol) in dry toluene (6.0 mL) was slowly added and the mixture was stirred at 80 °C for 98 h. The mixture was cooled down to room temperature and poured dropwise into a stirred solution of methanol:concentrated HCl (4:1, v/v) (50 mL) to form a red precipitate. It was filtered off, washed with water (3 × 10 mL) and dried *in vacuo*. The crude product was dissolved in chloroform (30 mL), stirred for 4 h, concentrated to a small volume (~ 3 mL) and added dropwise into vigorously stirred methanol (20 mL) to form red precipitate. The precipitate was filtered off, washed with methanol and dried *in vacuo* to afford a red solid (64 mg, 84%), (sample SK-182A).

Analysis: The unpurified sample SK-182A was analysed by GPC using THF and chloroform as eluents. The GPC analysis showed that the material represented a mixture of the monomer, trimer, pentamer and some longer oligomers. The sample preparation for the GPC analysis is the same as in previous synthesis SK-181.

GPC (THF): M_w = 2,194 Da, M_n = 2,301 Da, PDI = 1.04. Detailed analysis: broad unresolved signal at M_n > 2,300 Da, then Peak 1 (M_w = 1,863 Da, M_n = 1,856; pentamer), Peak 2 (M_w = 1,211 Da, M_n = 1,211 Da, trimer), Peak 3 (M_w = 620 Da, M_n = 613 Da, monomer).

GPC (chloroform): broad unresolved signal at M_n > 2,300 Da, then Peak 1: M_w = 1,881, M_n = 1,867, pentamer), Peak 2 (M_w = 1,169 Da, M_n = 1,156 Da, trimer), Peak 3: M_w = 508, M_n = 500 Da , monomer).

This unpurified sample (SK-182A) was combined with the similar sample SK-181A (previous synthesis) and extracted with methanol, acetone, and chloroform sequentially (for 24 h each). In each case the solvents were evaporated and the residues were dried *in vacuo* to afford:

(B): methanol-soluble fraction, 27 mg (~18%);

(C): acetone-soluble fraction, 23 mg (~16%);

(B): chloroform-soluble fraction, 33 mg (22%), **DDO-PFon-L**;

(E): insoluble compound as a red solid in a thimble, 30 mg (20%), **DDO-PFon-i**.

DDO-PFon-L:

MALDI-TOF: *m/z* (relative intensity, assignment) 1,252 (100%, trimer), 1,616 (90%, tetramer), 1,981 (50%, pentamer), 2,345 (40%, hexamer), 2,710 (30%, heptamer), 3,075 (20%, octamer).

UV-Vis (in chloroform): Figure 6.18 shows electron absorption spectra of methanol (B)/ acetone (C)/chlrotoform-soluble fractions (D), as well as monomer **6.21**. Bathochromic shifts from (B) to (D) indicate an increase of molecular weight of the products in fractions from methanol to chloroform. Fraction (B) seems mainly a mixture of monomer(s), fraction (C) is mainly a mixture of dimers/trimers.

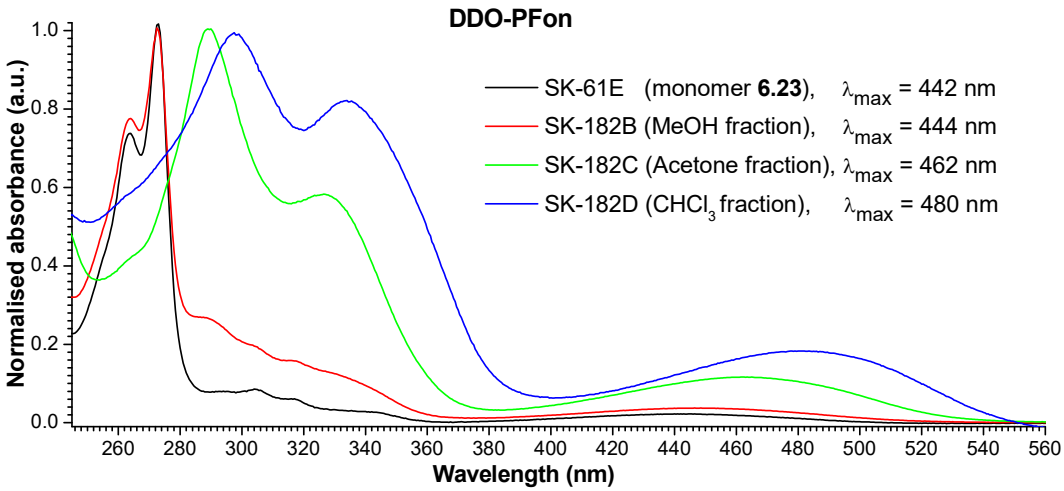

Figure 6.18 UV-Vis electron absorption spectra of soluble fractions of oligofluorenones **DDO-PFon** and monomer **6.21** in chloroform.

Poly(4-dodecyloxyfluorenone), DDO-PFon

Exp no: MRT-03

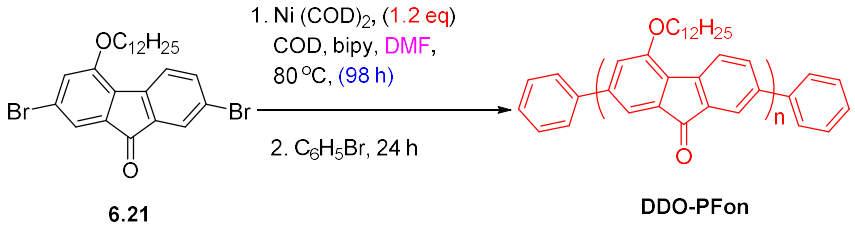

6.21 DDO-PFon

In a glove box under a nitrogen atmosphere, bis(1,5-cylcooctadiene)nickel(0), $Ni(COD)_2$, (322 mg, 1.17 mmol), 1,5-cyclooctadiene (0.1 mL, 1.13 mmol), 2,2'-bipyridyl (181 mg, 1.15 mmol), 2,7-dibromo-4-dodecyloxyfluorene (**6.21**) (510 mg, 0.97 mmol) and dry DMF (10

mL) were charged into 25 mL two neck round bottom flask. The flask was closed with a stopper and a septum and transfered to a fume hood for polymerisation. It was purged with argon for 5 min and the mixture was then stirred at 80 °C for 98 h. Bromobenzene (0.01 mL) was added as end-capper and the mixture was stirred at 80 °C for additional 18 h. The mixture was cooled down to room temperature and poured dropwise into a stirred solution of methanol:concentrated HCl (4:1, v/v) (50 mL) to form a dark red precipitate. After stirring for 1 h, the solid was filtered off, washed with methanol (5 mL) and dried *in vacuo* to give a dark red crude product (443 mg, 120%). It was extracted in a Soxhlet apparatus with acetone (18 h) to remove by-products and low molecular weight fractions. The residue was extracted with chloroform for 12 h, the solution was concentrated to a small volume (~4 mL) and added dropwise into vigorously stirred methanol (75 mL). The precipitate was filtered off, washed with methanol and dried *in vacuo* to afford polymer **DDO-PFon** as a red solid (182 mg, 51%).

GPC (THF): M_w = 6,100 Da, M_n = 5,800 Da, PDI = 1.05.

^{1}H NMR (400 MHz, ($CDCl_3$): δ (ppm) 7.78–7.77 (m, 1H), 7.67–7.64 (m, 1H), 7.53–7.51 (m, 1H), 7.47–7.30 (m, 1H), 7.21–7.16 (m, 1H), 4.18 (m, 2H), 1.96 (m, 2H), 1.55–1.27 (m, 18H), 0.85 (m, 3H, CH_3).

Poly(4-dodecylthiofluorenone), DDS-PFon

Exp no: MRT-02

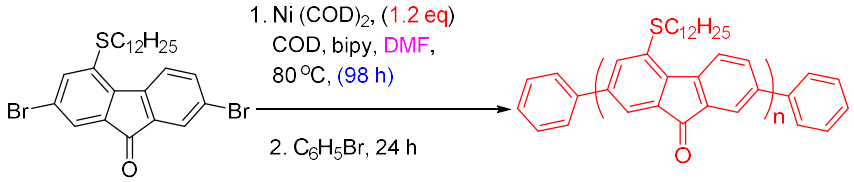

6.22 DDS-PFon

In a glove box under a nitrogen atmosphere, of bis(1,5-cylcooctadiene)nickel(0), $Ni(COD)_2$, (312 mg, 1.13 mmol), 1,5-cyclooctadiene (0.12 mL, 0.97 mmol), 2,2'-bipyridyl (175 mg, 1.12 mmol), 2,7-dibromo-4-dodecylthiofluorenone (**6.22**) (510 mg, 0.97 mmol) and dry DMF (10 mL) were charged into 25 mL two neck round bottom flask. The flask was closed with a stopper and a septum and transfered to a fume hood for polymerisation. It was purged with argon for 5 min and the mixture was then stirred at 80 °C for 98 h. Bromobenzene (0.01 mL) was added as end-capper and the mixture was stirred at 80 °C for additional 18 h. The mixture was cooled down to room temperature and poured dropwise into a stirred solution of methanol:concentrated HCl (4:1, v/v) (50 mL) to form a dark red precipitate. After stirring for 1 h, the solid was filtered off, washed with methanol (5 mL) and dried *in vacuo* to give a dark

red crude product (453 mg, 125%). It was extracted in a Soxhlet apparatus with acetone (18 h) to remove by-products and low molecular weight fractions. The residue was extracted with chloroform for 12 h, the solution was concentrated to a small volume (~4 mL) and added dropwise into vigorously stirred methanol (75 mL). The precipitate was filtered off, washed with methanol and dried *in vacuo* to afford polymer **DDS-PFon** as a red solid (151 mg, 44%).

GPC (THF): M_w = 6,200 Da, M_n = 5,600 Da, PDI = 1.10.

^{1}H NMR (400 MHz, ($CDCl_3$): δ (ppm) 8.18–8.11 (m, 1H), 8.02–7.97 (m, 1H), 7.79–7.70 (m, 1H), 7.63–7.59 (m, 1H), 7.51–7.49 (m, 1H), 3.08 (m, 2H), 1.77–1.75 (m, 2H), 1.51–1.23 (m, 18H), 0.86 (s, 3H, CH_3).

Poly(4-dodecylsulfonylfluorenone), DDSO$_2$-PFon

Exp no: MRT-01

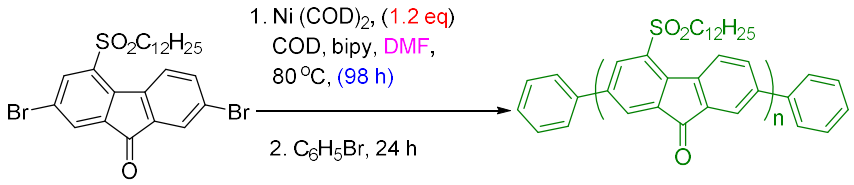

6.23 **DDSO$_2$-PFon**

In a glove box under a nitrogen atmosphere, bis(1,5-cylcooctadiene)nickel(0), Ni(COD)$_2$, (290 mg, 1.0 mmol), 1,5-cyclooctadiene (0.12 mL, 1.0 mmol), 2,2'-bipyridyl (165 mg, 1.0 mmol), 2,7-dibromo-4-dodecylsulphonylfluorenone (**6.23**) (510 mg, 0.8 mmol) and dry DMF (10 mL) charged into 25 mL two neck round bottom flask. The flask was closed with a stopper and a septum and transfered to a fume hood for polymerisation. It was purged with argon for 5 min and the mixture was stirred at 80 °C for 98 h. Bromobenzene (0.01 mL) was added as end-capper and the mixture was stirred at 80 °C for additional 18 h. The mixture was cooled down to room temperature and poured dropwise into a stirred solution of methanol:concentrated HCl (4:1, v/v) (50 mL) to form a dark red precipitate. After stirring for 1 h, the solid was filtered off, washed with methanol (5 mL) and dried *in vacuo* to give a dark red crude product (641 mg, 91%). It was extracted in a Soxhlet apparatus with acetone (18 h) to remove by-products and low molecular weight fractions. The residue was extracted with chloroform for 12 h, the solution was concentrated to a small volume (~4 mL) and added dropwise into vigorously stirring methanol (75 mL). The precipitate was filtered off, washed with methanol and dried *in vacuo* to afford polymer **DDSO$_2$-PFon** as a red solid (112 mg, 33%).

GPC (THF): M_w = 5,300 Da, M_n = 4,700 Da, PDI = 1.12.

^{1}H NMR (400 MHz, ($CDCl_3$): δ (ppm) 8.65–8.44 (m, 2H), 8.24 (s, 1H), 7.93 (s, 1H), 7.77 (d, 1H), 3.29 (m, 2H), 1.86 (s, 2H), 1.41–1.22 (m, 18H), 0.86 (s, 3H, CH_3).

References

1 A .C. Grimsdale, K. L. Chan, R. E. Martin, P. G. Jokisz, and A. B. Holmes, *Chem. Rev*., **2009**, *109*, 897–1091. (DOI: 10.1021/cr000013v).

2 A. Mishra, C.-Q. Ma, and P. Bäuerle, *Chem. Rev*., **2009**, *109*, 1141–1276. (DOI: 10.1021/cr8004229)

3 I. F. Perepichka and D. F. Perepichka (Eds), *Handbook of Thiophene-Based Materials: Applications in Organic Electronics and Photonics*, (Two-Volumes Set*, Vol. 1: Synthesis and Theory, Vol. 2: Properties and Applications*), Wiley, **2009**, 910 pp.

4 A. J. Blayney, I. F. Perepichka, F. Wudl, and D. F. Perepichka, *Isr. J. Chem*., **2014**, *54*, 674–688. (DOI: 10.1002/iJch.201400067).

5 Y. Olivier, D. Niedzialek, V. Lemaur, W. Pisula, K. Müllen ,U. Koldemir, J. R. Reynolds, R. Lazzaroni, J. Cornil, and D. Beljonne, *Adv. Mater*., **2014**, *26*, 2119–2136. (DOI: 10.1002/adma.201305809).

6 X. Zhaoab and X. Zhan, *Chem. Soc. Rev*., **2011**, *40*, 3728–3743. (DOI: 10.1039/c0cs00194e).

7 H. T. Nicolai, M. Kuik, G. A. H. Wetzelaer, B. de Boer, C. Campbell, C. Risko, J. L. Brédas, and P. W. M. Blom, *Nature Mater*., **2012**, *11*, 882–887. (DOI:10.1038/nmat3384).

8 S. Kola, J. Sinha, and H. E. Katz, *J. Polym. Sci. B: Polym. Phys*., **2012**, *50*, 1090–1120. (DOI: 10.1002/polb.23054).

9 C. Wang, H. Dong, W. Hu, Y. Liu, and D. Zhu, *Chem. Rev*., **2012**, *112*, 2208–2267. (DOI: org/10.1021/cr100380z).

10 J. Choi, K.-H. Kim, H. Yu, C. Lee, H. Kang, I. Song, Y. Kim, J. H. Oh, and B. J. Kim, *Chem. Mater*., **2015**, *27*, 5230−5237. (DOI: 10.1021/acs.chemmater.5b01274).

11 J. Lee, M. Jang, S. M. Lee, D. Yoo, T. J. Shin, J. H. Oh, and C. Yang, *ACS Appl. Mater. Interf*., **2014**, *6*, 20390–20399. (DOI:10.1021/am505925w).

12 W. Li, L. Yan, H. Zhou, and W. You, *Chem. Mater*., **2015**, *27*, 6470–6476. (DOI: 10.1021/acs.chemmater.5b03098).

13 A. P. Kulkarni, C. J. Tonzola, A. Babel, and S. A. Jenekhe, *Chem. Mater*., **2004**, *16*, 4556–4573. (DOI: 10.1021/cm049473l).

14 Y. Zhu, M. M. Alam, and S. A. Jenekhe, *Macromolecules*, **2003**, *36*, 8958–8968. (DOI: 10.1021/ma0348021).

15 C. J. Tonzola, M. M. Alam, B. A. Bean, and S. A. Jenekhe, *Macromolecules*, **2004**, *37*, 3554–3563. (DOI: 10.1021/ma035971o).

16 S. Hayashi, N. Nishioka, H. Nishiyama, and T. Koizumi, *Synth. Metals*, **2012**, *162*, 1485–1489. (DOI:10.1016/j.synthmet.2012.06.029).

17 M. Strukelj, F. Papadimitrakopoulos, T. M. Miller, and L. J. Rothberg, *Science*, **1995**, *267*, 1969–1972. (DOI: 10.1126/science.267.5206.1969).

18 F. Uckert, Y-H. Tak, K. Müllen, and H. Bässler, *Adv. Mater*., **2000**, *12*, 905–908. (DOI: 10.1002/1521-4095(200006)12:12<901).

19 M. Jandke, P. Strohriel, S. Berleb, E. Werner, and W. Brütting, *Macromolecules*, **1998**, *31*, 6434–6443. (DOI: 10.1021/ma9806054).

20 N. C. Greenham, S. C. Moratti, D. D. C. Bradley, R. H. Friend, and A. B. Holmes, *Nature*, **1993**, *365*, 628–630. (DOI:10.1038/365628a0).

21 A. M. Scott and M. R. Wasielewski, *J. Am. Chem. Soc*., **2011**, *133*, 3005–3013. (DOI: org/10.1021/ja1095649).

22 F. Uckert, Y-H. Tak, K. Müllen, and H. Bässler, *Adv. Mater.*, **2000**, *12*, 905–908. (DOI: 10.1002/1521-4095(200006)12:12<905).

23 T. Lee, C. A. Landis, B. M. Dhar, B. J. Jung, J. Sun, A. Sarjeant, H. J. Lee, and H. E. Katz, *J. Am. Chem. Soc*., **2009**, *131*, 1692–1705. (DOI: 10.1021/ja807219x).

24 H. Usta, C. Risko, Z. Wang, H. Huang, M. K. Deliomeroglu, A. Zhukhovitskiy, A. Facchetti, and T. J. Marks, *J. Am. Chem. Soc*., **2009**, *131*, 5586–5608. (DOI: 10.1021/Ja809555c).

25 S. Zecchin, G. Shiavon, R. Tomat, and G. Zotti, *J. Electroanal. Chem*., **1986**, *215*, 377–383. (DOI:10.1016/0022-0728(86)87030-9).

26 A. Cihaner, S. Tirkes, and A. M. Onal, *J. Electroanal. Chem*., **2004**, *568*, 151–156. (DOI:10.1016/J.Jelechem.2004.01.027).

27 F. Uckert, S. Setayesh, and K. Müllen, *Macromolecules*, **1999**, *32*, 4519–4524. (DOI: 10.1021/ma990157f).

28 L. Oldridge, M. Kastler, and K. Müllen, *Chem. Commun*., **2006**, 885–887. (DOI: 10.1039/B516078B).

29 S. Panozzo, J.-C. Vial, Y. Kervella, and O. Stephan, *J. Appl. Phys*., **2002**, *92*, 3495–3502. (DOI: 10.1063/1.1502920)

30 P. Sonar, T. J. Ha, and A. Dodabalapur, *Chem. Commun*., **2013**, *49*, 1588–1590. (DOI: 10.1039/C2CC37131F).

31 Z. Ying-ping, P. Chun-yue, Z. Zhen-hua, L. Bo, H. Yue-hui, Z. Ke-chao, Z. Yi, L. Yong-fang, *J. Centr. South Univ. Technol*., **2010**, *17*, 269–276. (DOI: 10.1007/s11771−010−0041−3).

32 S. Hayashi, N. Nishioka, H. Nishiyama, and T. Koizumi, *Synth. Metals*, **2012**, *162*, 1485–1489. (DOI: org/10.1016/J.synthmet.2012.06.029).

33 D. A. Patrick, J. E. Hall, B. C. Bender, D. R. McCurdy, D. W. Wilson, F. A. Tanious, S. Saha, and R. R. Tidwell, *J.Med.Chem*.,**1999**, *34*, 575–583. (DOI:10.1016/S0223-5234(00)80027-6).

34 I. F. Perepichka, A. F. Popov, T. V. Orekhova, M. R. Bryce, M. A. M. Andrievskii, S. A. Batsanov, J. A. K. Howard, and N. I. Sokolov, *J. Org. Chem*., **2000**, *65*, 3053–3063. (DOI: 10.1021/jo991796r).

35 T. Ishiyama, M. Murata, and N. Miyaura, *J. Org. Chem*., **1995**, *60*, 7508–7510. (DOI: 10.1021/Jo00128a024).

36 J. H. Ahn, C. Wang, I. F. Perepichka, M. R. Bryce, and M. C. Petty, *J. Mater. Chem*., **2007**, *17*, 2996–3001. (DOI: 10.1039/B700047B).

37 S. Y. Cho, A. C. Grimsdale, D. J. Jones, S. E. Watkins, and A. B. Holmes, *J. Am. Chem. Soc*., **2007**, *129*, 11910–11911.(DOI: 10.1021/ja074634i).

38 J. Pommerehne, H. Vestweber, W. Guss, R. F. Mahrt, H. Bassler, M. Porsch, and J. Daub, *Adv. Mater*., **1995**, *7*, 551–554. (DOI**:**10.1002/adma.19950070608).

39 R. Cervini, X. C. Li, G. W. C. Spencer, A. B. Holmes, S. C. Moratti, and R. H. Friend, *Synth. Metals*, **1997**, *84*, 359–360. (DOI:10.1016/S0379-6779(97)80781-3).

40 N. C. Greenham, S. C. Moratti, D. D. C. Bradley, R. H. Friend, and A. B. Holmes, *Nature*, **1993**, *365*, 628–630. (DOI:10.1038/365628a0).

Overall conclusion

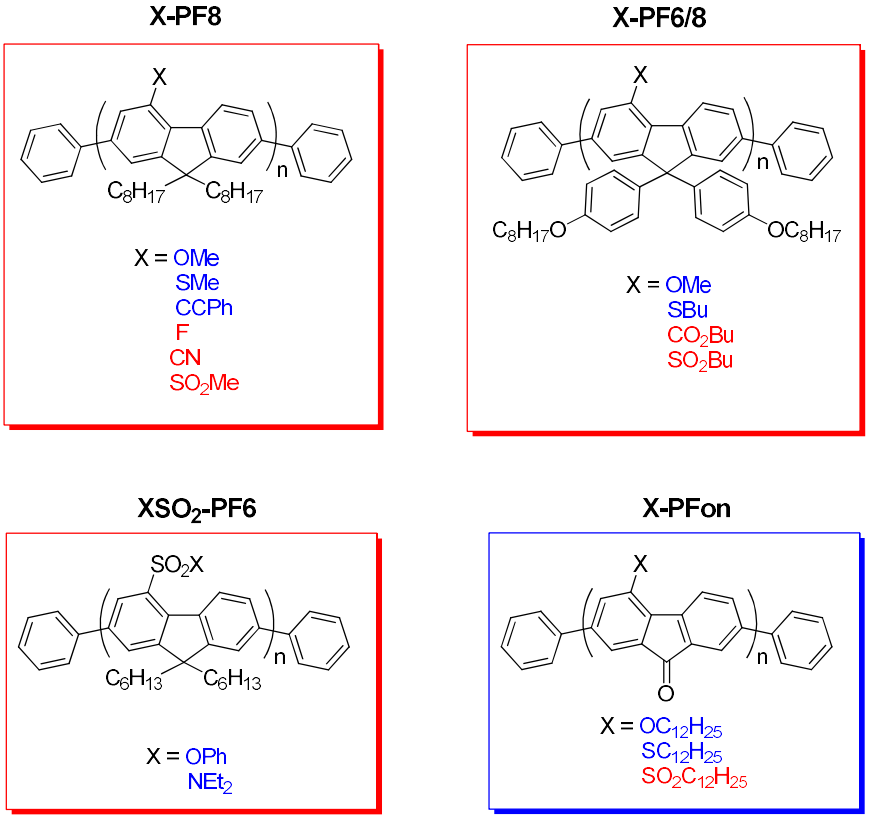

In this work we have successfully developed a novel class of light-emitting polyfluorenes functionalised with different groups a position 4 of the fluorene moieties. We have elaborated several different synthetic methodologies to introduce wide range of both electron-donating (and electron-withdrawing substituents into position 4 of the 2,7-dibromofluorene monomers with alkyl and alkoxyaryl solubilising groups (at C-9). Their Ni(0) mediated Yamamoto polymerisation gave high molecular weight homopolymers, which emitted bright blue light with high efficiencies in both the solution and the solid state.

Such a functionalisation of polyfluorenes allowed efficient tuning the HOMO and LUMO energy levels of the polymers (up to ca 0.7 eV), whereas the band gaps and the emission wavelengths of the polymers remained almost unchanged (λ_{PL} were varied in the range of 415–435 nm in solution and 428–445 in films), thus all novel 4-functionalised polyfluorenes (**X-PF8**, **X-PF6/8** and **XSO$_2$-PF6**) emitted in the blue region characteristic for unsubstituted polymers **PF8**, **PF6/8** and **PF6**. Consequently, the functionalisation of polyfluorenes in position 4 represents an efficient way for fine tuning the energy levels in this class of blue-emitting electroluminescent homopolymers for adjusting them to the work

functions of the electrodes used in the PLED devices and for controlling the mobility of the charge carriers (both holes and electrons).

Moreover, as a huge number of different copolymers with incorporated fluorene building blocks have been (and are) studied and used as materials for OLED, OPV and other optoelectrionic applications, elaborated in this work convenient methods of synthesis of a wide range of 4-functionalised fluorene monomers substantially expand the possible structural variations in such copolymers for a precise tuning their electronic and optical properties.

The synthetic methods toward 4-functionalised fluorenes have been expanded for synthesis of similar fluorenones and a series of soluble 4-functionalised polyfluorenones (**X-PFon**) have been successfully prepared. Strong electron-withdrawing effect of the carbonyl groups in the polyfluorenones resulted in materials with high electron affinities (LUMO = –(3.11–3.51 eV) and narrow band gaps (E_g^{opt} = 2.18–2.27 eV, in films) that makes them attractive candidates as electron-transporting polymers.

We believe that the results of this work will have a large impact on further development of novel fluorene-based semiconductive materials for various applications in organic electronics.